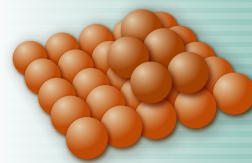
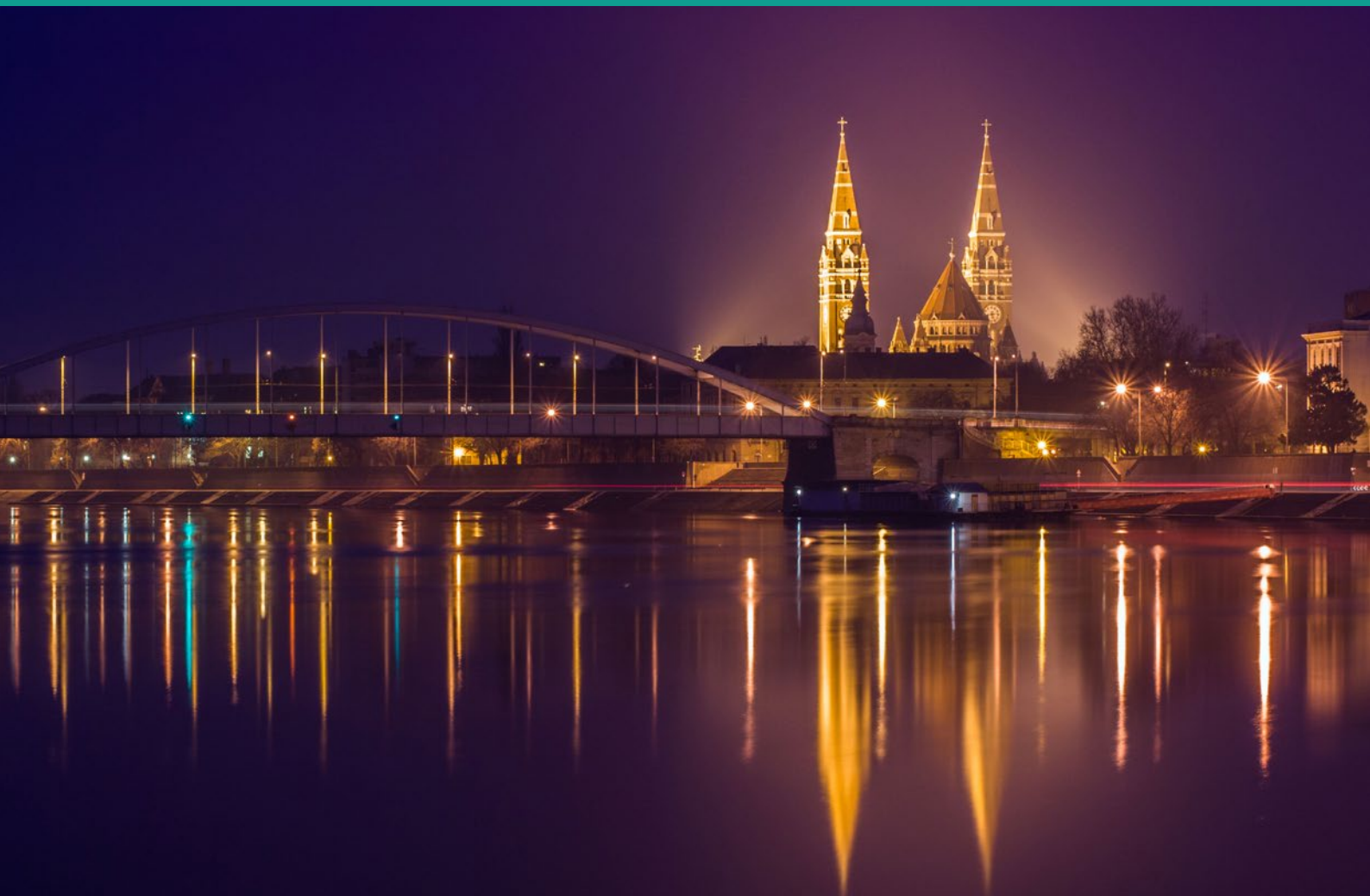


ecoss 33
27 AUG. – 1 SEPT. 2017
SZEGED, HUNGARY



33rd EUROPEAN CONFERENCE ON SURFACE SCIENCE



ABSTRACT BOOK

www.ecoss2017.org



CONFERENCE SECRETARY: Régió-10 Ltd. • Dugonics sq. 12, H-6720 Szeged, Hungary

Phone/fax: +36 62 710 500 • E-mail: ecoss33secretariat@regio10.hu • www.regio10.hu



Type of presentations

- Plenary lecture **Plen**
- Invited lecture **I**
- Keynote lecture **K**
- Oral presentation **O**
- Poster presentation **PS**

Communication code

Mon – day of the presentation

9:00 – time of the presentation

O – type of the presentation

CORR – “Corrosion at atomic level” session

● Color code session

Mon-9:00-O-CORR ●

SCIENTIFIC TOPICS

- BAND** ● Band structure of solid surfaces
- BIMS** ● Bimetallic surfaces and alloy nanocrystals
- CATH** ● Catalytic 2D-model studies under high pressures
- CATL** ● Catalytic 2D-model studies at low pressures
- COMP** ● Computational surface chemistry and physics
- CORR** ● Corrosion at atomic level
- EG2D** ● Epitaxial growth and modification of 2D materials
- ELAM** ● Electron attachment of adsorbed molecules
- ELCH** ● Electrochemistry at surfaces
- ENER** ● Surfaces for energy production and harvesting
- GRAP** ● Graphene and carbon-based 2D films
- LASE** ● LASER pulses for surface electron dynamics
- MAGN** ● Surface and molecular magnetism
- MOLA** ● Ultrathin two-dimensional molecular self-assembly
- NAEX** ● Novel advancement of experimental methods
- ORGS** ● Organic molecules on solid surfaces
- OXID** ● Oxide surfaces and ultrathin oxide films
- PISC** ● Photo-Induced Surface Chemistry
- SAMA** ● Structural analysis and manipulation on atomic scale
- SEMI** ● Semiconductor surfaces and ultrathin layers













| PLENARY LECTURES | | | 19 |
|-------------------------|--|----------------------|-----------|
| Behm R J | Nanostructured metal surfaces – from surface science to electrochemistry / electrocatalysis | Fri-11:20-Plen-7 | 20 |
| Campbell C T | Adsorption calorimetry techniques on well-defined surfaces and their application in understanding catalysis, photovoltaics and atomic-layer deposition | Fri-9:20-Plen-5 | 21 |
| Kuk Y | Understanding bulk properties from surfaces of high temperature superconductors | Wed-14:00-Plen-3 | 22 |
| Molinari E | Illuminating nanosystems at surfaces | Fri-10:10-Plen-6 | 23 |
| Raval R | Supramolecular and covalent assembly of molecules at surfaces: chirality, complexity and diversity | Wed-14:50-Plen-4 | 24 |
| Somorjai G A | Surface science approach to the molecular level integration of the principles in heterogeneous, homogeneous, and enzyme catalysis | Mon-9:30-Plen-1 | 25 |
| Wolf M | Ultrafast dynamics of excited states and light induced processes at surfaces | Mon-10:40-Plen-2 | 26 |
| KEYNOTE LECTURES | | | 27 |
| Netzer F P | Metal-supported 2D oxide systems: strong versus weak substrate coupling | Wed-16:00-K-OXID ● | 28 |
| Osvay K | The ELI Research Infrastructure and implementation status | Mon-11:30-K-ELI-ALPS | 29 |
| Schauer mann S | Partial selective hydrogenation of acrolein over model Pd catalysts: a mechanistic IRAS and molecular beam study | Tue-16:40-K-CATL ● | 30 |
| Steinrück H-P | Chemical reactions in ionic liquids monitored through the gas (vacuum)/liquid interface | Wed-9:40-K-NAEX ● | 31 |
| Tanemura M | Towards the low temperature growth of transfer free graphene | Wed-11:20-K-GRAP ● | 32 |
| INVITED LECTURES | | | 33 |
| Asscher M | Buffer layer assisted deposition as a tool for basic catalysis and photo-induced surface science studies | Tue-16:00-I-PISC ● | 34 |
| Bergmann K | Manipulation of interface-induced Skyrmions studied with STM | Tue-10:40-I-MAGN ● | 35 |
| Biró L P | SPM characterization and processing of 2D materials | Tue-15:00-I-EG2D ● | 36 |
| Comelli G | Graphene growth on Ni (111) | Thu-10:40-I-GRAP ● | 37 |
| Duò L | Tailoring the Properties of Oxide/Metal Interfaces: from Metallic to Graphitic Buffer Layers | Tue-14:00-I-OXID ● | 38 |
| Foster A S | Molecularly functionalized surfaces and interfaces | Wed-10:40-I-COMP ● | 39 |
| Gellman A J | Alloy surface science spanning composition space | Wed-9:00-I-BIMS ● | 40 |
| Gregoratti L | Novel solutions for near ambient pressure in-situ photoelectron spectro-microscopy | Tue-9:40-I-NAEX ● | 41 |
| Hermansson K | Multiscale modelling of reactive metal oxide interfaces | Thu-10:40-I-OXID ● | 42 |

| | | | |
|------------------|---|--------------------|----|
| Jelinek P | High-resolution AFM/STM/IETS imaging and its applications | Tue-10:40-I-NAEX ● | 43 |
| Kühnle A | Generic nature of long-range repulsion in molecular self-assembly on a bulk insulator surface | Mon-15:00-I-ORGS ● | 44 |
| Lesiak B | Surfaces of nanocarbon-based materials – chemical and structural analysis by electron spectroscopic methods | Wed-9:40-I-GRAP ● | 45 |
| Lindsay R | Using surface science to understand corrosion | Tue-9:00-I-CORR ● | 47 |
| Marbach H | Towards the controlled fabrication of well defined nanostructures: a surface science approach to electron beam lithograp | Thu-16:00-I-ELAM ● | 48 |
| Matolin V | Single-atom Pt-cerium oxide catalysts | Tue-9:00-I-ENER ● | 49 |
| Miwa J A | Electronic properties of high density doping profiles in semiconductors | Thu-9:00-I-SEMI ● | 50 |
| Neyman K M | Efficient computational engineering of bimetallic nanocrystals | Tue-15:00-I-BIMS ● | 51 |
| Nowicki M | Electrochemical formation of nanostructures monitored by EC-STM and CV | Tue-14:00-I-ELCH ● | 52 |
| Rupprechter G | Spectroscopy and microscopy of catalytic processes on well-defined surfaces: from UHV to operando conditions | Thu-9:40-I-CATH ● | 53 |
| Sadowski J | (Ga,Mn)As as a canonical dilute ferromagnetic semiconductor – electronic structure, surface effects & magnetism in low dimensional structures | Thu-15:00-I-SEMI ● | 55 |
| Surnev S | 2D ternary oxide layers: new paradigmas of structure and stoichiometry | Wed-9:00-I-OXID ● | 56 |
| Suzer S | Investigation of Ionic Liquid Interfaces using time- and position-resolved XPS | Mon-14:00-I-NAEX ● | 57 |
| Szanyi J | The mechanism of CO ₂ reduction over Pd/Al ₂ O ₃ : a combined steady state isotope transient kinetic analysis (SSITKA) and operando FTIR investigation | Thu-15:00-I-CATH ● | 58 |
| Taleb-Ibrahimi A | Electronic structure of quantum materials and perspectives with ultra-high brilliant sources | Mon-15:00-I-BAND ● | 59 |
| Trenary M | Spectroscopic characterization of reaction pathways over a Pd-Cu(111) single-atom alloy | Mon-14:00-I-CATL ● | 60 |
| Vedmedenko E Y | Information and energy storage in magnetic skyrmions and helices: role of oscillating Dzyaloshinskii-Moriya interactions | Thu-14:00-I-ENER ● | 61 |
| Weinelt M | Ultrafast magnetization dynamics and its signature in the transient electronic structure | Thu-9:00-I-LASE ● | 62 |
| Wang J | Manipulation of individual atoms/molecules on surfaces of 2D atomic crystals: from Kondo effect to reversible single spin control | Mon-14:00-I-SAMA ● | 63 |

ORAL PRESENTATIONS

64

| | | | |
|--------------------|---|---------------------|----|
| Aguilar P C | Scanning tunnelling spectroscopy of BiTeCl | Wed-11:00-0-BAND ● | 65 |
| Akhtar N | Self-cleaning oxide surfaces as optical windows used in environmental surveillance | Tue-11:40-0-OXID ● | 66 |
| Alev O | Enhanced gas sensing properties of Cu-doped ZnO nanorods | Tue-16:40-0-OXID ● | 67 |
| Andryushechkin B V | Structure of the Ag(111)-p(4x4)-O phase: Ag ₆ model or multilayer oxide? | Wed-11:20-0-OXID ● | 68 |
| Arafune R | Spectroscopic investigation of surface opto-spin-current on Ir(111) covered by graphene | Mon-14:40-0-BAND ● | 69 |
| Arasu N P | Conductance of aromatic and antiaromatic molecules | Tue-9:20-0-ORGS ● | 70 |
| Arguelles E F | Nuclear bound states of H ₂ on a stepped metal surface | Wed-9:00-0-COMP ● | 71 |
| Ayani C G | Symmetry reduction on metal supported graphene by intercalation of Pb | Tue-10:40-0-EG2D ● | 72 |
| Balajka J | TiO ₂ rutile (011) exposed to liquid water | Thu-9:40-0-OXID ● | 73 |
| Balog R | Switching the reactivity of graphene on Ir(111) by hydrogen intercalation | Wed-10:40-0-GRAP ● | 74 |
| Bana H V | Transition from sulfided molybdenum clusters to monolayer MoS ₂ on Au(111) | Tue-11:00-0-EG2D ● | 75 |
| Barroo C | Real-time observation of diffusive processes by field emission microscopy | Mon-15:20-0-CATL ● | 76 |
| Bauer A | Suppressed rotational oscillation by protonation of single triazatruxene molecules on Ag(111) | Wed-11:20-0-ORGS ● | 77 |
| Bayat A | X-ray absorption study of a barium titanate derived quasicrystal on Pt(111) | Wed-16:20-0-SAMA ● | 78 |
| Beinik I | Interaction of water with anatase TiO ₂ (001)-1x4 | Thu-10:00-0-OXID ● | 79 |
| Belza W | Morphology and stability of thin para-hexaphenyl layer grown on atomically flat surfaces of TiO ₂ (110) | Thu-10:40-0-SEMI ● | 80 |
| Blomberg S | In situ structural studies and gas phase visualization of model catalysts at work | Thu-14:40-0-CATH ● | 81 |
| Bondarchuk A | Ionic liquid thin films on the HOPG and VN surfaces: in-situ electrochemical XPS study | Tue-11:20-0-ELCH ● | 83 |
| Cai L | Competition between hydrogen bonds and coordination bonds steered by the surface molecular coverage | Thu-16:20-0-ORGS ● | 84 |
| Calloni A | Structure and electronic properties of Zn-tetra-phenyl-porphyrins single- and multi-layer films grown on Fe (001)-p(1x1)O | Tue-11:00-0-ORGS1 ● | 85 |
| Camuka H | Temperature-induced transformation of electrochemically formed hydrous RuO ₂ layers over Ru(0001) model electrodes | Tue-17:40-0-OXID ● | 86 |
| Canimkurbey B | Ta ₂ O ₅ :PMMA composite dielectric layer for ambipolar organic field effect transistors | Wed-16:00-0-ORGS ● | 87 |

| | | | |
|---------------------|--|---|-----|
| Carey S J | Energetics of adsorbed molecules and molecular fragments on Nickel (111) by microcalorimetry | Thu-14:20-0-ORGS  | 88 |
| Cassidy A | Synthesis and characterization of patterned graphene oxide | Wed-16:20-0-GRAP  | 89 |
| Catrou P | Ultrathin Fe films on SrTiO ₃ (001): growth, interfacial interaction and electronic structure | Wed-9:40-0-OXID  | 90 |
| Chan W-Y | Sharpness-induced energy shifts of quantum well states in Pb islands on Cu(111) | Tue-9:00-0-NAEX  | 91 |
| Cirera B | Chemical transformation and magnetic induced properties of a fluorinated tetraphenylporphyrin on Au(111) | Tue-11:20-0-ORGS1  | 92 |
| Cyganik P | Self-assembled monolayers – the impact of the binding group on structure and stability | Tue-17:20-0-MOLA  | 94 |
| De La Morena R M O | Peekaboo on the nanoscale: self-assembled monolayers of 1, 3, 5-tris(4-carboxyphenyl)benzene (H3BTB) on silver | Tue-17:00-0-MOLA  | 95 |
| Deák L | The interaction of hydrogen, water and carbon monoxide with rhodium covered TiO ₂ (110) surfaces | Tue-15:20-0-OXID  | 97 |
| Del Cueto M | Shaping surface landscapes with molecules: rotationally induced diffraction of H ₂ on LiF(001) under fast grazing incidence conditions | Wed-16:00-0-SAMA  | 98 |
| Demir Ü | One-pot electrochemical fabrication of reduced graphene oxide-metal/metal oxide nanocomposites for catalytic, sensor and energy storage applications | Tue-11:40-0-ELCH  | 99 |
| Deuermeier J | Energy band alignment at the nanoscale | Wed-10:40-0-BAND  | 100 |
| Di Giovannantonio M | Tracking on-surface chemical reactions for the bottom-up fabrication of graphene nanoribbons and open-shell polymers | Tue-11:40-0-ORGS2  | 101 |
| Diño W A | Morphology effect on proton dynamics in Nafion® 117 and sulfonated polyether ether ketone (SPEEK) | Thu-15:20-0-ENER  | 103 |
| Dreiser J | Giant hysteresis of single-molecule magnets adsorbed on a non-magnetic insulator | Tue-9:40-0-MAGN  | 104 |
| Ebeling R | Chemical controlled electronic decoupling of three-dimensional molecules on surfaces investigated with LT-UHV-STM | Wed-16:40-0-ORGS  | 105 |
| Erdélyi Z | Size dependent spinodal decomposition in Cu-Ag nanoparticles | Tue-14:00-0-BIMS  | 106 |
| Faisal F | In-situ spectro-electrochemical infrared investigations at atomically-defined Pt/Co ₃ O ₄ (111) model catalysts | Tue-14:40-0-ELCH  | 107 |
| Farkas A P | Effect of gold on the adsorption properties of acetaldehyde on clean and h-BN covered Rh(111) surface | Mon-15:00-0-CATL  | 108 |
| Foelske-Schmitz A | X-ray photoelectron spectroscopy of ionic liquids – from half cell measurements to in situ electrochemical XPS studies | Tue-15:00-0-ELCH  | 109 |

| | | | |
|---------------|--|---------------------|-----|
| Fogg J | In situ X-ray scattering studies of the formation of a Pb/Au(111) Surface alloy in the electrochemical environment | Tue-16:00-0-ELCH ● | 110 |
| Franceschi G | The influence of surface atomic structure on solid state electrochemistry: oxygen exchange on SrTiO ₃ (110) surfaces | Wed-16:40-0-OXID ● | 111 |
| Fujii S | Single-molecule electronic study on nanographene | Tue-11:20-0-ORGS2 ● | 112 |
| Fukuda T | Site correlation of two-dimensional Cu-Ni alloys on Ni(110) | Tue-14:20-0-BIMS ● | 113 |
| Gajdics B | Computer simulation of spinodal decomposition in bimetallic nanoparticles | Wed-10:00-0-BIMS ● | 114 |
| Getzlaff M | Melting processes of 3D metal alloy nanoparticles deposited on surfaces | Tue-14:40-0-BIMS ● | 115 |
| Godlewski S | Site selective, reversible Diels-Alder reaction between polycyclic conjugated molecules and DB dimers on Ge(001):H | Tue-16:00-0-ORGS ● | 116 |
| Gottfried M J | Molecular topology and metal/organic interfaces | Tue-11:40-0-ORGS1 ● | 117 |
| Grønborg S S | Hydrogen-induced crystal reshaping and edge vacancy formation in MoS ₂ catalyst particles on Au(111) | Thu-9:00-0-CATH ● | 118 |
| Groot I M N | Seeing is believing: atomic-scale imaging of catalysts under reaction conditions | Mon-15:20-0-NAEX ● | 119 |
| Hagman B | In-situ study of the oxidation of Cu(100) by CO ₂ | Thu-10:40-0-CATH ● | 120 |
| Hamamoto Y | Interlayer states induced by image potential states in naphthalene on graphene | Tue-17:00-0-ORGS ● | 121 |
| Han S W | Low temperature CO oxidation catalyzed by iron oxide nanoparticles decorating internal part of mesoporous alumina bead | Tue-17:00-0-OXID ● | 122 |
| Harlow G S | In-situ x-ray scattering: nano-structured aluminum oxides | Tue-16:20-0-ELCH ● | 123 |
| Harsh R | Graphene functionalized with electron acceptor molecules | Tue-17:20-0-ORGS ● | 124 |
| Hejral U | Combining high energy X-Ray diffraction techniques with LASER-induced fluorescence in operando catalysis | Thu-14:20-0-CATH ● | 125 |
| Horakova K | H adsorption studies on the Zr(0001) surface | Tue-10:00-0-CORR ● | 126 |
| Hötger D | On-surface transmetalation of Fe-porphyrin network on Au(111) | Tue-10:40-0-ORGS1 ● | 127 |
| Humblot V | Arginine on Cu(110): several adsorption configurations for a single molecule | Thu-9:00-0-MOLA ● | 129 |
| Isshiki Y | Electronic structure of Au-C ₆₀ -Au single molecule junction fixed by current voltage characteristics and thermopower measurement | Tue-10:40-0-ORGS2 ● | 130 |
| Ito S | Solving mysteries in pure bismuth by quantum confinement | Wed-16:20-0-BAND ● | 131 |

| | | | |
|---------------|---|--------------------|-----|
| Jacobs L | Surface reactivity of Au-Ag and Pt-Rh during deNO _x reactions studied by field emission techniques | Tue-11:20-0-EG2D ● | 132 |
| Jain R | Near ambient pressure photoelectron spectroscopy studies of CO oxidation on Co ₃ O ₄ surfaces: electronic structure and mechanistic aspects of wet and dry CO oxidation | Thu-11:00-0-CATH ● | 133 |
| Jakub Z | Atomic scale STM and nc-AFM study of the Hematite (012) surface | Thu-11:40-0-OXID ● | 135 |
| Jankowski M | Controlling the growth of Bi(110) and Bi(111) films on an insulating substrate | Tue-14:20-0-EG2D ● | 136 |
| Jany B R | Formation of stable hexagonal (hcp) gold nanostructures in the process of self-assembling on Ge(001) surface | Thu-14:00-0-SEMI ● | 137 |
| Johánek V | Bulk hydroxylation and fast water splitting on highly reduced ceria | Thu-14:20-0-OXID ● | 139 |
| Jørgensen J H | Surface chemistry of coronene on a hydrogenated graphite surface | Tue-16:40-0-ORGS ● | 140 |
| Juhász L | Fabrication and investigation of porous gold nanoparticles passivated with TiO ₂ layer | Thu-16:20-0-ENER ● | 141 |
| Kang H | Stable hydrated protons on platinum surface | Thu-16:00-0-ENER ● | 142 |
| Ke C-R | In situ investigation of degradation at metal halide perovskite surfaces by near ambient pressure X-ray photoelectron spectroscopy | Thu-15:00-0-ENER ● | 143 |
| King M | Corrosion studies of lithium hydride thin films | Tue-9:40-0-CORR ● | 144 |
| Kishida R | Intramolecular cyclization of o-quinone amines with a focus on dopamine-quinone: a density functional theory based study | Thu-16:00-0-ORGS ● | 145 |
| Kizaki H | Ab-initio analysis of nitric oxide adsorption on an FeO ₂ terminated (001) surface of LaFeO ₃ | Tue-10:00-0-MAGN ● | 146 |
| Kleimeier N F | Unoccupied band structure of Si nanoribbons on Ag(110) studied by IPE | Wed-11:20-0-BAND ● | 148 |
| Kobayashi K | Theoretical study on spin states of photoelectrons emitted from spin-polarized surface states with a mirror symmetry | Mon-14:20-0-BAND ● | 149 |
| Kobayashi T | Ductility of thin films constituting organic light emitting diodes | Tue-15:20-0-ORGS ● | 150 |
| Kocán P | Control over self-assembly of phthalocyanine molecules via the electric field of an STM tip | Mon-14:40-0-ORGS ● | 151 |
| Kolsbjerg E L | Supramolecular corrals on surfaces resulting from aromatic interactions of non-planar triazoles | Thu-11:20-0-ORGS ● | 152 |
| Kovács I | Self-organization and electronic structure of thin and mono-molecular layer of Keggin-type Al ₁₃ -sulfate salt | Tue-17:40-0-MOLA ● | 153 |
| Kratzer M | Epitaxial growth of organic crystal networks on ultra-thin hexagonal boron nitride | Thu-15:20-0-ORGS ● | 154 |

| | | | |
|------------------|--|----------------------|-----|
| Krejčí O | Simultaneous high-resolution AFM/STM/IETS imaging of FePc on Au(111) | Mon-14:00-0-ORGS ● | 155 |
| Kremer G | Band structure of one single layer of silica on Ru(0001) | Tue-15:00-0-OXID ● | 156 |
| Krzyzewski F | Stability of vicinal crystal surfaces against step bunching: Atomistic scale model of unstable evaporation and growth | Wed-9:20-0-COMP ● | 157 |
| Kuehn S | The next generation of attosecond sources at ELI-ALPS | Mon-17:00-0-ELI-ALPS | 159 |
| Kyhl L | Reactivity of bi- and single layer graphene on Ir(111) towards hydrogen | Wed-11:00-0-GRAP ● | 160 |
| Lackner P | Water adsorption at the zirconia surface on Pt ₃ Zr | Tue-16:00-0-OXID ● | 161 |
| Lagoute J | Electronic interaction of organic molecules with nitrogen doped graphene | Wed-16:00-0-GRAP ● | 162 |
| Laker Z P L | Supramolecular assembly on top and underneath 2D materials: can molecules interact across a graphene barrier? | Tue-14:00-0-EG2D ● | 163 |
| Lambeets S V | Observation of oxygen spillover between different {012} and {113} Rh facets during adsorption and hydrogenation of CO ₂ | Tue-17:20-0-CATL ● | 165 |
| Leung L | Contrasting dynamics for aryl- and alkyl-halide surface-reaction at copper | Thu-16:20-0-CATL ● | 167 |
| Linpé W | An <i>in-situ</i> study of Sn deposition into nano-porous ordered anodic aluminum oxide | Tue-16:40-0-ELCH ● | 168 |
| Lisi S | Density driven sodium 2D phase transformation on epitaxial graphene | Thu-11:40-0-GRAP ● | 169 |
| Luches P | The interaction between cerium oxide and platinum studied by LEEM | Thu-14:00-0-OXID ● | 170 |
| Lundgren E | The misfit structure between the Pd(100) and PdO(101) under reaction conditions | Thu-11:40-0-CATH ● | 171 |
| Lykhach Y | Redox-mediated conversion of atomically dispersed platinum to sub-nanometer particles | Tue-9:40-0-ENER ● | 172 |
| Ma T | The formation mechanism of the p(2×3) reconstruction on Mo(112) surface | Wed-11:00-0-OXID ● | 173 |
| Majzik Z | Characterization of polycyclic conjugated hydrocarbons by means of NCAFM | Mon-14:40-0-SAMA ● | 174 |
| Martinez J I | Unveiling universal trends for the energy level alignment in organic/oxide interfaces | Thu-15:00-0-ORGS ● | 176 |
| Martín-Jiménez A | Bragg diffraction of surface state electrons | Tue-17:20-0-PISC ● | 178 |
| Matvija P | Real-space visualization of the pair correlation function in a 2D molecular gas | Tue-14:20-0-ORGS ● | 179 |
| Menyhárd M | Ion irradiation induced compound formation. | Thu-14:40-0-SEMI ● | 180 |

| | | | | |
|-------------|--|-------------------|---|-----|
| Meriggio E | Model oxide-supported enantioselective catalysts : interaction between TiO ₂ -supported Ni nanoparticles and a chiral modifier | Tue-17:20-0-OXID | ● | 181 |
| Merte R L | The structure of the SnO ₂ (110)-(4x1) surface | Thu-15:20-0-OXID | ● | 182 |
| Messaykeh M | Probing in situ the wetting at metal/oxide interface via plasmonics combined with photoemission | Tue-11:20-0-OXID | ● | 184 |
| Minkowski M | Many particle collective diffusion in an arbitrary one-dimensional potential landscape | Wed-9:40-0-COMP | ● | 185 |
| Montes E | Calculation of molecular conductance 'on the fly' | Wed-10:00-0-COMP | ● | 186 |
| Morbec J M | Adsorption of anthracene and pentacene on coinage metal surfaces: coverage effects and the role of the van der Waals interactions | Tue-10:00-0-ORGS | ● | 187 |
| Nakamura J | Oxygen reduction reaction by pyridinic nitrogen-containing carbon electrocatalysts | Tue-15:20-0-ELCH | ● | 188 |
| Nakashima S | Spin reorientation in fcc Fe thin films with Mn overlayer | Tue-9:00-0-MAGN | ● | 189 |
| Nakayama Y | Valence band structures of the single crystal pentacene | Wed-11:40-0-BAND | ● | 190 |
| Navarro J J | Covalent and periodic functionalization of graphene/ Ru(0001) | Tue-15:00-0-ORGS | ● | 192 |
| Norris A | Opening a pseudogap, and the rich interplay of Dirac fermions with singularities, doping and asymmetric potentials in graphene | Thu-11:20-0-GRAP | ● | 193 |
| Nürnberg D | Circular dichroism in laser induced electron emission from nanohelix arrays | Thu-9:40-0-LASE | ● | 194 |
| Ogawa S | Soft X-ray spectroscopic study of electronic structure of Pd nanoparticles | Wed-16:40-0-BAND | ● | 195 |
| Olbrich R | Surface stabilises ceria in unexpected stoichiometry | Thu-14:40-0-OXID | ● | 196 |
| Ondráček M | Switchable charge states in multi-ferrocene molecules | Tue-11:00-0-ORGS2 | ● | 197 |
| Ortega J E | Vicinal noble metal surfaces with densely kinked steps | Wed-16:40-0-SAMA | ● | 198 |
| Óvári L | Surface science perspectives at ELI Attosecond Light Pulse Source | Thu-10:00-0-LASE | ● | 199 |
| Paier J | Electron transfer between gold adatoms and the reduced CeO ₂ (111) surface: Lessons learned from static density functional theory | Wed-11:40-0-COMP | ● | 200 |
| Palacio I | Decoupling epitaxial graphene from metals by potential-controlled electrochemical oxidation | Wed-9:00-0-GRAP | ● | 201 |
| Palotás K | Revised Chen's derivative rule for efficient calculations of scanning tunneling microscopy | Wed-11:20-0-COMP | ● | 203 |
| Papp C | Sulfur-passivation of graphene-supported Platinum nanocluster arrays | Tue-16:20-0-CATL | ● | 204 |
| Park Y | Field-driven orientation of small polar molecules in the condensed phase | Thu-11:00-0-SEMI | ● | 205 |

| | | | |
|--------------|--|--------------------|-----|
| Pasquali L | Layer-resolved molecular organization of pentacene thin films for organic transistors by Resonant Soft X-ray Reflectivity | Wed-16:20-0-ORGS ● | 206 |
| Pászti Z | Influence of the multifunctional $Ti_{0.7}M_{0.3}O_2-C$ (M= W, Mo) composite supports on the electrochemical performance of Pt electrocatalysts | Thu-9:00-0-OXID ● | 207 |
| Pécz B | Nitride layers grown on patterned graphene/SiC | Thu-10:00-0-SEMI ● | 208 |
| Petukhov M | Titanium tetraisopropoxide adsorption and decomposition on Cu(111) | Thu-11:40-0-ORGS ● | 209 |
| Piccolo L | Non-noble intermetallic compounds as selective butadiene-hydrogenation catalysts: $Al_{13}Fe_4$ vs $Al_{13}Co_4$ | Thu-16:00-0-CATH ● | 210 |
| Polak M | Remarkable confinement effects on equilibrated adsorption, segregation and dimerization reaction predicted for alloy nanoparticles | Tue-17:40-0-BIMS ● | 211 |
| Popova O | Molecular chessboard assemblies sorted by site-specific interactions of out-of-plane d-orbitals with a semi-metal template | Thu-9:20-0-MOLA ● | 213 |
| Radovic M | Low-dimensional electron system at titanate surfaces and related interfaces: create and control | Wed-10:40-0-OXID ● | 214 |
| Rauls E | On-surface synthesis of free-base corroles: a combined theoretical and experimental characterization | Tue-14:00-0-ORGS ● | 215 |
| Resta A | Fast surface X-ray diffraction: gold epitaxy on MoS_2 | Tue-14:40-0-EG2D ● | 217 |
| Rice D | Multi-layered poly-functional microspheres for rapid multiplexed immunoassay | Thu-9:40-0-MOLA ● | 219 |
| Risse T | Oxidation reactions on Au surfaces: the role of water | Mon-14:40-0-CATL ● | 220 |
| Sabik A | Revealing phthalocyanine arrangements on Ag(100): From pure overlayer of CoPc and F_{16} CuPc to bimolecular heterostructures | Wed-9:00-0-ORGS ● | 221 |
| Sack C | $CeO_{2-x}(111)$, a model catalyst for the HCl oxidation | Tue-16:00-0-CATL ● | 222 |
| Saha P | Ultrathin film polymorphs of ferrocene derivatives assisted by functional groups and solvents | Thu-10:00-0-MOLA ● | 223 |
| Sakamoto K | Electronic properties of thallium single crystal thin film | Wed-16:00-0-BAND ● | 224 |
| Sandell A | Adsorption and photolysis of trimethyl acetate on $TiO_2(B)$ (001) studied with synchrotron radiation core level photoelectron spectroscopy | Tue-16:40-0-PISC ● | 225 |
| Sápi A | Silica-based catalyst supports are inert, are they not?: striking differences in ethanol decomposition reaction originated from meso- and surface-fine-structure evidenced by small-angle X-ray scattering | Tue-9:20-0-NAEX ● | 226 |
| Schumann F O | Phonons of ultrathin perovskite oxide films | Wed-10:00-0-OXID ● | 227 |
| Schweke D | The adsorption sites of CO_2 on cerium oxide studied using quantitative TPD | Thu-15:20-0-OXID ● | 228 |

| | | | |
|-------------------|---|--------------------|-----|
| Serrate D | Ferroelectricity at the atomic scale | Mon-15:20-0-SAMA ● | 229 |
| Shukla N | Enantiomeric separations of chiral pharmaceuticals using chiral tetrahedral Au nanoparticles | Wed-11:00-0-ORGS ● | 231 |
| Simic-Milosevic V | EnviroESCA – routine surface chemical analysis under environmental conditions for biological samples | Mon-14:40-0-NAEX ● | 232 |
| Simonsen F D S | Investigating superhydrogenated polycyclic aromatic hydrocarbons on graphite and their catalytic effect on interstellar H ₂ formation | Tue-9:40-0-ORGS ● | 233 |
| Simpson G J | Dipole-mediated single-molecule manipulation | Mon-15:00-0-SAMA ● | 234 |
| Such B | Adsorption of porphyrin-based dyes on TiO ₂ surfaces: STM study | Mon-14:20-0-ORGS ● | 235 |
| Suchkova S | Various organic adsorbates for Si(553)-Au surface functionalization | Thu-16:20-0-SEMI ● | 236 |
| Sun Z | Iron doping on cobalt oxide bilayers on Au(111): toward a model of synergistic catalytic effect in the oxygen evolution reaction | Tue-16:20-0-OXID ● | 237 |
| Syres K L | Reversible CO ₂ absorption with a superbasic ionic liquid [P66614] [Benzim] studied using near-ambient pressure X-ray photoelectron spectroscopy | Tue-16:20-0-ORGS ● | 238 |
| Szabelski P | Self-assembly of tritopic molecules on surfaces: structure and bonding from computer simulations | Tue-14:40-0-ORGS ● | 239 |
| Szajna K | Formation of highly-ordered molecular structures on ion beam modified TiO ₂ (110) surface – the role of wetting layer stability | Thu-11:20-0-SEMI ● | 240 |
| Tajiri H | Transmission X-ray diffraction for a real-time observation of thin-film growth | Mon-15:00-0-NAEX ● | 241 |
| Tálas E | Graphite oxide-TiO ₂ nanocomposite type photocatalyst for methanol photocatalytic reforming reaction | Tue-10:00-0-ENER ● | 242 |
| Tariq Q | Adsorption of a functionalized porphyrin on MgO(100) thin films: a high-resolution photoemission and X-ray absorption spectroscopy study | Wed-11:40-0-OXID ● | 243 |
| Tejeda A | Experimental valence band dispersion of CH ₃ NH ₃ PbI ₃ hybrid organic-inorganic perovskite | Thu-14:40-0-ENER ● | 244 |
| Tsaousis P | Co-adsorption of alanine and water on Ni(110) | Thu-14:00-0-ORGS ● | 245 |
| Tsud N | Bonding of biomolecules to cerium oxide: histidine and adenine | Wed-11:40-0-ORGS ● | 246 |
| Urgel J I | On-surface photo- and thermal-generation of higher acenes | Tue-17:00-0-PISC ● | 247 |
| Vad K | Surface atomic arrangement and grain boundary diffusion in nanolayers | Tue-9:40-0-BIMS ● | 249 |
| Verlhac B | Probing the exchange coupling through a Nc-functionalized STM | Tue-9:20-0-MAGN ● | 250 |

| | | | |
|-----------------------------|--|--------------------|------------|
| Wagner M | Imaging and manipulations of dissociated water on $\text{In}_2\text{O}_3(111)$ | Thu-9:20-0-OXID ● | 251 |
| Walczak L | Novel systems toward ambient pressure photoemission spectroscopy | Mon-14:00-0-BAND ● | 252 |
| Xie L | Structural transformation and stabilization of metal-organic motifs induced by halogen doping | Tue-11:00-0-ORGS ● | 253 |
| Yadav R P | Correlation between fractal and wettability of rippled silicon surfaces under ion beam irradiation | Thu-14:20-0-SEMI ● | 254 |
| Yamamoto S | Adsorption and reaction of CO_2 on graphene studied by ambient pressure XPS | Thu-9:20-0-CATH ● | 255 |
| Yamasue K | Atomic resolution imaging and carrier type determination of Molybdenum disulfide by noncontact scanning nonlinear dielectric microscopy | Thu-9:40-0-SEMI ● | 256 |
| Yanagisawa H | Optical control of Young's type interferometers for ultrafast electron pulses | Thu-10:40-0-LASE ● | 258 |
| Zabka W-D | From 2D to 3D Alumina: Interface Templated Growth of $\gamma\text{-Al}_2\text{O}_3(111)$ -like Films | Tue-14:40-0-OXID ● | 259 |
| Zaki E | Adsorption of CO and water on magnetite Fe_3O_4 surfaces | Thu-11:20-0-OXID ● | 260 |
| Zehra T | Graphene/doped graphene from adsorbed molecules | Thu-14:00-0-GRAP ● | 261 |
| Zhang T | Conclusively addressing the CoPc electronic structure: a joint gas-phase and solid-state photoemission and absorption spectroscopy study | Wed-9:20-0-ORGS ● | 262 |
| Zhou J | Simultaneously 2D spatially resolved activity and surface of a Pd(100) single crystal during CO oxidation | Thu-11:20-0-CATH ● | 263 |
| Zhu J | Tailoring the topology of low-dimensional organic nanostructures with surface templates | Wed-10:40-0-ORGS ● | 264 |
| Zhuravlev A G | Electronic states induced by cesium on atomically rough and flat GaAs(001) surfaces | Thu-16:00-0-SEMI ● | 265 |
| Zollner E M | C60 adsorption on a two-dimensional oxide quasicrystal | Thu-14:40-0-ORGS ● | 266 |
| POSTER PRESENTATIONS | | | 267 |
| Arguelles E F | Interstitial impurity induced magnetism on Lead oxide surface | Tue-PS1-01 | 268 |
| Attia S | Enantioselective reactions on chirally-modified model surfaces: a new molecular beam/surface spectroscopy apparatus | Tue-PS1-39 | 269 |
| Barroo C | Advancement of sample preparation for Atom Probe Tomography: Analysis of nanoporous and single-atom-alloy catalysts | Thu-PS2-27 | 270 |
| Basa P | Hybrid SEM/AFM metrology for complex surface characterization | Tue-PS1-02 | 271 |
| Bertóti I | Reduction and nitrogen implantation of graphene-oxide thin films in low pressure N-containing plasma | Thu-PS2-22 | 273 |

| | | | |
|----------------|---|------------|-----|
| Buchholz B | Nitrogen doping of titania nanomaterials using thermal and plasma activation | Tue-PS1-04 | 274 |
| Camilli L | Self-assembly of ordered graphene nanodot arrays | Tue-PS1-05 | 275 |
| Chrafi Y | Effect of conduction band non-parabolicity on the intersubband transitions in ZnO/Mg _x Zn _{1-x} O Quantum Well Heterostructures | Thu-PS2-47 | 276 |
| Cresi J S P | Structural and Electronic modifications induced by reduction in cerium oxide nanoparticles | Tue-PS1-38 | 277 |
| Csik A | Effect of growing conditions on surface modification of PbTe crystals caused by Ar ⁺ ion bombardment | Tue-PS1-06 | 279 |
| Datz D | Nano-spectroscopy of phonon-polariton modes in boron nitride nanostructures | Tue-PS1-07 | 280 |
| El Kharbachi A | Oxide layer growth and hydrogen transfer processes at the surface of tungsten | Thu-PS2-43 | 281 |
| Gajdics B | Stochastic kinetic mean-field model – a new atomic scale simulation method | Thu-PS2-10 | 282 |
| Gottfried M J | Synthesis, metalation and structures of tetrapyrroles at interfaces | Tue-PS1-09 | 283 |
| Grabau M | X-ray photoemission studies of liquid model systems for Pt-Ga and Pd-Ga bimetallic dehydrogenation catalysts | Thu-PS2-04 | 284 |
| Gubó R | Au-Pd nanoparticles and Au/Rh double layers on TiO ₂ (110) | Tue-PS1-10 | 285 |
| Halasi G | Hydrogenation of CO ₂ on Pt nanoparticles supported on NiO | Tue-PS1-11 | 286 |
| Han S W | Toluene total oxidation over NiO nanoparticles on mesoporous SiO ₂ : catalytic reaction at lower temperatures and repeated regeneration | Thu-PS2-39 | 287 |
| Henderson Z | <i>In-situ</i> observation of water-induced reordering in ultrathin ionic liquid films | Thu-PS2-33 | 288 |
| Hirayama T | Observation of shell structure in mixed Ar/Kr clusters studied by electron energy loss spectroscopy | Thu-PS2-46 | 289 |
| Hsia Y Y | Reforming of ethanol on Rh(111) surface and supported Rh nanoclusters | Thu-PS2-07 | 291 |
| Hurdax P | Charge transfer and orbital level alignment at inorganic/organic interfaces: the role of dielectric interlayers | Tue-PS1-12 | 292 |
| Isshiki Y | Evaluation of electronic structure of the single molecule junction based on current voltage characteristics and thermopower | Tue-PS1-13 | 293 |
| Jacobs L | Surface enrichment in gold/silver alloys: Study of the physicochemical influences using atom probe tomography | Tue-PS1-08 | 294 |
| Jankowski M | Thermally induced dewetting of three dimensional Cu islands on the Ag(111) surface | Thu-PS2-15 | 295 |

| | | | |
|----------------|---|------------|-----|
| Jannane T | The sol aging time impact on the structural, optical and electrical properties of ZnO thin films | Tue-PS1-14 | 296 |
| Juhász L | Morphology and optical properties of porous gold nanoparticles coated with alumina layer | Tue-PS1-15 | 297 |
| Kahaly M U | Photonic bandgap engineering and photo-induced emission in layered two-dimensional structures | Tue-PS1-16 | 298 |
| Kaku M | Photon-stimulated desorption processes of polymers by vacuum ultraviolet emissions from a laser-produced plasma | Thu-PS2-28 | 299 |
| Komoto Y | Single-molecule conductance measurement of Ru(bpy) ₃ derivative | Thu-PS2-34 | 300 |
| Kovacs I | Reaction pathways of adsorbed acetaldehyde on clean and modified Rh(111) surfaces | Tue-PS1-17 | 301 |
| Kumar S | Photo-switchable wettability and electric conductivity of Self-Assembled Dithienylethene Monolayers on Ag surface | Tue-PS1-18 | 302 |
| Laker Z P L | Monolayer-to-thin-film transition in supramolecular assemblies on graphene | Tue-PS1-19 | 303 |
| Lambeets S V | Chiral recognition using field ion and field emission microscopy | Thu-PS2-29 | 305 |
| Lamirand A D | Antiferromagnetic domains in epitaxial CoO ultra-thin layers grown on Pt(001) | Tue-PS1-20 | 307 |
| László B | Titanate nanotube supported plasmonic gold and rhodium particles for heterogeneous photocatalysis | Thu-PS2-41 | 308 |
| Lee H | Surface spectroscopic analysis of transition metal doped TiO ₂ nanoparticles | Thu-PS2-37 | 309 |
| Lenchuk O | Atomistic modeling of alkali metals (Li, Na, K) intercalation into graphite | Tue-PS1-21 | 310 |
| Li X | Adsorption of CO and H ₂ O on Fe ₃ O ₄ surfaces studied by density-functional theory | Tue-PS1-22 | 311 |
| Lin J L | Adsorption and thermal reaction of 1H-pyrazole on Cu(100) | Thu-PS2-06 | 312 |
| Lion J | Preformed cluster mobility as a probe for surface characterization | Thu-PS2-45 | 313 |
| López J C | Surface plasmons on aluminum particles and silicon nanocrystals in off- stoichiometric SiO ₂ Films used to increase the conversion efficiency in silicon solar cells | Thu-PS2-40 | 314 |
| Luna López J A | Multi-wall carbon nanotubes grown by USP-CVD: study of the growth time ratio against its length | Thu-PS2-21 | 315 |
| Marks K M | Adsorption and dehydrogenation of naphthalene on nickel(111) | Tue-PS1-24 | 317 |
| Menyhárd M | Ellipsometric and XPS study of Zr and ZrO ₂ | Tue-PS1-23 | 318 |

| | | | |
|-------------|--|------------|-----|
| Mohai M | XPS MultiQuant: multimodel XPS quantification software | Thu-PS2-09 | 319 |
| Mohamed F | Iron phthalocyanine on ultrathin alumina template | Thu-PS2-26 | 320 |
| Mohebbi E | Insight into surface-confined 2D polymerization of a 1,2-bis(4-bromophenyl)ethyne on Ag(110) surface | Tue-PS1-25 | 321 |
| Mohrhusen L | Electrostatic shielding versus sterical ligand stabilization: tunable nanocrystal stabilization mechanisms | Thu-PS2-18 | 322 |
| Mohtasebi A | Surface mobility and nucleation of a molecular switch: tetraaniline on hematite | Thu-PS2-30 | 323 |
| Muttaqien F | Formate decomposition dynamics on Cu(111): importance of CO ₂ bending vibrational mode | Tue-PS1-26 | 324 |
| Nagy G | Sol derived alumina and silica supported Au-Ag bimetallic catalysts: structure and activity in aerobic selective oxidation of benzyl alcohol | Tue-PS1-27 | 326 |
| Nakamura M | Effect of cationic species on the oxygen reduction reaction on Pt(111) electrode | Tue-PS1-28 | 327 |
| Nara J | First principles study on the interaction between hydrogen atoms and the graphene buffer layer grown on the SiC(0001) surface | Tue-PS1-29 | 328 |
| Navarro J J | Gold intercalation in graphene/Ir(111) | Tue-PS1-46 | 329 |
| Nemcsics Á | Particular behaviour of the GaAs wetting layer on AlGaAs substrate during droplet epitaxy | Thu-PS2-48 | 330 |
| Ogawa S | Soft X-ray spectroscopic study of electronic structure of Pd nanoparticles | Tue-PS1-33 | 331 |
| Olbrich R | Regular and disordered surface vacancies on a ceria film surface | Tue-PS1-30 | 332 |
| Otsuki K | Synthesis of Pd nanoparticles by solution plasma method | Thu-PS2-08 | 333 |
| Palotás K | Metastable skyrmionic spin structures with various topologies and their electron charge/spin transport properties | Thu-PS2-24 | 334 |
| Pászti Z | Oxygen reduction on carbon supported Pt _x Sn electrodes with optimized Pt/Sn surface composition prepared by controlled surface reactions | Tue-PS1-03 | 335 |
| Pavlov A V | Spin relaxation length for medium energy electrons in Pd and LiF ultrathin films | Tue-PS1-31 | 337 |
| Peltonen J | Paper-supported electrochemical analysis platform for ion and biosensing | Tue-PS1-52 | 339 |
| Penschke C | Reactivity of vanadium oxide monolayers on CeO ₂ (111) studied by density functional theory | Thu-PS2-11 | 340 |
| Pető G | Investigation of oxide dispersion strengthened steel by photoelectron emission, Mössbauer spectroscopy, and X-ray diffraction | Thu-PS2-25 | 341 |

| | | | |
|-------------------|--|------------|-----|
| Petukhov M | Surface fluorination by $C_{60}F_{18}$ molecules adsorption on copper (001) | Tue-PS1-32 | 342 |
| Plucienik A | Messenger atom action spectroscopy of solid surfaces | Thu-PS2-38 | 343 |
| Ramakrishnan S | Photon and electron induced chemistry of molecules embedded within amorphous solid water (ASW) | Tue-PS1-34 | 344 |
| Rezvani S J | Reversible interface formed on metal alloy oxide nanoparticles via lithiation | Thu-PS2-17 | 345 |
| Romanyuk O | <i>In situ</i> XPS study of Ni-catalyzed graphitization on nanocrystalline diamond surface | Thu-PS2-20 | 347 |
| Sagi R | Temperature effect on transport and charging of low-energy electrons interacting with amorphous solid water films | Thu-PS2-16 | 349 |
| Sala L A | Grafting unsaturated carbon groups on hydrogenated diamond under low-energy electron irradiation | Tue-PS1-35 | 350 |
| Santoni A | BaZrO ₃ inclusions in solution-derived YBa ₂ Cu ₃ O _{7-d} epitaxial thin films studied by X-Ray photoelectron spectroscopy | Thu-PS2-03 | 352 |
| Shibata M | Improvement in corrosion resistance of NiWP and NiWB films formed by electroless plating | Thu-PS2-05 | 353 |
| Shigeta Y | Influence of local surface potential on Kikuchi envelope and channeling of high-energy electrons on reconstructed surface | Thu-PS2-44 | 354 |
| Shin S | Effect of electric field on proton transfer at acid-base interface | Tue-PS1-36 | 356 |
| Simic-Milosevic V | New Instrumentation for spin-integrated and spin-resolved Momentum microscopy – METIS and KREIOS | Thu-PS2-01 | 357 |
| Starfelt S | STM and STS study of thin Ag films grown on the Ga/Si(111)- $\sqrt{3}\times\sqrt{3}$ surface | Tue-PS1-37 | 358 |
| Sulyok A | Grazing incident excitations on aluminum and silicon surface | Tue-PS1-51 | 359 |
| Suzuki T | Indium coverage on Si(111)- $\sqrt{7}\times\sqrt{3}$ -In surface | Tue-PS1-40 | 360 |
| Szendró M | Adhesion model of graphene islands on metal substrates based on Moiré-patterns | Tue-PS1-41 | 361 |
| Szenti I | Formation of carbon nanostructures on metal deposits prepared by EBID | Thu-PS2-32 | 362 |
| Szítás A | Adsorption, polymerization and decomposition of acetaldehyde on clean and carbon-covered Rh(111) surfaces | Tue-PS1-42 | 363 |
| Tagawa M | Collision-induced enhancement of polyimide corrosion in sub-low Earth orbit (LEO) space environment | Thu-PS2-12 | 364 |
| Tasič A | Investigation of carbendazim removal from water media by multiwalled carbon nanotubes and magnetite modified multiwalled carbon nanotubes | Thu-PS2-36 | 365 |

| | | | |
|--------------|--|------------|------------|
| Tejeda A | Gap opening in graphene buffer layer induced by structural superperiodicity | Thu-PS2-19 | 366 |
| Tóth J | Electron spectroscopic study of carbon fiber – polyacrylate composites | Tue-PS1-43 | 367 |
| Tőkési K | Energy loss function of Samarium Derived from Reflection Electron Energy Loss Spectroscopy | Thu-PS2-02 | 368 |
| Tsai C L | Fabrication and characterization of the substrateless GaN-on-Si LEDs with a metal can package | Thu-PS2-14 | 369 |
| Tsuruta R | Epitaxial growth of fullerene on the organic single crystal | Thu-PS2-35 | 370 |
| Uchida K | Plasmon-induced electron emission from a carbon nanotube under polarized laser: a real-time first-principles study | Thu-PS2-23 | 372 |
| Ueda Y | First-principle study of angle-resolved secondary electron emission from atomic sheets | Thu-PS2-42 | 373 |
| Vajdle O | Comparison of multiwalled carbon nanotubes modified with silver and gold particles as surface modifiers of carbon paste electrode for hydrodynamic chronoamperometric determination of H ₂ O ₂ | Tue-PS1-50 | 374 |
| Vari G | Interaction of Au, Rh and Au-Rh alloys with the hexagonal boron nitride monolayer studied on Rh(111) | Tue-PS1-44 | 375 |
| Wiegmann T | Transmission surface diffraction for operando studies of heterogeneous interfaces | Tue-PS1-45 | 377 |
| Wu Y C | Decomposition of methanol on vanadium nanoclusters supported by graphene grown on Ru(0001) | Tue-PS1-47 | 379 |
| Yaji K | Spin-orbital entanglement and optical spin control in solid surfaces | Tue-PS1-48 | 380 |
| Yamamoto S-I | Orange up-conversion in TiO ₂ -ZnO composite ceramics fabricated by metal organic decomposition | Tue-PS1-49 | 381 |
| Yavuz A | Perfluoropentacene films on gold surfaces grown by supersonic molecular beam deposition | Thu-PS2-31 | 383 |
| Yokota K | Surface degradation of fluoroethylenepropylene (FEP) films in sub-low earth orbit (LEO) environment; origin and mechanism | Thu-PS2-13 | 384 |
| INDEX | | | 386 |



33rd EUROPEAN CONFERENCE ON SURFACE SCIENCE

PLENARY LECTURES

Fri-11:20-Plen-7**Nanostructured metal surfaces – from surface science to electrochemistry / electrocatalysis**

Plenary lecture**Rolf Jürgen Behm***Institute of Surface Chemistry and Catalysis, Ulm University, D-89069 Ulm, Germany*

The Surface Science approach to Heterogeneous Catalysis, aiming at a fundamental understanding of catalytic surface reactions from studies of elementary reaction steps on structurally well defined model surfaces under idealized reaction conditions, has been extended significantly by modern developments. Nanostructuring and *in situ* spectroscopies allow the use of more complex, but nevertheless structurally well defined surfaces and more realistic reaction conditions. Likewise, progress in theory and computation allow the description of surface reactions in increasingly complex systems.

Similar strategies can be employed also for gaining insight into fundamental processes in electrochemical and electrocatalytic reactions on complex electrode surfaces. This will be illustrated for a number of electrochemical/-catalytic reactions. Furthermore, the role of surface restructuring under electrochemical reaction conditions will be elucidated. Finally, the potential of this approach, which aims at the description of the overall (electro-)catalytic behavior of the electrode on the basis of the reactivity of individual nanostructures, will be discussed.

Fri-9:20-Plen-5**Adsorption calorimetry techniques on well-defined surfaces and their application in understanding catalysis, photovoltaics and atomic-layer deposition***Plenary lecture***Charles T. Campbell***University of Washington, Department of Chemistry, Seattle, WA 98195-1700 USA*

David King and his group developed the first calorimeter that could measure heats of adsorption on the well-defined surfaces of single crystals with sufficient precision to reveal new understanding of surface chemistry, especially by determining the energies of adsorbed molecular fragments that are catalytic reaction intermediates and otherwise inaccessible experimentally. Since then, other groups including our own have adopted this technique and made substantial extensions, including: (1) heat detector replacement with a pyroelectric polymer ribbon that is pressed against the back of the sample, allowing routine measurements from 100 to 350 K with high precision (a standard deviation of 1.3 kJ/mol with gas pulses that contain only 1% of a monolayer), (2) adsorption energies on well-defined metal nanoparticles grown on single crystal oxides as a function of particle size, (3) metal adsorption and adhesion energies during thin film growth, (4) energetics of oxide-supported metal nanoparticles versus size which correlate with catalytic performance, (5) measurements of electrochemical adsorption and reactions at liquid/solid interfaces, and (6) transient measurements of heat-signal line-shapes during two-step reaction mechanisms (e.g., molecular adsorption followed by dissociation) that give the heats for both steps and the rate constant for the second step during every gas pulse. These extensions and their applications will be reviewed to assess the current state of adsorption calorimetry on single-crystal surfaces, and its future prospects. These energies of well-defined adsorbates provide crucial benchmarks for assessing the energy accuracy of quantum mechanical approximation like those in density functional theory (DFT). The same type of pyroelectric heat detector has also been extended to measurements of adsorption energies on thin films that have been deposited directly onto the detector's surface, affording a further 10-fold improvement in sensitivity but now limited to polycrystalline surfaces. Applications of this approach will be described which clarify: (1) metal/organic interfaces of importance in photovoltaics and LEDs, and (2) mechanistic and energetic details of thin-film growth by atomic layer deposition (ALD).

Work supported by NSF grant #CHE-1361939 and DOE-OBES grant #DE-FG02-96ER14630.

Wed-14:00-Plen-3**Electronic and phononic structure measurements on superconducting surfaces using scanning tunneling microscopy**

Plenary lecture

Young Kuk

Department of Physics and Astronomy, Seoul National University, Seoul 08826, South Korea

The ability to measure the electronic or phononic structure on a solid surface is a great help in understanding the bulk or surface properties of the solids. Although it has been widely used to measure the electronic structure of the surface using scanning tunneling spectroscopy, it is known that measurement of phonons is not easy. This is because the phonon signal is not well measured in the tunneling condition of scanning tunneling microscopy. In this talk, tunneling conditions capable of phonon measurement are presented and experimentally demonstrated. We will use this experimental method to understand the electrical structure of superconducting materials and to show STS results when the phonons contribute to the formation of electron pairs in those materials.

Fri-10:10-Plen-6

Illuminating nanosystems at surfaces

Plenary lecture

Elisa Molinari*

University of Modena and Reggio Emilia and CNR Nanoscience Institute, Modena, Italy

We are now used to consider first principles theories and simulations as reliable and predictive tools for many ground state problems in surface science. Describing excitations and their dynamics from first principles is much tougher, but extremely important to understand fundamental processes following e.g. photoexcitation, and for the theory of spectroscopies. I will present recent progress showing that we are now reaching predictivity and quantitative accuracy for realistic systems also in that case. I will focus on two case studies that we have recently explored:

- organic photovoltaic interfaces and model photosynthetic systems [1]: what controls the ultrafast charge separation processes after exciton generation ?
- graphene-based nanosystems at surfaces [2]: what is the role of screening and substrate effects on many-body interactions and exciton binding? what are the excitonic spectral signatures, and how can they help in understanding the self-assembly process at surfaces [2] ? how to identify plasmonic signatures [3]?

In both cases, ab-initio approaches beyond mean-field theories are needed. We use real-time time-dependent density functional theory when coupling to vibrations is critical for large systems, and many body perturbation theory in the GW and Bethe-Salpeter approaches when we need the highest accuracy in excitonic effects.

I will discuss how these approaches are helping us to address the above questions and have contributed to successful interpretation of experiments [1-2], and the challenges we see for the future.

* In collaboration with C. Cardoso, A. Ferretti, D. Prezzi, C.A. Rozzi, A. Ruini, D. Varsano. Computational developments are supported by the European Center for HPC applications 'MaX – materials at the exascale': www.max-centre.eu.

- [1] CA Rozzi, SM Falke, N Spallanzani, A Rubio, E Molinari, D Brida, M Maiuri, G Cerullo, H Schramm, J Christoffers, and C Lienau, *Nat Commun* 4, 1602 (2013); SM Falke, CA Rozzi, D Brida, M Maiuri, M Amato, E Sommer, A De Sio, A Rubio, G Cerullo, E Molinari, and C Lienau, *Science* 344, 1001 (2014).
- [2] P Ruffieux, J Cai, NC Plumb, L Patthey, D Prezzi, A Ferretti, E Molinari, X Feng, K Müllen, CA Pignedoli, and R. Fasel, *ACS Nano* 6, 6930 (2012); R Denk, M Hohage, P Zeppenfeld, J Cai, CA Pignedoli, H Söde, R Fasel, X Feng, KH Müllen, S Wang, D Prezzi, A Ferretti, A Ruini, E Molinari, and P Ruffieux, *Nat Commun* 5, 4253 (2014); A Batra, D Cvetko, G Kladnik, O Adak, C Cardoso, A Ferretti, D Prezzi, E Molinari, A Morgante, and L Venkataraman, *Chem Sci* 5, 4419 (2014); L Massimi, O Ourdjini, L Lafferentz, M Koch, L Grill, E Cavaliere, L Gavioli, C Cardoso, D Prezzi, E Molinari, A Ferretti, C Mariani, and MG Betti, *J Phys Chem C* 119, 2427 (2015).
- [3] L Bursi, A Calzolari, S Corni, and E. Molinari, Quantifying the Plasmonic Character of Optical Excitations in Nanostructures, *ACS Phot* 3, 520 (2016); R Zhang, L Bursi, JD Cox, Y Cui, CM Krauter, A Alessandro, A Manjavacas, A Calzolari, S Corni, E Molinari, EA Carter, FG Garcia de Abajo, H Zhang, and P Nordlander, *ACS Nano* 11, 7321 (2017).

Wed-14:50-Plen-4**Supramolecular and covalent assembly of molecules at surfaces: chirality, complexity and diversity**

Plenary lecture

Rasmita Raval

The Surface Science Research Centre, Department of Chemistry, University of Liverpool, L69 3BX, UK

The nanoscale details of how complex molecular organisations and architectures are nucleated, controlled and propagated at surfaces have now begun to emerge from scanning probe microscopy, a powerful range of surface science techniques and periodic density functional theory. Organised molecular assemblies give rise to important functions such as molecular recognition, chirality, adaptive behaviour and confined motion that are important in functional interfaces and new materials. Furthermore, complexity in organisational behaviour is found to be induced by simple initiators such as the molecular interaction with the surface, chemical fields or from fluctuating populations of differing molecules. Finally, the transition towards robust, covalent assemblies will be demonstrated via on-surface synthesis of macromolecules using clean, generic connection strategies that utilise the C-H bond as a synthon. Scanning tunneling microscopy reveals that covalent macromolecular heterostructures, displaying diverse compositions, structures and topologies, are created with ease from seven distinct building blocks, including porphyrins, pentacene and perylene. By exploiting differences in C-H bond reactivity, controlled synthesis of specific products, such as block and cross-linked copolymers, can be attained. Further, the symmetry and geometry of the molecules and the surface can be exploited to determine the outcome of the covalent bond forming reactions. This strategy opens up the capability to generate libraries of multivariate macromolecules directly at a surface that, in conjunction with nanoscale probing techniques, could accelerate the discovery of functional interfaces.

Mon-9:30-Plen-1**Surface science approach to the molecular level integration of the principles in heterogeneous, homogeneous, and enzyme catalysis**

Plenary lecture

Gabor A. Somorjai

University of California at Berkeley, USA

The surface science of chemical reactivity utilized single crystal surfaces to determine the atomic structures at interfaces responsible for rearrangements of molecules through changes at covalent or charge transfer (acid-base) bonds. The evolution of nanomaterials science has had a large impact on molecular catalysis science since most heterogeneous, homogeneous and enzyme catalysts are nanoparticles in the 0.8–10 nm range. Monometallic and bimetallic nanoparticles as well as core-shell structures and oxide-metal interfaces are used to study multipath catalytic reactions with high product selectivity. At the same time instruments were developed that can be employed to study catalysts under reaction conditions to monitor dynamic changes that occur during catalytic reactions, their atomic and molecular structure, and composition and oxidation state with high spatial and time resolution. These *in-situ* surface techniques include sum frequency generation vibrational spectroscopy, high pressure scanning tunneling microscopy along with synchrotron techniques of X-ray spectroscopies. Discoveries have included the size and shape dependence of turnover rates and product selectivity and other kinetic variables, the importance of oxide-metal interfaces in heterogeneous catalysis and the dominance of covalent bond and charged ion chemistry in transition metal and acid-base catalysis. Below 2 nm the metal nanoparticles have electronic structures that stabilize charge states, which can be used to heterogenize homogeneous catalysts. Enzymes can be immobilized on a DNA to aniline functionalized glass and they maintain most of their catalytic activity in this mode. Our aim is integration of the three fields of catalysis, heterogeneous, homogeneous and enzyme by developing hybrid systems and new instrument that permit studies of increased catalytic complexity.

Mon-10:40-Plen-2**Ultrafast dynamics of excited states and light induced processes at surfaces**

*Plenary lecture***Martin Wolf***Fritz Haber Institute of the Max Planck Society, Department of Physical Chemistry, 14195 Berlin, Germany*

Electronic excitations at surfaces can induce a rich variety of processes, including chemical reactions at surfaces, coherent lattice excitations (phonons) or ultrafast structural transitions of solids. These photoinduced processes occur on ultrafast (femto- to picosecond) timescales and are accompanied by pronounced changes of the electronic structure and occupation of electronic states. Recent advances in femtosecond time-resolved spectroscopy allow direct probing of the underlying fundamental steps and provide a mechanistic understanding of transfer of energy from the electronic system into nuclear motions.

In this talk, I will discuss two different experimental approaches to probe such transient electronic structure changes on ultrafast timescales employing time- and angle-resolved photoelectron spectroscopy (trARPES) and time-resolved resonant inelastic x-ray scattering (trRIXS). XUV based trARPES at 500 kHz repetition rate opens the perspective of excited state band mapping throughout the complete Brillouin zone and monitoring collective phonon dynamics through their influence on the electronic band structure. In particular, we investigate in detail the dynamics of the photo-induced phase transition of quasi-1D metal nanowires on In/Si(111) as prototypical example for order-order structural transition. On the other hand, experiments at the X-ray free electron laser LCLS performed with trRIXS provide direct insight into chemical bond formation in ultrafast surface reactions. These studies allow new insights into dynamics and details of the potential energy landscape.



33rd EUROPEAN CONFERENCE ON SURFACE SCIENCE

KEYNOTE LECTURES

Wed-16:00-K-OXID ● HALL-C**Metal-supported 2D oxide systems: strong versus weak substrate coupling***Keynote Lecture*Thomas Obermüller, [Falko P. Netzer](#), Svetlozar Surnev*Surface and Interface Physics, Institute of Physics, Karl-Franzens University Graz, A-8010 GRAZ, Austria*

Two-dimensional (2-D) transition metal oxide layers have attracted significant interest during the past decade due to their novel emergent properties and high potential for nanotechnology applications [1,2]. For practical reasons 2-D oxide layers are usually supported on metal surfaces. This leads to a coupling of the oxide overlayer to the metal substrate, often strong coupling, which creates a metal-oxide hybrid system with properties that are largely determined by the oxide-metal interface. Here, we report the formation of a 2-D W-oxide layer on a Ag(100) surface, where the oxide appears to be only weakly coupled to the substrate. The 2-D W-oxide layer has been prepared by vapor phase deposition of gas phase $(\text{WO}_3)_3$ clusters onto Ag(100) at 500°C substrate temperature. The WO_x grows in the form of a well-ordered incommensurate 2-D wetting layer, with mesoscopically large domains in a variety of azimuth orientations with respect to the substrate. The different azimuth orientations of the oxide domains can easily be recognized in LEED and in the STM by their different Moiré patterns. The overlayer lattice can be imaged with atomic resolution in the STM and analyzed using the Moiré formula, from which the square overlayer lattice constant can be accurately evaluated to $a = 3.72 \text{ \AA}$; this is close to the respective WO_3 bulk lattice constant. AES and XPS spectra indicate an overlayer stoichiometry close to WO_3 , although the W 4f peaks occur at a lower binding energy than characteristic for W^{6+} . A structure model in terms of a 2-D WO_x sheet is proposed. The oxide lattice is flexible as demonstrated by the easy distortion in the vicinity of defects. It is suggested that this WO_x sheet on Ag(100) behaves essentially like a decoupled 2-D oxide layer. However, despite this weak overlayer-substrate interaction, an interesting anisotropic behavior is observed for the growth of WO_3 beyond the monolayer, where unidirectional needle formation suggests a symmetry break of the square lattices. A second-order interfacial strain interaction effect is conjectured.

References:

- [1] G. Pacchioni, *Two-dimensional oxides: multifunctional materials for advanced technologies*. Chem. Eur. J. 18(2012) 10144
- [2] *Oxide materials at the two-dimensional limit*. F.P. Netzer, A. Fortunelli, Eds. (Springer Series in Materials Science, Vol. 234, Springer 2016)

Mon-11:30-K-ELI-ALPS CONGRESS HALL
The ELI Research Infrastructure and implementation status

Keynote Lecture**Károly Osvay***ELI-ALPS, ELI-HU Nonprofit Ltd, Szeged, Hungary*

The major research equipment of the European distributed research facility, the Extreme Light Infrastructure (ELI), are based on short pulse laser sources operating in the 100 W average power regime. The peak power and the repetition rate range from 1 TW at 100 kHz up to multiple PW at few Hz. The systems are designed for stable and reliable operation, yet to deliver pulses with unique parameters, especially with unmatched fluxes and extreme bandwidths. This exceptional performance will give ways to a set of secondary sources with incomparable characteristics, including light sources ranging from the THz to the X-ray spectral ranges, and particle sources.

The experimental activities in the ELI Attosecond Light Pulse Source (ELI ALPS) at Szeged, Hungary, will start with the installation of the two 100 kHz repetition rate, CEP stabilized lasers in Autumn 2017. The MIR laser produces 0.15mJ, shorter than 4-optical-cycle pulses tunable between 2.5–3.9 μm . The first stage of the HR laser will provide pulses around 1 μm with 1 mJ energy and pulse duration less than 6.2 fs. The systems will be optically synchronized to each other with a temporal jitter below 1 fs.

Along with the installation of the lasers, we will also start the assembly of the THz laboratory, the nano-plasmonic experimental areas, as well as the first high harmonic beamline. The XUV bursts of light with attosecond duration are expected to be generated by the Spring of 2018.

Tue-16:40-K-CATL ● HALL-E

Partial selective hydrogenation of acrolein over model Pd catalysts: a mechanistic IRAS and molecular beam study

Keynote Lecture

Karl-Heinz Dostert¹, Swetlana Schauerma², Casey O. Brien¹, H.-J. Freund¹

¹ Fritz-Haber-Institut, Berlin, Germany;

² Institute of Physical Chemistry, Christian-Albrechts-Universität zu Kiel, Germany

Identifying the surface processes governing the selectivity in hydrogenation of unsaturated carbonyl compounds on late transition metals is crucial for the rational design of new catalytic materials with the desired selectivity towards C=O vs. C=C bond hydrogenation. In our studies, we investigate mechanisms, kinetics and thermodynamics of heterogeneously catalyzed partial hydrogenation of unsaturated hydrocarbons on nanostructured model supported catalysts by combination of multi-molecular beam techniques, infrared reflection-absorption spectroscopy (IRAS) and single crystal adsorption calorimetry (SCAC). The ultimate goal of our research is obtaining detailed correlations between reactivity, selectivity and the particular structure of the catalytic surface turning over.

Specifically, we will present a mechanistic study on selective hydrogenation of acrolein over model Pd surfaces – both single crystal Pd(111) surface and Pd nanoparticles supported on a model oxide support.¹ We show for the first time that selective hydrogenation of the C=O bond in acrolein to form the desired reaction product – an unsaturated alcohol propenol – is possible over Pd(111) with nearly 100% selectivity. However, this process requires a very distinct modification of the Pd(111) surface with an overlayer of oxopropyl spectator species that are formed from acrolein during the initial stages of reaction and turn the metal surface highly selective towards propenol formation. By applying pulsed multi-molecular beam experiments and *in operando* IRAS we identified the chemical nature of the spectator and the reactive surface intermediate as oxopropyl and propenoxy species, respectively. The evolution of the surface concentration of the propenoxy intermediate monitored spectroscopically was found to closely follow the propenol formation rate detected in the gas phase.

While Pd(111) shows nearly 100% selectivity towards the desired hydrogenation of the C=O bond in the temperature range between 250 and 300 K, Pd nanoparticles were found to be much less selective towards this product.² *In-situ* detection of surface species shows that formation of oxopropyl overlayer is strongly hindered on Pd nanoparticles by acrolein decomposition to CO and ethylidyne-like species. We show that the extent of acrolein decomposition can be tuned by varying the particle size and the reaction temperature. As a result, significant production of propenol is observed over 12 nm Pd nanoparticles at 250 K, while smaller (4 and 7 nm) nanoparticles did not produce propenol at any of the temperatures investigated. The possible origin of particle size dependence of propenol formation is discussed. This work demonstrates that the selectivity in hydrogenation of acrolein is controlled by the relative rates of acrolein partial hydrogenation to oxopropyl surface species and of acrolein decomposition, which has significant implications for rational catalyst design.

References:

1. Dostert, K.-H.; O'Brien, C. P.; Ivars-Barceló, F.; Schauerma, S.; Freund, H.-J., Spectators Control Selectivity in Surface Chemistry: Acrolein Partial Hydrogenation over Pd. *Journal of the American Chemical Society* 2015, 137, 13496-13502.
2. O'Brien, C. P.; Dostert, K.-H.; Schauerma, S.; Freund, H.-J., Selective Hydrogenation of Acrolein over Pd Model Catalysts: Temperature and Particle-Size Effects. *Chemistry – A European Journal* 2016, 22, 15856-15863.

Wed-9:40-K-NAEX ● HALL-A

Chemical reactions in ionic liquids monitored through the gas (vacuum)/liquid interface

Keynote Lecture

[H.-P. Steinrück](#), I. Niedermaier, F. Maier

Physikalische Chemie II, Universität Erlangen-Nürnberg, Germany

We analyze the potential of X-ray photoelectron spectroscopy under UHV conditions to follow chemical reactions in ionic liquids *in situ*. Traditionally, only reactions occurring on solid surfaces were investigated by XPS *in situ*. This was due to the high vapor pressures of common liquids or solvents, which are not compatible with the required UHV conditions. It was only recently realized that the situation is very different when studying reactions in ILs, which have an inherently low vapor pressure, and first studies have been performed within the last years. Compared to classical spectroscopy techniques used to monitor chemical reactions, the advantage of XPS is that through the analysis of their core levels all relevant elements can be quantified and their chemical state can be analyzed under well-defined (ultraclean) conditions. In this contribution, we cover several different reactions which occur in the IL, with the IL, or at an IL/support interface, demonstrating the outstanding potential of *in situ* XPS to gain insights in liquid phase reactions in the near-surface region.

References:

H.-P. Steinrück, I. Niedermaier, F. Maier, „Chemical Reactions in Ionic Liquids Monitored through the Gas (Vacuum)/Liquid Interface“, J.Chem.Phys. 2017 (in press)

Wed-11:20-K-GRAP ● HALL-D

Towards the low temperature growth of transfer free graphene

Keynote Lecture

Masaki Tanemura¹, Riteshkumar Vishwakarma¹, Kazunari Takahashi¹,
Mona Ibrahim Araby¹, Yuji Wakamatsu¹, Golap Kalita¹, Mohamad Saufi Rosmi²,
Yazid Yaakob³, Masashi Kitazawa⁴

¹ Nagoya Institute of Technology, Japan; ² Universiti Pendidikan Sultan Idris, Malaysia;

³ Universiti Putra Malaysia, Malaysia; ⁴ Olympus Co. Ltd., Japan

The major concern in graphene research includes the low-temperature growth, transfer free growth onto the substrate and position control growth for a variety of practical applications. Although chemical vapor deposition (CVD) is well-known to provide the high quality graphene on the catalyst surface, the transfer process of graphene onto the desired substrate is unavoidable, making the position control of graphene difficult. By contrast, transfer free graphene growth and thus the position control of graphene growth is readily achievable by the solid phase reaction method, namely, simple annealing of the stacked carbon and catalyst metal films [1]. Here we report the transfer free graphene growth on SiO₂ covered Si (SiO₂/Si) and glass substrates at the temperature as low as 250 °C by simple vacuum annealing of the stacked carbon and catalyst metal films on the substrate [2].

The key to this approach is the selection of catalyst metal. In the previous papers, transfer free graphene was synthesized at high temperatures (>750 °C) using Cu, Ni and Co, which are typical catalysts for the CVD graphene growth [3-5]. By contrast, the metal catalyst employed here is not popular for CVD graphene growth [2]. A catalyst metal film (500 nm in thickness) was deposited onto an amorphous carbon (50 nm in thickness) coated SiO₂/Si and glass substrates by laser ablation method. The samples thus prepared were simply annealed at 250 °C under vacuum condition, and then the catalyst metal was removed by chemical etching. After this treatment, as seen in Raman spectrum (Fig. 1), the surface was characterized by the intense G and 2D peaks together with a small D peak, confirming the direct growth of multilayer graphene on the substrates. Although the domain size of the graphene formed was still small, 5–10 μm in an average at the moment, this approach will open up a new route for transfer free and position control graphene growth at low temperatures.

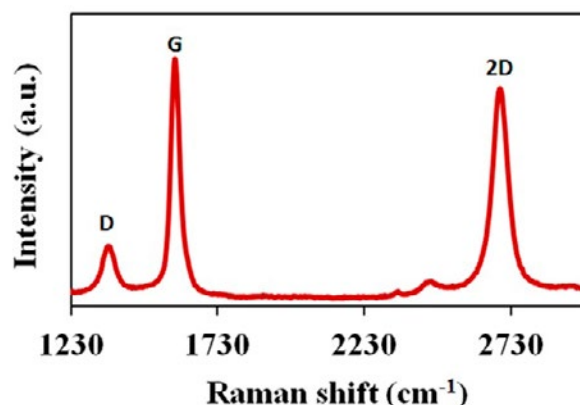


Figure 1. Typical Raman spectrum attained after the removal of the catalyst for the sample (glass substrate) annealed at 250 °C.

References:

- [1] M. Saufi Rosmi, M. Tanemura, et al., *Scientific Reports*, 4 (2014) 7563.
- [2] R. Vishwakarma, M. Tanemura, et al., *Scientific Reports*, 7 (2017) 43756.
- [3] R. Hirano, M. Tanemura, *Nanoscale* 4 (2012) 7791-7796.
- [4] G. Kalita, M. Tanemura, et al., *RSC Advances*, 4 (2014) 38450-38454.
- [5] M. Saufi Rosmi, M. Tanemura, et al., *RSC Advances*, 6 (2016) 82459-82466.



33rd EUROPEAN CONFERENCE ON SURFACE SCIENCE

INVITED LECTURES

Tue-16:00-I-PISC ● HALL-A

Buffer assisted growth of metallic nanoparticles and oxide films as a versatile ultraclean methodology for materials synthesis

PISC Photo-Induced Surface Chemistry

Micha Asscher, Liat Zilberberg, Serge Mitlin

Institute of Chemistry, The Hebrew University of Jerusalem, Israel

The growth of metallic nanoparticles and thin oxide films has been developed in recent years as a versatile methodology to prepare ultraclean metallic nanoparticles and thin oxide films, under ultra-high vacuum conditions. The metallic nanoparticles (NPs) are grown when clean metal elements are deposited on top of rare gas layers or water (Amorphous Solid Water – ASW). The size of the metallic NPs can be controlled in the size range of 3–150 nm by varying the evaporation rate, the film thickness and the cycles of deposition. We have recently demonstrated the dramatic enhancement photo-induced surface photochemistry led by hot electrons that are generated by shining UV on such metallic particles supported on an insulating substrate ($\text{SiO}_2/\text{Si}(100)$). [1]

When the metallic elements become reactive with respect to the buffer material (ASW), a complementary process may take place – Reactive Layer Assisted Deposition (RLAD). The result of RLAD is the formation of an ultrathin oxide film that can be manipulated to cover the metallic NPs and create new materials/properties. This procedure is similar to both Sol-Gel and the ALD, since one can control the oxide thickness at sub-nanometer level. It turns out that the driving force for the oxide formation is the oxidation/reduction potential relative to water. We have so far demonstrated such controlled growth of titania and alumina. The optical properties of embedded silver NPs within the thin oxide films has been studied. [2] The potential of such metal-oxide hybrid materials will be discussed.

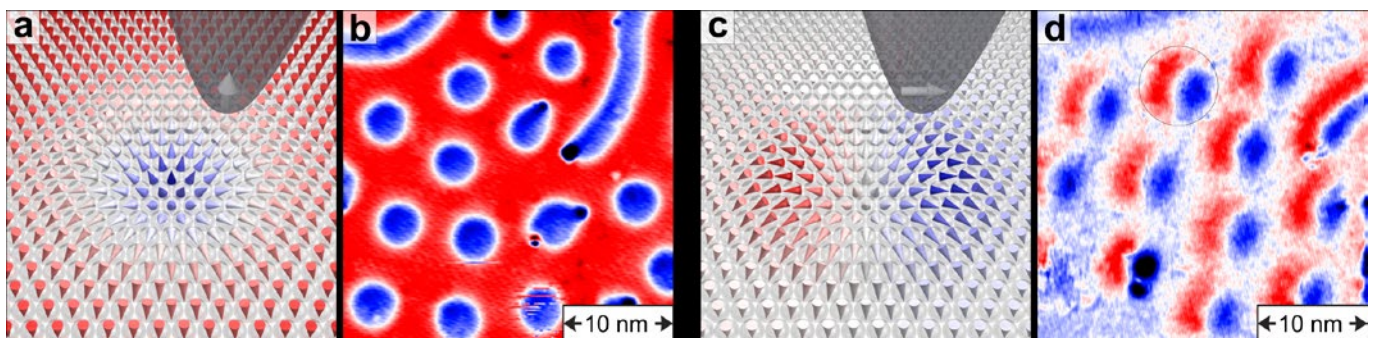
References:

- [1] Toker, G., Bospaly A., Zilberberg, L., Asscher, M. “Enhanced Photo Chemistry of Ethyl Chloride on Ag Nanoparticles”, *Nano Letters*, 15(2), 936-42 (2015).
- [2] Zilberberg, L., Mitlin, S., Shankar, H., Asscher, M., “Buffer Layer Assisted Growth of Ag Nanoparticles in Titania Thin Films”, *J. Phys. Chem. C*, 119(52), 28979-28991 (2015).

Tue-10:40-I-MAGN ● HALL-D**Manipulation of interface-induced Skyrmions studied with STM***MAGN Surface and molecular magnetism***Kirsten von Bergmann***Department of Physics, University of Hamburg, Germany*

Isolated magnetic skyrmions are envisioned as the basis for future spintronic devices. They can be stabilized by a favorable interplay of magnetic exchange, Dzyaloshinskii-Moriya interaction (DMI), anisotropy and Zeeman energy. The Fe/Ir(111) interface is known to exhibit strong DMI [1] and serves as an ideal basis to build up materials that host single skyrmions on the nanometer length scale. Such small magnetic objects can be imaged, characterized and manipulated using (spin-resolved) scanning tunneling microscopy (STM) [2].

Building upon the Fe/Ir(111)-interface a fine-tuning of the relevant magnetic energies is performed by adding metallic overlayers, by adsorption of hydrogen, or by a variation of the strain within the magnetic film. Magnetic field dependent STM measurements can be used to obtain the specific material parameters [3]. In addition, spectroscopy using a non-magnetic tip electrode reveals the correlation between the local magnetoresistance and the non-collinearity of the spin texture [4]. Such a read-out of the local magnetic state could be combined with the demonstrated reversible switching between skyrmion and ferromagnet by local electric fields [5].



References:

- [1] S. Heinze et al., *Nature Phys.* 7, 718 (2011).
- [2] K. von Bergmann et al., *J. Phys.: Condens. Matter* 26, 394002 (2014).
- [3] N. Romming et al., *Phys. Rev. Lett.* 114, 177203 (2015).
- [4] C. Hanneken et al., *Nature Nanotech.* 10, 1039 (2015).
- [5] P.-J. Hsu et al., *Nature Nanotech.* 12, 123 (2017).

Tue-15:00-I-EG2D ● HALL-E

SPM characterization and processing of 2D materials

EG2D Epitaxial growth and modification of 2D materials

L. P. Biró¹, P. Nemes-Incze¹, G. Z. Magda¹, P. Vancsó^{1,2}, G. Dobrik¹, A. A. Koós¹, Z. E. Horváth¹, J. Pető¹, G. I. Márk¹, Ph. Lambin², C. Hwang³, L. Tapasztó¹

¹ Institute of Technical Physics and Materials Science, Centre for Energy Research, Hungarian Academy of Sciences, Budapest, Hungary;

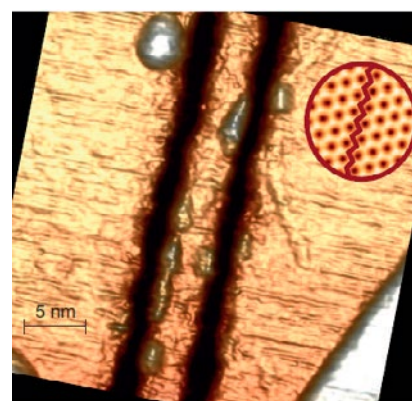
² Physics of Matter and Radiation, Physics Department, University of Namur, Namur, Belgium

³ Korea Research Institute of Standards and Science, Center for Nanometrology, Daejeon, South Korea

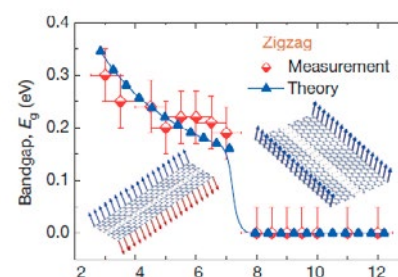
Graphene and the multitude of other 2D materials open a new era in materials science. Beyond the exotic changes in the properties of most materials when thinned down to a single atom/molecule thin layer, these materials offer for the first time the opportunity of building up novel materials by layering the individual 2D materials in so called Van der Waals heterostructures. Moreover, the CVD growth in large sheets of the 2D materials opens up the road towards the engineering on these novel, heterostructured materials in macroscopic sizes. Unfortunately, presently the CVD growth yields polycrystalline 2D sheets. Therefore it is crucial to be able to characterize by AFM, STM/STS the grain structure [1] and the properties of the grain boundaries [2]. In a next step, placing graphene on HOPG, or of MoS₂ on HOPG, generates a rich variety of phenomena which can be very conveniently investigated by STM and Raman microscopy [3]. On the other hand, the atomic scale details of the 2D materials, like: native point defects [4], or nanostructures, like graphene nanoribbons, realized by atomic scale, crystallographically controlled lithography [5] exhibit properties, which could hardly be characterized with other instruments than SPMs. We will overview some of the most significant results obtained in our laboratory in the characterization of the native point defects of TMDCs [4] and by scanning tunneling lithography of graphene [5].

References:

- [1] Nemes-Incze, P. et al. Revealing the grain structure of graphene grown by chemical vapor deposition. *Appl. Phys. Lett.* 99, 23104-1-23104-3 (2011).
- [2] Vancsó, P. et al. Effect of the disorder in graphene grain boundaries: A wave packet dynamics study. *Appl. Surf. Sci.* 291, 58–63 (2014).
- [3] Koós, A. A. et al. STM study of the MoS₂ flakes grown on graphite: A model system for atomically clean 2D heterostructure interfaces. *Carbon N. Y.* 105, 408–415 (2016).
- [4] Vancsó, P. et al. The intrinsic defect structure of exfoliated MoS₂ single layers revealed by Scanning Tunneling Microscopy. *Sci. Rep.* 6, 29726 (2016).
- [5] Magda, G. Z. et al. Room-temperature magnetic order on zigzag edges of narrow graphene nanoribbons. *Nature* 514, 608–611 (2014).



A 6.5-nm-wide graphene nanoribbon (GNR) with edges of precisely zigzag orientation, as shown by the inset in the upper right corner (300 mV, 2 nA). The GNR was patterned by scanning tunnelling lithography in a graphene sheet deposited on a Au(111) substrate



In zigzag graphene nanoribbons the band structure is governed by the emerging edge magnetism and a sharp semiconductor (antiferromagnetic) to metal (ferromagnetic) transition is revealed at ribbon widths of 7 nm.

Thu-10:40-I-GRAP ● HALL-A Graphene growth on Ni (111)

GRAP Graphene and carbon-based 2D films

Giovanni Comelli

Department of Physics, University of Trieste, via Valerio 2, I-34127 Trieste IOM-CNR Laboratorio TASC, in AREA Science Park, Basovizza, I-34149 Trieste

By means of joint Scanning Tunneling Microscopy (STM) experiments and Density Functional Theory (DFT) *ab initio* calculations, we have recently characterized the different chemisorbed configurations of epitaxial graphene coexisting on a Ni(111) single crystal surface [1], providing also an atomic scale description of the structure of their edges both *during* and *post* growth [2]. Here we demonstrate, both experimentally and theoretically, the catalytic role played by single metal adatoms during this spontaneous and technologically relevant growth process. The elusive catalytic action of individual Ni atoms at the edges of a growing graphene flake is directly captured by STM imaging at the ms time scale, thanks to the Fast-scan add-on module recently developed in our laboratory, which is capable of providing video rate STM movies of surface process. DFT calculations rationalise the experimental observations, yielding a full atomistic description of the growth mechanism, where the single atom Ni catalyst acts as a knitting needle, allowing new carbon stitches to be incorporated in the expanding graphene fabric. Our results represent a direct observation of a single atom catalyst *at work* during a surface catalysed process, providing straightforward evidence of the enhanced reactivity displayed by low-coordinated metal atoms in many model systems.

References:

- [1] F. Bianchini, L.L. Patera, M. Peressi, C. Africh and G. Comelli, *J. Phys. Chem. Lett.* 51, 467 (2014).
- [2] L.L. Patera, F. Bianchini, G. Troiano, C. Dri, C. Cepek, M. Peressi, C. Africh and G. Comelli, *Nano Lett.* 15, 56 (2015).

Tue-14:00-I-OXID ● HALL-C

Tailoring the properties of oxide/metal interfaces: from metallic to graphitic buffer layers

OXID Oxide surfaces and ultrathin oxide films

Lamberto Duò

Due to their extreme importance in nanotechnology, ultra-thin oxide films interfaced with metallic substrates have been extensively investigated during the last decade. Among these, epitaxial oxide layers deposited on 3d transition metals deserve particular attention because of the complex chemical reactions occurring at the oxide/substrate interface. As a matter of fact, the oxidizing atmosphere exploited during reactive deposition induces a severe oxidation of the substrate, modifying its chemical and structural identity [1].

In this framework, a method to control the physical and chemical characteristics of the oxide/metal interface is to insert a buffer layer between the metallic support and the oxide film. Buffer layers can be exploited to tune the chemical composition of the oxide/metal interface, protecting the substrate from oxidation. Moreover, metallic films developing metastable phases can be used as templates for the growth of epitaxial interfaces between metals and their native oxides. Finally, the development of peculiar magnetic coupling [2,3] can be observed by properly selecting the interlayer material.

In this contribution, the effects of either a nanometer-thick metallic film or a monolayer graphene intercalated at the oxide/metal interface will be elucidated by combining scanning tunneling microscopy with spin resolved electron spectroscopies. I will show how, by exploiting an appropriate buffer layer, it is possible to finely tune the chemical and structural properties of the oxide-metal interfaces, tailoring the magnetic properties of the oxide-metal superlattices.

References:

- [1] "Reactive metal–oxide interfaces: a microscopic view" A. Picone, M. Riva, A. Brambilla, A. Calloni, G. Bussetti, M. Finazzi, F. Ciccacci, L. Duò, Surf. Sci. Rep. 71 (2016) 32
- [2] "Magnetic properties of antiferromagnetic oxide materials: surfaces, interfaces and thin films", edited by L. Duò, M. Finazzi, F. Ciccacci (Wiley-VCH Verlag GmbH, Weinheim, Germany, 2010).
- [3] "Magnetic properties of interfaces and multilayers based on thin antiferromagnetic oxide films", M. Finazzi, L. Duò, F. Ciccacci, Surf. Sci. Rep. 64 (2009) 139.

Wed-10:40-I-COMP ● HALL-E

Molecularly functionalized surfaces and interfaces

COMP Computational surface chemistry and physics

Adam S. Foster^{1,2,3}

¹ COMP, Department of Applied Physics, Aalto School of Science, PO Box 11100, FI-00076 Aalto, Finland;

² Division of Electrical Engineering and Computer Science Kanazawa University, Kanazawa 920-1192, Japan;

³ Institute of Physical Chemistry, Johannes Gutenberg University Mainz, Duesbergweg 10-14, 55099 Mainz, Germany

Many ideas in next generation technology are predicated on atomic and molecular control of surfaces and interfaces. A natural route to providing this level of control is to design the interface directly using molecular building blocks via self-assembly. The molecular design process can either offer functionality directly, as in lubrication or electronics, or act as a template for the adsorption of the active atoms or molecules.

Using a combination of modelling approaches in partnership with Scanning Probe Microscopy experiments, in this work we consider several examples where the interface has been designed by the controlled assembly of molecular layers. We compare and contrast the adsorption and reaction mechanisms on metal and insulator systems [1, 2], and also explore the use of molecular templates to control the adsorption process [3, 4]. We build upon this to explore the limits of physical sensitivity in measurements on these assembled structures and consider new insights offered by modern machine learning simulation approaches.

References:

[1] J. Phys. Chem. C 120 (2016) 14730

[2] Nat. Commun. 7 (2016) 12711

[3] Nat. Commun. 7 (2016) 11559

[4] J. Phys. Chem. C (2016) 120 (2016) 8772

Wed-9:00-I-BIMS ● HALL-B

Alloy surface science spanning composition space

BIMS Bimetallic surfaces and alloy nanocrystals

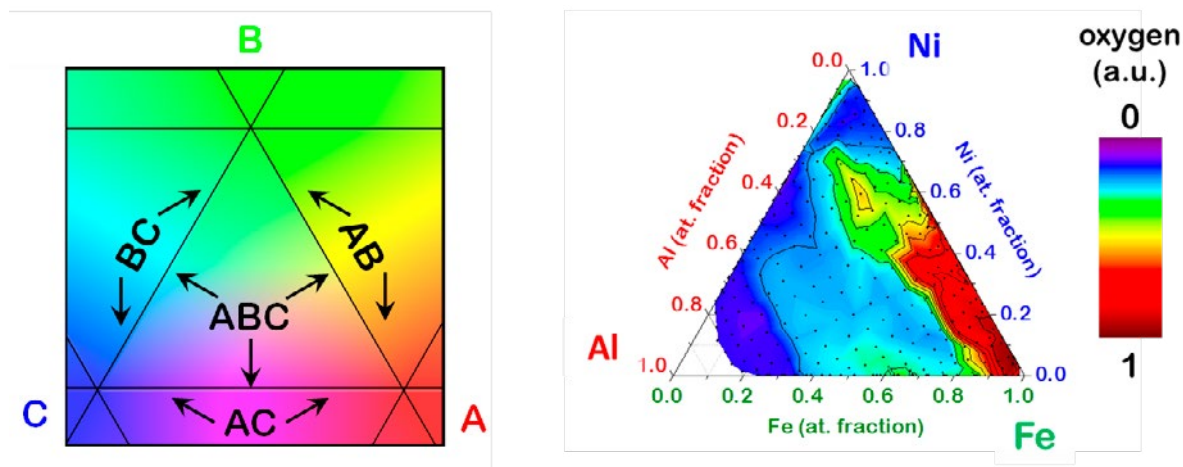
Andrew J. Gellman, James. B. Miller, Peter Kondratyuk, Mathew Payne, Irem Sen

Department of Chemical Engineering, Carnegie Mellon University, Pittsburgh, PA 15213, USA

One of the key challenges to systematic study of the composition dependence of the properties of multicomponent alloys is the need for experimental methods and simulation strategies that span multi-dimensional composition spaces comprehensively. We have addressed the experimental challenge by developing methods for preparation, characterization and property measurement on Composition Spread Alloy Films (CSAFs) (Figure 1, left). These are thin alloy films deposited with lateral composition gradients such that an entire ternary composition space can be represented in a 1 cm² thin film; $A_x B_y C_{1-x-y}$, $x = 0 \rightarrow 1$, $y = 0 \rightarrow 1-x$. By using a suite of spatially resolved analytical tools the alloy's physical characteristics (bulk composition, surface composition, electronic structure, phase, etc.) and its functional properties (catalytic activity, corrosion resistance, thermal conductivity, etc.) can be mapped across composition space (x, y) . The presentation will cover some of the methods and then illustrate their application to catalysis on $Ag_x Pd_{1-x}$ alloys and corrosion passivation of $Al_x Fe_y Ni_{1-x-y}$ alloys.

Our studies of alloy catalysis across alloy composition space have focused on correlating the electronic properties of alloys (d -band energies) with the barriers to elementary reaction steps extracted from reaction kinetics data. Using H_2 - D_2 exchange on $Ag_x Pd_{1-x}$ alloys we have measured the activation barrier to dissociative adsorption of H_2 , ΔE_{ads}^\ddagger , across alloy composition space and correlated this to the d -band energy. This experimentally tests the validity of the scaling relationships derived from electronic structure methods.

Our study of $Al_x Fe_y Ni_{1-x-y}$ corrosion in dry and humid air maps the critical aluminum concentration at which these alloys are passivated against corrosion across alloy compositions, $N_{Al}^*(x,y)$. In addition, this study maps the regions in which the various mechanisms of alloy passivation and corrosion are active (Figure 1, right). This yields by far the most comprehensive understanding of the influence of alloy composition on corrosion behavior yet obtained.



Tue-9:40-I-NAEX ● HALL-C

Novel solutions for near ambient pressure *in-situ* photoelectron spectro-microscopy

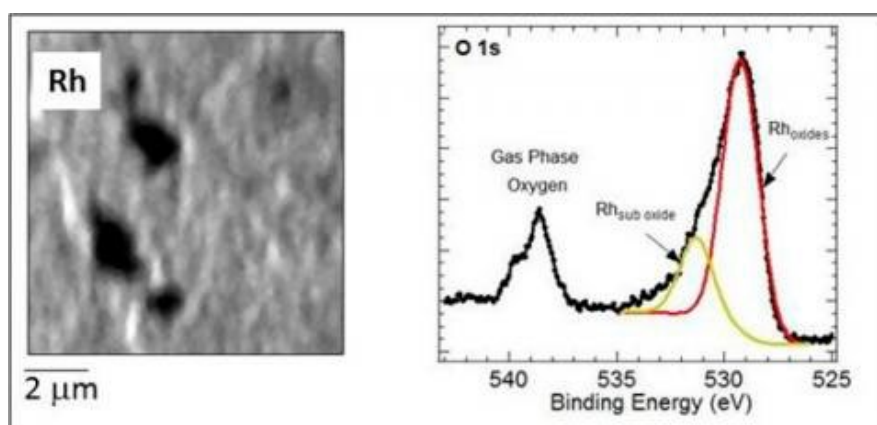
NAEX Novel advancement of experimental methods

Luca Gregoratti, M. Amati, H. Sezen, M. Al-Hada

Elettra – Sincrotrone Trieste ScPA Area Science Park SS14-Km 163.5 34149 Basovizza, Trieste, Italy

Monitoring *in-situ* the lateral distribution of the chemical state of surfaces and interfaces during catalytic and electrochemical reactions at sub micron level is of crucial importance for a large scale of phenomena (material gap). On the other hand the environmental conditions of the experiments should stay as close as possible to the operation conditions of devices/processes (pressure gap). The possibility to investigate chemical processes with X-ray photoelectron spectroscopy by combining both aspects is still a challenge for modern experimental setups.

The Escamicroscopy team of Elettra which operates a Scanning Photoemission Microscope (SPEM) has recently developed novel concepts for a new generation scanning photoelectron microscopes working under realistic pressure conditions. The first setup, called Dynamic High Pressure (DHP), generates high pressure pulsed gas packets directed to the sample; under the influence of gas pulses samples experience a several tens mbar pressure in a burst instant. The DHP has been already used for the characterization of electrochemical devices and catalytic materials and is now a standard option of the SPEM [1]. The most recent development is an effusive cell for near-ambient pressure SPEM where the highest static pressure achievable is around 1 mbar. Samples are encapsulated in a vacuum sealed cell and located behind a 200 μm diameter size pinhole through which the focused X-ray beam illuminates surfaces and photoelectrons reach the high vacuum path towards the electron analyzer [2]. The figure shows a photoemission map of a Rh surface exposed to 1 mbar O_2 partially oxidized and an O 1s core level spectrum of the surface showing also the gas phase spectrum of oxygen.



References:

- [1] Amati M et al. Journal of Instrumentation, Vol. 8 - 05, pp. T05001 (2013)
- [2] Sezen H. et al. Chem. Cat. Chem. DOI: 10.1002/cctc.201500637 in press (2015)

Thu-10:40-I-OXID ● HALL-C**Multiscale modelling of metal oxide interfaces and nanoparticles***OXID Oxide surfaces and ultrathin oxide films***Kersti Hermansson***Department of Chemistry-Ångström, Uppsala University, Uppsala, Sweden*

Redox-active metal oxide surfaces and interfaces – such as electrodes, catalysts, and sensors – play crucial roles in our society and in the development of new materials and greener technologies. In the scientific literature, a full arsenal of experimental methods are being used to help characterize such interfaces. At the same time, the number of theoretical studies in the literature steadily increases, providing mechanistic information at a detail that is hard to beat by experiment. *Are such theoretical results accurate enough?* Here the major challenges are (i) how to build a *structural model* that captures the complexity and imperfections of the real system at hand, and (ii) how to find an *interaction model/a materials relation* (say a DFT functional [1] or a force-field) that is good enough.

A 5 nm metal oxide nanoparticle may be very small to an experimentalist, but it contains many thousand atoms, making standard quantum-mechanical (e.g. regular DFT) methods totally unfeasible. Can force-field calculations be used instead? Well, mimicking the interactions and chemical properties *without explicit electrons* present is a formidable task, especially when the transfer of electrons is closely coupled to the material's functionality, as is the case for redox-active metal oxides. I will discuss some of our efforts in the development of a multiscale modelling approach for surfaces and interfaces of metal oxides (e.g. CeO₂, ZnO, MgO) – with and without interacting molecules (e.g. O₂ and water).

In summary, we combine a range of theoretical methods including DFT [2], tight-binding-DFT [3], and reactive force-field simulations [4] in a consistent multi-scale approach to examine the properties of oxide nanosystems. We generate images and spectra to make direct comparisons with the experimental counterparts (e.g. IRRAS spectra [5] and a new unpublished approach to predict vibrational spectra for OH-covered metal oxides), but we also generate properties that cannot be measured by experiments such as the water dipole moment enhancement on a surface (often much larger than in liquid water!). I will also inform about the European Materials Modelling Council (<https://emmc.info/>), and our efforts to promote the use of materials modelling in industry and the quality of the modelling results; the EMMC is open to everyone interested.

References:

- [1] G. G. Kebede, D. Spångberg, P. D. Mitev, P. Broqvist, K. Hermansson, "Comparing van der Waals DFT methods for water on NaCl(001) and MgO(001)", *The Journal of Chemical Physics* 146, 064703 (2017).
- [2] M. Hellström, D. Spångberg, K. Hermansson, "Treatment of Delocalized Electron Transfer in Periodic and Embedded Cluster DFT Calculations: The Case of Cu on ZnO (10-10)", *Journal of Computational Chemistry* 36, 2394 (2015).
- [3] J. Kullgren, M. J. Wolf, K. Hermansson, Ch. Köhler, B. Aradi, Th. Frauenheim, and P. Broqvist, "Self-Consistent-Charge Density-Functional Tight-Binding (SCC-DFTB) Parameters for Ceria in 0D to 3D". *J. Phys. Chem. C* 121, 4593–4607 (2017).
- [4] P. Broqvist, J. Kullgren, M. J. Wolf, A. C. T. van Duin, K. Hermansson, "A ReaxFF force-field for ceria bulk, surfaces and nanoparticles", *J. Phys. Chem. C* 119, 13598 (2015).
- [5] S. Hu, Z. Wang, A. Mattsson, L. Österlund, K. Hermansson, "Simulation of IRRAS Spectra for Molecules on Oxide Surfaces: CO on TiO₂(110)", *J. Phys. Chem. C* 119, 5403 (2015).

Tue-10:40-I-NAEX ● HALL-C

High-resolution AFM/STM/IETS imaging and its applications

NAEX Novel advancement of experimental methods

P. Jelinek

Institute of Physics of the Czech Academy of Sciences, Prague, Czech Republic

High-resolution AFM/STM/IETS imaging of molecules acquired functionalized tips [1] created a lot of excitement among researchers from many fields including material science, physics and chemistry. Here we will briefly describe a common underlying mechanism responsible for the unprecedented sub molecular contrast [2] including an efficient simulation approach of AFM/STM/IETS images. In next, we will also discuss applications of the technique achieving a precise identification of molecular products of on-surface reactions [3] or imaging electrostatic field of molecules with sub molecular resolution [4].

[1] R. Temirov et al, *New J. Phys.* 10, 053012 (2008); L. Gross et al, *Science* 325, 1110 (2009);
Ch. Chiang et al, *Science* 344, 885 (2014).

[2] P. Hapala et al, *Phys. Rev. B* 90, 085421 (2014); P. Hapala et al, *Phys. Rev. Lett.* 113, 226101 (2016)

[3] O. Stetsovych et al, *Nature Chemistry* (2016), DOI: 10.1038/nchem.2662

[4] P. Hapala et al, *Nature Commun.* 7, 11560 (2016).

Mon-15:00-I-ORGS ● HALL-B

Generic nature of long-range repulsion in molecular self-assembly on a bulk insulator surface

ORGS Organic molecules on solid surfaces

Julia L. Neff, [Angelika Kühnle](#), Hagen Söngen, Ralf Bechstein

*Institut für Physikalische Chemie, Johannes Gutenberg-Universität Mainz,
Duesbergweg 10–14, 55099 Mainz*

In this talk, we report upon long-range repulsion in molecular self-assembly on a bulk insulator surface. Using dynamic force microscopy operated under ultra-high vacuum conditions, we provide experimental evidence for long-range repulsion in molecular self-assembly of benzoic acid derivatives on calcite (10.4). We argue that this finding is not limited to the specific molecules tested, but is of generic nature. We discuss parameters that might affect a pronounced manifestation of this long-range repulsion during molecular self-assembly. These parameters need to be considered when aiming for taking advantage of rationally designing the balance between attractive short-range and repulsive long-range interactions in molecular self-assembly.

Wed-9:40-I-GRAP ● HALL-D
Surfaces of nanocarbon-based materials – chemical and structural analysis by electron spectroscopic methods
GRAP Graphene and carbon-based 2D films

Beata Lesiak-Orłowska

Institute of Physical Chemistry, Polish Academy of Sciences, Kasprzaka 44/52, 01-224 Warsaw, Poland

The wide range of applications of nanocarbon-based materials like polymers, carbon nanotubes (CNTs), graphene oxide (GO), reduced graphene oxide (RGO) decorated metal and metal oxide nanoparticles in (photo)catalysis, electronics, nanomedicine, energy storage and production, *etc.* has been recently reported. Due to these materials high biological compatibility, mechanical, thermal, dielectric and optical properties they are especially useful in nanomedicine application as specimens applied for implants, platforms for attaching nanoparticles and molecules for drug delivery, specimens designed for sensors, photothermal and photodynamic therapy. Controlling the shape, size of nanoparticles, their dielectric medium and integration with other nanostructures is of particular importance to tailor their properties. The objective is to demonstrate the capabilities of electron spectroscopic methods (X-ray photoelectron spectroscopy - XPS, (reflected) electron energy loss spectroscopy – (R)EELS) for investigating the structural and chemical properties of surfaces and interfaces of hybrid materials. Examples on selected samples like polymers, MWCNTs, GO, RGO, functionalised and decorated with nanoparticles of metal (Pd, AuPd) and metal oxide (ZrO_2) present possibilities of utilising electron spectroscopic methods as a complementary tool for a wide range of surface analyses, beside quantification and chemical bond description, *e.g.* quantification of hydrogen content (Fig. 1), quantification of an average number of layers in graphene nanostacking structures (Fig. 2), surface morphology (element coverage, concentration profile, nanoparticle size, overlayers thickness) [1-5], dielectric and optical properties (extinction coefficient, index of refraction and reflectivity) and in-depth profile analyses. Exemplary application of these methods to materials applied as catalysts in a reaction of electro-oxidation of a formic acid may reveal the reasons for their activity and stability.

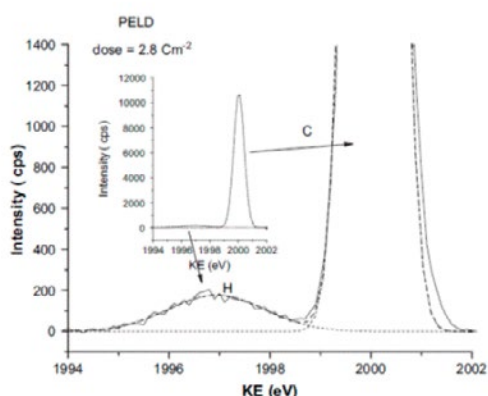


Fig. 1. Exemplary REELS spectrum recorded at electron kinetic energy (KE) of 2000 eV from a low density polyethylene (PELD) indicating components from hydrogen and carbon resulting from a recoil effect [3].

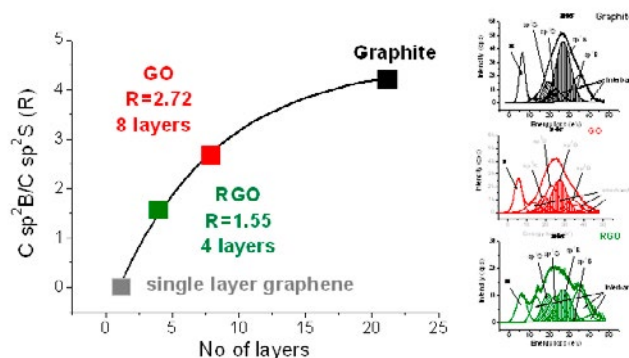


Fig. 2. Evaluation of an average number of graphene layers in stacking nanostructures of GO and RGO using the REELS spectra $\pi+\sigma$ components of $C\ sp^2$ hybridised surface and bulk plasmons [2].

References:

1. Stobinski L, Lesiak B, Kövér L, Tóth J, Biniak S, Trykowski G, Judek J (2010) Multiwall Carbon Nanotubes Purification and Oxidation by Nitric Acid Studied by the FTIR and Electron Spectroscopy Methods. *J Alloys Comp* 501:77-84.
2. Stobinski L, Lesiak B, Malolepszy A, Mazurkiewicz M, Mierzwa B, Zemek J, Jiricek P, Bielezapka I (2014) Graphene Oxide and Reduced Graphene Oxide Studied by XRD, TEM and Electron Spectroscopy Methods. *J Electron Spectrosc Rel Phenom* 195:145-154.
3. Lesiak B, Zemek J, Houdkova J (2008) Hydrogen detection and quantification at polymer surfaces investigated by elastic peak electron spectroscopy (EPES). *Polymer* 49:4127-4132.
4. Lesiak B, Mazurkiewicz M, Malolepszy A, Stobinski L, Mierzwa B, Mikolajczuk-Zychora A, Juchniewicz K, Borodzinski A, Zemek J, Jiricek P (2016) Effect of the Pd/MWCNTs anode catalysts preparation methods on their morphology and activity in direct formic acid fuel cell. *Appl Surf Sci* 387:929-937.
5. Malolepszy A, Mazurkiewicz M, Stobinski L, Lesiak B, Kövér L, Tóth J, Mierzwa B, Borodzinski A, Nitze F, Wågberg T (2015) Deactivation resistant Pd-ZrO₂ supported on multiwall carbon nanotubes catalyst for direct formic acid fuel cells. *Int J Hydrogen Energy* 40:16724-16733.

Tue-9:00-I-CORR ● HALL-B
Using surface science to understand corrosion

CORR Corrosion at atomic level

[R. Lindsay](#)¹, [M. Acres](#)¹, [H. Hussain](#)¹, [C.A. Muryn](#)², [E.A. Ahmad](#)³, [N.M. Harrison](#)³

¹ *Corrosion and Protection Centre, School of Materials, The University of Manchester, Sackville Street, Manchester, M13 9PL, UK*

² *Chemistry and Photon Science Institute, Alan Turing Building, The University of Manchester, Oxford Road, Manchester, M13 9PL, UK*

³ *Department of Chemistry, Imperial College London, Exhibition Road, London SW7 2AZ, UK*

Material degradation resulting from corrosion is an omnipresent concern. Not only is there a huge economic cost, estimated to be ~ €2 trillion per annum globally, but it can also lead to destruction of the environment, as well as the loss of life. Given this importance, there is a large ongoing effort to understand and control corrosion, with both academic and industry based researchers active in this area. Significant advances have been achieved, including the development of innovative corrosion control solutions. Atomic scale, mechanistic insight into pertinent phenomena, however, often remains elusive, hindering further progress. Such work is clearly the domain of the surface scientist, but it has not proven to be the most fashionable topic to date.

In this talk, our recent efforts to begin to understand corrosion using a surface science approach will be discussed. The primary focus will be internal oilfield corrosion, where dissolved CO₂/H₂S are the primary corrosive agents. More specifically, STM/LEED/XPS, supported by ab initio modelling, of the interaction of H₂O/CO₂/O₂/H₂S with Fe(110) will be described. STM images demonstrate that even under extremely low exposures (from an engineering perspective), significant modification of the substrate surface structure does occur, and is dependent on adsorbate identity. Intriguingly, however, for H₂O/CO₂/O₂ adsorption, XPS data indicate that the surface chemistry is apparently essentially invariant, i.e. all surfaces are simply decorated with chemisorbed O's. Data for H₂S also suggest that in the low exposure regime simple chemisorption of S occurs. In sharp contrast, much higher exposures of H₂S result in a range of surface phases, including the formation of hexagonal nano-pillars, demonstrating the complexity of the adsorption process.

Thu-16:00-I-ELAM ● HALL-C**Towards the controlled fabrication of well-defined nanostructures: a surface science approach to electron beam lithography***ELAM Electron attachment of adsorbed molecules*

Hubertus Marbach

Lehrstuhl für Physikalische Chemie II, Friedrich-Alexander Universität Erlangen-Nürnberg, Egerlandstr.3, D-91058, Erlangen, Germany

With the availability of localized electron probes, e.g., in scanning electron microscopy (SEM), it became possible to apply Focused Electron Beam Induced Processing (FEBIP) techniques for the lithographic fabrication of nanostructures.^{1,2} In Electron Beam Induced Deposition (EBID) adsorbed precursor molecules are locally dissociated by the impact of the electron beam leaving a deposit of the non-volatile dissociation products on the surface.¹ Even though EBID is applied for the repair of lithographic masks in semiconductor industry it usually lacks in the purity of the fabricated structures, e.g., the metal content from metalorganic compounds is usually rather poor. With our surface science approach to FEBIP, i.e., to perform the electron irradiation in an ultra-high vacuum (UHV) environment, we were able to overcome this hitherto existing limitation.²⁻⁶ With Fe(CO)₅ as precursor clean iron deposits were fabricated and characterized in terms of their electric⁴ and magnetic properties.⁵ It turned out that catalytic processes, like autocatalytic growth (AG) of the iron precursor can occur already at room temperature in UHV and might be actively used for the deposition of clean metallic nanostructures. Recently, we were able to expand the family of FEBIP techniques to Electron Beam Induced Surface Activation (EBISA).²⁻⁹ Thereby, in a first step, the chemical properties of the surface itself are modified via the e-beam such that it becomes active towards the decomposition of certain precursor molecules. In a second step, the surface is exposed to the precursor which decomposes at the preirradiated areas and eventually continues to grow autocatalytically. We demonstrated the feasibility of EBISA with Fe(CO)₅ for different oxide surfaces^{3,6}, expand it to porphyrin layers on various substrates^{7,8} and even to surface-anchored metal-organic frameworks (SURMOFs). It will be discussed that organic layers as substrates are suitable to reduce proximity effects and thus to increase the resolution of the written FEBIP structures. In this regard, we were able to fabricate iron line deposits on a SURMOF with width clearly below 10 nm. Notably, the EBISA process is not limited to Fe(CO)₅ but also works for Co(CO)₃NO.^{8,9} In a more vivid picture one might think of the electron beam as a pen and the precursor molecules as ink in the FEBIP process. The underlying surface chemistry, the physical processes and in particular the potential for applications of EBISA will be discussed.

References:

- [1] 1 a) van Dorp, W. F.; Hagen, C. W., *J. Appl. Phys.* 104, 081301 (2008); b) Utke, et al., *J. Vac. Sci. Technol. B*, 26, 1197 (2008); c) S. J. Randolph et al., *Crit. Rev. Solid State Mater. Sci.* 31, 55 (2006)
- [2] H. Marbach, *Applied Physics A*, 117, 987 (2014).
- [3] a) M.-M. Walz et al., *Ang. Chem. Int. Ed.*, 49, 4669 (2010) and b) *PCCP*, 13, 17333 (2011), c) *App. Phys. Lett.*, 100, 053118 (2012).
- [4] F. Porrati et al., *J. Phys. D: Appl. Phys.* 44 (2011) 425001
- [5] F. Tu et al., *Nanotechnology*, 27 (2016) 355302
- [6] F. Vollnhals et al., *J. Phys. Chem. C*, 117, 17674 (2013)
- [7] F. Vollnhals et al., *Langmuir*, 29, 12290 (2013)
- [8] M. Drost et al., *Small Methods*, DOI: 10.1002/smt.201700095 (2017)
- [9] F. Vollnhals et al., *Beilstein J Nanotech.* 5, 1175(2014)

Tue-9:00-I-ENER ● HALL-A

Single-atom Pt-cerium oxide catalysts

ENER Surfaces for energy production and harvesting

Vladimir Matolin

Charles University, Faculty of Mathematics and Physics, V Holesovickach 2, Praha 8, 18000 Czech republic

An important part of fundamental research in catalysis is based on theoretical and modelling foundations which are closely connected with studies of single-crystalline model catalyst surfaces. These so-called model catalysts are often prepared in the form of epitaxial thin films, and characterized using advanced material characterization techniques. This concept is providing the fundamental understanding and the knowledge base needed to tailor the design of new heterogeneous catalysts with improved catalytic properties. The present contribution is devoted to development of a model catalyst system of CeO₂ on a Cu(111) substrate.

Single-atom catalysts maximize the utilization of supported precious metals by exposing every single metal atom to reactants. To avoid sintering and deactivation at realistic reaction conditions, single metal atoms are stabilized by specific adsorption sites on catalyst substrates. We show by combining photoelectron spectroscopy, scanning tunneling microscopy and density functional theory calculations that Pt single atoms on ceria are stabilized by the most ubiquitous defects on solid surfaces—monoatomic step edges. Pt segregation at steps leads to stable dispersions of single Pt²⁺ ions in planar PtO₄ moieties incorporating excess O atoms and contributing to oxygen storage capacity of ceria [1,2]. We experimentally control the step density on our samples, to maximize the coverage of monodispersed Pt²⁺ and demonstrate that step engineering and step decoration represent effective strategies for understanding and design of new single-atom catalysts.

We have demonstrated the promising properties of the Pt-CeO₂ thin films as electrocatalysts in proton exchange membrane fuel-cell technology, specifically their superior noble metal efficiency. The high performance was shown for the anode catalyst with 2 micro g Pt/cm² which contained Pt²⁺ ions only. The catalyst with so small Pt loading can be considered as “almost Pt free” [3].

References:

- [1] Dvorak, F; Camellone, MF; Tovt, A; Tran, N-D; Negreiros, FR; Vorokhta, M; Skala, T; Matolinova, I; Myslivecek, J; Matolin, V; Fabris, S, „Creating single-atom Pt-ceria catalysts by surface step decoration“, Nat. Commun., 7 (Feb): Art. No. 10801, 2016.
- [2] Bruix, A; Lykhach, Y; Matolinova, I; Neitzel, A; Skala, T; Tsud, N; Vorokhta, M; Stetsovych, V; Sevcikova, K; Myslivecek, J; Fiala, R; Vaclavu, M; Prince, KC; Bruyere, S; Potin, V; Illas, F; Matolin, V; Libuda, J; Neyman, KM, „Maximum Noble-Metal Efficiency in Catalytic Materials: Atomically Dispersed Surface Platinum“, Angew. Chem.-Int. Edit., 53: 10525–10530, 2014
- [3] Fiala, R; Figueroba, A; Bruix, A; Vaclavu, M; Rednyk, A; Khalakhan, I; Vorokhta, M; Lavkova, J; Illas, F; Potin, V; Matolinova, I; Neyman, KM; Matolin, V, “High efficiency of Pt²⁺- CeO₂ novel thin film catalyst as anode for proton exchange membrane fuel cells”, Appl. Catal. B-Environ., 197: 262–270, 2016.

Thu-9:00-I-SEMI ● HALL-D**Electronic properties of ultra sharp dopant profiles in Silicon***SEMI Semiconductor surfaces and ultrathin layers*

Jill A. Miwa

Department of Physics & Astronomy, Aarhus University, Aarhus, Denmark

Atomically precise lithography of phosphorus δ -layers in silicon (Si:P δ -layers) has led to the fabrication of atomic-scale devices including, the world's narrowest conducting wire [1] and the single-atom transistor [2]. These Si:P δ -layers are comprised of an ultra-sharp, ultra-dense P dopant layer buried beneath a crystalline Si surface, and exhibit quantum properties. Motivated by the successful fabrication of atomic-scale devices, the composition and structure of Si:P δ -layers have been studied down to the atomic limit by both secondary ion mass spectrometry and scanning tunnelling microscopy [3], and their band structure thoroughly investigated by different theoretical methods [4]. The calculations predict that confinement of the P dopants to a single atomic plane beneath the Si surface leads to a lowering and discretization of the conduction band (CB) resulting in two parabolic-like states dispersing across the Fermi level, referred to as 1Γ and 2Γ . These states give the Si:P δ -layers metallic character, and are responsible for the transport properties observed in atomic-scale devices. Angle-resolved photoemission spectroscopy (ARPES) measurements can provide direct access to the electronic properties of the Si:P δ -layers [5]. Our ARPES measurements of the Si:P δ -layers reveal a surprising result: a third parabolic-like state at the Fermi level. The origin of this third state is related to an extreme underestimation of the theoretical strength of the material dielectric constant. This result allows us to reconcile an apparently contradicting picture of the physics of Si:P δ -layers. We are able to make a crucial revision of the electronic structure of these systems, and provide a more accurate description of the states involved in the transport properties of atomic-scale devices.

References:

- [1] B. Weber, S. Mahapatra, H. Ryu, S. Lee, A. Fuhrer, T.C.G. Reusch, D.L. Thompson, W.C.T. Lee, G. Klimeck, L.C.L. Hollenberg, M.Y. Simmons, *Science*, 335, 64 (2012).
- [2] M. Fuechsle, J.A. Miwa, S. Mahapatra, H. Ryu, S. Lee, O. Warschkow, L.C.L. Hollenberg, G. Klimeck, M.Y. Simmons, *Nat. Nano.* 7, 242 (2012)
- [3] J.G. Keizer, S.R. McKibbin, M.Y. Simmons, *ACS Nano*, 9, 7080 (2015)
- [4] D.W. Drumm, A. Budi, M.C. Per, S.P. Russo, L.C.L. Hollenberg, *Nanoscale Res. Letts.* 8, 111 (2013)
- [5] J.A. Miwa, Ph. Hofmann, M.Y. Simmons, J.W. Wells, *PRL*, 110, 136801 (2013)

Tue-15:00-I-BIMS ● HALL-A

Efficient computational engineering of bimetallic nanocrystals

BIMS Bimetallic surfaces and alloy nanocrystals

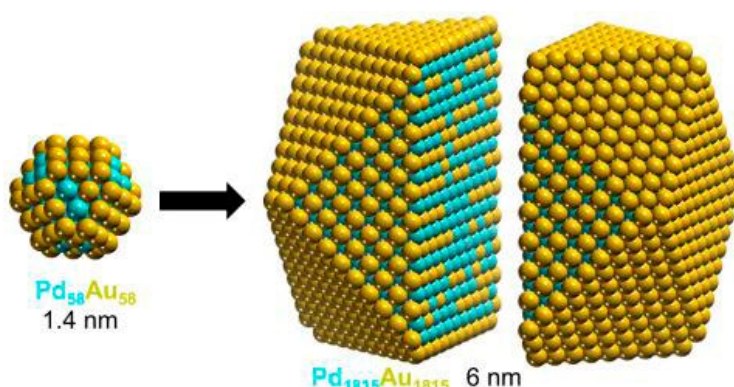
Konstantin M. Neyman

Departament de Ciència dels Materials i Química Física and Institut de Química Teòrica i Computacional, Universitat de Barcelona, Barcelona 08028, Spain ICREA (Catalan Institution for Research and Advanced Studies), Barcelona 08010, Spain

Metal nanoparticles are key components of many functional materials, including catalysts. However, applications of monometallic particles are limited by often insufficiently versatile properties of them. Properties of mixed-metal nanoparticles (nanoalloys) can be tuned for a given application much easier. Yet, it is very laborious to determine the atomically resolved composition (chemical ordering) in nanoalloys, which is required for rationalizing their reactivity and other functionalities.

We developed a method to optimize chemical ordering in crystalline nanoalloys using density functional calculations [1,2], which is applicable to various combinations of transition metals with each other and with s,p-elements [1-6]. The method allows one to predict energetically stable atomically resolved structures of bimetallic nanocrystals, which can be manufactured. I will outline the method and illustrate its applications to technologically important archetypal nanoalloys of Pd [1,2], Pt [3-5] and Ni [6].

Our new method enables generating databases of structures and energies of bimetallic nanoalloys spanning the Periodic Table. Its simplicity and reliability allows to provide researchers with unique opportunity to efficiently perform simulations of various nanoalloys with thousands of atoms. Applications of the method can not only radically accelerate design of tailor-made nanoalloys but also deepen the general understanding of chemical bonding in nanoalloys.



References:

- [1] S.M. Kozlov, G. Kovács, R. Ferrando, K.M. Neyman. How to determine accurate chemical ordering in several nanometer large bimetallic crystallites from electronic structure calculations. *Chemical Science* 6 (2015) 3868
- [2] G. Kovács, S.M. Kozlov, K.M. Neyman. Versatile optimization of chemical ordering in bimetallic nanoparticles. *J. Phys. Chem. C* 121 (2017), doi: 10.1021/acs.jpcc.6b11923
- [3] G. Kovács, S.M. Kozlov, I. Matolínová, M. Vorokhta, V. Matolín, K.M. Neyman. Revealing chemical ordering in Pt-Co nanoparticles using electronic structure calculations and X-ray photoelectron spectroscopy. *Phys. Chem. Chem. Phys.* 17 (2015) 28298
- [4] M. Vorokhta, I. Khalakhan, M. Václavů, G. Kovács, S.M. Kozlov, P. Kúš, T. Skála, N. Tsud, J. Lavková, V. Potin, I. Matolínová, K.M. Neyman, V. Matolín. Surface composition of magnetron sputtered Pt-Co thin film catalyst for proton exchange membrane fuel cells. *Appl. Surf. Sci.* 365 (2016) 245
- [5] A. Neitzel, G. Kovács, Y. Lykhach, S.M. Kozlov, N. Tsud, T. Skála, M. Vorokhta, V. Matolín, K.M. Neyman, J. Libuda. Atomic ordering and Sn segregation in Pt-Sn nanoalloys supported on CeO₂ thin films. *Top. Catal.* (2017), doi: 10.1007/s11244-016-0709-5
- [6] A. Wolfbeisser, G. Kovács, S.M. Kozlov, K. Föttinger, J. Bernardi, B. Klötzer, K.M. Neyman, G. Rupprechter. Surface composition changes of CuNi-ZrO₂ catalysts during methane decomposition. *Catal. Today* 283 (2017) 134

Tue-14:00-I-ELCH ● HALL-D

Electrochemical formation of nanostructures monitored by EC-STM and CV

ELCH Electrochemistry at surfaces

B. Madry¹, M. Nowicki¹, K. Wandelt¹ Institute of Experimental Physics, University of Wrocław, Pl. M. Borna 9, 50-204 Wrocław, Poland;² Institute of Physical and Theoretical Chemistry, University of Bonn, Wegelerstr. 12, 53115 Bonn, Germany

The selforganization of molecules at metal/electrolyte and, in particular, metal-on-metal/electrolyte interfaces is a scientifically and technologically interesting approach to form ordered molecular structures under controlled electrochemical parameters. We have used scanning tunneling microscopy (STM) and cyclic voltammetry (CV) to investigate *in-situ* the self-assembly of sulfate and redox-active Tetra (N-methyl-1-pyridyl) porphyrins (TMPyP) on Cu layers deposited on Au(111). The STM images enabled the characterization of the molecular overlayer on under- and over-potential deposited Cu layers with submolecular resolution. Cu/Au(111) with adsorbed sulfate anions exhibits different long range ordered structures, which depend on the local coverage of Cu layer governed by the electrode potential [1-3]. The first Cu layer grows stepwise, first up to 2/3ML [1] and then to a complete Cu monolayer (1ML) covered by a $(\sqrt{3}\times\sqrt{3})R30^\circ$ - and $(\sqrt{3}\times\sqrt{7})R19^\circ$ -sulfate structure [2,3], respectively (Fig.1 a,b). A sulfate induced Moiré superstructure is visible on multilayer Cu deposits (Fig. 1c) similar but not identical to that observed on bulk Cu(111) [2]. On the negatively polarized electrode the coadsorption of copper cations, sulfate anions, water, and/or hydronium cations induces a “charge inversion” effect within the interface layers. This serves as a substrate for adsorption of large solvated organic TMPyP cations. STM images recorded within the submonolayer Cu coverage (2/3ML) indicate no porphyrin adsorption. Single TMPyP molecules (Fig. 2) as well as an ordered molecular layer, exhibiting domain structure, were imaged after the formation of the complete pseudomorphic Cu monolayer. At multilayer Cu coverages randomly distributed porphyrin molecules were observed. This suggests a reduced mobility of TMPyP associated with the formation of cation-anion pairs. The change from “drastic” to “moderate” tunneling conditions leads to the removal of porphyrin species from the sulfate/copper coadsorption layer and *vice-versa*. The charge transfer within the interface is discussed. The results are compared to EC-STM and CV data obtained for porphyrins deposited on Cu(111) [4].

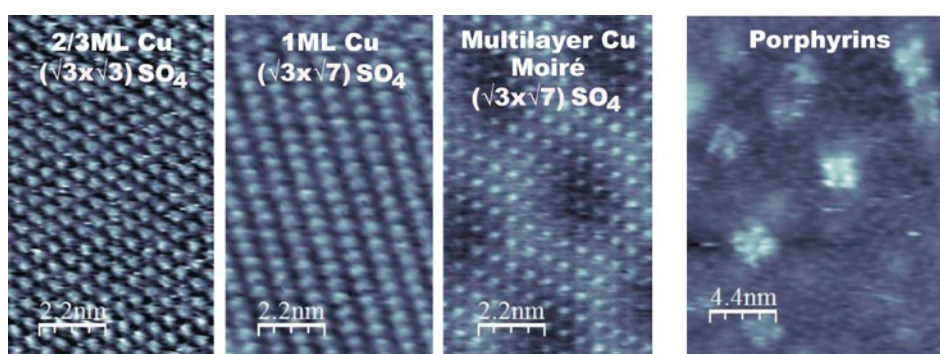


Fig.1a-c

Fig.2

References:

- [1] Z. Shi, S. Wu, J. Lipkowski, *Electrochimica Acta* 40 (1995) 9.
- [2] B. Madry, K. Wandelt, M. Nowicki, *Surface Science* 637-638 (2015) 77.
- [3] B. Madry, K. Wandelt, M. Nowicki, *Electrochimica Acta* 217 (2016) 249.
- [4] N.T.M. Hai, K. Wandelt, P. Broekmann, *Journal of Physical Chemistry C* 112 (2008) 10176.

Thu-9:40-I-CATH ● HALL-B

Spectroscopy and microscopy of catalytic processes on well-defined surfaces: from UHV to operando conditions

CATH Catalytic 2D-model studies under high pressures

Günther Rupprechter, Christoph Rameshan, Karin Föttinger, Yuri Suchorski

Institute of Materials Chemistry, Technische Universität Wien, 1060 Vienna, Austria

Our group's philosophy is to study catalytic surface reactions on heterogeneous catalysts *via a two-fold approach*, employing both *surface science based planar model catalysts* as well as *industrial-grade catalysts* [1]. For both, the focus is on examining *active functioning catalysts* under *operando* conditions, at (near) atmospheric pressure and at elevated temperature.

In particular for ultrahigh vacuum (UHV) based model catalysts that has been a challenge, requiring application of *in situ surface spectroscopy*, such as sum frequency generation (SFG) laser spectroscopy, polarization-modulation infrared reflection absorption spectroscopy (PM-IRAS) and near atmospheric pressure x-ray photoelectron spectroscopy (NAP-XPS). To image ("see") ongoing surface reactions by *in situ surface microscopy*, photoemission electron microscopy (PEEM) was applied to polycrystalline samples [2]. For technological catalysts, analogous *operando* studies were performed by Fourier transform infrared spectroscopy (FTIR), x-ray absorption spectroscopy (XAS), NAP-XPS, and X-ray diffraction (XRD) [3].

This two-fold approach may yield a glimpse on the catalytically relevant atomic and electronic surface structure of catalysts, as well as of molecular details that steer reaction activity and, even more important, reaction selectivity. Among the systems studied are

- i) CO oxidation and $\text{H}_2/\text{CO}/\text{O}_2$ reaction (PROX) on Co_3O_4 and CoO thin films, grown in UHV on Ir(100), and on commercial cobalt oxides, and
- ii) CO oxidation on (quasi) unsupported and oxide supported noble metals.

For the cobalt oxide catalysts the *in situ* (operando) studies revealed the reaction-induced formation of the active phase and the presence of intermediates/spectators (adsorbed CO, carbon, carbonates, hydroxyls) [4]. We have also directed substantial efforts towards surface microscopy, utilizing PEEM to obtain locally-resolved kinetic information on CO oxidation on polycrystalline noble metal foil and on surfaces modified by sputtering, oxidation or "powders" of a second noble metal [5]. Despite the micrometre resolution limit, PEEM provided valuable information on the kinetics of specific surface terminations and on long-ranging metal-support interactions.

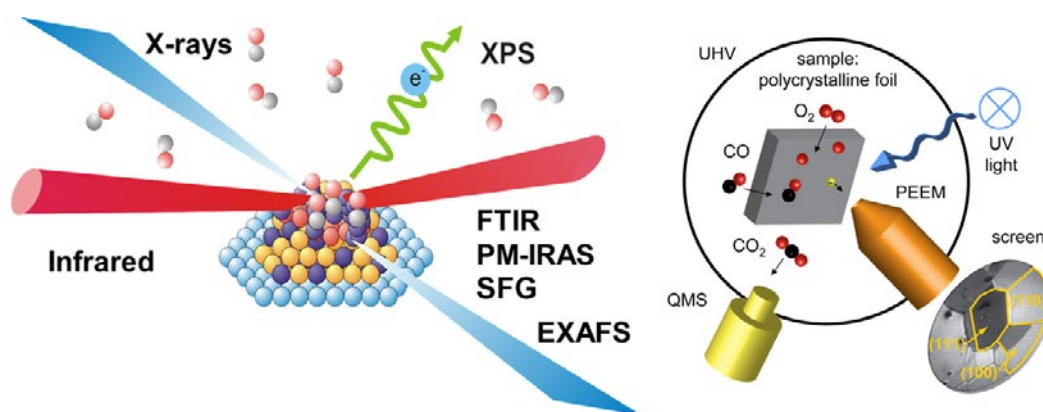


Figure 1 Schematics of spectroscopic and microscopic studies of functioning catalysts [1-3].

Supported by the Austrian Science Fund (FWF) via SFB-F45 FOXSI, DK+ Solids4Fun, ComCat and DryRef.

References:

- [1] G. Rupprechter, Textbook on Surface and Interface Science, K. Wandelt (Editor), Wiley-VCH, Weinheim, 2016, 459-527 (ISBN: 978-3-527-41158-0).
- [2] Y. Suchorski, G. Rupprechter, Surface Science 643, 52 (2016).
- [3] K. Föttinger, G. Rupprechter, Accounts of Chemical Research, 47 (2014) 3071–3079.
- [4] L. Lukashuk; K. Föttinger; E. Kolar; C. Rameshan; D. Teschner; M. Hävecker; A. Knop-Gericke; N. Yigit; H. Li; E. McDermott; M. Stöger-Pollach; G. Rupprechter, Journal of Catalysis 344,1 (2016).
- [5] M. Datler, I. Bepalov, G. Rupprechter, Y. Suchorski, Catalysis Letters 145, 1120 (2015).

Thu-15:00-I-SEMI ● HALL-D

(Ga,Mn)As as a canonical dilute ferromagnetic semiconductor – electronic structure, surface effects & magnetism in low dimensional structures

SEMI Semiconductor surfaces and ultrathin layers

Janusz Sadowski^{1,2,3}

¹ Institute of Physics, Polish Academy of Sciences, Warszawa, Poland;

² Linnaeus University, Kalmar Sweden;

³ MAX IV laboratory, Lund University, Sweden

After over two decades of extensive research activity (Ga,Mn)As - a solid solution of GaAs - the common semiconductor used in nowadays optoelectronic structure, and Mn - a magnetic transition metal has established its position of a canonical dilute ferromagnetic semiconductor (DFS). In comparison to other DFS materials such as (Pb,Sn,Mn)Te, (Ga,Mn)N, (Ge,Mn)Te; GaMnAs has a remarkably high ferromagnetic phase transition temperature (T_c) - close to 200 K and exhibits a number of very interesting magnetic properties, e.g. anomalous and planar Hall effect, voltage and pressure controlled ferromagnetism etc., which in many cases inspired a search of similar phenomena in conventional metallic ferromagnets. However in spite of an extensive research activity, a fundamental issue related to the origin of ferromagnetic phase in (Ga,Mn)As, namely the presence/absence of Mn-related impurity band (IB) in the GaAs host electronic structure has remained controversial/unresolved until recently. There have been a lot of contradicting literature reports supporting either the presence or the absence of IB in Mn-doped GaAs. We believe that our recent angle resolved photoemission spectroscopy (ARPES) experiments performed for clean samples (either with on-line MBE system vacuum connected to the ARPRES station, or with the samples transferred to ARPES setup in a vacuum suitcase) have ultimately clarified this situation in favor of the *absence* of IB in (Ga,Mn)As. In the second part of the talk the interesting magnetic and transport properties of low dimensional (2D and 1D) structures based on (Ga,Mn)As will be reviewed, with special focus on hexagonal wurtzite phase, in which this compound has not been investigated until very recently.

Wed-9:00-I-OXID ● HALL-C**2D ternary oxide layers: new paradigmas of structure and stoichiometry***OXID Oxide surfaces and ultrathin oxide films*

Svetlozar Surnev

Surface and Interface Physics, Institute of Physics, Karl-Franzens University Graz, A-8010 Graz, Austria

Two-dimensional (2D) oxide materials have tremendous potential in fundamental research and cutting edge technologies owing to their outstanding physical and chemical properties, which makes them excellent candidates for a wide range of applications including power harvesting, hydrogen storage, fuel cells, gas sensors, advanced electronic and spintronic devices, and nanocatalysis. To gain a fundamental understanding of the novel properties, afforded by the reduced dimension of oxide nanostructures, structurally well-defined model systems have been utilized, typically in the form of ultrathin oxide films epitaxially grown on single crystal metal surfaces. To date, most of the studies have been focussed on binary 2D oxides, but the increased interest in more complex oxide materials, such as ternary or multicomponent oxides with a broader range of functionalities, requires an adequate understanding of their properties at the nanoscale, which is still scarce. One reason for this is that the preparation of ternary oxide nanolayers with well-defined structure and stoichiometry is more challenging than for binary oxides, which requires the development of new fabrication strategies, where suitable thermodynamic and kinetic parameters have to be optimized in a narrow multi-parameter space to obtain structures with desired stoichiometry and 2D morphology. Moreover, the elucidation of their structural properties at the atomic level is experimentally and theoretically more demanding than for the binary oxides.

Here, I review the advance of fabrication of *2D ternary oxide layers* supported on single crystal metal surfaces and the atomic level understanding of their atomic structure and stoichiometry with the help of state-of-art surface science techniques in combination with density functional theory calculations. Specifically, new oxide preparation approaches for *metal tungstates* (MWOx), utilizing the on-surface solid-state chemical reaction between well-defined 2D binary metal oxide and tungsten oxide phases, are presented. The successful implementation of these fabrication methods is demonstrated for prototypical 2D ternary oxide layers, with different W-O coordination spheres. Depending on the oxygen chemical potential three different types of MWOx nanolayers form, where the W atoms exhibit low (3-fold) [1,2], intermediate (4-fold) [3] and high (up to 6-fold) [2,4] oxygen coordination. Structure models of 2D MWOx phases are discussed in the light of new building architecture concepts with no analogues in the bulk.

References:

- [1] S. Pomp, D. Kuhness, G. Barcaro, L. Sementa, V. Mankad, A. Fortunelli, M. Sterrer, F.P. Netzer, S. Surnev, *J. Phys. Chem. C* 120 (2016) 7629.
- [2] N. Doudin, D. Kuhness, M. Blatnik, F.P. Netzer, S. Surnev, *J. Phys.: Condens. Matter* (2017), in press.
- [3] M. Denk, D. Kuhness, M. Wagner, S. Surnev, F.R. Negreiros, L. Sementa, G. Barcaro, I. Vobornik, A. Fortunelli, F.P. Netzer, *ACS Nano* 8 (2014) 3947.
- [4] N. Doudin, S. Pomp, M. Blatnik, R. Resel, M. Vorokhta, J. Goniakowski, C. Noguera, F. P. Netzer, S. Surnev, *Surf. Sci.* 659 (2017) 20

Mon-14:00-I-NAEX ● HALL-D

Investigation of ionic liquid interfaces using time- and position-resolved XPS

NAEX Novel advancement of experimental methods

Sefik Suzer

Bilkent University, Chemistry Department, 06800 Ankara, Turkey

X-ray photoelectron spectroscopy (XPS), a chemical analysis tool, is utilized for investigation of charge screening at the interfaces of devices containing ionic liquids in between metal electrodes configured in different geometries. The first device is fabricated on a porous polymer surface which is infused with an ionic liquid (IL). The IL provides a sheet of conducting layer to the otherwise insulating polymer film, and enables monitoring charging and screening dynamics at the polymer + IL / air interface in a laterally resolved fashion across the electrodes. Time-resolved measurements are also implemented by recording several peaks of the IL, while imposing 10^{-3} to 10^{+3} Hz square-wave-pulses (SQW) across the electrodes in a source-drain geometry. Variations in the binding energy of the measured peaks (Au4f, C1s, N1s and F1s) reflects directly the local electrical potential, and allow us visualize screening of the otherwise built-in local voltage drop on and across the electrodes. In the second geometry the IL in the form of liquid drop is the conducting medium between the electrodes, where both electrochemical reaction products are monitored with XPS, in addition to tapping into the charging behavior of the interfaces. Impact of our findings with the presented structures and variants of XPS measurements on understanding of various electrochemical concepts will be discussed.

**This work is partially supported by TUBITAK through Grant No. 215Z534*

Thu-15:00-I-CATH ● HALL-A

The mechanism of CO₂ reduction over Pd/Al₂O₃: a combined SSITKA and operando FTIR investigation

CATH Catalytic 2D-model studies under high pressures

Janos Szanyi, Xiang Wang, Hui Shi

Institute for Integrated Catalysis, Pacific Northwest National Laboratory, RICHLAND, WA 99352, USA

Understanding the critical steps involved in the heterogeneous catalytic CO₂ reduction has attracted a lot of attention recently. In order to fully understand the mechanism of this reaction the determination of both the rate-determining steps and reaction intermediates are vital. Steady-State Isotopic Transient Kinetic Analysis (SSITKA) is one of the most powerful techniques used to investigate the elementary steps under steady-state reaction conditions. This technique provides valuable information on mean resident lifetime of surface intermediates, surface concentrations of adsorbed reactant species and an upper bound of the turnover frequency. Coupling SSITKA with *operando*-FTIR spectroscopy allows us to discriminate between active and spectator species present on the catalytic surface under steady state reaction conditions. In the present work *operando* SSITKA experiments coupled with transmission FTIR, mass spectrometry (MS) and gas chromatography (GC) were performed to probe both the chemical nature and kinetics of reactive intermediates over a Pd-Al₂O₃ catalysts and provide a clear mechanistic picture of the CO₂ hydrogenation reaction by revealing the rate-determining steps for CH₄ and CO production. Figure 1 shows normalized real-time signals for the decay and increase of methane (a) and carbon-monoxide (b) in the effluent at 533 K reaction temperature after the feed gas was switched at 0 s from CO₂/H₂/Ar mixture to ¹³CO₂/H₂ mixture. With increasing temperature, the decay of CH₄ and CO get faster. By integration under the decay curves, the mean surface-residence times (τ_{CH_4} and τ_{CO}), the abundance of adsorbed surface intermediates leading to CH₄ and CO products (θ_{CH_4} and θ_{CO}) at 533-573 K were calculated. At low temperature, CO₂ methanation is slower than the reverse water-gas shift reaction, but became faster as the temperature was increased over 563 K. The similar apparent activation energies obtained for the hydrogenation of adsorbed CO and for the formation of CH₄ indicates that the hydrogenation of CO is the rate-determining step during the CO₂ methanation reaction. Moreover, the similar apparent activation energies estimated for the consumption of adsorbed formates (FTIR) and for the formation of CO (MS), indicates that the H-assisted decomposition of formates is the rate determining step in the reverse water gas shift reaction. The rate-determining step for CO formation is the conversion of adsorbed formate, while that for CH₄ formation is the hydrogenation of adsorbed carbonyl. The balance of the hydrogenation kinetics between adsorbed formates and carbonyls governs the selectivities to CH₄ and CO. We applied this knowledge to design catalysts and achieved high selectivities to desired products.

Mon-15:00-I-BAND ● HALL-E

Electronic structure of quantum materials and perspectives with ultra-high brilliant sources

BAND Band structure of solid surfaces

Amina Taleb-Ibrahimi

UR1-CNRS/ Synchrotron SOLEIL, L'Orme des Merisiers, Saint-Aubin, 91192 Gif sur Yvette, France

For tomorrow's electronics new materials are attracting the scientific community. The new materials of the moment are quantum materials which exhibit rather unusual states: Dirac materials, topological states, Weyl semimetals...

The applications of these unusual states are yet to come but it is predicted that they will be as revolutionary as lasers or computer chips a hundred years ago. They could be the basis for a form of information processing and possibly the future quantum computer.

The relevance of the properties of these states in these systems is intimately linked to the quality of the materials. So this has pushed the community to investigate new methods of fabrication of these materials and correlate the structure quality and the physical properties as electronic, magnetic, transport and others.

In this presentation, I would like to give an overview of my research work performed the last 3-4 years. This work concerns mainly the investigation of 2D materials as graphene and semiconductor thin films with topological order. Together with other surface science techniques, angular resolved photoemission using synchrotron radiation has given a boost to the field. I will try to give a vision of the future capabilities of ultrabright photon sources to the technique and to the science in this domain.

Mon-14:00-I-CATL ● HALL-A

Spectroscopic characterization of reaction pathways over a Pd-Cu(111) single-atom alloy

CATL Catalytic 2D-model studies at low pressures

Michael Trenary, Christopher M. Kruppe, Joel D. Krooswyk

Department of Chemistry, University of Illinois at Chicago

Low coverages of catalytically active metals deposited onto less active metal surfaces can form single atom alloys (SAAs), which often display unique catalytic properties. Such alloys are particularly attractive for selective hydrogenation reactions. It is therefore of interest to probe the surface structure and chemistry of such alloys in the presence of gas phase reactants. We have used polarization dependent reflection absorption infrared spectroscopy (PD-RAIRS) to monitor the *in-situ* hydrogenation of acetylene to ethylene over a Pd/Cu(111) SAA surface. The coverage and morphology of the deposited Pd is characterized with Auger spectroscopy (AES), temperature programmed desorption (TPD) of H₂ and CO, and PD-RAIRS of CO. After exposing clean Cu(111) and Cu(111) with various Pd coverages to 10 L of CO at 100 K, the RAIR spectra show that the surface is largely unchanged by the presence of less than 0.5 ML of Pd. In the presence of 1×10^{-2} Torr of CO at 300 K, significant CO coverages are only achieved when Pd is present on the surface. The Pd coverage determined from CO peak areas obtained with RAIRS yields a value lower by about a factor of two than the Pd coverage obtained with AES. This is attributed to the presence of both surface and subsurface Pd, with only the former detectable by RAIRS of CO, but both detectable with AES. Surface species and gas phase products of C₂H₂ hydrogenation are monitored between 180 and 500 K on clean Cu(111) and Pd/Cu(111). With a total pressure of 1 Torr and a C₂H₂:H₂ ratio of 1:100, annealing a SAA-Pd/Cu(111) surface to 360 K results in complete conversion of all gas phase C₂H₂ to gas phase ethylene (C₂H₄), without producing any gas phase ethane (C₂H₆). The hydrogenation reaction is accompanied by acetylene coupling reactions that occur both on clean Cu(111) and on Pd-Cu(111).

Thu-14:00-I-ENER ● HALL-B

**Information and energy storage in magnetic skyrmions and helices:
role of oscillating Dzyaloshinskii-Moriya interactions**

ENER Surfaces for energy production and harvesting

Elena Y. Vedmedenko

University of Hamburg, Jungiusstr. 11, 20355 Hamburg, Germany

One of the most exciting recent developments in nanomagnetism concerns topologically non-trivial magnetic configurations acting as quasiparticles. Among these quasiparticle excitations are three- or two-dimensional magnetic skyrmions [1], one-dimensional topological solitons [2-4] and zero-dimensional monopoles, which can also be bound by one-dimensional Dirac strings [5]. Once created, magnetic quasiparticles can only be erased with effort from a surface [1-5]. This makes them valuable for the application in future data storage devices but also poses fundamental questions on the microscopic reasons for the topological stability. Here, analytical and numerical analyses are used to study the dynamics and life-times of skyrmions [1], topological solitons [2-4] and bound monopoles [5] in continuous and structured magnetic thin films. Additional attention is paid to the interaction between magnetic quasiparticles [5]. It is shown that the main reason for the enhanced stability is a dynamical behavior of an energy barrier rather than its height [1,2,5]. Interactions between quasiparticles, e.g. in spin-ices, are defined by the characteristic tension-to-mass ratio proportional to the fine structure constant and lattice parameters [5]. On the basis of this analysis, a theoretical concept of the energy storage at the nanoscale is proposed [2,5] and compared with recent experiments. A mesoscopic experimental illustration of the principle of the energy storage will be shown.

References:

- [1] J. Hagemeyer, N. Romming, K. von Bergmann, E. Y. Vedmedenko, and R. Wiesendanger, "Stability of single skyrmionic bits", *Nature Comms.* 6, 9455 (2015).
- [2] E. Y. Vedmedenko and D. Altwein, "Topologically Protected Magnetic Helix for All-Spin-Based Applications", *Phys. Rev. Lett.* 112, 017206 (2014).
- [3] L. Zhou, J. Wiebe, S. Lounis, E.Y. Vedmedenko, F. Meier, S. Blügel, P. H. Dederichs and R. Wiesendanger, "Strength and directionality of surface Ruderman–Kittel–Kasuya–Yosida interaction mapped on the atomic scale", *Nature Phys.* 6, 187 (2010).
- [4] M. Menzel, Y. Mokrousov, R. Wieser, J. E. Bickel, E. Y. Vedmedenko, S. Blügel, S. Heinze, K. von Bergmann, A. Kubetzka, and R. Wiesendanger, "Information Transfer by Vector Spin Chirality in Finite Magnetic Chains", *Phys. Rev. Lett.* 108, 197204 (2012).
- [5] E. Y. Vedmedenko, "Dynamics of Bound Monopoles in Artificial Spin Ice: How to Store Energy in Dirac Strings", *Phys. Rev. Lett.* 116, 077202 (2016).

Mon-14:00-I-SAMA ● HALL-C

**Manipulation of individual atoms/molecules on surfaces of 2D atomic crystals:
from Kondo effect to reversible single spin control**

SAMA Structural analysis and manipulation on atomic scale

Hong-Jun Gao, [Yeliang Wang](#)

Institute of Physics & University of Chinese Academy of Sciences, China

Control over charge and spin states at the single molecule level is crucial not only for a fundamental understanding of charge and spin interactions but also represents a prerequisite for development of molecular electronics and spintronics. While charge manipulation has been demonstrated by gas adsorption and atomic manipulation, the reversible control of a single spin of an atom or a molecule has been challenging. In this lecture, I will present a demonstration about a robust and reversible spin control of a single magnetic metal-phthalocyanine molecule via attachment and detachment of a hydrogen atom, with manifestation of switching of Kondo resonance. Low-temperature atomically resolved scanning tunneling microscopy was employed. Using density functional theory calculations, the spin control mechanism was revealed, by which the reduction of spin density is driven by charge redistribution within magnetic 3d orbitals rather than a change of the total number of electrons. This process allows spin manipulation at the single molecule level, even within a close-packed molecular array, without concern of molecular spin exchange interaction. Moreover, I will talk about 2D templates of PtSe₂ and CuSe recently developed for selective self-assembly of molecules nanoclusters, as well as for the functionalization of the same substrate with two different species. This work opens up a new opportunity for quantum information recording and storage at the ultimate molecular limit.

In collaboration with S.X. Du, Y.L. Wang, L.W. Liu, K. Yang, L.L. Jiang, Y. Shao, J.C. Lu, J.B. Pan et al. from Institute of Physics, CAS; X. Lin, Y.Y. Zhang from University of Chinese Academy of Sciences, CAS; S. Pantelides from Vanderbilt University, US; A. Castro Neto from University of Singapore; M. Ouyang from Maryland University, US; and Sokrates Pantelides from Vanderbilt University.

References:

- [1] L. Gao, S.X. Du, H.-J. Gao et al. *Phys. Rev. Lett.* 99, 106402 (2007).
- [2] L.W. Liu, K. Yang, Y.H. Jiang, S.X. Du, and H.-J. Gao et al. *Scientific Report* 3, 1210 (2013).
- [3] L.W. Liu, S.X. Du, and H.-J. Gao et al. *Phys. Rev. Lett.* 99, 106402 (2015).
- [4] L.L. Jiang, H.-J. Gao, and F. Wang et al. *Nature Materials* 15, 840 (2016).
- [5] X. Lin, and H.-J. Gao et al. *Nature Materials* (2017) (In press).

Thu-9:00-I-LASE ● HALL-E

Ultrafast magnetization dynamics and its signature in the transient electronic structure

LASE Laser pulses for surface electron dynamics

Martin Weinelt

Fachbereich Physik, Freie Universität Berlin, Arnimallee 14, 14195 Berlin, Germany

The past years have witnessed strongly increasing efforts to push solid-state spin dynamics and magnetism into the ultrafast realm, that is, to time scales below 10 ps. This goal is all but straightforward. First, the ultrafast regime coincides with the time scales set by the strengths of two fundamental spin interactions, exchange and spin-orbit coupling. Second, many relaxation phenomena of electrons and phonons occur on same, ultrafast time scales, *e.g.*, electron-electron thermalization and electron-phonon equilibration. Still, fundamental questions need to be addressed: On which timescale do the band structure and spin polarization of a ferromagnet change after femtosecond laser excitation and how do they affect the magnetization dynamics? To answer these questions we perform time-, spin-, and angle-resolved photoemission experiments with optical laser pulses and higher-order harmonic radiation.

We have studied ultrafast demagnetization in thin films of the local-moment ferromagnets Gadolinium and Terbium, prepared as epitaxial films on a W(110) substrate. In the lanthanides equilibration of the laser excited state involves more than one timescale, because optical transitions occur in the valence band but the magnetic moment is dominated by the localized $4f$ electrons. Following excitation by fs near-infrared pulses, we directly map the transient exchange splitting of the Gd and Tb valence bands near the center of the bulk Brillouin zone. Simultaneously we record the magnetic linear dichroism of the $4f$ photoemission line. This allows us to compare the magnetization dynamics of $4f$ core and $5d6s$ valence electrons in one measurement [1]. Varying starting temperature (40, 100, 200 K) and photon energy of the pump pulse (0.95 vs. 1.55 eV) we observe distinct changes in magnetization dynamics on the ultrafast timescale. demagnetization [3]. To probe the spin polarization, we utilized the unique magnetic properties of the $5d_{z^2}$ surface states on Gd(0001) and Tb(0001), which mirror the magnetism of the bulk. In spin- and time-resolved photoemission we confirm that the exchange splitting of the Gd and Tb surface state follows that of the $5d6s$ valence bands (black open circles). In contrast, the spin polarization of the surface state appears to reflect the magnetization of the $4f$ core levels [2]. Interestingly, the spin polarization decays with $\tau \sim 15$ ps in Gd, while it exhibits sub-picosecond dynamics in Tb ($\tau \sim 0.4$ ps). These results question the interpretation of XMCD data, which show comparable ultrafast decay constants of $\tau \sim 0.8$ ps in both Gd and Tb.

References:

- [1] B. Frietsch, J. Bowlan, R. Carley, M. Teichmann, S. Wienholdt, D. Hinzke, and U. Nowak, K. Carva, P. M. Oppeneer, and M. Weinelt, *Nature Communications* 6, 8262 (2015)
- [2] B. Andres, M. Christ, C. Gahl, J. Kirschner, M. Wietstruk, and M. Weinelt, *Phys. Rev. Lett.* 115, 207404 (2015)
- [3] M. Wietstruk, A. Melnikov, C. Stamm, T. Kachel, N. Pontius, M. Sultan, C. Gahl, M. Weinelt, H. A. Dürr, and U. Bovensiepen, *Phys. Rev. Lett.* 106, 127401 (2011).



33rd EUROPEAN CONFERENCE ON SURFACE SCIENCE

ORAL PRESENTATIONS

Wed-11:00-O-BAND ●

Scanning tunnelling spectroscopy of BiTeCl

BAND Band structure of solid surfaces

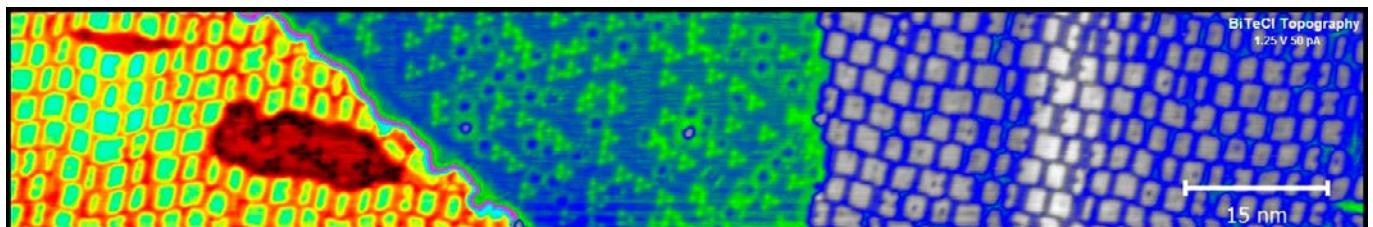
P. Casado Aguilar^{1,2}, Andrew Norris¹, C.G.Ayani¹, E.V. Chulkov¹, R. Miranda¹,
A. L. Vázquez de Parga^{1,2}

¹ Universidad Autonoma de Madrid (Spain);

² IMDEA nanociencia Madrid (Spain)

Owing to its inversion asymmetry, strong polarization and spin-orbit coupling (SOC), BiTeCl is a candidate spintronic compound [1-3] and a reported inversion asymmetric topological insulator (IATI) [4]. Furthermore, the accidental presence of a Bi₂TeCl crystal structure, a predicted weak topological insulator (WTI) [5], and exposed quasi 2D Bi bi-layers [6], provide for a rich environment for studying exotic topological phenomena.

We investigate the topological and electronic properties of BiTeCl, a tri-layered, non-centro symmetric, polar semi-conductor, whose large band-gap renders it immune from RT thermal excitations using spectroscopic imaging scanning tunneling microscopy (SI-STM). We confirm and contest several key reported points including; termination dependent electronic structures, band gap inconsistencies, and the highly contested issue of the presence or lack of a non-trivial topological state. Preliminary evidence suggests signatures of at least one topologically non-trivial state. We therefore discuss these aforementioned inconsistencies, alongside presenting entirely new structures, defects and evidence of sub-band structure.



References:

- [1] K. Ishizaka et al., Nature Materials 10, 521–526 (2011)
- [2] A. Crepaldi et al., Phys. Rev. Lett. 109, 096803
- [3] Y. Kohsaka et al., Phys. Rev. B 91, 245312
- [4] Y. L. Chen et al., Nature Physics 9, 704–708 (2013)
- [5] P. Tang et al., Phys. Rev. B 89, 041409(R)
- [6] I.K.Drozdov et al., Nature Physics 10, 664–669 (2014)
- [7] Y. J. Yan et al. Journal of Physics: Condensed Matter Vol27, (47)

Tue-11:40-O-OXID ●**Self-cleaning oxide surfaces as optical windows used in environmental surveillance***OXID Oxide surfaces and ultrathin oxide films*Naureen Akhtar, Bodil Holst*Department of Physics and Technology, University of Bergen, Norway*

Owing to its excellent mechanical and thermal properties as well as optical performance, sapphire (crystalline Al_2O_3 , alpha alumina) is extensively used as window in optical sensors for harsh conditions, for example underwater surveillance in the oil industry. However, under these conditions the sapphire surfaces are continuously exposed to oil and other fouling mixtures, which can lead to contamination of the window surface. Hence, making the surface underwater oleophobic would be highly desirable.

We found out that a sapphire surface can change from oleophilic to superoleophobic depending on the crystal miscut, polishing method and initial cleanliness state when submerged in water[1]. Moreover, giving the surface the hydrophilic character improves the underwater oleophobic character. This could be understood in the context of underwater superoleophobic surfaces found in nature that exhibit higher propensity for trapping water. Inspired by the underwater superoleophobic self-cleaning surfaces found in nature such as fish scales, sapphire surfaces are further developed for maintenance free solutions for permanent underwater installation of optical instrumentation.

References:

- [1] Akhtar, N., Holm, V. R., Thomas, P. J., Svardal, B., Askeland, S. H., & Holst, B. (2015). Underwater Superoleophobic Sapphire (0001) Surfaces. *The Journal of Physical Chemistry C*, 119(27), 15333-15.

Tue-16:40-O-OXID ●

Enhanced gas sensing properties of Cu-doped ZnO nanorods*OXID Oxide surfaces and ultrathin oxide films*

Onur Alev, Imren Torun, Zafer Ziya Öztürk

Gebze Technical University

Recently, gas sensors have attracted increasing interest due to their extensive applications in air quality control, environmental monitoring, disease diagnoses and quality control of foods [1]. Metal-oxide (MOXs) based amperometric gas sensors are the most promising devices among different types of gas sensors due to their high sensitivity, easy fabrication and low cost capability [2]. Sensing mechanism of the MOXs is based on reactivity of the surface materials to incoming analyte gases where electron transfer between gas molecules and the chemisorbed oxygen species plays a key role leading to a change of the conductivity on the surface [3]. Therefore, sensing properties are related to the morphology and sensing material itself. In order to achieve high performance gas sensors, various approaches have been made including fabrication of nanostructures, loading of noble metal as catalyst, formation of heterostructures and doping [4]. Among them, doping into MOXs nanocrystals is one of the most promising method to alter the structure, grains size, carrier concentration, distribution of oxygen component, which lead an enhanced gas sensing performance [5].

In this study, $Zn_{x-1}Cu_xO$ ($x= 0 - 5\%$) nanorods (NRs) were synthesized on glass substrate coated with ZnO seed layer via hydrothermal route. Scanning electron microscopy (SEM), energy-dispersive electron spectroscopy (EDS) elemental mapping and X-ray diffraction (XRD) techniques were used to investigate the crystal structure and morphology of nanorods. Presence of Cu was observed on EDS mapping results proportionally to doping concentration. Moreover, no other peaks corresponding to Cu related compounds were observed in the XRD patterns. However, a low angle shift was detected. The gas sensing performance of the devices were investigated against hydrogen, volatile organic compounds (VOCs) and nitrogen dioxide (NO_2) at different operation temperatures. Sensor responses showed that Cu doping positively effects the sensing properties of ZnO NRs, such as sensor response, selectivity and operation temperature. Enhanced sensing properties can be attributed to the incorporation of Cu^{+2} with ZnO which induces a change in carrier concentration and distribution of oxygen component. It can also be concluded that doping concentration directly effects the sensing properties, especially selectivity.

References:

- [1] E. Comini, Metal oxide nanowire chemical sensors: innovation and quality of life, *Materials Today* 19(10) (2016) 559-567.
- [2] G. Korotcenkov, B.K. Cho, Metal oxide composites in conductometric gas sensors: Achievements and challenges, *Sensors and Actuators B: Chemical* 244 (2017) 182-210.
- [3] A. Mirzaei, S.G. Leonardi, G. Neri, Detection of hazardous volatile organic compounds (VOCs) by metal oxide nanostructures-based gas sensors: A review, *Ceramics International* 42(14) (2016) 15119-15141.
- [4] K. Wetchakun, T. Samerjai, N. Tamaekong, C. Liewhiran, C. Siriwong, V. Kruefu, A. Wisitsoraat, A. Tuantranont, S. Phanichphant, Semiconducting metal oxides as sensors for environmentally hazardous gases, *Sensors and Actuators B: Chemical* 160(1) (2011) 580-591.
- [5] C. Wang, X. Cui, J. Liu, X. Zhou, X. Cheng, P. Sun, X. Hu, X. Li, J. Zheng, G. Lu, Design of Superior Ethanol Gas Sensor Based on Al-Doped NiO Nanorod-Flowers, *ACS Sensors* 1(2) (2016) 131-136.

Wed-11:20-O-OXID ●**Structure of the Ag(111)-p(4x4)-O phase: Ag₆ model or multilayer oxide?***OXID Oxide surfaces and ultrathin oxide films*

[B.V. Andryushechkin](#), [V.M. Shevlyuga](#), [T.V. Pavlova](#), [G.M. Zhidomirov](#), [K.N. Eltsov](#)

A.M. Prokhorov General Physics Institute of Russian Academy of Sciences, Russia

Oxygen adsorption on the Ag(111) has been a subject of many papers since the 1970s. A significant progress in the understanding of the system has been achieved in the 2000s after the application of scanning tunneling microscopy in a combination with DFT calculations [1-4]. As a result, the Ag_{1.83}O oxide-like model appeared for the p(4x4) phase [1]. The authors in Ref.[2] also reported the observation of the disordered phase at low oxygen coverage and describe it as an array of chemisorbed oxygen atoms with saturation coverage of 0.06 ML. Lately a new structural model for the p(4x4) phase containing two triangles of six silver atoms within the unit cell has been suggested [3,4]. According to the model, the oxygen coverage in the p(4x4) phase is equal to 0.375 ML.

Recently, we reexamined the disordered phase with LT-STM and obtained the high-quality atomic resolution images showing trefoil-like structures instead of the simple dark spots [5]. A thorough DFT analysis of the structures showed that each object is an oxide-like ring of six oxygen atoms surrounding the vacancy in the upper Ag(111) layer. Therefore, the coverage of the disordered phase in the new model appears to be 6 times larger than in the previous models.

In this work, we have found out that the density of dark objects in STM images just before the p(4x4) phase formation is equal to 0.10-0.11 ML. Therefore, the total oxygen coverage in the p(4x4) phase should be at least larger than 0.60-0.66 ML. For further coverage calibration, we measured integrals under TDS curves for the Ag(111) surface totally covered either with the disordered phase or the p(4x4) phase and found that total oxygen coverage for the p(4x4) should be at least 3 ML. All these data are not in line with a simple Ag₆ model considering the reconstruction of the upper silver layer. We believe that the p(4x4) phase is a multilayer oxide film. On the base of the DFT-simulation, we proposed a new sandwich-like model in which lower and upper oxide layer are reconstructed, with the arrangement of silver atoms like in the Ag₆ -model. The internal oxide layers preserve the structure of the (111) plane of bulk Ag₂O.

This work was supported by Grant No. 16-12-10546 of the Russian Science Foundation.

References:

- [1] C. I. Carlisle et al., Phys. Rev. Lett. 84, 3899 (2000).
- [2] C. Carlisle et al., Surf. Sci.470, 15 (2000).
- [3] M. Schmid et al., Phys. Rev. Lett. 96, 146102 (2006).
- [4] J. Schnadt et al., Phys. Rev. Lett. 96, 146101 (2006).
- [5] B.V. Andryushechkin et al., Phys. Rev. Lett. 117, 056101 (2016).

Mon-14:40-O-BAND ●**Spectroscopic investigation of surface opto-spin-current on Ir(111) covered by graphene***BAND Band structure of solid surfaces*[Ryuichi Arafune](#)¹, [Takeo Nakazawa](#)², [Noriaki Takagi](#)², [Maki Kawai](#)³¹International Center for Materials Nanoarchitectonics, National Institute for Materials Science, Japan;²Department of Advanced Materials Science, The university of Tokyo, Japan;³Institute for Molecular Science

Spin-current plays one of the most substantial roles in spintronics. Both two classes of spin-current, pure-spin-current and spin-polarized current, are important. The former is a non-equilibrium distribution where electrons with spin "up" propagate in one direction whereas those with spin "down" propagate in the opposite direction and not accompanied by a net charge transfer. The latter is the charge transfer with the co-oriented spins. By using angle resolved one- and two- photon photoemission spectroscopy, we have investigated the opto-spin-current generated at surfaces via spin orbit interaction. In this talk, we have demonstrated that changing light polarization enable us to switch the opto-spin-current characteristics; opto-pure-spin-current and spin-polarized photocurrent. The sample is Ir(111) covered by graphene. The Rashba-type band splitting has been found in the image potential states as well as the spin-split surface resonances in the occupied region. The optical direct transition between the spin-polarized states excited by the linear polarized light results in the opto-pure-spin-current, and the circularly polarized light excitation causes the spin-polarized photocurrent.

Tue-9:20-O-ORGS ●

Conductance of aromatic and antiaromatic molecules

ORGS Organic molecules on solid surfaces[N. P. Arasu](#), [H. Vázquez](#)*Institute of Physics, Academy of Sciences of the Czech Republic – Prague, Czech Republic*

Aromatic and antiaromatic molecules are cyclic, planar and have π conjugated systems. They are governed by Hückel's rule, which states that a system is aromatic if it has $4n+2$ electrons and antiaromatic if it has $4n$ electrons contributing to the molecular π system.

Antiaromatic systems were predicted to be more conducting [1]. Indeed, a decrease in the single molecule conductance was correlated with increased aromaticity [2]. However, due to the challenging synthesis of stable antiaromatic compounds, this relationship was only established for aromatic and non-aromatic molecules. Recently, a stable antiaromatic compound was synthesized and its conducting properties studied [3]. Its single molecule conductance was found to be 20 times higher than the aromatic counterpart. In this talk, I will describe our study on the electronic structure and conductance of aromatic and antiaromatic molecular junctions. We use DFT and NEGF methods to calculate the transmission spectra of a pair of structurally similar aromatic and antiaromatic molecules. Corrections to the DFT molecular levels bring the calculated conductance values in good agreement with experiment. We find that the higher conductance of the antiaromatic molecule is due to the LUMO-derived resonance closer to the Fermi level.

References:

- [1] R. Breslow, D.R. Murayama, S. Murahashi and R. Grubbs, *J. Am. Chem. Soc.*, 95 (20), 6688 (1973); R. Breslow and F.W. Foss, *J. Phys.: Condens. Matter*, 20, 374104 (2008).
- [2] W. Chen, H. Li, J.R. Widawsky, C. Appayee, L. Venkataraman, and R. Breslow, *J. Am. Chem. Soc.*, 136 (3), 918 (2014); Z. Xie, X.L. Ji, Y. Song, M.Z. Wei, and C.K. Wang, *Chem. Phys. Lett.*, 639, 131 (2015).
- [3] S. Fujii, S. Marqués-González, J. Y. Shin, H. Shinokubo, T. Masuda, T. Nishino, N.P. Arasu, H. Vázquez, and M. Kiguchi, (submitted).

Wed-9:00-O-COMP ●**Nuclear bound states of H₂ on a stepped metal surface***COMP Computational surface chemistry and physics*

[Elvis F. Arguelles](#)¹, [Hideaki Kasai](#)², [Katsuyuki Fukutani](#)³, [Ayako Yajima](#)⁴,
[Kousuke Nakayama](#)⁴, [Seiji Yamashita](#)⁴, [Wilson Agerico Dino](#)¹

¹ Department of Applied Physics, Osaka University;

² National Institute of Technology, Akashi College;

³ Institute of Industrial Science, The University of Tokyo;

⁴ Kawasaki Heavy Industries

We investigate the dynamics of the nuclear spin states of H₂ under the influence of a highly anisotropic potential induced by the stepped Pd(210) by first principles calculations based on the density functional theory (DFT). Previous temperature programmed desorption (TPD) study has shown that molecular adsorption of H₂ is only possible after the accumulation of atomic hydrogen on Pd(210) [1]. Further, H₂ has been shown to be at a chemisorption state on top of the step-edge Pd atom, contrary to flat transition metal surfaces where the adsorption is governed by weak van der Waals interaction. Our calculated orientation-dependent potential energy surface (PES) shows that H₂ adsorption is highly anisotropic and molecular orientation parallel to the surface plane is energetically favored. From this PES, we calculate the bound nuclear spin states of H₂ on Pd(210) and show that the desorption is significantly favored for para-H₂ isomers [2].

References:

[1] P.K. Schmidt, et al., Phys. Rev. Lett. 87(2001) 096103-1

[2] E. Arguelles, et al., submitted

Tue-10:40-O-EG2D ●

Symmetry reduction on metal supported graphene by intercalation of Pb

*EG2D Epitaxial growth and modification of 2D materials*C.G.Ayani¹, J.J. Navarro^{1,2}, F. Calleja¹, A.L. Vázquez de Parga^{1,2}, R. Miranda^{1,2}¹ IMDEA Nanociencia, Cantoblanco 28049, Madrid, Spain;² Departamento de Física de la Materia Condensada and IFMAC, Universidad Autónoma de Madrid, Cantoblanco 28049, Madrid, Spain

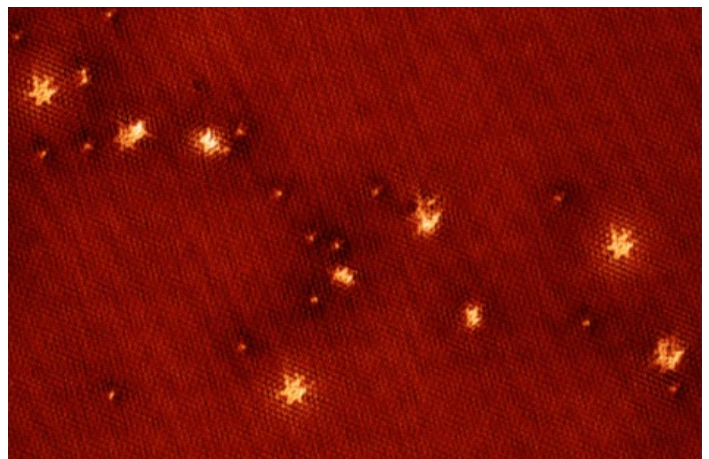
Monolayer graphene supported on metallic substrates is a wonderful test bench to alter graphene's electronic properties, exploiting the potential landscape created by the moiré patterns derived from the lattice mismatch between graphene and the metal. However, interaction with the metal often leads to the suppression of many interesting effects, like the inter- or intra-valley scattering processes present in the case of non-metallic substrates [1]. A possible way to decouple graphene from the substrate is the intercalation of an atomic layer of a different element between them [2-6].

Here we study the graphene/Pb/Ir(111) system and show that, under certain growth conditions, lead enters through graphene-free patches and intercalates between graphene and iridium preserving the original 9.3×9.3 incommensurated moiré structure [7]. Our STM and LEED measurements allow us to determine the atomic structure of the interlayer, that turns out to be a $c(2 \times 4)$ -2Pb commensurated with iridium. In addition we observe inter-valley scattering processes, which indicate that lead decouples graphene from the metallic substrate preserving its sub-lattice symmetry [8].

Figure: Pb intercalated graphene showing $\sqrt{3} \times \sqrt{3}$ pattern: STM atomically resolved image of graphene/Pb/Ir(111) at 1.2K. The whole image corresponds to a lead intercalated region of the sample. For a certain set of parameters (7 mV, 1 nA) $\sqrt{3} \times \sqrt{3}$ patterns are revealed, confirming elastic electron scattering processes.

References:

- [1] G.M. Rutter et al, Science 317, 219 (2007)
- [2] I. Gierz et al, PRB 81, 235408 (2010)
- [3] L. Huang et al, APL 99, 163107 (2011)
- [4] M. Gyamfi et al, PRB 85, 205434 (2012)
- [5] L. Meng et al, APL 100, 083101 (2012)
- [6] J. Mao et al, APL 100, 093101 (2012)
- [7] A.T. N'Diaye et al. NJP 10, 043033 (2008)
- [8] I. Brihuega et al. PRL 101, 206802 (2008)



Thu-9:40-O-OXID ● TiO₂ rutile (011) exposed to liquid water

OXID Oxide surfaces and ultrathin oxide films

Jan Balajka¹, Ulrich Aschauer², Annabella Selloni³, Michael Schmid¹, Ulrike Diebold¹

¹ Institute of Applied Physics, TU Wien, Austria;

² Departement für Chemie und Biochemie, Universität Bern, Switzerland;

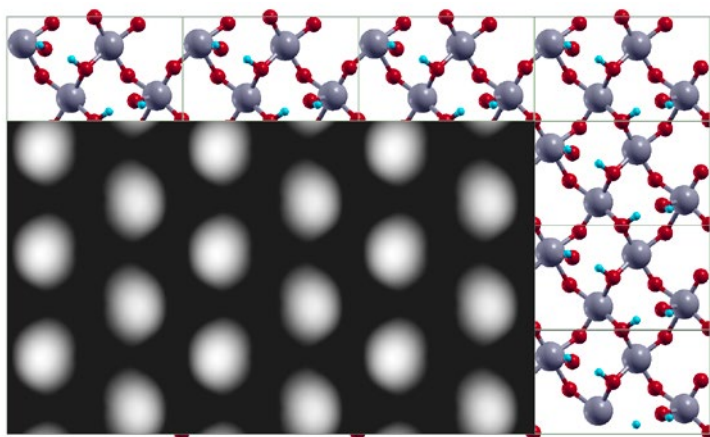
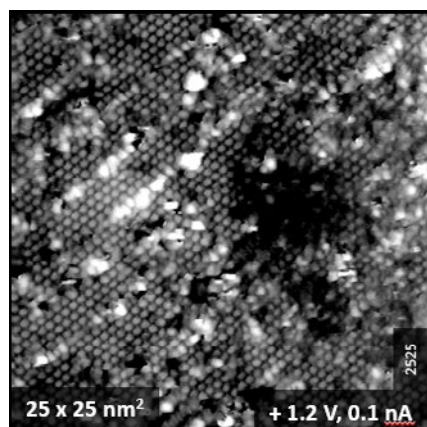
³ Department of Chemistry, Princeton University, NJ, USA

The interaction of water with titanium dioxide (TiO₂) is of significant interest as the TiO₂-water interface occurs in many practical applications such as photocatalytic water splitting. At present, most surface-science studies involve the interaction of gas-phase H₂O with TiO₂. Here we interface the TiO₂ surface with liquid water in order to approach application-relevant conditions.

The (011) surface is the second-lowest energy termination of TiO₂ rutile and frequently found on equilibrium-shape nanoparticles. When prepared by conventional techniques in UHV the (011) surface exhibits a (2×1) reconstruction. Based on DFT predictions [1], the (2×1) reconstruction is no longer favorable in liquid water environment and undergoes restructuring into a bulk-terminated (1×1) structure.

In the experiment, a TiO₂ rutile (011) crystal was prepared and characterized with STM, XPS, LEIS, and LEED in a dedicated UHV chamber, equipped for controlled and clean transfer of samples to and from a liquid environment. After the sample was first immersed and then removed from water, it was analyzed with the same UHV techniques.

The results indicate surface restructuring upon contact with liquid water. An overlayer with a “c(2×1)” symmetry is observed, which on the basis of STM analysis and DFT calculations can only be attributed to dissociated water on top of the (1×1) surface. Unlike the (2×1) reconstruction, the (1×1) surface has equivalent adsorption sites with correct density and symmetry. Domains of similar width are formed within the OH overlayer, which results in a splitting of LEED spots. The possibility of contaminant induced-restructuring was excluded based on XPS and LEIS measurements.



References:

- [1] U. Aschauer, A. Selloni, Phys.Rev.Lett. 106 (2011), 166102.

Wed-10:40-O-GRAP ●**Switching the reactivity of graphene on Ir(111) by hydrogen intercalation***GRAP Graphene and carbon-based 2D films*

[R. Balog](#)¹, [L. Kyhl](#)¹, [J. Jorgensen](#)¹, [A. Cassidy](#)¹, [A. G. Cabo](#)², [L. Hornekær](#)^{1,2}

¹ Dept. of Physics and Astronomy, University of Aarhus, Aarhus C, Denmark;

² iNANO, University of Aarhus, DK-8000 Aarhus C, Denmark

The functionalization of graphene with hydrogen enables a variety of new phenomena to appear such as *e.g.* band-gap opening, enhanced spin-orbit coupling and ferromagnetic order in single sided hydrogenated graphene. The appearance of these phenomena, however, strongly depends on the type of hydrogen structures, formation of which is often driven by the graphene-substrate interactions. [1,2] Moreover, the possibility for graphene to act as a hydrogen storage medium has led to several studies[3,4]. The reaction between gas phase atomic hydrogen and graphene on Ir(111) can at certain conditions allow formation of a highly periodic hydrogen structures, that are fully determined by the graphene-iridium interfacial properties. However, a quasi free-standing graphene can be prepared on Ir(111) upon hydrogen intercalation. The presence of hydrogen at the interface in turn dictates how graphene reacts towards atomic hydrogen bombardment from above – leading to the formation of different type of hydrogen structures when compared to the non-intercalated case. In addition, the modified interfacial properties also show a distinct reactivity towards vibrationally excited $H_2^{\#}$, [5] Understanding the reactivity of graphene towards hydrogen and the role of underlying substrates in these reactions is important for the realization of *e.g.* carbon-based hydrogen storage materials.

References:

- [1] J. Jorgensen et.al, ACS Nano , 10, 10798 (2016)
- [2] R. Balog, et.al, ACS Nano 7, 3823 (2013)
- [3] H. McKay et.al, Phys. Rev. B, 81, 075425 (2010)
- [4] Y. Miura, et.al, J Appl. Phys., 93, 3395 (2003)
- [5] L. Kyhl, et. al, (in preparation)

Tue-11:00-O-EG2D ●**Transition from Sulfided Molybdenum clusters to monolayer MoS₂ on Au(111)***EG2D Epitaxial growth and modification of 2D materials*

Elisabetta Travaglia¹, Harsh Bana¹, Paolo Lacovig², Luca Bignardi², Rosanna Larciprete³, Alessandro Baraldi^{1,2,4}, Silvano Lizzit²

¹ Physics Department, Via Valerio 2, 34127 Trieste, University of Trieste, Italy

² Elettra - Sincrotrone Trieste S.C.p.A., AREA Science Park, S.S. 14 km 163.5, 34149 Trieste, Italy.

³ CNR-Institute for Complex Systems, Via Fosso del Cavaliere 100, 00133 Roma, Italy.

⁴ IOM-CNR, Laboratorio TASC, AREA Science Park, S.S. 14 km 163.5, 34149 Trieste, Italy.

Nowadays, the growth of 2D materials via different synthetic approaches and the achievement of structure-property correlations of monolayer, bilayer, and multilayer sheets [1] are important challenges in materials science. Transition metal dichalcogenides (TMDCs) are one of the most promising 2D materials that could find application in new-generation electronic and optoelectronic devices [2]. Molybdenum disulfide (MoS₂) is one of the most representative members of TMDCs, due to its uncommon size dependent properties: in fact, it displays a change from indirect to direct band gap when going from its bulk to the monolayer form [3]. Among the various approaches attempted to grow MoS₂ monolayers, the one consisting in the deposition of Mo atoms on Au(111) at room temperature, followed by annealing, both performed in H₂S atmosphere, showed promising results [4].

Here we present a high energy resolution X-ray photoelectron spectroscopy study (HR-XPS), carried out at the SuperESCA beamline of Elettra, the Italian synchrotron radiation facility, on the growth of MoS₂ on Au(111) performed with the aforementioned growth method. The XPS technique, used also in its fast modality to follow transient processes (Fast-XPS), allowed us to detect the different species present on the surface and to follow their evolution during annealing. The HR-XPS spectra of the Au 4f core level besides decreasing in intensity, showed the appearance of a new component upon MoS₂ growth, caused by the MoS₂-substrate interaction. This interaction is detected also in the S 2p core level region, where the component related to the bottom sulfur layer, which is in contact with gold, is shifted with respect to the top sulfur layer of the 'S-Mo-S' sandwich structure.

References:

- [1] M. Xu, T. Liang, M. Shi, and H. Chen, *Chem. Rev.*, 113, (2013), 3766.
- [2] Q. H. Wang, K. Kalantar-Zadeh, A. Kis, J. N. Coleman and M. S. Strano, *Nat Nanotech.*, 7, (2012), 699.
- [3] K.F. Mak, C. Lee, J. Hone, J. Shan, and T. F. Heinz, *Phys. Rev. Lett.*, 105, (2010) 136805.
- [4] S. Sørensen, H. G. Fuchtbauer, A. K. Tuxen, A. S. Walton and J. V. Lauritsen, *Acs Nano*, 7, (2014) 6788.

Mon-15:20-O-CATL ●**Real-time observation of diffusive processes by field emission microscopy***CATL Catalytic 2D-model studies at low pressures*

Cédric Barroo^{1,2}, Yannick De Decker^{2,3}, Thierry Visart de Bocarmé^{1,2}

¹ *Chemical Physics of Materials and Catalysis, Université libre de Bruxelles, CP243, 1050 Brussels, Belgium;*

² *Interdisciplinary Center for Nonlinear Phenomena and Complex Systems (CENOLI), Université libre de Bruxelles (ULB), 1050 Brussels, Belgium;*

³ *Non Linear Physical Chemistry Unit, Université libre de Bruxelles, CP231, 1050 Brussels, Belgium*

Probing the reactions and their dynamics at the scale of a single nanoparticle remains challenging, due to the scarcity of high-resolution techniques. Field emission microscopy (FEM) is a powerful technique for studying the dynamics of catalytic reaction taking place at the surface of a nanosized metal tip which acts as a catalyst. The dynamics is probed in real-time and during ongoing reactive processes. In this context, we used FEM to study the hydrogenation of NO₂ on Pt model catalysts. By exploiting the nanoscale resolution capabilities of the FEM, the reaction can be probed down to 10 nm².

The reaction was followed by recording the FEM patterns appearing dynamically on the screen of the microscope. Time series were extracted from videos (at 50 fps) and established by probing the mean brightness over regions of interest. The dynamic of the process was analyzed by measuring the variations of grey levels with time, image by image. The catalytic hydrogenation of NO₂ was monitored in real time. On Pt at 390 K, amongst several non-linear behaviors, self-sustained periodic oscillations were observed. Transient phenomena were also monitored with an acquisition rate up to 10,000 fps. These experiments at high temporal resolutions show the presence of propagating processes at the surface of the catalyst. This observation proves that the consecutive catalytic ignition of the active facets is due to a coupling via surface diffusion. The propagation of chemical waves on a single facet of the nanocrystal is also observed. These waves take the form of target patterns, which are observed for the first time at the nanoscale, on areas as small as some 100 surface atoms. The velocity of the observed waves is of the order of a few μm/s, which is in good agreement with previous studies of catalytic reactions at the mesoscale. A discussion of the emergence of oscillations is proposed.

Field emission techniques are powerful techniques in the field of catalysis, and by exploiting the nanoscale resolution of the FEM, it is possible to obtain a better understanding of catalytic systems down to the molecular level.

References:

- [1] C. Barroo, Y. De Decker, T. Visart de Bocarmé and P. Gaspard. Fluctuating Dynamics of Nanoscale Chemical Oscillations: Theory and Experiments. *J. Phys. Chem. Lett.*, 2015, 6, 2189-2193
- [2] C. Barroo, Y. De Decker, T. Visart de Bocarmé and N. Kruse. Emergence of Chemical Oscillations from Nanosized Target Patterns. *Phys. Rev. Lett.* 117, 144501 (2016)

Wed-11:20-O-ORGS ●

Suppressed rotational oscillation by protonation of single triazatruxene molecules on Ag(111)

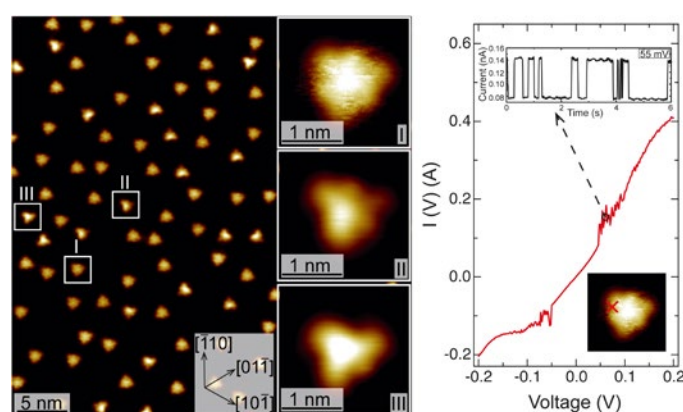
ORGS Organic molecules on solid surfaces

Anja Bauer¹, Florian Singer¹, Philipp Eler¹, Markus Maier², Rainer Winter², Yuriy Dedkov¹, Mikhail Fonin¹

¹ Department of Physics, University Konstanz, D-78457 Konstanz

² Department of Chemistry, University Konstanz, D-78457 Konstanz

The opportunity of tuning the electric and magnetic properties [1] as well as the control of the translational [2] and rotational motion of molecules on surfaces [3], [4] is of great interest since it lays a foundation for the fabrication of molecule-based functional devices. Here, we investigated triazatruxene (TAT) molecules on Ag(111) by low temperature scanning tunneling microscopy (STM) and spectroscopy (STS). After the deposition of TAT molecules by means of electrospray ionization (ESI) on Ag(111), STM measurements show an assembly of individual molecules with roughly equidistant spacings, emerging upon the interaction of molecules with the two-dimensional electron gas of the Ag(111) surface. Further measurements reveal three different types of molecular appearance which we assign to the non-, single- and double-protonated TAT. STS and time resolved current measurements at individual non-protonated molecules reveal characteristic excitations above a certain threshold energy showing a telegraph noise behaviour with the period depending both on voltage and current. We attribute these findings to the tip-induced rotational oscillation of the molecules between two distinct states which can be as well resolved in topography measurements at tunneling voltages below threshold. Protonation, however, leads to an efficient suppression of the rotational oscillation and the overall mobility of the molecules. By applying voltage pulses directly on the TAT molecules, we are able to switch on and off the rotational oscillation in a controlled manner. This process seems to be reversible with a greatly suppressed probability for tip-induced protonation.



References:

- [1] B. Borca, V. Schendel, R. Pétuya, I. Pentegov, T. Michnowicz, U. Kraft, H. Klauk, A. Arnau, P. Wahl, U. Schlickum, K. Kern, *ACS Nano* 9, 12506 (2015)
- [2] I. Swart, T. Sonnleitner, J. Niedenführ, J. Repp, *Nano Letters* 12, 1070 (2012)
- [3] A. Krönlein, J. Kügel, K.A. Kokh, O.E. Tereshchenko, M. Bode, *J. Phys. Chem.* 120, 13843 (2016)
- [4] H.W. Kim, M. Han, H.-J. Shin, S. Lim, Y. Oh, K. Tamada, M. Hara, Y. Kim, M. Kawai, Y. Kuk, *Phys. Rev. Lett.* 106, 146101 (2011)

Wed-16:20-O-SAMA ●**X-ray absorption study of a barium titanate derived quasicrystal on Pt(111)***SAMA Structural analysis and manipulation on atomic scale*

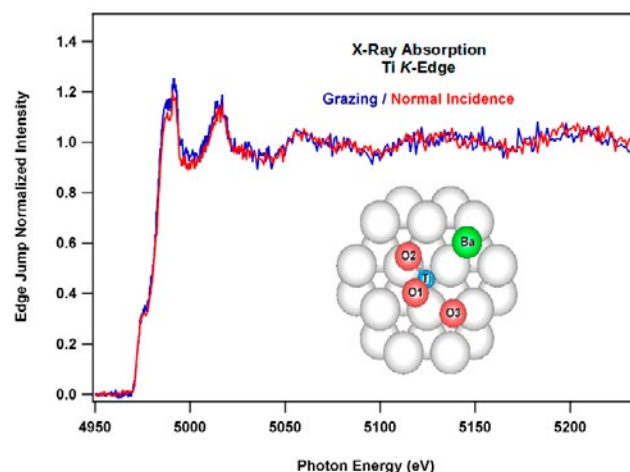
[Alireza Bayat](#)¹, [Stefan Förster](#)¹, [Eva Maria Zollner](#)¹, [Christoph Dresler](#)¹, [Wolf Widdra](#)^{1,2}, [Paula Huth](#)³, [Reinhard Denecke](#)³, [Angelika Chasse](#)¹, [Karl-Michael Schindler](#)¹

¹ *Institut für Physik, Martin-Luther-Universität, Halle-Wittenberg, D-06120 Halle, Germany;*

² *Max-Planck-Institut für Mikrostrukturphysik, D-06120 Halle, Germany;*

³ *Wilhelm-Ostwald-Institut für Physikalische und Theoretische Chemie, Universität Leipzig, D-04103 Leipzig, Germany*

The discovery of an aperiodic barium titanate derived quasicrystalline film on a periodic platinum substrate opened a new field in science and technology [1]. The key point of understanding physical and chemical properties as well as potential future applications of such systems is to determine its geometric structure. The equivalent of a monolayer of barium titanate was deposited on a clean Pt(111) substrate using MBE in an O₂ atmosphere. The quasicrystalline layer was then obtained through a two-step dewetting-rewetting process, annealing in O₂ at 1020 K and subsequent annealing in vacuum at 1120 K [2]. From this sample X-ray absorption spectra at the Ti K-edge (4990 eV - 5250 eV) were recorded at the KMC-1 beamline, BESSY, Berlin (Fig. 1). Missing pre-edge features of the XANES spectrum at around 4965 eV favor the exclusion of 4- and 5-fold O coordination of Ti [3]. EXAFS modulations have been analyzed using FEFF calculations. The analysis reveals that the Ti-Pt nearest neighbor distances are in the range of 2.65 - 2.75 Å. Furthermore, three different O atoms have been found in the first coordination shell. The EXAFS modulations in normal and grazing incidences suggest that two O atoms are close to in-plane with respect to Ti at distances of 1.70 Å and 2.57 Å. The third O atom is found to be out-of-plane at a distance of 2.58 Å. Although the quasicrystalline structure of the overlayer suggests that the Ti atoms occupy multiple sites above the Pt surface, a model with a single site (close to 3-fold hollow, Fig. 1) could be composed, which describes the experimental modulation functions surprisingly well (R-factor 0.12), better than any other single site model. Within this model contributions of atoms at distances up to 5.6 Å to Ti could mainly be assigned to scattering from substrate Pt atoms. In addition, a weak contribution at 3.24 Å could be assigned to Ba atoms. Any other atom above 5.6 Å is too far away to contribute significantly to EXAFS modulations. Further implications of this model for the geometric structure of the quasicrystalline layer will be discussed.



Ti K-edge x-ray absorption of a barium titanate derived quasicrystalline layer on Pt(111) including a structural model

References:

- [1] S. Förster et al., *Nature*, 502 (2013) 215.
 [2] S. Förster et al., *Annalen der Physik*, 529 (2016) 1600250.
 [3] B. Ravel et al., *Ferroelectrics*, 206-207 (1998) 407.

Thu-10:00-O-OXID ●**Interaction of water with anatase TiO₂(001)-1x4***OXID Oxide surfaces and ultrathin oxide films*

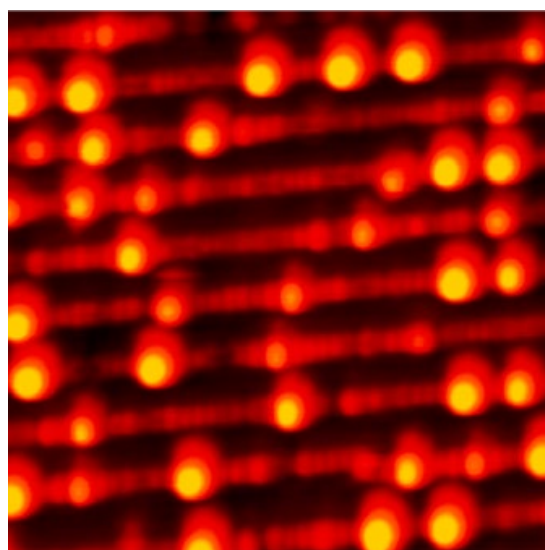
Igor Beinik, Kræn Christoffer Adamsen, Stig Koust, Jeppe V. Lauritsen, Stefan Wendt

Interdisciplinary Nanoscience Center (iNANO), Aarhus University, Gustav Wieds Vej 14, DK-8000 Aarhus C, Denmark

The interaction of water with titanium dioxide (TiO₂) is pivotal for many practical applications of this material in heterogeneous catalysis because water is almost always present either as a reactant or a product in many catalytic reactions. In our model study, we focus on the anatase polymorph of TiO₂ that has demonstrated a higher catalytic activity in water splitting than rutile and is generally considered as a more technologically relevant polymorph. The nanocrystals of anatase that are present in powder catalysts normally expose a high fraction of low surface energy (101) facets and a significantly smaller fraction of high energy, but supposedly more reactive (001) facets. The (001) facet is intrinsically unstable and reconstructs upon annealing in vacuum forming 1x4 reconstructed terraces, where rows of bridging oxygen atoms in [100] and [010] directions are replaced by TiO₃ units [1]. This kind of reconstruction has been found both on the (001) facets of anatase single crystals and nanoparticles [2], however the interaction of water with this surface has been significantly less investigated.

In the present work, we study the adsorption and dissociation of water on the anatase (001) 1x4 reconstructed surface by means of STM, TPD, and synchrotron core-level and valence band PES under UHV conditions. Our results show that water dissociates to some extent even at 120 K and that low water exposures (up to 3 L) at this temperature results in a mixture of molecularly and dissociatively adsorbed molecules. A systematic analysis of the data obtained using all three techniques leads us to a conclusion that the A-TiO₂(001)-1x4 surface is rather reactive - in agreement with an earlier study [3] we find that water dissociates at the ridges of the 1x4 reconstruction. Moreover, the 1x4 reconstruction remains stable upon water exposures at least up to ~45 L (at 120 K). However, after desorption of a multilayer ice film, the ridges themselves contain a high number of defects (see the STM image in Fig. 1), which remain stable up to 800 K. The nature of these defects will be discussed.

Figure 1: A typical STM image of the anatase (001) 1x4 reconstructed surface after desorption of multilayer ice film recorded at room temperature.

**References:**

- [1] Lazzeri, M. & Selloni, A. Phys. Rev. Lett. 87, 266105 (2001).
- [2] Yuan, W. et al. Nano Letters 16, 132–137 (2016).
- [3] Blomquist, J., et al. J Phys Chem C 112, 16616–16621 (2008).

Thu-10:40-O-SEMI ●**Morphology and stability of thin para-hexaphenyl layer grown on atomically flat surfaces of TiO₂(110)***SEMI Semiconductor surfaces and ultrathin layers*

Wojciech Bełza, K. Szajna, D. Wrana, K. Cieřlik, F. Krok

Marian Smoluchowski Institute of Physics, Jagiellonian University, 30-348 Krakow, ul. Lojasiewicza 11, Poland

The growing interest in organic and molecular electronics and its technological applications encourages search for best suitable molecule-substrate systems. In particular for films composed of rod-like molecules (like oligo-phenylenes), the molecular orientation with respect to the substrate is crucial.

We report on the investigation of the nucleation process of *para*-hexaphenyl (6P) molecules, consisting of six interlinked phenyl rings, deposited on atomically flat TiO₂(110) (1x1) surfaces prepared by cycles of Ar⁺ sputtering at room temperature (RT) and subsequent annealing at 1050 K. Sub-monolayer films of 6P (from 0,1 ML to 1 ML) were prepared by use of organic molecular beam epitaxy at RT. The surface morphology of the developed structures were investigated *in situ* by means of non-contact atomic force microscopy (ncAFM), scanning tunneling microscopy (STM) and *ex situ* by tapping-mode AFM. Additionally, for the surface reconstruction examination, we used a Low Energy Electron Diffraction (LEED) technique.

It has been found that the evaporation of sub-monolayer 6P coverages on flat TiO₂(110) resulted in the formation of molecular nanowires built of 6P molecules and a wetting layer consisting of lying molecules. We present that the molecularly-resolved imaging proved that the wetting layer is a well-ordered straight striped structure of molecular rows of molecules aligned side-by-side with the average distance of 0,65 nm corresponding to the distance of atomic rows of TiO₂(110) substrate surface (Figure 1). This wetting layer is a thermodynamically unstable structure and the molecular stripes rearrange at the timescale depending on the substrate surface quality, to form the structure following the shape of the TiO₂(110) terrace edges. Finally, an air-exposure of the sample induces a decomposition of the wetting layer and molecular clusters formation.

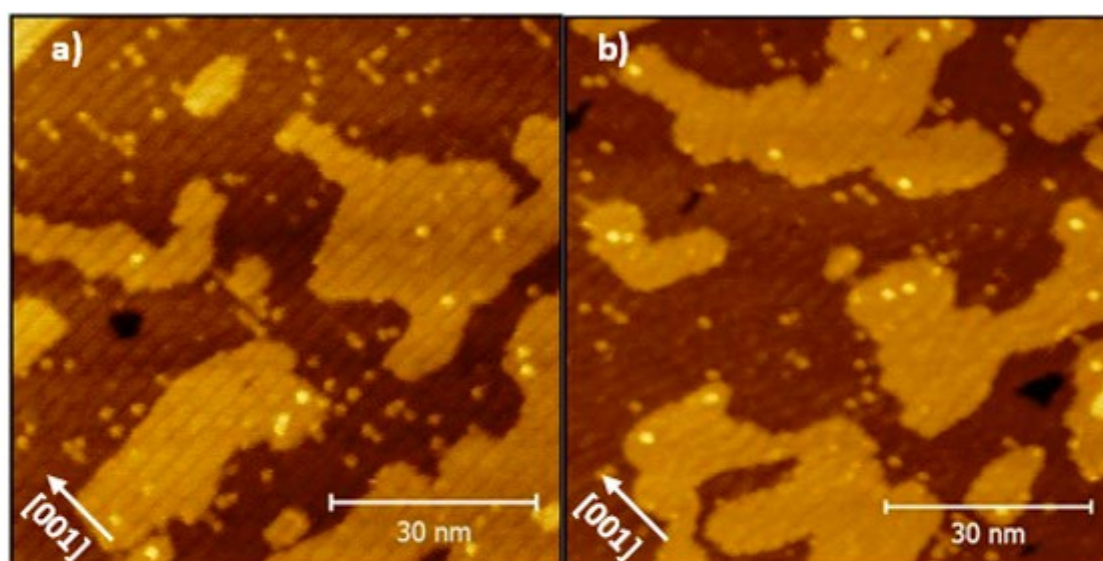


Figure 1. STM images of the wetting layer consisting of side-by-side aligned 6P molecules: a) 80x80 nm image taken few hours after 6P deposition; b) 80x80 nm image taken 1 day after 6P deposition.

Thu-14:40-O-CATH ●***In situ* structural studies and gas phase visualization of model catalysts at work*****CATH Catalytic 2D-model studies under high pressures***

[Sara Blomberg](#)¹, [J. Zetterberg](#)², [J. Zhou](#)², [J. Gustafson](#)¹, [E. Lundgren](#)¹

¹ Div. Synchrotron Radiation Research, Lund University, Sweden;

² Div. Combustion Physics, Lund University, Sweden

Catalysis is widely used in the production process of chemicals, pharmaceuticals, and fuels. In an industrial catalyst the heterogeneous catalytic reaction proceeds via adsorption on surfaces of catalytic active nanoparticles embedded in an insulating porous oxide. The materials system of a catalyst is therefore complex in particular when operating under harsh conditions and at elevated temperatures. Simplified model systems such as single crystals are therefore used to gain reliable knowledge on the catalytically active surface on the atomic scale studied under Ultra High Vacuum (UHV) conditions [1]. The well-defined surface of a single crystal enables detailed studies of specific properties such as adsorption sites or surface structures that are expected to be present on the active catalytic nanoparticles in an industrial catalyst, and how these properties contribute to the catalytic activity. The drawback with this approach is the difficulty to conclude if the properties found on a single crystal surface under UHV conditions also are applicable for nanoparticles and under harsh conditions. As a consequence, a number of *in situ* experimental techniques have been developed operating at more realistic condition to extend the fundamental knowledge on catalytic reactions and to bridge the pressure gap.

In this contribution we present results from Ambient Pressure X-ray Photoelectron Spectroscopy (APXPS) for surface and gas-phase studies and Planar Laser-induced Fluorescence (PLIF) for gas phase visualization, see Figs. 1a) and d), during the CO oxidation over a Pd(100) surface under semi-realistic conditions.

The APXPS experiments were carried out by slowly increasing the temperature of the Pd(100) in a 1:1 ratio of CO and O₂ at different total pressures [2]. We observe a pressure dependent CO desorption temperature, and therefore a pressure dependent ignition temperature of the reaction. The increasing light-off temperature of the catalyst is observed in conjunction with an increasing oxygen coverage on the surface measured immediately after the light-off. A surface oxide, which is formed at a coverage of 0.8 ML of oxygen was never observed in a 1:1 ratio of CO and O₂ at pressures up to 1 mbar. Exposing the crystal to a more oxygen rich environment at a ratio of 1:4 of CO and O₂ results in an active surface and the formation of a surface oxide. Remarkably, no CO could be detected neither in the gas phase nor adsorbed on the surface after the ignition of the reaction, despite a highly active surface, see Fig. 1c). A similar situation was also observed when CO oxidation over Rh(100) was studied using APXPS[3].

The absence of CO during the APXPS *in situ* studies during CO oxidation highlight the importance of the change of the gas phase in the presence of an active catalyst to enable a correlation between the surface structure of the catalyst and the measured catalytic activity. To investigate the gas phase in more detail, we have developed PLIF for applications in catalysis. In PLIF, a laser is used to excite a gas molecule of interest in the vicinity (~0.3 mm) of the catalyst surface. By using a laser sheet, the gas phase is probed, non-intrusively, in two dimensions, allowing for 2D detection of the emitted fluorescence light. The result is an image of the gas distribution in the reactor of the probed gas with an updating frequency of 10 Hz, see Figs. 1e-h).

PLIF was used to study *in situ* the change of the gas phase during CO oxidation over Pd(100), where the images visualize the build-up of a boundary layer of CO₂ close to the active surface, see Fig. 1 f) and h), and the reaction is mass transfer limited by the diffusion of CO. Within this boundary layer the gas composition is significantly different as compared to the composition detected at the outlet of the reactor by a mass spectrometer (MS)[4]. A detailed analysis of the CO gas phase reveals a depletion region

of CO 0.3 mm above the sample where the partial pressure of CO is approximately 80% lower as detected 10 mm from the sample surface or by the MS[5]. The drastic drop in the CO pressure close to the surface explain the absent CO emission in the APXPS experiments, since the resulting partial pressure of CO is below the detection limit of the APXPS. PLIF opens the door to a number of new fundamental studies and applications [6], which will be discussed in the contribution.

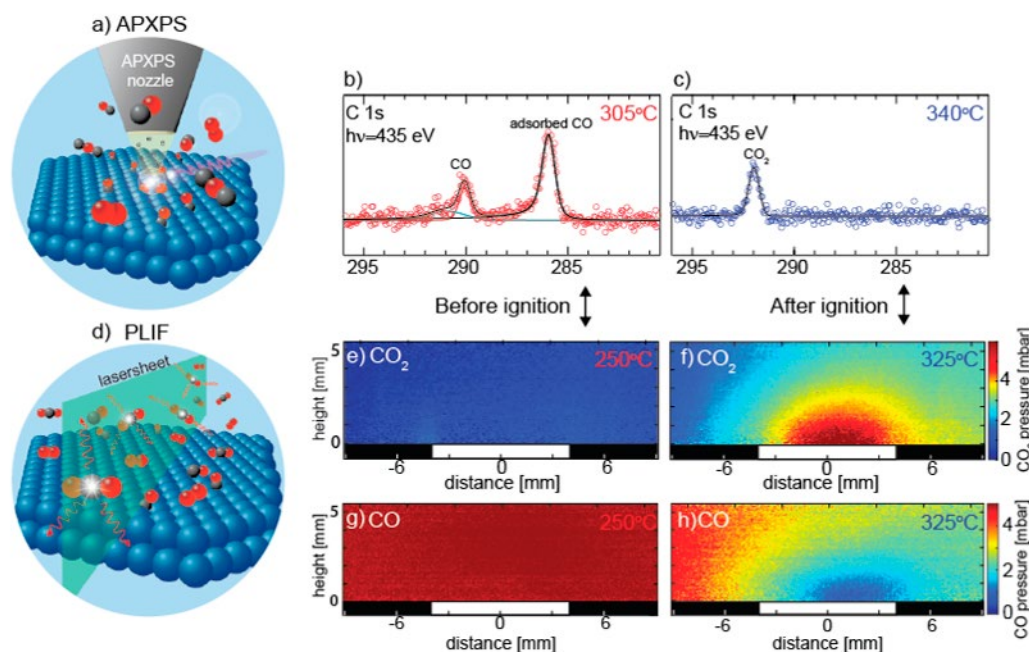


Figure 1. a) APXPS operating at semi-realistic conditions used to probe a model catalyst surface for structure and gas determination. b) C 1 s before ignition. c) C 1 s after ignition. Note the absence of CO in the gas phase or at the surface. d) A laser sheet probes the gas phase when PLIF is used to generate a 2D image of the gas distribution. The 2D CO₂ distribution e) before and f) after ignition. The CO distribution g) before and after h) after ignition

References:

- [1] G. Ertl, Reactions at solid surfaces, Wiley, Hoboken, N.J., 2009.
- [2] S. Blomberg et al. In Situ X-Ray Photoelectron Spectroscopy of Model Catalysts: At the Edge of the Gap, *Phys Rev Lett*, 110 (2013) 117601.
- [3] J. Gustafson et al. A high pressure x-ray photoelectron spectroscopy study of CO oxidation over Rh(100), *J Phys-Condens Mat*, 26 (2014).
- [4] J. Zetterberg et al. Spatially and temporally resolved gas distributions around heterogeneous catalysts using infrared planar laser-induced fluorescence. , *Nat Commun*, 6 (2015) 7076.
- [5] S. Blomberg et al. Real-Time Gas-Phase Imaging over a Pd(110) Catalyst during CO Oxidation by Means of Planar Laser-Induced Fluorescence, *Acs Catalysis* 5 (2015) 2028-2034.
- [6] Sara Blomberg et al *J. Phys.: Condens. Matter* 28 (2016) 453002

Tue-11:20-O-ELCH ●

Ionic liquid thin films on the HOPG and VN surfaces: *in-situ* electrochemical XPS study

ELCH Electrochemistry at surfaces

A. Bondarchuk, M. Panhwer, T. Rojo, R. Mysyk, E. Goikolea

CIC energiGUNE, Miñano, Alava, Spain

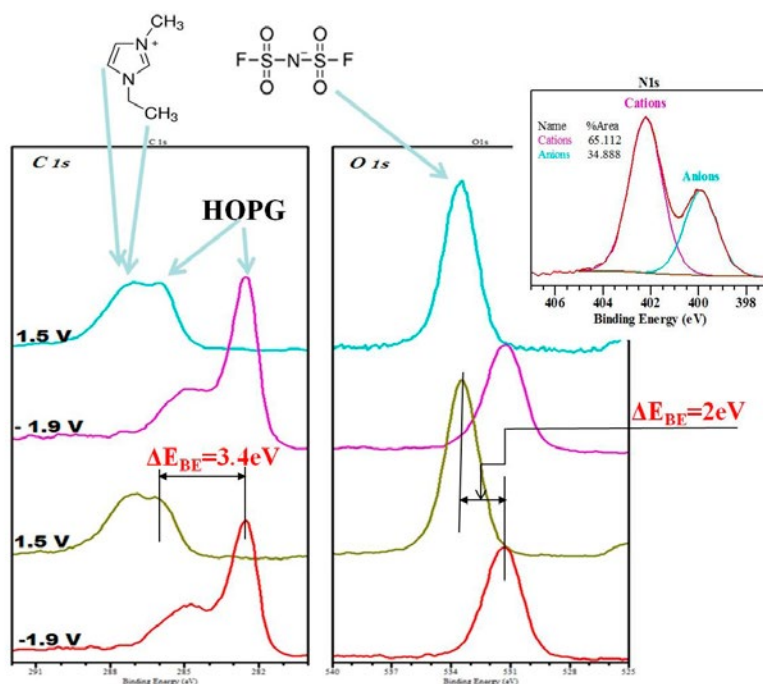
Interest in ionic liquids (IL) for electrochemical devices, such as batteries and supercapacitors can be attributed to their large electrochemical windows (up to ~6 V), thermal stability, low volatility and inherently high conductivity. However, the application of ILs for the device, has been limited for several reasons but especially because the electrolyte-electrode interface is not as well-defined.

To assess electrolyte-solid state interface under in-operando conditions ultra thin films of [EMI+][FSI-] ionic liquid of varying thickness were deposited on the surfaces of HOPG and VN film. The IL was deposited via thermal evaporation under UHV conditions. The deposited IL thin films were characterized by means of the *in-situ* XPS and *ex-situ* AFM (but under inert atmosphere of Ar). Electrochemical characterizations of the IL thin films were performed in the UHV apparatus using two-electrode set-up with a counter electrode made out of activated carbon.

At the interface with polycrystalline VN film the XPS revealed ordering of the IL in the direction perpendicular to the interface – alternating layers of cations and anions with cations adjacent to the substrate. In contrast, at the interface with HOPG the IL structure was similar to that in the bulk. The AFM data confirm “droplet on layer” growth model of the IL on the surface of HOPG.

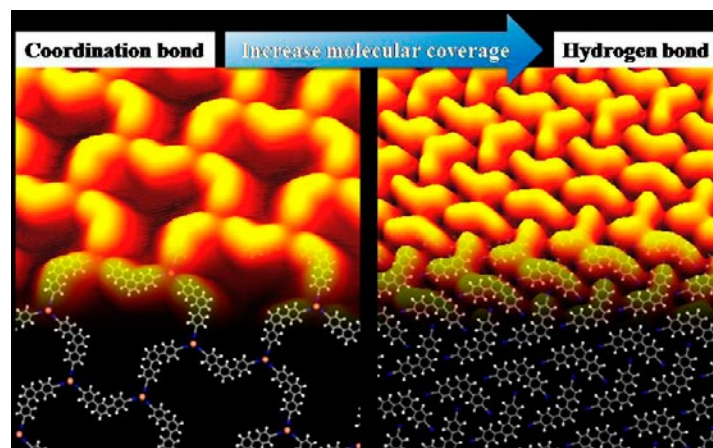
In-situ XPS measurements of the IL film at the cathodic (-1.9 V) and anodic (+1.5 V) revealed: 1) potential drop across the IL film and 2) reversible variation of the intensity of the XPS spectral lines (F1s, S2p, O1s, N2p and C1s) when the cell potential changes from positive to negative and back (See Fig.1). A model describing the potential/charge profile across the IL-solid interface and the potential driven lateral dynamics of the IL will be discussed.

Fig.1. *In-situ* electrochemical XPS. C1s and O1s spectra of the [EMI][FSI] thin film deposited on HOPG. The spectra were taken at the alternating surface potential measured wrt the grounded counter electrode (activated carbon). Inset shows a N1s spectrum taken at the OCP (open circuit potential) with two peaks correspondent to anion and cation components of the IL. The peaks' intensity ratio is close to the IL formula predicted value of 2 and does not change upon biasing.



Thu-16:20-O-ORGS ●**Competition between hydrogen bonds and coordination bonds steered by the surface molecular coverage***ORGS Organic molecules on solid surfaces*Liangliang Cai, Qiang Sun, Wei Xu*College of Materials Science and Engineering, Tongji University, Shanghai 201804*

In addition to the choices of metal atoms/molecular linkers and surfaces, several crucial parameters, including surface temperature, molecular stoichiometric ratio, electrical stimulation, concentration, and solvent effect for liquid/solid interfaces, have been demonstrated to play key roles in the formation of on-surface self-assembled supramolecular architectures. Moreover, self-assembled structural transformations frequently occur in response to a delicate control over those parameters, which, in most cases, involve either conversions from relatively weak interactions to stronger ones (e.g., hydrogen bonds to coordination bonds) or transformations between the comparable interactions (e.g., different coordination binding modes or hydrogen bonding configurations). However, intermolecular bond conversions from relatively strong coordination bonds to weak hydrogen bonds were rarely reported. Moreover, to our knowledge, a reversible conversion between hydrogen bonds and coordination bonds has not been demonstrated before. Herein, we have demonstrated a facile strategy for the regulation of stepwise intermolecular bond conversions from the metal–organic coordination bond (Cu–N) to the weak hydrogen bond (CH \cdots N) by increasing the surface molecular coverage. From the DFT calculations we quantify that the loss in intermolecular interaction energy is compensated by the increased molecular adsorption energy at higher molecular coverage. Moreover, we achieved a reversible conversion from the weak hydrogen bond to the coordination bond by decreasing the surface molecular coverage.

**Fig. 1** Bond conversion from coordination bond to hydrogen bond steered by surface molecular coverage

Keywords:

bond conversion, hydrogen bond, metal–organic coordination bond, self-assembly, scanning tunneling microscopy

References:

- [1] Liangliang Cai, Qiang Sun, Meiling Bao, Honghong Ma, Chunxue Yuan, and Wei Xu. *ACS Nano*. 2017, DOI: 10.1021/acsnano.6b08374.

Tue-11:00-O-ORGS1 ●

Structure and electronic properties of Zn-tetra-phenyl-porphyrins single- and multi-layer films grown on Fe (001)-p(1x1)O*ORGS Organic molecules on solid surfaces*A. Calloni¹, L. Floreano², R. Yivlialin¹, G. Bussetti¹, A. Goldoni³, A. Verdini², A. Picone¹, A. Brambilla¹, M. Finazzi¹, L. Duò¹, F. Ciccacci¹¹ Department of Physics, Politecnico di Milano, p.za Leonardo da Vinci 32, I-20133, Milano, Italy;² TASC Laboratory, Istituto Officina dei Materiali-CNR, ss-14 km 163.5, I-34149, Trieste, Italy;³ ST-INSTM Laboratory, Sincrotrone Trieste S.C.p.A. ss-14 km 163.5, I-34149, Trieste, Italy

Porphyrins have attracted the interest of researchers in different fields: chemistry, biology, physics, material science and technology due to the enormous variations of the molecular reactivity obtained by simply changing the peripheral radical groups and/or the inner metal atom. Thin porphyrin films have been grown on metals, semiconductors or organic-compatible substrates in view of possible applications in scalable organic-based devices (sensors, solar cells, etc.). In those cases, the interaction with the substrate can significantly perturb the reactivity of the porphyrin and the properties of the hypothetical device. A viable strategy to passivate the surface of the substrate is the introduction of an ultra-thin metal oxide (MO) layer prior to the growth of the molecular film. Since MO thin films represent an extremely wide class of compounds, we decided to focus our attention on the well characterized Fe(001)-p(1x1)O system, where the presence of oxygen atoms residing in the fourfold-symmetry surface hollow sites, i.e. slightly above the Fe(001) surface layer, might help decoupling the porphyrins from the metallic substrate. We studied the growth of the prototypical Zn-tetra-phenyl-(meso) porphyrin (ZnTPP) molecule on Fe-p(1x1)O with a variety of experimental techniques: scanning tunneling microscopy (STM), low-energy electron diffraction (LEED) and near edge X-ray adsorption spectroscopy (NEXAFS) for the morphology of the films and the ordering of the molecules; photoemission, inverse photoemission (PES,IPES) and scanning tunneling spectroscopy (STS) for the electronic structure. In the monolayer range, we observed the formation of a commensurate (5x5) superstructure composed by flat-lying molecules completely wetting the MO surface, while for a higher thickness of the ZnTPP layer a more compact configuration is observed, possibly allowed by the tilting of the inner ring of the molecule. Our spectroscopic results [1] are compared with those obtained by growing ZnTPP films either on Si(111) 7x7, clean Fe(001) or Au(001). On Fe(001)-p(1x1)O, sharp spectroscopic features are detected, together with the HOMO and LUMO levels of the ZnTPP molecule, suggesting that the ultra-thin oxygen layer significantly reduces the molecule-substrate interaction.

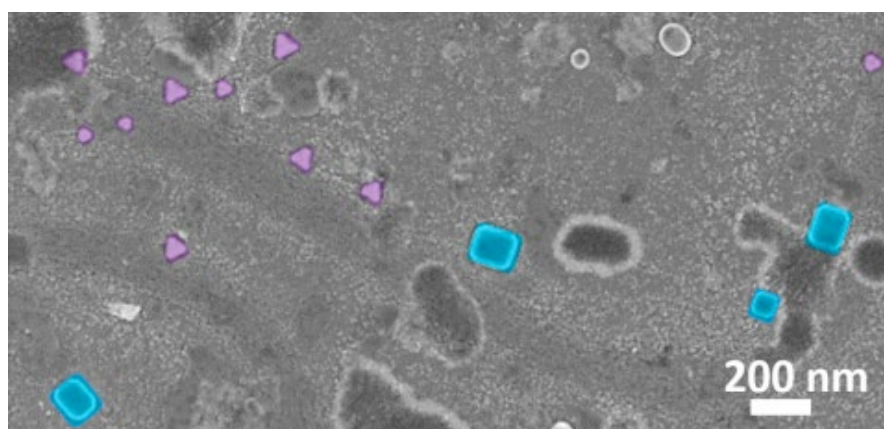
References:

- [1] G. Bussetti, A. Calloni et al. Appl. Surf. Sci. 390 (2016) 856-862; G. Bussetti, A. Calloni et al. Beilstein J. Nanotechnol. 7 (2016) 1527-1531

Tue-17:40-O-OXID ●**Temperature-induced transformation of electrochemically formed hydrous RuO₂ layers over Ru(0001) model electrodes***OXID Oxide surfaces and ultrathin oxide films*Hava Camuka, Philipp P. Krause, Thomas Leichtweiss, Herbert Over*Physikalisch-Chemisches Institut, Justus-Liebig-Universität Gießen, Heinrich-Buff-Ring 17, 35392 Gießen, Germany*

One of the most extensively studied metal oxides for use in electrochemical capacitors is hydrous ruthenium dioxide powder with a pseudocapacitance of with about 800–1000 F/g. Catalyst screening suggests that hydrous RuO₂ also performs well as an oxidation catalyst at room temperature. The catalytic properties of hydrous RuO₂ are so far not well understood due to its complex amorphous structure. In order to improve molecular understanding of hydrous RuO₂, a model system with preferably low structural and morphological complexity is required. This contribution presents a model system using single crystalline Ru(0001) as a template on which hydrous RuO₂ is electrochemically formed.

The hydrous RuO₂ layer on Ru(0001) and its temperature induced transformation under ultra-high vacuum and atmospheric conditions are comprehensively characterized by scanning electron microscopy and X-ray photoemission spectroscopy. The hydrous RuO₂ layer grows with an intricate morphology governed by the presence of step bunching regions of the Ru(0001) surface. Lastly, we studied the formation of RuO₂ crystallites aligned along the high symmetry direction of Ru(0001) (highlighted in the SEM micrograph) formed by the decomposition of the hydrous RuO₂ layer upon annealing at 200 °C. These particles form preferentially at step edges and step bunching regions and are distributed evenly across the sample surface. This model system is used to study the catalytic CO oxidation and ethanol oxidation in the next step.



References:

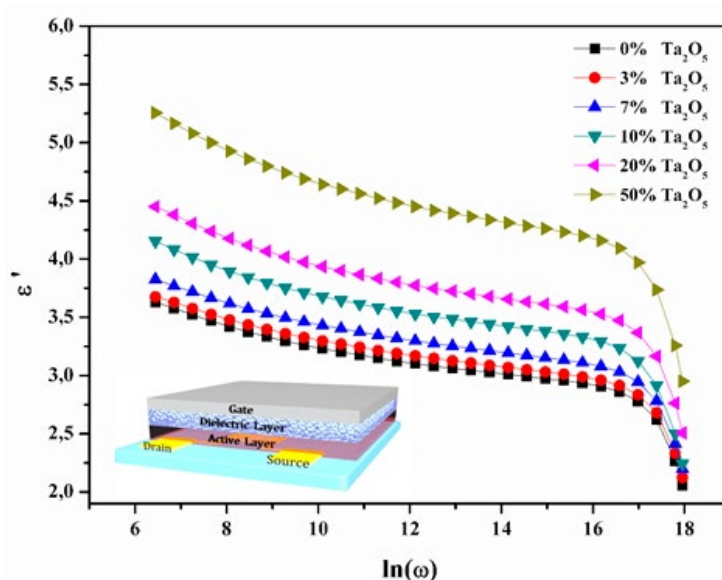
P.P.T. Krause, H. Camuka, T. Leichtweiss, H. Over, Temperature-induced Transformation of Electrochemically Formed Hydrous RuO₂ Layers over Ru(0001) Model Electrodes, *Nanoscale* 8 (2016) 13944-13953.

Wed-16:00-O-ORGS ●

Ta₂O₅: PMMA composite dielectric layer for ambipolar organic field effect transistors*ORGS Organic molecules on solid surfaces*Betül Canımkuşbey^{1,2}, Çiğdem Çakırlar¹, Serkan Büyükköse¹, Elif Altürk Parlak³, Zafer Ziya Öztürk¹, Savaş Berber¹¹ Department of Physics, Gebze Technical University, 41400, Kocaeli, Turkey² Department of Physics, Amasya University, 05100, Amasya, Turkey;³ TÜBİTAK MAM Material Institute, Photonic Technologies Laboratory, 41470 Gebze, Kocaeli, Turkey;

High-k inorganic dielectrics are ideal candidates for fabrication of high-capacitance organic field effect transistors (OFETs) [1]. However, deposition of inorganic dielectrics require expensive equipment and high temperature processes which is not compatible with flexible substrates. On the other hand, polymer dielectrics have relatively low dielectric constants and good mechanical properties. The combination of inorganic-organic materials as gate dielectrics is considered as a promising solution to get better OFET performance [2].

In this work, Ta₂O₅ nanoparticles are dispersed in a poly (methyl methacrylate) (PMMA) matrix to form a high-k nanocomposite dielectric layer. OFETs were fabricated using a solution-processed semiconductor P-SBTBDT which is a medium band gap polymer [3]. Dielectric constant of PMMA:Ta₂O₅ nanocomposites was found to increase with the increasing concentration of Ta₂O₅ in PMMA. Devices with up to 10 wt% concentration of Ta₂O₅ exhibited a typical p-type OFET behavior. Whereas, the devices with 10 wt% and higher concentration of Ta₂O₅ showed electron mobility in addition to hole mobility. Further, electron mobility was found to increase with increasing concentration of Ta₂O₅. The hole mobility of device with 0 wt% concentration is $\sim 3 \times 10^{-3}$ cm²/Vs. Besides hole and electron mobility values were found to be about 1.5×10^{-3} and 5×10^{-3} cm²/Vs at 70 wt% concentration of Ta₂O₅, respectively.



References:

- [1] Rocío Ponce Ortiz, Antonio Facchetti, and Tobin J. Marks, High-k Organic, Inorganic, and Hybrid Dielectrics for Low-Voltage Organic Field-Effect Transistors, *Chem. Rev.* 2010, 110, 205–239
- [2] Amjad Rasula, Jie Zhangc, Dan Gamotac, Manish Singhb, Christos Takoudisb, *Thin Solid Films*, Volume 518, Issue 23, 30 September 2010, Pages 7024–7028 Flexible high capacitance nanocomposite gate insulator for printed organic field-effect transistors
- [3] Hande Unay, Naime A. Unlu, Gonul Hizalan, Serife O. Hacıoglu, Dilber Esra Yildiz, Levent Toppare, Ali Cirpan, Benzotriazole and Benzodithiophene Containing Medium Band Gap Polymer for Bulk Heterojunction Polymer Solar Cell Applications, *Journal of Polymer Science, Part A: Polymer Chemistry* 2015, 53, 528–535

Thu-14:20-O-ORGS ●**Energetics of adsorbed molecules and molecular fragments on Nickel (111) by microcalorimetry***ORGS Organic molecules on solid surfaces*[Spencer J. Carey](#), [Wei Zhao](#), [Zhongtian Mao](#), [Wei Zhang](#), [Charles T. Campbell](#)*University of Washington, Washington, USA*

Nickel is one of the most commonly used catalysts for industrial reactions. We will present here experimental measurements of the energetics of adsorbed methyl, formate, water, methanol, benzene, and phenol on Ni(111). These systems have been widely studied with experimental and theoretical methods, but their energetics have not been previously measured. A complete understanding of these energetics is crucial for developing better catalysts and more accurate theoretical methods. Single crystal adsorption calorimetry (SCAC) allows for the direct measurements of surface reaction heats by using a pulsed molecular beam, a 1 μ m thick Ni(111) crystal, and a heat transducer. By analyzing how the heat of adsorption changes as a function of temperature and coverage, heats of formation and bond enthalpies of each of these molecules and molecular fragments on Ni(111) are determined. These measured energies provide important experimental benchmarks that are compared with quantum mechanical calculations. We will also provide a comparison of these energetics on Ni(111) to previous measurements on Pt(111). This knowledge provides insight into the thermodynamic distinctions between these two catalysts, which explain differences in their catalytic activities and selectivities.

Wed-16:20-O-GRAP ●**Synthesis and characterization of patterned graphene oxide***GRAP Graphene and carbon-based 2D films*

[Cassidy, A](#)¹, [T. Angot](#)², [E. Salomon](#)², [Régis Bisson](#)², [L. Hornekær](#)¹

¹ Department of Physics and Astronomy, University of Aarhus, DK-8000 Aarhus C, Denmark;

² PIIM/CNRS Laboratory, Saint Jérôme, Aix-Marseille Université, France

Creating sp³ defect sites in an otherwise perfect sp² graphene lattice, in a controlled manner, has been shown to introduce a band gap in the electronic structure of graphene.(1) Here, we exploit the moire lattice which emerges following the epitaxial growth of graphene on an Ir(111) surface to create localized graphene oxide nano-islands, in patterned formation, on the graphene basal plane. We demonstrate, experimentally, that the Ir surface beneath the graphene facilitates formation of new types of carbon-oxygen bonds, previously not considered in graphene oxide, in regions where the carbon atoms lie in a graphane-like configuration above Ir atoms. Precise control over the graphene oxide growth conditions allows for selective oxygen atom addition to carbon atoms at specific sites in the moire pattern.

The addition of oxygen species to graphene, and the formation of graphene oxide, is actively pursued to produce well-dispersed graphene sheets from graphite crystals in solution.(2) The controlled formation of the oxide and, in particular, the production of lightly oxidized graphene sheets, is of significant benefit during the subsequent reduction step and the synthesis of reduced graphene oxide.(3) Hence, it is important to understand the multitude of ways in which O species can covalently bond to the graphene basal plane. It was recently suggested, through DFT calculations, that O atoms can add to the graphene basal plane through formation of enolate moieties and here we show tentative experimental evidence in support of that theory.(4) Using scanning tunneling microscopy we show that graphene prepared on Ir(111) selectively bonds to oxygen atoms in areas where the moire lattice facilitates the formation of a graphane-like structure. A similar method has previously been used to produce patterned C-H bonds in the same graphene system.(5) The new bond formation is further characterized using x-ray photoelectron spectroscopy and high-resolution energy-loss spectroscopy. The etching of graphene oxide nano-islands through thermal annealing is also considered.

References:

- (1) Balog, R.; Jørgensen, B.; Nilsson, L.; Andersen, M.; Rienks, E.; Bianchi, M.; Fanetti, M.; Laegsgaard, E.; Baraldi, A.; Lizzit, S.; et al. Bandgap Opening in Graphene Induced by Patterned Hydrogen Adsorption. *Nat. Mater.* 2010, 9, 315–319.
- (2) Eda, G.; Chhowalla, M. Chemically Derived Graphene Oxide: Towards Large-Area Thin-Film Electronics and Optoelectronics. *Adv. Mater.* 2010, 22, 2392–2415.
- (3) Kumar, P. V.; Bardhan, N. M.; Tongay, S.; Wu, J.; Belcher, A. M.; Grossman, J. C. Scalable Enhancement of Graphene Oxide Properties by Thermally Driven Phase Transformation. *Nat. Chem.* 2014, 6, 151–158.
- (4) Jung, J.; Lim, H.; Oh, J.; Kim, Y. Functionalization of Graphene Grown on Metal Substrate with Atomic Oxygen: Enolate vs Epoxide. *J. Am. Chem. Soc.* 2014, 136, 8528–8531.
- (5) Jørgensen, J. H.; Čabo, A. G.; Balog, R.; Kyhl, L.; Groves, M. N.; Cassidy, A. M.; Bruix, A.; Bianchi, M.; Dendzik, M.; Arman, M. A.; et al. Symmetry-Driven Band Gap Engineering in Hydrogen Functionalized Graphene. *ACS Nano* 2016, 10, 10798–10807.

Wed-9:40-O-OXID ●**Ultrathin Fe films on SrTiO₃(001): growth, interfacial interaction and electronic structure***OXID Oxide surfaces and ultrathin oxide films*

[Pierre Catrou](#), [Gabriel Delhay](#)e, [Jean-Christophe Le Breton](#), [Sylvain Tricot](#), [Pascal Turban](#), [Bruno Lépine](#), [Philippe Schieffer](#)

Université de Rennes 1, Institut de Physique de Rennes, UMR UR1-CNRS 6251, Département Matériaux Nanosciences, F-35042 Rennes Cedex, France

Metal/perovskites interfaces have received considerable attention because of their technological importance in many applications. For example, the non-volatile resistive switching devices have been studied extensively, because of their potential applications for next generation nonvolatile resistance random access memory [1]. Besides, perovskite-based extrinsic multiferroic materials exhibiting an interfacial magnetoelectric coupling have also attracted much attention for their scientific and technological interest with a view to developing novel multifunctional devices [2]. Although many studies have been carried out on resistance switching processes or on magnetoelectric coupling in metal/perovskites devices, there is still little information about the mechanisms governing the interface formation.

Here we report a detailed study on the initial growth and electronic properties of ultrathin Fe films on TiO₂-terminated SrTiO₃(001) surface using x-ray photoemission spectroscopy (XPS), x-ray photoelectrons diffraction (XPD) and reflection high-energy electron diffraction (RHEED) techniques. The Fe films were deposited by molecular beam epitaxy at room temperature on clean (carbon-free) Nb-doped SrTiO₃(001) substrate. The epitaxial growth of monocrystalline Fe on SrTiO₃ is obtained for iron coverages higher than 0.6 nm with the 45° in-plane rotated cube-on-cube epitaxy, *i.e.* (001)[110]Fe//(001)[100]SrTiO₃. In the first stage of growth (0 - 0.15 nm Fe) the Ti³⁺ and Ti²⁺ components appear in the Ti2p core-level XPS spectra. We assign these components to Ti ions surrounded by oxygen vacancies in the SrTiO₃ substrate close to the surface. Besides, we also observe that during the interface formation some Fe atoms are oxidized in the interface region, but in limited proportion. Concomitantly, we find that the deposition of the fraction of Fe monolayer pushes the surface conduction band of the SrTiO₃ below the Fermi level indicating that Fe deposition induces a metallization of the SrTiO₃(001) surface. We propose then that this surface downward band bending is related to the oxygen vacancies creation induced by the Fe atoms deposition. Finally, we have determined the Schottky barrier height (SBH) for the Fe/SrTiO₃(001) n-doped junctions from XPS measurements. We obtain a SBH value of ~0.2 eV indicating that the contact is ohmic as for Cr/SrTiO₃ junctions. These results disagree with theoretical works which shown that the SBH for the Fe/SrTiO₃ junctions should be higher than 1.0 eV [3]. The difference between the theoretical works and our data comes from the fact that the theoretical model does not take into account the presence of positively charged oxygen vacancies at the surface.

References:

- [1] R. Waser et al., *Adv. Mater.* 21, 2632 (2009)
- [2] N. A. Spaldin and M. Fiebig, *Science* 309, 391 (2005)
- [3] M. Mrovec et al., *Phys. Rev. B* 79, 245121 (2009)

Tue-9:00-O-NAEX ●

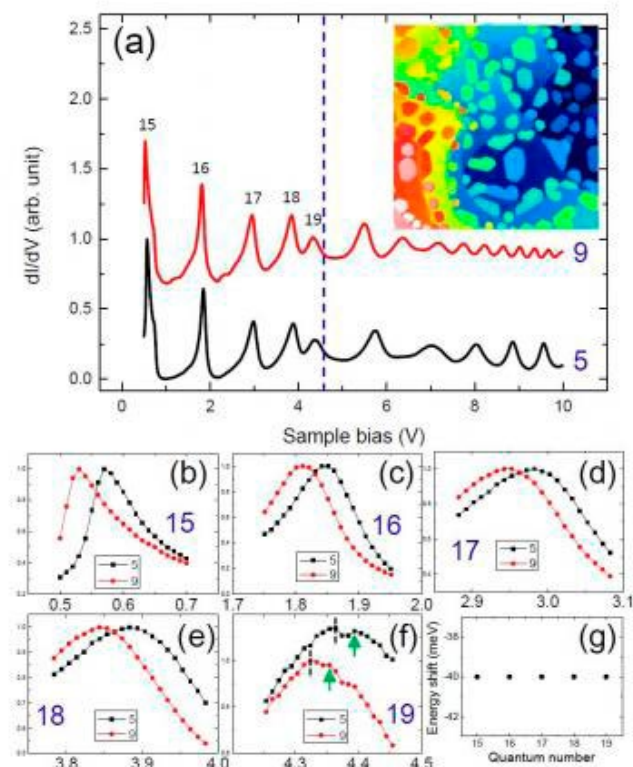
Sharpness-induced energy shifts of quantum well states in Pb islands on Cu(111)

*NAEX Novel advancement of experimental methods*Wen-Yuan Chan¹, Shin-Ming Lu¹, Wei-Bin Su¹, Chun-Chieh Liao^{1,2}, Germar Hoffmann³, Tsong-Ru Tsai², Chia-Seng Chang¹¹ Institute of Physics, Academia Sinica, Nankang, Taipei 11529, Taiwan, Republic of China;² Institute of Optoelectronic Sciences, National Taiwan Ocean University, Keelung 20224, Taiwan, Republic of China;³ Department of Physics, National Tsing Hua University, Hsinchu 30013, Taiwan, Republic of China

We elucidate that the tip sharpness in scanning tunneling microscopy (STM) can be characterized through the number of field-emission (FE) resonances. A higher number of FE resonances indicates higher sharpness. We observe empty quantum well (QW) states in Pb islands on Cu(111) under different tip sharpness levels. We found that QW states observed by sharper tips always had lower energies, revealing negative energy shifts. This sharpness-induced energy shift originates from an inhomogeneous electric field in the STM gap. An increase in sharpness increases the electric field inhomogeneity, that is, enhances the electric field near the tip apex, but weakens the electric field near the sample. As a result, higher sharpness can increase the electronic phase in vacuum, causing the lowering of QW state energies. Moreover, the behaviors of negative energy shift as a function of state energy are entirely different for Pb islands with a thickness of two and nine atomic layers. This thickness-dependent behavior results from the electrostatic force in the STM gap decreasing with increasing tip sharpness. The variation of the phase contributed from the expansion deformation induced by the electrostatic force in a nine-layer Pb island is significantly greater, sufficient to effectively negate the increase of electronic phase in vacuum.

References:

Nanotechnology 25 (2017) 095706



Tue-11:20-O-ORGS1 ●

Chemical transformation and magnetic induced properties of a fluorinated Tetraphenylporphyrin on Au(111)

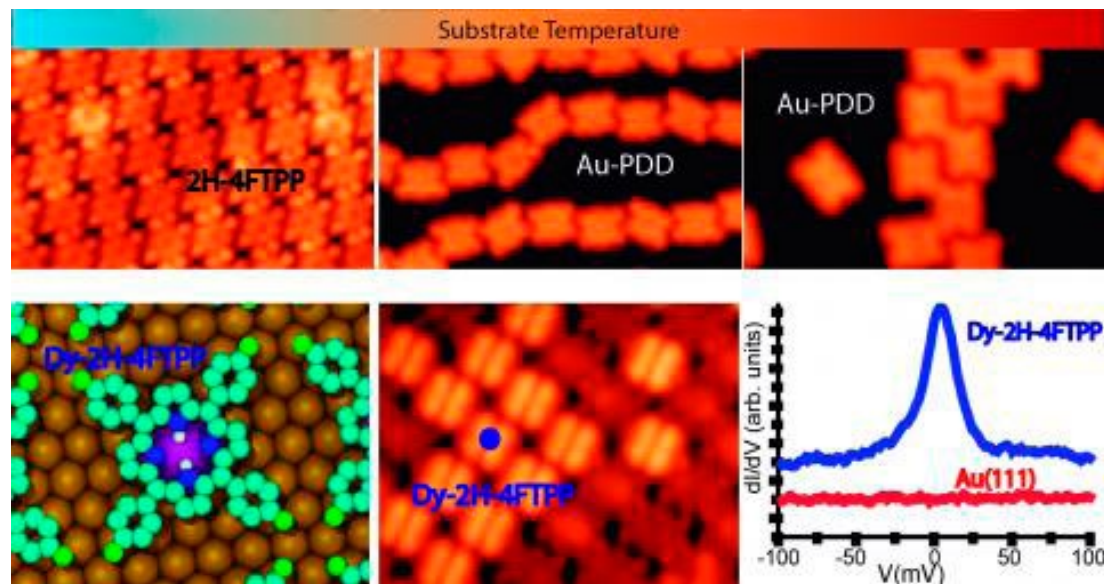
ORGS Organic molecules on solid surfaces

Borja Cirera¹, Roberto Otero¹, Jose Maria Gallego², David Ecija¹

¹ IMDEA Nanoscience, Departamento Física de la Materia Condensada, Universidad Autónoma de Madrid, 28049 Madrid, Spain

² Instituto de Ciencia de Materiales de Madrid, CSIC, 28049 Madrid, Spain

Porphyrins have attracted the attention of the scientific community due to their importance in biology as well as their potential for optoelectronic devices, bioprobes, sensors and catalysts. In particular, they are of great interest in surface science as their magnetic, electronic and chemical properties can be tailored at will for different purposes such as spintronics, information storage or sensing. Their terminal positions can be functionalized with different moieties to design diverse low dimensional nanoarchitectures with distinct intermolecular interactions: self-assembled arrays, metal-organic networks or covalent frameworks. Additionally, the central cavity acts as a chemical pocket that can incorporate a large variety of metal ions. In the last decade, many studies focused on the *in-situ* metalation with transition metals, but only recently lanthanides started to be investigated. This is particularly interesting as porphyrins can embrace the unique properties of the rare-earth metals, such as the high single-ion magnetic anisotropy arising from the protected 4f electron shell.



Here we present a thorough scanning tunneling microscopy (STM) study of the 5,10,15,20-tetrakis (4fluorophenyl)-21,23H-Porphyrin (4FTPP) on the Au(111) surface. First the topologic and electronic properties of intact species is determined, featuring the well-known characteristics of porphyrinoids such as the tautomerization of its central H atoms. Annealing the sample with self-assembled monomers at 625 K leads to the metalation of the tetrapyrrole macrocycle with surface Au adatoms and the chemical transformation of the units, resulting in planarized porphyrin derivatives (Au-PDD). The mechanism, via a dehydrogenative ring-closure intramolecular reaction, yields four types of products which self-assemble into two different supramolecular architectures: i) One-dimensional chains confined in the hcp and fcc regions of the herringbone reconstruction and ii) Large porous supramolecular islands.

Further annealing at 725 K overcomes the energy barrier of intermolecular reactions and Au-PDD covalent tapes are obtained through the formation of C-C coupling.

Alternatively, we explored the metalation of intact 4FTPP species on Au(111) by dosing dysprosium (Dy) atoms. Due to the larger ionic radius of Dy atoms in comparison with other transition metals they coordinate out of the main plane of the monomer and two intermediate metalation states are observed: Dy-2H-4FTPP and Dy-1H-4FTPP, in coexistence with fully metalated Dy-4FTPP. The Dy-2H-4FTPP species exhibits a strong Kondo signal, and the analysis of the broadening of the Kondo resonance versus temperature indicates a Kondo temperature of 100 K. Interestingly, the Kondo signal can be switched off by vertical manipulation, irreversibly changing the Dy-2H-4FTPP into the Dy-1H-4FTPP and finally into the fully metalated Dy-4FTPP species.

These results introduce a new porphyrin derivative and demonstrate its potential for molecular self-assembly and on-surface synthesis. In addition, our results pave new avenues for the design of molecular magnets on surfaces.

Tue-17:20-O-MOLA ●**Self-assembled monolayers – the impact of the binding group on structure and stability***MOLA Ultrathin two-dimensional molecular self-assembly*Jakub Ossowski, [Piotr Cyganik](#), Tomasz Żaba, Anna Krzykawska*Smoluchowski Institute of Physics Jagiellonian University, 30-348, Kraków, Poland*

Self-assembled monolayers (SAMs) are considered to be one of the most prototypical systems for investigating organic nanostructures and their potential application in nanotechnology and molecular electronics. The key feature in this type of material is the chemical bonding between the molecules and respective substrate. So far, the overwhelming majority of studies have been performed using sulphur as the binding group atom, which covalently binds the desired molecule to the metal substrate, making this system a reference standard for other types of SAMs. In this presentation we will compare standards based on sulfur with analogue SAMs based on selenium [1-3], carbon [4] and carboxylate group [5] indicating differences in 2D structure and in stability of binding with the most common metal substrates such as Au(111) and Ag(111). By combination of microscopic and spectroscopic study we will propose a general mechanism responsible for the film stability at the molecule-metal interface.

References:

- [1] J. Ossowski et al. *Angew. Chem. Int. Ed.* 2015, 54, 1336.
- [2] J. Ossowski et al. *ACS Nano* 2015, 9, 4508.
- [3] J. Ossowski et al. *J. Phys. Chem. C* 2017, 121, 459.
- [4] T. Zaba et al. *J. Am. Chem. Soc.* 2014, 136, 11918
- [5] A. Krzykawska et al. *Chem. Comm.* 2017 accepted

Tue-17:00-O-MOLA ●

Peekaboo on the nanoscale: self-assembled monolayers of 1, 3, 5-tris(4-carboxyphenyl)benzene (H3BTB) on Silver

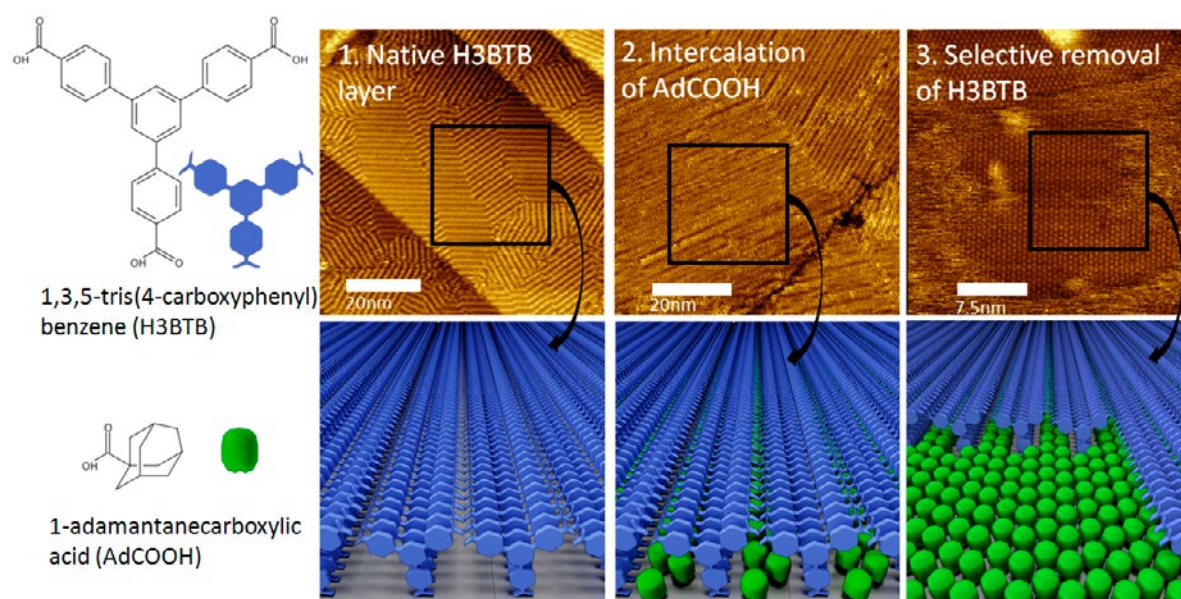
MOLA Ultrathin two-dimensional molecular self-assembly

Rodrigo Mateo Ortiz de la Morena¹, Hannah Aitchison¹, Hao Lu², Michael Zharnikov², Manfred Buck¹

¹ EaStCHEM School of Chemistry, University of St Andrews, North Haugh, St Andrews KY16 9ST, United Kingdom

² Angewandte Physikalische Chemie, Universität Heidelberg, Im Neuenheimer Feld 253, 69120 Heidelberg, Germany

Aromatic carboxylic acids (ACAs) have been in the focus as key constituents of both 3D frameworks and 2D networks on surfaces. In contrast, self-assembled monolayers (SAMs) of ACAs, where molecules adopt an upright orientation and exhibit a dense packing, have been studied very little. Only very recently it has been demonstrated in molecularly resolved studies^{1,2,3} that ACAs form high quality layers on copper and silver, thus, suggesting that the versatility of this class of compounds can also be exploited for the design of SAMs.



H3BTB, which has been used as linker in metal-organic frameworks⁴ (MOFs) and in 2D supramolecular networks⁵, exhibits an interesting case as its geometry should result in a more open SAM structure compared to other oligophenylene SAMs¹. Here we report our studies of H3BTB SAMs formed from solution on a Ag modified Au(111)/Mica substrate. Scanning tunnelling microscopy (STM), X-ray photoelectron spectroscopy (XPS), and near-edge X-ray absorption spectroscopy (NEXAFS) reveal that H3BTB adsorbs in a monopodal geometry, and yields a highly crystalline layer in which the molecules arrange in rows due to the strong π - π interactions between the molecules. Thus forming a SAM which exhibits nanochannels (1 in Figure), the possibility of intercalating a second species (2 in Figure) opens up. To establish this the native H3BTB SAM was exposed to a solution of either 1-adamantanecarboxylic acid or 1-adamantanethiol. While the SAM appears unchanged when imaged by STM the appearance of a sulphur peak in the XPS spectra when using the adamantanethiol or a change in the carboxylate signal

when using 1-adamantanecarboxylic acid suggest the presence of adamantane molecules. Imaging under conditions where the H3BTB molecules are removed reveals the adamantane molecules. Unexpectedly, they form a dense layer (3 in Figure) which is explained by the nanochannels representing a reservoir from which, due to a delicate balance of competing enthalpic factors, the molecules are expelled.

References:

1. H. Aitchison, H. Lu, S. W. L. Hogan, H. Früchtl, I. Cebula, M. Zharnikov, M. Buck. *Langmuir*, 2016, 32, 9397
2. H. Aitchison, H. Lu, M. Zharnikov, M. Buck. *J. Phys. Chem. C*, 2015, 119 (25), pp 14114–14125
3. C. Shen, I. Cebula, C. Brown, J. Zhao, M. Zharnikov, M. Buck. *Chem. Sci.*, 2012, 3, 1858-1865
4. S. R. Caskey, A. G. Wong-Foy, A. J. Matzger *Inorg. Chem.*, 2008, 47, 7751
5. C. N. Morrison, S. Ahn, J. K. Schnobrich, A. J. Matzger, *Langmuir*, 2011, 27, 936

Tue-15:20-O-OXID ●**The interaction of hydrogen, water and carbon monoxide with rhodium covered TiO₂(110) surfaces***OXID Oxide surfaces and ultrathin oxide films*László Deák¹, Imre Szenti², Zoltán Kónya¹¹ MTA-SZTE Reaction Kinetics and Surface Chemistry Research Group, Hungary, 6720 Szeged, Rerrich B. sqr. 1.² University of Szeged, Department of Applied and Environmental Chemistry, Hungary, 6720 Szeged, Rerrich B. sqr. 1.

The spillover of hydrogen including the diffusion of H atoms from the metal particles of a catalyst to the support is of great importance in catalysis, hydrogen storage and gas-sensorics [1]. On metal oxide supports the spilt-over hydrogen can form OH groups similar to the reaction of metal covered titania with water, which phenomena have attracted interest regarding the photocatalytic activity of TiO₂ for water-splitting [2] and water gas shift (WGS) reaction [3]. The reactions of D₂, H₂ and H₂O with a nearly stoichiometric TiO₂(110) surface covered by rhodium particles and the effect of CO on these processes has been investigated by TPD, AES and sensitive temperature-programmed work function (WF) measurements.

One monolayer (ML) of Rh saturated with deuterium at 270 K gave D₂ TPD features with T_p=370 and 450 K, corresponding to desorption from the metal and support, respectively. Isotope mixing with H₂ resulted in the release of HD at about 30 K higher temperatures. Saturating the Rh by CO at 330 K completely blocked the uptake of hydrogen on the metal and consequently eliminated the peak at 450 K attributed to spilt-over hydrogen. At 270 K, under the effect of CO exposure the pre-adsorbed hydrogen could be removed from the metal, but the TPD feature for spilt-over hydrogen was still observed. Decreasing the adsorption temperature to 200 K, CO replaced only partly the pre-adsorbed hydrogen which was accompanied by a considerable decrease in the adsorption bond energy of the other part remained on the metal. The co-adsorbed CO could not cease the spillover of H atoms towards the support. TiOx overlayers produced by stepwise heating of the titania-supported Rh particles suppressed the H₂ uptake of the metal, but the spillover of hydrogen from the Rh particles covered partially by TiOx towards the support proceeded.

The adsorption of water at 200 K on the nearly stoichiometric TiO₂(110) gave H₂O TPD peaks at 227 and 380 K, attributable to molecular water desorption and recombination reaction of surface hydroxide groups, respectively. The release of H₂ peaked at 326 K indicated that adsorbed water reacted with the defect sites of titania, leaving oxygen on the surface. Saturation of the titania by water decreased the WF by 1.47 eV. The desorption states observed below and over 300 K have positive outward dipole moments, contributing to the WF change by -0.65 and -0.82 eV, respectively. In the presence of 1 ML Rh a new H₂ TPD state developed with T_p=580 K. It is associated with the reaction of water at the titania-Rh interface, the length of which could be maximized by pre-heating the titania supported Rh layer to 700-750 K. Importantly, this interfacial state could be formed in the presence of adsorbed CO, which has also reactivity towards the interface.

References:

[1] R. Prins, Chem. Rev., 112 (2012) 2714-2738.

[2] Y. Zhu, D. Liu, M. Meng, Chem. Commun., 50 (2014) 6049.

[3] J. A. Rodriguez, S. Ma, P. Liu, J. Hrbek, J. Evans, M. Pérez, Science 318 (2007) 1757.

Wed-16:00-O-SAMA ●**Shaping surface landscapes with molecules: rotationally induced diffraction of H₂ on LiF(001) under fast grazing incidence conditions***SAMA Structural analysis and manipulation on atomic scale*

[M. del Cueto](#)¹, [A. S. Muzas](#)¹, [M. F. Somers](#)², [G. J. Kroes](#)², [C. Díaz](#)^{1,3,4}, [F. Martín](#)^{1,3,5}

¹ Departamento de Química, Módulo 13, Universidad Autónoma de Madrid, 28049 Madrid, Spain;

² Leiden Institute of Chemistry, Gorlaeus Laboratories, Leiden University, P.O. Box 9502, 2300 RA Leiden, The Netherlands;

³ Condensed Matter Physics Center (IFIMAC), Universidad Autónoma de Madrid, 28049 Madrid, Spain;

⁴ Institute for Advanced Research in Chemical Science (IAChem), Universidad Autónoma de Madrid, 28049 Madrid, Spain;

⁵ Instituto Madrileño de Estudios Avanzados en Nanociencia (IMDEA-Nanociencia), Cantoblanco 28049 Madrid, Spain

Following the observation in 2007 of atomic and molecular diffraction by surfaces under fast (0.2-20 keV) grazing (1-3°) incidence conditions [1, 2], the potential to characterize surface properties with more accuracy than with traditional atomic diffraction techniques was immediately realized.

As in traditional low energy diffraction, most experiments of diffraction under fast grazing incidence (DFGI) have been performed by using light atomic projectiles, mainly H and He, since their internal structure is preserved upon scattering by the surface, thus simplifying the analysis of the measured spectra. Nevertheless, DFGI has also been reported by using H₂ and D₂ molecular projectiles, although the complications arising from the additional degrees of freedom (molecular rotation and vibration) and the lack of theoretical support to understand their role in this context has prevented further developments in this direction.

One of the main problems in interpreting H₂ DFGI experiments is that the initial ro-vibrational state of the molecule is not known. Lack of knowledge on the actual projectile ro-vibrational distributions and the role played by vibrational and rotational excitations in DFGI is therefore the current bottleneck in the field, which prevents experimentalists from exploiting the huge potential of molecular projectiles.

In this context, help from theoretical modeling with real predictive power is crucial to guide experimental research. This modeling requires, at least, the evaluation of accurate potential energy surfaces (PES) to describe the H₂-surface interaction and the solution of the time-dependent Schrödinger equation (TDSE) that governs the scattering dynamics in which all the H₂ molecules degrees of freedom are taken into account.

We show that diffraction strongly depends on the initial H₂ rotational state, while it barely depends on the initial vibrational excitation. This behavior is entirely due to elastic scattering processes in which the initial rotational angular momentum of H₂ is preserved, thus greatly simplifying the analysis of the observed spectra. At specific incidence directions, the appearance of high-order diffraction peaks reveals a high degree of rotational excitation in the incident molecular beam, which must therefore be taken into account to correctly interpret experimental spectra, but provides, in the absence of inelastic processes, the ideal scenario for a detailed characterization of the surface. These conclusions are supported by the good agreement between our results and those of recent experimental measurements [3].

References:

[1] A. Schüller et al. 2007 Phys. Rev. Lett. 98 016103

[2] P. Rousseau et al. 2007 Phys. Rev. Lett. 98 016104

[3] P. Rousseau et al. 2008 J. Phys. Conf. Ser.133 012013

Tue-11:40-O-ELCH ●

One-pot electrochemical fabrication of reduced graphene oxide-metal/metal oxide nanocomposites for catalytic, sensor and energy storage applications

ELCH Electrochemistry at surfaces

Ümit Demir, Tuba Öznülüer, Hülya Öztürk Doğan, Bingül Kurt Urhan

Department of Chemistry, Faculty of Sciences, Atatürk University, Erzurum, Turkey 25240

Graphene-based nanocomposites show great potential in photocatalysis, photoelectrochemical cells, dye-sensitized solar cells, energy storage and sensors applications [1]. Especially, the hybrid composites that are formed by the anchoring of metal (Me) or metal oxide (MeO) with graphene or GO have been the most studied research topic in the recent years due to the enhanced electrical and electronic properties and the synergistic effect between graphene and Me or MeO. However, those composites were generally prepared by chemical and solvothermal methods that carried out in presence of high concentration of protective and reducing agents and requires multiple steps and externally supplied energy. Therefore, it is of great importance to develop facile and feasible synthetic routes in order to fabricate graphene-based nanocomposites with novel and enhanced properties.

We report the one-pot electrochemical strategy to fabricate electrochemically reduced graphene oxide (ERGO)-Me/MeO nanocomposites and their applications in catalytic, sensor and energy storage. This approach is based on the combination of electrochemical reduction of GO [2] and Me ions in the presence or absence of dissolved oxygen [3] from the same solution. Unlike existing approaches, the present approach is simple and allows us to fabricate Me or MeO decorated ERGO hierarchical structures directly onto substrates, which are highly desirable for many applications.

The nanoscale structure, morphology and chemical compositions of the as-electrodeposited nanocomposites (ERGO-Ni and ERGO-ZnO) were characterized by field emission scanning electron microscopy (FE-SEM), X-ray diffraction (XRD), Raman spectroscopy and X-ray photoelectron spectroscopy (XPS). Our results indicate that the direct electrochemical fabrication of ERGO-Ni and ERGO-ZnO nanostructures on conductive substrates is a convenient and low-temperature route to large-scale production and is also expected to be applicable to the synthesis of other metal oxide structures.

Photocatalytic, capacitive, and electrochemical sensing behavior of the nanocomposites were explored using cyclic voltammetry, UV-Vis absorption and reflection spectroscopy and photocurrent measurements. Electrochemical and photocurrent measurements revealed that those nanocomposites are promising candidates for the catalysis and sensor applications.

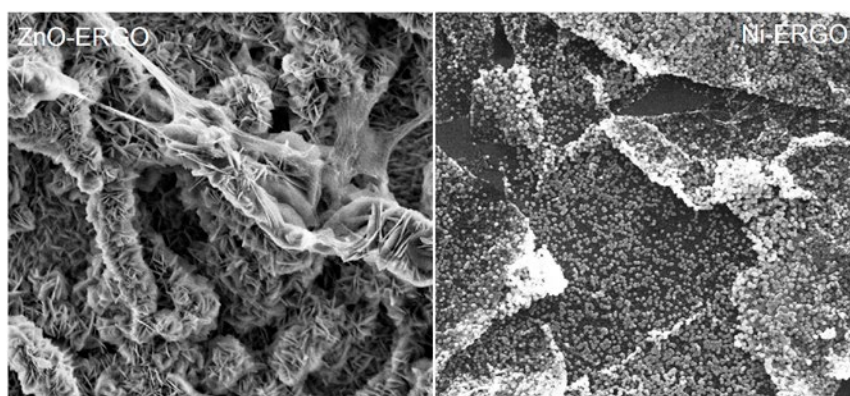


Figure. SEM images of ZnO and Ni decorated ERGO structures

References:

- [1] I. V. Lightcap, P. V. Kamat. *Acc. Chem. Res.*, 2013, 46 (10), 2235–2243
- [2] H. Öztürk Doğan, D. Ekinci, Ü. Demir, *Surface Sci.*, 2013, 611, 54-59-
- [3] C. Kartal, Y. Hanedar, T. Öznülüer, Ü. Demir, *Langmuir*, DOI: 10.1021/acs.langmuir.7b00340.

Wed-10:40-O-BAND ● Energy band alignment at the nanoscale

BAND Band structure of solid surfaces

[Jonas Deuermeier](#)¹, [Elvira Fortunato](#)¹, [Rodrigo Martins](#)¹, [Andreas Klein](#)²

¹ i3N/CENIMAT, Department of Materials Science, Faculty of Science and Technology, Universidade NOVA de Lisboa and CEMOP/UNINOVA, Campus de Caparica, 2829-516 Caparica, Portugal;

² Department of Materials and Earth Sciences, Technische Universität Darmstadt, Jovanka-Bontschits-Straße 2 D-64287 Darmstadt, Germany

The energy band alignments at interfaces often determine the electrical functionality of a device. Along with the size reduction into the nanoscale, functional coatings become thinner than a nanometer. With the traditional analysis of the energy band alignment by in situ photoelectron spectroscopy, a critical film thickness is needed to determine the valence band offset. By making use of the Auger parameter, it becomes possible to determine the energy band alignment to coatings, which are only a few Ångström thin. This is demonstrated with experimental data of Cu₂O on different kinds of substrate oxide materials and discussed taking into account dielectric constants and changes to the cation coordination in the film material.

Tue-11:40-O-ORGS2 ●**Tracking on-surface chemical reactions for the bottom-up fabrication of graphene nanoribbons and open-shell polymers***ORGS Organic molecules on solid surfaces*

[Marco Di Giovannantonio](#)¹, [Okan Deniz](#)¹, [José Ignacio Urgel](#)¹, [Shantanu Mishra](#)¹, [Roland Widmer](#)¹, [Samuel Stolz](#)¹, [Pascal Ruffieux](#)¹, [Roman Fasel](#)¹, [Matthias Muntwiler](#)², [Tim Dumslaff](#)³, [Uliana Beser](#)³, [Akimitsu Narita](#)³, [Klaus Müllen](#)³

¹ EMPA – Swiss Federal Laboratories for Materials Science and Technology, Überlandstrasse 129, 8600, Dübendorf, Switzerland;

² Paul Scherrer Institute, WSLA/122 5232 Villigen PSI Switzerland;

³ Max Planck Institute for Polymer Research, Ackermannweg 10, D-55128 Mainz, Germany

The formation of extended covalent molecular structures with low dimensionality is an exciting scientific challenge and technological prospect, aiming to realize organic analogues of graphene exploiting a bottom-up approach. On-surface synthesis has demonstrated the possibility of realizing a variety of 1D and 2D structures with atomic precision upon careful choice and functionalization of the precursor molecules[1,2]. However, precise control over the growth processes is not always achieved, leading to undesired final products that negatively affect the properties of the desired nanostructure. A detailed understanding of the reaction pathways may lead to the optimization of the reaction conditions, allowing for the rational choice of proper reactant molecules and the control of the parameters during the activation of the surface-confined reactions.

In this view, we performed combined investigation of novel systems by means of scanning tunneling microscopy (STM), noncontact atomic force microscopy (nc-AFM), fast X-ray photoelectron spectroscopy (fast-XPS) and density functional theory (DFT) calculations. The growth of (i) 9-atom wide armchair graphene nanoribbons (9-AGNRs)[3] and (ii) indenofluorene-based polymers will be discussed. In the first case, fast-XPS measurements provide insights into the sequence of surface-confined reactions producing 9-AGNRs from iodine and bromine-containing precursors. Our results enlighten all the chemical states appearing during the transformation, the corresponding temperatures of transition, and the reaction kinetics, demonstrating the advantages in the use of iodine as substituent halogen to promote the aryl-aryl coupling and obtaining longer ribbons. Moreover, the connection between cyclodehydrogenation and halogen desorption reactions will be discussed (Figure 1a). The second part of the talk will focus on open-shell structures, which received extreme interest because of their unusual properties, such as narrow frontier-orbital energy gaps and strong absorption in the visible spectrum[4]. The synthesis and characterization of novel nanostructures containing indenofluorene units, which are predicted to possess biradical character, has been achieved using precursor molecules containing methyl groups. A detailed investigation of the morphology and electronic properties of polymers containing various relative arrangement of six- and five-member rings will be presented (Figure 1b).

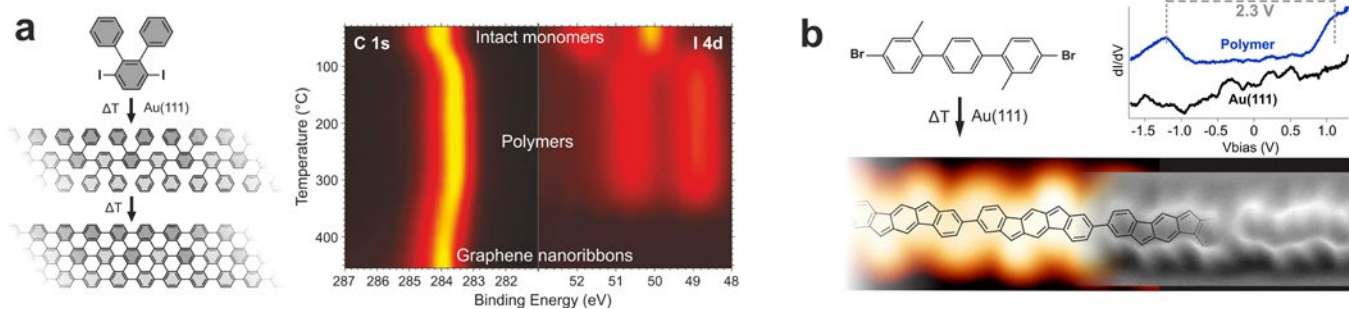


Figure 1. On-surface synthesis and characterization of 9-AGNRs (a) and indenofluorene-based polymers (b).

References:

- [1] On-Surface Synthesis; Gourdon, A., Ed.; *Advances in Atom and Single Molecule Machines*; Springer International Publishing: Cham, 2016.
- [2] Cai, J.; Ruffieux, P.; Jaafar, R.; Bieri, M.; Braun, T.; Blankenburg, S.; Muoth, M.; Seitsonen, A. P.; Saleh, M.; Feng, X.; Müllen, K.; Fasel, R. *Nature* 2010, 466 (7305), 470.
- [3] Talirz, L.; Söde, H.; Dumslaff, T.; Wang, S.; Sanchez-Valencia, J. R.; Liu, J.; Shinde, P.; Pignedoli, C. A.; Liang, L.; Meunier, V.; Plumb, N. C.; Shi, M.; Feng, X.; Narita, A.; Müllen, K.; Fasel, R.; Ruffieux, P. *ACS Nano* 2017, 11, 1380.
- [4] Rudebusch, G. E.; Zafra, J. L.; Jorner, K.; Fukuda, K.; Marshall, J. L.; Arrechea-Marcos, I.; Espejo, G. L.; Ponce Ortiz, R.; Gómez-García, C. J.; Zakharov, L. N.; Nakano, M.; Ottosson, H.; Casado, J.; Haley, M. M. *Nat. Chem.* 2016, 8 (8), 753.

Thu-15:20-O-ENER ●**Morphology effect on proton dynamics in Nafion® 117 and sulfonated polyether ether ketone (SPEEK)***ENER Surfaces for energy production and harvesting*

Jun Xing Leong^{1,2}, [Wilson Agerico Diño](#)^{2,3,4}, Azizan Ahmad⁵, Wan Ramli Wan Daud^{1,6}, Hideaki Kasai^{7,8}

¹ Fuel Cell Institute, Universiti Kebangsaan Malaysia, 43600 UKM Bangi, Selangor, Malaysia;

² Department of Applied Physics, Osaka University, Suita, Osaka 565-0871, Japan;

³ Center for Atomic and Molecular Technologies, Osaka University, Suita, Osaka 565-0871, Japan;

⁴ Joining and Welding Research Institute, Osaka University, Ibaraki, Osaka 567-0047, Japan;

⁵ School of Chemical Sciences and Food Technology, Faculty of Science and Technology, Universiti Kebangsaan Malaysia, 43600 UKM Bangi, Selangor, Malaysia;

⁶ Department of Chemical and Process Engineering, Universiti Kebangsaan Malaysia, 43600 UKM Bangi, Selangor, Malaysia;

⁷ Institute of Industrial Science, The University of Tokyo, Meguro, Tokyo 153-8505, Japan;

⁸ National Institute of Technology, Akashi College, Akashi, Hyogo 674-8501, Japan

We report results of our experimental and theoretical studies on the dynamics of proton conductivity in Nafion® 117 and self-fabricated sulfonated polyether ether ketone (SPEEK) membranes. Knowing that the presence of water molecules in the diffusion process results in a lower energy barrier, we determined the diffusion barriers and corresponding tunneling probabilities of Nafion® 117 and SPEEK system using a simple theoretical model that excludes the medium (water molecules) in the initial calculations. We then propose an equation that relates the membrane conductivity to the tunneling probability. We recover the effect of the medium by introducing a correction term into the proposed equation, which takes into account the effect of the proton diffusion distance and the hydration level. We have also experimentally verified that the proposed equation correctly explain the difference in conductivity between Nafion® 117 and SPEEK. We found that membranes that are to be operated in low hydration environments (high temperatures) need to be designed with short diffusion distances to enhance and maintain high conductivity.

Tue-9:40-O-MAGN ●

Giant hysteresis of single-molecule magnets adsorbed on a nonmagnetic insulator

MAGN Surface and molecular magnetism

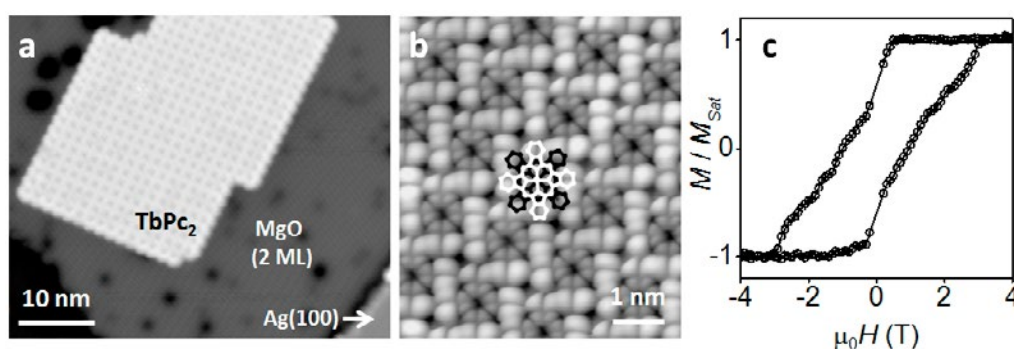
Christian Wäckerlin¹, Jan Dreiser^{1,2}, Fabio Donati¹, Aparajita Singha¹, Romana Baltic¹, Stefano Rusponi¹, Katharina Diller¹, François Patthey¹, Marina Pivetta¹, Harald Brune¹, Yanhua Lan³, Svetlana Klyatskaya³, Mario Ruben³

¹ Institute of Physics (IPHY), Ecole Polytechnique Fédérale de Lausanne (EPFL) Station 3, CH-1015 Lausanne (Switzerland);

² Swiss Light Source, Paul Scherrer Institut CH-5232 Villigen PSI (Switzerland);

³ Institute of Nanotechnology, Karlsruhe Institute of Technology (KIT) D-76344 Eggenstein-Leopoldshafen (Germany)

Single-molecule magnets (SMMs) are molecular coordination complexes which exhibit magnetic bistability [1-3] manifested in the appearance of a magnetic hysteresis. They are attracting much interest because of their potential for device applications in molecular spintronics or quantum computing. In order to exploit them in such applications it is necessary to distribute the molecules, e.g., on a flat surface [4,5] to make them addressable one-by-one. However, recent research has shown that the interaction with the surface often suppresses the magnetic hysteresis, and in particular no significant remanence, important for storage applications, has been observed in any surface-deposited SMM down to liquid-helium temperatures. Here we show by scanning tunneling microscopy (Fig. 1a,b) and x-ray magnetic circular dichroism that adding an ultrathin magnesia (MgO) film between TbPc₂ molecules [3] and the Ag(100) substrate leads to a record large magnetic hysteresis (Fig. 1c) [6] which is even enhanced compared to the case of bulk molecules. In particular, for the first time a significant magnetic remanence is observed. We attribute the strong hysteresis enhancement to the preservation of molecular symmetry because of the weak adsorption, to the deceleration of spin-flip processes owing to the MgO tunnel barrier as well as to the low phonon density of states at low energies in MgO.



References:

- [1] R. Sessoli, D. Gatteschi, A. Caneschi, and M. A. Novak, *Nature* 365, 141 (1993).
- [2] D. Gatteschi, R. Sessoli, and J. Villain, *Molecular Nanomagnets* (Oxford University Press, 2006).
- [3] N. Ishikawa, M. Sugita, T. Ishikawa, S. Koshihara, and Y. Kaizu, *J. Am. Chem. Soc.* 125, 8694 (2003).
- [4] M. Mannini, F. Pineider, P. Sainctavit, C. Danieli, E. Otero, C. Sciancalepore, A. M. Talarico, M.-A. Arrio, A. Cornia, D. Gatteschi, and R. Sessoli, *Nat Mater* 8, 194 (2009).
- [5] J. Dreiser, *J. Phys.: Condens. Matter* 27, 183203 (2015).
- [6] C. Wäckerlin, F. Donati, A. Singha, R. Baltic, S. Rusponi, K. Diller, F. Patthey, M. Pivetta, Y. Lan, S. Klyatskaya, M. Ruben, H. Brune, and J. Dreiser, *Adv. Mater.* 28, 5195 (2016).

Wed-16:40-O-ORGS ●**Chemical controlled electronic decoupling of three-dimensional molecules on surfaces investigated with LT-UHV-STM***ORGS Organic molecules on solid surfaces*

[René Ebeling](#)¹, [Shigeru Tsukamoto](#)², [Vasile Caciuc](#)², [Nicolae Atodiresei](#)², [Stefan Blügel](#)², [Rainer Waser](#)¹, [Silvia Karthäuser](#)¹

¹ Forschungszentrum Jülich GmbH, Peter Grünberg Institut – Elektronische Materialien (PGI-7), Jülich, Germany;

² Forschungszentrum Jülich GmbH, Peter Grünberg Institut – Quanten-Theorie der Materialien (PGI-1 / IAS-1), Jülich, Germany

To improve the resolution of two-dimensional molecules adsorbed on metallic surfaces recorded by STM, very thin electronic decoupling layers (i.e. NaCl, graphene, hexagonal boron nitride, transition metal dichalcogenides or oxides [1,2,3]) between the metallic substrate and the molecule are used. Thereby the direct coupling of the molecular states, i.e. originating from aromatic hydrocarbons, with the electronic states of the metal surface is suppressed, giving rise to the orbital resolution with STM [4]. As an alternative we present chemical decoupling by the adsorption of three-dimensional molecules directly onto a metallic surfaces. The adsorption behavior and the exact geometry of single target molecules on atomically flat surfaces of Pt(111) are investigated by LT-UHV-STM. For this purpose 2,7-Dibenzyl 1,4,5,8-naphthalenetetracarboxylic diimide (BNTCDI), which consists of a large pi-conjugated backbone and two phenyl rings each connected with a methylene-linker to the central part, has been studied. According to the high resolution STM images, the naphthoic diimide backbone of the molecule adsorbs flat on the substrate while the two benzyl groups build one line together with the backbone and the atomic nodal plane can be identified located at the C atoms of the phenyl rings. That points to phenyl groups standing vertically on the substrate leading to a full electronic decoupling of the benzyl groups.

References:

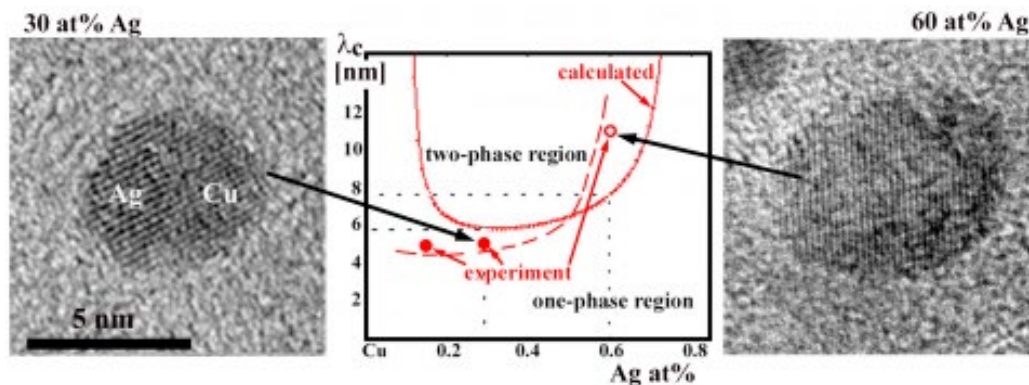
- [1] Repp, J., Meyer, G., Stojkovic, S., Gourdon, A., Joachim, C., Molecules on insulating films: Scanning-tunneling microscopy imaging of individual molecular orbitals, *Phys. Rev. Lett* 94, 026803 (2005).
- [2] Kumar, A., Banerjee, K., Liljeroth, P., Molecular assembly on two-dimensional materials, *Nanotechnology* 28, 082001 (2017).
- [3] Paßens, M., Moors, M., Waser, R., Karthäuser, S., Charge transport across the C60/TiO ultrathin film interface, *J. Phys. Chem. C* 121, 2815-2821 (2017).
- [4] de Oteyza, D., Gorman, P., Chen, Y.-C., Wickenburg, S., Riss, A., Mowbray, D., Ethin, G., Pedramrazi, Z., Tsai, H.Z., Rubio, A., Crommie, M., Fischer, F., Direct imaging of covalent bond structure in single-molecule chemical reactions, *Science* 340, 1434-1437 (2013).

Tue-14:00-O-BIMS ●

Size dependent spinodal decomposition in Cu-Ag nanoparticles

*BIMS Bimetallic surfaces and alloy nanocrystals*Zoltán Erdélyi¹, B. Gajdics¹, J.J. Tomán¹, G. Radnóczy², E. Bokányi², F. Misják²¹ Department of Solid State Physics, University of Debrecen, P.O. Box 2, H-4010 Debrecen, Hungary² Research Centre for Energy Research, Hungarian Academy of Sciences, H-1525 Budapest, PO Box 49, Hungary

Nanoparticles are of considerable interest, owing to their size-dependent properties, different from those of bulk materials. For revealing internal atomic processes in them, individual nanoparticles of Cu-Ag alloys were grown by direct current (DC) magnetron sputtering. Phase-separation during growth in Cu-Ag particles was found to be size- and composition-dependent. Particles below 5 nm in diameter grow as a solid solution of the components for all compositions (15–80 at% Ag). In the low Ag content range (15 and 30 at% Ag) phase-separation occurs only for particles above 5 nm in diameter. The separation into Cu-rich and Ag-rich domains, when observed, takes place by spinodal decomposition for all particle sizes. In particles undergoing incomplete coalescence, phase-separation occurs even if the diameter of the colliding particles is below 5 nm. In the higher Ag content range (60–80 at%), however, no phase-separation is observed until coalescence sets in. Lattice parameter measurements in alloy particles of 30 at% Ag revealed that the miscibility gap in individual particles varies between 70 and 90 at%. Calculation of the composition dependence of the critical length for spinodal decomposition based on the Cahn-Hilliard theory provided quantitative explanation for the observed phenomena. [1] Besides, computer simulations using the Stochastic Kinetic Mean Field model (<http://skmf.eu>, open source) [2] have also been performed which confirmed the results of the analytical calculations.



References:

- [1] G. Radnóczy, E. Bokányi, Z. Erdélyi, F. Misják, ACTA MATERIALIA 123: pp. 82-89. (2017)
 [2] Erdélyi Z, Pasichnyy M, Bezpalcuk V, Tomán JJ, Gajdics B, Gusak AM, COMPUTER PHYSICS COMMUNICATIONS 204: pp. 31-37. (2016)

Tue-14:40-O-ELCH ●

In-situ* spectro-electrochemical Infrared investigations at atomically-defined Pt/Co₃O₄(111) model catalystsELCH Electrochemistry at surfaces*Firas Faisal¹, Olaf Brummel¹, Manon Bertram¹, Corinna Stumm¹, Jörg Libuda^{1,2}¹ Department Chemie und Pharmazie, Friedrich-Alexander-Universität Erlangen-Nürnberg, Erlangen, Germany;² Erlangen Catalysis Resource Center Friedrich-Alexander-Universität Erlangen-Nürnberg, Erlangen, Germany

Electrocatalysts are often highly complex nanomaterials, both with respect to their composition and structure. In order to understand structure-property relationships in electrocatalysis, we follow a surface-science-based model approach. Complex model catalysts are prepared and characterized under ultra-high vacuum conditions and, subsequently, transferred to the electrochemical environment to study electrocatalytic reaction.

In this work, we explore Pt nanoparticles (NPs) supported on a reducible oxide, a common approach in heterogeneous catalysis that has also been transferred to electrocatalysis more recently.[1] We prepared highly ordered thin films of Co₃O₄(111) on Ir(100) [2] under ultra-high-vacuum (UHV) conditions and deposited Pt NPs by physical vapor deposition. The model systems were characterized with broad range of surface science methods. Subsequently, the model systems were transferred from UHV into the spectro-electrochemical cell and back without exposure to ambient conditions. As a test reaction, we used the electrooxidation of CO which was monitored *in-situ* by electrochemical infrared-reflection absorption spectroscopy (EC-IRRAS) in thin film configuration. All samples were characterized by low-energy electron diffraction (LEED) and Auger electron spectroscopy (AES) before and after the electrochemical experiments.

We identified a pH and potential window in which the Co₃O₄(111) film is stable in the electrochemical environment. This allows us to explore potential-dependent differences in the CO site occupation on the Pt/Co₃O₄ model catalyst. The behavior was compared to that of a Pt(111) reference sample under identical conditions. Specifically, we observed a strong suppression of bridging CO on Pt facets and identify additional strongly bound CO at low coordinated Pt sites. The latter persists at the electrode up to high electrode potentials. Additionally, we identify an electronic metal support interaction between the Co₃O₄(111) support and the Pt particles, which leads to a suppression of CO adsorption for very small Pt particles.

References:

[1] O. Brummel, F. Waidhas, F. Faisal, R. Fiala, M. Vorokhta, I. Khalakhan, M. Dubau, A. Figueroba, G. Kovács, H. A. Aleksandrov, G. N. Vayssilov, S. M. Kozlov, K. M. Neyman, V. Matolín, and J. Libuda, *J Phys Chem C*, 2016, 120 (35), 19723–19736

[2] K. Heinz, L. Hammer, *J Phys Condens Matter*, 2013, 25(17), 173001

Mon-15:00-O-CATL ●**Effect of gold on the adsorption properties of acetaldehyde on clean and h-BN covered Rh(111) surface****CATL Catalytic 2D-model studies at low pressures**

Arnold Péter Farkas^{1,3}, **Ádám Sztás**², **Gábor Vári**², **László Óvári**¹, **András Berkó**¹,
János Kiss¹, **Zoltán Kónya**^{1,2}

¹MTA - SZTE Reaction Kinetics and Surface Chemistry Research Group of the Hungarian Academy of Sciences at the University of Szeged, Szeged (Hungary);

²University of Szeged, Department of Applied and Environmental Chemistry – Szeged (Hungary);

³ELI-ALPS, ELI-HU Non-profit Ltd.- Szeged (Hungary)

In the case of gold catalysts, the most dramatic and well-known factors influencing the catalytic activity are the size and shape of the nanoparticles. Control of the particle size is possible with a plenty of physical (e.g.: evaporation, laser ablation) and chemical (e.g.: electro, photo- or colloid chemical) methods. On gold evaporated Rh(111) surface we can count also with the “self-organization” of bimetallic layers. In this case, nano-range ordering of the alloyed layer was detected by STM, where the lateral extension of the uniform commensurate (2×1) domains was around $4 \times 4 \text{ nm}^2$ [1]. The h-BN/Rh(111) system is also interesting for size controlling due to the self-organized superstructure of boron nitride on a Rh(111) surface described in [2–4].

In this study measurements performed in an UHV chamber equipped with facilities for Auger electron spectroscopy (AES), high-resolution electron energy loss spectroscopy (HREELS) and temperature-programmed desorption (TPD). STM, XPS and low energy ion scattering spectroscopy (LEIS) measurements were carried out to characterize the gold nanoparticles on clean and BN covered Rh(111). Our main purpose was to follow the effects of gold on the adsorption properties of acetaldehyde on clean and h-BN nanomesh covered Rh(111). In our preliminary work we observed that the dissociation reaction of ethanol stopped at formation of hydrogen and acetaldehyde on Au/h-BN/Rh(111). In contrast to the behavior found for the substrate metal, we didn't observe any sign of CO evolution. In our ongoing study we followed the adsorption and reactions of acetaldehyde on Au/Rh(111) and Au/h-BN/Rh(111). The product distribution showed a completely different picture in the case of clean and gold domain covered Rh(111). This suggests that hollow and bridge sites on rhodium play an important role in the dissociation process toward CO production, namely the production of carbon monoxide inhibited by the gold domains. Our measurements with acetaldehyde on Au/h-BN/Rh(111) strengthened the observation that the lack of possible adsorption sites eliminates the formation of CO. Nevertheless increased coverage of gold enhanced the amount of adsorbed aldehyde at low temperature. This trend turned back at higher gold coverage. The size of nanoparticles and possibly the charge on gold particles also influenced the position of the CO HREELS peak after adsorption of CO on Au/h-BN/Rh(111).

References:

- [1] L. Óvári, A. Berkó, G. Vári, R. Gubó, A.P. Farkas, Z. Kónya, Phys. Chem. Chem. Phys. 18 (2016) 25230.
- [2] M. Corso, W. Auwärter, M. Muntwiler, A. Tamai, T. Greber, J. Osterwalder, Science 303 (2014) 217.
- [3] Matthew C. Patterson, Bradley F. Habenicht, Richard L. Kurtz, Li Liu, Ye Xu, Phillip T. Springer, Phys Rev B.89 (2014) 205423.
- [4] A.P. Farkas, P. Török, F. Solymosi, J. Kiss, Z. Kónya, Appl. Surf. Sci. 354 (2015) 367.

Tue-15:00-O-ELCH ●**X-ray photoelectron spectroscopy of ionic liquids – from half cell measurements to *in situ* electrochemical XPS studies***ELCH Electrochemistry at surfaces*[Annette Foelske-Schmitz](#)¹, [Markus Sauer](#)¹, [Daniel Weingarh](#)², [Rüdiger Kötz](#)³¹ Vienna University of Technology;² Heraeus Holding GmbH;³ Paul Scherrer Institute

X-ray Photoelectron Spectroscopy (XPS) investigations of the liquid/ultra-high vacuum (UHV) interface have been of fundamental interest for several decades [1]. In these and subsequent studies, charging was observed and XP spectra were commonly referenced to the C 1s line [2]. Ionic liquids (IL) are particularly interesting to study as their negligible vapor pressure allows for XPS measurements without need of complex experimental setups. Again charging was reported to occur and the C 1s line of aliphatic chains was suggested to be used as internal reference [3].

Weingarh et al. developed an *in situ* electrochemical (EC) XPS cell and followed charging phenomena by recording the open circuit potential (OCP) under X-ray illumination using a twin anode [4]. It is well established that the OCP reflects the potential difference between an electrode and an electrolyte. In electrochemical equilibrium the OCP is constant, however, expected to change if physical or chemical properties of the two phases are changed.

Conversely, BE measurements may allow for determination of the OCP in one half-cell if significant charging of the IL caused by the X-ray induced photoemission can be excluded in course of the measurement. Since significant charging could not be observed by means of *in situ* EC XPS using a small spot monochromatic X-ray source directed to the bulk of the IL [5], we have further investigated double layer phenomena by means of XPS using a mono source. Recorded core level data of [EMIM][TFSI] on different substrates before and after 4h of irradiation indicates that significant charging does not occur in course of the measurement. Binding energies, however, were found to vary by 0.4 eV among the used substrates, thus confirming that the potential drop at the substrate/IL interface determines the OCP and therewith the BE values measured at the IL/UHV interface.

In the course of the presentation, recent XPS data of IL/UHV interfaces will be presented and elucidated by means of existing literature.

[1] H. Siegbahn, K. Siegbahn, J. Electron Spectrosc. Relat. Phenom., 1973, 2 319

[2] R. Moberg, F. Bökman, O. Bohman, H.O.G. Siegbahn, J. Am. Chem. Soc., 1991, 113, 3663-3667

[3] I.J. Villar-Garcia, E.F. Smith, A.W. Taylor, F. Qiu, K.R.J. Lovelock, R.G. Jones, P. Licence, Phys. Chem. Chem. Phys., 2011, 13, 2797-2808

[4] A. Foelske-Schmitz, D. Weingarh, A. Wokaun, R. Kötz, ECS Electrochem. Lett., 2013, 2, H13-H15

[5] D. Weingarh, PhD thesis, 2013, ETH NO. 21213

Tue-16:00-O-ELCH ●

***In situ* X-ray scattering studies of the formation of a Pb/Au(111) surface alloy in the electrochemical environment**

ELCH Electrochemistry at surfaces

Joshua Fogg¹, Christopher Lucas¹, Yvonne Grunder¹, Natasa Vasiljevic²

¹ University of Liverpool, Department of Physics, United Kingdom;

² School of Physics, University of Bristol, United Kingdom

The development of new functional materials is transforming many technological areas of great interest from electronics and catalysis to detection and bio-sensing. Pivotal to these advancements is surface alloying and self-organisation phenomena, driven by surface stress and elastic interactions in metals. Much has been explored experimentally in Ultra-High Vacuum and theoretically, however in terms of practical applications, little has been done. Electrochemistry is the ideal science to exploit the chemistry and physics of such functional materials. In general, alloying between two surfaces is driven by negative enthalpy of mixing and the lowering of surface free energy. Nevertheless, it can be observed even in systems where alloying does not occur in the bulk phase when confined to a few surface layers.

The Au(111)/Pb underpotential deposition (UPD) system has been intensively studied using multiple techniques including STM, AFM and surface X-ray surface diffraction. The rotated hexagonally close packed incommensurate formed on the surface can be considered a model UPD system. However, during the stripping of the UPD layer studies have been inconsistent. STM studies conducted by Green et al.[1] and later by Nutariya et al.[2] found suggestions of Au/Pb alloying evidenced by damage to the Au(111) surface layer after stripping of the Pb UPD structure. Nevertheless, other studies were unable to detect such evidence.

In this talk *in-situ* X-ray scattering studies of the formation of a Pb-Au(111) surface alloy will be presented. For this system, the alloy was prepared in the electrochemical environment and resonant x-ray scattering methods were utilised to identify the onset of surface alloying and correlate the changes in surface stress with the out of plane surface structure. A brief comparison with other surface alloy systems will be given.

References:

[1] M.P. Green and K.J. Hanson, Surf. Sci. 259, L743 (1991).

[2] J. Nutariya, J. Velleuer, W. Schwarzacher, and N. Vasiljevic, ECS Trans. 28, 15 (2010).

Wed-16:40-O-OXID ●**The influence of surface atomic structure on solid state electrochemistry: oxygen exchange on SrTiO₃(110) surfaces***OXID Oxide surfaces and ultrathin oxide films*

Michele Riva¹, [Giada Franceschi](#)¹, Markus Kubicek², Xianfeng Hao³, Stefan Gerhold¹, Giada Franceschi¹, Michael Schmid¹, Herbert Hutter², Juergen Fleig², Cesare Franchini³, Bilge Yildiz⁴, and Ulrike Diebold¹

¹ Institute of Applied Physics, TU Wien, Wiedner Hauptstraße 8-10, 1040 Wien, Austria;

² Institute of Chemical Technology and Analytics, TU Wien, Getreidemarkt 9, 1060 Wien, Austria;

³ University of Vienna, Faculty of Physics Center for Computational Material Science, Sensengasse 8, 1090 Vienna, Austria;

⁴ Laboratory of Electrochemical Interfaces, Department of Nuclear Science Engineering, MIT, 77 Massachusetts Avenue, Cambridge, MA 02139, U.S.A

Perovskite oxides are widely used and studied materials for enabling oxygen reduction and evolution reactions, which limit the efficiency of energy conversion technologies, including fuel cells, electrolyzers and photo-/electrochemical water splitting. In solid-state electrochemistry, most often the reactivity on perovskite oxides is interpreted in terms of the availability of surface oxygen vacancies, or the ease of electron transfer. Intriguingly, none of these standard reactivity models consider the role of the precise atomic structure of surfaces.

In the present contribution, I will show that the surface atomic structure can play a crucial role in affecting oxygen exchange on the prototypical perovskite SrTiO₃ [1]. In doing so, we take advantage of our ability to reproducibly and reversibly prepare SrTiO₃(110) with several different surface phases, by adjusting the chemical potential of Sr and Ti [2,3]. All the structures are based on families with $(n \times 1)$ and $(2 \times m)$ symmetries, with their surface layers composed of tetrahedrally-, and octahedrally-coordinated Ti atoms, respectively [4,5]. Using a host of surface science techniques (STM, LEED, XPS, etc.) we find that these structures are remarkably stable under realistic conditions for oxygen-exchange reactions. The ¹⁸O exchange was quantified with two different ion-based spectroscopy techniques, which revealed that the reactivity of these two reconstructions differs by a factor of three.

From DFT calculations and electron spectroscopic measurements we rule out that this difference is due to oxygen vacancies or the variations in work function or surface potential, that would affect the availability of electrons on this material. Instead we find that the interaction with molecular oxygen is determined by the structural details of the surface: Our results reveal the polyhedral flexibility up to the ideal coordination limit as an important and new factor that governs the surface reactivity to oxygen exchange reactions on perovskite oxides [1].

References:

- [1] Riva et al., submit. to Nat. Mater. (2016)
- [2] Wang et al., Appl. Phys. Lett. 100, 051602 (2012)
- [3] Wang et al., Phys. Rev. Lett. 111, 056101 (2013)
- [4] Enterkin et al., Nat. Mater. 9, 245 (2010)
- [5] Wang et al., Nano Lett. 16, 2407 (2016)

Tue-11:20-O-ORGS2 ● Single-molecule electronic study on nanographene

ORGS Organic molecules on solid surfaces

Shintaro Fujii, Manabu Kiguchi

Department of Chemistry, Graduate School of Science, Tokyo Institute of Technology,
2-12-1 W4-10 Ookayama, Meguro-ku, Tokyo 152-8551 (Japan)

Graphene is a zero-gap semiconductor and its low-energy π -state is characterized by electron-hole symmetry and linear conduction and valence bands within the nearest-neighbor tight-binding approximation. The thickness on the atomic scale, high carrier mobility, high thermal conductivity, and ambipolar transfer characteristics make graphene attractive for many electronic applications. However, despite its outstanding properties, one of the hurdles for graphene to be useful as an electronic material is the lack of an electronic gap. One of the ways to open a gap in its electronic spectra is to reduce the width of the graphene [1]. Recent advances in surface chemical reactions allows us to precisely prepare graphene with nanosized widths called graphene nanoribbons (GNRs) [2]. Despite the development of the synthetic method for GNRs, its transport property remains largely unexplored due to the lack of appropriate technology platform to make electronic contact with individual GNRs and measure its electric current.

Here, we present single-molecule transport study on GNRs using scanning tunneling microscopy-based break junction (STM-BJ [3]) technique. The GNRs were prepared by surface assisted polymerization of halogenated acene derivatives on Au(111) 2 (Fig. 1a,b). STM-BJ measurements on individual GNRs revealed that single-molecule junctions were formed between the Au surface and the Au-STM tip, and the individual GNRs were highly conductive (Fig. 1c). Length analysis of the GNRs indicates that prepared molecular junctions correspond to dimer and tetramer of the precursors (Fig. 1d). In summary, the STM-BJ method was applied to clarify the transport property of individual GNRs. Based on the statistical analysis of the single-molecule conductance and the molecular length, it is shown that the individual GNRs consisting of dimer and tetramer of the precursor are highly conductive with the electronic conductance of 0.1 and 0.4 G_0 ($G_0 = 2e^2/h$).

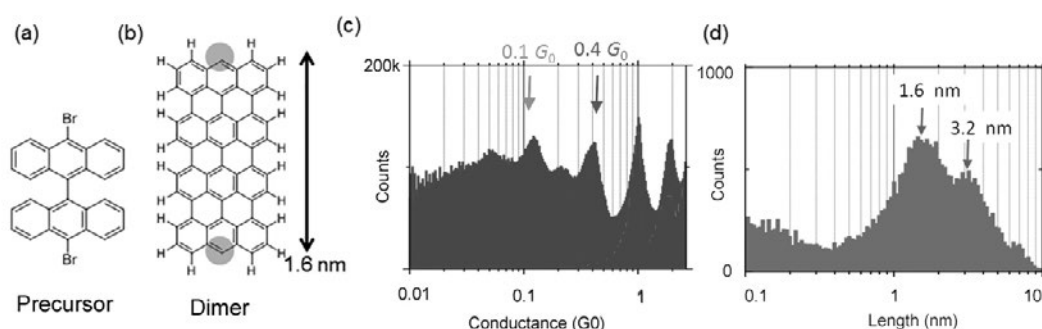


Figure 1. (a) Precursor of GNR (Acene derivative) (b) Dimer of the precursor (c,d) Histograms of single-molecule conductance and molecular length of GNRs ($V = 200$ mV, 16000 spectra).

References:

- (1) Fujita, M.; Wakabayashi, K.; Nakada, K.; Kusakabe, K. *Journal of the Physical Society of Japan* 1996, 65, 1920-1923.
- (2) Cai, J.; Ruffieux, P.; Jaafar, R.; Bieri, M.; Braun, T.; Blankenburg, S.; Muoth, M.; Seitsonen, A. P.; Saleh, M.; Feng, X.; Mullen, K.; Fasel, R. *Nature* 2010, 466, 470-473.
- (3) Fujii, S.; Tada, T.; Komoto, Y.; Osuga, T.; Murase, T.; Fujita, M.; Kiguchi, M. *J Am Chem Soc* 2015, 137, 5939-5947.

Tue-14:20-O-BIMS ● Site Correlation of Two-dimensional Cu-Ni Alloys on Ni(110)

BIMS Bimetallic surfaces and alloy nanocrystals

T. Fukuda¹, I. Kishida², K. Umezawa³

¹ Department of Physical Electronics and Informatics, Graduate School of Engineering, Osaka City University, Osaka 558-8585, Japan;

² Department of Mechanical and Physical Engineering, Graduate School of Engineering, Osaka City University, Osaka 558-8585, Japan;

³ Faculty of Liberal Arts and Sciences, Osaka Prefecture University, Sakai 599-8531, Japan

Cu-Ni alloy is an ubiquitous material and it is employed extensively as coinages and pipings known as cupronickel. It has a fcc structure with any fraction of constituents, i.e., an all proportional solid solution. However, the mixing energy for Cu impurity in bulk Ni and vice versa are positive, indicating potential phase separation of constituent elements at low temperatures, known as spinodal decomposition. Of course for bulk alloys marginal diffusion at low temperatures prohibits the decomposition and no clear evidence of the phase separation was reported so far. For surface alloys enhancement of diffusion due to the lower coordination of surface atoms would promote diffusion even at low temperatures and the phase separation will take place. In addition, because individual Cu and Ni can be discriminated by scanning tunneling microscopy (STM), [1] the phase separation would be unambiguously observed. Here we report a positive correlation of Cu and Ni within the $[1-10]$ row in the two-dimensional alloy on the Ni(110) surface and it is a direct evidence of the positive mixing energy between Cu and Ni even for the surface atoms.

Two-dimensional Cu-Ni alloy films were grown by depositing Cu on the Ni(110) surface at moderate temperatures that displaces substrate Ni with impinged Cu and Cu was instead embedded into the top surface layer. No island formation nor bulk diffusion were seen. An STM observation such as shown in Fig. 1 clearly demonstrates individual Cu and Ni as dark and bright sites, respectively. By counting the nearby Cu and Ni for distances up to 10 units cells we could extract the correlation lengths. For the $[001]$ direction no correlation was found, whereas for the close packed $[1-10]$ direction apparent positive correlation was seen and it is depicted in Fig. 2 for Cu. Our results can be compared with the one-dimensional Ising model. From the exact solution of the site correlation as an exchange energy for 1/2 Ising spin, we could draw the Cu-Cu energy of 15.7 meV at the Cu coverage of 0.5.

References:

[1] T. Fukuda, K. Iwamoto, H. Nakayama, and K. Umezawa, Phys. Rev. B 78, 195422 (2008).

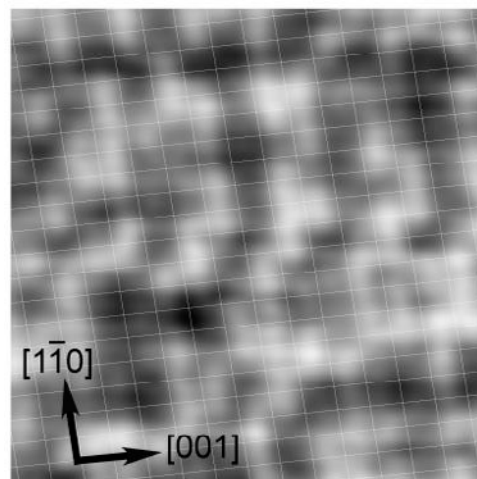


Fig. 1 A typical Cu deposited Ni(110) surface. Cu coverage is 0.49 ML.

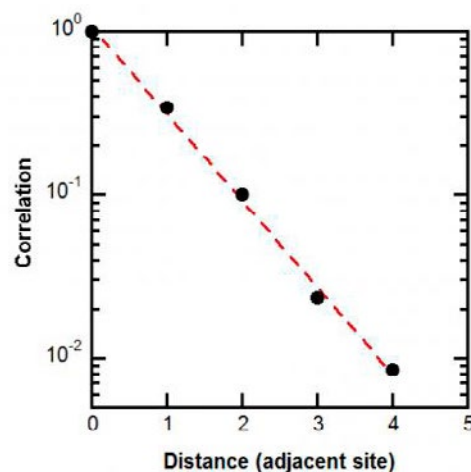


Fig. 2 Site correlation for Cu along the $[1 -1 0]$ direction. Cu coverage is 0.49 ML.

Wed-10:00-O-BIMS ●**Computer simulation of spinodal decomposition in bimetallic nanoparticles***BIMS Bimetallic surfaces and alloy nanocrystals*

Bence Gajdics^{1,2}, **János J. Tomán**¹, **Fanni Misják**³, **György Radnóczy**³, **Zoltán Erdélyi**¹

1 Department of Solid State Physics, University of Debrecen, Debrecen, Hungary;

2 Groupe de Physique des Matériaux, Université de Rouen Normandie, Rouen, France;

3 Research Centre for Energy Research, Hungarian Academy of Sciences, Budapest, Hungary

To investigate stochastic processes on atomic scale, one possible simulation method is the Stochastic Kinetic Mean Field (SKMF) model, which technique is based on the mean-field approach [1]. We introduced a dynamic Langevin noise to make it capable to study processes, such as phase separation and spinodal decomposition. [2,3] Phase separation have been studied in bimetallic Ag-Cu alloy hemispherical particles [4]. The spontaneous formation of two-phase nanoparticles is size- and composition-dependent. Computer simulations by SKMF model confirmed the size-dependency and reproduced the experimentally observed internal structure of the particles. [5]

References:

[1] Martin G., Atomic mobility in Cahn's diffusion model, Phys. Rev. B 41, 2279-2283 (1990)

[2] Erdélyi Z, Pasichnyy M, Bezpalcuk V, Tomán J, Gajdics B, Gusak A, Stochastic Kinetic Mean Field Model, Computer Physics Communications 204:31-37. (2016)

[3] <http://skmf.eu>

[4] Radnóczy G, Bokányi E, Erdélyi Z, Misják F, Size dependent spinodal decomposition in Cu-Ag nanoparticles, Acta Materialia 123:82-89. (2017)

[5] Gajdics B, Tomán JJ, Misják F, Radnóczy Gy, Erdélyi Z, Spinodal decomposition in nanoparticles – experiments and simulation, Manuscript submitted for publication (2017)

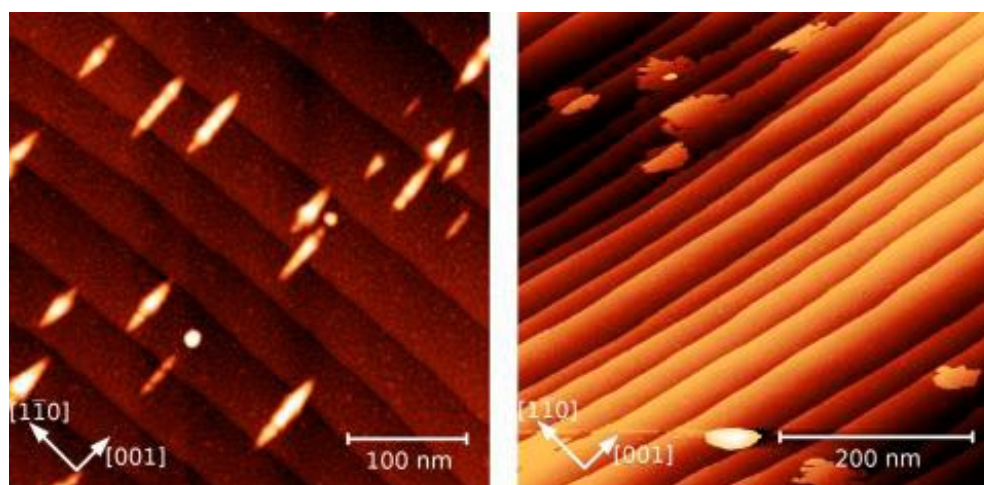
Tue-14:40-O-BIMS ●**Melting processes of 3D metal alloy nanoparticles deposited on surfaces***BIMS Bimetallic surfaces and alloy nanocrystals***Mathias Getzlaff, Hendrik Bettermann***Institute of Applied Physics and Nanotechnology, University of Düsseldorf, Universitätsstr. 1, D-40225 Düsseldorf, Germany*

Nanoparticles with diameters below 100nm exhibit properties which differ from that of macroscopic objects. One important reason for this behavior is due to the high ratio of surface-to-volume atoms. Additionally, most of the properties of nanoparticles significantly depend on their size. For the corresponding determination it is therefore essential to work with size-selected particles. For alloy systems the stoichiometry also plays an important role.

For any technological application nanoparticles have to be embedded into a matrix or deposited on a surface. Generally, a subsequent tempering occurs during the preparation of devices. Due to that reason it is important to know the changes of the nanoparticles' properties like shape induced by the heating process.

In this contribution we report on the temperature dependent shape of size-selected deposited nanoparticles consisting of different stoichiometries of the 3d metals Fe, Co, and Ni. This investigation is carried out by STM. The larger nanoparticles are produced by an arc cluster ion source (ACIS) and mass-filtered by an electrostatic quadrupole. These particles exhibit diameters from 5 to 15 nm. Smaller particles are prepared by a magnetron sputter source and are mass-selected using a quadrupole mass filter. All nanoparticles are prepared and deposited under UHV and softlanding conditions on a W(110) surface. Therefore, oxidation and contamination are avoided. Subsequently, they are tempered *in situ* by a resistive heater integrated in the manipulator. The heating process is varied in final temperature and time. The melting point itself and processes near that temperature are found to depend on the clusters' diameter and the material components inside the particles. The influence of the anisotropy of the W(110) surface also plays an important role.

Two examples are shown in the Figure below. The left one demonstrates the shape after the heating process of Fe₅₀Co₅₀ nanoparticles. It is evident that in this case an uniaxial anisotropy of the melted particles occurs. The right image shows the result after heating Fe₅₀Ni₅₀ particles. Now, a rather different result can be observed with a nearly isotropic melting behavior.



Tue-16:00-O-ORGS ●

Site selective, reversible Diels-Alder reaction between polycyclic conjugated molecules and DB dimers on Ge(001):H**ORGS Organic molecules on solid surfaces**

Szymon Godlewski¹, Marek Kolmer¹, Mads Englund², Hiroyo Kawai³, Rafal Zuzak¹, Aran Garcia-Lekue⁴, Antonio Echavaren⁵, Diego Peña⁶, Dolores Pérez⁶, Enrique Guitián⁶, Christian Joachim⁷, Daniel Sanchez-Portal^{2,4}, Mark Saeys⁸, Marek Szymonski¹

¹ Centre for Nanometer-Scale Science and Advanced Materials, NANOSAM, Faculty of Physics, Astronomy and Applied Computer Science, Jagiellonian University, Łojasiewicza 11, PL 30-348 Krakow, Poland;

² Centro de Fisica de Materiales CSIC-UPV/EHU, Paseo Manuel de Lardizabal 5, E-20018, Donostia-San Sebastian, Spain;

³ Institute of Materials Research and Engineering, 2 Fusionopolis Way, Innovis, #08-03, Singapore 138634, Singapore. E-mail: kawaih@imre.a-star.edu.sg;

⁴ Donostia International Physics Center, Paseo Manuel de Lardizabal 4, 20018, Donostia-San Sebastian, Spain;

⁵ Institute of Chemical Research of Catalonia (ICIQ), Av. Països Catalans 16, 43007 Tarragona, Spain;

⁶ Centro Singular de Investigación en Química Biolóxica e Materiais Moleculares (CiQUS) C/ Jenaro de la Fuente s/n Campus Vida, Universidad de Santiago de Compostela, 15782 Santiago de Compostela, Spain;

⁷ Nanosciences Group & MANA Satellite, CEMES-CNRS, 29 rue Jeanne Marvig, F-31055 Toulouse, France; International Center for Materials Nanoarchitectonics (MANA), National Institute for Materials Science (NIMS), 1-1 Namiki, Tsukuba, Ibaraki 305-0044, Japan;

⁸ Laboratory for Chemical Technology, Ghent University, Technologiepark 914, 9052 Ghent, Belgium

In recent years the on-surface, local chemistry attracts growing attention, inspired by the interest in fundamental processes occurring on surfaces, as well as by potential technological applications. In particular, the controlled and reversible bonding between single molecules and atoms could be advantageous in construction of prototypical molecular switches, rotors and electronic circuits. To control the electronic properties of organic species the isolation from the underlying substrate is required. This could be achieved by application of passivated surfaces that enable retention of originally designed properties [1-3].

Hydrogen passivated silicon and germanium surfaces are of particular interest enabling creation of atomic scale defects – hydrogen vacancies that could interact with organic molecules and form artificial wiring [4-5]. In the presentation we will demonstrate reversible Diels-Alder attachment of prototypical three-branch conjugated molecules to paired surface dangling bonds. We will show that molecules initially undergo the [4+2] cycloaddition forming chemical bonds with the unsaturated surface dangling bonds [6].

Further, it will be discussed that the bonds could be broken and restored using the low temperature scanning tunnelling microscope. We will demonstrate that at low temperature the molecules located on surface dangling bonds could be switched between the chemisorbed configuration and the physisorbed one held by van der Waals interactions only. Interestingly, the molecules adsorbed in the latter configuration could be controllably switched rotationally with the STM tip, which constitutes the first molecular switch on a passivated surface [7]. Further it will be shown that by tuning the structure of the molecules the attachment geometry could be controlled with high selectivity. Finally we will introduce prospects for utilization of the control over connecting individual molecules with surface single atoms.

This research was supported by the National Science Centre, Poland (contract no. UMO-2014/15/D/ST3/02975) and the 7th Framework Programme of the European Union Collaborative Project PAMS (contract no.610446).

References: [1] S. Godlewski et al. ACS Nano 7, 10105 (2013). [2] A. Bellec et al. Nano Lett. 9, 144 (2009). [3] S. Godlewski et al. Phys. Chem. Chem. Phys. 18, 3854 (2016). [4] M. Kolmer et al. Phys. Rev. B 86, 125307 (2012). [5] M. Kolmer et al. Nanoscale 7, 12325 (2015). [6] S. Godlewski et al. Phys. Chem. Chem. Phys. 18, 16757 (2016). [7] S. Godlewski et al. ACS Nano 10, 8499 (2016).

Tue-11:40-O-ORGS1 ● Molecular Topology and Metal/Organic Interfaces

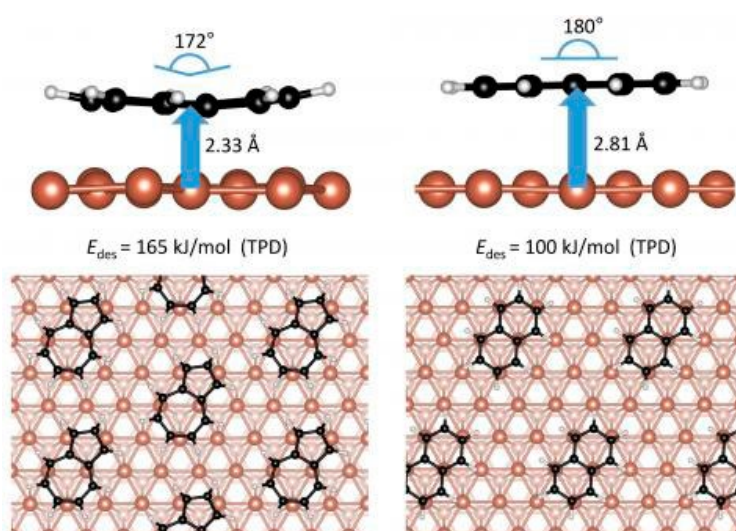
ORGS Organic molecules on solid surfaces

Benedikt P. Klein¹, J. Michael Gottfried¹, Nadine van der Heijden², Claudio K. Krug¹, Maik Schöniger¹, Phil Rosenow¹, Martin Schmid¹, Ralf Tonner¹, Ingmar Swart²

¹ Fachbereich Chemie, Philipps-Universität Marburg, Germany;

² Debye Institute for Nanomaterial Science, Utrecht University, The Netherlands

Interfaces between molecular organic semiconductors and metallic electrodes play a crucial role in the performance of organic electronic devices [1]. The understanding of their chemical, electronic and geometric structure is indispensable for the control of key parameters such as charge injection rates, which need to be optimized for the further rational development of organic electronics. Accordingly, model metal/organic interfaces with aromatic molecules have been a major research topic during the past decade. Up to now, the focus has been on aromatic systems with alternant topology such as pentacene. They typically have a uniform charge distribution and highly delocalized frontier orbitals. In contrast, aromatic systems with non-alternant topology have non-uniform charge distributions, which can result in considerable in-plane dipole moments, and more localized frontier orbitals. They also violate the Coulson-Rushbrooke pairing theorem and thus have shifted valence levels compared to isomers with alternant topology. Here, we present the first systematic surface-science studies of a non-alternant aromatic molecule. In particular, we focus on bicyclo[5.3.0]decapentaene (azulene) as the non-alternant counterpart of naphthalene on Cu(111) and Ag(111). On the basis of extensive NEXAFS, PES, TPD, nc-AFM and STM data, we show that the non-alternant topology results in much stronger and more localized interaction with metal surfaces, especially in the case of Cu(111). Complementary periodic DFT calculations provide insight into the surface chemical bond and charge redistribution between surface and molecule. A major part of the localized interaction is the donation of electron density into the molecular LUMO. This leads to in-plane and out-of-plane deformations of the adsorbed non-alternant system, while the alternant isomer is less distorted.



References:

- [1] J. M. Gottfried, Quantitative Model Studies for Interfaces in Organic Electronic Devices, *New J. Phys.* 18 (2016) 113022.

Thu-9:00-O-CATH ●**Hydrogen-induced crystal reshaping and edge vacancy formation in MoS₂ catalyst particles on Au(111)***CATH Catalytic 2D-model studies under high pressures*

[Signe S. Grønberg](#), [Norberto Salazar](#), [Albert Bruix](#), [Jonathan Rodriguez-Fernandez](#),
[Sean D. Thomsen](#), [Bjørk Hammer](#), [Jeppe V. Lauritsen](#)

iNANO, Aarhus University, Denmark

MoS₂ nanoclusters compose the active phase of the hydrodesulfurization catalyst which enables sulfur removal from crude oil. New legislations on sulfur impurity levels in diesel in EU and US demands still lower sulfur content which increases the requirements for even more effective catalyst. The key to increase the catalytic activity is to understand the catalytic mechanism which has been the subject of extensive studies during the preceding decades.

Scanning tunneling microscopy (STM) is an outstanding tool for investigating atomic scale morphology of MoS₂ based nanoclusters in model systems under ultra-high vacuum (UHV) conditions. Under real catalytic conditions, however, the catalyst functions under high temperatures and high pressure of H₂ (300–400 °C, 50–100 bar), conditions which rules out the usage of any scientific characterization technique on the working industrial catalyst. This leaves us with some open questions: Is the structure of the nanoclusters observed under UHV in fact representative for real catalyst under the industrial working conditions? Does the edge structure, stoichiometry or even the entire particle shape change under these reductive conditions?

In this study we report STM studies of structural changes of a model system of Au-supported MoS₂ nanoparticles(1) after exposure to a post-synthesis anneal in a H₂ atmosphere of 10⁻⁴ mbar at 400 °C to mimic the conditions present in the real catalyst. In spite of the still relatively low pressure these conditions turn out to be sufficient for the implementation of interesting morphology changes. Through atomic resolved STM images we find that the reductive conditions indeed change the equilibrium shape of the triangular MoS₂ nanocluster into a truncated triangular to hexagonal shape, introducing a new edge termination (S-edge) to the cluster. This suggests that the S-edge is relatively more stable under reductive conditions resulting in a post-synthesis change in cluster shape. Furthermore the original shape can be partly restored by subsequent H₂S anneal.

In addition we study Co promoted MoS₂-based nanoclusters (CoMoS) under same conditions. CoMoS is the catalytic active phase used in the industry as it is more catalytic active than pure MoS₂. The as-synthesized hexagonal CoMoS nanoclusters shows no clear change of shape from the H₂ anneal, however the appearance of the S-edge of the CoMoS nanocluster changes drastic which is addressed to partial removal of sulfur from the S-edge(2). Catalytically this is a very interesting observation as such reduced edges contain more coordinatively unsaturated sites which are believed to play an essential role for the catalytic activity.

Our study hereby reveals the occurrence of interesting changes of cluster morphology under hydrogen exposure at elevated temperature. These changes may be crucial for a correct description of the catalytic mechanism.

References:

- [1] S. Helveg, J. V. Lauritsen, E. Lægsgaard, I. Stensgaard, J. K. Nørskov, B. S. Clausen, H. Topsøe and F. Besenbacher. *Physical Review Letters* 84, 951 (2000).
- [2] A. Bruix, J. V. Lauritsen, B. Hammer, *Faraday Discussion Catalysis* 2016.

Mon-15:20-O-NAEX ●**Seeing is believing: atomic-scale imaging of catalysts under reaction conditions***NAEX Novel advancement of experimental methods*

Irene M.N. Groot

Leiden Institute of Chemistry, Leiden University, the Netherlands

The atomic-scale structure of a catalyst under reaction conditions determines its activity, selectivity, and stability. Recently it has become clear that essential differences can exist between the behavior of catalysts under industrial conditions (high pressure and temperature) and the (ultra)high vacuum conditions of traditional laboratory experiments. Differences in structure, composition, reaction mechanism, activity, and selectivity have been observed. These observations indicated the presence of the so-called pressure gap, and made it clear that meaningful results can only be obtained at high pressures and temperatures. However, most of the techniques traditionally used to study catalysts and their reactions were designed to operate under (ultra)high vacuum conditions. To bridge the pressure gap, the last years have seen a tremendous effort in designing new instruments and adapting existing ones to be able to investigate catalysts *in situ* under industrially relevant conditions.

In this talk, I will give an overview of the *in situ* imaging techniques we use to study the structure of model catalysts under industrial conditions of atmospheric pressures and elevated temperatures. We have developed set-ups that combine an ultrahigh vacuum environment for model catalyst preparation and characterization with a high-pressure flow reactor cell, integrated with either a scanning tunneling microscope or an atomic force microscope. With these set-ups we are able to perform atomic-scale investigations of well-defined model catalysts under industrial conditions. Additionally, we combine the structural information from scanning probe microscopy with time-resolved mass spectrometry measurements on the gas mixture that leaves the reactor. In this way, we can correlate structural changes of the catalyst due to the gas composition with its catalytic performance. Furthermore, we use other *in situ* imaging techniques such as transmission electron microscopy, surface X-ray diffraction, and optical microscopy, all combined with mass spectrometry.

This talk highlights a short overview of the instruments we developed and illustrates their performance with results obtained for different model catalysts and reactions. As a proof of principle, results for the fruit fly of surface science, i.e. CO oxidation, will be shown. But additionally, results for more complex reactions such as NO oxidation and reduction, Fischer-Tropsch synthesis, and hydrodesulphurization will be discussed.

Thu-10:40-O-CATH ●***In-situ study of the oxidation of Cu(100) by CO₂******CATH Catalytic 2D-model studies under high pressures***

[Benjamin Hagman](#)¹, [Alvaro P. Borbon](#), [Andreas Schaefer](#)¹, [Lindsay Merte](#)³, [Mikhail Shipilin](#)¹, [Chu Zhang](#)¹, [Ethan Crumlin](#)⁴, [Hendrik Grönbeck](#)², [Edvin Lundgren](#)¹, [Johan Gustafson](#)¹

¹ Lund University, Sweden;

² Chalmers University of Technology, Sweden;

³ MAX IV Laboratory;

⁴ Lawrence Berkeley National Laboratory;

In the light of the increasing CO₂ levels in the atmosphere and its relation to global warming, an interest to achieve a carbon-neutral society has risen. A promising approach for this is to recycle CO₂ instead of releasing it into the atmosphere. Due to the inertness of CO₂, this is a rather difficult task, but already today, industrial production of methanol is performed over Cu-based catalysts with CO₂ as the main source of carbon. However, as for many other catalytic reactions, the fundamental knowledge about this process is limited. The present contribution will discuss the interaction of CO₂ with Cu(100). We observe Cu oxide formation as we expose the Cu(100) surface to CO₂, indicating the CO₂ dissociate and desorb as CO, leaving atomic oxygen at the surface. We see a change of the CO₂ dissociation as the oxygen coverage approach 0.25 ML.

We will present a combined APXPS and DFT study of dissociative adsorption of CO₂ on Cu(100) and compare the resulting structures with those formed by exposure to O₂. We have followed the evolution of the O 1s signal in situ as the surface was exposed to 300 mTorr CO₂ at sample temperatures of 100°C and 200°C. At lower exposures, a peak towards lower binding energy is observed. As the exposure is increased a new component at higher binding energy is observed, which increases in intensity while the low binding energy component gradually disappears. We assume that the difference in binding energy comes from a change in adsorption site for the surface oxygen. If Cu(100) is exposed to O₂, the oxygen will adsorb at the four-fold hollow sites at low coverage¹. At an increasing coverage, however, this surface becomes unstable, and the will gradually reconstruct into a (2√2x√2)R45° missing-row structure, where every fourth Cu row in either [010] or [001] direction is removed from the surface layer¹. This structure is complete at a coverage of 0.5 ML. For XPS, it has previously been found that the O 1s peak, corresponding to chemisorbed O, shifts gradually towards higher binding energy with increasing oxygen coverage. This is interpreted as different adsorption geometries of the oxygen in the reconstructed and unreconstructed surface². By comparing the oxidation with CO₂ and O₂, we propose that the origin of the growth of the higher binding energy component is that the oxygen atoms changes from being 4-fold to 3-fold coordinated to Cu atoms.

For the adsorption process, we see a decrease in the oxygen uptake adsorption rate as the coverage approaches 0.25 ML. Our DFT results suggest that CO₂ can adsorb and dissociate on the clean surface, but not on the (2x2) structure, which is the most stable structure at an O coverage of 0.25 ML. This disagrees with our experimental results, where the saturation coverage is 0.5 ML. However, the CO₂ can dissociate at a coverage above 0.25 ML if there are patches of oxygen deficient copper surface, which could be realized by oxygen clusters of a denser c(2x2) structure and oxygen deficient regions in-between. B. Eren, et. al., observe a similar phenomenon, at room temperature, as they saw that at ~1/3 ML the surface becomes poisoned by the atomic oxygen on the surface³.

References:

- [1] C. Gattinoni, A. Michaelides, Atomistic details of oxide surfaces and surface oxidation: the example of copper and its oxides, *Surf. Sci. Rep.*, 2015, 70, 424-447.
- [2] H. Tillborg, et al., O/Cu(100) studied by core level spectroscopy, *Surf. Sci.*, 1992, 270, 300-304.
- [3] B. Eren, et al., Dissociative Carbon Dioxide Adsorption and Morphological Changes on Cu(100) and Cu(111) at Ambient Pressures, *J. Am. Chem. Soc.* 2016, 138, 8207–8211.

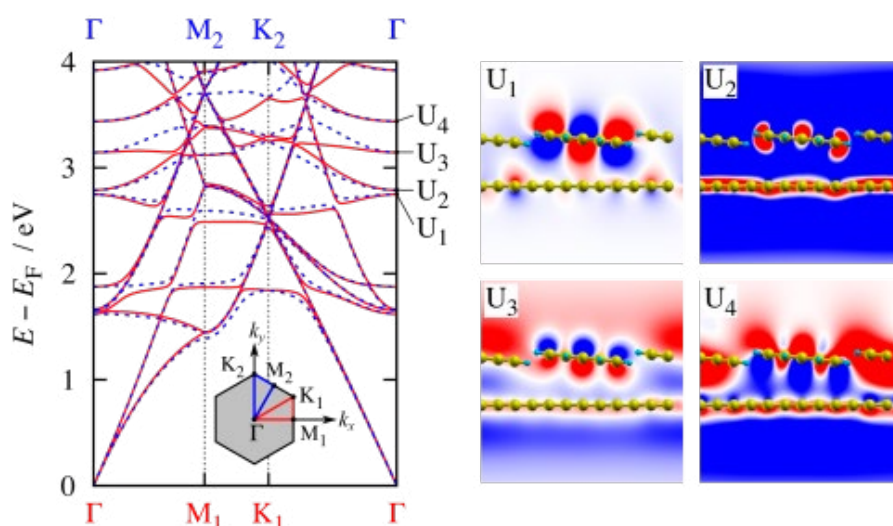
Tue-17:00-O-ORGS ●

Interlayer states induced by image potential states in naphthalene on graphene

ORGS Organic molecules on solid surfaces

Yuji Hamamoto¹, Sasfan Arman Wella¹, Hiroyuki Sawada¹, Nana Kawaguchi², Fahdzi Muttaqien¹, Kouji Inagaki¹, Ikutaro Hamada¹, Yoritada Morikawa¹¹ Department of Precision Science and Technology, Graduate School of Engineering, Osaka University² Department of Applied Chemistry, Graduate School of Engineering, Osaka University

The image potential states (IPSs) characterized by a Rydberg series of unoccupied states appear universally on metal surfaces. In particular, the IPSs induced on graphene play an essential role in the emergence of interlayer states with a nearly-free-electron feature in a variety of graphitic materials such as graphite, carbon nanotube bundles and C60 fullerite solids. Here we theoretically demonstrate that the concept of the IPS-derived interlayer states is also applicable to the problems of molecular adsorption on solid surfaces, taking naphthalene on graphene as an example. Experimentally, the adsorption of naphthalene on highly oriented pyrolytic graphite (HOPG) has been investigated intensively thus far. Recent scanning tunneling microscopy (STM) measurements have revealed that the adsorbed naphthalene form a well-ordered superstructure, in which each molecule is tilted with respect to the surface [1]. Moreover, the results of angle-resolved two-photon photoemission spectroscopy suggest that the naphthalene adsorption has little influence on the transport properties of the lowest IPS [2]. To elucidate the origin of these peculiar behaviors, we investigate the geometrical and electronic structures of naphthalene on graphene from first principles using the van der Waals density functional method [3]. We show that the naphthalene molecules are stabilized by forming a superstructure with the $2\sqrt{3}\times 2\sqrt{3}$ periodicity and a tilted adsorption structure, in good agreement with the STM results on HOPG. More intriguingly, our results predict that intermolecular interaction induces IPS-like states on the naphthalene overlayer, which are quite analogous to the graphene IPSs. In the adsorbed system, the naphthalene IPSs hybridize with the IPSs derived from graphene to form interlayer states with anisotropic effective mass reflecting the molecular structure of adsorbed naphthalene. By using STM simulations, we also show that one of the hybrid IPSs manifest itself as a set of oval protrusions in the STM image, which is similar to an experimental result on HOPG previously attributed to the LUMO of naphthalene [1].



References:

- [1] T. Yamada, Y. Takano, M. Isobe, K. Miyakubo, T. Munakata, Chem. Phys. Lett. 546, 136 (2012).
- [2] T. Yamada, M. Isobe, M. Shibuta, H. S. Kato, and T. Munakata, J. Chem. Phys. C 118, 1035 (2013).
- [3] M. Dion, H. Rydberg, E. Schröder, D. C. Langreth, and B. I. Lundqvist, Phys. Rev. Lett. 92, 24601 (2004); I. Hamada, Phys. Rev. B 89, 121103(R) (2014)

Tue-17:00-O-OXID ●

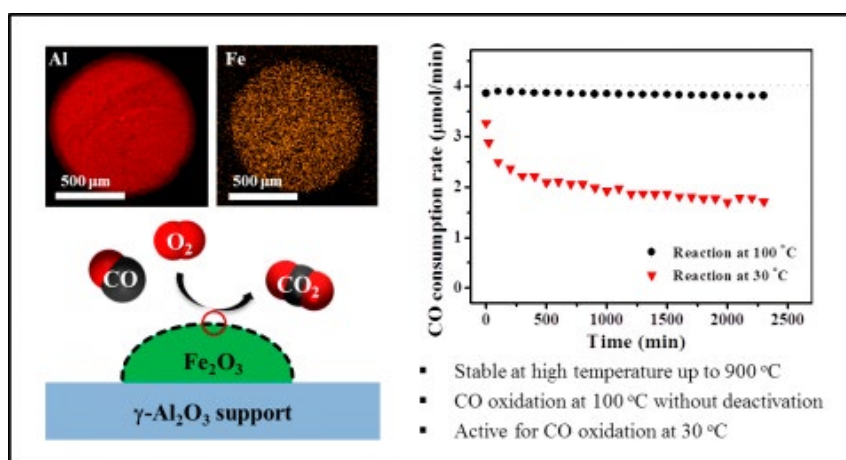
Low temperature CO oxidation catalyzed by iron oxide nanoparticles decorating internal part of mesoporous alumina bead*OXID Oxide surfaces and ultrathin oxide films*

Sang Wook Han¹, Il Hee Kim¹, Ho Jong Kim¹, Byeong Jun Cha¹, Chan Heum Park¹,
Jae Hwan Jeong¹, Tae Gyun Woo¹, Hyun Ook Seo^{2*}, Young Dok Kim^{1*}

¹ Department of Chemistry, Sungkyunkwan University, 16419 Suwon, Republic of Korea;

² Department of Chemistry and Energy Engineering, Sangmyung University, 03016 Seoul, Republic of Korea

Using a chemical vapor deposition method with regulated sample temperatures under atmospheric conditions, we were able to deposit iron oxide nanoparticles with a lateral size of less than 1 nm at the internal part of a mesoporous Al_2O_3 bead (size of ~ 1 mm). The iron oxide-deposited Al_2O_3 catalyst showed a CO oxidation activity even at room temperature. This catalyst did not show significant deactivation at 100 °C with increasing reaction time. and the catalyst showed high activity for CO oxidation even after harsh thermal treatment at ~ 900 °C, (i.e., the structure of the catalysts could be maintained under very harsh treatment conditions). We show that our catalysts have the potential for application as oxidation catalysts in industrial processes due to the simplicity of their fabrication process as well as the high and stable catalytic performance.



Tue-16:20-O-ELCH ●

In-situ X-ray scattering: nano-structured aluminum oxides**ELCH Electrochemistry at surfaces**

G.S. Harlow¹, N.A. Vinogradov², R. Felici³, F. Carla³, J. Evertsson¹, L. Rullik¹, W. Linepé¹, E. Lundgren¹

¹ Division of Synchrotron Radiation Research, Lund University, SE-22100 Lund, Sweden;

² MAX IV Laboratory, SE-22594, Lund, Sweden;

³ ESRF – The European Synchrotron, 71 Avenue des Martyrs, 38000 Grenoble, France

Traditional surface science studies have been quite successful in determining several surface structures for alumina films, in particular those grown on NiAl, where the bulk structure consists of a combination of several building blocks but the surface Al atoms are found to occupy sites with either tetrahedral or pyramidal coordination [1]. However, the naturally forming ‘native oxide’ layers are found to be largely amorphous. The thickness of these layers can be increased electrochemically, i.e. by the industrial process of anodization, and to some extent the degree of crystallinity found depends on the applied voltage [2]. This type of oxide layer is called an anodic barrier layer and forms in neutral type electrolytes. In acidic electrolytes a porous oxide film is found, in which case the oxide has many nanometer sized pores, the basis for most industrial aluminum coloring. Furthermore, under certain conditions these pores are found to be self-ordering [3]. They form hexagonal arrays and the pore diameter can be tuned by changes in potential, making excellent nanoscale templates.

We have investigated the formation and self-ordering behavior of porous type anodic alumina films *in situ*, using Grazing Transmission Small-Angle X-Ray Scattering (GTSAXS). We observe that the in-plane arrangement of the nanopores is independent of substrate crystallographic orientation whereas the oxide growth rate is not. The self-ordering behavior is studied in a variety of electrolytes and at several potentials in-order to explore the dynamics of self-ordering both below and above the breakdown potential (UB) at which the optimal ordering is achieved [4]. It is also possible to follow the chemical etching of the oxide (pore widening) and subsequent metal deposition within the nanopores. This experimental approach can be applied to the study of a large variety of electrochemically produced materials such as magnetic nanowires, novel solar cell designs and catalysts.

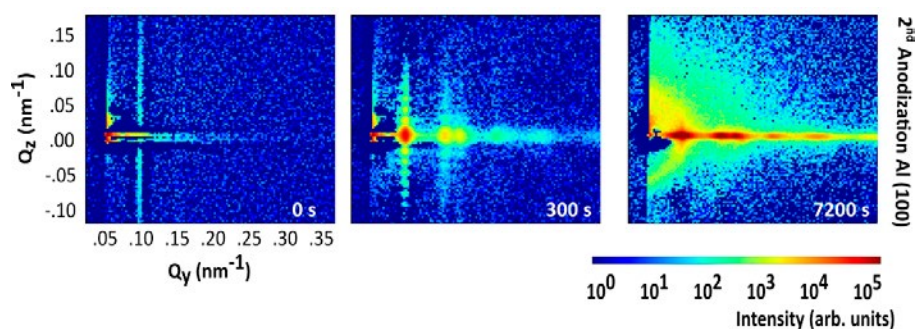


Fig. 1: Time evolution of the GTSAXS pattern during a second anodization of a Al(100) substrate aluminum.

References:

- [1] G. Prevot, et al. Phys. Rev. B, 85, 205450 (2012)
- [2] J.W. Diggle, et al. Chem. Revs., 69(3), 365 (1969)
- [3] H. Masuda, K. Fukuda, Science. 268, 1466–1468 (1995)
- [4] Chu S.Z, et al. A. J. Electrochem Soc., 153, B384 (2006)

Tue-17:20-O-ORGS ●

Graphene functionalized with electron acceptor molecules*ORGS Organic molecules on solid surfaces*

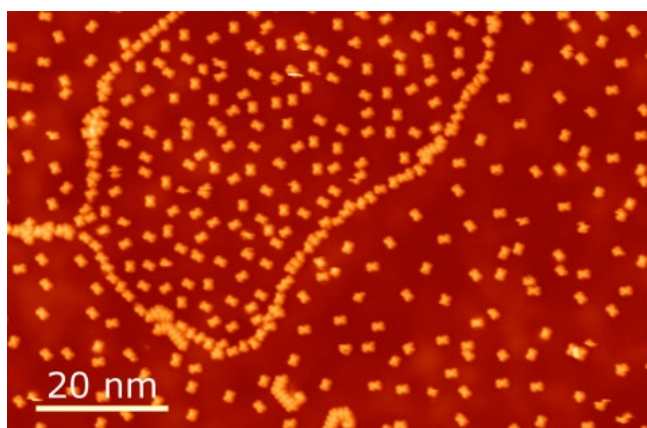
[Rishav Harsh](#)¹, [C. Chacon](#)¹, [V. Repain](#)¹, [Y. Girard](#)¹, [A. Bellec](#)¹, [S. Rousset](#)¹, [F. Joucken](#)²,
[J. Lagoute](#)¹

¹ *Laboratoire Matériaux et Phénomènes Quantiques, UMR 7162 CNRS/Université Paris Diderot, Paris, France;*

² *Research Center in Physics of Matter and Radiation (PMR), Université de Namur, Namur, Belgium*

Graphene exhibits exceptional electronic, thermal and mechanical properties. The control of its physical properties is a major challenge for the realization of future graphene based components. In this context, the functionalization with organic molecules has gained considerable attention. This functionalization can be covalent or non-covalent. The latter is based on the interaction between the pi-electrons of graphene and physisorbed molecules. In that context, electron acceptor and electron donor molecules have been studied as they are expected to lead to a tunable electronic doping of graphene. The molecule/graphene interaction is driven by the electronic interaction but also the structural orientation and organization of the molecule. The extent of pi-interaction between graphene and the guest molecule depends on the nature of substrate underneath graphene, inter-molecule interaction energy, surface morphology and defects present within.

Here, we study a model system of an electron acceptor type molecule (F4-TCNQ) on multilayer graphene grown on Silicon Carbide. We use scanning tunneling microscopy and spectroscopy at 5 K under ultra-high vacuum conditions to systematically study the coverage dependence of the assembly of molecules on graphene as well as their electronic energy levels. Despite a weak molecule-graphene interaction, series of experiments performed with different amounts of molecule coverage suggest an influence of the surface structure (moiré, defects) on the molecular arrangement. Moreover, scanning tunneling spectroscopy (STS) reveal a shifting of the energy levels for the molecular states depending on the local organization and inter-molecule interaction.



Thu-14:20-O-CATH ●**Combining high energy X-Ray diffraction techniques with LASER-induced fluorescence in operando catalysis****CATH Catalytic 2D-model studies under high pressures**

[Uta Hejral](#)¹, [J. Gustafson](#)¹, [S. Albertin](#)¹, [O. Balmes](#)², [J. Zhou](#)³, [T. Wiegmann](#)^{4,5}, [J. Drnec](#)⁴, [S. Blomberg](#)¹, [M. Shipilin](#)¹, [S. Pfaff](#)³, [J. Zetterberg](#)³, [E. Lundgren](#)¹

¹ Division of Synchrotron Radiation Research, Lund University, Lund, Sweden;

² MaxIV Laboratory, Lund, Sweden;

³ Division of Combustion Physics, Lund University, Lund, Sweden;

⁴ Beamline ID31, European Synchrotron Radiation Facility (ESRF), Grenoble, France;

⁵ Institute of Experimental and Applied Physics, Kiel University, Kiel, Germany;

Catalysts are widely employed in fuel cells, vehicle exhaust control systems and chemical industry. To improve their performance, the interplay between catalyst structure, the surrounding gas phase and catalytic activity needs to be understood.

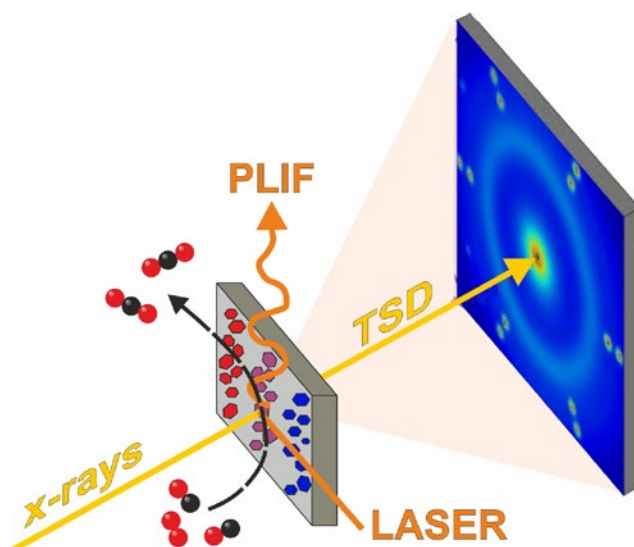
High Energy Surface X-Ray Diffraction (HESXRD) is a powerful technique that allows for studying the catalyst structure during reaction conditions with sub-second time resolution [1, 2]. Planar Laser Induced Fluorescence (PLIF), on the other hand, yields direct information on the gas composition close to the catalyst surface and hence spatially resolves its catalytic activity [3]. In previous experiments we have successfully combined HESXRD and PLIF, but were greatly limited in parameter space due to the alignment sensitivity of HESXRD, which makes the combination of both techniques difficult and a ramping of temperature – an essential variable to vary when mimicking realistic reaction conditions – impossible.

Transmission Surface Diffraction (TSD) is a novel and promising operando technique which provides with μm spatial resolution information on sample structures in a LEED-like manner [4]. Besides, its reduced sensitivity to sample alignment makes it very attractive for its combination with PLIF, which will allow the direct correlation between catalyst structure and catalytic activity also during harsh reaction conditions.

Here we present the first data obtained from TSD during catalytic CO oxidation on model catalyst systems. We compare them to previous results obtained from HESXRD and discuss future possibilities arising from the combination of TSD and PLIF.

References:

- [1] High-energy surface x-ray diffraction for fast structure determination, J. Gustafson et al., *Science* 343, 758 (2014).
- [2] Tracking the Shape-Dependent Sintering of Platinum-Rhodium Model Catalysts under Operando Conditions, U. Hejral et al., *Nature Comm.* 7, 10964 (2016).
- [3] 2D and 3D Imaging of the Gas Phase close to an Operating Model Catalyst by Planar Laser Induced Fluorescence, S. Blomberg et al., *J. of Phys.: Condens. Matter* 28, 453002 (2016).
- [4] Transmission Surface Diffraction for Operando Studies of Heterogeneous Interfaces, F. Reikowski et al., *J. Phys. Chem. Lett.* 8, 1067 (2017).



Tue-10:00-O-CORR ● H adsorption studies on the Zr(0001) surface

CORR Corrosion at atomic level

[Katerina Horakova](#)¹, [Stanislav Cichon](#)¹, [Jan Lancok](#)¹, [Irena Kratochvilova](#)¹, [Vladimir Chab](#)¹, [Petr Sajdl](#)², [Luca Floreano](#)³, [Alberto Verdini](#)³, [Marcos Dominguez Rivera](#)^{1,3}

¹ Institute of Physics, the Czech Academy of Sciences, 182 21 Prague 8, Czechia;

² University of Chemistry and Technology Prague, 166 28 Prague 6, Czechia;

³ CNR-IOM Laboratorio Nazionale TASC, Basovizza SS14, km 163.5, I-34012 Trieste, Italy

Atomically resolved STM (Scanning Tunneling Microscopy) and PES (Photoelectron Spectroscopy) were applied to study a surface of the Zr(0001) single crystal and its interaction with H. Zirconium is used as a getter, for hydrogen storage or in corrosion resistant alloys in nuclear reactors where a failure mechanism was found directly related to the presence of H. To develop new protective coatings of claddings, the knowledge of the Zr H interaction is the crucial step for theory, data interpretation and technology. A limited work is reported on well-defined Zr/H systems due to high affinity of Zr to many gases and other contaminants. Thus, examination of a Zr-H surface under controlled conditions is quite difficult.

In our work, the Zr surface was cleaned with repeating ion bombardment and annealing at 750 °C in UHV conditions. LEED (Low Energy Electron Diffraction) shows simple (1×1) patterns and the Zr 3d peak at 179.1 eV (A in Fig.1a) exhibits a shoulder shifted ~ 0.3 eV to higher BE (Binding Energy). STM images display a high density of steps at terraces ~ 1 μm in diameter. The surface was unstable, full of moving objects. By the minutes, the shoulder is replaced with a new peak B at higher BE (0.6 eV) and the surface becomes more stable.

The surface was exposed to H₂ gas and the Zr 3d peak was monitored. Typically, two new peaks were identified: B and C at 1.4 eV higher BE (Fig.1b). Repeating H exposure, the ratio between the peaks was not reproduced. We selected the B peak intensity as a normalisation factor. Fig. 1 also shows spectra acquired at the beginning and at the end of the 10 hours aging experiment for both surfaces. The clean surface is typical with the metallic peak A and the shoulder originating from surface steps and defects. BE of the shoulder gradually moves to the B peak value interpreted as diffusion of H stored in the bulk to the surface region.

H adsorption produces significant increase of B and C peaks. We suggest that C is due to Zr H bond. With increasing time, the H from Zr H dissolves in the bulk (decrease of C) forming a solid solution reflected with increase of B. It coincides with the increase of A intensity.

The hydrogen content of this probed region is strongly influenced with adsorption of a small amount of Si that erases any signal connected with H. Fig. 2 demonstrates the disappearance of the H induced feature from the valence band of the Zr(0001)-1×1 surface with adsorption of 0.5 ML of Si in a new structure 2√3×2√3. Concurrently, B and C peaks are fully suppressed in the Zr 3d peak envelope.

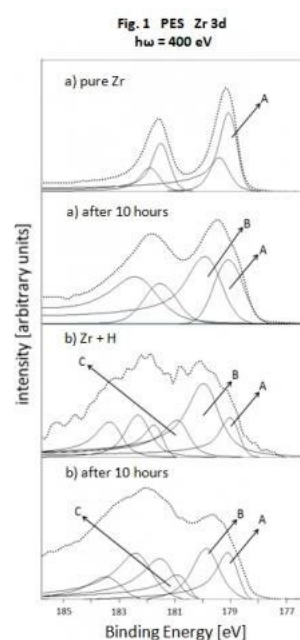


Fig. 1 PES Zr 3d
 $h\nu = 400$ eV

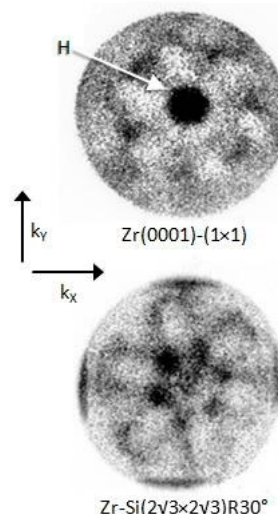


Fig. 2 PES valence band
 $h\nu = 21.2$ eV
BE ~ 1 eV

Tue-10:40-O-ORGS1 ●

On-surface transmetalation of Fe-porphyrin network on Au(111)

ORGS Organic molecules on solid surfaces

Diana Hötger¹, Claudius Morchutt¹, Patrick Alexa¹, Doris Grumelli², Jan Dreiser³, Sebastian Stepanow⁴, Markus Etzkorn¹, Rico Gutzler¹, and Klaus Kern^{1,5}

¹ Max Planck Institute for Solid State Research, 70569 Stuttgart, Germany;

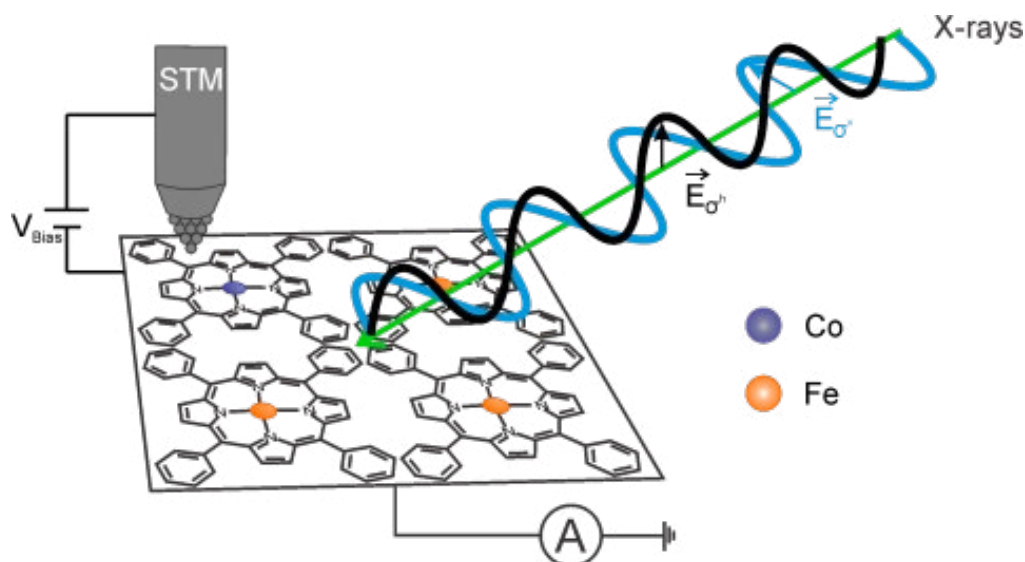
² Universidad Nacional de La Plata – CONICET, 1900 La Plata, Argentina;

³ Paul Scherrer Institute, Swiss Light Source, 5232 Villigen, Switzerland;

⁴ Swiss Federal Institute of Technology Zurich, 8093 Zürich, Switzerland;

⁵ Ecole Polytechnique Fédérale de Lausanne, 1015 Lausanne, Switzerland

Porphyrins are a widely studied molecular class offering a tremendous range of functions in diverse domains such as biologic systems and technologically relevant devices. In particular the metalated state is a suitable building block for nanomaterials used for applications in the fields of catalysis, sensors and (opto)electronics. The metal-organic complex offers a multiplicity of functional groups and metal centers resulting in a large tool box for steering the electronic structure commensurate to the needs of the application. Especially its reactivity, stability and convertibility make it a promising molecule for the use as electrocatalyst.[1,2] On-surface metalation is a routinely used synthesis to create metalloporphyrins under vacuum conditions at the vacuum/solid interface. The predominantly discussed cation insertion into free-base porphyrins at surfaces has recently been extended to metal exchange reactions. Two studies describe the replacement of Ni and Co by Cu, which is supplied through the adatom gas on the copper surface, in ultra-high vacuum.[3,4] A third study describes the exchange at the solid/liquid interface, in which Zn is replaced by Cu.[5]



Here we investigate a self-assembled porphyrin network on Au(111). The utilized metalloporphyrin chelates either Fe or Cu in the tetrapyrrole ring and was functionalized by either phenyl or pyridyl groups at the periphery. In a second step cobalt is sublimed onto the network at room temperature. The effect of cobalt deposition on topography and electronic structure is studied by scanning tunneling microscopy (STM) supported by scanning tunneling spectroscopy (STS) and x-ray absorption spectroscopy (XAS). The topography remains almost unchanged while the electronic structure of the metal centers changes

dramatically. Sublimation of Co spontaneously substitutes Fe/Cu and occupies its place in the tetrapyrrole ring on the Au(111) surface explaining the strong change of the electronic structure. Transmetalation upon cobalt deposition occurs partially in both the phenyl and pyridyl functionalized porphyrin network. The second metal atom is deposited in an active way in contrast to the two published studies making use of the adatom gas of Cu(111) and annealing temperatures to initiate the substitution reaction.[3,4] The back reaction, Co substitution by additionally sublimed Fe is not observed. Transmetalation mechanisms are well-studied in solution but are hardly transferable to on-surface metalloporphyrins due to reduced flexibility. We are proposing a SE2-like transmetalation mechanism involving a cis-transition state involving both metal centers.

References:

- [1] Auwärter, et al.; Porphyrins at interfaces. *Nat. Chem.* 7, 105–120 (2015).
- [2] Gottfried, J. M.; Surface chemistry of porphyrins and phthalocyanines. *Surf. Sci. Rep.* 70, 259–379 (2015).
- [3] Doyle, C. M. et al.; Ni–Cu ion exchange observed for Ni(ii)–porphyrins on Cu(111). *Chem. Commun.* 50, 3447 (2014).
- [4] Shen, K. et al.; On-surface manipulation of atom substitution between cobalt phthalocyanine and the Cu(111) substrate. *RSC Adv.* 7, 13827–13835 (2017).
- [5] Franke, M. et al.; Zinc Porphyrin Metal-Center Exchange at the Solid-Liquid Interface. *Chem. - A Eur. J.* 22, 8520–8524 (2016).

Thu-9:00-O-MOLA ●

Arginine on Cu(110): several adsorption configurations for a single molecule

MOLA Ultrathin two-dimensional molecular self-assembly

Roberta Totani¹, Vincent Humblot¹, Christophe Méthivier¹, Claire-Marie Pradier¹, Hervé Cruguel², Alberto Verdini³, Luca Floreano³, Albano Cossaro³

¹ Laboratoire de Réactivité de Surface - UMR CNRS 7197, Université Pierre et Marie Curie, UPMC Paris 6, 4 place Jussieu, 75252 Paris Cedex 05, France;

² Institut des NanoScience de Paris, Université Pierre et Marie Curie, UPMC Paris 6, 4 place Jussieu, 75252 Paris Cedex 05, France;

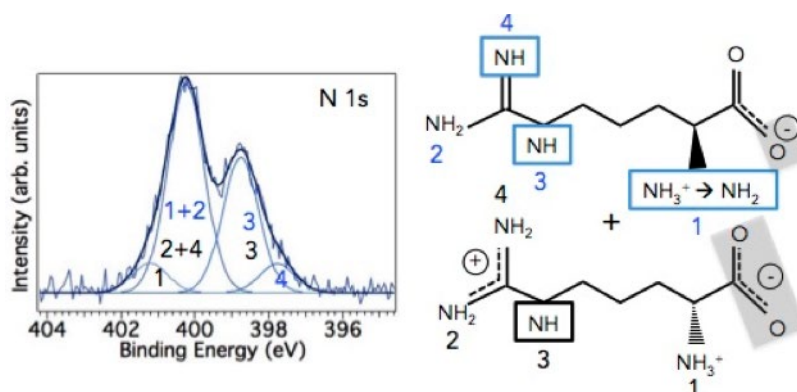
³ CNR-IOM, Laboratorio TASC, Basovizza SS 14, Km 163.5, 34149 Trieste, Italy

The investigation on thin films of biomolecules deposited on metal single crystal surfaces is a key point in the design of biocompatible innovative materials. Studies of amino acids adsorption on metallic single crystals are relevant model studies to understand interfacial processes with occurrence of complex adsorption mechanisms and geometries.

Arginine is an amino acid characterized by a 3-aliphatic carbon side chain and a guanidinium functional group ($\text{HNC}(\text{NH}_2)_2$). Our interest in arginine is motivated by its presence in the tri-peptide RGD (arginine-glycine-aspartic acid), known in the context of biotechnologies for its capacity to promote cell adhesion or other peptides sequences for specific molecular recognition or cell interactions. Therefore RGD is often currently employed for biomaterials functionalization. With the intention of realizing a complete characterization of RGD on a copper surface, we started from the study of the adsorption mechanisms of arginine on a Cu(110) surface, with a conventional surface science approach but with a non-traditional preparation method for the molecular layer. Considering that arginine is a rather delicate molecule and is not easily sublimated in the UHV chamber, an electrospray ionization (ESI) device is used to introduce ionized molecules with no damage.

We have thus combined experimental analyses techniques, such as XPS, STM and NEXAFS together with DFT simulations to investigate the adsorption of arginine/Cu(110). NEXAFS spectra indicate preferential anchoring points of the carboxylate group along the $\langle 110 \rangle$ crystallographic axis, while STM results depict the lack of a long-range order in arginine pattern with a preferential growth direction along the $\langle 110 \rangle$ axis. By means of XPS (Fig.1) and DFT results, we discovered that arginine is present on the surface in different chemical configurations, depending on the protonated/deprotonated state of its carboxylic and amine groups. Since, in turn, the protonation/deprotonation of the different functionalities depends on their interaction with the surface, this indicates that different adsorption configurations characterize arginine molecules on Cu(110). So, even if the interaction with the substrate is strong enough to influence the molecular ordering, the different chemical configurations prevent to establish periodic intermolecular interactions and thus inhibit the creation of a 2D regular pattern.

Figure 1. Left: N 1s XPS spectrum of arginine. Right: different chemical configurations of the adsorbed molecule. Species interacting with the surface are inside boxes or highlighted in grey.



Tue-10:40-O-ORGS2 ●

Electronic structure of Au-C₆₀-Au single molecule junction fixed by current voltage characteristics and thermopower measurement

ORGS Organic molecules on solid surfaces

Yuji Isshiki, Yuki Komoto, Shintaro Fujii, Manabu Kiguchi

Tokyo Institute of technology, Department of Chemistry, Tokyo, Japan

The electronic structure of molecular junctions has significant impacts on their transport properties which have been expected to apply molecular devices such as switching, and transistor devices [1]. Despite the decisive role of the electronic structure, a complete characterization of the electronic structure remains a challenge. This is because there is no straightforward methods of measuring electron structure for an individual molecule trapped in a nanoscale gap between two metal electrodes. Herein, a comprehensive approach to obtain a detailed description of the electronic structure in single molecule junctions based on the analysis of current–voltage (I-V) and thermoelectric characteristics is described. It is shown that the electronic structure of the prototypical C₆₀ single-molecule junction trapped between Au electrodes (Au-C₆₀-Au) can be resolved by analyzing complementary results of the I-V and thermoelectric measurement. The conductance and I-V measurement revealed that the Au-C₆₀-Au single-molecule junction displayed high (H) and low (L) conductance states ($H = 0.033G_0$ and $L = 0.003G_0$) and the high electronic conductance of the H state was owing to a large electronic coupling between the molecule and the Au electrodes. The thermoelectric measurement indicated that the Au-C₆₀-Au single molecule junction possessed a Seebeck coefficient of $-12 \mu\text{V/K}$. By analyzing the complementary I-V and thermoelectric measurement, we found that charge transport was mediated by a LUMO, whose energy level was $+0.5\sim 0.6 \text{ eV}$ above the Fermi level of the Au electrode (Figure 1). By combining the results of the I-V and thermoelectric measurements, the electronic structure of the C₆₀ single-molecule junction was determined.

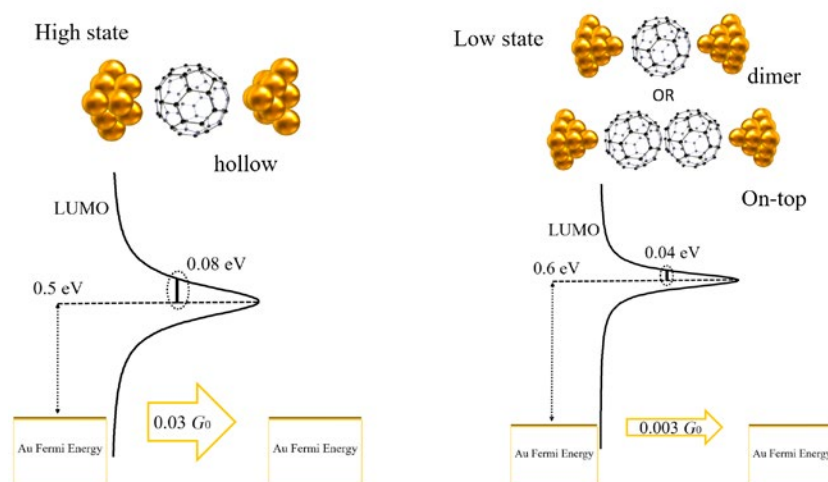


Figure 1. Energy level diagram of the H and L states of the Au-C₆₀-Au single molecule junction. Inset indicates possible structural models (i.e., hollow and on-top adsorption models) of the H and L states

References:

- [1] S. Fujii, T. Tada, Y. Komoto, T. Osuga, T. Murase, M. Fujita, M. Kiguchi, *J. Am. Chem. Soc.* 137 5939-5947 (2015)
 [2] Y. Komoto, Y. Isshiki, S. Fujii, T. Nishino, M. Kiguchi, *Chem. Asia J.* 12, 440-445 (2017)

Wed-16:20-O-BAND ●**Solving mysteries in pure bismuth by quantum confinement***BAND Band structure of solid surfaces*

[Suguru Ito](#)¹, [Ro-Ya Liu](#)¹, [Takashi Someya](#)¹, [Baojie Feng](#)², [Masashi Arita](#)², [Akari Takayama](#)³, [Wei-Chuan Chen](#)⁴, [Takushi Iimori](#)¹, [Hirofumi Namatame](#)², [Masaki Taniguchi](#)², [Cheng-Maw Cheng](#)⁴, [Shu-Jung Tang](#)⁵, [Fumio Komori](#)¹, [Katsuyoshi Kobayashi](#)⁶, [Tai-Chang Chiang](#)⁷, [Iwao Matsuda](#)¹

¹ Institute for Solid State Physics, University of Tokyo; ² Hiroshima Synchrotron Radiation Center;

³ Department of Physics, University of Tokyo; ⁴ National Synchrotron Radiation Research Center;

⁵ Department of Physics and Astronomy, National Tsing Hua University; ⁶ Department of Physics, Ochanomizu University; ⁷ Department of Physics, University of Illinois at Urbana-Champaign

Bismuth (Bi) has been providing an irreplaceable playground in condensed matter physics owing to its several extreme properties such as the huge spin-orbit coupling, the semimetallic bulk with very low carrier densities, and the three-dimensional Dirac-like dispersion. A direct band mapping by angle-resolved photoelectron spectroscopy (ARPES) has revealed many interesting phenomena on Bi. However, because of an uncertainty relation of photoelectrons, ARPES has a clear limitation in measuring three-dimensional bands, which has left some important questions of Bi elusive. In this talk, we introduce how our novel quantum-confinement approach with ARPES can solve mysteries in Bi.

Firstly we describe our method based on our recent result which determined the topology of Bi [1]. Although Bi is a central element in designing topological materials, the topology of its pure crystal has long been controversial. The three-dimensional Dirac-like dispersion of Bi is so sharp against a momentum resolution expected in usual ARPES that the bulk bands have never been clearly detected [2]. This is fatal because the band gap of Bi is very small (~10 meV [3]) and a slight energy shift in bulk bands can easily transform a topologically nontrivial case into a trivial case. Here we overcame the difficulty by simultaneously observing evolutions of surface and quantized bulk bands formed in Bi thin films with increasing thicknesses. Such quantized states are two-dimensional states which can be clearly observed in ARPES but still possess information of the bulk in the evolution against thicknesses. Following the evolutions with analyses on the phase shift of confined wave functions enabled us to precisely determine the connection between surface and bulk bands, which is an unambiguous evidence of the nontrivial topology [1].

Furthermore we apply our approach to another important open question in Bi: a semimetal-to-semiconductor (SMSC) transition in the ultrathin film. A combination between the small carrier densities and quantization of bulk bands can result in the transition [4]. Despite experimental efforts for half a century, the whole picture has still been contentious [5]. The biggest reason is the existence of metallic surface states, which counteract the insulating bulk when a thickness decreases. In addition, a strain effect from the substrate can contribute to the transition but has never been discussed based on experimental results. By explicitly considering these effects, we extend our quantum-confinement approach to reveal a whole picture of the SMSC transition. Especially, after we identify a strain effect from the evolution of surface states, we quantify the influence on the transition by including the relaxation against thicknesses in the phase analyses on quantized levels. These results reveal a microscopic origin of the SMSC transition and provide a firm ground to achieve the consensus view.

References:

- [1] S. Ito et al., Physical Review Letters 117, 236402 (2016).
- [2] Y. Ohtsubo et al., New Journal of Physics 15, 033041 (2013).
- [3] L. Aguilera et al., Physical Review B 91, 125129 (2015).
- [4] V. Sandomirskii, Soviet Physics JETP 25, 101 (1967).
- [5] K. Zhu et al., Physical Review B 94, 121401(R) (2016).

Tue-11:40-O-EG2D ●**Surface reactivity of Au-Ag and Pt-Rh during deNOx reactions studied by field emission techniques***EG2D Epitaxial growth and modification of 2D materials*Luc Jacobs, Cédric Barroo, Natalia Gilis, Sten Lambeets, Eric Genty, Thierry Visart De Bocarmé*Chemical Physics of Materials and Catalysis, Université Libre de Bruxelles, Faculty of Sciences, CP 243, 1050-Brussels, Belgium*

The main objective of this work is the surface characterisation of binary alloys of interest in heterogeneous catalysis, such as AuAg (8,8 at. % of Ag) and PtRh (17,4 at. % of Rh), using field emission techniques during ongoing catalytic reactions. The catalytic properties of these alloys are most promising in the domain of nitrogen oxides abatement (deNOx reactions). This is made possible by the combination of two metals exhibiting intrinsically different properties, giving rise to new interesting catalytic properties compared to those of single metal catalysts.

Tip-samples are produced by electrochemical etching, and characterised with atomic resolution by Field Ion Microscopy (FIM). For this, a series of *in-situ* treatments is necessary to obtain high quality pictures of the samples. Field Emission Microscopy (FEM) is then used to image the sample in real time, during the ongoing processes.

The systems of interest for the deNOx reactions correspond to the $\text{N}_2\text{O}+\text{H}_2/\text{AuAg}$ and $\text{NO}_2+\text{H}_2/\text{PtRh}$ systems. The AuAg system can also be seen as a model reaction to understand the formation of O(ads) species at the surface of Au-based catalysts, important to understand more complex reactions. The reaction dynamics are followed by local changes of brightness reflecting variations in electron emission of the different crystallographic planes. In fact, at constant electric field and temperature, electron emission from the sample depends on the presence or absence of adsorbates.

To study the AuAg system, different ratios of the $\text{N}_2\text{O}/\text{H}_2$ mixture, as well as linear variations in temperature, were applied to the AuAg tips. The dissociation of N_2O and its reaction with H_2 are observed in the temperature range 300–320 K, proving the activity of gold-based catalyst at low temperature. The results suggest a localized dissociative adsorption phenomenon for N_2O and H_2 . The presence of O-enriched zones and neighbouring H-enriched zones lead to the formation of reactive interfaces where the adsorbed species are supposed to react. This forms a pattern which systematically appears with the same 3-fold symmetry as the underlying surface. It seems that the composition of the gas phase does not influence the observed reaction patterns, indicating a strong dependence of the reaction pathway on the state of the surface. O-enriched zones appear darker due to the increased surface work function in the presence of oxygen adsorbates. It has to be noted that dissociative adsorption of N_2O takes place preferentially over the roughest facets, {210}.

In the case of the PtRh system, a NO_2 base pressure is introduced in the reaction chamber and leads to a significant brightness decrease on the FE pattern, indicating NO_2 dissociative adsorption. Gradual increase of H_2 pressure at different temperatures leads to the formation of spikes in the brightness signal, sign of a reactive behaviour. At the temperature of 425 K, self-sustained periodic oscillations can be observed in the brightness signal.

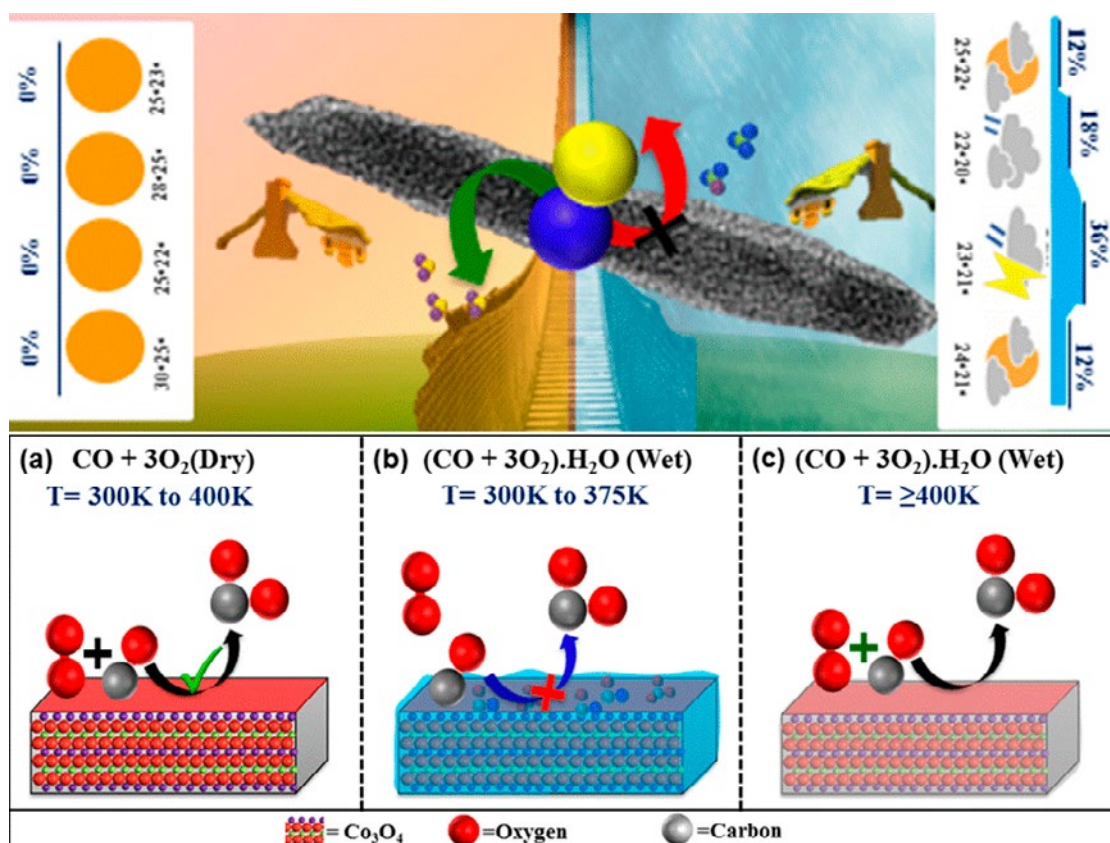
Thu-11:00-O-CATH ●

Near ambient pressure photoelectron spectroscopy studies of CO oxidation on Co_3O_4 surfaces: electronic structure and mechanistic aspects of wet and dry CO oxidation

CATH Catalytic 2D-model studies under high pressures

Ruchi Jain¹, Chinnakonda S. Gopinath^{1,2*}¹ Catalysis Division, National Chemical Laboratory, Dr. Homi Bhabha Road, Pune 411 008, India;² Centre of Excellence on Surface Science, National Chemical Laboratory, Pune 411 008, India

Near ambient pressure photoelectron spectroscopy (NAPPEs) is a powerful tool that is inherently surface sensitive, and oxidation state specific, with the ability to probe sample surfaces at pressures closer to ambient pressure. Catalytic activity, electronic structure and the mechanistic aspects of Co_3O_4 nanorod surfaces has been explored for the CO oxidation in dry and wet atmosphere by NAPPEs with conventional X-ray (Al $k\alpha$) and ultraviolet sources (He-I). Comparative NAPPEs studies enable to understand the elucidation of the catalytic reaction pathway and the evolution of various surface species. Our findings from NAP-UPS results support Co_3O_4 NR as the most active metal oxides for CO oxidation at room temperature in the absence of water vapour. However, in the presence of water vapor the reaction is not active around ambient temperature and up to 375 K due to the surface hydroxylation and associated electronic structure changes.



Presence of water with CO+O₂ plummet the catalytic activity due to the change in electronic nature from predominantly oxide (without water in feed) to few intermediates covered Co₃O₄ surface. The surface OH group hampers catalysis by reducing the active site for reactant (CO) adsorption and creates pseudo three-fold sites which promote the formation of carbonate and formate intermediate. CO oxidation activity is partially regained above 375 K underscores the dissociative water adsorption poisons the surface below 375 K and water desorption above the boiling point leads to activity resumption. This is fully supported by the changes observed in the work function of Co₃O₄ NR in the presence of wet (H₂O+CO+O₂) compared to dry (CO+O₂) reaction conditions. Work function decreases under the wet reaction condition underscores the contaminated surface is more stable than the reactive surface with high work function. Likely, the VB potential shifts depending on the reaction environment underscoring the changes in electronic environment in the presence of reactant species.

References:

- [1] Xie, X.; Li, Y.; Liu, Z.-Q.; Haruta, M.; Shen, W., Low-temperature oxidation of CO catalysed by Co₃O₄ nanorods. *Nature* 2009, 458, (7239), 746-749
- [2] Roy, K.; Vinod, C. P.; Gopinath, C. S., Design and Performance Aspects of a Custom-Built Ambient Pressure Photoelectron Spectrometer toward Bridging the Pressure Gap: Oxidation of Cu, Ag, and Au Surfaces at 1 mbar O₂ Pressure. *J. Phys. Chem. C* 2013, 117, (9), 4717-4726.
- [3] Roy, K.; Gopinath, C. S., UV Photoelectron Spectroscopy at Near Ambient Pressures: Mapping Valence Band Electronic Structure Changes from Cu to CuO. *Anal. Chem.* 2014, 86, (8), 3683-3687.
- [4] Jain, R.; Gnanakumar, E S.; Gopinath, C S.; Mechanistic Aspects of Wet and Dry CO Oxidation on Co₃O₄ Nanorod Surfaces: A NAP-UPS Study. *ACS Omega*, 2017, 2 (3), pp 828–834

Thu-11:40-O-OXID ●**Atomic scale STM and nc-AFM study of the Hematite (012) surface***OXID Oxide surfaces and ultrathin oxide films*

[Zdenek Jakub](#)¹, Florian Kraushofer¹, Magdalena Bichler², Jan Hulva¹, Michael Schmid¹, Ulrike Diebold¹, Peter Blaha², Gareth S. Parkinson¹

¹ Institute of Applied Physics, TU Wien;

² Institute of Materials Chemistry, TU Wien

For its abundance, low cost, stability and environmental benignity, hematite ($\alpha\text{-Fe}_2\text{O}_3$) is a promising material for utilization in a wide range of fields, including as a photoanode for photoelectrochemical water splitting [1]. Although (012) is known to be one of the most stable surfaces of hematite, the atomic-scale structure remains unknown. Here we present the first-ever atomic-scale scanning tunneling microscopy (STM) and non-contact atomic force microscopy (nc-AFM) study of the surface.

Our data suggests that a bulk termination model for the oxidized (1x1) surface is plausible, but images of the reduced (2x1) surface are inconsistent with any of the previously proposed structural models. Based on the experimental data we propose a new model for the (2x1), whose plausibility is supported by our DFT calculations.

We also present the results of H_2O adsorption studies on both surface terminations and discuss the data in the context of previously published results [2].

References:

- [1] Parkinson, G.S., Iron oxide surfaces. Surface Science Reports.
- [2] Henderson, M.A., S.A. Joyce, and J.R. Rustad, Interaction of water with the (1x1) and (2x1) surfaces of alpha-Fe₂O₃(012). Surface Science, 1998. 417(1): p. 66-81.

Tue-14:20-O-EG2D ●

Controlling the growth of Bi(110) and Bi(111) films on an insulating substrate

EG2D Epitaxial growth and modification of 2D materials

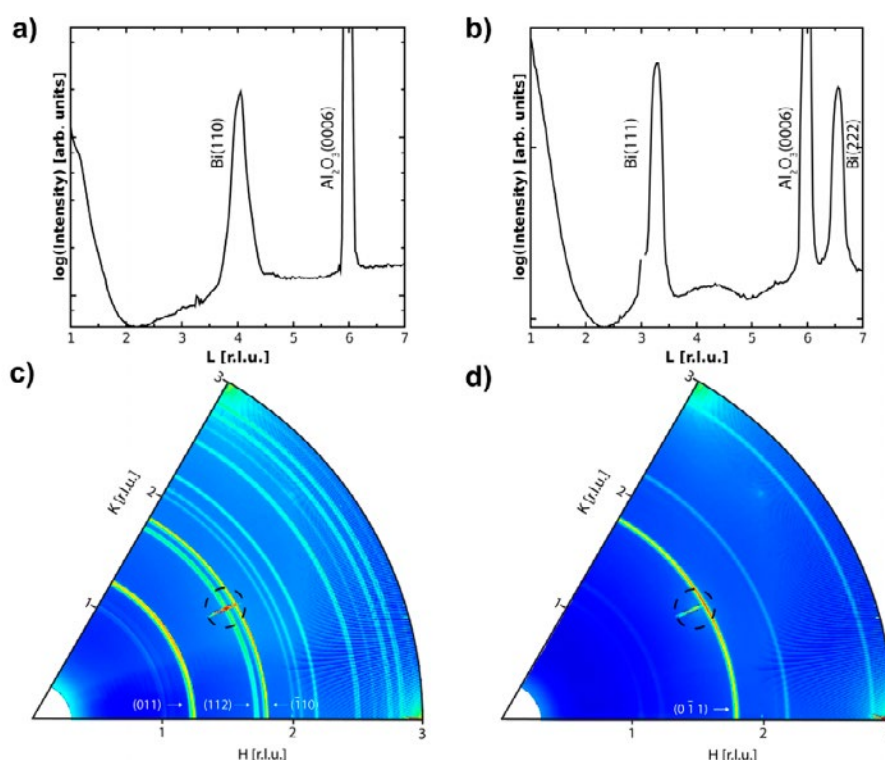
Maciej Jankowski¹, Daniel Kamiński², Kurt Vergeer³, Marta Mirolo¹, Francesco Carla¹, Guus Rijnders³, Tjeerd R J Bollmann³

¹ ESRF-The European Synchrotron, 71 Avenue des Martyrs, F-38000 Grenoble, France;

² Department of Chemistry, University of Life Sciences in Lublin, 20-950, Poland;

³ University of Twente, Inorganic Materials Science, MESA+ Institute for Nanotechnology, PO Box 217, NL-7500AE Enschede, The Netherlands

Nanostructured ultrathin bismuth films [1,2] have attracted a lot of interest as they reveal exotic functional properties that do not exist in bulk. The material properties are advantageous for the realization of e.g. spin based electronic devices, magnetoresistance effects and topological insulators (TI). To develop and optimize TIs towards applications, thin films of high quality are a necessity, as otherwise the exotic electronic properties are hampered by bulk conduction. To minimize the contribution of the substrate, an atomically well defined insulating substrate is essential for both future electronic applications as well as to get a deeper understanding of Bi thin films growth controllability. In this study we demonstrate by Surface X-ray Diffraction (SXRD) the controlled growth of thin Bi(110) and Bi(111) films on such a substrate: atomically smooth insulating sapphire (α -Al₂O₃(0001)).



References:

- [1] E.I. Rogacheva, et al., Appl. Phys. Lett. 82, 2628 (2003).
- [2] Y.W. Wang, et al., Appl. Phys. Lett. 88, 143106 (2006).
- [3] I.K. Drozdov, et al., Nat Phys. 10, 664-669 (2014).
- [4] M. Jankowski, et al., Nanotechnology 28 (2017) 155602.

Thu-14:00-O-SEMI ●**Formation of stable hexagonal (hcp) gold nanostructures in the process of self-assembling on Ge(001) surface***SEMI Semiconductor surfaces and ultrathin layers***B.R. Jany¹, N. Gauquelin², T. Willhammar², M. Nikiel¹, K.H.W. van den Bos², A. Janas¹, K. Szajna¹, J. Verbeeck², S. Van Aert², G. Van Tendeloo², F. Krok¹**¹ Marian Smoluchowski Institute of Physics Jagiellonian University, Lojasiewicza 11, PL-30348 Krakow, Poland;² EMAT University of Antwerp, Groenenborgerlaan 171, BE-2020 Antwerp, Belgium

Nano sized gold has become an important material in various fields of science and technology such as nanoelectronics, catalysis, nanophotonics and medicine, where control over the size and crystallography of the structures is desired to tailor the functionality. The hexagonal closed packed (hcp) structure of gold is a very unique and unusual phase, since gold naturally adopts face centered cubic phase (fcc). The Au/Ge(001) surface itself is also very interesting for the applications of future mono-molecular devices since it may exhibit 1D and 2D conductivity channels in form of atomic chains [1] and subsurface layer [2].

In the presentation, we will report on studies concerning post-annealing induced nanostructures formation after room temperature deposition of thin film of Au on (2x1) Ge(001) in UHV. Deposition of 6 ML of Au by MBE resulted in the formation of a continuous Au overlayer as checked by RHEED to be crystalline. Just after deposition, the samples were post-annealed in UHV to temperatures ranging from 473 K to 773 K with different cooling rates. The self-organized structures, in form of Au nanoislands, were formed due to the surface diffusion of Au adatoms on Au rich surface and Ostwald ripening process [3]. The nanostructures were characterized by EBSD/SEM (Electron Back Scatter Diffraction/Scanning Electron Microscopy) and Atomically resolved HAADF STEM (High Angle Annular Dark Field Scanning Transmission Electron Microscopy), see Fig. 1.

It has been found that there exists preferential island orientation along crystallographic direction of the substrate surface as provided by diffraction methods (EBSD), the epitaxial relations have been determined. For an annealing temperature close to the eutectic temperature of Au/Ge system (634 K), change in size and shape of the Au nanoislands is observed as well as the appearance of the hexagonal phase of gold, indicating eutectic melting of the system. The chemical composition of the leading Au/Ge interface was uncovered using quantitative atomically resolved HAADF-STEM and indicate the absence of alloying. The crystallographic structure of the Au islands and the presence of hexagonal gold as well as the Au/Ge interface were studied in details by atomically resolved HAADF-STEM. The studies at atomic level allowed us to uncover the mechanism of Au hcp phase formation and to derive the phase diagram for Au hcp nanostructures appearance on Ge(001) surface[4].

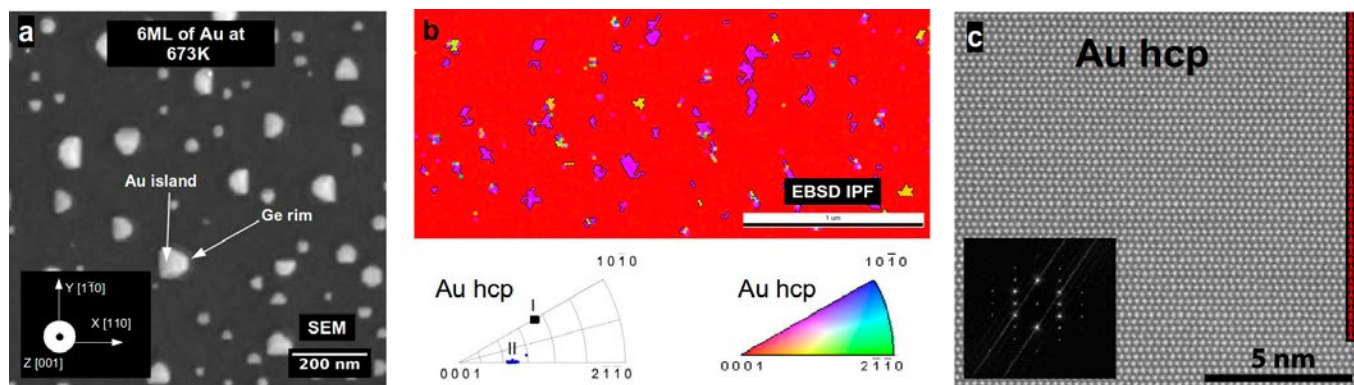


Fig. 1 Au hcp nanostructures formed on Ge(001) surface, a) SEM micrographs, b) EBSD/SEM Inverse Pole Figures (IPF) showing two main orientations of Au hcp crystallites, c) Atomically resolved HAADF STEM showing directly Au hcp phase.

References:

- [1] C. Blumenstein, et al. *Nat Phys* 7, 776-780 (2011).
- [2] F. Krok et al. *Beilstein Journal of Nanotechnology* 5, 1463-1471 (2014).
- [3] M. Nikiel et al. *CrystEngComm* 18, 5674 (2016).
- [4] B.R. Jany et al., *Sci. Rep.* 7, 42420 (2017).

Thu-14:20-O-OXID ●

Bulk hydroxylation and fast water splitting on highly reduced ceria

OXID Oxide surfaces and ultrathin oxide films

Viktor Johánek¹, Filip Dvořák¹, Josef Mysliveček¹, Andrii Tovt¹, Tomáš Skála^{1,2}, Lucie Szabová³, Matteo Farnesi Camellone³, Stefano Fabris³

¹ Department of Surface and Plasma Science, Charles University in Prague, V Holesovickach 2, 180 00 Prague 8, Czech Republic;

² Sincrotrone Trieste, Strada Statale 14, km 163.5, 34149 Basovizza-Trieste, Italy;

³ Centro DEMOCRITOS - Istituto Officina dei Materiali, Consiglio Nazionale delle Ricerche, c/o Scuola Internazionale Superiore di Studi Avanzati SISSA, Via Bonomea 265, 34136 Trieste, Italy

Interaction of cerium oxide (ceria) with water is a key process involved in many applications of ceria-based catalysis. A combination of experimental model study (TPD, XPS/SRPES, LEED, STM) with theory (ab-initio calculations) has been employed to get a detailed insight into the reaction of water with ceria at various levels of reduction (spanning from CeO_2 to Ce_2O_3). Reduced thin films of ceria were prepared by high temperature interfacial reaction of Ce with CeO_x layer which produces oxides with specific concentration and coordination of surface oxygen vacancies [1,2].

Upon increasing the degree of ceria reduction, we observe a transition from slow surface water splitting to fast and efficient water dissociation leading to hydrogen production (hence the water dissociation is irreversible) and ceria re-oxidation. The observed reaction yields exceed the oxide surface capacity. It is shown that the fast dissociation of water is associated with the appearance of bixbyite $c\text{-Ce}_2\text{O}_3$ phase in the ceria layers and to the close-packed structure of oxygen vacancies allowing diffusion and accommodation of OH species in Ce_2O_3 bulk. This bulk hydroxylation is proved absent in less-reduced ceria structures, where surface hydroxyl groups and hydrogen ad-atoms preferentially recombine reversibly to produce water. The presented study clearly demonstrates that the coordination of oxygen vacancies in ceria represents a crucial parameter to be considered in understanding and tuning the functionality of ceria-based catalysts.

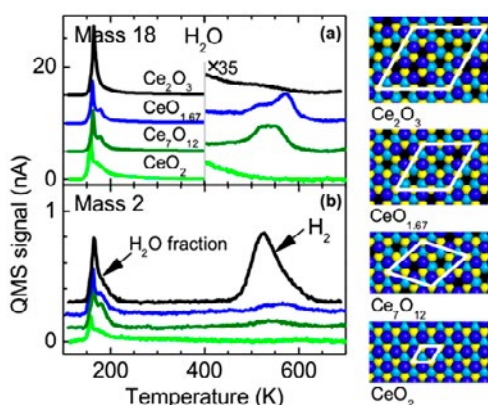


Fig. 1: Thermal desorption spectra of water on ordered reduced ceria thin films— $c\text{-Ce}_2\text{O}_3(4\times 4)$, $\text{CeO}_{1.67}(3\times 3)$, $i\text{-Ce}_7\text{O}_{12}(\sqrt{7}\times\sqrt{7})$, and reference $\text{CeO}_2(111)$. TPD spectra of H_2O (mass 18) and H_2 (mass 2) are shown. Right panel: Surface model of the above ceria structures; black areas are oxygen vacancies, white outlines represent the surface unit cells.

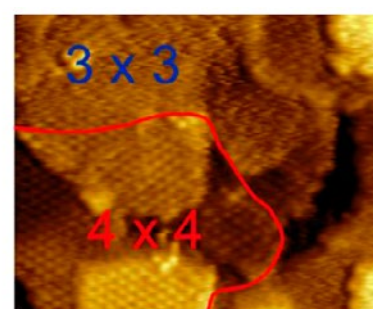


Fig. 2: STM image of the coexistence of the $c\text{-Ce}_2\text{O}_3(4\times 4)$, $\text{CeO}_{1.67}(3\times 3)$ phases on partially re-oxidized $c\text{-Ce}_2\text{O}_3$ sample. Size $40\times 50\text{ nm}^2$.

References:

- [1] V. Stetsovych et al.: "Epitaxial Cubic Ce_2O_3 Films via Ce– CeO_2 Interfacial Reaction," *J. Phys. Chem. Lett.* 4 (6), 2013, pp. 866–871
- [2] T. Duchoň et al.: "Ordered Phases of Reduced Ceria As Epitaxial Films on $\text{Cu}(111)$," *J. Phys. Chem. C* 118 (1), 2014, pp. 357–365

Tue-16:40-O-ORGS ●

Surface chemistry of coronene on a hydrogenated graphite surface

ORGS Organic molecules on solid surfaces

Jakob Holm Jørgensen¹, Anders Witte Skov², Liv Hornekær^{1,2}

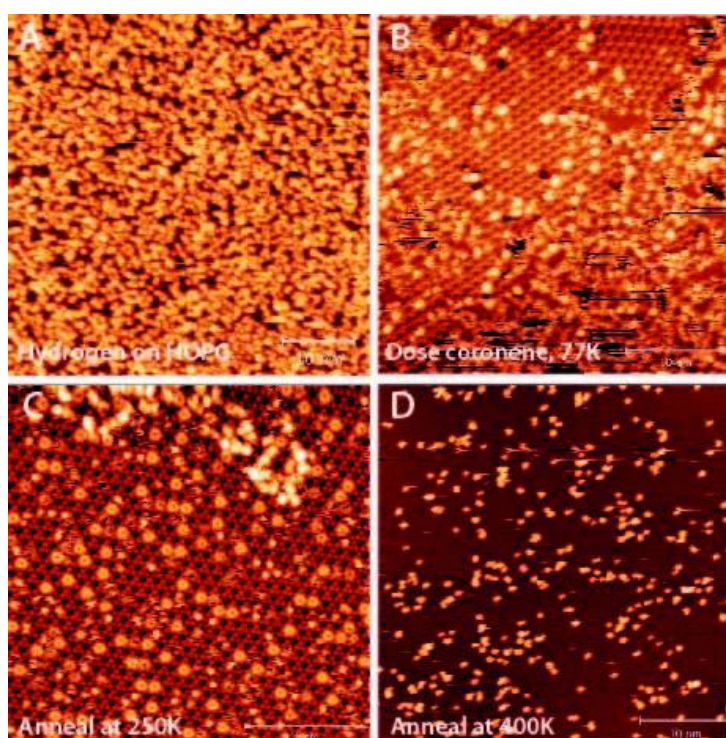
¹ Interdisciplinary Nanoscience Center iNANO, Aarhus University, Denmark;

² Institute for Physics and Astronomy, Aarhus University, Denmark

Carbon exists in abundance in the interstellar medium (ISM), for instance as carbonaceous grains in the interstellar dust. Of high significance is also the polycyclic aromatic hydrocarbons (PAH) which accounts for around 10% of the observed carbon in the space. Both of these carbon sources are thought to play important roles in the chemical environment of the ISM. For instance observational[1] as well as laboratory[2] studies have suggested PAHs to be a potential catalyst for the formation of H₂ from atomic hydrogen – a crucial step for the synthesis of complex organic molecules.

In this study a surface science approach is taken to study the interaction and chemistry between hydrogen and carbonaceous materials. Here, highly oriented pyrolytic graphite (HOPG) is used as a model surface for carbonaceous grains and coronene as a representative PAH [3]. Using low temperature scanning tunneling microscopy (LT-STM) it is found that coronene deposited on a hydrogen-functionalized HOPG substrate is mobile on the surface at 77K but shows very limited to no reactivity towards the adsorbed hydrogen. However, at increasing temperatures the coronene picks up hydrogen from graphite surface, and thus becomes super-hydrogenated. Based on temperature dependent STM studies the temperature range at which the reaction occurs is identified as well as the most reactive site of the coronene molecules is elucidated.

These measurements thus shed light on the dynamics and chemical reactivity of PAHs on a carbonaceous surface in the ISM.



References:

[1] Astronomy and Astrophysics 397 (2003) 623-634

[2] Faraday Discuss., 2014,168, 223-234

[3] Phys. Chem. Chem. Phys., 2014,16, 3381-3387

Thu-16:20-O-ENER ●**Fabrication and investigation of porous gold nanoparticles passivated with TiO₂ layer***ENER Surfaces for energy production and harvesting*L. Juhász¹, B. Parditka¹, C. Cserhádi¹, S. S. Shenouda², Z. Erdélyi¹¹ Department of Solid State Physics, University of Debrecen, Bem sqr. 18/b, H-4026 Hungary;² Department of Physics, Faculty of Education, Ain Shams University, Cairo, Egypt

Porous nanoparticles are very popular because of their high surface volume ratio, moreover they have stronger plasmonical properties than their solid counterparts. Porous gold nanoparticles were fabricated on SiO₂/Si as well as on sapphire substrates with solid state dewetting and dealloying methods. It is well known that the surface of porous gold nanoparticles can be passivated with a thin alumina layer, which results in good thermal stability of the nanoporous morphology. Morphology and optical properties of porous gold nanoparticles were investigated. They were coated with thin (~5-7 nm) TiO₂ layer using plasma-enhanced atomic layer deposition (ALD) method. Investigations by scanning electron microscopy (SEM) showed that the particles preserved their initial state even after annealing in the temperature range of 350 °C to 900 °C. Optical studies showed that the TiO₂ coating shifts the dipole plasmon peak to the higher (red) wavelength range due to the change of the refractive index. The samples were annealed for one hour in air at different temperatures from 350 °C to 900 °C. A blue-shift of the dipole plasmon peak has been observed already at low temperatures. The blue-shift is influenced by the annealing temperature and the thickness of the TiO₂ coating. At higher temperature (above 700 °C) the TiO₂ coating lost its thermal stability and the morphology as well as the optical properties suffer significant change. In the presentation we will compare the effect of the Al₂O₃ and the TiO₂ coatings on the change of the morphology and optical properties of porous gold nanoparticles.

Thu-16:00-O-ENER ● Stable hydrated protons on platinum surface

ENER Surfaces for energy production and harvesting

Youngsoon Kim, [Heon Kang](#)

Department of Chemistry, Seoul National University, Gwanak-ro 599, Seoul 151-747, Republic of Korea

Understanding the nature of hydrated protons at water/metal interfaces is fundamentally important in wide variety of research subjects, including heterogeneous catalysis, corrosion, and electrochemical processes in acidic environments. We explored the stability of hydrated protons on a Pt(111) surface formed by coadsorption of atomic hydrogen and water in ultrahigh vacuum (UHV) condition. Mass spectrometry and reflection absorption infrared spectroscopy (RAIRS) experiments showed clear evidence that hydrogen atoms are ionized to hydrated protons on the Pt surface. The surface-bound protons exist in multiply hydrated (H_5O_2^+ , H_7O_3^+ and H_9O_4^+) forms rather than as hydronium (H_3O^+) ion.[1] Upon the addition of water overlayer, the surface-bound protons transformed to a different structure, which is considered to be fully-hydrated protons in three-dimension. Proton migration through ≤ 20 water layers was observed by detecting proton transfer to ammonia molecules adsorbed onto the water film. The results suggest that surface hydrated protons may be key intermediates in the electrochemical interconversion between atomic hydrogen adsorbates and bulk-solvated protons in the Volmer reaction.

References:

- [1] Kim, Y.; Shin, S.; Kang, H., Zundel-like and Eigen-like Hydrated Protons on a Platinum Surface. *Angew. Chem. Inter. Ed.* 2015, 54, 7626-7630.

Thu-15:00-O-ENER ●***In situ* investigation of degradation at metal halide perovskite surfaces by near ambient pressure X-ray photoelectron spectroscopy*****ENER Surfaces for energy production and harvesting***

[Jack Chun-Ren Ke](#)¹, [Alex S. Walton](#)², [David J. Lewis](#)³, [Aleksander A. Tedstone](#)⁴, [Paul O'Brien](#)⁵, [Andrew G. Thomas](#)⁶, [Wendy R. Flavell](#)¹

¹ School of Physics and Astronomy and Photon Science Institute, the University of Manchester, Oxford Road, Manchester M13 9PL, UK;

² School of Chemistry and Photon Science Institute, the University of Manchester, Oxford Road, Manchester M13 9PL, UK;

³ School of Materials, the University of Manchester, Oxford Road, Manchester M13 9PL, UK;

⁴ School of Chemistry, the University of Manchester, Oxford Road, Manchester M13 9PL, UK;

⁵ School of Chemistry and Materials, the University of Manchester, Oxford Road, Manchester M13 9PL, UK;

⁶ School of Materials and Photon Science Institute, the University of Manchester, Oxford Road, Manchester M13 9PL, UK

Metal halide perovskites have emerged as the highly promising light absorbers of the photovoltaic devices due to excellent absorptivity and carrier diffusion length, which allows satisfactory power conversion efficiency to be achieved by utilising a small amount of raw material. Nevertheless, poor stability has limited their advancement for commercialisation, which has resulted in enormous worldwide research effort in the reduction of degradation at the perovskite materials. Consequently, understanding the degradation mechanism of the perovskite materials is of paramount importance to further improve the stability of perovskite solar cell.

Near-ambient pressure X-ray photoelectron spectroscopy (NAPXPS) plays a vitally important role in *in situ* investigation of surface degradation, especially for surface sensitive materials like metal halide perovskites. In this study, two different perovskite materials are examined by NAPXPS during exposure to water vapour, organic lead perovskite ($\text{CH}_3\text{NH}_3\text{PbI}_3$) and 'all-inorganic' tin caesium double perovskite (Cs_2SnI_6). The former is the most widely used type of organometal halide perovskite, and is highly unstable in air containing water vapour, whilst the latter was proposed to address the toxicity and instability issues. In the case of $\text{CH}_3\text{NH}_3\text{PbI}_3$, samples were prepared *in situ* inside the spectrometer, and these pristine samples were monitored during their exposure to 9 mbar water vapour.[1] This allows us to distinguish unambiguously between alternative mechanisms for the degradation reaction. As expected, the results show significant differences between the two perovskite materials. Following the same level of water vapour exposure, NAPXPS spectra reveal that the organic (nitrogen-containing) part in $\text{CH}_3\text{NH}_3\text{PbI}_3$ is almost completely removed,[1] whereas the inorganic counterpart (Cs) in Cs_2SnI_6 does not undergo any significant change.[2] The outcomes demonstrate that the surfaces of Cs_2SnI_6 are far more stable than $\text{CH}_3\text{NH}_3\text{PbI}_3$, consistent with the relative bulk stabilities.

References:

[1] C.R. Ke, A.S. Walton, D.J. Lewis, A.A. Tedstone, P. O'Brien, A.G. Thomas, W.R. Flavell, *Chemical Communications*, (2017), 53, 5231-5234. (DOI: 10.1039/c7cc01538k)

[2] C.R. Ke, D.J. Lewis, A.S. Walton, P. O'Brien, A.G. Thomas, W.R. Flavell, in preparation for publication.

Tue-9:40-O-CORR ●
Corrosion studies of Lithium Hydride thin films

CORR Corrosion at atomic level

James Tonks, [Martin King](#), Ewan Galloway

AWE, University of Surrey, Guildford, UK

Thin films of LiH and its corrosion products were studied using temperature programmed decomposition (TPD), x-ray photoelectron spectroscopy (XPS) and Auger electron spectroscopy (AES). Thin films were grown on Ni(100) in an ultra high vacuum system using an electron beam evaporator. Characteristic Li KLL AES peaks were identified for Li, LiH, Li₂O and LiOH which facilitated identification of thin film composition. XPS of the O 1s region revealed three distinct chemical shifts which were attributed to Li₂O, LiOH and chemisorbed H₂O. We show that exposing LiH to very low H₂O partial pressures results in formation of LiOH/Li₂O domains on LiH. We also show that these XPS peaks can be linked to reaction mechanisms in the TPD profiles. TPD traces have been explicitly modelled to determine the activation energies of the reactions and compare favourably with previous measurements on bulk LiH samples.

Thu-16:00-O-ORGS ●**Intramolecular cyclization of o-quinone amines with a focus on dopamine-quinone: a density functional theory based study***ORGS Organic molecules on solid surfaces*Ryo Kishida¹, Hideaki Kasai^{2,3,4}¹ Department of Applied Physics, Osaka University, Osaka, Japan;² National Institute of Technology, Akashi College, Japan;³ Center for International Affairs, Osaka University;⁴ Institute of Industrial Science, The University of Tokyo

Oxidation of dopa, dopamine, or similar *p*-substituted phenols/catechols to form corresponding *o*-quinones finally results in generation of dark pigment called melanin. Recently, melanin formed from dopamine (dopamine-melanin or polydopamine) has been attracting considerable attention in the field of materials and surface science. Dopamine-melanin possesses versatile adhesive properties and then can be used as interface layers for a wide range of surfaces regardless of organic or inorganic materials. The structure of dopamine-melanin or other melanins has been extensively investigated both in the context of chemistry and physics. The above-mentioned *o*-quinones are usually converted into cyclic structures via intramolecular cyclization. However, a recent experiment shows uncyclized structures in dopamine-melanin [1]. Furthermore, an *o*-quinone resulting from dopamine oxidation, i.e., "dopamine-quinone", has been shown to slowly cyclize as compared to the case of "dopa-quinone" [2].

In the present study, we conducted a mechanistic study on cyclization of *o*-quinones with the aid of density functional theory based calculation [3]. Motivated by previous experiments [1,2], we compared the cyclization of (a) dopamine-quinone with its analogues, i.e., (b) dopaquinone, (c) *N*-methyl-dopamine-quinone, and (d) *N*-formyl-dopamine-quinone. Cyclizations of these molecules result in formation of five-membered rings. We also calculated cyclization processes of (a') - (d') the methylene (-CH₂-)inserted derivatives, corresponding to six-membered rings. We found that the five-membered ring formations require higher activation energies as compared to the cases of six-membered ring formation. Our computational results also show that the activation barriers increase in the following order of cases: (b) < (c) < (a) < (d) and (b') < (c') < (a') < (d').

As the factors affecting the cyclization of *o*-quinones, we will discuss electron transfer, properties of molecular orbitals, and transition state structures in the reaction.

References:

[1] J. Liebscher et al., *Langmuir* 29 (2013) 10539.[2] E.J. Land et al., *Arkivoc* xi (2007) 23.[3] R. Kishida et al., *Int. J. Quant. Chem.* (under revision).

Tue-10:00-O-MAGN ●

Ab-Initio analysis of nitric oxide adsorption on an FeO₂-terminated (001) surface of LaFeO₃**MAGN Surface and molecular magnetism**

Hidetoshi Kizaki, Yoshitada Morikawa

Department of Precision Science and Technology, Graduate School of Engineering, Osaka University, Japan

Studying nitric oxide (NO) adsorption is of fundamental importance for the reduction of nitroxide (NO_x) automotive emissions using precious metals such as Rh, Pt and Pd supported on ceramics. In general, precious metals are very effective at reducing NO_x. However, the use of these materials is limited because of their restricted availability and high cost. Notably, several studies have described the reactivity towards NO_x reduction in host perovskite materials. Above all, iron-based materials have been shown to be superior candidates. According to Reddy et al., the catalytic activity of Fe₂O₃ (10 wt%) supported on Al₂O₃ and ZrO₂ for the NO + CO reaction is the most reactive catalyst among various metal oxide surfaces[1]. Nevertheless, the question of how Fe-containing oxide supports affect the NO_x reduction remains unclear. Hence, a study of NO chemical reactions on an Fe-based oxide surface, such as an Fe-terminated LaFeO₃ support, could offer a means to identify an alternative NO_x reduction path relevant to the design of more intelligent catalysts. LaFeO₃ is known to be anti-ferromagnet with a Néel temperature of 738 K[2]. Since the NO_x reduction is drastically activated at around 200 °C and shows low catalytic activity at low temperature for automotive emissions, it is of increased importance to take the magnetic properties of interface into account. Thereafter, to demonstrate the adsorption properties of NO on an FeO₂-terminated surface of LaFeO₃, investigating the magnetic properties of not only the anti-ferromagnetic LaFeO₃ slab but also the adsorbate molecule is crucial. However, as far as we know, there are no discussions on its magnetism.

In this study, the adsorption of NO on an FeO₂-terminated (001) surface of LaFeO₃ is studied based on spin-polarized ab-initio calculations. The plane-wave pseudo-potential density functional theory method as implemented in the Quantum-ESPRESSO package was used throughout the calculations[3]. The Perdew-Burke-Ernzerhof-Generalized Gradient Approximation was employed for the exchange-correlation functional. The adsorption energies, $E_{\text{ads}} = E(\text{NO adsorbed slab}) - E(\text{slab}) - E(\text{NO})$, on the FeO₂ terminated LaFeO₃ (001) surface with and without oxygen vacancies (VO) were evaluated.

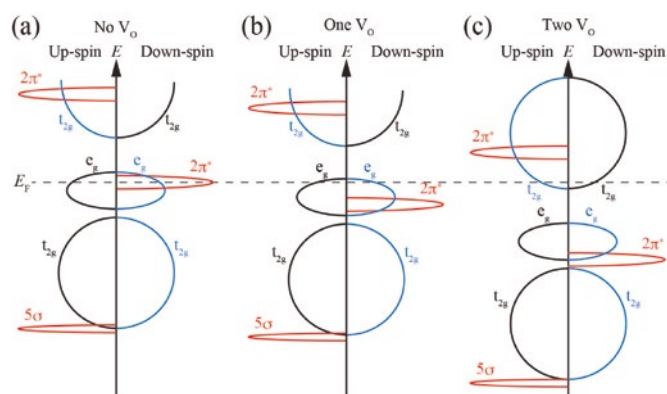


Fig. 1: Schematic illustration of the DOS of the Fe¹ and Fe¹ atoms on the 1 L and molecular orbital of the adsorbed NO w/ and w/o V_O. Black, blue and red solid lines denote the Fe¹, the Fe¹ and molecular orbital of NO, respectively.

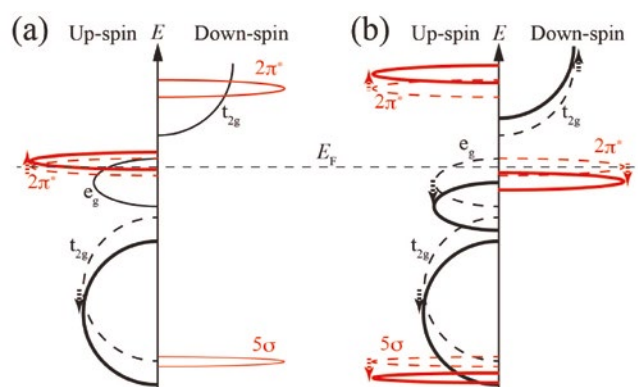


Fig. 2: Schematic illustration of the DOS of the Fe¹ atom and the adsorbed NO molecule with parallel spin coupling (a) and that with anti-parallel spin coupling (b).

Consequently, the calculated adsorption energies of NO are approximately between -1.1 and -1.4 eV on a pristine FeO_2 -terminated surface. For the surface with an VO concentration of 25% with respect to the surface O in the 1st FeO_2 layer, the adsorption energy of NO is -1.35 eV, which is closer to that without any V_{O} . For a surface slab with a V_{O} concentration of 50 % in the 1st FeO_2 layer, however, the adsorption energy of NO is enhanced to -2.17 eV. We show that the interaction between the $2\pi^*$ orbital of NO and the occupied part of the Fe $3d$ states governs the bonding and magnetic properties of NO on the FeO_2 -terminated surface as shown in Fig. 1. As a whole, the anti-parallel spin coupling between the adsorbed NO and the Fe bonded to the NO was realized because of the interaction between the $2\pi^*$ orbital of NO and the Fe $3d$ states as shown in Fig. 2. This energy gain in magnetic interaction contributes to the E_{ads} and reaction barrier for the NO adsorption. Thus, the consideration of such magnetic interactions is indispensable to discussing the catalytic activity on transition metal oxide surfaces.

References:

- [1] B. V. Reddy and S. N. Khanna, Phys. Rev. Lett. 93 (2004) 068301.
- [2] D. Treves, J. Appl. Phys. 36 (1965) 1033.
- [3] <http://www.quantum-espresso.org>

Wed-11:20-O-BAND ●**Unoccupied band structure of Si nanoribbons on Ag(110) studied by IPE***BAND Band structure of solid surfaces*[Nils Fabian Kleimeier](#), [Gabi Wenzel](#), [Helmut Zacharias](#)*Westfälische Wilhelms-Universität, Münster, Germany*

Slowly evaporating Si onto the (110) surface of a Ag(110) single crystal leads to the formation of atomically perfect pentagonal chains of Si that are globally aligned along the [-110] direction of the silver surface. Although the occupied band structure of these nanoribbons has been investigated thoroughly, the unoccupied bands have so far not been studied with momentum-resolved methods.

We employ k-resolved inverse photoemission spectroscopy (KRIPES) to determine the unoccupied band structure of these nanoribbons on Ag(110) in ultra-high vacuum. Electrons from a modified Erdman-Zipf electron gun are used to excite the sample and the emitted photons are detected in a Geiger-Müller tube with acetone as counting gas and a CaF₂ entrance window acting as a bandpass filter around $h\nu=9.9$ eV.

The band structure is investigated in both ΓX and ΓY direction (along the nanoribbons and perpendicular to them, respectively). These measurements reveal two clearly visible states around the Γ -point of the Ag(110) that disperse strongly along the ΓX -direction and show no dispersion in the ΓY -direction, as expected for quantum confinement states in 1D-materials. Moreover a linear continuation of the Dirac-cone like feature around the X-point of the surface Brillouin zone of the Ag(110) crystal is found.

Mon-14:20-O-BAND ●**Theoretical study on spin states of photoelectrons emitted from spin-polarized surface states with a mirror symmetry***BAND Band structure of solid surfaces*[Katsuyoshi Kobayashi](#)¹, [Koichiro Yaji](#)², [Kenta Kuroda](#)², [Fumio Komori](#)²¹ *Department of Physics, Ochanomizu University, Japan*² *Institute for Solid State Physics, The University of Tokyo, Japan*

Recently the spin-polarized surface states formed by spin-orbit interaction attract much attention. Such surface states are fundamental ingredients in topological insulators and Rashba systems. Recent experiments of photoelectron emission of topological insulators show that 100% polarized electrons are emitted by irradiating linearly polarized light, and the spin direction of electrons is completely reversed by changing the polarization of light from p to s [1]. This phenomenon was qualitatively explained using the wave functions of initial states in which spin states and orbital symmetry are coupled [2]. The key property for the 100 % polarization to occur is the mirror symmetry of the system.

In this presentation, we show a theoretical calculation of this phenomenon with explicit account of final states obtained by a density-functional method. We develop a method for calculating spin states of electrons excited by light. The method is simple and effective for low energy excitation. This method is applied to the Bi(111) surface. Spin expectation values of electrons emitted from surface states of Bi(111) surfaces reproduce experimental ones measured as a function of the polarization angle of incident light. We explain the asymmetry observed in photoelectron intensity between time-reversed states in two-dimensional Brillouin zone by breaking time-reversal symmetry in photoemission process.

References:

[1] C. Jozwiak, et al.: Nat. Phys. 9, 293 (2013).

[2] K. Yaji, et al.: Nat. Commun. 8, 14588 (2017).

Tue-15:20-O-ORGS ●

Ductility of thin films constituting organic light emitting diodes

ORGS Organic molecules on solid surfaces

Toshiro Kobayashi¹, Munkhzul Munkhtsog¹, Makoto Okada², Yuichi Utsumi², Hideaki Kanematsu³, Tsuyoshi Masuda⁴

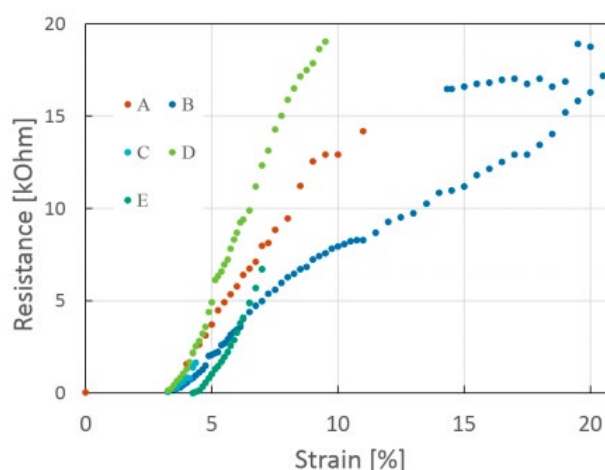
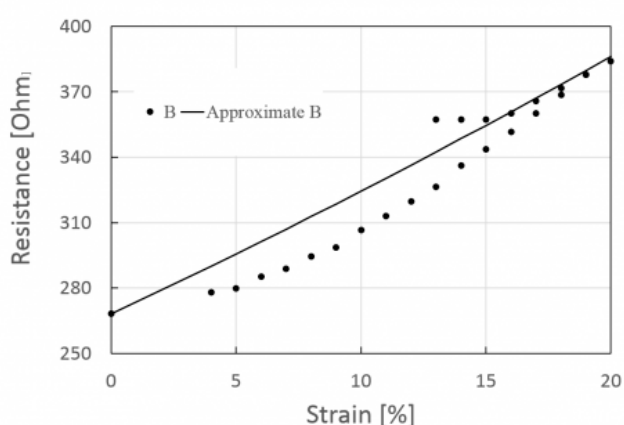
¹ Department of Electronics & Control Engineering, National Institute of Technology, Tsuyama College, Okayama, Japan

² Laboratory of Advanced Science and Technology for Industry, University of Hyogo, Hyogo, Japan

³ Department of Materials Science & Engineering, National Institute of Technology, Suzuka College, Mie, Japan

⁴ Q-Light co., Ltd., Iwate, Japan

This paper describes an evaluation method of the mechanical properties and electrical characteristic of thin films constituting organic semiconductor, and the test result of the relation between cracking and the electrical resistance of the films. The final target of the present research is the improvement of flexibility of organic devices, flexible displays and flexible organic light emitting diodes (OLEDs). The purpose of this study is to understand the vulnerable parts of the constituent materials of OLED quantitatively, further the guideline for designing OLED structure will be obtained. A few types of PEDOT:PSS were coated on polyethylene naphthalate (PEN) substrate by spin coating method, and two layer thin film structures PEN/Alq3/Al, and PEN/CBP/Al were prepared by vacuum deposition method. Then electrical resistance and cracking of the films were investigated. As a result, it was found that the PEDOT:PSS films do not cause cracking and the electrical resistance increased theoretically by around 10% of strain. Regarding the two layer thin films, cracking initiated at a strain of around 4% then the electrical resistance started increasing. The reason has suggested that cracking was caused by the strain resulting in cracking with forming network shape. Furthermore it was found that the aspect of the cracking depends on the underlayers suggesting the effect of adhesion of the films.



Mon-14:40-O-ORGS ●**Control over self-assembly of phthalocyanine molecules via the electric field of an STM tip****ORGS Organic molecules on solid surfaces**

Peter Matvij¹, Pavel Kocán¹, Pavel Sobotík¹, Barbara Pieczyrak², Leszek Jurczyszyn², Filip Rozbořil¹, Ivan Ošťádal¹

¹ Charles University in Prague, Czech Republic;

² Institute of Experimental Physics, University of Wrocław, Poland

Ordered layers of organic molecules are usually grown on weakly interacting surfaces, typically those of metal mono-crystals. An interesting alternative, consistent with silicon technologies, is represented by silicon surfaces passivated by metal mono-layers. Such surfaces carry interesting electronic properties, e.g. the Rashba-type spin-split bands in the case of Tl/Si(111)-(1×1) [1].

We use the scanning tunneling microscopy (STM) to study field-dependent assembly of copper phthalocyanine (CuPc) molecules on the Tl/Si(111)-(1×1) surface. Previously we reported that the surface is inert to adsorbates [2]. We demonstrate that the electric force can be used to control the assembly of molecules and switch between phases on areas of hundreds of nm² with a switching time of less than 1 ms. With help of ab-initio calculations and kinetic Monte Carlo simulations we explain the mechanism of the STM tip influence on assembly of the molecules by means of electrostatic interactions.

Two aspects are important for explanation of observed morphologies and dynamic behavior – 1) molecular assembly as a result of high density and steric repulsion, and 2) the charge rearrangement induced by adsorption of the molecules on the substrate.

This work was supported by Czech Science Foundation (contract no. 16-15802S) and by the Charles University in Prague (project GAUK No. 326515).

References:

- [1] K. Sakamoto, T. Oda, A. Kimura, Y. Takeichi, J. Fujii, R. I. G. Uhrberg, M. Donath, and H. Woong, *J. Electron Spectros. Relat. Phenomena* 201, 88 (2015).
- [2] P. Matvija, P. Sobotík, I. Ošťádal, and P. Kocán, *Appl. Surf. Sci.* 331, 339 (2015).

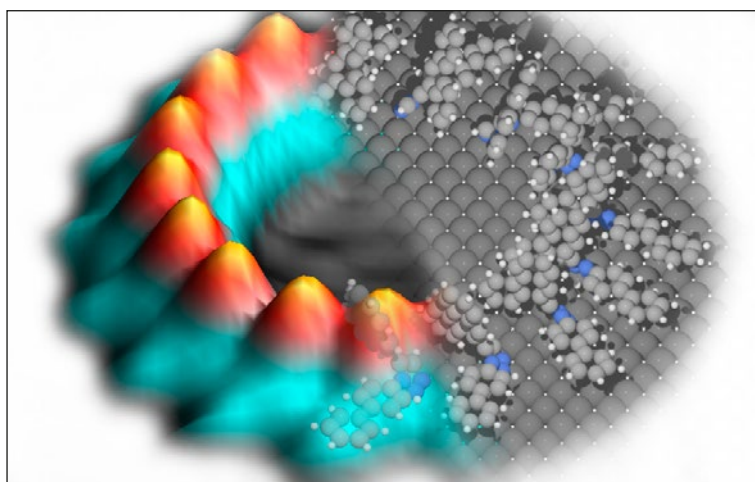
Thu-11:20-O-ORGS ●**Supramolecular corrals on surfaces resulting from aromatic interactions of non-planar triazoles***ORGS Organic molecules on solid surfaces*

Siddharth J. Jethwa, Esben L. Kolsbjerg, Bjørk Hammer, Trolle R. Linderoth

Interdisciplinary Nanoscience Center (iNANO), Department of Physics and Astronomy, Aarhus University, Aarhus, Denmark

Molecular self-assembly on surfaces has been studied with great interest over the previous 20 years with a view towards the formation of functional two-dimensional nanostructures using the bottom-up approach. One example is pores of assemblies that can be used to selectively expose active surface sites or host guest molecules via specific interactions and thus have a range of potential applications in catalysis,[1-3] for instance by encapsulation of organic compounds on surfaces[4]. Such two-dimensional corral structures can be formed on various transition metal surfaces from functionalized molecules normally governed by in-plane interactions. Interaction forces between aromatic moieties, often referred to as π - π interactions, are an important element in stabilising complex supramolecular structures. For supramolecular self-assembly occurring on surfaces, where aromatic moieties are typically forced to adsorb co-planar with the surface, the possible role of intermolecular aromatic interactions is much less explored.

Here we report on unusual, ring-shaped supramolecular corral surface structures resulting from adsorption of a molecule with non-planar structure, allowing for intermolecular aromatic interactions. The discrete corral structures are observed using high-resolution Scanning Tunnelling Microscopy (STM) and the energetic driving forces for their formation are elucidated using Density Functional Theory (DFT) calculations and Monte Carlo (MC) simulations. The individual corrals involve between 11–18 molecules bound through triazole moieties to a ring-shaped ensemble of bridge site positions on (111) surfaces of copper, silver or gold. The curvature required to form the corrals is identified to result from the angle-dependence of aromatic interactions between molecular phenanthrene moieties. The study provides detailed quantitative insights into triazole-surface and aromatic interactions and illustrates how they may be used to drive surface supramolecular self-assembly.



References:

- [1] J. S. Seo, D. Whang, H. Lee, S. I. Jun, J. Oh, Y. J. Jeon and K. Kim, *Nature*, 2000, 404, 982-986.
- [2] B. Kesanli and W. Lin, *Coordination Chemistry Reviews*, 2003, 246, 305-326.
- [3] M. O. Lorenzo, S. Haq, T. Bertrams, P. Murray, R. Raval and C. J. Baddeley, *The Journal of Physical Chemistry B*, 1999, 103, 10661-10669.
- [4] E. N. Yitamben, L. Niebergall, R. B. Rankin, E. V. Iski, R. A. Rosenberg, J. P. Greeley, V. S. Stepanyuk and N. P. Guisinger, *The Journal of Physical Chemistry C*, 2013, 117, 11757-11763.

Tue-17:40-O-MOLA ●**Self-organization and electronic structure of thin and mono-molecular layer of Keggin-type Al₁₃-sulfate salt***MOLA Ultrathin two-dimensional molecular self-assembly*Imre Kovács¹, András Stirling², Zoltán Schay³¹ Technical Institute, University of Dunaújváros, H-2401, Dunaújváros Hungary

E-mail: amerigo1960@gmail.com; kovacsimre@uniduna.hu;

² Institute of Organic Chemistry, Research Centre for Natural Sciences, Hungarian Academy of Sciences, Budapest, Hungary

E-mail: stirring.andras@ttk.mta.hu;

³ Department of Surface Chemistry and Catalysis, Centre for Energy Research, Hungarian Academy of Sciences, Budapest, Hungary

E-mail: schay@mail.kfki.hu

The Keggin-type aluminum polyhydroxy cation, $[\text{AlO}_4\text{Al}_{12}(\text{OH})_{24}(\text{H}_2\text{O})_{12}]^{7+} - (\text{Al}_{13})$ is the most frequently used modifier in preparing pillared layer clays. It is also used in wastewater cleaning processes. This curious compound was prepared and crystallized in the form of a sulfate salt. The crystal structure of this salt was analyzed by X-ray diffraction analysis. While the structural analysis of intercalated clays is difficult on model surfaces, such as HOPG, scanning tunneling microscopy provides detailed insights. The main purpose of this study is to characterize the two-dimensional self-assembled structure of the Keggin-type Al_{13} ions and to arrange them artificially in new 1D or 2D structure.

Samples for imaging were prepared by depositing Al_{13} -sulfate solution onto freshly cleaved HOPG surface. This surface exhibits small patches of oriented rod-like crystallites consisting of several, parallel lines, often twin structures. These rough patterns separate the well-ordered flat monolayer regions with corrugation of 2-3 Å.

Coadsorption of surfactant SDS and the Keggin-salt can form various surface patterns, depending on the applied conditions. These motifs and their possible origins will be discussed.

Scanning tunneling spectroscopic (STS) measurements over the fresh Al_{13} -Keggin layer have shown a characteristic negative differential resistance (NDR) peak at around 1.4 V sample bias. In interpreting this finding we applied XPS measurement and DFT calculations. A detailed explanation will be presented in this study.

Thu-15:20-O-ORGS ●**Epitaxial growth of organic crystal networks on ultra-thin hexagonal boron nitride***ORGS Organic molecules on solid surfaces*

[Markus Kratzer](#)¹, [Aleksandar Matković](#)¹, [Jakob Genser](#)¹, [Daniel Lüftner](#)², [Radoš Gajić](#)³, [P. Puschnig](#)², [C. Teichert](#)¹

¹ *Institute of Physics, Montanuniversität Leoben, Franz-Josef Straße 18, 8700 Leoben, Austria;*

² *Institute of Physics, Karl Franzens University of Graz, NAWI Graz, Univ. Pl 5, A-8010 Graz, Austria;*

³ *University of Belgrade, Institute of Physics, Pregrevica 118, Belgrade 11080, Serbia*

For organic thin film electronic devices, the interface of the organic film and the substrate is essential for their performance. So-called van der Waal (vdW) substrates are anticipated to be advantageous for organic thin film electronics. These vdW substrates exhibit in general very smooth surfaces and no dangling bonds. As a result the interface between vdW substrate and organic thin film is molecularly smooth and is essentially free of charge traps. On the one hand, organic semiconductor films are typically soft and therefore are well suited for mechanically flexible electronics. On the other hand, two-dimensional (2D) vdW materials offer mechanical flexibility and good interfacing with organic semiconductors. Therefore it is straight forward to use a combination of 2D vdW materials as substrates/electrodes with organic layers as active element in organic semiconductor devices [1].

Here, we investigated hexagonal boron nitride (hBN) as an ultra-thin dielectric vdW substrate for the epitaxial growth of highly ordered crystalline networks of the organic semiconductor parahexaphenyl (6P). 6P is a typical representative of small aromatic organic semiconductor molecules and is therefore suitable as model system. 6P layers were vapor deposited by hot-wall epitaxy onto hBN/SiO₂/Si substrate stacks which were prepared by mechanical exfoliation. The resulting morphologies have been investigated using atomic force microscopy. Needle-like crystallites of 6P with their long axes oriented five degrees off the hexagonal boron nitride zigzag directions were observed [2]. This finding together with the adsorption site determined by density functional theory simulations revealed the formation of a (-629) contact plane of bulk 6P. Adjustment of deposition temperature and the hBN thickness lead to ordered networks of needle-like crystallites of up to several tens of micrometers length. A profound understanding of the organic crystallite growth and ordering on ultra-thin vdW dielectric substrates is a step towards field effect devices whose performance is only limited by the intrinsic properties of the organic semiconductor and not by grain-boundaries or the organic-gate dielectric interface.

References:

[1] M. Kratzer, C. Teichert, *Nanotechnology* 27, 292001 (2016).

[2] A. Matković, J. Genser, D. Lüftner, M. Kratzer, R. Gajić, P. Puschnig, C. Teichert, *Sci. Rep.* 6, 38519 (2016).

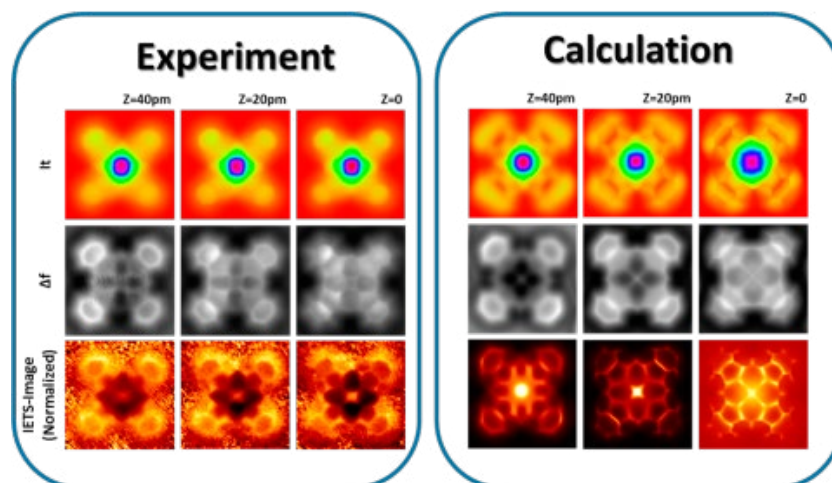
Mon-14:00-O-ORGS ●

Simultaneous high-resolution AFM/STM/IETS imaging of FePc on Au(111)

ORGS Organic molecules on solid surfaces

Bruno de la Torre^{1,2}, Ondřej Krejčí^{1,3}, Martin Švec^{1,2}, Giuseppe Foti¹, Héctor Vázquez¹, Radek Zbořil², Pavel Jelínek^{1,2}¹ Institute of Physics of the CAS, Prague, Czech Republic;² Regional Centre of Advanced Technologies and Materials, Palacký University, Olomouc, Czech Republic;³ Department of Surface and Plasma Science, Charles University, Prague, Czech Republic

The recent progress in scanning probe microscopy provided unprecedented atomic resolution of single organic molecules on surfaces. Namely, the submolecular resolution was achieved in AFM [1], STM [2] and also IETS [3] mode employing functionalized tips. The origin of the submolecular contrast can be rationalized by a simple mechanical model introducing a lateral bending of a flexible tip apex [4,5]. However direct experimental evidence correlating the AFM/STM/IETS imaging mechanisms has been missing so far. Here we present simultaneous high resolution AFM/STM/IETS imaging of iron(II) phthalocyanine (FePc) on Au(111) surface acquired with CO-functionalized probe. The acquired data demonstrate unambiguously the common imaging mechanism of the modes. We will show that not only renormalization of the frustrated translational mode [5], but also renormalization of the amplitude of IETS signal affect the IETS imaging. We also propose a simple model designed to capture variations in the amplitude of the IETS signal, which permits us to reproduce the experimental findings. The validity of our model is verified not only by the agreement with experimental measurements but also by ab-initio IETS calculations based on non-equilibrium Green's function.



References:

- [1] L. Gross et al., Science 325,1110 (2009).
- [2] C. Weiss et al., Phys. Rev. Lett. 105, 086103 (2010).
- [3] C.I. Chiang et al Science 344, 885 (2014).
- [4] P. Hapala et al., Phys. Rev. B 90, 085421 (2014).
- [5] P. Hapala et al., Phys. Rev. Lett. 113, 226101 (2014).

Tue-15:00-O-OXID ●

Band structure of one single layer of silica on Ru(0001)

OXID Oxide surfaces and ultrathin oxide films

Geoffroy Kremer¹, Yannick Fagot-Revurat², Muriel Sicot², Bertrand Kierren², Daniel Malterre², Luc Moreau², Simone Lisi³, Johann Coraux³, Pascal Pochet⁴, Yannick J. Dappe⁵, Patrick Le Fèvre⁶, François Bertran⁶, Julien Rault⁶

¹ Institut Jean Lamour, UMR 7198, Université de Lorraine/CNRS, BP 70239, F-54506 Vandoeuvre-les-Nancy, France;

² Institut Jean Lamour, UMR 7198, Université de Lorraine/CNRS, BP 70239, F-54506 Vandoeuvre-les-Nancy, France;

³ Univ. Grenoble Alpes, Inst. NEEL, F-38000 Grenoble, France;

⁴ CEA, INAC-SP2M, F-38054 Grenoble, France;

⁵ SPEC (CNRS URA2464), SPCSI, IRAMIS, CEA Saclay, 91191 Gif-Sur-Yvette, France;

⁶ SOLEIL, L'Orme des Merisiers, Saint-Aubin, BP 48, F-91192 Gif sur Yvette, France

Two-dimensional materials like graphene, transition metal dichalcogenides and ultrathin oxides have revealed unique properties very different from bulk. As an example, new quasi-2D phases of atomically thin silica films have been discovered recently [1,2]. Reduced dimensionality is expected to ease structural phase transitions, a desirable characteristics in view of faster and less energy costly applications. Although the structural properties of ultrathin silica phases have been characterized, experimental electronic properties of this material are yet to be explored, especially the band structure.

In this framework, we have investigated the electronic properties of one single layer of silica epitaxially grown on Ru(0001).

The samples were grown *in situ* under UHV environment. Silica was grown on a single crystalline Ru(0001) surface which was first exposed to oxygen to obtain a 3O-(2x2)/Ru(0001) superstructure [3]. The atomic structure of one monolayer of crystalline silica was studied by high-resolution X-ray Photoemission Spectroscopy (HR-XPS), low energy electron diffraction (LEED) and low-temperature scanning tunneling microscopy (LT-STM). LEED patterns revealed a (2x2) lattice consistent with crystalline silica and in agreement with our STM images and previous works [1-4]. The electronic properties of the monolayer of silica over Ru(0001) were studied by means of high-resolution Angle Resolved Photoemission Spectroscopy (HR-ARPES, see Figure below). The band structure exhibits bands related to the presence of silica with a clear (2x2) periodicity. This study provide insightful understanding on the electronic properties of the atomic oxide layer and metal-oxide electronic coupling.

References:

- [1] S. Shaikhutdinov et al, *Advanced Materials* 25, (2012), 49
- [2] S. Shaikhutdinov et al, *Physical Review Letters* 95, (2005), 076103
- [3] S. Mathur et al, *Physical Review B* 92, (2015), 161410(R)
- [4] B. Yang et al, *Physical Chemistry Chemical Physics* 14, (2012), 11344

Band structure of one ML of ultrathin silica on Ru(0001)

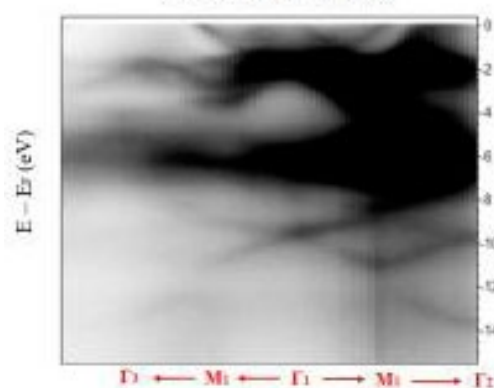


Figure : ARPES spectra of a single layer of crystalline silica on Ru(0001)

Wed-9:20-O-COMP ●

Stability of vicinal crystal surfaces against step bunching:
atomistic scale model of unstable evaporation and growth

COMP Computational surface chemistry and physics

Filip Krzyzewski¹, Hristina Popova², Anna Krasteva³, Magdalena Załuska-Kotur¹,
Vesselin Tonchev²¹ Institute of Physics, Polish Academy of Sciences, Warsaw, Poland;² Institute of Physical Chemistry, Bulgarian Academy of Sciences, Sofia, Bulgaria;³ Institute of Electronics Bulgarian Academy of Sciences, Sofia, Bulgaria;

We recently proposed an atomistic scale model of vicinal crystal growth at vicinal surfaces [1,2]. Since no step-step interaction was incorporated in the model we observed step bunches consisting of both macro- and mono-steps. Step bunching (SB) was obtained due to the application of one of two instability sources: down step diffusional bias (δ) or infinite inverse Ehrlich-Schwoebel effect [3]. We studied scaling of time evolution of bunch size (N) [1,2] and other quantities (macrostep size and terrace width) which describe character of the surface shape.

Here we develop further this model and report results from stability analysis of evaporation and vicinal growth destabilized by diffusional bias. We show that system is destabilized by both bias directions during evaporation as well as growth process. The approach is briefly as follows – using the time-scaling of the bunch size obtained in [1, 2] we probe the surface stability for many parameter values for times that would result in the same number of steps according to the time-scaling of N . The resulting plots of the bunch size as a function of the model parameters such as diffusion-to-kinetics rates ratio (n_{DS}) and sustained surface concentration (c_0), show where the system is most unstable against step bunching with step-up and step-down direction of the bias. We also show that time scaling exponent of bunch size is $\frac{1}{2}$ and is independent on external force orientation as well as it does not depend on the direction of steps movement. We show four different curves for time scaling of bunch sizes. Each curve corresponds to different case of system evolution: growth at step-down (SD) or step-up (SU) bias and sublimation at those two bias directions.

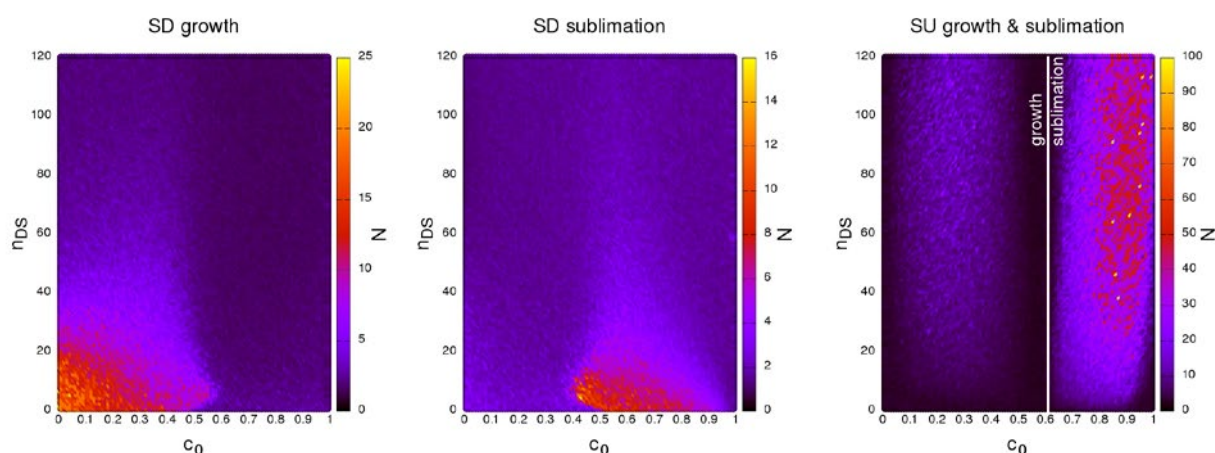


Fig. 1 Stability diagrams of bunch size dependent in the space on surface atom concentration and diffusion rate in the case of growth at SD bias (left) sublimation at SD bias (centre) and growth and sublimation at SU bias (right)

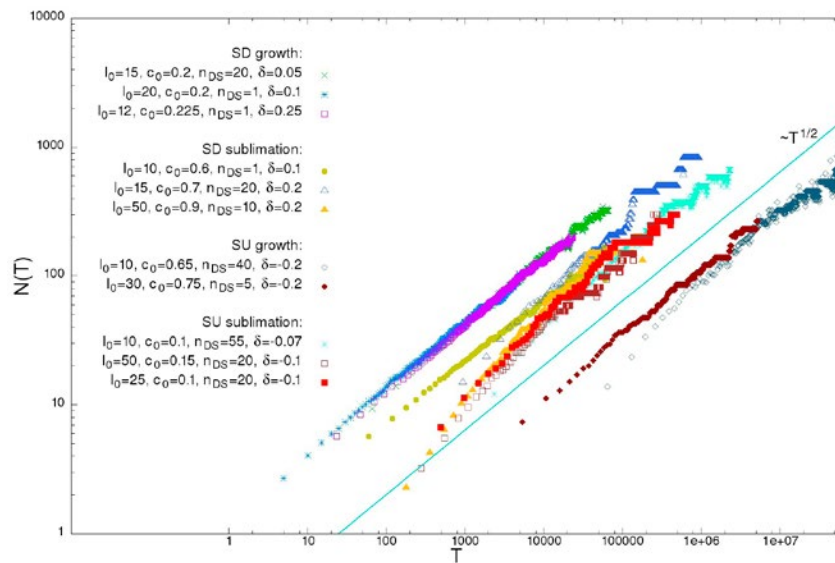


Fig. 2 Time dependent bunch size in four investigated cases.

References:

- [1] A. Krasteva et al., AIP Conf. Proc. 1722, (2016) 220014
- [2] F. Krzyżewski et al., arXiv preprint arXiv:1601.07371 (2016), J. Cryst. Growth accepted
- [3] R. L. Schwoebel, E. J. Shippy J. Appl. Phys. 37, 3682 (1966)

Mon-17:00-O-ELI-ALPS**The next generation of attosecond sources at ELI-ALPS****ELI-ALPS**

[S. Kuehn](#), [T. Csizmadia](#), [B. Farkas](#), [M. Fule](#), [M. Dumergue](#), [S. Kahaly](#), [B. Major](#), [S. Mondal](#), [P. Tzallas](#), [P. Antici](#), [D. Charalambidis](#), [P. Dombi](#), [F. Lepine](#), [L. Fulop](#), [G. Meszaros](#), [K. Osvay](#), [G. Sansone](#), [K. Varju](#)

ELI-ALPS, ELI-Hu Nonprofit Ltd., Budapesti ut 5, H-6728 Szeged Hungary

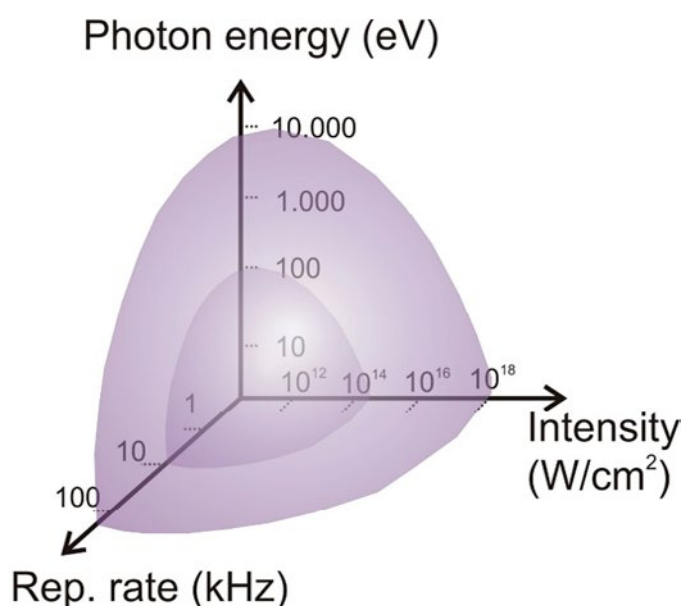
The research infrastructure at ELI-ALPS is based on four main laser sources: three operating in the regime of 100 W average power in the near-infrared (NIR) and one at 10 W in the mid-IR (MIR). These systems are designed to deliver pulses with unique parameter combinations of pulse duration, repetition rate and pulse energy delivered in stable and reliable operation. The outstanding performance of the primary laser pulses will enable the operation of secondary sources with exceptional characteristics, achieving a remarkable spectral range from the THz to the X-ray wavelengths of synchronized pulses, and even particles. This goal is achieved with the highest quality primary laser sources and expertly designed, innovative high-harmonic beamlines. The generation of high flux attosecond pulse trains and isolated attosecond pulses is a central target that will be realized using high-harmonic generation from gas and plasma targets. These efforts will extend the experimental range of activities in attoscience in three strategic directions as graphically presented in fig. 1:

- Spectral bandwidth: Few-cycle pulses from the terahertz/infrared up to the petahertz/ultraviolet, and attosecond pulses from extreme-ultraviolet up to soft and hard x-ray wavelengths,
- Pulse energy: Attosecond pulses with GW peak powers.
- Repetition rate: An impressive pulse rate up to 100 kHz.

The secondary sources will be equipped with a set of optical delay lines and diagnostic devices enabling the users to perform experiments on various types of targets using the precisely synchronized above light sources. A time-preserving monochromator will enable spectral selection of the pulse wavelength. Special, dedicated end stations are also being developed, including a Reaction Microscope, a Condensed matter end station, Velocity Map Imaging Spectrometers and a Magnetic Bottle Electron Spectrometer equipped with target areas, while user-owned end stations can be installed at any of the beam lines.

The experimental activities will commence with the commissioning of the two 100 kHz repetition rate laser systems. Along with the lasers, we will also start the assembly of the high harmonic beamlines and the THz laboratory which will provide the first opportunities for research activities. I will highlight the opportunities for condensed matter and AMO sciences as the full capacity of ELI-ALPS will become available.

Fig. 1: Extension of the experimentally available activity range for the three strategic directions of Attoscience at ELI-ALPS.



Wed-11:00-O-GRAP ●

Reactivity of bi- and single layer graphene on Ir(111) towards hydrogen

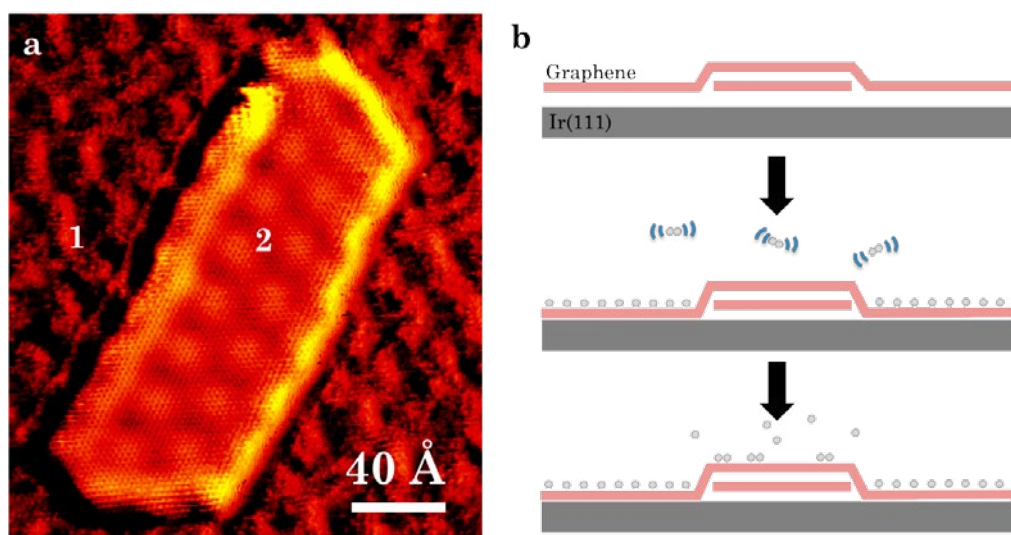
GRAP Graphene and carbon-based 2D films

[Line Kyhl](#)¹, [Jakob Holm Jørgensen](#)¹, [Andrew Cassidy](#)², [Liv Hornekær](#)², [Richard Balog](#)²

¹ Interdisciplinary Nanoscience Center (iNANO), Aarhus University, Denmark;

² Institute of Physics and Astronomy, Aarhus University, Denmark

The adsorption of atomic hydrogen on graphene on Ir(111) is a hot topic in the area of graphene band gap engineering [1,2]. Recently, it was shown that also vibrationally excited H_2 molecules can dissociate and chemisorb on graphene on Ir(111) in an adsorption structure favored by the moiré pattern [3]. While in a single layer graphene the H addition is catalyzed by the presence of the underlying Ir substrate, the reactivity towards vibrationally excited H_2 is fully deactivated in bilayer graphene. This introduces a new arena for the selective functionalization of single layer, non-freestanding graphene as opposed to bilayer graphene. Nanoislands of un-functionalized bilayer (and trilayer) graphene embedded in a surface of hydrogen functionalized single layer graphene can thus be prepared as shown by scanning tunneling microscopy in Fig. 1a (number of layers are indicated). The multilayer nanoislands remain, however, reactive towards *atomic* H with a hydrogen adsorption structure that depends on the orientation of the layers. Fig. 1b sketches the sideview of a bilayer graphene nanoisland before (top) and after exposure to vibrationally excited H_2 (middle) and subsequently atomic H (bottom). Additionally, our preliminary results opens for the interpretation that, in some cases, the exposure of atomic H on bilayer graphene on Ir(111) induces a complete sp^2 to sp^3 rehybridization yielding the electronically insulating structure diamane [4].



References:

- [1] J. H. Jørgensen, et al., ACS nano 10, 10798 (2016).
- [2] R. Balog, et al., Nature Materials 9, 315 (2010).
- [3] L. Kyhl, et al. Physical Review Letters (2017) Submitted.
- [4] D. Odhkuu, D. Shin, R. S. Ruoff, and N. Park, Scientific reports 3 (2013).

Tue-16:00-O-OXID ●

Water adsorption at the Zirconia Surface on Pt₃Zr

OXID Oxide surfaces and ultrathin oxide films

Peter Lackner¹, Jan Hulva¹, Joong-Il J. Choi^{1,2}, Eva-Maria Köck³, Simon Penner³, Bernhard Klötzer³, Ulrike Diebold¹, Gareth Parkinson¹, Michael Schmid¹

¹ Institute of Applied Physics, TU Wien, Vienna, Austria;

² Institute for Basic Science, KAIST, Daejeon, Republic of Korea;

³ Institute of Physical Chemistry, Leopold Franzens University Innsbruck, Innsbruck, Austria

Surface-science studies of zirconia (ZrO₂) with conduction-dependent techniques like scanning tunneling microscopy (STM) are hindered by its band gap of >5 eV. Thin and ultra-thin film model systems offer a possibility to circumvent this problem. A ZrO₂(111) trilayer can be formed via oxidation of Pt₃Zr(0001) single crystals [1]. As the oxide contains Zr from the top layers of the crystal, a pure Pt layer forms between the ZrO₂ trilayer above and Pt₃Zr layers below. The Pt layer at the interface contracts, forming a reconstruction with misfit dislocations. The ZrO₂ trilayer shows a ($\sqrt{19} \times \sqrt{19}$)R23.4° superstructure with 12 Zr atoms in every unit cell. It is strongly buckled; additionally it shows in-plane distortions above Pt dislocation lines, thus creating different adsorption locations.

We have employed this ZrO₂/Pt₃Zr system as a model system for water adsorption on zirconia, combining temperature-programmed desorption (TPD), X-ray photoelectron spectroscopy (XPS), and STM. In TPD, $\approx 90\%$ of the adsorbed D₂O contributes to the monolayer peak at 180 K. This corresponds to an adsorption energy of 0.57 ± 0.05 eV, which is in agreement with infrared-spectroscopy measurements on polycrystalline ZrO₂ at near-ambient conditions (E_{ads} ≈ 0.60 eV for most of the monolayer range). This indicates that the ZrO₂/Pt₃Zr ultra-thin oxide is a valid model system for bulk ZrO₂, and we argue that this should also apply to other reactions without a net charge transfer. According to XPS, the D₂O that desorbs in the monolayer peak is bound in molecular form, again in agreement with infrared-spectroscopy on polycrystalline ZrO₂. The remaining 10% of D₂O are bound in the form of hydroxyls. They have higher binding energies, which leads to a tail in the TPD spectrum reaching up to 550 K. STM shows that the highest adsorption energies occur above Pt dislocations. Repeated TPD measurements lead to a decrease of the monolayer peak area and to an increase of the tail area. Thus, repeated exposure to water changes the surface structure, creating adsorption sites with higher adsorption energies.

Supported by the Austrian Science Fund (FWF; project F45).

References:

[1] Antlanger et al., Phys. Rev. B 86, 035451 (2012).

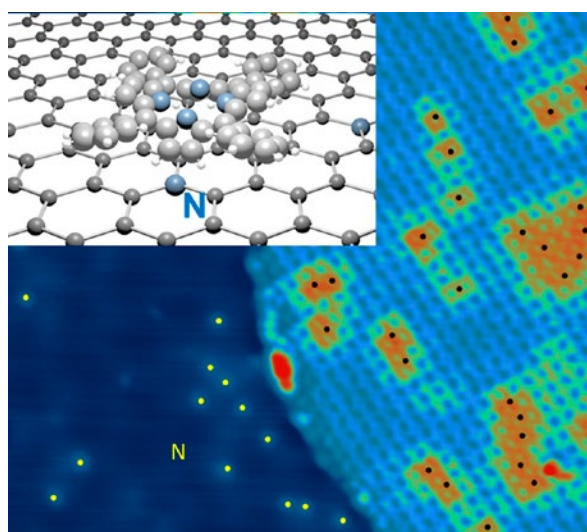
Wed-16:00-O-GRAP ●**Electronic interaction of organic molecules with nitrogen doped graphene***GRAP Graphene and carbon-based 2D films*

[Jérôme Lagoute](#)¹, [V. D. Pham](#)¹, [F. Joucken](#)², [V. Repain](#)¹, [C. Chacon](#)¹, [A. Bellec](#)¹, [Y. Girard](#)¹, [S. Rousset](#)¹

¹ *Laboratoire Matériaux et Phénomènes Quantiques (MPQ), CNRS/Université Paris diderot, Paris, France;*

² *Research Center in Physics of Matter and Radiation (PMR), Université de Namur, Namur, Belgium*

Tailoring the properties of graphene is of fundamental interest to uncover new functionalities and open new opportunities for graphene based applications. Among the possible strategies explored, substitutional doping obtained by replacing some carbon atoms by foreign atoms has focused tremendous efforts. In this context, nitrogen doping appears to be particularly interesting as it allows to perform n-doping with minor structural perturbations. This doping induces a shift of the Dirac point and the formation of localized electronic states [1]. Concerning chemical reactivity, the doping also modifies the interaction of graphene with molecules. To probe this effect at the molecular level, scanning tunneling microscopy (STM) and spectroscopy (STS) experiments have been performed with electron acceptor (porphyrin) [2,3] and electron donor molecules deposited on nitrogen doped graphene. Local spectroscopy allows to measure resonances arising from the molecular states and to reveal a weak electronic coupling between graphene and molecules. The doping sites induce a downshift of the energies of the molecular electronic states revealing a local charge transfer. Using molecular manipulation with the STM tip molecules can be removed to reveal the underlying substrate and correlate the electronic features of the molecules with the presence of nitrogen atoms below. In order to obtain a more complete picture of the role of nitrogen doping on the interaction of graphene with molecules, we have recently investigated the case of electron acceptor molecules that will be discussed.



STM image of porphyrin molecules on nitrogen doped graphene

References:

- [1] Joucken F. et al., *Sci. Rep.* 5, 14564 (2015)
- [2] Pham V. D. et al., *ACS Nano* 8, 9403 (2014)
- [3] Pham V. D. et al., *Sci. Rep.* 6, 24796 (2016)

Tue-14:00-O-EG2D ●

Supramolecular assembly on top and underneath 2D materials: can molecules interact across a graphene barrier?

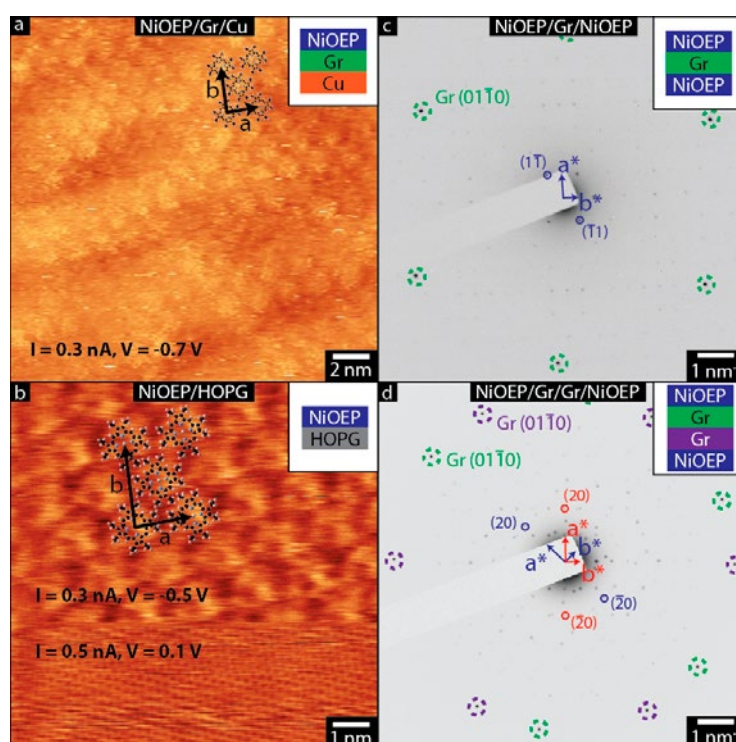
EG2D Epitaxial growth and modification of 2D materials

Zachary P. L. Laker¹, Harry Pinfold², Xue Xia¹, Giovanni Costantini², Neil R. Wilson¹

¹ Department of Physics, University of Warwick, Coventry, CV4 7AL;

² Department of Chemistry, University of Warwick, Coventry, CV4 7AL

Directed assembly of molecules on surfaces occurs due to a combination of molecule-molecule and molecule-substrate interactions, and is utilized in the formation of molecular thin films for a wide variety of purposes. Molecule-molecule interactions involve electrostatic, hydrogen-bonding and van der Waals (vdW) forces, whilst molecule-substrate interactions are typically governed by the electronic and topographic properties of the substrate. Recently, the use of 2D materials, such as graphene, as molecular substrates has received increasing attention.[1,2] 2D materials have strong in-plane bonding but only weak out-of-plane interactions. These weak interactions can encourage crystalline 2D supramolecular assembly without epitaxy,[3] with incommensurate substrate and molecular lattices. As graphene is a single atom thick, it can be considered as both a 2D substrate and a membrane, with identical top and bottom crystalline surfaces. This presents the intriguing question: to what extent can inter-molecular interactions extend across the graphene membrane?



Using a combination of transmission electron microscopy (TEM) and scanning tunneling microscopy (STM), we study the molecular level structure of self-assembled nickel(II) octaethylporphyrin (NiOEP) on metal-supported and freestanding graphene. STM measurements show that NiOEP assumes a flat 2D lattice on both Cu-supported graphene and on HOPG, in agreement with previous reports.[4] TEM measurements of NiOEP deposited on both the top and bottom faces of freestanding graphene reveal the same 2D molecular lattice, with spacings of (2.31 ± 0.01) nm by (1.52 ± 0.01) nm and a lattice angle of $(89.5 \pm 0.1)^\circ$.

There is no epitaxial alignment between the graphene and molecular layers but, crucially, the two molecular films are aligned with respect to each other. By contrast, when the molecular layers are separated by two layers of graphene, they are randomly oriented with respect to each other and with respect to the graphene. The same results – ordered 2D molecular layer on each graphene surface, but aligned only when separated by monolayer graphene – are obtained for self-assembled octaethylporphyrin (OEP) without a metal center. These results demonstrate that graphene is at least partially transparent to intermolecular interactions, which are rendered ineffective once the barrier width is increased to two layers of graphene. This new phenomenon of molecular alignment through 2D films gives a new tool for the study and design of nanostructured films, and demonstrates how molecular interactions can extend across the otherwise impermeable graphene membrane.

References:

- [1] Macleod, J. M. & Rosei, F. Molecular self-assembly on graphene. *Small* 10, 1038–1049 (2014).
- [2] Zhou, Q. et al. Switchable supramolecular assemblies on graphene. *Nanoscale* 6, 8387 (2014).
- [3] Marsden, A. J. et al. Growth of Large Crystalline Grains of Vanadyl-Phthalocyanine without Epitaxy on Graphene. *Adv. Funct. Mater.* (2016).
- [4] Ogunrinde, A., Hips, K. W. & Scudiero, L. A scanning tunneling microscopy study of self-assembled nickel(II) octaethylporphyrin deposited from solutions on HOPG. *Langmuir* 22, 5697–5701 (2006).

Tue-17:20-O-CATL ●

Observation of oxygen spillover between different {012} and {113} Rh facets during adsorption and hydrogenation of CO₂

CATL Catalytic 2D-model studies at low pressures

Sten V. Lambaerts¹, Cédric Barroo², Sylwia Owczarek³, Eric Genty¹, Natalia Gilis¹,
Luc Jacobs¹, Thierry Visart de Bocarmé²

¹ Chemical Physics of Materials (CPMCT), Université libre de Bruxelles (ULB), Faculty of Sciences, CP243, 1050 Brussels, Belgium;

² Chemical Physics of Materials (CPMCT) and Interdisciplinary Center for Nonlinear Phenomena and Complex Systems (CENOLI) Université libre de Bruxelles (ULB), Faculty of Sciences, CP243, 1050 Brussels, Belgium;

³ Institute of Experimental Physics, University of Wrocław, Wrocław, Poland

In heterogeneous catalysis, one way to develop better catalysts is to acquire a thorough understanding of the reaction steps at the surface, down to the molecular level. The focus is put on particle shape, size and local surface composition, features that can show mutual effects on each other. In the context of CO₂ valorisation, this work addresses the CO₂ adsorption as well as the interaction of H₂/CO₂ gas mixtures on single nano-sized rhodium crystals, using field ion microscopy (FIM), field emission microscopy (FEM) and 1-Dimensional Atom Probe (1DAP). The structure of the model catalyst is characterized with atomic resolution by FIM. CO₂ adsorption and hydrogenation processes are studied in FEM mode, during the ongoing processes at 700K. Reactive behaviours are monitored by following the evolution of the FEM pattern due to the variations of the local work function. Observed phenomena have been compared with the adsorption of other O-containing species such as CO, N₂O and O₂.

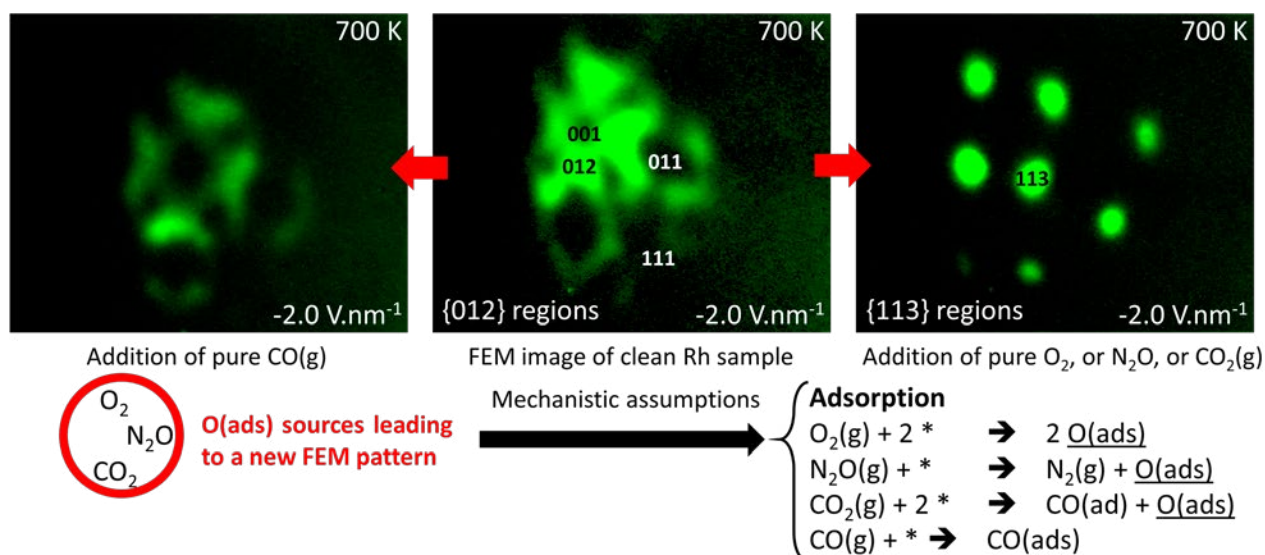


Figure 1. FEM pattern transformations and mechanistic suggestions.

The FEM pattern of a clean Rh-sample features bright area corresponding to facets of {012} orientations surrounding a central (001) pole (Fig1-centre). During CO₂ exposure, their brightness drastically decreases and remains dark, reflecting the CO₂ dissociative adsorption and the formation of O(ads) species. The presence of O(ads) at the surface also induces a new FEM pattern where {113} facets become the most visible. The pattern reflects the formation of subsurface oxygen O(sub) beneath the {113} facets (Fig1-right),

inducing a decrease of their work function. This is confirmed by comparative studies with N_2O , O_2 and CO adsorptions on Rh. To study the hydrogenation of CO_2 , pure H_2 gas is introduced in the chamber, while the pressure of CO_2 is kept constant. Reaction phenomena, reflected by variations in the brightness pattern, were observed from 650 to 700 K. H_2 adsorption leads to the formation of $H(ads)$ species, subsequently reacting with $O(ads)$ to form $H_2O(ads)$ that readily desorbs. Similar reaction phenomena were observed with N_2O+H_2/Rh and O_2+H_2/Rh systems in the same temperature range, but not with the $CO+H_2/Rh$ system (Fig1-left): this indicates the absence of CO dissociation on Rh under the reaction conditions and shows the crucial role of $O(ads)$ in the mechanism. Our observations are in line with the occurrence of the Reverse Water Gas Shift reaction ($CO_2(g)+H_2(g) \rightarrow CO(g)+H_2O(g)$). Direct local chemical analyses performed by 1DAP revealed the presence of rhodium oxides species – RhO^{2+} and RhO_2^{2+} – as well as CO_2 and its dissociation products. CO^{2+} , CO^+ and O^+ , are detected in the first layers of a (115) facet of the Rh nanoparticle during an exposure to pure CO_2 at 325K.

Thu-16:20-O-CATL ●**Contrasting dynamics for aryl- and alkyl-halide surface-reaction at copper***CATL Catalytic 2D-model studies at low pressures*

[Lydie Leung](#), [Matthew J. Timm](#), [Kelvin Anggara](#), [Tingbin Lim](#), [Zhixin Hu](#), [John C. Polanyi](#)

Lash Miller Chemical Laboratories, Department of Chemistry, University of Toronto, 80 St. George Street, Toronto, Ontario, M5S 3H6, Canada

Electron-induced carbon-halogen bond-breaking in aryl molecules adsorbed on copper has been shown to be mainly localized to an adjacent copper site $\sim 3\text{-}4$ Å away. Here we contrast the reaction of phenyl and pentyl bromide on Cu(110), studied by scanning tunneling microscopy (STM) at 4.6 K. On electron-impact the atomic Br was observed in this work to recoil along the C-Br bond-direction giving localized reaction for phenyl bromide (PhBr) whereas Br from pentyl bromide (PeBr) recoiled in the majority of cases to substantially larger distances of 10-20 Å.

The molecular dynamics of these electron-induced reactions were computed using an Impulsive-Two-State model, in which the systems resided in an anionic excited state for a time, t^* , and then returned to the ground electronic state. It was found that for PhBr the molecule when excited for the minimum t^* required for C-Br bond-breaking gave the observed localized reaction. By contrast, two to three times the minimum t^* was required to account for the observed long-range recoil of the Br-atom from PeBr. The marked difference in the observed recoil distances for Br from PhBr and PeBr suggests that in the case of PeBr the system stays for a significantly longer time on the electronically excited state with extended repulsion between the Br and the pentyl radical.

Tue-16:40-O-ELCH ●

An *in-situ* study of Sn deposition into nano-porous ordered anodic aluminum oxide

ELCH Electrochemistry at surfaces

Weronica Linpé, G.S Harlow, J. Evertsson, U. Hejral, E. Lundgren

Division of Synchrotron Radiation Research, Lund University, SE-22100 Lund, Sweden

Aluminum and its alloys are used in a wide range of products and applications because of their characteristic properties: low density, high strength, good thermal conductivity and corrosion resistance. A native self-limited aluminum oxide is naturally formed on aluminum, protecting the metal from corrosion and has self-healing properties [1,2]. To increase the corrosion resistance, the thickness of the oxide layer can be increased by electrochemical means, a process called anodization [3], which forms a porous aluminum oxide with a thickness of several microns. However in recent years it has been discovered that, under certain electrochemical conditions, ordered nano-porous Anodic Aluminum Oxides (AAO) can be grown [4], which can be used as templates for nano structures, by the electro-deposition of metals into the nano-pores.

We have conducted *in situ* studies of the electro-deposition of Sn into ordered nano-porous AAO templates using Grazing Incidence Small Angle X-ray Scattering (GISAXS) and X-Ray Fluorescence (XRF) spectroscopy. The AAO templates were created by a two-step anodization process, where the second anodization step was continuously imaged using GISAXS to follow the growth of the AAO. To facilitate the deposition of metals into the pores, a widening of the pores and thinning of the barrier oxide layer was done by either a chemical etch or through stepping-down the anodization potential. Deposition of Sn into the AAO pores was done with an alternating potential. The deposition was studied *in situ* by anomalous GISAXS and XRF. Measurements were conducted at energies close to the x-ray adsorption edge for Sn at 29 keV and far away from the edge at 12 keV. While the anomalous GISAXS did not show significant changes during the deposition, the XRF clearly revealed an accumulation of Sn at the sample, and a clear change in color of the sample could be observed after the measurements. *Ex situ* FIB-SEM measurements supports the accumulation of Sn inside the pores.

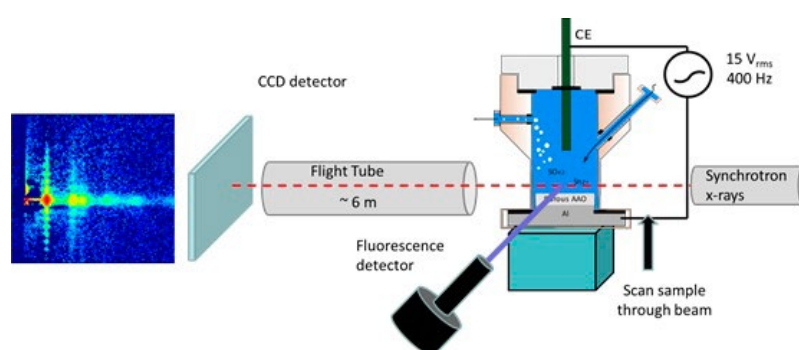


Figure 1: Illustration of the experimental setup. The left image shows a typical GISAXS image of the nano-porous AAO during a second anodization stage.

References:

- [1] L.P.H. Jeurgens, W.G. Sloof, F.D. Tichelaar, C.G. Borsboom, E.J. Mittemeijer, *Appl. Surf. Sci.* 144 (1999) 11
- [2] J. Evertsson et al *Appl. Surf. Sci.* 349 (2015) 826
- [3] F. Bertram et al, *J. Appl. Phys.* 116 (2014) 034902
- [4] W. Lee. and S.-J. Park, *Chem. Rev.* 114 (2014) 7487.

Thu-11:40-O-GRAP ●

Density driven sodium 2D phase transformation on epitaxial graphene

GRAP Graphene and carbon-based 2D films

Simone Lisi, Mazaleyra Estelle, Gomez-Herrero Ana-Cristina, Nguyen Van Dung, Guisset Valerie, David Philippe, Coraux Johann

Institut NEEL CNRS/UGA UPR2940, 25 rue des Martyrs BP 166, 38042 Grenoble cedex 9, France

Graphene is an easily accessible platform whose unique properties can accordingly be tailored along various strategies [1, 2]. Decorating graphene with adsorbates has been proven to be an efficient such strategy and, among the others, alkali metals (e.g. Li, Na, Cs, K) have been extensively explored due to their well known capability to transfer charges to graphene [3, 4]. Resolving and controlling the structure of alkali atom phases decorating graphene from atop (adsorbed) and below (intercalated) is of uttermost importance, as: i) it permits to rationalise and control the charge transfer, hence to control electronic doping and work-function; ii) it opens the way to breaking the equivalence of the two carbon sub-lattices in graphene, hence to generate the often elusive band-gap at the Dirac point.

We will present the so-far unknown [3] structural evolution, as a function of density, of a Na layer deposited on epitaxial graphene grown on an Ir(111) single crystal. By means of in-operando reflection high energy electron diffraction (RHEED) we discovered multiple periodicities in two-dimensional Na lattices, with a succession of plateaux in the evolution of the lattice parameter [5]. We interpret our observations as the evidence of a first order phase transition, whereby the repulsive Na-Na interactions lead the system to lock first on the Ir lattice, second on the graphene lattice, as the Na density increases. The second phase nucleates and progressively spreads in the first one, eventually replacing it.

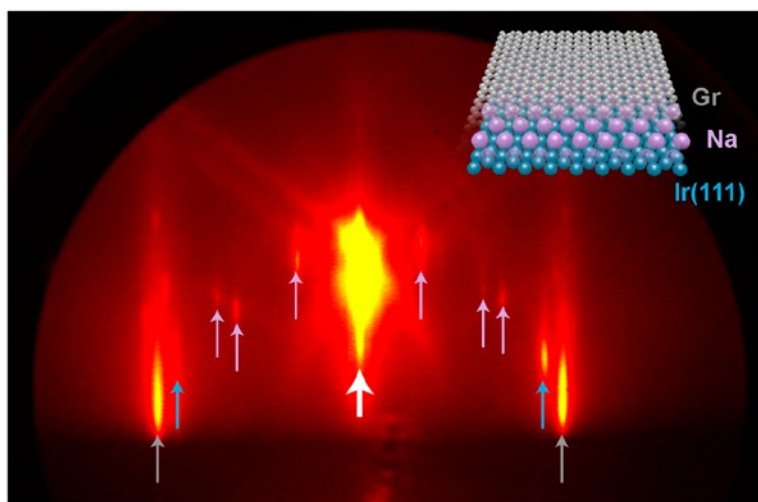


Figure 1. Representative RHEED pattern of graphene/Ir(111) during Na deposition (17.0keV electron beam primary energy, incidence angle $<5^\circ$, electron beam aligned along the (1,-2,1) direction with respect to the Ir(111) surface). Colored arrows highlight the contributions coming from graphene (grey), Na (purple) and Ir(111) (Blue). All the additional diffraction streaks, except for the specular one (pointed by the white arrow), are due to moiré interference effects.

References:

- [1] Balog, R. et al., Nature Materials, 9, 315 (2010)
- [2] Usachov, D. et al., Nano Letters, 11, 5401 (2011)
- [3] Papagno, M. et al., ACS Nano, 6, 199 (2012)
- [4] Struzzi, C. et al., Physical Review B, 94, 085427 (2016)
- [5] Lisi, S. et al. submitted

Thu-14:00-O-OXID ●**The interaction between cerium oxide and platinum studied by LEEM***OXID Organic molecules on solid surfaces*

Gabriele Gasperi^{1,2}, Paola Luches², Sergio Valeri¹, Marc Sauerbrey³, Jens Falta³, Jan Ingo Flege³

¹ Dipartimento di Scienze Fisiche, Informatiche e Matematiche, Università degli Studi di Modena e Reggio Emilia, Italy;

² Istituto Nanoscienze, Consiglio Nazionale delle Ricerche, Modena, Italy;

³ Institute of Solid State Physics, University of Bremen, Germany

Cerium oxide combined with platinum nanoparticles is a material in which the synergy between the two constituents provides additional functionalities, very interesting for catalytic applications. To obtain an atomic scale description of the interaction between the metal and the oxide, and thus understand the origin of properties which arise from their combination, the system can be studied in the form of an inverse model catalyst, i.e. as ultrathin epitaxial oxide films on metal single crystals.

With this aim we studied cerium oxide films grown on the Pt(111) surface. We have shown in previous work that films of subnanometer thickness have a much higher reducibility than the surface of thicker films and we ascribed this evidence to the interaction with platinum [1]. In the present work we used low-energy electron microscopy (LEEM) and spatially-resolved low-energy electron diffraction (μ -LEED) to characterize the as-grown inverse model catalyst [2] and study in real-time the morphological and structural modifications occurring in the system during reduction and oxidation. The reduction was induced by thermal annealing in ultra-high vacuum and in hydrogen partial pressure, and by deposition of metallic cerium on the surface of thicker films. From the comparison of the structural and morphological evolution in the three cases we obtain important information on the interaction between platinum and cerium oxide. An example of the morphological modifications observed after thermal reduction and reoxidation is shown in Figure 1.

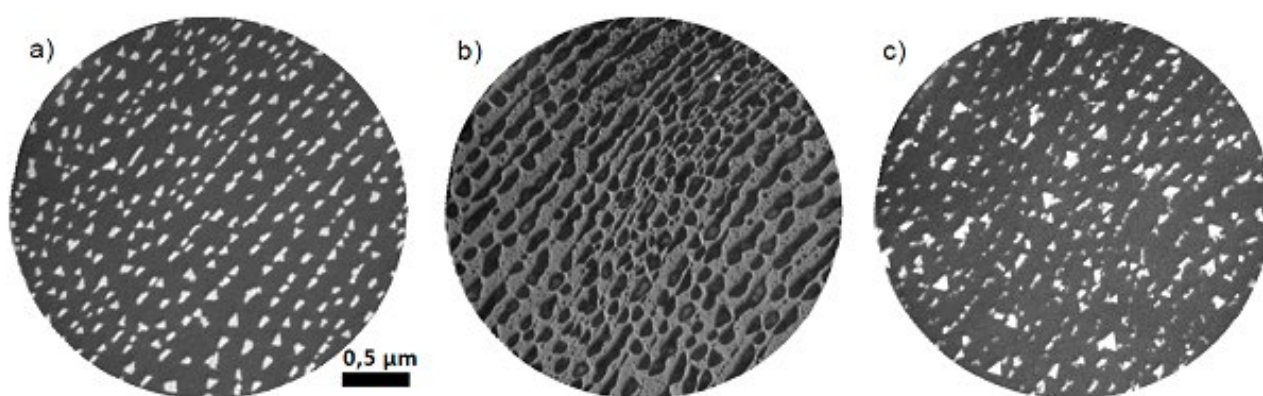


Figure 1: LEEM images acquired at $E=12,0$ eV on a cerium oxide sample grown at 770 °C on Pt(111): a) as-grown; b) after the reducing treatment in UHV; c) after re-oxidation.

References:

[1] G. Gasperi et al., Phys. Chem. Chem. Phys. 18, 20511 (2016).

[2] M. Sauerbrey et al., Top. Catal. (2016), DOI: 10.1007/s11244-016-0716-6.

Thu-11:40-O-CATH ●**The misfit structure between the Pd(100) and PdO(101) under reaction conditions***CATH Catalytic 2D-model studies under high pressures*

M. Shipilin¹, Edvin Lundgren¹, M. Shipilin¹, A. Stierle^{2,3,4}, L. R. Merte¹, J. Gustafson¹, U. Hejral¹, N. M. Martin^{1,5}, C. Zhang¹, D. Franz³, V. Kilic⁴,

¹ Division of Synchrotron Radiation Research, Lund University, Lund, Sweden;

² Physics Department, University of Hamburg, Hamburg, Germany;

³ Deutsches Elektronen-Synchrotron (DESY), Hamburg, Germany;

⁴ Physics Department, University of Siegen, Siegen, Germany;

⁵ Competence Centre for Catalysis, Chalmers University of Technology, Göteborg, Sweden

The details of the oxygen induced ($\sqrt{5}\times\sqrt{5}$)R27° structure on Pd(100) [1-3] was studied by Surface X-Ray Diffraction (SXR) during the catalytic oxidation of CO using a pressure of 200 mbar and a temperature of 300°C. It is shown that the misfit of the PdO(101) layer on the Pd(100) gives rise to a diffraction pattern deviating from that of a perfect ($\sqrt{5}\times\sqrt{5}$)R27° due to a lattice mismatch between the PdO(101) and the Pd(100) in essentially one direction. The presence of four rotated domains significantly complicates the high resolution SXR diffraction pattern, a pattern not observed in standard Low Energy Electron Diffraction (LEED) due to the lower resolution. To reproduce the observed diffraction pattern, we constructed a number of different models of larger PdO(101) unit cells including various types of mismatch. By comparing the calculated diffraction patterns to the observed pattern, we find that only a model including a periodic rigid shift of the Pd and O atoms in the PdO(101) in the incommensurate direction (the [011] substrate direction) explains the experimental diffraction pattern [4]. Surprisingly, despite the fact that the SXR data is recorded under harsh reaction conditions, the results are in qualitative agreement with Scanning Tunneling Microscopy (STM) observations performed under Ultra High Vacuum (UHV) conditions.

References:

[1] M. Todorova, et al., Surf. Sci. 541 (2003) 101.

[2] P. Kostelnik, et al., Surf. Sci. 601 (2007) 1574.

[3] M. Shipilin et al, Surf. Sci. 630 (2014) 229.

[4] M. Shipilin et al, Surf. Sci. 660 (2017) 1.

Tue-9:40-O-ENER ●

Redox-mediated conversion of atomically dispersed platinum to sub-nanometer particles

ENER Surfaces for energy production and harvesting

Yaroslava Lykhach¹, Alberto Figueroba², Tomáš Skála³, Tomáš Duchoň³, Nataliya Tsud³, Marie Aulická³, Armin Neitzel¹, Kateřina Veltruská³, Kevin C. Prince⁴, Vladimír Matolín³, Konstantin M. Neyman^{2,5}, Jörg Libuda^{1,6}

¹ Lehrstuhl für Physikalische Chemie II, Friedrich-Alexander-Universität Erlangen-Nürnberg, Egerlandstrasse 3, 91058 Erlangen, Germany;

² Departament de Ciència dels Materials i Química Física and Institut de Química Teòrica i Computacional, Universitat de Barcelona, c/ Martí i Franquès 1, 08028 Barcelona, Spain;

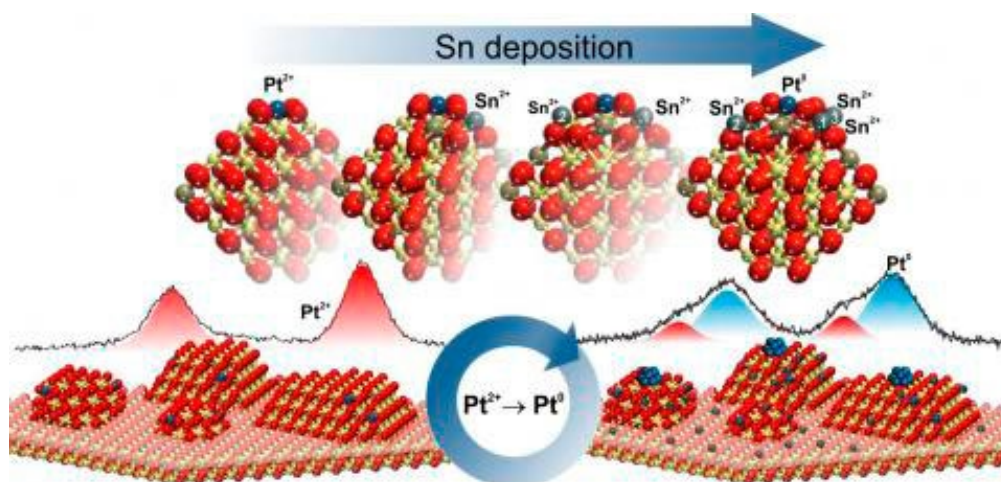
³ Charles University, Faculty of Mathematics and Physics, Department of Surface and Plasma Science, V Holešovičkách 2, 18000 Prague, Czech Republic;

⁴ Elettra-Sincrotrone Trieste SCpA and IOM, Strada Statale 14, km 163.5, 34149 Basovizza-Trieste, Italy;

⁵ ICREA (Institució Catalana de Recerca i Estudis Avançats), Pg. Lluís Companys 23, 08010 Barcelona, Spain;

⁶ Erlangen Catalysis Resource Center, Friedrich-Alexander-Universität Erlangen-Nürnberg, Egerlandstrasse 3, 91058 Erlangen, Germany

Redox interactions in the metal-oxide systems can be utilized to design advanced materials for applications in catalysis. In our studies, we show that sub-nanometer Pt particles on ceria can be formed by reduction of atomically dispersed Pt²⁺ species triggered by the interaction with reducing agents, e.g. Sn. The sequence of reactions involves oxidation of Sn⁰ to Sn²⁺ coupled with the reduction of Ce⁴⁺ to Ce³⁺. Consecutively, the redox coupling between the Ce³⁺ and Pt²⁺ species triggers the reduction of Pt²⁺ species yielding sub-nanometer Pt particles. By means of synchrotron radiation photoelectron spectroscopy, resonant photoemission spectroscopy, and angle-resolved X-ray photoelectron spectroscopy, we followed the conversion of Pt²⁺ species as a function of the Sn concentration in the Pt–CeO₂ films. The onset of the reduction of Pt²⁺ species was found to be directly related to the concentration of Ce³⁺ centers which, in turn, is controlled by the concentration of Sn²⁺ cations in the Pt–CeO₂ film. On average, formation of 6 Ce³⁺ centers, corresponding to the adsorption of 3 Sn atoms, gives rise to the reduction of one Pt²⁺ species. According to density functional modeling, adsorption of three Sn atoms in the vicinity of the Pt²⁺ species results in a rearrangement of the local coordination accompanied by substantial destabilization of the Pt²⁺ species with respect to the adsorption of Pt⁰ atoms.



Wed-11:00-O-OXID ●**The formation mechanism of the p(2×3) reconstruction on Mo(112) surface***OXID Oxide surfaces and ultrathin oxide films*Teng Ma, Xue Bao*Shenyang Agricultural University*

Oxygen induced reconstruction and oxidation of Mo(112) surface has shown various surface structures in model catalysis and surface studies. Because of its complexity, the p(2 × 3) reconstruction has been modeled as several patterns and its formation mechanism was not well clarified. In this report, a critical precursor or the unfinished of p(2 × 3) reconstruction has been observed during the evolution processes by using STM, XPS and HREELS methods. For the Mo(112) surface exposed to 5.0×10^{-8} mbar O₂, the p(2×3) reconstruction is a complex and stepwise process, during which the clean metallic surface experience the initial oxidation to form dispersed oxide particles at nanoscale, and then consecutive reduction and structural rearrangement of molybdenum oxides to the ordered nanostructures. The features of surface structures are also temperature-dependent, a mixture of dispersed nanoparticles of molybdenum oxide and one-dimensional nanostructures occurs in the [-1-11] direction after O₂ dose at 605 K, while two-dimensional nanostructures or the p(2×3) reconstruction occurs until above 710 K. Our findings would give a good explanation about some hurdled questions about the appearance of p(1×3) features in the LEED patterns and antidomain dislocations in the STM images of the p(2×3) reconstruction.

References:

1. J. Seifert and H. Winter, Surf. Sci. 2013, 610, L1-L5.
2. S. Kaya, J. Weissenrieder, D. Stacchiola, et.al., Surf. Sci. 2008, 602, 3338-3342;
3. M. Sierka, T.K. Todorova, J. Sauer, et.al., J. Chem. Phys. 2007,126, 234710.

Mon-14:40-O-SAMA ●

Characterization of polycyclic conjugated hydrocarbons by means of NCAFM

SAMA Structural analysis and manipulation on atomic scale

Zsolt Majzik¹, Niko Pavliček¹, Manuel Vilas-Varela², Nikolaj Moll¹, Dolores Pérez², Enrique Guitián², Gerhard Meyer¹, Diego Peña², Leo Gross¹

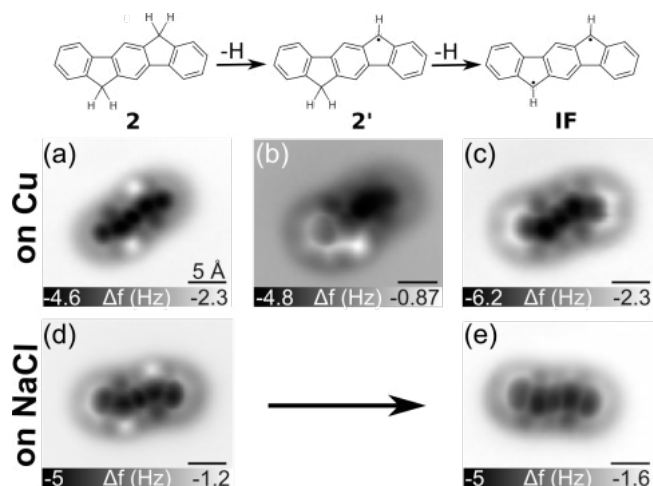
¹ IBM Research-Zurich, 8803 Rüschlikon, Switzerland;

² CIQUS and Departamento de Química Orgánica, Universidade de Santiago de Compostela, Santiago de Compostela 15782, Spain

Aromaticity is one of the most relevant yet intriguing concepts in chemistry. In 1931, Hückel suggested his wellknown rule to explain the “extra stability” of planar monocyclic molecules that contain $[4n+2]$ π -electrons in a conjugated system. With some limitations, the concept was later extended to polycyclic conjugated hydrocarbons (PCHs), based on the number of Clar sextets, or the presence of conjugated circuits with $[4n + 2]$ π -electrons within a particular structure. In 1967, Breslow introduced the term antiaromaticity as the inverse to aromaticity, in order to explain the destabilization of molecules with $[4n]$ π -electrons in a cyclic conjugated system [1]. Among PCHs with antiaromatic character, indeno[1,2-b]fluorene (**IF**) is a remarkable example. Compare to pentacene, the most prominent p-type organic semiconductor with five linearly fused six-membered rings and 22 π -electrons in its larger aromatic conjugate circuit ($[4n + 2]$, $n = 5$), **IF** presents a 6-5-6-5-6 fused-ring motif and a formally antiaromatic 20 π -electron conjugate system ($[4n]$, $n = 5$). The **IF** closed-shell structure with a central para-quinodi methane core and two Clar sextets might be in resonance with the **IF'** open-shell diradical structure with three sextets [2,3]. As a result, unsubstituted **IF** is presumed to be an extremely reactive PCH and in fact it has never been synthesized or even detected. Advances in atomic force microscopy (AFM), particularly resolving and modifying the structure of molecules at the atomic scale [4], have opened new routes in the chemistry of highly reactive compounds [5,6].

Here we present the generation and characterization of indeno[1,2-b]fluorene (**IF**) for the first time. We deposited custom synthesized precursor, 6H,12Hindeno[1,2-b]fluorene (**2**) molecules on Cu(1 1 1) partly covered by bilayer NaCl islands. A Cu tip was positioned above the center of a precursor molecule **2** at a tip height corresponding to an STM setpoint of $V = 0.1$ V and $I = 1$ pA. Then the feedback loop was opened, the tip was retracted by few Å to keep the current below $I = 0.1$ nA and the sample voltage V was increased until a step change in the tunneling current occurred indicating a manipulation event. Typically, dehydrogenation occurred for sample voltages above +3.5 V on both surfaces being consistent with previous experiments to remove a single H from CH₂ groups [6]. On Cu(111) two hydrogens were removed sequentially, giving rise to two distinct steps in current, whereas on 2ML NaCl two dehydrogenations happened simultaneously (Figure).

To learn more about the aromaticity of **IF**, we imaged the first negative ion resonance (NIR) at positive sample bias and compared the image with calculated STM images. The experimentally observed image at the first NIR is in good agreement with the simulated LUMO STM map of the molecule. Therefore, the orbital map confirms the success of our on-surface syntheses of **IF** and the molecule preserves the closed-shell character predicted for the free molecule on NaCl. Our bond-order analyses indicates that on Cu(1 1 1) the electronic configuration of **IF** is significantly altered due to strong chemisorption to the substrate.



References:

- [1] Breslow, R.; Brown, J.; Gajewski, J. J.: *J. Am. Chem. Soc.* 1967, 89, 4383
- [2] Kubo, T.: *Chem. Lett.* 2015, 44, 111
- [3] Fukuda, K.; Nagami, T.; Fujiyoshi, J.; Nakano, M.: *J. Phys. Chem. A* 2015, 119, 10620
- [4] Gross, L.; Mohn, F.; Moll, N.; Liljeroth, P.; Meyer, G.: *Science* 2009, 325, 1110
- [5] Schuler, B.; Fatayer, S.; Mohn, F.; Moll, N.; Pavlicek, N.; Meyer, G.; Pena, D.; Gross, L.: *Nat. Chem.* 2016, 8, 220–224
- [6] Pavlicek, N.; Mistry, A.; Majzik, Z.; Moll, N.; Meyer, G.; Fox, D. J.; Gross, L.: *Nat. Nanotechnol.* 2017, 12, 308–311

Thu-15:00-O-ORGS ●**Unveiling universal trends for the energy level alignment in organic/oxide interfaces***ORGS Organic molecules on solid surfaces*Jose Ignacio Martinez¹, Sylvie Rangan², Charles Ruggieri², Robert Bartynski², Fernando Flores³, Jose Ortega³¹ Dept. Nanostructures, Surfaces, Coatings and Molecular Astrophysics, Institute of Materials Science of Madrid (ICMM-CSIC), Sor Juana Inés de la Cruz 3, ES-28049 Madrid (Spain);² Dept. Physics and Astronomy, and Laboratory for Surface Modification, Rutgers, The State University of New Jersey, Piscataway, NJ 08854-8019 (USA);³ Dept. Condensed Matter Theoretical Physics and Condensed Matter Physics Center (IFIMAC), Universidad Autónoma de Madrid, ES-28049 Madrid (Spain)

Due to their extended pi-systems, polyaromatic molecules appear as convenient organic semiconductor materials for many technological applications such as organic electronics and optoelectronics. [1] Besides, hybrid organic-inorganic materials consisting of the combination of organic semiconductors and transition metal oxides have attracted great interest due to their complementary properties. In this contribution we present a comprehensive analysis of the energy level alignment at the interface between an organic monolayer (PTCDA, ZnTPP and TCNQ) and a prototypical oxide surface, TiO₂(110), looking for universal behaviors. PTCDA shows a physisorbed interaction with TiO₂ and a small interface dipole potential with its HOMO energy level located in the oxide energy gap and the LUMO energy level located above the oxide conduction band minimum, E_c. We analyze how the interface barrier depends on an external bias potential between the organic layer and the oxide surface, D, and find for this interface that the screening parameter $S = d(E_c - \text{HOMO})/dD$ is close to 1. In the second case, the ZnTPP monolayer shows a moderate chemisorbed interaction with some charge transfer from the molecule to the oxide and a significant interface dipole potential, in such a way that S decreases to around 0.8.[2] In the TCNQ/TiO₂(110) case, the TCNQ molecules present a strong chemical interaction with the oxide; the LUMO energy level is located in the oxide energy gap in such a way that one electron is transferred from the oxide to the organic molecule; we also find that in this case $S \sim 0.5$. [3] All those cases can be integrated within a universal behavior when $(E_c - \text{HOMO})$ is calculated as a function of D (see Figure); that function presents a zig-zag curve with a central part having a S-slope, and two plateaus associated with either the LUMO or the HOMO energy levels crossing the oxide Fermi level. In these plateaus, a Coulomb blockade regime appears and a space charge layer appears in the oxide surface.

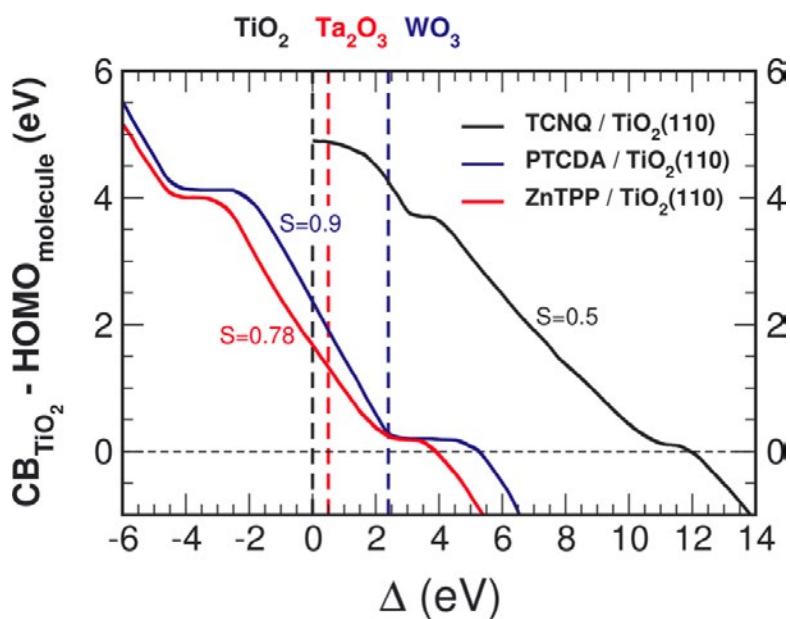


Figure: For the PTCDA, ZnTPP and TCNQ on $TiO_2(110)$ interfaces the oxide conduction band edge, $CB(TiO_2)$, minus the molecule HOMO level at RT conditions is depicted as a function of the relative positioning of the organic molecule w.r.t. the oxide energy levels

References:

- [1] a) Forrest, S. R. Chem. Rev. 1997, 97, 1793; b) Kabra, D.; et al. Adv. Mater. 2010, 22, 3194; c) Li, H.; et al. Chem. Mat. 2014, 26, 631; d) Meyer, J.; et al. Adv. Mater. 2012, 24, 5408; e) Sessolo, M.; et al. Adv. Mater. 2011, 23, 1829.
- [2] Rangan, S.; et al. JPCC 2016, 120, 4430.
- [3] Martínez, J. I.; et al. JPCC 2015, 119, 22086.

Tue-17:20-O-PISC ● Bragg diffraction of surface state electrons

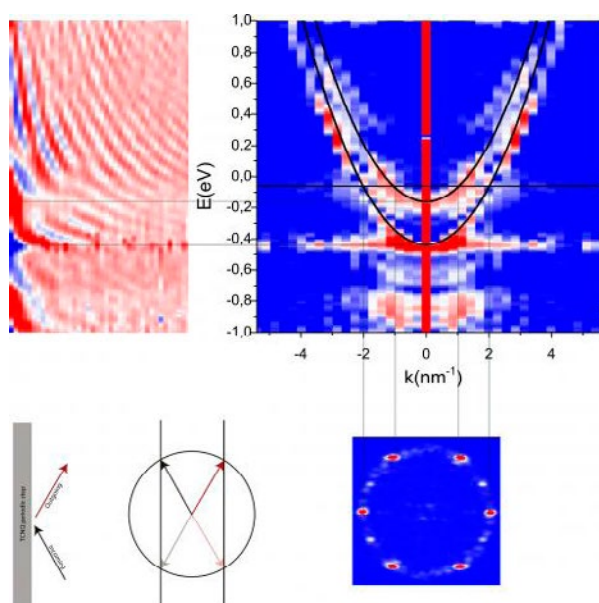
PISC Photo-Induced Surface Chemistry

[Alberto Martín-Jiménez](#), [David Écija](#), [Rodolfo Miranda](#), [Roberto Otero](#)

IMDEA-Nanoscience, Universidad Autónoma de Madrid C/Faraday 9, Madrid, Spain, 28049

STM has become a very powerful technique for studying quasi-particle interference of 2D materials. Quantum interference of scattered electrons results in standing wave patterns which correspond to Local Density of States (LDOS) maps at given energies. In previous experiments, the scattering centers were either randomly distributed over the surface, or an ordered array of them was created by atomic manipulation. In the former case, the need to observe several oscillations of the standing wave pattern between the scatterers required the they should be spaced by distances significantly larger than the wavelength of the surface state electrons, where as in the latter case, the scatterers are kept at distances of the order of the lattice pare meter of surface atoms, and therefore are small compared with the wavelength of surface state electrons.

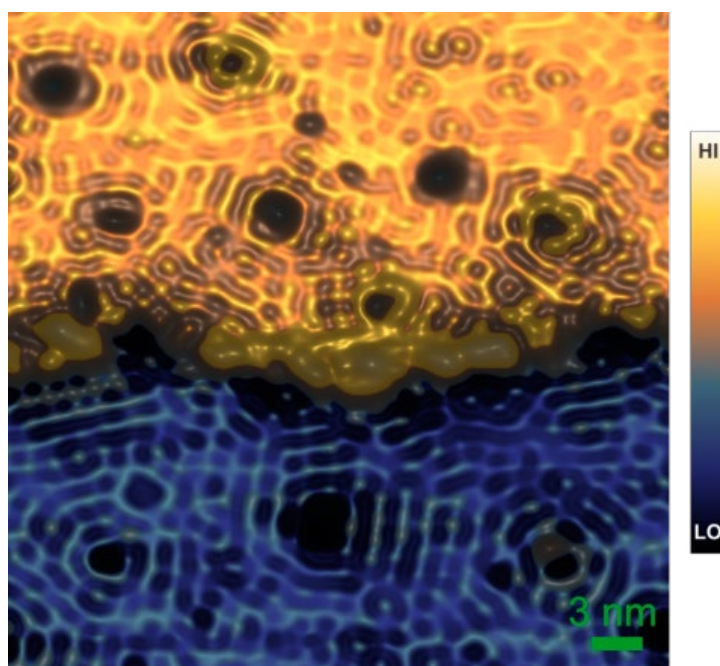
Here we present an experimental study on the standing wave pattern produced by the interaction of the surface state electrons of the Cu(111) surface with the ordered edges of TCNQ (tetracyanoquinodimethane) self-assembled islands, which present a periodicity of about 3.5 nm, very close to the Fermi wavelength of surface state electron. Energy-resolved 2D maps clearly indicate that the molecular island edge acts as a diffraction nano-grating, leading to a discrete set of preferred scattering orientations which can be described by Bragg coherent diffraction from a periodic set of scatterers. Moreover, such effect leads to the existence of electronic sub-bands corresponding to different diffraction indices, which are accessible through a Fourier analysis of STS spectra recorded along lines perpendicular to the step edge. These experiments are thus equivalent to a 2D LEED experiment performed by STM, and opens the possibility to build monochromators and filters for electrons in 2DEGs in analogy with optical devices.



Tue-14:20-O-ORGS ●**Real-space visualization of the pair correlation function in a 2D molecular gas***ORGS Organic molecules on solid surfaces*Peter Matvija, Filip Rozbořil, Pavel Sobotík, Ivan Ošťádal, Pavel Kocán*Faculty of Mathematics and Physics, Charles University, Prague, Czech Republic*

Properties of matter in fluid phases, determined by the interactions between particles, can be described by the pair correlation function. The function is defined as ensemble-averaged particle density (PD) at a given position relative to a reference molecule. We demonstrate that the scanning tunneling microscope (STM) is capable to directly visualize the PD in the real space in the case of two-dimensional (2D) molecular gas on weakly interacting surfaces.

We use the STM to study highly mobile molecules of fluorinated copper phthalocyanine on the Si(111)/Ti-(1×1) surface. A slow mechanism of STM imaging results in the time-averaging of molecular occurrence under the STM tip. The obtained image represents a map of local density of the 2D gas (see the figure). We show that in the proximity of fixed molecules the images represent directly the pair correlation function. We support the data interpretation by lattice-gas kinetic simulations and we use the method to analyze interactions between the molecules and surface defects.



Thu-14:40-O-SEMI ●
Ion irradiation induced compound formation*SEMI Semiconductor surfaces and ultrathin layers*

G. Battistig¹, [M. Menyhard](#)¹, S. Gurban¹, A. Racz¹, A Sulyok¹, Z. Zolnai¹, G. Vertesy¹,
A. Németh²

¹ Institute for Technical Physics and Materials Science, Centre for Energy Research, Hungarian Academy of Sciences;

² Wigner Research Centre for Physics, Institute of Particle and Nuclear Physics, Hungarian Academy of Sciences

Ion irradiation produces various defects on the surface and in surface close regions. A special type of defect is produced if an interface is subjected to ion irradiation; in this case a mixture of atoms of the neighbor regions forms. Such regions possess high internal energy which drives various relaxations resulting in atomic rearrangements even at room temperature. During the relaxation of the intermixed region compound formation might occur. The formation of stable compounds of high heat of formation as well as the formation of metastable compounds has been reported. The compounds in many cases form three-dimensional nanoparticles but intermixing of the components through continuous layer formation was also reported.

In this contribution we will report ion irradiation-induced compound formation observed on C/Ni, Si/Cr, C/Si, C/Ta and Si/C interfaces. The variety of heats of formation as well as differences in the stability of the compounds resulted in intermixed regions with different micro and nanostructures. The morphology of the produced compound also varies considerably. We have observed either layer type growth or the formation of a matrix enriched by embedded compound nanoparticles. We will attempt to define classes of compound formation based on the physical and chemical properties of the intermixing elements.

Tue-17:20-O-OXID ●**Model oxide-supported enantioselective catalysts: interaction between TiO₂-supported Ni nanoparticles and a chiral modifier***OXID Oxide surfaces and ultrathin oxide films***Elisa Meriggio^{1,2}, Christophe Méthivier¹, Gregory Cabailh², Xavier Carrier¹, Vincent Humblot¹**¹ Sorbonne Universités, UPMC Univ. Paris 06, UMR CNRS 7197, Laboratoire de Réactivité de Surface - 4 place Jussieu, 75252 Paris Cedex 05, France;² Sorbonne Universités, UPMC Univ. Paris 06, UMR CNRS 7588, Institut des NanoSciences de Paris - 4 place Jussieu, 75252 Paris Cedex 05, France

Enantioselective heterogeneous catalysis is a promising method for the synthesis of enantiopure chiral compounds for fine chemical, pharmaceutical and agrochemical industries. One successful approach involves the modification of a metal surface by a chiral modifier. Nevertheless, despite its great potential and economic advantages, only a small number of successful systems have been developed so far [1]. Moreover, most of fundamental works have been devoted to model systems based on single crystal metal surfaces while the role of the oxide support in supported metal catalysts have usually been overlooked. However, to date, fundamental questions remain on the role of the oxide support on the chiral induction during the reaction. A detailed understanding of the reaction mechanism and the mode of action of the chiral modifier requires therefore knowledge of the interactions at a molecular level between the three partners: oxide support, metal nanoparticles and chiral modifier. In this respect, surface science techniques provide fundamental insights into the physics and chemistry of such systems.

In this work TiO₂ single crystals, nickel nanoparticles (NPs) and tartaric acid (TA) have been chosen as model oxide support, metal nanoparticles and chiral modifier, respectively. Deposition of nickel and tartaric acid are performed by evaporation on a rutile TiO₂(110) single crystal under ultra-high vacuum condition. The so-obtained surfaces are then fully characterised by combining several *in situ* surface science techniques such as Scanning Tunnelling Microscopy (STM), X-Ray Photoemission Spectroscopy (XPS) and High Resolution Electron Energy Loss Spectroscopy (HR-EELS) in order to probe the surface organization and chemical state of both Ni NPs and TA.

At early stages of growth, we show that nickel forms small clusters of uniform size, in agreement with thermodynamic expectations. By increasing the deposition time and hence the coverage, the cluster density rather than the island size increases.

Tartaric acid is then deposited on (i) the clean TiO₂ surface and (ii) on the Ni/TiO₂ system, for different TA coverage values at a given Ni NP coverage. By monitoring the C 1S peak we are able to study the influence of several key parameters on TA deposition: surface structure, surface hydration, Ni density and type of TA enantiomer. By means of complementary STM and HREELS data is possible to gain insight on the chemical state, adsorption geometry and 2D organisation of tartaric acid enabling to decipher the interactions between the partners.

References:

[1] K. Ding, Y. Uozumi, Handbook of Asymmetric Heterogeneous Catalysis, Wiley-VCH, 2008.

Thu-15:20-O-OXID ●**The structure of the SnO₂(110)-(4×1) surface***OXID Oxide surfaces and ultrathin oxide films*

[L.R. Merte](#)¹, [M. S. Jørgensen](#)², [K. Pussi](#)³, [J. Gustafson](#)⁴, [M. Shipilin](#)⁴, [A. Schaefer](#)⁴,
[C. Zhang](#)⁴, [J. Rawle](#)⁵, [C. Nicklin](#)⁵, [G. Thornton](#)⁶, [R. Lindsay](#)⁷, [B. Hammer](#)², [Edvin Lundgren](#)⁴

¹ Chalmers University of Technology, Gothenburg, Sweden;

² Aarhus University, Aarhus, Denmark;

³ LUT School of Engineering Science, Lappeenranta, Finland;

⁴ Lund University, Lund, Sweden;

⁵ Diamond Light Source, Didcot, UK;

⁶ University College London, London, UK;

⁷ University of Manchester, Manchester, UK

SnO₂ is an important material for a number of applications, including gas sensing and catalysis [1], and its usefulness is in many cases related to the oxide's reducibility. However, a detailed understanding of some of the functions of the material is missing due to an incomplete understanding of the structures of different SnO₂ surfaces under different conditions. The most stable termination plane of rutile SnO₂ is the (110), which is similar to TiO₂(110) and RuO₂(110) [1]. Reduction of the SnO₂(110) surface by heating or sputtering and annealing leads to formation of several ordered and disordered phases, the most well-ordered of which is the (4×1).

The surface structure of the SnO₂(110)-(4×1) has been studied previously by several methods, and a model consisting of in-plane oxygen vacancies appeared initially to explain the reconstruction. However, observations of defects in the structure by STM [4] as well as theoretical modeling by DFT [5] cast doubt on this model, and it was suggested instead that the structure consists of a reduced SnO overlayer, though the atomic structure remained unclear.

We have studied the SnO₂(110)-(4×1) reconstruction by a combination of Surface X-Ray Diffraction (SXRD), X-Ray Absorption Spectroscopy (XAS), Density Functional Theory (DFT), and quantitative Low Energy Electron Diffraction (LEED). The SXRD measurements indicate that the Sn sublattice of the structure consists of a single atomic layer atop the SnO₂(110) surface in a quasi-hexagonal arrangement. While the oxygen atoms are more difficult to observe in SXRD, XAS directly indicates the presence of Sn(II) in the structure, suggesting an oxygen depleted Sn_xO_y structure. Using an evolutionary algorithm based on density functional theory calculations, an Sn₆O₆ overlayer was identified that agrees well with the SXRD measurements and is predicted to be more stable than any other calculated structure over a wide range of oxygen chemical potentials. LEED-IV calculations for the structure show excellent agreement with experiment and simulated STM images agree well with those published previously.

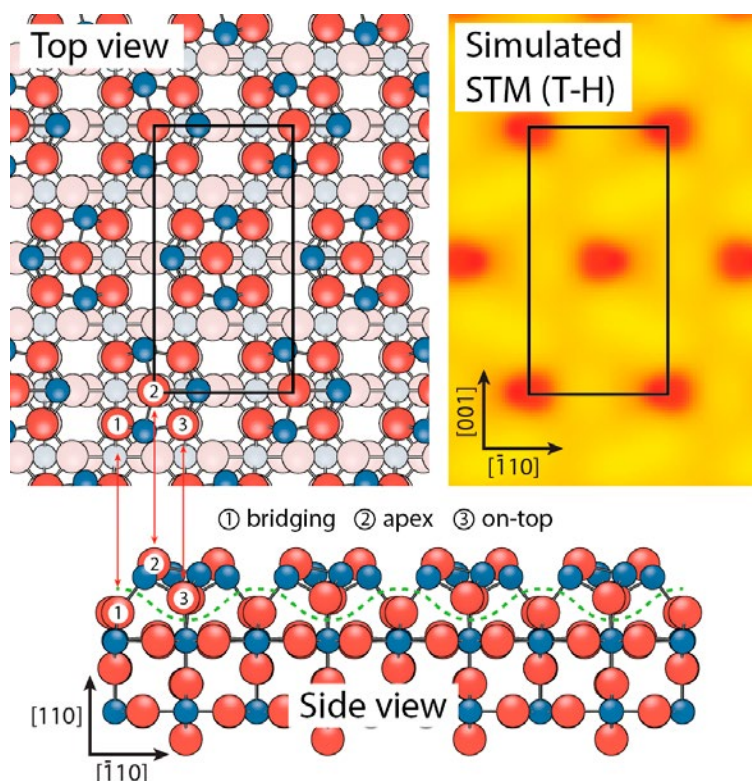


Figure: Model of the $\text{SnO}_2(110)\text{-}4\times 1$ structure

References:

- [1] M. Batzill and U. Diebold, The surface and materials science of tin oxide. *Prog. Surf. Sci.* 2005, 79, 47–154.
- [2] F. H. Jones, R. Dixon, J. S. Foord, R. G. Egdell and J. B. Pethica, The surface structure of $\text{SnO}_2(110)$ (4×1) revealed by scanning tunneling microscopy. *Surf. Sci.* 1997, 376, 367–373.
- [3] A. Atrei, E. Zanazzi, U. Bardi and G. Rovida, The $\text{SnO}_2(110)(4\times 1)$ Structure Determined by LEED Intensity Analysis. *Surf. Sci.* 2001, 475, L223–L228.
- [4] M. Batzill, K. Katsiev and U. Diebold, Surface Morphologies of $\text{SnO}_2(110)$. *Surf. Sci.* 2003, 529, 295–311.
- [5] J. Oviedo and M. J. Gillan, Reconstructions of strongly reduced $\text{SnO}_2(110)$ studied by first-principles methods. *Surf. Sci.* 2002, 513, 26–36.

Tue-11:20-O-OXID ●

Probing *in situ* the wetting at metal/oxide interface via plasmonics combined with photoemission

OXID Oxide surfaces and ultrathin oxide films

M. Messaykeh¹, R. Lazzari¹, J. Jupille¹, G. Cabailh¹, T.-H.L Le¹, J. Goniakowski¹, C. Noguera¹, S. Chenot¹, A. Koltsov², J.-M. Maigne²

¹ Institut des NanoSciences de Paris, CNRS UMR7588, Sorbonne Universités, Université Paris VI, 75005 Paris, France;

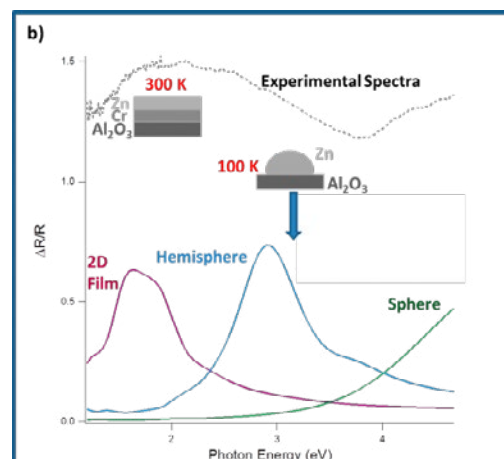
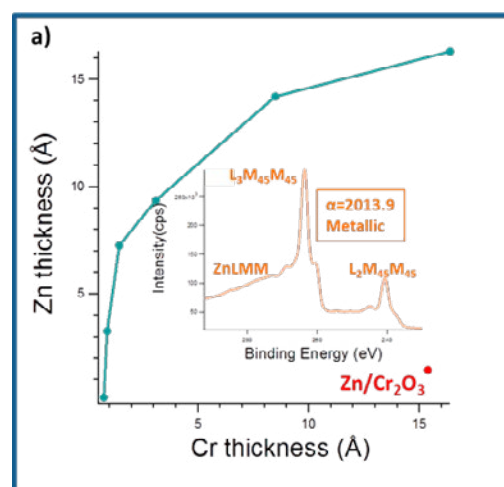
² Arcelor Mittal Maizières Research, 57280 Maizières-lès-Metz, France

The *in situ* and real time characterization of the wetting of a surface by growing films is a crucial issue in surface science [1]. We address herein the case by combining plasmonics sensitivity to morphology (UV-vis Surface Differential Reflectivity Spectroscopy, SDRS [2]) and X-ray Photoelectron Spectroscopy (XPS) sensitivity to chemistry to study the effect of a metallic buffer (Cr) on a metal/oxide interface (Zn/a-Al₂O₃(0001)). The system is inspired by the new Advanced High Strength Steel grades used in the automotive industry. However, its drawback is to exhibit segregated oxide adlayers (here alumina) that prevent the adhesion of Zn necessary in the galvanization process.

Our fundamental study performed at 300 K involves (i) Cr/Al₂O₃ film growth for different thicknesses of Cr and (ii) deposition of Zn (16Å) overlayer on top. Cr allows Zn sticking on Al₂O₃ at 300 K while much lower temperature (100K) is required to reach a sizeable condensation of Zn on bare alumina [2,3]. At early stages of growth, SDRS shows that Cr forms initially 3D clusters that cover partially the surface of alumina until an early percolation for kinetic reasons. Photoemission points at Cr in metallic state and the lack of reduction of alumina. Only a reaction limited to surface OH is detected. Concerning Zn sticking, the thickness of deposited Zn determined through XPS correlates with the Cr thickness (Fig. a). Both the shape of the Zn LMM Auger transition and the Auger parameter ($\alpha=2013.9\text{eV}$) highlight metallic zinc (Inset of Fig. a). Consistently, dielectric simulation of experimental SDRS of a Zn film grown over a thick Cr deposit that completely covers alumina (Fig. b) reveals a 2D morphology (that contrasts with the 3D growth on alumina at 100 K, Fig. b) in agreement with *ab initio* predictions on Zn/Cr/Al₂O₃ [4]. Finally, Zn is shown, both experimentally and theoretically [4], to poorly wet oxidized Cr. The contrasted behavior of Zn wetting over metallic and oxidized Cr highlights the interest of optics and photoemission combination in the case of the *in situ* study of the wetting/adhesion during the growth of thin films.

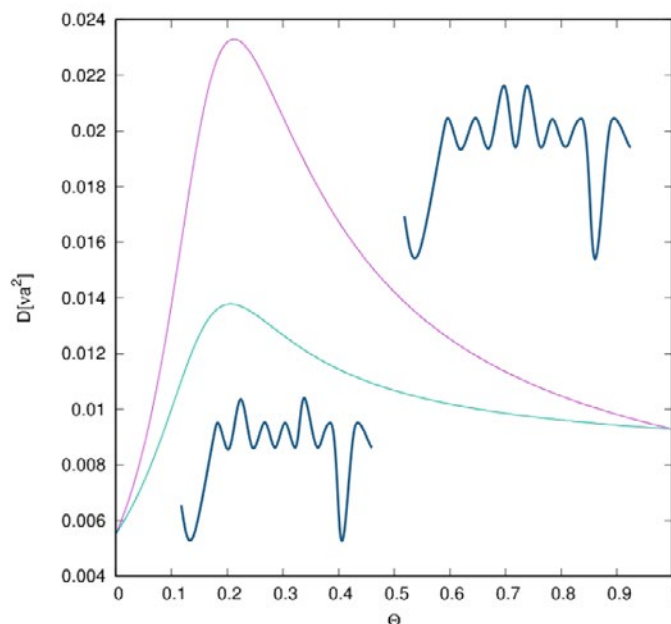
References:

- [1] G. Renaud et al. , Science 300 (2003) 1416.
- [2] R. Lazzari et al. , J. Phys. Chem. C 118 (2014) 7032.
- [3] Le et al, J. Phys. Chem. C accepted (2017)
- [4] Le et al., J. Phys. Chem. C 120 (2016) 9836.



Wed-9:40-O-COMP ●**Many particle collective diffusion in an arbitrary one-dimensional potential landscape***COMP Computational surface chemistry and physics*Marcin Mińkowski, Magdalena A. Załuska-Kotur*Institute of Physics Polish Academy of Sciences*

We present the general expression for collective diffusion coefficient of non-interacting particles in an arbitrary one-dimensional energetic potential. The result is derived by means of a variational approach to diffusion [1,2] and is expressed as a function of the jump rates between the potential minima, temperature and coverage. Quasi-one-dimensional diffusion occurs in real systems at low temperatures, when jumps along one of the directions are much more probable than those along the other directions. An example of such a system are Pb atoms on Si(553)-Au surface [3]. The result is compared with the expression obtained by effective-medium approximation [4], which takes into account the correlation only between two neighbouring potential minima involved in the jump. The diffusion coefficient obtained in the variational approach takes into account long-range correlations, which are particularly important in non-homogenous systems. That gives more accurate values of diffusion coefficients than effective-medium approximation. Our formulas are able to distinguish potentials which differ only by the sequence of energetic barriers.



References:

- [1] M. A. Załuska-Kotur, Z. W. Gortel, Phys. Rev. B 76, 245401 (2007)
- [2] M. Mińkowski, M. A. Załuska-Kotur, Surf. Sci. 642, 22 (2015)
- [3] P. Nita, K. Palotás, M. Jałochowski, M. Krawiec, Phys. Rev. B, 165426 (2014)
- [4] K. Mussawisade, T. Wichmann, K. W. Kehr, J. Phys.: Condens. Matter 9, 1181-1189 (1997)

Wed-10:00-O-COMP ● Calculation of molecular conductance 'on the fly'

COMP Computational surface chemistry and physics

[Enrique Montes](#), [Héctor Vázquez](#)

Institute of Physics Czech Academy of Sciences – Prague, Czech Republic

We present a computational scheme based on DFT to compute the conductance of single-molecule junctions 'on the fly'. We carry out Nose-Hoover molecular dynamics simulations of a molecular junction at room temperature in the canonical ensemble and apply an approximation to estimate its conductance from the electronic structure of the molecule.

In the talk I will describe its implementation in the SIESTA code [1]. The methodology is implemented inside the coordinate relaxation cycle of the SIESTA algorithm, after each self-consistent loop. After calculating conductance in the approximate scheme, the Nose scheme updates the coordinates and continues with the normal calculation path. After the whole molecular dynamics run, SIESTA has a normal exit, writing an additional file that contains the calculated conductance for each MD step.

I will discuss details of the implementation and compare calculation times with standard transport simulations. I will illustrate the method for a pair of molecular junctions, having a conjugated ring and methyl sulfide linkers [2]. In one of the molecules, the orientation of the metal-molecule bond with respect to the pi system is locked by chemical design, hindering rotations of the conjugated core.

References:

- [1] J. M. Soler, E. Artacho, J. D. Gale, A. García, J. Junquera, P. Ordejón, and D. Sánchez-Portal, *J. Phys.: Condens. Matt.* 14, 2745-2779 (2002).
- [2] Y. S. Park, J. R. Widawsky, M. Kamenetska, M. L. Steigerwald, M. S. Hybertsen, C. Nuckolls, and L. Venkataraman. *JACS* 131, 10820 (2009).

Tue-10:00-O-ORGS ●

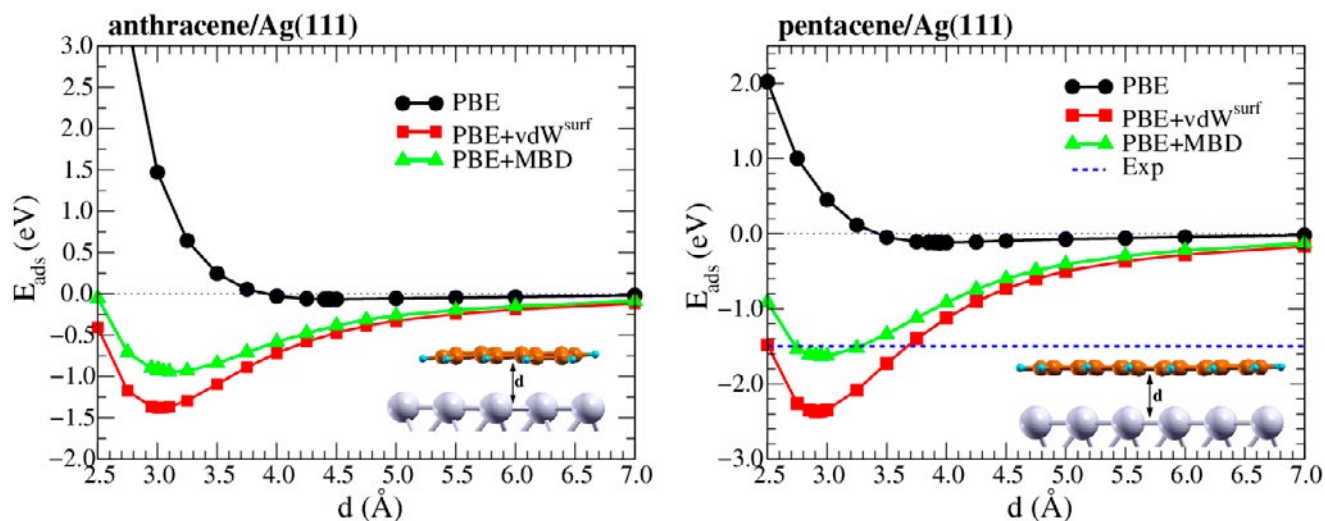
Adsorption of anthracene and pentacene on coinage metal surfaces: coverage effects and the role of the van der Waals interactions

ORGS Organic molecules on solid surfaces

Juliana M. Morbec, Peter Kratzer

Faculty of Physics, University of Duisburg-Essen, Duisburg, Germany

Understanding the interactions between metal surfaces and organic molecules—such as anthracene and pentacene, which have great potential for optoelectronic applications—is essential for electric contacts in organic electronics. In this work we use first-principles calculations to investigate the adsorption of anthracene and pentacene on coinage metal surfaces (especially Ag(111)), examining the effects of the van der Waals (vdW) interactions on the structural and electronic properties of these systems. We consider different coverages to disentangle the energy contributions to the molecule-molecule and molecule-surface interactions. Our results show, for example, that vdW interactions strongly affect the stability and structural properties of both anthracene/Ag(111) and pentacene/Ag(111), but have little effect on the electronic properties of these systems once the correct geometry has been obtained [1]. We found, in particular, that the inclusion of vdW interactions is crucial to correctly describe the flat adsorption geometry of anthracene/Ag(111) observed in experiments [2]. Moreover, we found that the adsorption of anthracene induces a larger reduction in the work function of the Ag(111) surface than pentacene, which is consistent with the stronger physisorption character observed in anthracene/Ag(111) [1]. We will also discuss the change in the work function and adsorption energy as function of the coverage.



Adsorption energies of anthracene/Ag(111) and pentacene/Ag(111)

References:

- [1] Juliana M. Morbec and Peter Kratzer, *J. Chem. Phys.* 146, 034702 (2017). [2] T. Shimooka et al., *Langmuir* 17, 6380 (2001).

Tue-15:20-O-ELCH ●

Oxygen reduction reaction by pyridinic nitrogen-containing carbon electrocatalysts*ELCH Electrochemistry at surfaces*Riku Shibuya¹, Junji Nakamura², Yuto Shimoyama¹, Takahiro Kondo²¹ Graduate School of Pure and Applied Sciences, University of Tsukuba;² Faculty of Pure and Applied Sciences, University of Tsukuba

Nitrogen containing carbon materials have been reported to show catalytic activities such as an oxygen reduction reaction (ORR) in fuel cells. Among several types of nitrogen species in carbon materials, pyridinic nitrogen (nitrogen atom bound to two C atoms) was found to create ORR active sites in our previous work [1]. We then try to prepare catalytically active carbon surfaces covered with pyridinic nitrogen-containing aromatic molecules with high density. Here we report model catalyst studies using HOPG (highly oriented pyrolytic graphite) electrode covered with pyridinic nitrogen-containing aromatic molecules (dibenz[a,c]acridine (DA) molecule). The DA molecules were deposited on HOPG with different coverage by simply dropping solutions of the DA molecules at room temperature. Scanning tunneling microscopy (STM) measurements revealed that a well-ordered two-dimensional structure of DA monolayer is formed on HOPG surfaces with high densities via π - π interaction, rather than aggregates to form three-dimensional clusters. The nitrogen concentration of the DA-covered HOPG surfaces was estimated to be 0.5~1.5 at.% by XPS. The DA-covered HOPG model catalysts revealed activities of ORR. The specific activity per pyridinic nitrogen atom was estimated to be 0.08 ($\text{e sec}^{-1} \text{pyriN}^{-1}$) at 0.5 eV, which is comparable to that for pyridinic nitrogen incorporated graphene sheets (0.07 ~ 0.14 ($\text{e sec}^{-1} \text{pyriN}^{-1}$))[1]. The current densities at 0.1, 0.2, and 0.3 V vs RHE were in proportional to the surface coverage of DA molecules, indicating that the ORR active site was created by DA molecule adsorbed on HOPG. The present studies clearly show that fixing nitrogen-containing aromatic molecules on graphitic carbon materials is one of promising approaches to prepare active ORR carbon catalysts.

References:

[1] D.Guo, R.Shibuya, T.Kondo, J.Nakamura, et al., Science, 351 (2016), 361-365.

Tue-9:00-O-MAGN ●**Spin reorientation in fcc Fe thin films with Mn overlayer***MAGN Surface and molecular magnetism*[S. Nakashima](#), [T. Miyamachi](#), [Y. Takahashi](#), [F. Komori](#)*Institute for Solid State Physics (ISSP), University of Tokyo, 5-1-5 Kashiwanoha, Kashiwa – Chiba (Japan)*

In magnetic multilayers, interfaces play a key role in determining the overall magnetic properties which are of fundamental interest and of technological importance for device applications. The magnetic properties, e.g., magnetic moment, magnetic anisotropy and exchange interaction, rely much on their interfacial conditions such as intermixing and roughness. One of the interesting effects induced by the presence of the interface is a change of the magnetic anisotropy due to adsorbates and overlayers, which is known as a spin reorientation transition (SRT) and has been studied over two decades. The structure and intermixing at the interface can be investigated during its formation process by the deposition of the overlayer atoms using scanning tunneling microscopy (STM) on an atomic scale.

In the present study, we combine STM and X-ray magnetic circular dichroism (XMCD) to make clear the correlation between the interface structure in an atomic scale and magnetic anisotropy for a ferromagnetic (FM) film with anti-ferromagnetic (AFM) overlayers. We chose an fcc Fe thin film on Cu(001) as a FM layer and Mn overlayers as AFM layers. The electronic and magnetic properties of the fcc Fe films are sensitive to the surface structural changes [1,2]. The Mn overlayers with a thickness between 0.5 and 5 monolayer were grown at room temperature in an ultrahigh vacuum. In the Fe fcc phase, the topmost two Fe layers couple ferromagnetically with the magnetic easy axis perpendicular to the surface plane. We found the Mn overlayers modified the magnetic properties of the Fe and induced SRT to the in-plane magnetization by XMCD. Atomically-resolved STM observations revealed that Mn and Fe atoms were mixed at the interface. The observed SRT was driven by the formation of alloy layers at the Mn/Fe interface, which depends on the amount of the deposited Mn atoms.

References:

- [1] T. Miyamachi et al., Phys. Rev. B 94, (2016) 045439.
- [2] R. Vollmer et al., Phys. Rev. B 61, (2000) 1303.

Wed-11:40-O-BAND ●**Valence band structures of the single crystal pentacene***BAND Band structure of solid surfaces*

Masataka Hikas¹, Yasuo Nakayama¹, Koki Yoshida¹, Mimi Murata¹, Yuta Mizuno², Shinichiro Ideta³, Kiyohisa Tanaka³, Nobuo Ueno², Takahiro Ueba³, Satoshi Kera^{2,3}

¹ Department of Pure and Applied Chemistry, Tokyo University of Science, Japan;

² Graduate School of Advanced Integration Science, Chiba University, Japan;

³ Institute for Molecular Science, National Institutes of Natural Sciences (IMS), and SOKENDAI, Japan

Charge carrier transport mechanisms in pi-conjugated molecular solids still involve essential questions unsolved in spite of recent successful application of organic electronic devices utilizing these organic molecules as semiconductor materials. Valence electronic structures of the molecules determine the transport phenomena and thus are important subjects in both fundamental and practical viewpoints. Pentacene (C₂₂H₁₄) is one of the most representative organic semiconductor materials exhibiting large charge carrier mobility. The valence electronic structures of the single crystal of this molecule have therefore been of great interest as key knowledge to resolve intrinsic nature of the transport mechanisms in the organic semiconductor materials. In the present work, the valence band structures of the single crystal pentacene are demonstrated by means of two sample charging-durable methodologies, photoconductivity-assisted angle-resolved ultraviolet photoelectron spectroscopy (ARUPS) [1] and photoelectron yield spectroscopy (PYS) [2].

The single crystal samples of pentacene were prepared through recrystallization in a purified nitrogen stream. Oblong plates of the crystal were taken out to the ambient condition (*ex-situ* samples) or were transferred to a glove box filled with N₂ (*in-situ* samples), and subsequently posted onto pieces of conductive carbon tape to bound onto Au-coated Si substrates. ARUPS measurements were conducted by A-1 analyzer (MB Scientific) at IMS under illumination of cw laser light (405 nm) for relieving photoemission-induced sample charging. PYS measurements were carried out by a home-built system where the photoelectron yield is counted as the electric current by a precise ammeter.

Figure 1 shows an ARUPS spectral image of an *ex-situ* pentacene single crystal (Pn-SC) sample taken along a diagonal direction of the surface Brillouin zone at room temperature [3]. The excitation photon energy was set at 10 eV for the sake of probing a deeper region through the surface first molecular layer containing ca. 2% oxidized species [4] due to exposure the Pn-SC surface to the ambient condition [5]. The ARUPS results clearly exhibit that the highest-occupied molecular orbital (HOMO) of the Pn-SC forms two valence bands with significant energy-momentum dispersion. Intermolecular transfer integral and hole effective mass values of the Pn-SC are evaluated to be -0.043 eV and 3.43-times electron rest mass, respectively, at the valence band maximum. Cooling the temperature to 110 K expands the width of the valence bands, which accordingly leads enhancement and reduction of the transfer integral and effective mass, respectively, by ca. 20%, as shown in Fig. 2. The threshold ionization energy of the Pn-SC are determined to be 4.95 eV by PYS results, which is slightly greater than that of the bulk film of pentacene. Accurate valence band structures of the *in-situ* Pn-SC samples are also discussed in this contribution.

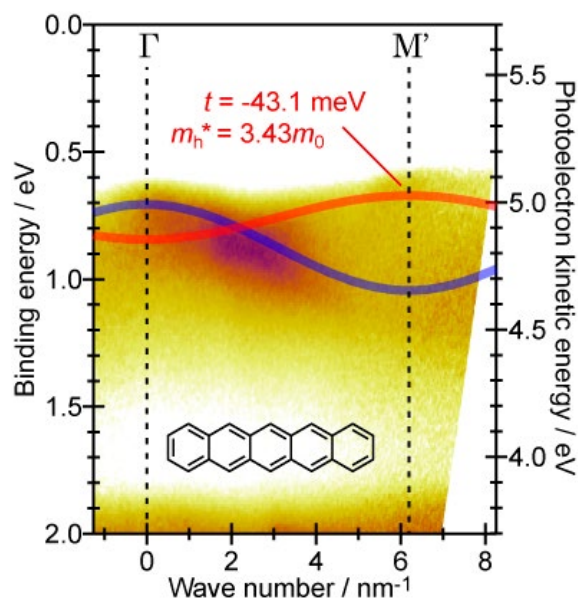


Fig. 1: ARUPS image of the Pn-SC taken at RT. The shallower and deeper valence bands are shown in red and blue, respectively. (t : transfer integral, m_h^* : hole effective mass, m_0 : electron rest mass)

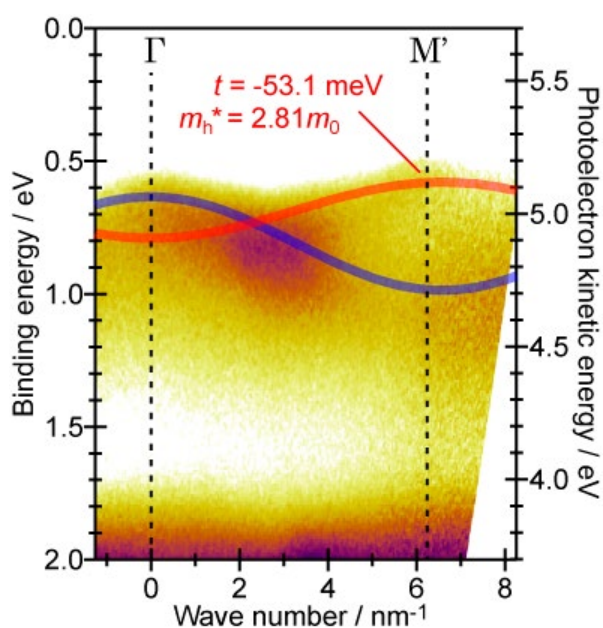


Fig. 2: ARUPS image of the Pn-SC taken at 110 K.

References:

- [1] S. Machida, et al., Phys. Rev. Lett. 104 (2010) 156401.
- [2] Y. Nakayama, et al., Appl. Phys. Lett. 92 (2008) 153306.
- [3] Y. Nakayama, et al., J. Phys. Chem. Lett. 8 (2017) 1259.
- [4] Y. Nakayama, et al., J. Phys.: Cond. Matter 28 (2016) 094001.
- [5] Y. Mizuno, et al., Mol. Cryst. Liq. Cryst. in press (DOI: 10.1080/15421406.2017.1302001).

Tue-15:00-O-ORGS ●

Covalent and periodic functionalization of graphene/Ru(0001)*ORGS Organic molecules on solid surfaces*

Juan Jesús Navarro^{1,2}, Fabián Calleja², Rodolfo Miranda^{1,2}, Emilio M. Pérez^{2,3},
Amadeo L. Vázquez de Parga^{1,2}

¹ Departamento de Física de la Materia Condensada and IFIMAC, Universidad Autónoma de Madrid, Spain;

² IMDEA Nanociencia, Madrid, Spain;

³ Departamento de Química, Universidad Autónoma de Madrid, Spain

The organic covalent functionalization of graphene with long-range periodicity could pave the way to control the electronic, optical, or magnetic properties of graphene-based devices, a subject of great interest. In this work we describe a method for the covalent modification of graphene with strict spatial periodicity at the nanometer scale under ultra-high vacuum conditions. The periodic landscape is provided by a single monolayer of graphene grown on Ru(0001) that presents a moiré pattern arising from the mismatch between the carbon and ruthenium lattices [1]. The moiré contains periodically arranged areas where the graphene–ruthenium interaction is enhanced and show higher chemical reactivity, a fact that we exploit to attach cyanomethyl radicals ($\text{CH}_2\text{CN}\cdot$) produced by homolytic breaking of acetonitrile (CH_3CN) [2]. This process presents a 90% yield and 97% site-selectivity of $\text{CH}_2\text{CN}\cdot$ molecules that bind covalently to graphene following the moiré lattice, as revealed by our STM study. This method in principle could be extended to other organic nitriles, paving the way for the attachment of functional molecules.

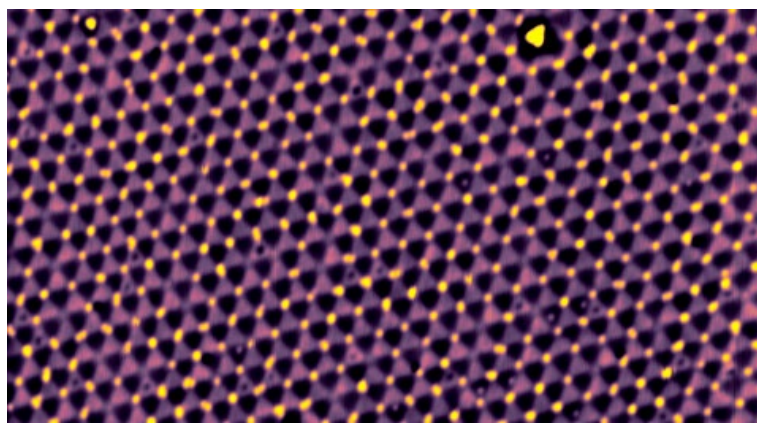


Figure 1. 70 nm × 30 nm STM topographic image of covalently functionalized graphene/Ru(0001). $\text{CH}_2\text{CN}\cdot$ molecules are attached following the moiré periodicity with 90% yield and 97% site-selectivity.

References:

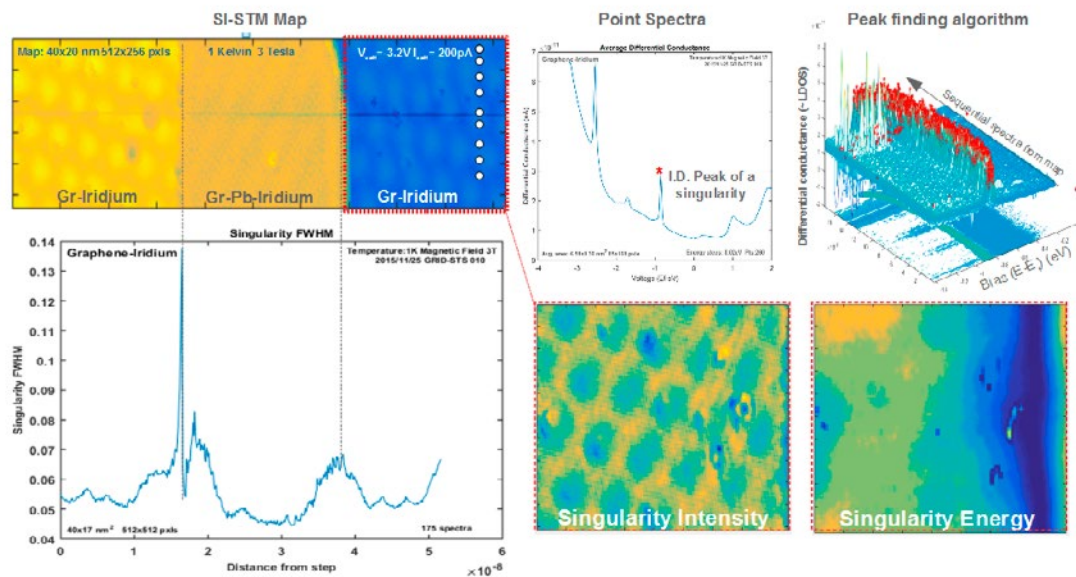
- [1] A.L. Vázquez de Parga et al. Phys. Rev. Lett. 100, 056807 (2008) [2] J.J. Navarro et al. Nano Lett. 16, 355-361 (2016)

Thu-11:20-O-GRAP ●**Opening a pseudogap, and the rich interplay of Dirac fermions with singularities, doping and asymmetric potentials in graphene****GRAP Graphene and carbon-based 2D films**

Andrew Norris, F. Calleja, J.J. Navarro, A.L. Vázquez de Parga, R. Miranda

Imdea Nanoscience (Universidad de Autonoma) Spain

A growing range of materials exhibit low-energy fermionic excitations that behave as massless Dirac particles, including d-wave superconductors, topological insulators and graphene. These materials share a significant number of common properties whose Dirac nature is controlled by specific symmetries [1]. Emergent areas of exploration including mass acquisition, confinement, and interaction enhancement are just some of the avenues expected to reveal exotic and novel quantum phases [2]. We report experimental results on the rich interplay of Dirac electrons, with singularities in the density of states (VHS), chemical doping, and asymmetric potentials using spectroscopic imaging scanning tunneling microscopy (SI-STM). We find evidence of a pseudo-gap, charge localisation, unusual interference patterns, and detail the properties and responses of the aforementioned singularities to potentials and doping which leads to a range of effects including a suspected charge density wave (CDW). We reveal, the non-equivalent response of each singularity to the potential energy landscape indicative of a certain degree of autonomy, and close by discussing potential origins and consequences of this well controlled, yet rich, Graphene [3] playground for other Dirac systems.

**Figure:** Singularities on Graphene

References:

- [1] "Dirac Materials", T. Wehling, A.M. Black-Schaffer, A.V. Balatsky *Advances in Physics*, Vol. 63, Iss. 1 (2014)
- [2] The electronic properties of graphene AHC Neto, F Guinea, NMR Peres, KS Novoselov, AK Geim *Reviews of modern physics* 81 (1), 109
- [3] F.Calleja et al. *Nature Physics* 11,43–47 (2015)

Thu-9:40-O-LASE ●**Circular dichroism in laser induced electron emission from nanohelix arrays**

LASE Laser pulses for surface electron dynamics[Daniel Nürenberg](#)¹, [Andrew Mark](#)², [Matthias Kettner](#)¹, [Peer Fischer](#)², [Helmut Zacharias](#)¹¹ *Physikalisches Institut, Westfälische Wilhelms-Universität Münster, Germany;*² *Max Plank Institut für intelligente Systeme, Stuttgart, Germany*

We investigate the electron emission from chiral metallic nanostructures triggered by fs laser radiation. Circularly polarized pulses from an optical parametric chirped pulse amplifier (OPCPA) were used to irradiate arrays of metallic nanohelices on silicon surfaces. We find a strong asymmetry regarding to left and right circularly polarized excitation in the electron yield in accordance to the handedness of the helices. The emission can be interpreted in terms of a non-equilibrium heating of the electron gas by surface plasmon excitation. Simulations of the surface plasmons correlate the polarization dependence of the photosignal to the field enhancement on the nanostructures.

Wed-16:40-O-BAND ●

Soft X-ray spectroscopic study of electronic structure of Pd nanoparticles

BAND Band structure of solid surfaces

Satoshi Ogawa¹, Kenta Otsuki¹, Shinya Yagi^{1,2}¹ Energy Engineering, Graduate School of Engineering, Nagoya University, Japan;² Institute of Materials and Systems for Sustainability, Nagoya University, Japan

In order to clarify the anomalous hydrogen absorption property of the Pd nanoparticles (NPs), we have investigated the electronic structure of the Pd NPs by the soft X-ray spectroscopy. Pd bulk exhibits the clear and sharp plateau region in the pressure-composition isotherm (PCI) of the hydrogen absorption. In contrast, the plateau is ambiguous in the PCI of the Pd NPs i.e. the plateau has the slope and the narrower width compared with that of the bulk one [1,2]. One of the suggested origins is the change of the electronic structure around the fermi level by the formation of the NPs [1]. We have carried out near Pd L₃-edge X-ray absorption fine structure (Pd L₃-edge NEXAFS) and X-ray photoelectron spectroscopy (XPS) measurements to investigate the unoccupied d-states and the valence band structure around the fermi level of the Pd NPs, respectively.

Pd L₃-edge NEXAFS measurements were carried out with Material Chemical State-Structural Analysis II at BL6N1, Aichi Synchrotron Radiation Center. The NEXAFS spectra were obtained by the total electron yield method using the drain current under the high vacuum ($\sim 5 \times 10^{-8}$ Pa). Figure 1 shows the Pd L₃-edge NEXAFS spectra of the Pd NPs and Pd sheet (Pd bulk). All spectra in Figure 1 were normalized with respect to height of the edge jump. The intensity of the white line in the L₃-edge NEXAFS spectrum reflects the DOS of the unoccupied d-state in the simple approximation. It can be seen that the intensity of the white line of Pd NPs is slightly lower than that of Pd bulk. This result represents that the unoccupied d-states near the Fermi level has decreased by the formation of Pd NPs which explains qualitatively that the hydrogen absorption amount of Pd NPs is lower than that of bulk. The unoccupied d-states are fulfilled by the electron of the hydrogen during the hydrogen absorption of Pd [3]. The decrease of the unoccupied d-DOS leads the decrease of the amount of the permitted hydrogen in the crystal lattice of Pd. The results of the valence band XPS will be also shown at the presentation.

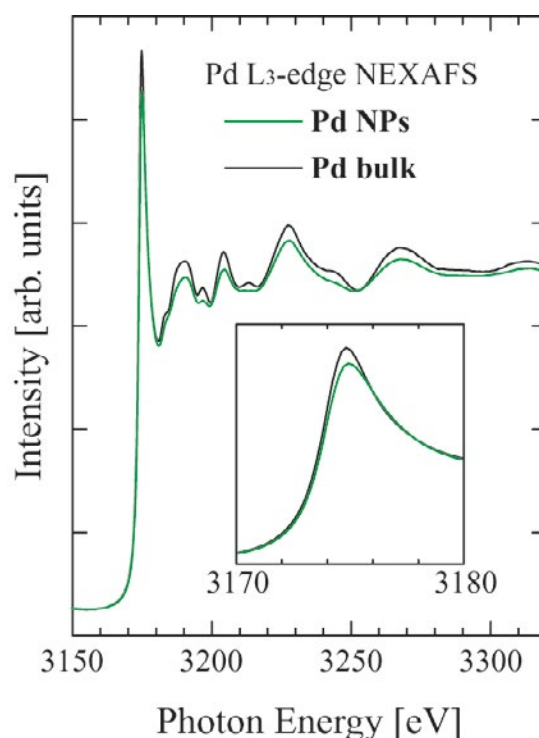


Figure 1. Pd L₃-edge NEXAFS of the Pd NPs and Pd bulk.

References:

- [1] M. Yamauchi, R. Ikeda, H. Kitagawa, and M. Takata, J. Phys. Chem. C 112, 3294 (2008).
- [2] S. Ogawa, T. Fujimoto, T. Kanai, N. Uchiyama, C. Tsukada, T. Yoshida and S. Yagi, e-J. Surf. Sci. Nanotech. 13, 343 (2015).
- [3] C. D. Gelatt, Jr., H. Ehrenreich, J.A. Weiss, Phys. Rev. B 17, 1940 (1978).

Thu-14:40-O-OXID ●**Surface stabilises ceria in unexpected stoichiometry***OXID Oxide surfaces and ultrathin oxide films*

[Reinhard Olbrich](#)¹, [Gustavo E. Murgida](#)², [Valeria Ferrari](#)², [Clemens Barth](#)³, [Ana M. Llois](#)², [Michael Reichling](#)¹, [M. Veronica Ganduglia-Pirovano](#)⁴

¹ *Fachbereich Physik, Universität Osnabrück, Barbarastr. 7, 49076 Osnabrück, Germany*

² *Departamento de Física de la Materia Condensada, GlyA, CAC-CNEA, 1650 San Martín, Buenos Aires, Argentina; Consejo Nacional de Investigaciones Científicas y Técnicas - CONICET, C1033AAJ Buenos Aires, Argentina*

³ *Aix-Marseille University, CNRS, CINaM UMR 7325, 13288 Marseille, France*

⁴ *Instituto de Catálisis y Petroleoquímica, Consejo Superior de Investigaciones Científicas-CSIC, 28049 Madrid, Spain*

By annealing a 180 nm thick ceria film [1] in an ultra-high vacuum (UHV) environment at various temperatures up to 1100K, we stabilize periodic structures representing ceria reduction stages ranging from CeO_2 to Ce_2O_3 . These surface reconstructions are revealed by direct imaging with a non-contact atomic force microscope (NC-AFM). An accurate understanding of the surface reconstructions is achieved by combining high-resolution NC-AFM imaging with extensive spin-polarized DFT+U calculations [2]. Starting from $(1 \times 1) \text{CeO}_2$ we identify four reconstructions namely $(\sqrt{7} \times \sqrt{7})\text{R}19.1^\circ \text{Ce}_7\text{O}_{12}$, $(\sqrt{7} \times 3)\text{R}19.1^\circ \text{Ce}_3\text{O}_5$, $(\sqrt{3} \times \sqrt{3})\text{R}30^\circ \text{Ce}_3\text{O}_5$, and $(1 \times 1) \text{Ce}_2\text{O}_3$.

The $(\sqrt{7} \times 3)\text{R}19.1^\circ$ reconstruction is most interesting as it is the only phase that has an oblique rather than a hexagonal structure, and theoretical modeling shows that this phase appears at the surface but cannot be stabilized in a bulk structure. We also observe that some phases coexist on the same terraces [3].

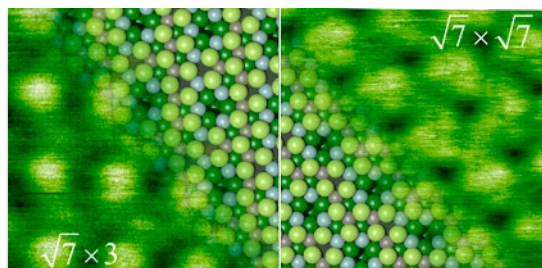
The sequence of occurrence of the observed phases at evaluated temperature is explained employing DFT and thermodynamic modeling whereby also the coexistence of phases and the missing observation of the (3×3) phase, which has been observed in other experiments [4,5], can be understood.

These results help understanding the surface defect structure which is of paramount importance in catalytic and sensor applications exploiting the high oxygen storage capacity of ceria [5].

Acknowledgment: Support from the COST Action CM1104 is gratefully acknowledged.

References:

1. Olbrich, R., et al., A well-structured metastable ceria surface. *Applied Physics Letters*, 2014. 104: p. 081910.
2. Murgida, G.E. and M.V. Ganduglia-Pirovano, Evidence for subsurface ordering of oxygen vacancies on the reduced $\text{CeO}_2(111)$ surface using density-functional and statistical calculations. *Physical Review Letters*, 2013. 110(24): p. 246101.
3. Olbrich, R., et al., Surface Stabilizes Ceria in Unexpected Stoichiometry. *The Journal of Physical Chemistry C*, 2017. 121(12): p. 6844-6851.
4. Duchoň, T., et al., Ordered Phases of Reduced Ceria As Epitaxial Films on $\text{Cu}(111)$. *Journal of Physical Chemistry C*, 2014. 118(1): p. 357-365.
5. Höcker, J., et al., Unraveling the Dynamic Nanoscale Reducibility ($\text{Ce}^{4+} \rightarrow \text{Ce}^{3+}$) of CeOX-Ru in Hydrogen Activation. *Advanced Materials Interfaces*, 2015. 2(18): p. 1500314.



Tue-11:00-O-ORGS2 ●
Switchable charge states in multi-ferrocene molecules

ORGS Organic molecules on solid surfaces

Jan Berger¹, Martin Ondráček¹, Oleksandr Stetsovych¹, Martin Švec¹, Irena Stará², Ivo Starý², Pavel Jelínek¹

¹ Institute of Physics, Czech Academy of Sciences, Cukrovarnická 10/112, 162 00 Praha 6, Czech Republic;

² Institute of Organic Chemistry and Biochemistry, Czech Academy of Sciences, Flemingovo náměstí 542/2, 166 10 Praha 6, Czech Republic

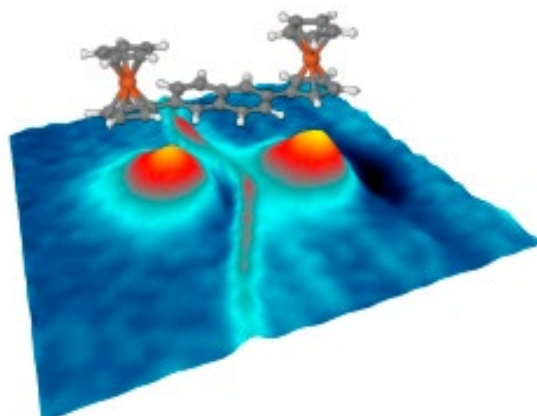
Molecular electronics is an envisioned field of electronics which would allow the ultimate miniaturization and new functionalities by using molecules as building blocks of electronic devices. Gaining a control over the charge state of a single molecule would be an important milestone on the way towards such technology. Ferrocene-based molecules are known to be stable in different redox states, which makes them promising as candidates for quantum cellular automata units. Previous works demonstrated charging single metal adatoms [1], molecules or their clusters on insulating films [2] as well as charging of large self-assembled islands of molecules by scanning tunneling microscopy (STM) or non-contact atomic force microscopy (nc-AFM) [3].

Here we will present experimental evidence of controlling multiple charge states on single of 2,6-bis(ferrocenyl)naphthalene ("bis-ferrocene") or 3,6,3',6'-tetraferrocene-9,9'-bis-fluorenylidene ("tetraferrocene") molecules deposited on an insulating NaCl film, actualized by means of nc-AFM. We succeeded to control the multiple charge states including their reversible transfer within a single molecule between different redox centers. The maximal number of charging events we were able to observe in succession corresponded to the multiplicity of ferrocene centers within the probed molecule. The induced charged states featured prominent fingerprints in both the frequency shift and energy dissipation channels. In order to corroborate the experimental evidence, we have developed a theoretical model that simulates the response of an oscillating AFM probe to the switching of the molecular charge, in particular to the hopping of the charge between the redox centers. This hopping is presumably stimulated by the oscillation of the probe itself and therefore correlated to it, resulting in a strong signal detected by the microscope. Our model is akin to but different from the one we have previously published for periodic charging and discharging of molecules or quantum dots by means of STM/nc-AFM [4].

A 3D representation of constant-height nc-AFM data (frequency shift) taken over a bis-ferrocene molecule is shown in the figure, together with a schematic model of the molecule. The linear feature corresponds to the boundary at which the charge tends to switch between the two ferrocene redox centers.

References:

- [1] J. Repp et al., *Science* 305, 493-495 (2004).
- [2] W. Steurer et al., *Nature Comm.* 6, 8353 (2015).
- [3] P. Rahe et al., *Nano Letters* 16, 911-916 (2016).
- [4] M. Ondráček et al., *Nanotechnology* 27, 274005 (2016).



Wed-16:40-O-SAMA ●

Vicinal noble metal surfaces with densely kinked steps

SAMA Structural analysis and manipulation on atomic scale

G. Vasseur¹, J. E. Ortega^{1,2,3}, J. Lobo-Checa⁴, I. Piquero-Zulaica², A. El-Sayed⁵, Z. Abd-el-Fattah⁵, M. Corso², F. Schiller²

¹ Donostia International Physics Center DIPC, San Sebastian, Spain;

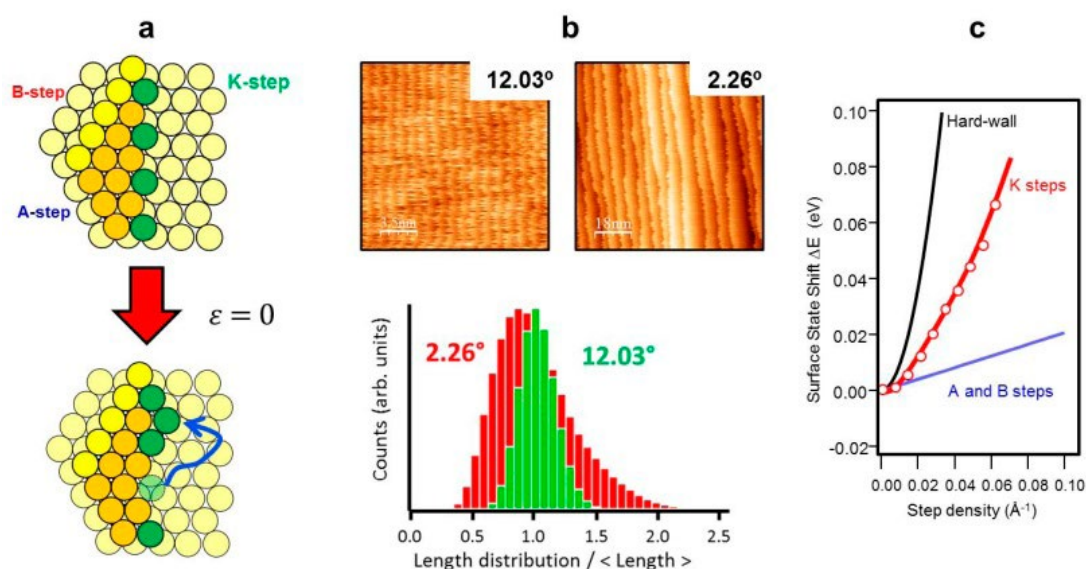
² Centro de Fisica de Materiales, CFM-CSIC, San Sebastian (Spain);

³ Departamento de Fisica Aplicada I, Universidad del Pais Vasco, San Sebastian (Spain);

⁴ Instituto de Ciencia de Materiales de Aragon (ICMA), Universidad de Zaragoza (Spain);

⁵ Physics Department, Faculty of Science, Al-Azhar University, Cairo (Egypt);

The thermal excitation of step-edge atoms into kinks is the essence of the step dynamics on a crystal surface. At a vicinal surface with high step densities, kinks also influence the equilibrium shape at finite temperature. As shown in Fig. 1a, in fcc $-(111)$ vicinal planes steps oriented along the $[11-2]$ direction exhibit a 100% kinked step-edge (K-type), where out-protruding step-edge atoms have no direct nearest-neighbors parallel to the step. Remarkably, as sketched in the same Fig. 1a, in such K-steps thermal excitations have zero energy cost, allowing meandering and roughening of steps without energy penalty. We have investigated Ag crystals curved around the (654) direction, which allows one to probe with STM and Angle Resolved Photoemission (ARPES) all K-type surfaces from the (111) plane up to 18 deg vicinal angles. In Fig. 1b we show characteristic STM images and terrace-width distribution histograms. A remarkably neat transformation is observed from low to high step-densities, suggesting a dramatic transition in step interactions, from purely entropic, at low step-densities, to strongly elastic, at high step-densities. In Fig. 1c we show the energy shift of the Shockley band measured with ARPES across the curved sample. Large shifts are found compared to close-packed steps, indicating strong repulsive scattering due to a larger electric dipole at K-type steps. On the other hand, with the kinked Au(16,15,14) surface we explored on-surface synthesis of organic nanowires and nanostripes. In all cases, the connection of STM and ARPES results with the particular step energetics and dynamics of K-type vicinal surfaces will be discussed.



Thu-10:00-O-LASE ●**Surface science perspectives at ELI Attosecond Light Pulse Source***LASE Laser pulses for surface electron dynamics*

László Óvári^{1,2}, Péter Dombi^{1,3}, Dimitris Charalambidis¹

¹ ELI-ALPS, ELI-HU Non-profit Ltd., Szeged, Hungary;

² MTA-SZTE Reaction Kinetics and Surface Chemistry Research Group, Szeged, Hungary;

³ MTA "Lendület" Ultrafast Nanooptics Group, Wigner Research Centre for Physics, Budapest, Hungary

Photoemission has long been an efficient way for the investigation of ultrafast surface phenomena. In a pump-probe approach using visible or near UV femtosecond pulses, two (or three) photon photoemission can reveal the energy spectrum of occupied and unoccupied electronic states as well as the lifetime of intermediate states. By means of two dimensional position sensitive detectors the dispersion characteristics of different states can also be addressed, although often in a restricted k space and energy range due to the low acceptance angles of the analyzers and the photon energy limited to the few eV range. Other goals in current photoemission research are availability of lateral resolution for the analysis as well as to obtain information about the spin state of electrons. With gas high harmonic generation (GHHG) XUV pulses of attosecond duration can be obtained opening new possibilities for surface science. In addition, photoelectrons are ideal probes for ultrafast plasmonic phenomena [1] and with state-of-the-art probing of nanooptical near-fields, novel applications in integrated optics, sensorics and spectroscopy can emerge.

The ELI Attosecond Light Pulse Source (ELI-ALPS), located in Szeged, will offer the surface science and plasmonics communities a state-of-the-art end station incorporating all the above mentioned capacities. The core of the instrument will be a photoemission electron microscope (PEEM) capable of laterally resolved imaging. It will be complemented by both an electrostatic and a time-of-flight analyzer to provide energy resolved images. Moreover, an imaging spin filter will be available for spin, energy, and laterally resolved detection at the same time. Instead of lateral imaging, small spot ARPES can also be performed at the end-station (optionally with spin filtering) with enhanced angle resolution in a nearly 2 Pi solid angle. The end-station will include an UHV system with various possibilities for sample preparation and characterization.

Superior sensitivity will be secured by the usage of a state-of-the-art a high repetition rate (100 kHz) excitation source. A 100 W near IR laser, emitting carrier-envelope phase (CEP) stabilized pulses of <6.2 fs duration will drive a GHHG beamline, which will produce isolated attosecond pulses and attosecond pulse trains with photon energies up to ~150 eV. Both NIR and the XUV pulses, with adjustable delay, will be available for the surface science end station. For measurements requiring XUV pulses of narrow spectral bandwidth, the beamline will be equipped with a time compensating monochromator.

The possible use of the end station will be illustrated in this presentation discussing a measurement aiming at the determination of plasmonic field enhancement at nanostructures mapping also the angular distribution of photoelectrons.

References:

[1] P. Rácz et al., Nano Lett. 17, 1181-1186 (2017).

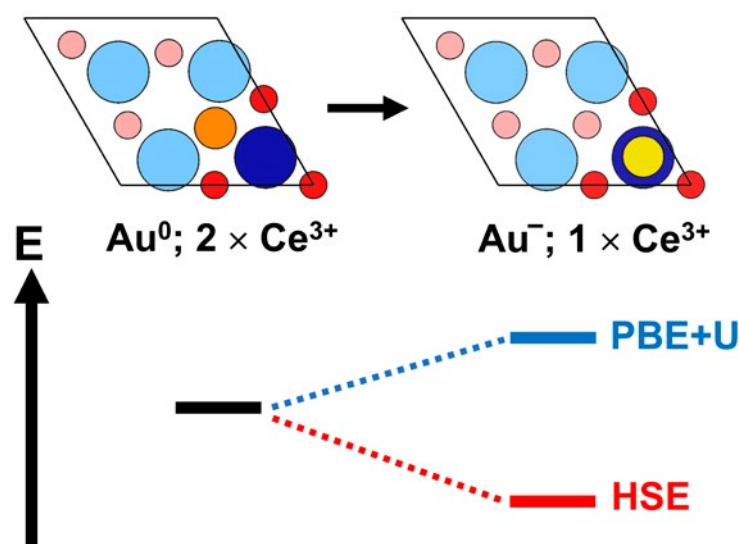
Wed-11:40-O-COMP ●**Electron transfer between gold adatoms and the reduced CeO₂(111) surface:
Lessons learned from static density functional theory***COMP Computational surface chemistry and physics*

Christopher Penschke, Joachim Paier

Institut für Chemie, Humboldt-Universität zu Berlin, Unter den Linden 6, 10099 Berlin

Oxygen point defects in reducible oxide surfaces like ceria play a crucial role, when it comes to redox catalysis [1]. The activity of these surfaces may be drastically enhanced upon deposition of noble metals like gold [2]. The theoretical description of these complex systems involving electron transfer in the redox chemistry, however, represents a formidable task [3].

We present a detailed analysis of results obtained using density functional theory within the so-called DFT+*U* approach and hybrid functionals. The order by energy of donor (i.e. Ce³⁺ 4f¹) and acceptor (i.e. Au⁰ 6s¹) levels matters and affects the stability of Au atoms adsorbed on a reduced CeO₂(111) surface. Benchmark *GW* calculations corroborate results obtained with hybrid functionals [4].



PBE+U(4.5) and the HSE hybrid functional give qualitatively different results for a Au atom adsorbed on a Ce³⁺ ion.

References:

- [1] J. Paier, C. Penschke, and J. Sauer, *Chem. Rev.*, 113 3949 (2013).
- [2] M. Haruta and M. Date, *Appl. Catal. A-Gen.*, 222 427 (2001).
- [3] Y. Pan, N. Nilius, H.-J. Freund, J. Paier, C. Penschke, J. Sauer, *Phys. Rev. Lett.*, 111 206101 (2013); *E*: 115 269901 (2015).
- [4] C. Penschke and J. Paier, *Phys. Chem. Chem. Phys.* 2017, DOI: 10.1039/C7CP01785E

Wed-9:00-O-GRAP ●**Decoupling epitaxial graphene from metals by potential-controlled electrochemical oxidation****GRAP Graphene and carbon-based 2D films**

[Irene Palacio](#)¹, [Gonzalo Otero-Irurueta](#)^{1,2}, [Concepción Alonso](#)³, [José I. Martínez](#)¹, [Elena López-Elvira](#)¹, [Isabel Muñoz-Ochando](#)⁴, [Horacio J. Salavagione](#)⁴, [María F. López](#)¹, [Mar García-Hernández](#)¹, [Javier Méndez](#)¹, [Gary J. Ellis](#)⁴, [José A. Martín-Gago](#)¹

¹ Institute of Materials Science of Madrid (ICMM-CSIC), Sor Juana Inés de la Cruz 3, 28049 Madrid, Spain;

² Centre for Mechanical Technology and Automation (TEMA), Dept. Mechanical Engineering, University of Aveiro, 3810-193 Aveiro, Portugal;

³ Dept. Applied Physical-Chemistry, Autonomous University of Madrid, 28049 Madrid, Spain;

⁴ Institute of Polymer Science and Technology (ICTP-CSIC), Juan de la Cierva 3, 28006 Madrid, Spain

The catalytic role of metallic substrates is a perfect starting point for growing high quality graphene layers by thermal decomposition of aromatics [1]. However, metallic substrates quench the outstanding properties that make graphene the most promising material for future applications. Thus, protocols to transfer graphene to different technologically relevant substrates are mandatory. These transfer processes are cost inefficient and some can severely degrade the properties of graphene by introducing structural and chemical defects. As an alternative, we propose a novel, less invasive approach that is easily scalable. We target pristine graphene sheets grown on metals and employ electrochemical oxidation at controlled potentials to introduce a single atom-thick hydroxide decoupling layer. To fully understand this decoupling a multi-technique characterization (STM, AFM, XPS and Raman) combined with theoretical studies (*ab-initio* calculations) of each step of the process has been undertaken.

Epitaxial graphene was grown on Pt(111) and Ir(111) in UHV by thermal decomposition of aromatics. Fig. 1a shows a representative STM image ((4x4)nm², I=4nA, V=10mV) of a typical Moiré obtained for Gr on Pt(111) [2]. After *in-situ* characterization the sample was removed from UHV and studied by XPS, AFM and Raman spectroscopy before and after electrochemical treatments. O1s XPS spectrum show the sandwich hydroxide layer found after the electrochemical treatment (Fig.1b) responsible for decoupling graphene from the metal surface, as verified by the radical changes in the Raman spectra (Fig 1c, before (black curve) and after (red curve) electrochemical oxidation. The decoupling of the graphene sheet from the metallic substrate is clear by the emergence of D, G and 2D bands). From AFM the overall topography implies that around 90% of the surface is decoupled, and *ab-initio* calculations clearly show that intercalation of a single atom-thick hydroxide layer can induce a structural separation of the graphene with respect to the surface. This work suggests that suitably optimized electrochemical treatments may provide interesting alternatives to standard transfer protocols for graphene and other 2D materials prepared on diverse metal surfaces.

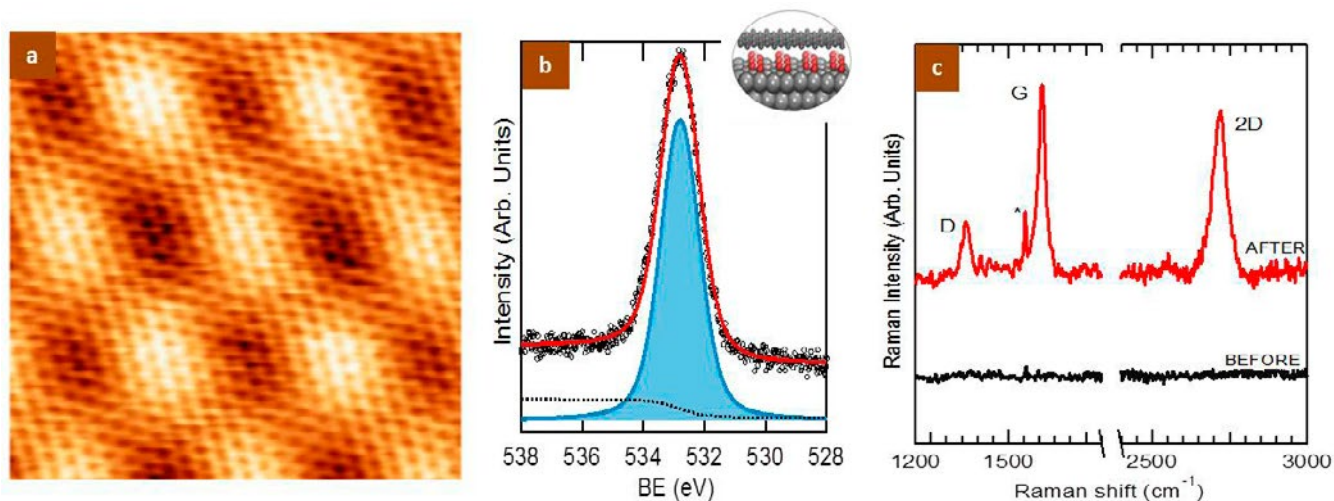


Figure 1: a) STM image of Gr/Pt(111) showing a characteristic Moiré ((4x4)nm², I=4 nA, V=10 mV). b) O1s XPS spectrum after the electrochemical treatment and a soft annealing of a Gr/Pt(111) sample. The peak can be fitted with one main component that corresponds to the hydroxide species. Inset: optimized representative Gr/Pt₂(OH)@Pt(111) interface. c) Raman spectra of graphene on Pt(111) before (black curve) and after (red curve) electrochemical oxidation.

References:

- [1] Otero, G. et al., Phys. Rev. Lett. 105 (2010) 216102.
- [2] Merino, P. et al., ACS Nano 5, (2011) 5627.

Wed-11:20-O-COMP ●

Revised Chen's derivative rule for efficient calculations of scanning tunneling microscopy

COMP Computational surface chemistry and physics

Krisztián Palotás^{1,2,3}, Gábor Mándi³

¹ Institute of Physics, Slovak Academy of Sciences, Bratislava, Slovakia;

² MTA-SZTE Reaction Kinetics and Surface Chemistry Research Group, University of Szeged, Szeged, Hungary;

³ Department of Theoretical Physics, Budapest University of Technology and Economics, Budapest, Hungary

Chen's derivative rule for electron tunneling is revised [1] for the purpose of computationally efficient calculations of scanning tunneling microscopy (STM). New features include (i) the weighting of tunneling matrix elements of different tip-orbital characters by an arbitrary energy-independent choice or based on first-principles data, (ii) arbitrary tip geometrical orientations, and (iii) the possibility of quantitative analysis of tip-orbital interference contributions. The model has initially been applied to two functionalized surfaces where quantum interference effects play an important role in the STM imaging and the Tersoff-Hamann model fails to describe the correct STM contrast under certain conditions: N-doped graphene [2] and a magnetic Mn_2H complex on the Ag(111) surface [3]. For both of these surface structures, the importance of interference between s and p_z tip orbitals is highlighted that cause a significant contrast change in the STM images [1]. Moreover, the revised Chen's method has recently been applied to validate a newly proposed structural model for the magnetite Fe_3O_4 (110) surface with two-fold oxygen vacancies [4], and to study surface defects in the organic perovskite $\text{CH}_3\text{NH}_3\text{PbBr}_3$ [5].

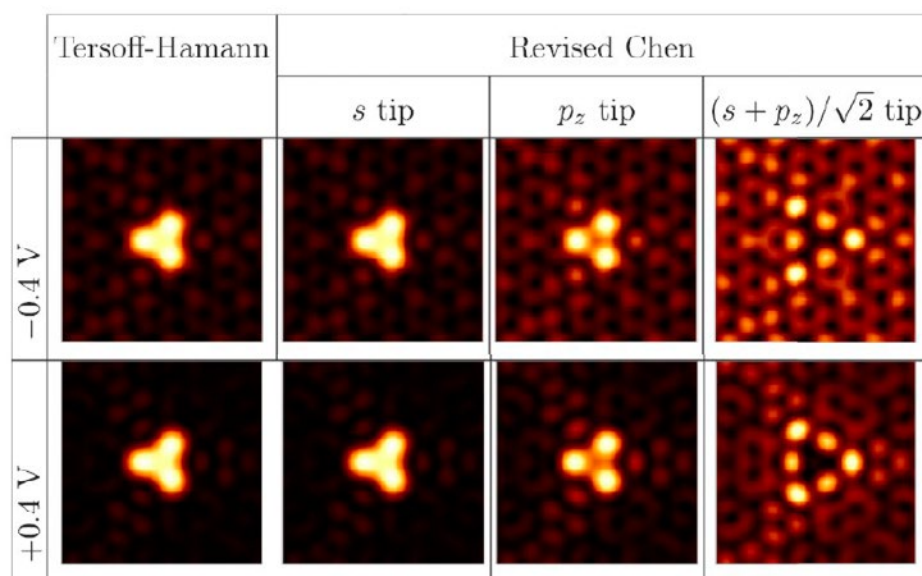


FIG: Constant-height STM images of N-doped graphene calculated by using Tersoff-Hamann and revised Chen's methods with s , p_z and $(s+p_z)/\sqrt{2}$ tip orbital compositions [1].

References:

- [1] G. Mándi, K. Palotás, Phys. Rev. B 91, 165406 (2015).
- [2] M. Telychko et al., ACS Nano 8, 7318 (2014).
- [3] T. Sachse et al., New J. Phys. 16, 063021 (2014).
- [4] B. Walls et al., Phys. Rev. B 94, 165424 (2016).
- [5] Y. Liu et al., ACS Nano 11, 2060 (2017).

Tue-16:20-O-CATL ●**Sulfur-Passivation of Graphene-Supported Platinum Nanocluster Arrays***CATL Catalytic 2D-model studies at low pressures*

Fabian Düll, Christian Papp, Florian Späth, Udo Bauer, Philipp Bachmann,
Johann Steinhauer, Hans-Peter Steinrück

*Lehrstuhl für Physikalische Chemie II, Friedrich-Alexander-Universität Erlangen-Nürnberg,
Egerlandstr. 3, 91058 Erlangen, Germany*

Poisoning of heterogeneous catalysts by sulfur and sulfur-containing compounds is of high importance for various processes in industry and therefore a hot topic in catalysis for decades. Platinum is a widespread catalyst material for various applications and sulfur a common impurity in many feedstocks.

Utilizing the intrinsic Moiré pattern that is formed by graphene on Rh(111) as a template and chemically inert support, platinum nanocluster arrays were grown. These clusters were then poisoned by sulfur via thermal reduction of SO_2 .^[1] To understand the changes that occur upon sulfur poisoning the adsorption and desorption of the common probe molecule CO were investigated. The changes in the adsorption behavior for several preadsorbed sulfur coverages were investigated with in situ high-resolution X-ray photoelectron spectroscopy. Three different CO species can be distinguished; top and bridge bonded CO on terrace sites and CO at step sites. Sulfur blocks those adsorption sites to different degrees. While on-top and step sites are highly affected, bridge sites are affected to a lower degree. These results will be compared to measurements on the stepped Pt(322) and Pt(355) surfaces.^[2,3] Upon annealing CO on the sulfur poisoned clusters, a displacement of sulfur from step to terrace sites by CO is observed around 330 K. This displacement is reversed after desorption of the CO.

References:

- [1] Streber, R.; Papp, C; Lorenz, M; Bayer, A; Denecke, R; Steinrück, H.-P. Chem. Phys. Lett. 2008, 452, 94–98
- [2] Streber R., Papp C., Lorenz M.P.A., Wickert S., Schöppke M., Denecke R. and Steinrück H.-P J. Phys.: Condens. Matter 2009, 21, 134018 [3] C. Papp Cat. Lett. 2017, 2, 147.

Thu-11:00-O-SEMI ●**Field-driven orientation of small polar molecules in the condensed phase***SEMI Semiconductor surfaces and ultrathin layers*

[Youngwook Park](#), [Hani Kang](#), [Heon Kang*](#)

Department of Chemistry, Seoul National University, 1 Gwanak-ro, Gwanak-gu, Seoul 08826, South Korea;

Controlling the spatial orientation of molecules is an important research subject in molecular science and engineering. The manipulation of molecular orientation in condensed phases, however, has been very limited. We present a novel method to reorient polar molecules from randomly oriented to almost perfectly aligned states by applied electrostatic field.^[1] The method utilizes an ice film nanocapacitor^[2] to apply intense external electric field (on the order of $10^8 \text{ V}\cdot\text{m}^{-1}$) across a thin film of matrix-isolated molecules. Asymptotically perfect alignment along the field direction was achieved for small polar molecules, including formaldehyde, water, ammonia and hydrogen chloride. The field alignment was monitored by reflection-absorption infrared (RAIR) spectroscopic measurement with p-polarized light and the unidirectional Stark shift of molecular vibrational bands.^[1] The reorientation process was found to be reversible with respect to field changes, even for formaldehyde, which is not a free rotor in the noble gas matrices. Ammonia molecule, which is nearly a free rotor in the condensed matrices, exhibited the pendular state spectroscopic features^[3] with the removal of rovibrational structures during the field alignment. In addition, RAIR spectral features indicate that the shape of the symmetric double-well potential of umbrella vibration was changed by applied electric field. The field-driven reorientation of molecules in the inert matrices is expected to offer a new platform for molecular spectroscopic studies and the manipulation of molecules in condensed phases.

References:

- [1] Y. Park, H. Kang, H. Kang, "Brute Force Orientation of Matrix-Isolated Molecules: Reversible Reorientation of Formaldehyde in an Argon Matrix toward Perfect Alignment," *Angew. Chem. Int. Ed.* 2017, 56, 1046.
- [2] S. Shin, Y. Kim, H. Kang, H. Kang, "Effect of Electric Field on Condensed-Phase Molecular Systems. I. Dipolar Polarization of Amorphous Solid Acetone," *J. Phys. Chem. C* 2015, 119, 15588.
- [3] J. M. Rost, J. C. Griffin, B. Friedrich, D. R. Herschbach, "Pendular States and Spectra of Oriented Linear Molecules," *Phys. Rev. Lett.* 1992, 68, 1299.

Wed-16:20-O-ORGS ●**Layer-resolved molecular organization of pentacene thin films for organic transistors by Resonant Soft X-ray Reflectivity***ORGS Organic molecules on solid surfaces*

Raffaella Capelli¹, Luca Pasquali^{2,3}, Marco Vittorio Nardi⁴, Tullio Toccoli⁴, Roberto Verucchi⁴, Franco Dinelli⁵, Caterina Gelsomini², Konstantin Koshmak¹, Angelo Giglia¹, Stefano Nannarone¹

¹ CNR - Istituto Officina dei Materiali S.S. 14, km 163.5 in Area Science Park I-34012, Trieste, Italy;

² Dipartimento di Ingegneria 'Enzo Ferrari' Università di Modena e Reggio Emilia Via Vivarelli 10 41125, Modena, Italy;

³ Department of Physics, University of Johannesburg, PO Box 524, Auckland Park, 2006, South Africa;

⁴ IMEM-CNR, Istituto Materiali per Elettronica e Magnetismo, sede di Trento, Via alla Cascata 56/C, Povo Trento, Italy;

⁵ CNR- Istituto Nazionale di Ottica Area della ricerca di Pisa - Via G. Moruzzi 1 Località S. Cataldo 56124, Pisa, Italy

Reflectivity is typically carried out in the hard X-rays to study morphology of interfaces and structure of layered systems, where electron density contrast between materials is exploited. In the soft X-rays, reflectivity at resonance provides additional advantages in terms of atomic and depth-resolved investigation of the chemical, structural and magnetic properties of a variety of systems, including organic materials. The technique is non-destructive. The sampling depth is not limited to the near-surface region, as for electron yield spectroscopies, but deep buried interfaces can be accessed as well (several tenths of nm). In particular, we developed a protocol [1,2] to get simultaneous quantitative information on the structure, interface morphology, chemical properties and optical anisotropies of layered materials with sub-nm depth resolution. The method is based on the quantitative prediction of the spectral line-shape across specific elemental edges through: 1) the simulation (from the first principles) of the dielectric tensor of each material in a stack; 2) the simulation of the propagation of the electromagnetic field in the layers and the computation of the (anisotropic) optical properties (reflectivity, transmission); 3) the comparison and fitting of the simulation to the experiment.

Soft X-ray reflectivity at carbon K-edge with linearly polarized photons is used here to study Pentacene thin films produced by Supersonic Molecular Beam Deposition (SuMBD) on SiO₂. SuMBD allows a precise control of molecular directionality and velocity during growth, with the formation of highly flat organic layers that present enhanced electronic transport properties in organic thin film transistors [3]. Films of different thickness, up to 20 nm, are examined. It is observed that molecules adopt a standing orientation, with the tilt angle of the long molecular axis with respect to the substrate normal that progressively reduces with the increasing film thickness. This is expected to influence the molecular reciprocal interaction and the charge transport parallel to the dielectric substrate in devices. The effect of the deposition of an Au electrode overlayer on top of the organic film is also studied, as far as the organic molecular organization below the metal contact is concerned. It is found that the pentacene molecules at the buried interface with Au assume a flat orientation, that propagates two-tree layers into the organic film. This can have a strong impact on charge injection at electrodes. We believe that studies of this type, aiming at understanding the molecular orientation at deep buried interfaces, are fundamental to finely tune organic thin film thickness and growth modes and to guide optimization of devices architectures.

References:

[1] L. Pasquali et al., Phys Rev B, 2014, 89, 45401.

[2] R. Capelli et al., J Chem Phys, 2016, 145, 024201

[3] T. Toccoli et al., Appl. Phys. Lett. 2006, 88, 132106; Yu Wu et al., Phys. Rev. Lett. 2007, 98, 076601

Thu-9:00-O-OXID ●

Influence of the multifunctional $\text{Ti}_{0.7}\text{M}_{0.3}\text{O}_2\text{-C}$ ($\text{M} = \text{W}, \text{Mo}$) composite supports on the electrochemical performance of Pt electrocatalysts

OXID Oxide surfaces and ultrathin oxide films

Ádám Vass¹, Zoltán Pászti¹, Irina Borbáth¹, István Bakos¹, István Sajó², András Tompos¹

¹ Institute of Materials and Environmental Chemistry, Research Centre for Natural Sciences, HAS, Budapest, 1519, Hungary

² University of Pécs, Szentágotthai Research Centre, Pécs, H-7624, Hungary

A promising step towards a novel class of fuel cell electrocatalysts is the application of multifunctional mixed oxide-carbon composite supports. The preparation and the thorough characterization of Pt electrocatalysts deposited onto $\text{Ti}_{0.7}\text{M}_{0.3}\text{O}_2\text{-C}$ ($\text{M} = \text{W}, \text{Mo}$) composites is presented. The necessary conditions for exclusive incorporation of W and Mo dopant into the TiO_2 -lattice of mixed oxide were determined [1-3]. A characteristic feature of the cyclic voltammograms (CVs) of the $\text{Pt}/\text{Ti}_{(1-x)}\text{M}_x\text{O}_2\text{-C}$ catalysts is the appearance of a redox peak pair in the so-called hydrogen region [3]. The peak in the anodic branch of the voltammograms above 350 mV can not be assigned solely to the support or to the platinum, thus it can be the result of some collective effect of the support and the Pt. Upon using different potential limits during the cyclic polarization the nature of the redox pre-peak characteristic to the W- and Mo-containing composite supported Pt catalysts was clarified. This anodic peak was connected to the oxidation of tungsten or molybdenum bronzes $\text{H}_x\text{M}\text{O}_3$ formed via the hydrogen spillover. Upon using of $\text{Pt}/\text{Ti}_{0.7}\text{W}_{0.3}\text{O}_2\text{-C}$ catalysts cathodic counterpart (i.e. the current peak of the formation of the tungsten bronzes) of this anodic peak coincides with the hydrogen-adsorption peaks of the platinum. However, on Mo-containing composite supported catalysts a clearly distinguishable cathodic peak could be observed in the so called double layer region on the CVs. On account of the spillover effect oxophilic dopant-containing composites improved the catalytic activity in the hydrogen oxidation reaction (HOR) with respect to conventional Pt/C catalysts. In addition, the mixed oxide component increased the CO tolerance under simulated CO poisoning conditions by providing adsorbed hydroxyl species (OH_{ads}) for CO oxidation at very low electrode potentials. The assessment of the electrochemical properties of the composite supported catalysts revealed a clear correlation between the degree of M dopant incorporation, hydrogen spillover effect, stability and CO tolerance. No significant difference in the activity, short-term stability and CO tolerance was found between the tungsten- and molybdenum-containing $\text{Ti}_{0.7}\text{M}_{0.3}\text{O}_2\text{-C}$ composite supported Pt catalysts, if the oxophilic doping metals were completely incorporated. Better performance of the $\text{Pt}/\text{Ti}_{0.7}\text{M}_{0.3}\text{O}_2\text{-C}$ catalysts in a single cell test device using hydrogen containing 100 ppm CO compared to the reference Pt/C and PtRu/C (Quintech) catalysts was also demonstrated [3].

References:

- [1] D. Gubán, I. Borbáth, Z. Pászti, I.E. Sajó, E. Drotár, M. Hegedűs, A. Tompos, Appl. Catal. B- Environ. 2015, 174, 455-470.
- [2] Á. Vass, I. Borbáth, Z. Pászti, I. Bakos, I.E. Sajó, P. Németh, A. Tompos, React. Kinet. Mech. Cat. 2017, DOI: 10.1007/s11144-017-1155-5.
- [3] D. Gubán, A. Tompos, I. Bakos, Á. Vass, Z. Pászti, E.Gy. Szabó, I.E. Sajó, I. Borbáth, Int. J. Hydrogen Energy 2017, DOI: 10.1016/j.ijhydene.2017.03.080

Thu-10:00-O-SEMI ●**Nitride layers grown on patterned graphene/SiC***SEMI Semiconductor surfaces and ultrathin layers*

[B. Pécz](#)¹, [A. Kovács](#)², [R. E. Dunin-Borkowski](#)², [R. Yakimova](#)³, [H. Behmenburg](#)⁴, [C. Giesen](#)⁴, [M. Heuken](#)⁴

¹ Institute for Technical Physics and Materials Sci., Research Centre for Natural Sciences, Hungarian Academy of Sciences, 1121 Budapest, Konkoly-Thege u. 29-33, Hungary;

² Ernst Ruska-Centre for Microscopy and Spectroscopy with Electrons, Peter Grünberg Institute, Forschungszentrum Jülich, D-52425, Germany;

³ Department of Physics, Chemistry and Biology, Linköping University, S-581 83 Linköping, Sweden;

⁴ AIXTRON SE Kaiserstrasse 98, 52134, Herzogenrath, Germany

Self-heating of high power devices is a major problem in GaN high electron mobility transistors (HEMT), in which the power reached the values of 10 W/mm (the length of the gate in mm). Implementation of graphene layers in gallium nitride heterostructure growth can solve the self-heating problem in nitride-based high-power electronic and light-emitting optoelectronic devices.

Now we explore the possibilities of nitride layer growth on graphene/SiC. The task is challenging thanks to the lack of chemical reactivity between the two materials. Therefore instead of direct growth on graphene we present how high quality nitrides can be grown on patterned graphene/SiC templates. The grown samples are analysed by transmission electron microscopy (TEM). The dislocation density is practically the same as in GaN grown on SiC. The results show, that the used graphene is a multilayer of 3-5 graphene sheets, but this is advantageous for the high heat conductivity [1]. The nitride heterostructures deposited on patterned graphene layers are grown via lateral overgrowth, which results in the formation of a single-crystalline GaN layer that has a relatively low defect density and a smooth surface. Fig.1 shows the interface region over the SiC at the edge of the graphene stripe. AlN could nucleate on bare (and a little bit over-etched) SiC and overgrow the graphene pads laterally. After about one micron growth of GaN on AlN buffer the surface is completely smooth [1]. Optimization of the plasma etching process and growth procedure promises to offer a simple route to produce nitride based device structures with better thermal management due to graphene layer incorporation.

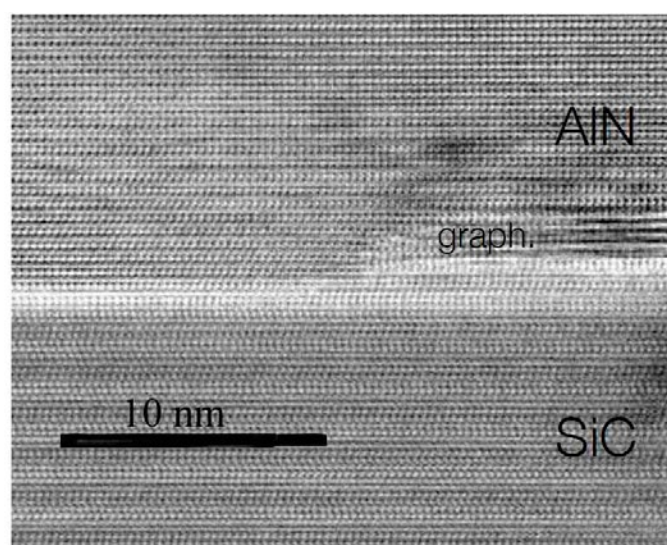


Fig. 1: BF STEM image of the sample: AlN buffer layer grown on patterned graphene/SiC.

References:

A. Kovács, M. Duchamp, R.E. Dunin-Borkowski, R. Yakimova, P.L. Neumann, H. Behmenburg, B. Foltynski, C. Giesen, M. Heuken and B. Pécz, *Advanced Materials Interface*, 2 (2015), 1400230

Thu-11:40-O-ORGS ●**Titanium tetraisopropoxide adsorption and decomposition on Cu(111)***ORGS Organic molecules on solid surfaces*

[Mikhail Petukhov](#)¹, [P. Bernal](#)¹, [S. Bourgeois](#)¹, [B. Domenichini](#)¹, [D. Vantalon](#)², [P. Lagarde](#)²

¹ ICB, UMR 6303 CNRS-Université de Bourgogne Franche-Comté, Dijon, France;

² Synchrotron SOLEIL, L'Orme des Merisiers, Saint-Aubin, Gif-sur-Yvette, France

Titanium tetraisopropoxide $\text{Ti}(\text{OC}_3\text{H}_7)_4$ (TTIP) is the predominant precursor used in chemical vapour deposition methods to synthesize titanium dioxide thin films. Study of adsorption, decomposition of TTIP molecules and kinetic mechanisms underlying the synthesis of TiO_2 on metal surfaces has a top interest for various applications.

TTIP molecules have been deposited on copper substrate Cu(111) with submonolayer and monolayer coverage at low temperature (150K), room temperature and elevated temperatures (up to 800K) and studied by variable temperature scanning tunneling microscope (VT STM), X-ray photoelectron spectroscopy (XPS), low electron energy diffraction (LEED) and X-ray absorption spectroscopies (XANES & EXAFS, LUCIA beamline, SOLEIL).

Adsorption and assembling of entire molecules are observed at low temperatures. At room temperature, STM reveals an assembling of TTIP molecular fragments. XPS analysis confirms presence of ligand groups bonded to $(\text{Ti}-\text{O}_x)$ molecular center, indicating a partial decomposition process confirmed by EXAFS spectroscopy. TTIP molecules start to decompose completely on copper surface at temperatures higher than 600 K. After cooling down from 800 K, STM images at room temperature evidently demonstrate formation of titanium oxide islands with hexagonal structure (Figure 1; STM image $30 \times 24 \text{ nm}^2$; $U_b=400 \text{ mV}$; $I_t=0.8 \text{ nA}$) confirmed by surface EXAFS. Besides, XPS analysis proves appearance of a new state of Ti2p levels with lower binding energy (456.3 eV for Ti2p3/2), than those of regular titanium dioxide (458.8 eV) or entire TTIP molecule adsorbed on copper surface (459.4 eV).

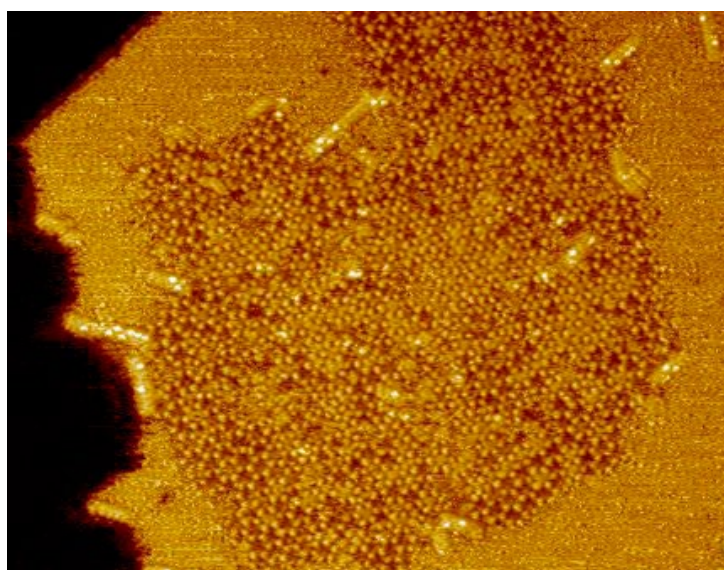


Figure 1: STM image of TiO_x islands having hexagonal structure on Cu(111): $30 \times 24 \text{ nm}^2$; $U_b=400 \text{ mV}$; $I_t=0.8 \text{ nA}$

Thu-16:00-O-CATH ●**Non-noble intermetallic compounds as selective butadiene-hydrogenation catalysts: $\text{Al}_{13}\text{Fe}_4$ vs $\text{Al}_{13}\text{Co}_4$** **CATH Catalytic 2D-model studies under high pressures**

[Laurent Piccolo](#)¹, [Emilie Gaudry](#)², [Julian Ledieu](#)², [Vincent Fournée](#)², [Lidiya Kibis](#)³

¹ Univ Lyon, Université Claude Bernard - Lyon 1, CNRS, IRCELYON - UMR 5256, 2 Avenue Albert Einstein, F-69626 VILLEURBANNE CEDEX, France;

² Institut Jean Lamour, UMR 7198 CNRS & Université de Lorraine, Parc de Saurupt, CS 50840, F-54011 Nancy, France;

³ Boreskov Institute of Catalysis SB RAS, Lavrentieva 5 & Novosibirsk State University, Pirogova St. 2, Novosibirsk 630090, Russia

Non-noble complex intermetallic compounds have shown promising properties as inexpensive catalyst alternatives to Pt-group metals for alkyne [1] and alkene [2-4] partial hydrogenation. In this work, the gas-phase hydrogenation of 1,3-butadiene over the $\text{Al}_{13}\text{Fe}_4(010)$ and $\text{Al}_{13}\text{Co}_4(100)$ surfaces was investigated in the 0.2–2 kPa range at 20–200 °C in a batch-type reactor coupled with an ultrahigh-vacuum setup allowing for Auger electron spectroscopy and low energy electron diffraction. The results were also compared with those obtained for Pd(100) in the same conditions.

Clean $\text{Al}_{13}\text{Fe}_4(010)$ is initially as active as Pd and 100% selective to butenes, including at room temperature (RT), with sequential conversions of butadiene to butenes, and butenes to butane [2,3]. The main difference with Pd comes from the butenes distribution, with a *cis/trans* 2-butene ratio larger than unity for Al-Fe while it is near zero for Pd. This result can be explained in terms of active site isolation and steric constraints upon π -allylic precursors to 2-butenes [3]. The sensitivity of the Al-Fe surface to oxygen-containing gas impurities, forming an aluminum oxide overlayer at high coverage, leads to gradual deactivation under reaction conditions, which is the main issue for the practical use of non-noble metal catalysts. However, the alloy surface can be fully regenerated through high-temperature annealing [3].

While both $\text{Al}_{13}\text{Fe}_4$ and $\text{Al}_{13}\text{Co}_4$ have been claimed to be efficient for partial acetylene hydrogenation [1], $\text{Al}_{13}\text{Co}_4(100)$ appears more stable but much less active than $\text{Al}_{13}\text{Fe}_4(010)$ for butadiene partial hydrogenation. Although the bulk structures of the two compounds are similar, their surface structures and compositions, as determined by a combination of surface-science experiments and *ab initio* calculations, substantially differ [5]. The influence of these structural differences will be discussed in the light of recent density-functional-theory calculations.

References:

[1] M. Armbrüster et al., Nat. Mater. 11 (2012) 690

[2] L. Piccolo, Chem. Commun. 49 (2013) 9149

[3] L. Piccolo, L. Kibis, J. Catal. 332 (2015) 112

[4] L. Piccolo, L. Kibis, M.C. DeWeerd, E. Gaudry, J. Ledieu, V. Fournée, ChemCatChem (2017), doi: 10.1002/cctc.201601587

[5] E. Gaudry et al., Phys. Rev. B 94 (2016) 165406

Tue-17:40-O-BIMS ●

Remarkable confinement effects on equilibrated adsorption, segregation and dimerization reaction predicted for alloy nanoparticles

BIMS Bimetallic surfaces and alloy nanocrystals

[Micha Polak](#), [Leonid Rubinovich](#)

Department of Chemistry, Ben-Gurion University of the Negev, Beer-Sheva 84105, Israel

A new nano-confinement effect on equilibrated reactions (NCECE) was predicted by us some years ago using statistical-mechanics principles¹. Thus, the involvement of very small numbers of reacting molecules in a closed space can considerably affect the chemical-equilibrium via mixing-entropy variations. In particular, canonical partition-function based computations reveal significant increase of the reaction extent and equilibrium constant for the case of exothermic reactions as compared to the corresponding macroscopic system (the thermodynamic limit, TL). Since that first work we published several articles dealing with NCECE predictions for „ordinary“ chemical reactions²⁻³. Most recently, we investigated the effect for nanoconfined adsorption (NCEA). Quiet remarkably, adsorption isotherms computed for H_2 / *Ti*-doped graphene as a model nanosystem exhibit fundamental deviations from the “macroscopic” Langmuir isotherm (Fig.1), namely, system-size dependent significant enhancement of surface coverage. In addition, the talk will incorporate three novel manifestations of the effect predicted for alloy nanoparticle systems:

Adsorption isochores: CO on Pt-Ru(111) islands

Equilibrium CO site populations computed for Pt_6Ru_3 and Pt_3Ru surface alloy vs. alloy surface islands, with reported DFT energetics as input, consistently exhibit extra coverage ($\Delta\Theta$) compared to the TL, especially for the dominant Ru on-top sites. The NCEA decreases with increasing system-size and $\Delta\Theta_{surf-alloy} \neq \Delta\Theta_{alloy-surf}$ due to different adsorption energies.

Surface segregation of Si impurity in Fe (bcc) rhombic dodecahedra

In view of the general analogy between gas molecule adsorption on a surface and elemental surface segregation from the material interior, possible NCECE effects were explored also for the latter. A key prediction is the significant lowering of residual Si concentration in rhombic-dodecahedral nanoparticle cores due to the enhancement of its surface segregation compared to the TL. Considering the known strong effects of Si impurities on Fe properties this result can have some practical implications.

Dimerization reaction of Ir within dilute Pd - Ir cuboctahedra⁴

Up to ~ 60% increase in the dimerization extent, as compared to the macroscopic TL, is predicted (Fig.2). When subsurface sites are preferential for the dimerization, catalytic properties of Pd - Ir nanoparticles can possibly be affected. The dual role of configurational entropy, namely mixing of Ir/Ir₂ vs. Pd/Ir will be elucidated.

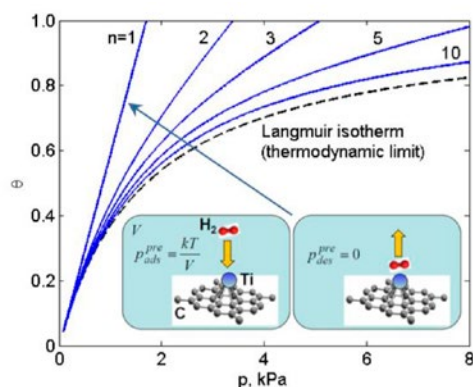


Fig.1 NCEA-induced enhancement of H_2 physisorption on Ti in doped graphene as reflected in adsorption isotherms computed assuming single molecule per surface site for different system sizes ($T = 300$ K). Inset: strong pressure fluctuations in the smallest nanosystem.

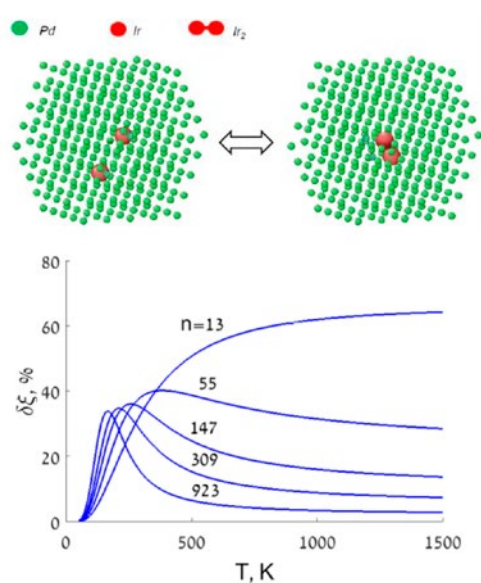


Fig.2 Top: Illustration of $2Ir \leftrightarrow Ir_2$ equilibrated dimerization inside the 309-atom core of Pd surface-segregated 561-atom $Pd-Ir$ cubooctahedron. Bottom: The temperature dependence of the dimerization extent relative increase computed for several core sizes.

References:

1. M. Polak and L. Rubinvich, Nano Letters 8, 3543 (2008).
2. M. Polak and L. Rubinvich, Surf. Sci. 641, 294 (2015).
3. L. Rubinvich and M. Polak, Nano Letters 13, 2247 (2013).
4. M. Polak and L. Rubinvich, Int. J. Nanomater. Nanotechnol. Nanomed. 3(1) 023 (2017).

Thu-9:20-O-MOLA ●

Molecular chessboard assemblies sorted by site-specific interactions of out-of-plane d-orbitals with a semi-metal template

MOLA Ultrathin two-dimensional molecular self-assembly

A. Waeckerlin¹, O. Popova¹, S. Fatayer³, T. Nijs¹, S. Nowakowska¹, S. F. Mousavi¹,
A. Ahsan¹, T. A. Jung⁴, C. Wäckerlin⁵

¹ Department of Physics, University of Basel, Klingelbergstrasse 82, 4056 Basel, Switzerland;

² Laboratory for Thin Films and Photovoltaics, Empa, Swiss Federal Laboratories for Materials Science and Technology, 8600 Dübendorf, Switzerland;

³ Departamento de Física Aplicada, Instituto de Física Gleb Wataghin, Universidade Estadual de Campinas, Campinas 13083-859, Brazil;

⁴ Laboratory for Micro- and Nanotechnology, Paul Scherrer Institute 5232 Villigen, PSI, Switzerland;

⁵ Nanoscale Materials Science, Empa, Swiss Federal Laboratories for Materials Science and Technology, 8600 Dübendorf, Switzerland;

The self-assembly of single component porphyrin or phthalocyanine (Pc) layers at different surfaces is a straight forward approach to obtain highly ordered 2D periodicity. In this work we show a conceptually new approach to produce 2D chessboard patterns from bi-component mixtures in absence of functionalization of the molecular modules by functional groups towards their supramolecular organization. Specifically, we show that mixtures of CuPc + MnPc and CuPc + CoPc sort into highly ordered Cu/Mn and Cu/Co chessboard arrays on the p(10x10)-Bi/Cu(100) semimetal template (Figure 1). The p(10x10) Bi-reconstructed Cu(100) substrate which is key to the sorting mechanism is very different from other metal/noble metal substrates, as it is characterized by a periodic array of square pockets and a low density of electronic states around the Fermi level. As we show, site-specific interactions between the central transition-metal ions and the substrate lead to preferred adsorption sites of the metal-Pcs with out-of-plane 3d states. Therefore MnPc and CoPc if combined with CuPc mix into chessboard layers due to their out-of-plane 3d states around the Fermi level and the absence of these states for CuPc. If both molecules have out-of-plane 3d states around the Fermi level (CoPc + MnPc mixture), no chessboard layer is formed.

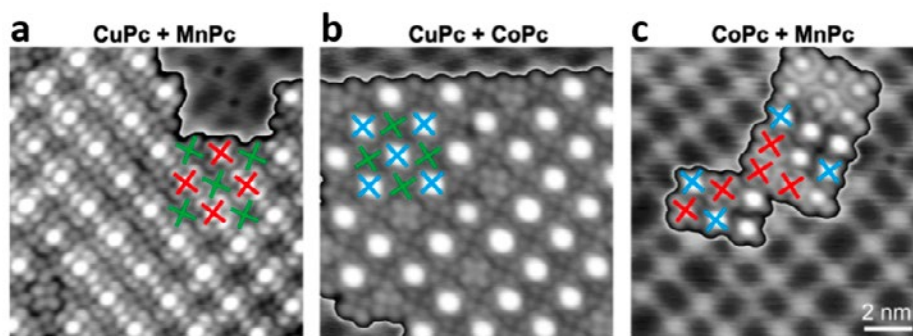


Fig.1. STM images binary mixtures of metal phthalocyanines on p(10×10)-Bi/Cu(100). Images of (a) CuPc + MnPc, b) CuPc+ CoPc and c) CoPc + MnPc. The crosses assign the type of molecule (CuPc – green, CoPc – blue, MnPc – red) and their orientation. CuPc + MnPc and CuPc + CoPc mixtures assemble into a chessboard arrays, but CoPc + MnPc does not. The scale bar applies to all images.

References:

[1] A. Wäckerlin, et al., Nano Letters 17, 1956 (2017)

Wed-10:40-O-OXID ●**Low dimensional electron system at titanates surfaces and related interfaces:
Create and control***OXID Oxide surfaces and ultrathin oxide films*

Milan Radovic

Swiss Light Source, Paul Scherrer Institut

Transition Metal Oxides (TMOs) exhibit unique and multifunctional electronic properties (such as high-temperature superconductivity, colossal magnetoresistance, metal-insulator transitions, etc.) directly related to the spin and orbital degrees of freedom of the transition metal d-states. Furthermore, their iso-structural nature permits realization of heterostructures where novel unexpected electronic properties take place. Engineering transition metal oxide surfaces and interfaces carries the potential for achieving new physical properties that radically differ from those of the constituent bulk materials. This is the case of oxide-lowDEGs, which recently showed extraordinary occurrences, including interfacial superconductivity, magnetism, large tuneable spin-orbit coupling and indications of topological states. In my talk, I will present recent spin resolved Angle Resolved Photoemission Spectroscopy (ARPES) measurements of the low dimensional electron gas at SrTiO₃ [1, 2, 3], TiO₂-anatase [4] and LAO/STO [5] interface showing that these systems have capability for the realization of TMO based electronic device.

References:

- [1] N. C. Plumb, M. Salluzzo, E. Razzoli, M. Månsson, M. Falub, J. Krempasky, C. E. Matt, J. Chang, J. Minár, J. Braun, H. Ebert, B. Delley, K.-J. Zhou, C. Monney, T. Schmitt, M. Shi, J. Mesot, C. Quitmann, L. Patthey, M. Radović, *Phys. Rev. Lett.* 113, 086801 (2014).
- [2] A. F. Santander-Syro, F. Fortuna, C. Bareille, T. C. Rodel, G. Landolt, N. C. Plumb, J. H. Dil, and M. Radovic, *Nature Materials*, 13, 1085–1090 doi:10.1038/nmat4107 (2014).
- [3] Z. Wang, S. McKeown Walker, A. Tamai, Z. Ristic, F.Y. Bruno, A. de la Torre, S. Ricco, N.C. Plumb, M. Shi, P. Hlawenka, J. Sanchez-Barriga, A. Varykhalov, T.K. Kim, M. Hoesch, P.D.C. King, W. Meevasana, U. Diebold, J. Mesot, M. Radovic, and F. Baumberger, *Nature Materials* 15, 835–839 (2016) doi:10.1038/nmat4623 (2016).
- [4] Z. Wang, Z. Zhong, S. McKeown Walker, Z. Ristic, J.-Z. Ma, F. Y. Bruno, S. Riccò, G. Sangiovanni, G. Eres, N. C. Plumb, L. Patthey, M. Shi, J. Mesot, F. Baumberger and M. Radovic, Atomic scale lateral confinement of a two-dimensional electron liquid in anatase TiO₂, *Nano Letters* 17 (4), pp 2561–2567 (2017).
- [5] N. C. Plumb, M. Kobayashi, M. Salluzzo, E. Razzoli, C. Matt, V. N. Strocov, K.-J. Zhou, C. Monney, T. Schmitt, M. Shi, J. Mesot, L. Patthey, M. Radovic, Evolution of the SrTiO₃ Surface Electronic State as a Function of LaAlO₃ Overlayer Thickness, *Applied Surface Science* Volume 412, Pages 271–278 (2017).

Tue-14:00-O-ORGS ●**On-surface synthesis of free-base corroles: a combined theoretical and experimental characterization***ORGS Organic molecules on solid surfaces*

[Eva Rauls](#)¹, [H. Aldahhak](#)², [M. Paszkiewicz](#)³, [F. Allegretti](#)³, [D. A. Duncan](#)⁴, [S. Tebi](#)⁴, [P. S. Deimel](#)³, [P. Casado Aguilar](#)³, [Y. Zhang](#)³, [A. C. Papageorgiou](#)³, [R. Koch](#)⁴, [J. V. Barth](#)³, [W. G. Schmidt](#)², [S. Müllegger](#)⁴, [W. Schöfberger](#)⁵, [F. Klappenberger](#)³, [U. Gerstmann](#)²

¹ *Det teknisk-naturvitenskapelige Fakultet, Universitetet i Stavanger, Norway;*

² *Lehrstuhl für Theoretische Materialphysik, Universität Paderborn, Germany;*

³ *Festkörperphysik, Universität Linz, Austria;*

⁴ *Physik Department E20, Technische Universität München, Germany;*

⁵ *Institut für Organische Chemie, Universität Linz, Austria*

Corroles are structurally closely related to the well-known porphyrins with their aromatic tetrapyrrole macrocycles. They have a lower symmetry and a smaller congested cavity. This and the resulting changes in the electronic structure promote the stabilization of metal ions in exceptionally high oxidation states. Therefore, corroles are distinctive candidates for various biomedical, catalytic, or solar cell applications. During the past decade, extensive studies regarding the synthetic aspects as well as the activity of different corrole-chelated metal ions have been reported. Only few studies, however, have been performed on well-defined model systems where corroles are adsorbed onto clean substrates under ultrahigh vacuum (UHV) conditions.

Combining dispersion-corrected density-functional theory (DFT) calculations, temperature-programmed desorption (TPD) measurements, scanning tunneling microscopy (STM), X-ray spectroscopic signature (XPS), near-edge X-ray absorption fine structure (NEXAFS) spectroscopy measurements and simulations, we characterize the chemical state and the conformation of the free-base corrole 5,10,15-tris(pentafluorophenyl)corrole (3H-TpFPC) adsorbed on a Ag(111) surface and unravel annealing induced chemical reactions.

Our novel method to simulate the XPS and the NEXAFS signatures of the C1s and N1s edges facilitates a thorough interpretation of the spectral features and predict new molecular chemical states arising at elevated temperatures.

We reveal a formation of on-surface stable corrole radicals by a site-specific cleavage of a pyrrole N-H bond triggered by annealing to 330 K. The molecular species adsorbs with a near-to-planar macrocycle tilted approximately 20° with respect to the surface plane contrasting the typical saddle-shape conformation of related porphyrin species. The tilted adsorption geometries enable the molecules to aggregate in non-trivial interwoven monolayer structures. After annealing to 430 K, a thermally induced regioselective cyclization (ring closure) reaction between the phenyl ring and the pyrrolic moiety, mediated by the radical cascade, has been reported. The ring-closed radicals form a highly symmetric regular monolayer structure describing a hexagonal lattice. Our calculations resolve the packing motif and predict the molecular conformations within the structure.

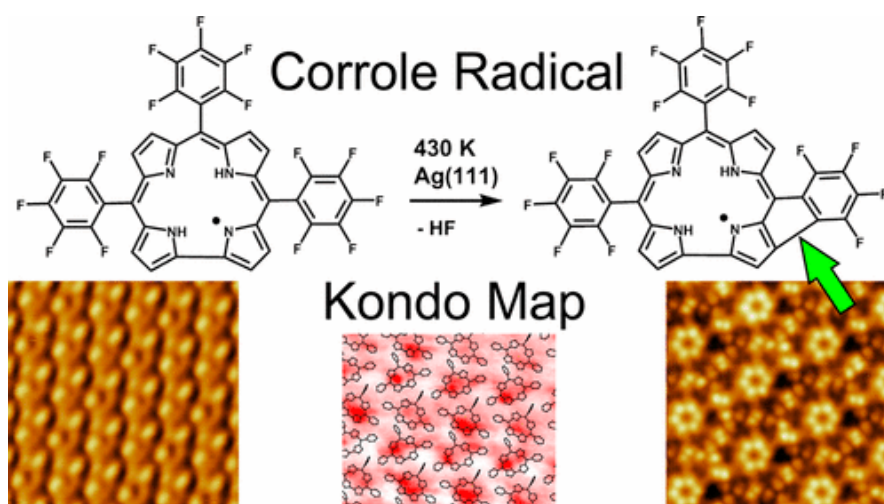


Figure Corrole Phases on Ag(111)

References:

- S. Tebi, H. Aldahhak, G. Serrano, W. Schoefberger, E. Rauls, W. G. Schmidt, R. Koch, and S. Müllegger, "Manipulation resolves non-trivial structure of corrole monolayer on Ag(111)", *Nanotechnology* 27, 025704 (2016).
- H. Aldahhak, M. Paszkiewicz, F. Allegretti, D. Duncan, S. Tebi, P. Deimel, P. A. Casado, Y. Zhang, A. Papageorgiou, R. Koch, J. Barth, W. G. Schmidt, S. Muellegger, W. Schoefberger, F. Klappenberger, E. Rauls, U. Gerstmann, "X-Ray Spectroscopy of Thin Film Free-Base Corroles – a Combined Theoretical and Experimental Characterization", submitted to *J. Phys. Chem C*, DOI: 10.1021/acs.jpcc.6b09935 (2017).
- S. Tebi, M. Paszkiewicz, H. Aldahhak, F. Allegretti, P. Deimel, P. A. Casado, D. Duncan, W. G. Schmidt, J. Barth, R. Koch, U. Gerstmann, E. Rauls, F. Klappenberger, W. Schoefberger, S. Muellegger, "On-Surface Site-Selective Cyclization of Corrole Radicals", *ACS Nano*, DOI: 10.1021/acsnano.7b00766 (2017).

Tue-14:40-O-EG2D ●

Fast surface X-ray diffraction: Gold epitaxy on MoS₂

EG2D Epitaxial growth and modification of 2D materials

Andrea Resta¹, M. Narayanan-nair¹, Y. Garreau¹, A. Taleb¹, A. Vlad¹, A. Coati¹, Tejada A², Y. Garreau³

¹ Synchrotron SOLEIL – L'Orme des Merisiers – Saint-Aubin;

² Laboratoire de Physique des Solides, CNRS-UMR 8502 Orsay France;

³ Univ Paris Diderot, Sorbonne Paris Cite, MPQ, CNRS,UMR 7162, F-75205 Paris 13, France

Metal to semiconductor junction is a long lasting research topic, that recently with the uprising fields of two dimensional materials find new challenges [1, 2, 3]. In this prospective investigating atomic structure and growth at the metal to 2D material interface can provide relevant information. More specifically we investigate the growth of gold under ultra high vacuum (UHV) condition on MoS₂ by surface x-ray diffraction, grazing incidence small angle scattering and scanning tunneling microscope and high resolution core level spectroscopy. The substrate is 2H-MoS₂ (0001) single crystal synthetically grown and commercially available. The single crystal was prepared by cleaving in air and then quickly transferred into the UHV chamber, followed by degassing at 400 C. The gold was deposited by physical vapor deposition while the substrate held at room temperature. The diffraction experiment reveal highly oriented particles, see image 1.A) The in-plane map (HK) taken at L=0.15 shows the diffraction spots specific for the Au(111) surface orientation, which is further sustained by the out of plane maps where the crystal truncation rods of the particle's to MoS₂ interface surface coincide with the aforementioned Au(111) surface orientation. It is therefore possible to orient the particles with respect to the substrate. Thanks to two-dimensional detector it is easily accessible to study the L dependence of the gold signal and its evolution upon annealing from the 4D data collected in a map.

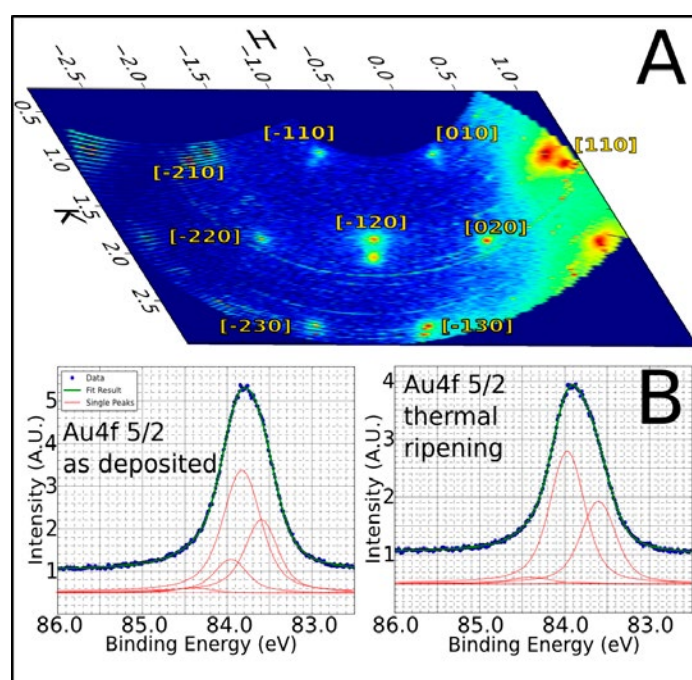


Figure: A) Here reported the in-plane [HK] cut in the reciprocal space. In the map are visible the signal from the substrate and from the gold particles in the vicinity. In the B) field is reported the Au 4f 5/2 signal registered for the gold[4] as deposited and for the ripened particles after an annealing at 400 C.

Moreover thanks to the the high resolution granted by the two dimensional detectors it is possible to obtain unique information on the embedded gold/MoS₂ interface otherwise hidden to the probe microscopy techniques. In the field B of the image is reported the particles ripening after thermal treatment observed by high resolution core level spectroscopy. The spectra are de-convoluted with four peaks and in agreement with the signals development observed in the SXR D experiments. Through those techniques it is therefore possible to follow growth and ordering of nanoparticles as well as the reordering/reshaping occurring upon annealing.

References:

- [1] Igor Popov, Gotthard Seifert, and David Tománek, Phys Rev. Lett.108 (2012) 156802
- [2] Maximilian Donath, Felix Hennersdorf and Jan J. Weigand Chem. Soc. Rev., (2016) page 45
- [3] David Tománek Phys.: Condens. Matter 27 (2015) 133203
- [4] Yoshikazu Ishikawa, Shigehumi Onodera, Keisuke Tajima Solid State Communications, 38,(1980) pp.595-598

Thu-9:40-O-MOLA ●

Multi-layered poly-functional microspheres for rapid multiplexed immunoassay

MOLA Ultrathin two-dimensional molecular self-assembly

Daragh Rice^{1,2,3}, M. Gleeson^{1,2}, K. O'Dwyer^{1,2}, R. Mouras^{1,2}, N. Liu^{1,2}, T. Soulimane^{1,3}, S. A. M. Tofail^{1,2}, C. Silien^{1,2}

¹ Bernal Institute, University of Limerick, Limerick, Ireland;

² Department of Physics, University of Limerick, Limerick, Ireland;

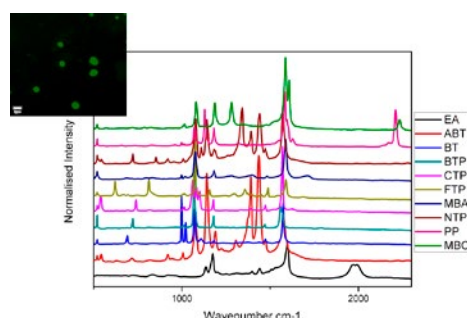
³ Department of Chemical Sciences, University of Limerick, Limerick, Ireland

Early detection of diseases such as pancreatic cancer and neurodegenerative disease (Alzheimer's or Parkinson disease) is a prerequisite for our health and well-being and enables fast and more effective treatments. Yet, biomarkers of such diseases are usually present at very low concentration in samples (blood, serum and saliva) and thus rapid, highly sensitive and accurate detection methods are needed.

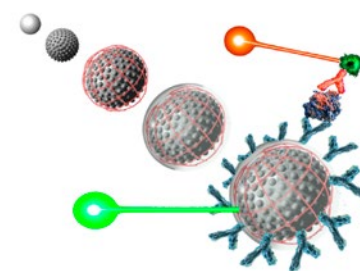
We are developing poly-functional multi-layered silica micro beads, which use SERS[1] and fluorescence for multiplexed immunoassays with dual mode recognition. Surface enhanced Raman spectroscopy, with its high sensitivity, chemical specificity and capacity for multiplex detection [2], provides a powerful tool for accurate identification of the beads and fluorescence immunoassay detection ensures highly selective biomarker detection and quantification. The beads incorporate a nanostructured silver layer gownned at the surface of a porous silica microsphere by a new single-step electroless plating method. The silver layer is functionalized with thiol- or thioacetate-based self-assembled monolayers that act as active Raman reporters. Polyelectrolyte multilayers and mine-functionalized silica shells encapsulate these reporters and act as immunoassay substrate, on which monoclonal antibodies are covalently attached.

Here, we will discuss the growth protocols and in particular the optimization of the nanostructured silver film and of the silica shell, to maximize the SERS signals and maintain the integrity of the Raman reporters during encapsulation and immunoassay detection. We will show that our beads affords multiplex detection and accurate diagnostics of clinical samples including. To further fasten the identification in these multiplex assay, we show that the beads also exhibit strong resonant coherent anti-Stokes Raman scattering (CARS). The assay is currently being developed as a diagnostic for pancreatic cancer by targeting three blood based biomarkers.

Figure 1 (LHS): SERS spectra of ten fully functionalized particles obtained using a Jobin-Yvon LabRAM HR confocal Raman microscope using 532 nm laser. Spectra were collected with 1 s acquisition time and 0.06 mW laser power. The insert shows an SEM image of a fully functionalised 1 μm size silica bead.



(Inset) Laser Scanning confocal microscopy fluorescence image of fluorescent microspheres following formation of an Immunocomplex for TNF- α with a secondary fluorescent tagged antibody (RHS): Schematic repre



References:

- [1] Li, J.-F., et al., Core-Shell Nanoparticle-Enhanced Raman Spectroscopy. *Chemical Reviews*, 2017.
 [2] Li, J., et al., Surface-Enhanced Raman Scattering Active Plasmonic Nanoparticles with Ultrasmall Interior Nanogap for Multiplex Quantitative Detection and Cancer Cell Imaging. *Analytical Chemistry*, 2016. 88(15): p. 7828-7836.

Mon-14:40-O-CATL ●**Oxidation reactions on Au surfaces: the role of water***CATL Catalytic 2D-model studies at low pressures*Raphael Moreira, [Thomas Risse](#), Erik Meyer*Institut für Chemie und Biochemie, Freie Universität Berlin,
Takustr. 3, 14195 Berlin, Germany*

Nanoporous gold has emerged as a very promising catalysts for a variety of catalytic processes. In recent years' significant efforts have been made to elucidate the role of structural aspects as well as admixtures of a second metal, oftentimes silver, which remains in the systems produced by corrosion of an appropriate alloy such as AuAg. Investigations on well-defined single crystalline model systems provide evidence that the reactivity of nanoporous gold can be rationalized by the properties of low index Au surfaces. However, various open questions still remain such as the role of the second metal, steps or the importance of water for the understanding of the catalytic properties.

In this contribution, we will present results for different oxidation reaction on Au single crystal surfaces using molecular beam techniques combined with *in-situ* IR spectroscopy. In particular, we will focus on the role of water for two different oxidation reactions namely CO oxidation and oxidative coupling of alcohols. As Au surfaces do not dissociate molecular oxygen under UHV conditions the experiment utilize an effusive beam of atomic oxygen as created by a thermal cracker. We will discuss the steady state reactivity as well as transient kinetics of the oxidation reactions under isothermal conditions using pulsed beams and combine these with IR spectroscopic results to elucidate the nature of possible surface species. The transient kinetics observed in these experiments provide clear evidence for a complex reaction scenario than anticipated even for a simple oxidation such as the reaction of CO by oxygen atoms. The mechanistic implications of water on the reaction mechanism become even more intricate for more complex reactions such as the oxidative coupling of alcohols for which water as a reaction product may play an important role. Depending on the conditions chosen to run the experiment water can increase or decrease the reactivity or change the selectivity of the process. Possible scenarios to understand these results will be discussed taking theoretical considerations into account.

Wed-9:00-O-ORGS ●**Revealing phthalocyanine arrangements on Ag(100):
from pure overlayer of CoPc and F₁₆CuPc to bimolecular heterostructures***ORGS Organic molecules on solid surfaces*Agata Sabik, Piotr Mazur, Franciszek Gołek, Grażyna Antczak*Institute of Experimental Physics, Department of Physics and Astronomy, University of Wrocław, Poland*

Metal phthalocyanines (MPc) are macrocyclic coordinative compounds, with remarkable chemical and thermal stability, which have been widely studied as the suitable candidates for organic electronic devices. Variety of molecular compositions are available and provide broad array of MPc (opto)electronic and magnetic properties. It is also possible to tune material properties by preparation of the layer which consists of MPc blend. The commonly performed fundamental studies on the adsorption of MPc on monocrystalline metal and semiconductor surfaces are indirect way to get better insight into organic nanotechnology.

In this work we have utilized scanning tunneling microscopy (STM) and low energy electron diffraction (LEED) to determine the structural properties of cobalt phthalocyanine (CoPc) and prefluorinated copper phthalocyanine (F₁₆CuPc) on the Ag(100) surface. For coverages close to monolayer both studied systems form long-range ordered structures which are detected by LEED. Their alignments (with respect to the [110] silver crystallographic direction) was investigated by STM. The local lateral molecular arrangements depend on the molecule composition.

Finally, we co-adsorb CoPc and F₁₆CuPc on the Ag(100) surface. We demonstrate that adsorption of CoPc-F₁₆CuPc blend also leads to formation of ordered structure, visible in both STM and LEED investigations. The difference in the STM appearance of central part of the molecule allows us to distinguish each MPc in the bimolecular heterostructure. The blend consists of molecular chessboard in which CoPc and F₁₆CuPc arrange in alternating manner.

This work has been supported by National Science Center, Poland within the project number 2015/19/N/ST3/01044.

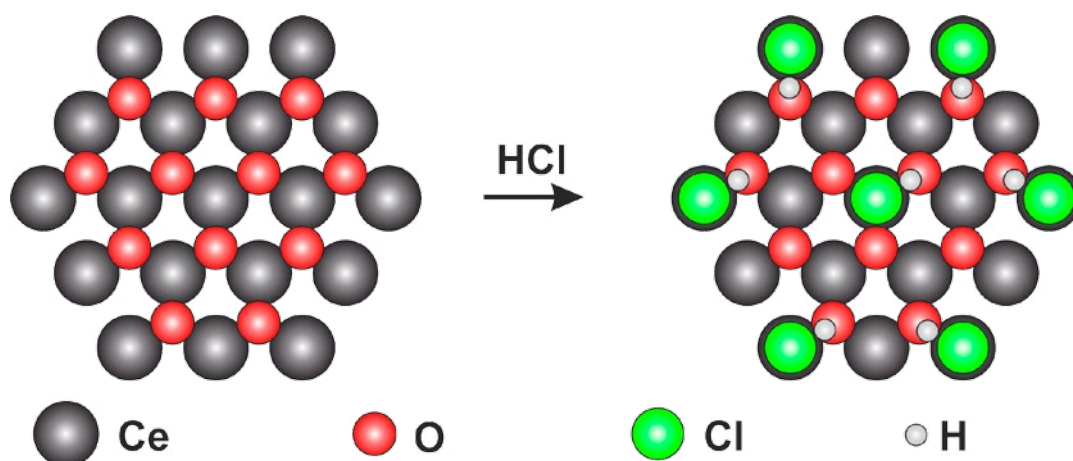
Tue-16:00-O-CATL ●

CeO_{2-x}(111), a model catalyst for the HCl oxidation*CATL Catalytic 2D-model studies at low pressures*Christian Sack¹, Herbert Over¹, Pablo Lustemberg², María Verónica Ganduglia Pirovano³¹ *Physikalisch-Chemisches Institut, Justus-Liebig-Universität Gießen, Heinrich-Buff-Ring 17, 35392 Gießen, Germany;*² *Instituto de Física Rosario (IFIR-CONICET), Bv. 27 de Febrero 210bis, S2000EZP Rosario, Santa Fe, Argentina;*³ *Institute of Catalysis and Petrochemistry, Spanish Council for Scientific Research, Marie Curie, 2. Cantoblanco, 28049 Madrid, Spain*

CeO_{2-x} is capable of catalyzing the reaction of HCl and O₂ to form Cl₂ and H₂O, a process which is of great industrial interest. Amrute *et al.* published a DFT based catalytic cycle for the HCl oxidation over CeO₂(111) together with FTIR measurements of nano particle CeO₂ powders [1].

In this contribution we provide first surface science experiments, in combination with DFT modeling and calculations, for the HCl oxidation on crystalline CeO_{2-x}(111) films with 1.5 < x < 2.0. The goal is to achieve a deeper insight into the elementary steps of the catalytic cycle and the active sites of the CeO_{2-x}(111) model system. CeO_{2-x}(111) samples were grown on a Ru(0001) substrate, samples with lower oxygen content were created via soft sputtering the ceria film. HCl adsorbs on the ceria surface at room temperature forming an ordered ($\sqrt{3} \times \sqrt{3}$)R30° overlayer structure, which was monitored with LEED. Supported by DFT calculations, we propose a first explanation for the overlayer structure, where Cl can either adsorb on-top of a Ce position, being stabilized by a neighboring hydroxide species, or on surface oxygen vacancies. Under UHV conditions, Cl is stable on the surface up to temperatures between 700 K and 900 K, depending on the degree of reduction of the ceria film. The concentration of surface Cl was quantified with XPS, where we can show that the maximum Cl surface concentration depends critically on the defect chemistry of the ceria film.

Our present understanding of the surface science experiments for HCl-CeO₂(111) will be critically compared to the reaction mechanism proposed by Amrute *et al.* [1].



References:

[1] A.P. Amrute *et al.* *Journal of Catalysis* 286 (2012) 287–297.

Thu-10:00-O-MOLA ●

Ultrathin film polymorphs of ferrocene derivatives assisted by functional groups and solvents

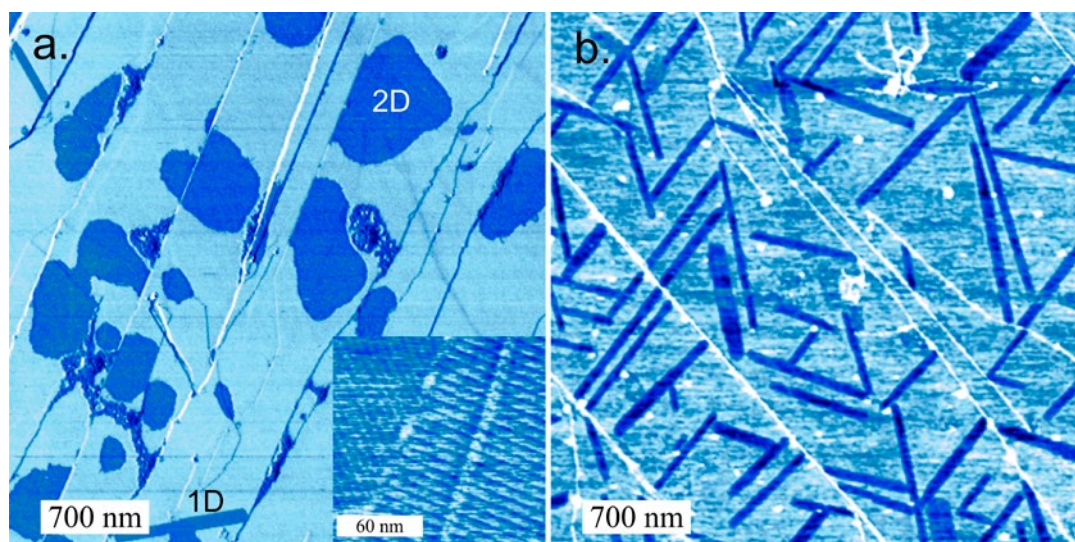
MOLA Ultrathin two-dimensional molecular self-assembly

Prithwidip Saha, Vinithra G, Himani Malik, Ramesh Ramapanicker, Thiruvancheril G. Gopakumar

Department of Chemistry, Indian Institute of Technology Kanpur, India

Ferrocene (Fc) derivatives are well known for its highly tunable electronic properties, which gain attention in molecular thin film based devices.¹⁻² Due to high thermal instability and diffusion on surfaces,³ formation of ordered pattern of Fc molecules are challenging at room temperature. This adverse effect in turn reduces its applicability in electronics, which rely on defect free ordered adlayer. To overcome this difficulty, we have introduced functional moiety with possible donor hetero atoms in view of hydrogen bonding stabilization between molecules.

Ultrathin films prepared by drop casting method of several Fc derivatives are investigated on highly oriented pyrolytic graphite (HOPG) using Atomic Force Microscope. Different kinds of ordered self-assembled patterns like one dimensional (1D) and 2D assemblies are observed at sub-monolayer coverage. Upon incorporation of different functional groups within the Fc derivatives, we show a control on the selectivity of 1D-islands over 2D domains,⁴ which is understood using previous theoretical calculations.⁵ We also show nature of solvent plays a vital role in controlling the growth of Fc derivatives at sub-monolayer coverage. Molecules drop-casted from methanol shows typically 2D growth (Figure a and its inset), while high boiling solvent shows extended 1D growth (Figure b). We interpret this observation is due to competitive kinetic and thermodynamic control.



References:

- [1] Yokota, Y.; Fukui, K.-I.; Enoki, T.; Hara, M. *J. Phys. Chem. C*, 111, (2007), 7561–7564.
- [2] Fabre, B. *Acc. Chem. Res.* 43, (2010), 1509–1518.
- [3] Braun, K.-F.; Iancu, V.; Pertaya, N.; Rieder, K.-H.; Hla, S.-W. *Phys. Rev. Lett.* 96, (2006), 246102.
- [4] Saha, P.; Yadav, K.; Chacko, S.; Philip, A. T.; Ramapanicker, R.; Gopakumar, T. G. *J. Phys. Chem.* 120, (2016), 9223–9228.
- [5] Bogdanovic, G. A.; Novakovic, S. B. *Cryst. Eng. Commun.* 13, (2011), 6930–6932.

Wed-16:00-O-BAND ●**Electronic properties of thallium single crystal thin film***BAND Band structure of solid surfaces*

[Kazuyuki Sakamoto](#)¹, [Mutsuki Iwaoka](#)², [Mariko Koga](#)², [Yuchi Yaoita](#)², [Yituo Zhang](#)², [Yasmine Sassa](#)³, [Jun Fujii](#)⁴, [Yasuo Yoshida](#)⁵, [Yukio Hasegawa](#)⁵, [Satoru Ichinokura](#)⁶, [Ryota Akiyama](#)⁶, [Shuji Hasegawa](#)⁶

¹ Department of Materials Science, Chiba University, Chiba 263-8522, Japan;

² Department of Nanomaterials Science, Chiba University, Chiba 263-8522, Japan;

³ Department of Physics and Astronomy, Uppsala University, S-75121 Uppsala, Sweden;

⁴ TASC Laboratory, IOM-CNR, SS 14, km 163.5, I-34012 Trieste, Italy;

⁵ Institute for Solid State Physics, The University of Tokyo, Kashiwa 277-0882, Japan;

⁶ Department of Physics, The University of Tokyo, Tokyo 113-0033, Japan

Heavy element single crystals show interesting physical phenomena owing to their strong spin-orbit coupling. For example, Bi single crystal shows spin-polarized surface electronic bands [1], and Pb and Tl show superconductivity at 7.2 K [2] and 2.4 K [3], respectively. Of these three heaviest non-radioactive elements, the electronic band structures of Bi and Pb, which are indispensable to have a proper understanding on their physical properties, have been studied in details both experimentally and theoretically. In contrast to these two elements, however, there is no experimental study on the electronic structure of Tl single crystal. The main reason of this lack is that there was no Tl single crystal that is large enough to perform angle-resolved photoelectron spectroscopy (ARPES) measurement. In our study, we have succeeded to grow a Tl single crystal thin film, which is large enough to perform ARPES measurement, on a Ag(111) substrate. The formation of Tl single crystal film was confirmed by the observation of sharp spots and low background intensity in low-energy electron diffraction (LEED), and the atomic structure using scanning tunneling microscopy (STM). The spin-splitting band predicted theoretically at the H point of the Brillouin zone [4] was clearly observed in the ARPES measurement, and the obtained Fermi surface shows good agreement with that of the theoretically Fermi surface in the A-H-L plane [4]. However, although the electronic structure was measured with different photon energy, there was only negligible difference in both electronic structure and Fermi surface. In this presentation, we will show detailed electronic structure of Tl single crystal film grown on a Ag(111) substrate, and discuss the origin of the negligible dispersion along the surface normal direction. We will also show the superconducting phase transition of this Tl thin film, and discuss the possibility of being topological superconductor.

References:

[1] Yu. M. Koroteev et al., Phys. Rev. Lett. 93, 046403 (2004).

[2] W. L. McMillan, Phys. Rev. 167, 331 (1968).

[3] T. Imamura, K. Okamoto, M. Saito, and M. Ohtsuka, J. Phys. Soc. Jpn, 40, 1256 (1976).

[4] R. Heid and K.-P. Bohnen, Phys. Rev. B 81, 174527 (2010).

Tue-16:40-O-PISC ●**Adsorption and photolysis of trimethyl acetate on TiO₂(B) (001) studied with synchrotron radiation core level photoelectron spectroscopy***PISC Photo-Induced Surface Chemistry*

[Anders Sandell](#)¹, [Andreas Schaefer](#)², [Davide Ragazzon](#)¹, [Mari Helene Farstad](#)³,
[Anne Borg](#)³

¹ Dept. of Physics and Astronomy, Uppsala University, P. O. Box 516, SE-75120 Uppsala, Sweden;

² Dept. of Synchrotron Radiation Research, Lund University, P. O. Box 118, SE-22100 Lund, Sweden;

³ Dept. of Physics, Norwegian University of Science and Technology (NTNU), NO-7491 Trondheim, Norway

Titanium dioxide (TiO₂) appears in four natural polymorphs: rutile, anatase, brookite and B-phase. TiO₂ has a wide range of applications of which the surface chemical properties are for example exploited within the fields of thermal catalysis, photocatalysis, and photoelectrochemistry. Specifically, devices based on TiO₂ are used in water splitting, degradation of organic pollutants, hydrophilic coatings and dye-sensitized solar cells. Due to its open structure, TiO₂(B) has recently mostly been associated with energy storage applications, particularly as electrode material for rechargeable Li ion batteries. Little is known about surface thermal and photochemical phenomena of TiO₂(B). This shortcoming has so far been, due to difficulties in the realization of TiO₂(B) samples for surface science studies. Recent experiments have however shown that it is possible to obtain TiO₂(B) in the form of ultrathin films. The films have been formed in ultrahigh vacuum (UHV), which ensures optimal purity and clean surfaces. TiO₂(B) films have been formed on both Pt(111), Pt(110) and Au(111) and STM images reveal that the films comprise large domains of TiO₂(B)(001) [1,2].

In this contribution, the first experimental study of the adsorption of a carboxylic acid, trimethyl acetic acid (TMAA, (CH₃)₃CCOOH), on TiO₂(B)(001) is presented. Synchrotron radiation photoelectron spectroscopy has been used to explore the adsorption and photooxidation of the formed trimethyl acetate (TMA). The TiO₂(B)(001) substrate was realized in the form of 2 nm thick film on Au(111). The TMA species adopt the bidentate bonding configuration with a thermal stability comparable to that on rutile TiO₂(110) [3]. Photolysis using both UV light and soft x-rays was employed and compared to the reaction on the reduced rutile TiO₂(110) surface. A kinetic analysis suggests that the initial photoreaction rate for TMA on the TiO₂(B) thin film is two times higher than that on the reduced rutile surface. The different photoactivities are discussed on the basis of the influence from reduced Ti species [4,5].

References:

- [1] A. Vittadini, F. Sedona, S. Agnoli, L. Artiglia, M. Casarin, G.A. Rizzi, M. Sambì, G. Granozzi, *ChemPhysChem* 11 (2010) 1550.
- [2] D. Ragazzon, M.H. Farstad, A. Schaefer, L.E. Walle, P. Uvdal, A. Borg, A. Sandell, *Surface Science* 633 (2015) 102.
- [3] J. M. White, M. A. Henderson, *J. Phys. Chem. B* 109 (2005) 12417.
- [4] Z.-T. Wang, N. A. Deskins, M. A. Henderson, I. Lyubinetsky, *Phys. Rev. Lett.* 109 (2012) 266103.
- [5] A. Sandell, D. Ragazzon, A. Schaefer, M. H. Farstad and A. Borg, *Langmuir* 32 (2016) 11456.

Tue-9:20-O-NAEX ●

Silica-based catalyst supports are inert, are they not?:**Striking differences in ethanol decomposition reaction originated from meso- and surface-fine-structure evidenced by small-angle X-ray scattering***NAEX Novel advancement of experimental methods*

András Sápi¹, Dorina G. Dobó^{1,2}, Dániel Sebők³, Gyula Halasi¹, Koppány L. Juhász¹, Ákos Szamosvölgyi¹, Péter Pusztai¹, Erika Varga⁴, Ildikó Kálomista⁴, Gábor Galbács⁴, Ákos Kukovecz^{1,2}, Zoltán Kónya^{1,3}

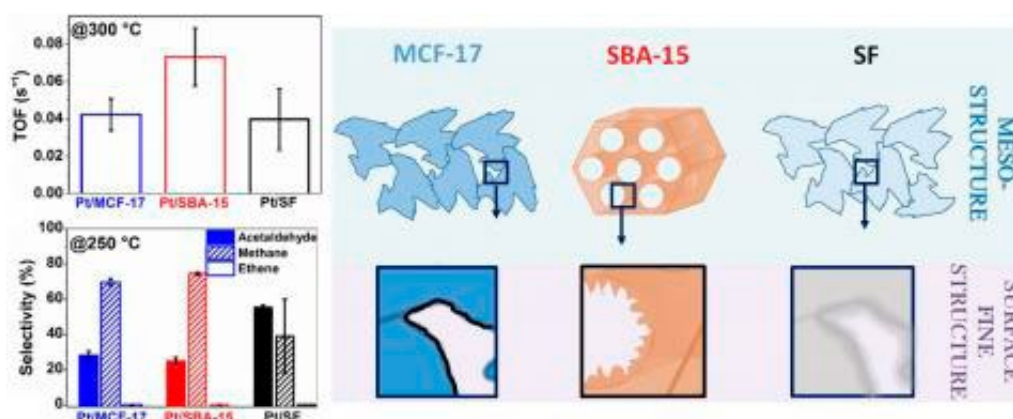
¹ Department of Applied and Environmental Chemistry, University of Szeged, Rerrich B. square 1, 6720 Szeged, Hungary;

² MTA-SZTE "Lendület" Porous Nanocomposites Research Group, University of Szeged, H-6720 Szeged, Hungary;

³ Department of Physical Chemistry and Material Science, University of Szeged, H-6720 Szeged, Hungary;

⁴ Department of Inorganic and Analytical Chemistry, University of Szeged, H-6720 Szeged, Hungary

6.6 nm Pt nanoparticles with narrow size distribution were anchored on mostly identical, amorphous silica supports (SBA-15, MCF-17, Silica Foam) and were tested in ethanol decomposition reactions at < 300 °C. The reaction on the Pt/SBA-15 was ~2 times faster (0.073 molecules•site⁻¹•s⁻¹) compared to Pt/MCF-17 (0.042 molecules•site⁻¹•s⁻¹) and Pt/SF (0.040 molecules•site⁻¹•s⁻¹) at 300 °C. In the case of Pt/SF, selectivity towards acetaldehyde was ~2 times higher compared to the Pt/MCF-17 and Pt/SBA-15 catalysts. In the case of Pt/MCF-17 and Pt/SBA-15, the methane to acetaldehyde ratio was ~ 4 times higher compared to the Pt/SF catalyst. The ethene selectivity was ~1.5 times higher in the case of Pt/SBA-15 compared to Pt/MCF-17 and Pt/SF. Small Angle X-ray Scattering (SAXS) studies showed striking differences in the nature of the surface of the different silica supports, which may be responsible for the activation, and selectivity deviation in ethanol decomposition reactions. The SBA-15 has the most disordered mesostructure and SF has a fine surface structure with a diffuse phase boundary may resulted in the high activity and varying selectivity, respectively.



Wed-10:00-O-OXID ● Phonons of ultrathin Perovskite Oxide Films

OXID Oxide surfaces and ultrathin oxide films

F. O. Schumann¹, K. Meinel¹, W. Widdra^{1,2}

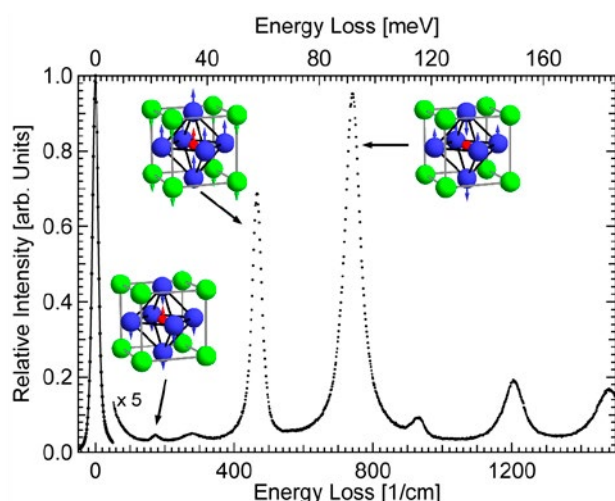
¹ Institute of Physics, Martin-Luther-Universität Halle-Wittenberg, Von-Danckelmann-Platz 3, 06120 Halle, Germany;

² Max Planck Institute of Microstructure Physics, Weinberg 2, 06120 Halle, Germany

Phonons and their softening are key elements for the understanding of phase transitions in ferroelectrics and multiferroics. In thin films, phonons as well as phase transition temperatures depend sensitively on the strain within the film. Here we report on high-resolution electron energy loss spectroscopy (HREELS) on the (001) surfaces of BaTiO₃, SrTiO₃ and the Ruddlesden-Popper series of Sr_{n+1}Ru_nO_{3n+1} with n of 1 and 2 (as can be seen in the figure for SrTiO₃). HREELS reveals three dipole-active phonon-polariton (Fuchs-Kliewer) modes, which are derived from the known transversal optical bulk phonons (sketched in the figure). In addition, it will be demonstrated that the complex dielectric function in the energy range from 4 to 1000 meV (30 to 8000 cm⁻¹) can be quantitatively extracted from the experimental loss function.

The full dielectric characterization for (001)-oriented single crystals of BaTiO₃ and SrTiO₃ with different intentional doping levels will be presented. The extracted surface dielectric function will be quantitatively compared with available bulk infrared data and allows the experimental determination of the surface-near doping level and a quantitative assessment of plasmonic contributions. For ultrathin films of BaTiO₃(001) as grown by MBE or magnetron sputtering on various substrates, HREELS data allow for the first time the determination of the complex dielectric functions of ultrathin oxide films down to single unit cell thicknesses. These data will be discussed with respect to a two-dimensional electron gas (2DEG) at the surface, electron-phonon coupling, as well as strain-driven phonon softening.

Support by the Sonderforschungsbereich SFB-762 "Functional oxide interfaces" is gratefully acknowledged.



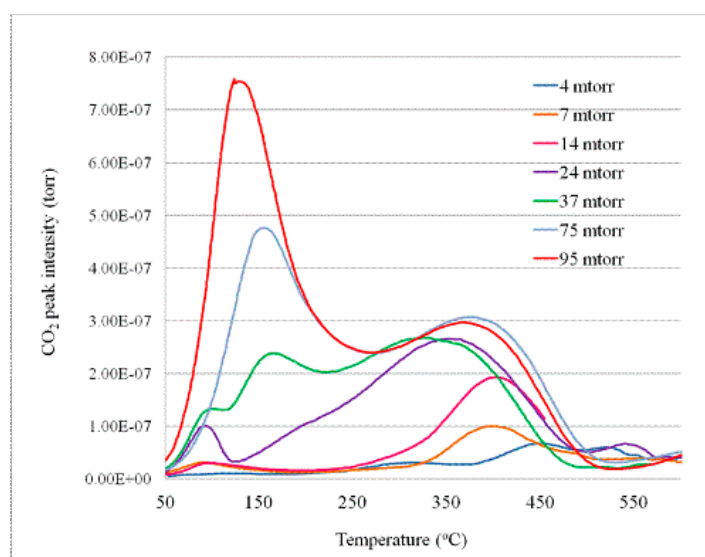
HREEL-spectra of STO at 300 K. The spectra consist of the three dipole-active phonon-polariton, marked by arrows and multiple losses. The vibration of the ions for the three modes are sketched (Sr green, Ti red, O blue).

Thu-15:20-O-OXID ●**The adsorption sites of CO₂ on cerium oxide studied using quantitative TPD***OXID Oxide surfaces and ultrathin oxide films*Daniella Schweke¹, Shimon Zalkind¹, Smadar Attia², Joseph Bloch¹ †¹ Nuclear Research Centre Negev, Beer-Sheva, Israel;² Fritz Haber Institute of the Max Planck Society, Berlin, Germany

† Deceased 24 April 2015

The adsorption of different amounts of CO₂ on powdered CeO₂ was studied, in near realistic conditions, using a system combining a volumetric gas adsorption facility with thermal programmed desorption (TPD) for residual gas analysis. Adsorption kinetics curves were obtained as a function of the CO₂ exposure pressure. The adsorption stage was followed by a TPD process to follow the rate of desorption as a function of sample temperature (in the range 310 and 930 K) for the different exposure pressures (as seen in Figure 1).

Several reproducible desorption peaks, associated with different adsorption sites, were clearly identified in the TPD spectrum. The activation energies and occupation of the various adsorption states were derived based on de-convolution of the TPD spectra. The distribution of increasing amounts of adsorbed CO₂ between the different adsorption sites on the oxide at 310 K was thus obtained and their sequence of occupation determined. An assignment for the different adsorption states, showing distinctive characteristics (such as red shifts and interaction between sites), is proposed. These results are correlated to the adsorption kinetics to get more insight about the mechanism for CO₂ adsorption on ceria.



Mon-15:20-O-SAMA ● Ferroelectricity at the atomic scale

SAMA Structural analysis and manipulation on atomic scale

José Martínez Castro^{1,2,3}, David Serrate^{3,4}, Marten Piantek^{3,4}, Sonja Schubert^{3,4},
Mats Persson^{5,6}, Cyrus F. Hirjibehedin^{1,2,7}

¹ London Centre for Nanotechnology, University College London (UCL), London WC1H 0AH, UK.

² Department of Physics & Astronomy, UCL, London WC1E 6BT, UK.

³ Instituto de Nanociencia de Aragón and Laboratorio de Microscopías Avanzadas, Universidad de Zaragoza, 50018 Zaragoza, Spain

⁴ Departamento de Física de la Materia Condensada, Universidad de Zaragoza, 50009 Zaragoza, Spain

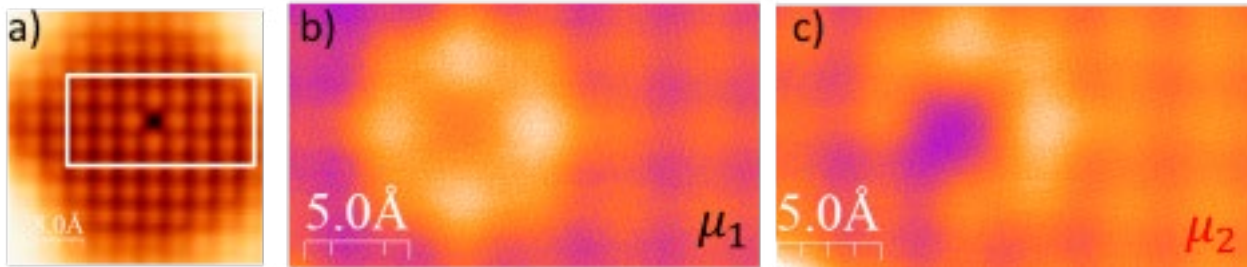
⁵ Surface Science Research Centre and Department of Chemistry, University of Liverpool, Liverpool, L69 3BX, UK

⁶ Department of Applied Physics, Chalmers University of Technology, SE-412 96, Göteborg, Sweden

⁷ Department of Chemistry, UCL, London WC1H 0AJ, UK.

Ferroelectricity at the nanometer scale is a long-standing goal in materials science. The smallness of ferroelectric domains today is limited by the resolution of AFM probes in contact mode on films with thickness of a few nm of ferroelectric materials [1]. Furthermore, ferroelectricity is intrinsically suppressed at the nanometer scale when a thin ferroelectric is sandwiched between metallic electrodes due to: (i) depolarization due to imperfect screening of the surface dipole by free charges at the metal [2]; (ii) quenching of the polar distortion by the energy gain due to electronic hybridization with the metal [3]. The key ingredient for ferroelectricity is the breaking of inversion symmetry of a polar insulator. In ferroelectric oxides, this breaking proceeds via a spontaneous structural transition where charged atoms can occupy bistable non-centrosymmetric positions. However, the symmetry breaking can be also induced by a compositional asymmetry, as shown for artificial tricolor superlattices [4]. We have recently reported that applying concepts of atomic scale engineering, it is possible to use the abrupt compositional discontinuity occurring at a surface to induce ferroelectricity in ultrathin ionic insulators. The distinct feature of Scanning Probe Methods in nanotechnology is its ability to *manipulate matter at the atomic scale* while probing simultaneously its mechanical, magnetic and electronic properties. In this way, we have been able to design the specific structural and compositional environment of atomic scale objects that provides a bistable electric polarization switchable by the electric field applied by a sharp metallic tip. In particular, ferroelectricity is strongly enhanced around single anion vacancies created by tip indentation onto bilayer films of binary rock-salts. The rock-salt is decoupled from the metallic bottom electrode by a copper nitride monolayer. The electric polarization is probed by a STM tip attached to a piezoelectric transducer (qPlus sensor) which allows for simultaneous tunneling current and force measurements: the local workfunction, atomically resolved Kelvin Probe Spectroscopy and non-contact AFM force spectroscopy. This principles can be applied to many different active layers that do not need to be necessarily ferroelectric in bulk phase.

Figure (a) shows a constant current STM topography of one anion vacancy. Figures (b) and (c) show tunneling conductance maps of this vacancy and its neighbouring atoms in the two different electric polarization states (μ_1 and μ_2). Note that the difference between (b) and (c) corresponds to tunneling electroresistance at the atomic scale.



References:

1. Garcia, V., et al., Giant tunnel electroresistance for non-destructive readout of ferroelectric states. *Nature*, 2009. 460(7251): p. 81-84.
2. Stengel, M. and N.A. Spaldin, Origin of the dielectric dead layer in nanoscale capacitors. *Nature*, 2006. 443(7112): p. 679-682.
3. Stengel, M., D. Vanderbilt, and N.A. Spaldin, Enhancement of ferroelectricity at metal-oxide interfaces. *Nat Mater*, 2009. 8(5): p. 392-397.
4. Rogdakis, K., et al., Tunable ferroelectricity in artificial tri-layer superlattices comprised of non-ferroic components. *Nature Communications*, 2012. 3: p. 1064.

Wed-11:00-O-ORGS ●

Enantiomeric Separations of Chiral Pharmaceuticals using Chiral Tetrahedral Au Nanoparticles

ORGS Organic molecules on solid surfaces

Nisha Shukla, D. Yang, Y. Zhao, A.J. Gellman

Carnegie Mellon University, Department of Chemical Engineering, Scott Hall, 5000 Forbes Avenue, Pittsburgh, PA-15213, USA

Chiral tetrahedral (24-sided) Au nanoparticles have been tested for their use as chiral separators of pharmaceutical drugs in solution phase. Tetrahedral Au nanoparticles were chirally modified with either D- or L-cysteine. They show enantioselective adsorption of pharmaceuticals such as propranolol hydrochloride (used for anxiety and high blood pressure) from a solution of racemic propranolol hydrochloride (PLL), thus leaving an enantiomeric excess in the solution phase [1]. This work indicates that chiral nanoparticles can be used for enantiomeric separation of real pharmaceutical drugs. A simple robust model has also been developed that allows extraction of the enantiospecific equilibrium constants for R- and S-PLL adsorption on the chiral tetrahedral Au nanoparticles. The model obviates the need for experimental determination of the surface area of absorbent Au nanoparticles which is extremely difficult to measure [2].

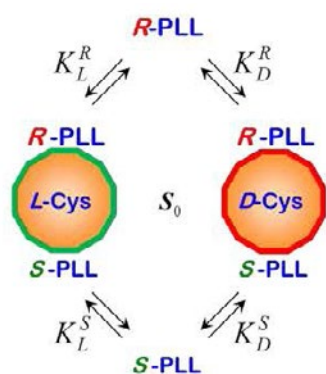


Illustration of the reversible equilibrium adsorption of R- and S-PLL on THT Au nanoparticles modified with L- or D-cysteine. The equilibrium constants are enantiospecific, $K_L^R = K_D^S \neq K_D^R = K_L^S$

References:

- [1] N. Shukla, D. Yang, A.J. Gellman, Surf. Sci. 2016, 648, 29-34.
 [2] N. Shukla, N. Ondeck, A.J. Gellman, Surf. Sci. 2014, 629, 15.

Mon-14:40-O-NAEX ●**EnviroESCA – Routine surface chemical analysis under environmental conditions for biological samples***NAEX Novel advancement of experimental methods*

Stephan Bahr¹, [Violeta Simic-Milosevic](#)², Andreas Thissen², Paul Dietrich², Marit Kjaervik³, Wolfgang Unger³

¹ *Enviro Analytical Instruments GmbH, Germany*

² *SPECS Surface Nano Analysis GmbH, Germany*

³ *Bundesanstalt für Materialforschung und -prüfung (BAM), Germany*

Since many decades XPS (or ESCA) is the well-accepted standard method for non-destructive chemical analysis of solid surfaces. To fulfill this task existing ESCA tools combine reliable quantitative chemical analysis with comfortable sample handling concepts, integrated into fully automated compact designs. Over the last years it has been possible to develop XPS systems, that can work far beyond the standard conditions of high or ultrahigh vacuum. Near Ambient Pressure (NAP) XPS has become a fastly growing field in research inspiring many scientist to transfer the method to completely new fields of application. Thus, by crossing the pressure gap, new insights in complicated materials systems have become possible using either synchrotron radiation or laboratory X-ray monochromators as excitation sources under NAP conditions.

Based on this experience SPECS Surface Nano Analysis GmbH has developed a revolutionary tool to realize the long existing dream in many analytical laboratories: reproducible chemical surface analysis under any environmental condition. EnviroESCA allows for different applications, like extremely fast solid surface analysis of degassing (but also non-degassing) samples, ESCA analysis of liquids or liquid-solid interfaces, chemical analysis of biological samples, materials and device analysis under working conditions. After introduction of the technological realization a comprehensive survey of results will be given starting from standard solid conductive samples under different pressure conditions, bulk insulators with environmental charge compensation applied, high throughput analysis of batches of similar objects, geological samples, chemical analysis of pharmaceuticals to the comparative analysis of ultrapure liquid water with different aqueous solutions.

The application of Near Ambient Pressure XPS to biological specimen from plants and animals, biofilms and bacteria, as well as food samples is a completely new field for electron spectroscopic studies of the surface chemical composition. An outlook is presented on the application to electrochemical and other in-operando devices. Finally the influence of the ambient conditions on quantification in XPS will be demonstrated and discussed.

This project has received funding from the EMPIR programme co-financed by the Participating States and from the European Union's Horizon 2020 research and innovation programme.

Tue-9:40-O-ORGS ●

Investigating superhydrogenated polycyclic aromatic hydrocarbons on graphite and their catalytic effect on interstellar H₂ formation*ORGS Organic molecules on solid surfaces*

Frederik S. Simonsen, Anders W. Skov, Pernille A. Jensen, Liv Hornekær

*Department of Physics and Astronomy, Ny Munkegade 120, Aarhus University, 8000 Aarhus (Denmark),
Frederik_doktor@phys.au.dk*

Scanning tunneling microscopy and temperature programmed desorption techniques have been used to investigate adsorption and abstraction of hydrogen atoms on the polycyclic aromatic hydrocarbon, coronene. Coronene molecules were exposed to different hydrogen fluences at dosing temperatures of 2300K and 1000K. Large fluences of hydrogen leave superhydrogenated coronene molecules which reveal stable configurations and indirect evidence of H₂ formation.

In certain regions of the interstellar medium (ISM), like photodissociation regions (PDRs), unexpectedly high abundances of molecular hydrogen, H₂, are observed. Because of relatively high H₂ destruction rates in these regions, the presently accepted formation routes on dust grains cannot exclusively account for the observed abundances[1]. Therefore new formation routes are needed and lately attention has been drawn towards molecules called polycyclic aromatic hydrocarbons (PAHs). PAHs are believed to account for up to 20% of the available carbon in the ISM and have been observed, with significantly large abundances, alongside H₂[2].

Here we investigate the adsorption and abstraction pattern of hydrogen/deuterium on coronene, C₂₄H₁₂. Both scanning tunneling microscopy (STM) and temperature programmed desorption (TPD) techniques have been used. Coronene monolayers were prepared on highly ordered pyrolytic graphite (HOPG) and exposed to different fluences of 2300K or 1000K H or D atoms.

STM images show bright spots on the coronene monolayers after hydrogenation indicating adsorption to coronene edges. TPD measurements show an exponential decay of pristine coronene with increasing D fluence again showing the adsorption process. TPD also reveals formation of fully deuterated coronene (C₂₄D₃₆), hence the original H atoms are substituted with D atoms i.e. by Eley Rideal abstraction reactions forming HD[3].

Density functional theory (DFT) calculations made for H-addition to coronene molecules predict that the barrier for adsorption is lowest at the outer edge of the coronene molecule[4]. Further more competing abstraction and adsorption channels with 0eV barriers should be present after only 3 H-additions to the coronene molecule. These tendencies can be recognized by both the STM images and the TPD measurements.

We observe superdeuterated coronene species which appear stable against further hydrogenation at intermediate D fluences. These stable configurations are observed only for the 1000K atom doses. Further investigation of the stable configurations examined binding energies of superhydrogenated coronene on an HOPG substrate. The difference in energies reveal buckling of the planar coronene molecule at intermediate superhydrogenations[5].

References:

- [1] Tielens, A., *Reviews of Modern Physics*, 85 (2013) 1021-1081
- [2] Habart, E.; et. al., *Astronomy and Astrophysics* 397 (2003) 623-634
- [3] Mennella, V., et. al. *The Astrophysical Journal Letters* 745 (2011) L2
- [4] Rauls, E.; and Hornekær L., *The Astrophysical Journal* 679 (2008) 531
- [5] Skov, Anders W., et al., *The Journal of Chemical Physics* 145.17 (2016) 174708.

Mon-15:00-O-SAMA ●
Dipole-mediated single-molecule manipulation*SAMA Structural analysis and manipulation on atomic scale*

[Grant J. Simpson](#)¹, Leonhard Grill¹, Víctor García-López²

¹ University of Graz, Graz, Austria;

² Rice University, Texas, USA, James Tour Rice University, Texas, USA

It has been long known that the scanning tunneling microscope (STM) is the perfect tool not only for imaging single molecules on surfaces, but also can be used to manipulate such molecules in a variety of ways. The classical method of lateral manipulation is either pushing or pulling via van der Waals interaction with the STM tip. In the current work it is shown that the electric field of the tip plays an important role when a dipole moment exists within a molecule. The dipolar nanocar, investigated here on the Ag(111) surface, displays rotational and translational motion under the influence of the electric field of the tip. Furthermore, the spatial dependence of the tip position with respect to the molecule reveals that the dipole moment of the molecule is the deciding factor for the direction of motion. The rotation and translation of the nanocar can therefore be carefully controlled.

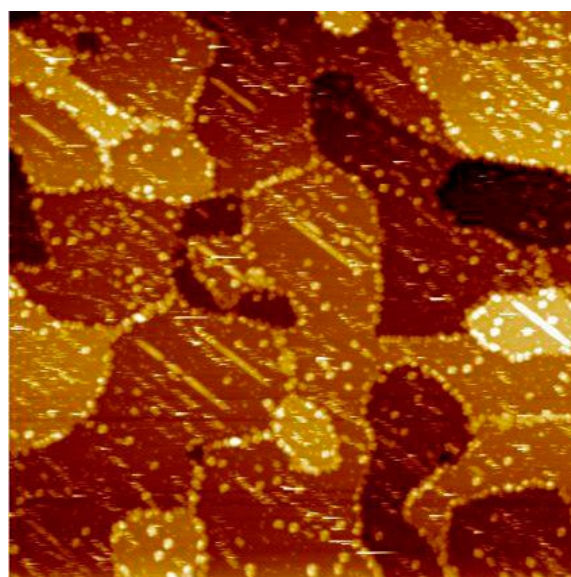
Mon-14:20-O-ORGS ●**Adsorption of porphyrin-based dyes on TiO₂ surfaces: STM study***ORGS Organic molecules on solid surfaces*

Łukasz Zajac¹, Bartosz Such¹, Piotr Olszowski¹, Łukasz Bodek¹, Szymon Godlewski¹, Res Jöhr², Thilo Glatzel², Ernst Meyer², Marek Szymonski¹

¹ Jagiellonian University, Institute of Physics, Lojasiewicza 11, 30-348 Krakow, Poland;

² University of Basel, Department of Physics, Klingelbergstrasse 82, 4056 Basel, Switzerland

In the presentation we will present the morphology of assemblies formed on titania surfaces by the typical organic dye molecules – Zn-porphyrins (Zn-TPP) at a coverage below a monolayer. The molecules of choice are widely used as dyes in the dye-sensitized solar cells and in many instances they are assumed to adopt a geometry perpendicular to the surface when equipped with a carboxylic anchoring group. In our experiments, we have explored adsorption behavior of Zn-TPP and carboxylic-substituted Zn-porphyrins (COOH-Zn-TPP) on two faces of rutile TiO₂: (110) and (011) [1,2]. The selected faces exhibit different reactivity since the position of Ti atoms in the structure are quite different: in (110) the Ti atoms are exposed for the interaction with the adsorbates, which makes the surface quite reactive while in the case of (011) face the Ti atoms are buried making the surface inert. We have found that on the (110) surface the molecules stay flat on the surface regardless of the presence of a carboxylic group, whereas in the case of (011) surface the interaction of the carboxylic group with the surface is sufficient to facilitate lifting the molecular board from the surface and forming one-dimensional structures stabilized by the pi-pi interactions between the molecules (see the figure below). Flat Zn-TPP molecules on (011) surface can be used, however, as a wetting layer for deposition of the alternative dyes, such as Cu and Zn phthalocyanines [3,4]. We will show that decoupling from the titania surface by the wetting layer allows for the growth of very well ordered structures. Additionally, we will present the structures formed by the Zn-TPP molecules on the (101) face of another form of titania: anatase. The molecules tend to adsorb preferentially on one type of terrace edges, which can be explained by steric considerations. At the level of a monolayer they form an ordered layer of flat molecules stabilized by intermolecular interactions.



References:

- [1] P. Olszowski, et al. *Journal of Physical Chemistry C*. 2015;119(37):21561–21566
- [2] L. Zajac, et al. *Applied Surface Science* 2016;379, 277–281
- [3] L. Zajac, et al. *Journal of Chemical Physics* 2015;143(22):224702
- [4] P. Olszowski, et al. *Beilstein Journal of Nanotechnology* 2017;8,99-107

Thu-16:20-O-SEMI ●**Various organic adsorbates for Si(553)-Au surface functionalization***SEMI Semiconductor surfaces and ultrathin layers*S. Suchkova¹, E. Speiser¹, S. Chandola¹, C. Hogan², F. Bechstedt³, N. Esser¹¹ Leibniz-Institut für Analytische Wissenschaften - ISAS - e.V., Interface Analytics Department, Schwarzschildstr. 8, 12489 Berlin, Germany;² Università di Roma "Tor Vergata", Via della Ricerca Scientifica 1,00133 Roma, Italy;³ Friedrich-Schiller-University Jena, Institut für Festkörpertheorie und -optik, Helmholtzweg 3, 07743 Jena

Organic functionalization of semiconductors is an important route towards the development of novel semiconductor-based devices [1,2]. In particular the self-assembled formation of ordered organic molecule structures on silicon is may lead to the formation of interfaces with excellent electrical electronic properties [3,4]. We investigate the adsorption such small organic molecules as toluene-3,4-dithiol (TDT), dopamine, and leucine by density functional theory (DFT) simulations. Here we propose a scheme for the surface modification of the stepped Si(553)-Au surface, tuning the chemical and electronic properties by site-specific adsorption of a small organic molecules.

Various adsorption geometries of TDT on the clean Si(553)-Au surface and on the terrace sites for H passivated step edge dangling bonds are analyzed. In spite of expectations, that molecular thiol groups of TDT will interact with Au chains, we show that the most reactive surface adsorption sites are the Si dangling bonds at the step edge before and the Si double bonds on honeycomb chains after H passivation, respectively. The analysis of the surface electronic band structure yields either metallic or insulating condition at the respective interfaces, depending on the adsorption geometry and coverage. Our approach offers atomic/molecular scale tuning of surface geometry and electronic properties by controllable molecular adsorption sites. Nanopatterned surface templates and a switching of chemical reactivity on the vicinal Si(553)-Au surface is suggested.

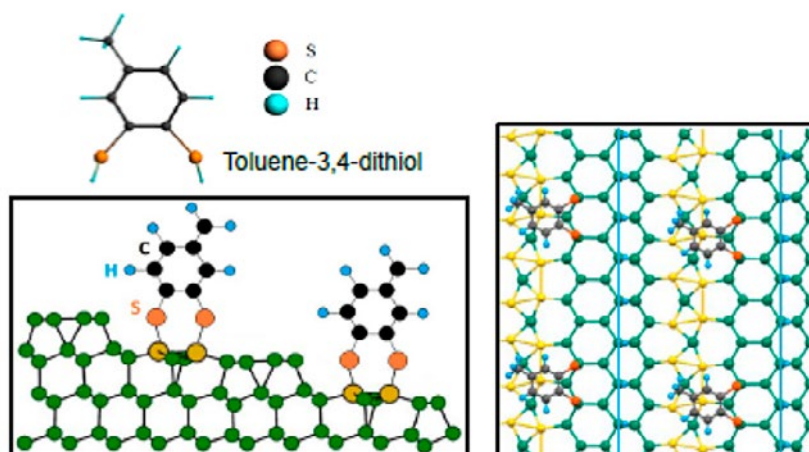


Figure: Adsorption sites of toluene-3,4-dithiol on H-passivated Si(553)-Au

References:

- [1] Schmidt, W., Seino, K., Preuss, M. et al., Appl. Phys. A (2006) 85: 387.
- [2] William J. I. DeBenedetti, Yves J. Chabal. J. Vac. Sci. Technol., A (2013) 31: 050826.
- [3] D.K. Aswala, S. Lenfanta, D. Guerina, J.V. Yakhmib, D. Vuillaumea. Anal. Chim. Acta (2006) 568: 84.
- [4] Kristina R. Rusimova, Peter A. Sloan, Nanotechnology (2017) 28: 054002.

Tue-16:20-O-OXID ●

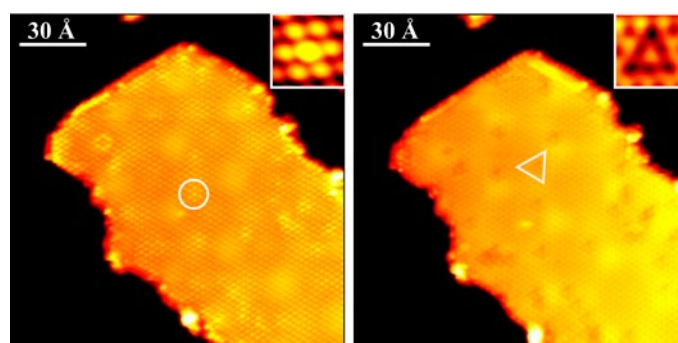
Iron doping on cobalt oxide bilayers on Au(111): toward a model of synergistic catalytic effect in the oxygen evolution reaction

*OXID Oxide surfaces and ultrathin oxide films*Zhaozong Sun, Jonathan Rodriguez-Fernandez, Jakob Fester, Jeppe V. Lauritsen*Interdisciplinary Nanoscience Center (iNANO), Aarhus University, 8000 Aarhus C, Denmark*

Iron doped cobalt oxides have revealed enhanced activity for promoting the oxygen evolution reaction (OER) compared with unary iron oxides and cobalt oxides, respectively¹. However, the nature of such synergistic catalytic effect and in particular the way iron species incorporate within cobalt oxides are only understood on a superficial level, which presents a significant obstacle to further exploration on rational design of efficient OER catalysts. Noble metal supported transition metal oxides have been previously applied as model catalysts, which enable the powerful surface science techniques, and successfully reveal the catalytic active sites and help researchers understand the catalytic process further².

Here, aiming to study the origin of the synergistic catalytic effect, we dope iron into well-characterized cobalt oxide bilayer nanoislands supported on a single crystal Au(111) substrate³. Atomic-resolved scanning tunneling microscopy (STM) and X-ray photoelectron spectroscopy (XPS) are used to compare the growth of cobalt oxide and mixed cobalt-iron oxide bilayers. We perform a comprehensive analysis of the influence of iron doping on the atomic structure of the nanoislands and oxidation states of both the dopant and host species.

We find that doped iron species easily integrate into the cobalt oxide nanoislands and adopt a high oxidation state. In atom-resolved STM images, the Co atoms surrounding the doped Fe appear brighter and form 6-fold flower-like features due to the local modification of electronic structure, which may indicate a changed chemical activity of these atoms. Imaging of the O lattice reveals that a similar effect is seen for the O atoms in proximity of the doped Fe which appear as 3-fold triangle-like features. Our XPS spectra imply that Co keeps the 2+ oxidation state whereas Fe, surprisingly, adopt a 3+ oxidation state in the binary oxide, in contrast to the oxidation state of 2+ in the pure iron oxide nanoislands grown under the same conditions, indicating that iron species in the cobalt-iron oxides have stronger oxidizing ability. Further water exposure experiments demonstrate that hydroxyl groups usually appear next to the doped iron sites while almost randomly distributed on the basal plane of pure cobalt oxide nanoislands, suggesting that iron species in the cobalt-iron oxide play an important role in promoting the catalytic activity.



References:

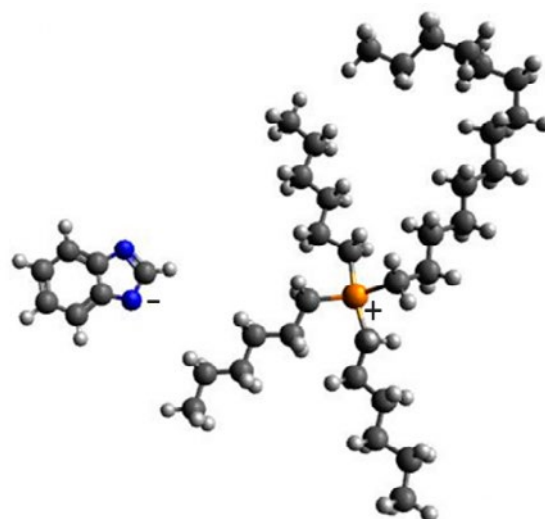
1. Burke, Michaela S., et al., *Journal of the American Chemical Society* 137.10 (2015): 3638-3648.
2. Fester, J., et al., *Nature Communications* 8 (2017): 14169.
3. Walton, Alex S., et al., *ACS Nano* 9.3 (2015): 2445-2453.

Tue-16:20-O-ORGS ●

Reversible CO₂ absorption with a superbasic ionic liquid [P66614] [Benzim] studied using near-ambient pressure X-ray photoelectron spectroscopy*ORGS Organic molecules on solid surfaces*Karen L. Syres¹, Zoë Henderson¹, Rebecca Taylor², Christopher Hardacre², Andrew G. Thomas²¹ The Jeremiah Horrocks Institute, University of Central Lancashire, Fylde Road, Preston, PR1 2HE, UK² School of Chemical Engineering and Analytical Science, The University of Manchester, Oxford Road, Manchester, M13 9PL, UK.

Ionic liquids have been widely investigated as potential CO₂ capture agents. The regeneration of some ionic liquids after CO₂ capture is a relatively low energy process compared to current industrial solutions such as monoethanolamine [1,2]. Recently a class of ionic liquids called superbasic ionic liquids (SBILs) have received considerable attention for CO₂ capture applications. SBILs have a deprotonated aromatic amine as the anion and their reaction with CO₂ leads to the formation of carbamate at one or more of the amine sites [3]. Studies of SBILs by various groups have shown an excellent capacity for CO₂ capture [1]. In addition these SBILs, unlike some other ILs, do not undergo a large increase in viscosity upon CO₂ saturation, which makes them potentially useful in large-scale applications. In an experimental and theoretical study of SBILs, tetra-alkylphosphonium benzimidazolium [P66614][Benzim] (see figure), was able to absorb equimolar quantities of CO₂ in the dry state, but when wet its capacity for CO₂ decreased [1-3].

The recent availability of near-ambient pressure X-ray photoelectron spectroscopy has opened up the possibility of measurements of solid and liquid surfaces in gas pressures of up to a few tens of mbar [4]. Here we examine the absorption and reaction of [P66614][Benzim] with CO₂ and a CO₂/water vapour mixture, using near-ambient pressure X-ray photoelectron spectroscopy. Results indicate a reaction between the CO₂ and aromatic nitrogen atoms to form a carbamate species. Competitive absorption between water and CO₂ indicates that CO₂ preferentially binds but water blocks aromatic nitrogen sites via hydrogen bonding. The CO₂ reaction appears to be reversible simply by evacuating the near-ambient pressure cell, restoring the ionic liquid to its original state.



References:

- [1] Taylor, S. F. R.; McCrellis, C.; McStay, C.; Jacquemin, J.; Hardacre, C.; Mercy, M.; Bell, R. G.; de Leeuw, N. H., CO₂ Capture in Wet and Dry Superbase Ionic Liquids. *Journal of Solution Chemistry* 2015, 44, 511-527.
- [2] Blanchard, L. A.; Hancu, D.; Beckman, E. J.; Brennecke, J. F., Green Processing Using Ionic Liquids and CO₂. *Nature* 1999, 399, 28-29.
- [3] Mercy, M.; Rebecca Taylor, S. F.; Jacquemin, J.; Hardacre, C.; Bell, R. G.; De Leeuw, N. H., The Addition of CO₂ to Four Superbase Ionic Liquids: A DFT Study. *Physical Chemistry Chemical Physics* 2015, 17, 28674-28682.
- [4] Jackman, M. J.; Thomas, A. G.; Murny, C., Photoelectron Spectroscopy Study of Stoichiometric and Reduced Anatase TiO₂(101) Surfaces: The Effect of Subsurface Defects on Water Adsorption at near-Ambient Pressures. *The Journal of Physical Chemistry C* 2015, 119, 13682-13690.

Tue-14:40-O-ORGS ●**Self-assembly of tritopic molecules on surfaces: Structure and bonding from computer simulations***ORGS Organic molecules on solid surfaces***Paweł Szabelski¹, Wojciech Rżysko², Damian Nieckarz³**

¹ Department of Theoretical Chemistry, Maria Curie-Skłodowska University, Pl. M.C. Skłodowskiej 3, 20-031 Lublin, POLAND;

² Department for the Modeling of Physico-Chemical Processes, Maria-Curie Skłodowska University, Pl. M.C. Skłodowskiej 3, 20-031 Lublin, POLAND;

³ Supramolecular Chemistry Laboratory, University of Warsaw, Biological and Chemical Research Centre, Ul. Żwirki i Wigury 101, 02-089 Warsaw, POLAND

Steering molecular organization in adsorbed overlayers is a challenging task which requires detailed information on intermolecular interaction patterns which are often dictated by molecular geometry, shape and distribution of functional groups. In this contribution we present the results of theoretical investigations aiming at identification of supramolecular 2D structures formed by tritopic tectons with different aspect ratios and differently assigned interaction directions. These structures were modeled using the Monte Carlo simulation method in which the tripod-shaped building blocks were treated as rigid planar structures composed of a few interconnected segments. The calculations were performed on a triangular lattice representing (111) crystalline surface. Molecules having active terminal arm segments with differently assigned interaction directions were used and their bonding in adsorbed overlayers was monitored [1-3]. For some of the building blocks additional off-lattice simulations were carried out to assess the effect of surface corrugation on the self-assembly. The obtained findings demonstrated that a suitable encoding of the interactions enables directing the self-assembly towards structures such as strings, ladders and periodic (also chiral) and aperiodic networks. The hints gained from the simulations can be helpful in tailoring molecular superstructures on solid substrates.

The financial support of the Polish National Science Centre (grant 2015/17/B/ST4/03616) is gratefully acknowledged.

References:

1. P. Szabelski, W. Rżysko, D. Nieckarz, *J. Phys. Chem. C*, 120 (2016) 13139.
2. W. Rżysko, D. Nieckarz, P. Szabelski, *J. Phys. Chem. C*, 121 (2017) 410.
3. P. Szabelski, D. Nieckarz, W. Rżysko, *Coll. Surf. A*, doi.org/10.1016/j.colsurfa.2017.04.009

Thu-11:20-O-SEMI ●

Formation of highly-ordered molecular structures on ion beam modified TiO₂(110) surface – the role of wetting layer stability

SEMI Semiconductor surfaces and ultrathin layers

K. Szajna¹, M. Kratzer², W. Bełza¹, D. Wrana¹, B. R. Jany¹, C. Teichert², F. Krok¹¹ Marian Smoluchowski Institute of Physics, Jagiellonian University, Krakow 30-348, Poland;² Institute of Physics, Montanuniversitat Leoben, Leoben 8700, Austria

We have investigated the morphology of ultra-thin organic films consisting of rod-like para-hexaphenyl (6P) molecules on ion beam modified TiO₂(110) surface. For the ion-beam modification, the TiO₂(110) substrate surface was irradiated with low energy, 2 keV, Ar ions at oblique (75°) incidence angle and elevated sample temperature. Under the applied experimental conditions, the ion bombardment of the titanium dioxide surface results in the formation of a nanoscale pattern with a regularly stepped ripples. Within one step, the local crystallinity of pristine TiO₂(110) was conserved as has been confirmed by atomically-resolved STM imaging and by low energy electron diffraction. The morphology of developed molecular structures were examined *in situ* with Kelvin probe force microscopy (KPFM) and *ex situ* with tapping mode atomic force microscopy (TM-AFM).

It has been found that the 6P evaporation of sub-monolayer coverage on rippled substrate results in the formation of large (100×300 nm²) anisotropic islands, of up-right standing 6P molecules, and a layer of lying molecules covering the whole TiO₂(110) substrate surface (beneath and around the islands – Fig. 1a). The lying 6P molecules play the role of a wetting layer of certain amount of molecules, above which, all subsequently adsorbed 6P molecules assemble in form of up-right standing 6P islands during the deposition process. However, the layer is kinetically unstable structure with low energy barrier of transformation into next stable phase, which can be induced by e.g. exposure to ambient air. As a result, we have observed a formation of smaller (20×70 nm²) up-right standing 6P islands between the larger ones (Fig. 1b). This significant surface redistribution of 6P molecules is clearly visible with KPFM imaging, where the relative difference in CPD signal between the 6P islands and surface changes from 30-50 mV to almost 500 mV.

Furthermore, we have observed that the 6P island elongation is directly correlated with the ripples' length¹ and the relative orientation of the ripple direction and origin atomic rows of pristine TiO₂(110) surface. It is possible to enhance the 6P islands elongation in a significant way by changing the direction of atomic rows (represented by [001]) from perpendicular to parallel orientation with respect to the ripples.

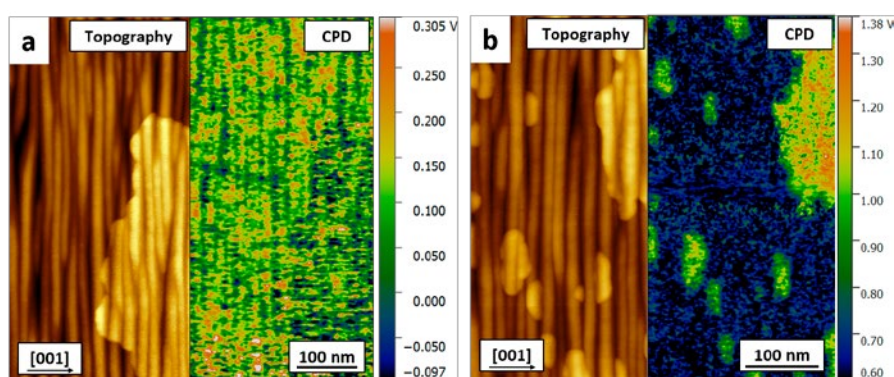


Figure 1. Topography (left) and CPD (right) images of the rippled TiO₂(110) substrate covered by 6P molecules **a**) before and **b**) after exposure to ambient air. The CPD images reveal a significant change in contrast between 6P islands and TiO₂(110) surface fully covered by **a**) 6P molecules and **b**) adsorbates from air.

References:

[1] M. Kratzer, D. Wrana, K. Szajna, F. Krok, C. Teichert, Phys. Chem. Chem. Phys., 16, 26112-26118 (2014)

Mon-15:00-O-NAEX ●**Transmission X-ray diffraction for a real-time observation of thin-film growth****NAEX Novel advancement of experimental methods**

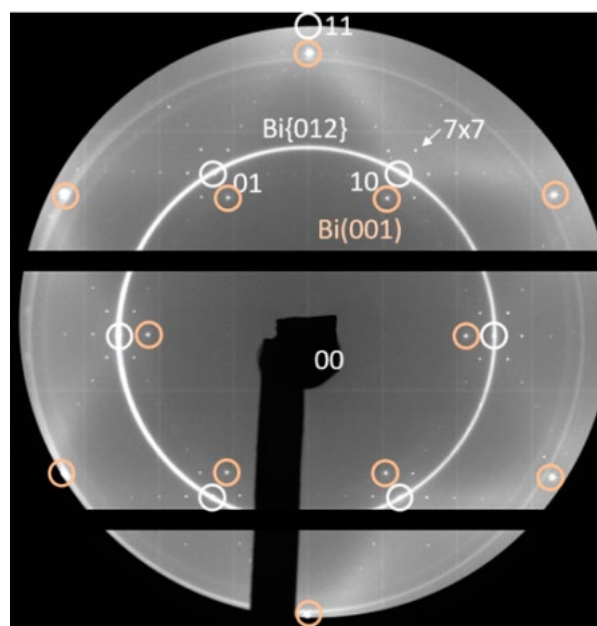
Hiroo Tajiri

Japan Synchrotron Radiation Research Institute/SPring-8

By virtue of recent advances of hybrid-type pixel array detectors in the X-ray region, a wide-range reciprocal space mapping by surface X-ray diffraction has been becoming usual since a diffraction measurement with the stationary mode[1] using two-dimensional(2D) detector has an experimental advantage of high-efficiency than a rocking mode.

Transmission X-ray diffraction(TXD) using 2D detector is one of the such experimental methods[2], and gives us a novel way to realize both quick and precise characterizations of nano- and thinfilm-structures grown on surface. Here, we observed an initial growth of ultrathin Bi film on clean Si(111)-7×7 in real-time by TXD. The ultrathin Bi film goes through phase transformation according to Bi film thickness[3].

The figure shows a typical TXD pattern of Bi thin-film epitaxially grown on Si(111)-7×7 in ultra-high vacuum at room temperature observed by a PILATUS-300K detector with 20 keV X-rays. The synchrotron experiment was performed at the beamline BL13XU in SPring-8. The sample was thinned at the center by chemical etching to reduce thermal diffuse scatterings from the substrate, which increase background noises. Both a Debye-ring from Bi{012} islands and diffraction spots from a Bi(001) film are clearly seen in addition to the fundamental spots of the Si(111) substrate indicated by circles. By real-time observations with 10s periods, we successfully traced the phase transformation of Bi film from Bi{012} to Bi(001). It is noteworthy that the super-structure with 7×7 periodicity has been kept at the interface even during Bi deposition, which is confirmed by its diffraction spot.



References:

- [1] E. Vlieg, *J. Appl. Crystallogr.* 30, 532 (1997).
- [2] H. Tajiri, O. Sakata, T. Takahashi, *Appl. Surf. Sci.* 234, 403 (2004).
- [3] T. Nagao et al., *Phys. Rev. Lett.* 93, 105501 (2004).

Tue-10:00-O-ENER ●

Graphite oxide-TiO₂ nanocomposite type photocatalyst for methanol photocatalytic reforming reaction

ENER Surfaces for energy production and harvesting

Árpád Turcsányi¹, Emília Tálás², Katalin Majrik², Zoltán Pásztai², Tamás Szabó¹, Attila Domján³, Judith Mihály², András Tompos², Imre Dékány¹

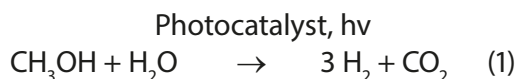
¹ Department of Physical Chemistry and Materials Science, University of Szeged, H-6720 Szeged, Aradi vértanúk tere 1, Hungary;

² Institute of Materials and Environmental Chemistry, Research Centre for Natural Sciences, Hungarian Academy of Sciences, H-1117 Budapest, Magyar tudósok körútja 2, Hungary;

³ NMR Research Group, Research Centre for Natural Sciences, Hungarian Academy of Sciences, H-1117 Budapest Magyar tudósok körútja 2, Hungary

Combination of highly graphitic carbon materials with a semiconductor has been reported to enhance the photocatalytic activity. The enhancement mechanism can be attributed to carbon materials, which (i) offer more active adsorption sites and photocatalytic reaction centers, (ii) suppress the recombination and prolong the lifetime of the photogenerated electron/hole pairs, (iii) narrow the band gap of photocatalyst, and (iv) act as photosensitizer for catalytic reaction [1]. Composites prepared from graphite oxide (GO) and TiO₂ have been found beneficial for hydrogen producing reactions [2,3].

In this work a series of GO/TiO₂ nanocomposite type of photocatalysts with different GO content was prepared from aqueous dispersions of Degussa P25 TiO₂ and exfoliated GO by heterocoagulation as described before [4]. The composites were tested in the photocatalytic reforming reaction of methanol (1) in liquid phase.



Our recent results revealed that the working conditions of the above reaction result in significant changes in the structural properties of the metal oxide-semiconductor catalyst systems with respect to the fresh photocatalysts [5]. Our aim was to clarify details of the carbon-semiconductor interaction in the working GO/TiO₂ catalyst; therefore we characterized both the fresh and recovered samples by bulk and surface characterization methods such as diffuse reflectance UV-Vis, ¹³C MAS NMR, ATR-IR spectroscopy and XPS.

The presence of GO increased the catalytic activity about three- fourfold; the H₂ evolution-GO content dependency showed a maximum, similarly as reported [2,3]. The preparation of the composite itself resulted in only little changes in the structure of GO, although chemical interaction between GO and TiO₂ was evidenced by both ATR-IR spectroscopy and XPS. However during the photocatalytic reaction all of the GO/TiO₂ samples darkened strongly indicating structural changes of GO. The XPS in accordance with ¹³C MAS NMR showed significant decrease of surface carbon content in the recovered sample of 10% GO on TiO₂ probable caused by the fragmentation and release of the GO sheets. In all cases significant reduction of GO occurred during the reaction. Meanwhile, both on recovered bare TiO₂ and GO/TiO₂ samples new bands appeared in the ATR-IR spectra which could be interpreted as surface -OCH₃ groups originated from the CH₃OH. Newly formed OH groups in the GO containing recovered samples were well-marked which probable connected to the activity increase. Details of the structure-activity relationship will be given in the lecture.

References

1. D. Chen, et al., Scientific Reports (2016) DOI: 10.1038/srep20335
2. W. Fan, et al., J. Phys. Chem. C 115 (2011) 10694.
3. P. Zeng, et al., J. Alloy Compd. 516 (2012) 85.
4. T. Szabó, et al. Colloid. Surf. A Physicochem. Eng. Aspects 433 (2013) 230.
5. Á. Vass, et al., Mater. Res. Bull. 83 (2016) 65.

Wed-11:40-O-OXID ●**Adsorption of a functionalized porphyrin on MgO(100) thin films: a high-resolution photoemission and X-ray absorption spectroscopy study***OXID Oxide surfaces and ultrathin oxide films*Quratulain Tariq, Matthias Franke, Daniel Wechsler, Hans-Peter Steinrück, Ole Lytken*Chair of Physical Chemistry II, Friedrich Alexander University Erlangen-Nürnberg, Germany*

The efficient functionalization of metal oxide surfaces by adsorption and covalent attachment of organic molecules has received considerable attention in emerging technologies, such as molecular electronics, catalysis and solar cells [1-3].

Tetrapyrrole derivatives, in particular porphyrins, are among the most promising compounds and can be modified synthetically by variation of the metal center, by attaching different substituents to the macrocycle, or by introduction of specific linker groups for the attachment on surfaces [4-5].

In present study, we report on the adsorption of a functionalized cobalt porphyrin bearing four carboxylic acid groups, 5,10,15,20-tetrakis (4-carboxyphenyl) porphyrin (CoTCPP), on ordered MgO(100) thin films grown on Ag(100). We have combined high-resolution synchrotron-radiation photoelectron spectroscopy (SRPES) and near-edge X-ray absorption fine structure (NEXAFS) spectroscopy to characterize the nature of the molecule-surface bonding as a function of coverage and temperature.

SRPES for different coverages of CoTCPP suggests a bidentate binding mode via the carboxylic group. For sub-monolayer coverages, NEXAFS reveals that CoTCPP adsorbs almost parallel to the oxide substrate, but as the coverage is increased, the angle to the surface plane also increases. Although, even for monolayer and higher coverages, CoTCPP never adopts a completely upright standing adsorption geometry. This project is supported by the DFG through FOR 1878 (funCOS).

References:

- [1] Liljeroth, P.; Nat. Nanotechnol. 2012, 7, 5.
- [2] Rochford, J.; Chu, D.; Hagfeldt, A.; Galoppini, E.; J. Am. Chem. Soc. 2007, 129, 4655.
- [3] Bentez, I. O.; Bujoli, B.; Camus, L. J.; Lee, C. M.; Odobel, F.; Talham, D. R.; J. Am. Chem. Soc. 2009, 124, 4363.
- [4] Gouterman, M.; J. Chem. Phys. 1959, 30, 1139.
- [5] Urbani, M.; Grätzel, M.; Nazeeruddin, M.K.; Torres, T., Chem. Rev. 2014, 114, 12330.

Thu-14:40-O-ENER ●**Experimental valence band dispersion of $\text{CH}_3\text{NH}_3\text{PbI}_3$ hybrid organic-inorganic perovskite***ENER Surfaces for energy production and harvesting*

M. Lee¹, A. Tejada¹, A. Barragán¹, M.N. Nair^{1,2}, V. Jacques¹, D. Le Bolloc'h¹, P. Fertey², K. Jemli³, F. Lédée³, G. Trippé-Allard³, E. Deleporte³, A. Taleb-Ibrahimi²

¹ Laboratoire de Physique des Solides, CNRS, U. Paris-Sud, U. Paris-Saclay, Bat. 510, 91405 Orsay, France;

² Synchrotron SOLEIL, Saint-Aubin, 91192 Gif-sur-Yvette;

³ Laboratoire Aimé Cotton, ENS Cachan, CNRS, U. Paris-Sud, U. Paris-Saclay, Bat. 505, 91405 Orsay, France

Organic-inorganic hybrid perovskites are promising absorber materials for low-cost photovoltaic solar cells or optoelectronic devices [1-4]. Among these perovskites, methylammonium triiodideplumbate ($\text{CH}_3\text{NH}_3\text{PbI}_3$, MAPbI_3 or MAPI) exhibits currently the highest efficiency. Here we have analyzed the structural transition in MAPI by X-ray diffraction at the β phase and we have correlated it to its electronic properties. Despite all the extensive work on hybrid organic-inorganic halide perovskites, their experimental band structure measured with k-resolution has remained elusive. Such an experimental determination is a necessary requirement for an accurate theoretical description and understanding of the system. The impact of the structural phase transitions on the band structure in the operation temperature range of solar cells needed also to be elucidated. Herein, we present the experimental determination of the band structure of MAPI with k resolution by angle-resolved photoemission at 170 K [5]. Our results show that the spectral weight is strongly affected by the cubic symmetry. Some deviations with respect to theoretical calculations are observed, which may help to reach a more precise description of this paradigmatic system of the hybrid perovskite family. The project leading to this application has received funding from the European Union's Horizon 2020 research and innovation programme under grant agreement No 687008 (GOTSolar).

References:

- [1] S.D. Stranks and H.J. Snaith, *Nature Nanotech* 10, 391 (2015).
- [2] M. Grätzel, *Nature Materials* 13, 838 (2014).
- [3] Y. Wei et al., *J. Phys. D: Appl. Phys.* 46, 135105 (2013).
- [4] H. Diab et al., *J. Phys. Chem. Lett.* 7, 5093 (2016).
- [5] M. Lee et al., (submitted).

Thu-14:00-O-ORGS ● Co-adsorption of alanine and water on Ni(110)

ORGS Organic molecules on solid surfaces

[Panayiotis Tsaousis](#)^{1,2}, [Alix Cornish](#)¹, [Richard Ed Nicklin](#)¹, [David Watson](#)³, [Georg Held](#)^{1,2}

¹ *University of Reading, Department of Chemistry, Whiteknights, Reading, Berkshire, RG6 6AH, UK;*

² *Diamond Light Source Ltd, Diamond House, Harwell Science and Innovation Campus, Didcot, Oxfordshire, OX11 0DE, UK;*

³ *University of Surrey, Department of Chemistry, Guildford, Surrey, GU2 7XH, UK*

Enantioselective catalysis is of key importance, since it can provide products with valuable biological activity. Alanine acts as a chiral modifier in the enantioselective hydrogenation of β -ketoesters over Ni catalysts [1].

The present study explores the chemical state and thermal stability of alanine and water on clean Ni{110} using Temperature Programmed Desorption (TPD), X-Ray Photoelectron Spectroscopy (XPS), Temperature Programmed-XPS (TP-XPS) and Near Edge X-Ray Adsorption Fine Structure Spectroscopy (NEXAFS). In addition, the co-adsorption of alanine and water on Ni{110} was also investigated. XPS results of alanine on clean Ni{110} at different coverages provide evidence that the amino acid exists in the chemisorbed layer mainly in its anionic form, forming three surface bonds: two via the carboxylate group and one through the amino group. In the multilayer, alanine is in its zwitterionic form. TP-XPS and TPD results show that the multilayer desorbs around 300 K while the chemisorbed alanine dissociates around 400-420 K (fig.1). The temperature is well above the temperature of the catalytic reactions and is the highest observed on any nickel surface [2].

The presence of multilayer water changes the chemical state of alanine, enhancing the formation of zwitterionic alanine. Low coverages of water influence the decomposition path of the amino acid, without changing its chemical state.

References:

- [1] CJ Baddeley, TE Jones, AG Trant, and KE Wilson. Fundamental investigations of enantioselective heterogeneous catalysis. *Topics in catalysis*, 54(19-20):1348–1356, 2011.
- [2] REJ Nicklin, A Cornish, A Shavorskiy, S Baldanza, K Schulte, Z Liu, RA Bennett, and G Held. Surface Chemistry of Alanine on Ni {111}. *The Journal of Physical Chemistry C*, 119(47):26566–26574, 2015.

Wed-11:40-O-ORGS ●

Bonding of biomolecules to cerium oxide: histidine and adenine

ORGS Organic molecules on solid surfaces

Nataliya Tsud¹, Sofia Bercha¹, Klára Ševčíková^{1,2a}, Robert G. Acres^{2b}, Mykhailo Vorokhta¹, Ivan Khalakhan¹, Martin Dubau¹, Iva Matolínová¹, Kevin C. Prince², Tomáš Skála¹, Vladimír Matolín¹

¹ Charles University, Faculty of Mathematics and Physics, Department of Surface and Plasma Science, V Holešovičkách 2, 18000 Prague 8, Czech Republic;

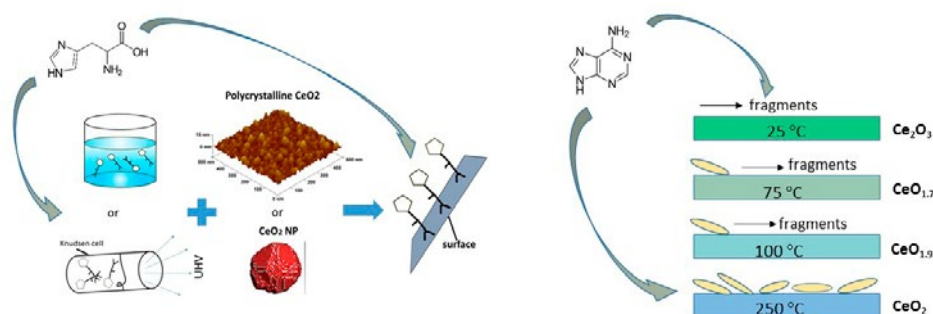
² Elettra-Sincrotrone Trieste S.C.p.A., in Area Science Park, Strada Statale 14, km 163.5, Basovizza (Trieste), 34149, Italy;

^a Present address: Institute of Physics AS CR, Na Slovance 2, 182 21 Prague 8, Czech Republic

^b Present address: Australian Synchrotron, 800 Blackburn Road, Clayton, VIC 3168, Australia

The interface formed between fundamental biomolecules and inorganic oxide surfaces has attracted considerable attention as a decisive factor in bio-application of nanostructured oxides. We report a study of the adsorption of histidine and adenine on a cerium oxide model support, by surface science techniques with the use of synchrotron radiation. The systematic approach was applied that considers different stoichiometry and morphology of cerium oxide films as well as two ways of molecular deposition (evaporation in vacuum and deposition from aqueous solution). As the nanostructured ceria films or powders for real bio-sensing systems contain small crystallites of CeO₂ and Ce³⁺ sites adjacent to oxygen vacancies and at grain edges and other defects, ordered stoichiometric, polycrystalline, porous, under stoichiometric and reduced cerium oxide thin films were chosen as model supports. The chemical state, coverage and bonding of the molecules were studied by synchrotron radiation photoelectron spectroscopy and resonance photoelectron spectroscopy; molecular orientation was examined by near edge X-ray absorption fine structure spectroscopy. In view of the importance of nanostructured cerium oxide in various biological and recently also in pharmacological applications, the primary objective of this work was to investigate the basic properties of cerium oxide films in their bonding with the biomolecules. On the well-ordered single crystalline ceria, histidine bonded via the deprotonated carboxylic acid group, the α amino nitrogen and the imidazole (IM) ring, with deprotonation of its amino nitrogen. On the polycrystalline oxide, surface bonding occurred via the carboxylic acid group only, and the IM formed intermolecular bonds. The presence of a “free” IM ring provides the possibility for further interaction or linkage with other molecules which may be targets for biosensors.

The adenine molecule chemisorbs on stoichiometric cerium oxide intact independent on oxide morphology and deposition technique. The reduced ceria surface was found to decompose the adenine molecule. We show that the stability of the molecules is strongly influenced by concentration of Ce³⁺ ions at the surface. These findings are very useful for understanding fundamental processes occurring at the adsorbate/substrate interface which are crucial to comprehend the impact of ceria in bio-applications.



Tue-17:00-O-PISC ●

On-surface photo- and thermal-generation of higher acenes

PISC Photo-Induced Surface Chemistry

José Ignacio Urgel¹, Shantanu Mishra¹, Hironobu Hayashi², Marco Di Giovannantonio¹, Carlo A. Pignedoli¹, Okan Deniz¹, Pascal Ruffieux¹, Hiroko Yamada^{2,3}, Roman Fasel¹

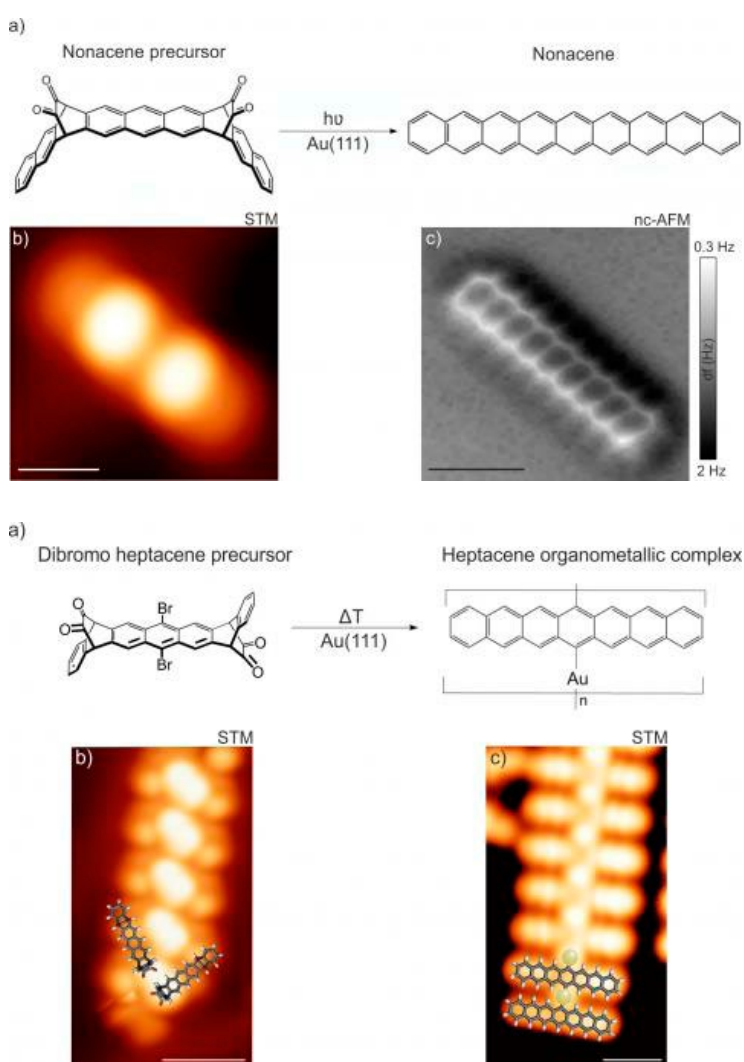
¹ Empa, Swiss Federal Laboratories for Material Science and Technology, 8600 Dübendorf, Switzerland;

² Graduate School of Materials Science, Nara Institute of Science and Technology (NAIST), 8916-5 Takayama-cho, Ikoma 630-0192 (Japan);

³ CREST, Japan Science and Technology Agency (JST), 4-1-8 Honcho, Kawaguchi, Saitama 332-0012 (Japan)

Over the last decades, large acenes and their derivatives have attracted enormous interest due to their unique physical properties and potential applications in opto- and molecular electronics [1]. Nevertheless, their synthesis, functionalization and characterization are ambitious and become more challenging considering the significant decrease in stability as the acene length is enlarged [2,3]. The emerging research domain of on-surface covalent synthesis bears promise to tackle this challenge. Pioneering work has shown that surface-assisted reactions allow synthesizing specific polyaromatic molecules and atomically precise covalent nanoarchitectures under ultrahigh vacuum (UHV) conditions using specifically designed molecular building blocks [4,5]. Important achievements comprise the formation of polyaromatic hydrocarbons, graphene nanoribbons or two-dimensional networks.

In this work we present a combined scanning tunneling microscopy (STM), scanning tunneling spectroscopy (STS), non-contact atomic force microscopy (nc-AFM) and density functional theory (DFT) study enlightening the photo-conversion of α -diketone protected nonacene and heptacene precursors into nonacene and heptacene species on a pristine Au(111) substrate. A quantitative analysis of the STM images reveals how the α -diketone bond dissociation is induced by visible-light irradiation giving rise to the formation of the targeted acene compounds whose chemical structure is unequivocally confirmed by nc-AFM. Moreover their electronic structure, studied by STS will be also presented. In addition, a thermal-conversion approach for Br-substituted α -diketone protected precursor was carried out. Annealing of the sample up to 460 K affords the formation of 1D Au-directed organometallic nanostructures.



A subsequent annealing to 535 K results in the thermal-conversion of monomers, (i.e. the cleavage of the α -diketone moieties) producing Au-directed heptacene organometallic complexes.

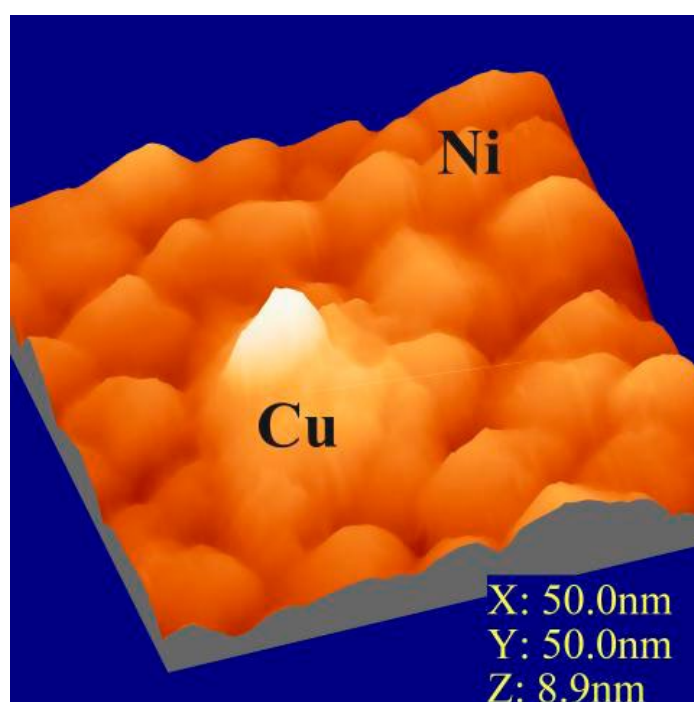
Our results introduce a novel strategy towards the design of large acenes and their derivatives using two different activation pathways, which prospects new avenues in the field of on-surface synthesis.

References:

- [1] Anthony John E., "The larger acenes: versatile organic semiconductors", *Angew. Chem. Int. Ed.*, Vol. 47, No. 3, (2008), pp 452-483.
- [2] Mondal R., Shah B. K., Neckers D. C., "Photogeneration of heptacene in a polymer matrix", *J. Am. Chem. Soc.*, Vol. 128, No. 30, (2006), pp 9612-9613.
- [3] Tönshoff, Christina, and Holger F. Bettinger. "Photogeneration of octacene and nonacene." *Angewandte Chemie International Edition* 49.24 (2010): 4125-4128.
- [4] Lindner R. and Kühnle A., "On-surface reactions", *Chemphyschem*, Vol. 16, No. 8, (2015), pp 1582-1592.
- [5] Krüger, Justus, et al. "Imaging the electronic structure of on-surface generated hexa-cene." *Chemical Communications* (2017).

Tue-9:40-O-BIMS ●**Surface atomic arrangement and grain boundary diffusion in nanolayers***BIMS Bimetallic surfaces and alloy nanocrystals*Viktor Takáts, [Kálmán Vad](#), Attila Csik, József Hakl*Institute for Nuclear Research, Hungarian Academy of Sciences, H-4001 Debrecen, P.O. Box 51, Hungary*

Surface atomic arrangement induced by grain boundary diffusion was studied in nanolayers by *in-situ* low energy ion scattering spectroscopy, X-ray photoelectron spectroscopy, scanning probe microscopy and *ex-situ* depth profiling based on ion sputtering. A new experimental approach of measurement of grain boundary diffusion coefficients was applied. In Ni/Cu bi-layers the appearing time of copper atoms diffused through the few nanometer thick nickel layer has been detected by low energy ion scattering with high sensitivity. The grain boundary diffusion coefficient can be directly calculated from this appearing time without using segregation factors in calculations. The temperature range of 423-463 K insures the pure C-type diffusion kinetic regime. The most important result is that surface coverage of Ni layer by Cu atoms reaches a maximum during annealing and stays constant if the annealing procedure is continued. Scanning probe microscope measurements show a Volmer-Weber type layer growth of Cu layer on the Ni surface in the form of Cu atomic islands. Depth distribution of Cu in Ni layer has been determined by SNMS depth profile analysis.



Tue-9:20-O-MAGN ●

Probing the exchange coupling through a Nc-functionalized STM

MAGN Surface and molecular magnetism

Benjamin Verlhac¹, Maider Ormaza¹, Nicolas Bachellier¹, Léo Garnier¹, Laurent Limot¹, Marie-Laure Bocquet², Nicolás Lorente³

¹ Université de Strasbourg, CNRS, IPCMS, UMR 7504, IPCMS, F-67000 Strasbourg, France;

² Ecole Normale Supérieure, Département de Chimie, ENS-CNRS-UPMC UMR 8640, 75005 Paris, France;

³ Centro de Física de Materiales CFM/MPC (CSIC-UPV/EHU), Paseo Manuel de Lardizabal 5, 20018 Donostia-San Sebastian, Spain

Recent advances in scanning tunneling microscopy (STM) offer the possibility of studying the interaction between elementary magnets – atoms and molecules. Here we focus on the interaction between a sandwich molecule, nickelocene (Nc, Fig. 1a), and a transition metal atom. Nc preserves its spin-1 character and uniaxial magnetic anisotropy upon adsorption in different metallic environments [1]. The adsorbed molecule presents efficient inelastic spin-flip excitations as evidenced with inelastic electron tunneling spectroscopy (IETS). In particular we manage to transfer the Nc on the tip apex of the microscope preserving its properties. Taking advantage of this portable source of inelastic excitations, we use IETS to spatially probe the magnetic coupling of the Nc at the tip apex to a second spin impurity, a Fe atom on a Cu(100) surface (Fig. 1b). The electronic transport through these coupled spins also reveals an asymmetry in the differential conductance [2], which is related to the sign of the coupling (ferromagnetic or antiferromagnetic). Our findings are discussed in view of density functional theory calculations, which mimic the STM junction.

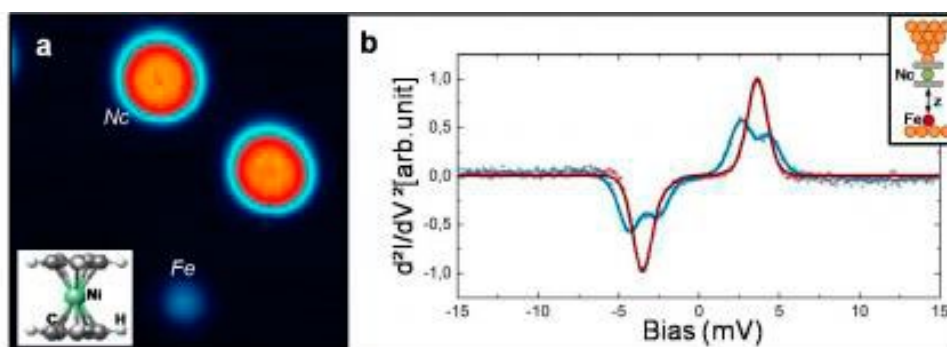


Figure 1: a) STM image of nickelocene and of a Fe atom. Inset: Chemical structure of Nc. b) Numerical derivative of dI/dV spectra taken with a Nc-terminated tip over a Fe atom (red: $z=280$ pm; blue: $z=130$ pm).

References:

[1] Ormaza et al., NanoLett.17, 1877 (2017)

[2] Muenks et al., Nat. Commun.8, 14119 (2017)

Thu-9:20-O-OXID ●**Imaging and manipulations of dissociated water on $\text{In}_2\text{O}_3(111)$** *OXID Oxide surfaces and ultrathin oxide films*

[Margareta Wagner](#)¹, [Martin Setvín](#)¹, [Steffen Seiler](#)², [Lynn A. Boatner](#)³, [Michael Schmid](#)¹, [Bernd Meyer](#)², [Ulrike Diebold](#)¹

¹ *Institut für Angewandte Physik, TU Wien, Austria;*

² *Computer Chemistry Center, FAU Erlangen-Nürnberg, Germany;*

³ *Materials Science and Technology Division, ORNL, Tennessee, USA*

Indium oxide is one of the most important transparent conductive oxides (TCOs), and commonly used as a contact and sensor material. Here, the adsorption of water is investigated with low temperature STM/AFM, XPS and DFT. Above 100 K dissociative adsorption of water on $\text{In}_2\text{O}_3(111)$ single crystals is observed. At room temperature the surface is saturated with three dissociated water molecules per unit cell, symmetrically arranged around the six-fold coordinated In atoms. The fully hydroxylated surface shows a (1×1) structure with respect to the clean $\text{In}_2\text{O}_3(111)$ surface. This leads to a well-ordered, hydroxylated surface where the three terminal OH groups plus the three protons (forming surface OH groups) are imaged together as one bright triangle in STM. The internal structure is revealed by AFM measurements, and manipulations with the STM tip, where surface OH groups can be individually removed.

Mon-14:00-O-BAND ●**Novel systems toward ambient pressure photoemission spectroscopy*****BAND Band structure of solid surfaces*****Lukasz Walczak***R&D Department, PREVAC Sp. z o.o., Rogow, Poland*

Nowadays, the complexity of materials and their surfaces is expanded across a wide range of topics, including surface science, catalysis, corrosion, photoelectrochemical energy conversion, battery technology, or energy-saving technologies [1-5]. An unique and exceedingly flexible analysis cluster with a detection system is needed for this applied research. Here the examples of innovative, compact ambient pressure X-ray spectroscopy systems with a some experimental results. One of the example will be a laboratory based high pressure x-ray photoelectron spectroscopy (HPXPS). The focus is on the usability of the system for various types of studies relevant for high level research for photo-catalytic reactions, light harvesting and solar cell development [6]. Further examples will be the advanced HP cell with the ambient pressure X ray spectroscopy system and flexible gas inlet system to allow for frontier research on gas-solid interactions. Systems are equipped with the possibility of process automatization in different environments. Additional it will be presented a spectrometer for the ambient pressure photoemission spectroscopy with a new monochromatic source, in order to permit complete characterization of the energy, angular, and later resolutions using different metal samples at different pressures.

References:

1. S. Bengió, et al. Surf. Sci. 646, 126 - 131 (2016)
2. B. Eren et al. Science 29, 475-478 (2016)
3. Z. Duan et al. J. of Solid St. Electrochem. 19, 2265 - 2273 (2015)
4. K. Samson et al. ACS Catalysis, 4, 373 - 374 (2014)
5. C. S. Gopinath et al. ChemCatChem 7, 588 – 594 (2015)

Tue-11:00-O-ORGS ●

Structural transformation and stabilization of metal-organic motifs induced by halogen doping

ORGS Organic molecules on solid surfaces

Igor Beinik, Kræn Christoffer Adamsen, Stig Koust, Jeppe V. Lauritsen, Stefan Wendt

Interdisciplinary Nanoscience Center (iNANO) Aarhus University Gustav Wieds Vej 14 DK-8000 Aarhus C, Denmark

The interaction of water with titanium dioxide (TiO_2) is pivotal for many practical applications of this material in heterogeneous catalysis because water is almost always present either as a reactant or a product in many catalytic reactions. In our model study, we focus on the anatase polymorph of TiO_2 that has demonstrated a higher catalytic activity in water splitting than rutile and is generally considered as a more technologically relevant polymorph. The nanocrystals of anatase that are present in powder catalysts normally expose a high fraction of low surface energy (101) facets and a significantly smaller fraction of high energy, but supposedly more reactive (001) facets. The (001) facet is intrinsically unstable and reconstructs upon annealing in vacuum forming 1×4 reconstructed terraces, where rows of bridging oxygen atoms in [100] and [010] directions are replaced by TiO_3 units [1]. This kind of reconstruction has been found both on the (001) facets of anatase single crystals and nanoparticles [2], however the interaction of water with this surface has been significantly less investigated.

In the present work, we study the adsorption and dissociation of water on the anatase (001) 1×4 reconstructed surface by means of STM, TPD, and synchrotron core-level and valence band PES under UHV conditions. Our results show that water dissociates to some extent even at 120 K and that low water exposures (up to 3 L) at this temperature results in a mixture of molecularly and dissociatively adsorbed molecules. A systematic analysis of the data obtained using all three techniques leads us to a conclusion that the A- $\text{TiO}_2(001)-1 \times 4$ surface is rather reactive – in agreement with an earlier study [3] we find that water dissociates at the ridges of the 1×4 reconstruction. Moreover, the 1×4 reconstruction remains stable upon water exposures at least up to ~ 45 L (at 120 K).

However, after desorption of a multilayer ice film, the ridges themselves contain a high number of defects (see the STM image in Fig. 1), which remain stable up to 800 K. The nature of these defects will be discussed.

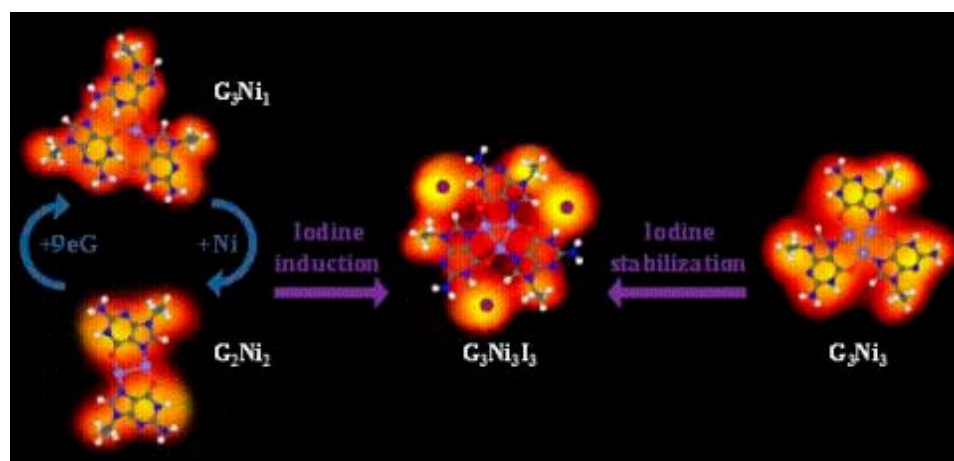


Figure 1: A typical STM image of the anatase (001) 1×4 reconstructed surface after desorption of multilayer ice film recorded at room temperature.

References:

- [1] Lazzeri, M. & Selloni, A. Phys. Rev. Lett. 87, 266105 (2001).
- [2] Yuan, W. et al. Nano Letters 16, 132–137 (2016).
- [3] Blomquist, J., et al. J Phys Chem C 112, 16616–16621 (2008).

Thu-14:20-O-SEMI ●**Correlation between fractal and wettability of rippled silicon surfaces under ion beam irradiation***SEMI Semiconductor surfaces and ultrathin layers***R. P. Yadav¹, Manvendra Kumar², S. N. Pandey¹, A. K. Mittal³**¹ Department of Physics, Motilal Nehru National Institute of Technology, Allahabad- 211004, India;² Nanotechnology Application Centre, University of Allahabad, Allahabad, 211002, India;³ Department of Physics, University of Allahabad, Allahabad, 211002, India

A correlation between fractal properties of rippled surface and wettability is presented on Si (100) surfaces, which have potential application in various fields like biosensing, optoelectronics and magnetic devices. Ripple patterns have been fabricated using 200 keV Ar⁺ ion beam at oblique incidence of angle 60 with fluences ranging from 3×10^{17} ions/cm² to 3×10^{18} ions/cm² and the surface morphologies were captured by atomic force microscopy (AFM). Fractal analysis is performed on these AFM images. The autocorrelation function analysis showed that the wavelength of ripple patterns varied with ion fluences. Height-height correlation function is used to estimate the roughness exponent for each surface. It is found that the roughness exponent increases with increase in ion fluence. Roughness exponent and fractal dimensions are found correlated with static water contact angle measurement. A sharp variation in contact angle values is found for low fractal dimensions. The larger values of interface width indicate the larger ripples on the surface. The contact angle on the water drop on such surface is observed to be lowest. It is found that the large ripples help in transforming the hydrophobic surface to a hydrophilic surface. Detailed analysis indicates that the fractal characterization can be useful as a tool for tailoring the wetting properties of solid surfaces.

Thu-9:20-O-CATH ●**Adsorption and reaction of CO₂ on graphene studied by ambient pressure XPS***CATH Catalytic 2D-model studies under high pressures*

[Susumu Yamamoto](#)¹, [Kaori Takeuchi](#)¹, [Ro-Ya Liu](#)¹, [Yuichiro Shiozawa](#)¹, [Takanori Koitaya](#)¹, [Takashi Someya](#)¹, [Keiichiro Tashima](#)², [Hirokazu Fukidom](#)², [Kozo Mukai](#)¹, [Shinya Yoshimoto](#)¹, [Maki Suemitsu](#)², [Jun Yoshinobu](#)¹, [Iwao Matsuda](#)¹

¹ *The Institute for Solid State Physics, The University of Tokyo, Japan;*

² *Research Institute of Electrical Communication, Tohoku University, Japan*

Graphene, a two dimensional honeycomb lattice of carbon atoms, has great promise as a catalyst support due to its high specific surface area and high electron mobility. The adsorption of molecules on the graphene surface is the most fundamental elementary process in catalytic reactions. Despite of importance, experimental studies to clarify the interaction of adsorbed molecules with graphene are still limited. Especially, it has been challenging to experimentally study the adsorption of molecules on graphene at ambient conditions where catalysts are operated.

In this study, we investigated the adsorption of CO₂ on graphene at near ambient conditions using ambient pressure X-ray photoelectron spectroscopy (AP-XPS). The experiments were performed using a newly developed AP-XPS apparatus [1] at the soft X-ray undulator beamline BL07LSU [2] of SPring-8. Monolayer epitaxial graphene on SiC(0001) was adopted as a model graphene surface. At near ambient conditions of 1.6 mbar CO₂ gas pressure and 175 K sample temperature, no CO₂ adsorption was observed on the pristine graphene, but CO₂ adsorption was observed on the oxygen-modified graphene surface. Therefore, the oxygen-modification of graphene enhances the adsorption energy of CO₂. The oxygen-species on the graphene surface was ascribed to epoxide by the XPS binding energies and its temperature stability. If time allows, we will introduce the hydrogenation reactions of CO₂ on metal nanoparticles supported on graphene.

This work was supported by the JST ACT-C project (Grant Number JPMJCR12YU), and carried out as joint research in the Synchrotron Radiation Research Organization and The Institute for Solid State Physics, The University of Tokyo.

References:

[1] T. Koitaya, S. Yamamoto et al., *Topics in Catalysis* 59, 526 (2016).

[2] S. Yamamoto et al., *J. Synchrotron Rad.* 21, 352 (2014).

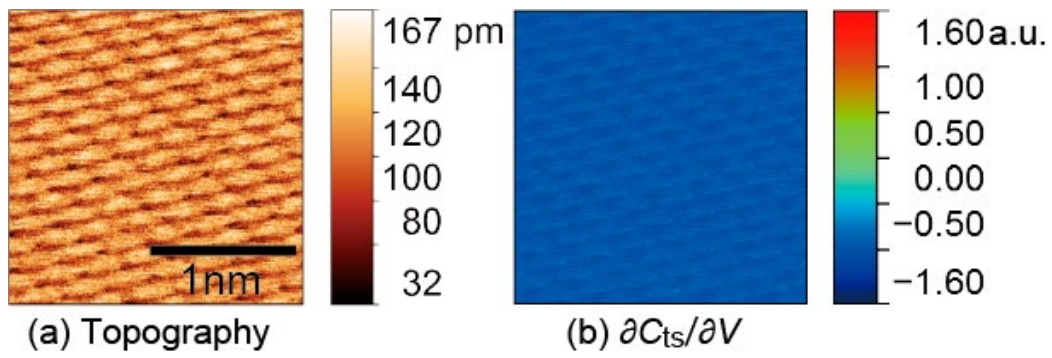
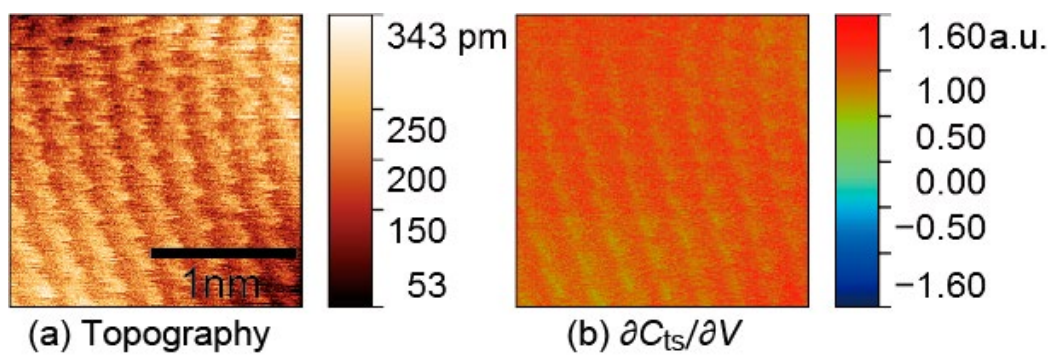
Thu-9:40-O-SEMI ●**Atomic resolution imaging and carrier type determination of Molybdenum disulfide by noncontact scanning nonlinear dielectric microscopy***SEMI Semiconductor surfaces and ultrathin layers*[Kohei Yamasue](#), [Yasuo Cho](#)*Research Institute of Electrical Communication*

In recent years, various layered materials have been extensively studied towards their future applications to functional devices. Like graphite and graphene, they show interesting properties especially when they are thinned down to a monoatomic layer. Among the layered materials, MoS₂ is known as a semiconductor. In particular, a monolayer MoS₂ has a direct transition band-gap promising for electronic and optical applications. Here we demonstrate that a MoS₂ surface and its charge distribution can be atomically resolved and, at the same time, its dominant carrier type can be determined in a nanoscale by noncontact scanning nonlinear dielectric microscopy (NC-SNDM) [1-3].

NC-SNDM is a scanning probe microscopy method measuring tip-sample capacitance variation to an external electric field ($\partial C_{ts} / \partial V$). In general, $\partial C_{ts} / \partial V$ is contributed from two different physical properties. One is a local nonlinear dielectric property characterized by nonlinear dielectric constants ($\epsilon_i, i = 3, 4, \dots$). In particular, ϵ_3 imaging is useful for determining the direction of spontaneous polarization or permanent dipole moments in a sample surface. The other comes from semiconductor properties. $\partial C_{ts} / \partial V$ can be directly interpreted as the derivative of a local capacitance-voltage characteristics emerging in a metal-insulator-semiconductor (MIS) system consisting of a conductive tip, vacuum-gap, and semiconductor sample in the measurement. Since $\partial C_{ts} / \partial V$ reflects the response of a depletion layer to an applied field below the tip, $\partial C_{ts} / \partial V$ provides local information of carrier type and density. Furthermore, topographic information can also be obtained by using ϵ_4 -feedback for noncontact tip-sample distance regulation.

We performed NC-SNDM imaging of n-type and p-type MoS₂ in an ultrahigh vacuum at room temperature. Figures 1 and 2 respectively show simultaneous NC-SNDM images of (a) topography and (b) $\partial C_{ts} / \partial V$ for n-type and p-type MoS₂. Both topographic images show atomic resolution. In addition, the polarity of $\partial C_{ts} / \partial V$ was basically negative and positive for n-type and p-type, respectively, as predicted from the derivative of local capacitance-voltage characteristics in n-type and p-type MIS systems. Furthermore, in an atomic scale, $\partial C_{ts} / \partial V$ was modulated through the intensity difference of ϵ_3 on each atomic site. This is attributable to electric polarization or local charge distribution of imaged atoms. Thus, these results indicate that NC-SNDM will provide rich information on the local electronic properties of layered semiconductor materials.

This work was partly supported by a Grant-in-Aid for Scientific Research (Nos. 15K04673, 16H02330) from the Japan Society for the Promotion of Science.

Fig. 1: NC-SNDM images of n-type MoS₂Fig. 2: NC-SNDM images of p-type MoS₂

References:

- [1] Y. Cho and R. Hirose, Phys. Rev. Lett. 99, 186101 (2007).
- [2] K. Ohara and Y. Cho, Nanotechnology 16, S54 (2005).
- [3] K. Yamasue et al., Phys. Rev. Lett. 114(22), 226103 (2015).

Thu-10:40-O-LASE ●**Optical control of Young's type interferometers for ultrafast electron pulses***LASE Laser pulses for surface electron dynamics*Hirofumi Yanagisawa^{1,2}¹ Max Planck Institute of Quantum Optics, D-85748 Garching, Germany;² Ludwig-Maximilians University, D-85748 Garching, Germany

Interference experiments with electrons in a vacuum can illuminate both the quantum and the nanoscale nature of the underlying physics. An interference experiment requires two coherent waves, which can be generated by splitting a single coherent wave using a double slit. If the slit-edge separation is larger than the coherence width at the slit, no interference appears. Here we have achieved optical control of the double-slit dimension using the simplest form of Young's interference, which is established via two electron beams from a nanometre-sized tip apex [1]. Applying high DC fields on the tip apex can drive electron tunnelling through the surface barrier, known as field emission. The field emission current density depends exponentially on area of the surface potential-energy barrier. As a result, the emission sites become localized on the nanometre scale, and it is possible to establish two emission sites within the coherence width of the electrons inside the tip. This kind of interference has never been observed other than at the tiny apex of a carbon nanotube with a radius of 5nm [1]. Therefore, careful material and tip designs are necessary for observing the interference via this method, and controlling the double-slit properties is very difficult. By using photo-assisted electron emission [2], and without changing the tip and materials, we could control the distance and opening-and-closing of the double slit, represented by the surface barriers, by respectively tuning the intensity and polarization of 7fs laser pulses that induce the photoexcitation [3-5]. We observed interference patterns from two electron beams from a comparatively large tungsten tip apex with a radius of curvature of approximately 100nm at room temperature, where interference has never been observed prior to this technique because of the large slit-edge separation. The underlying physics is derived by numerical modelling and shows that photo-excited electrons on the tip surface experience small slit-edge separation.

References:

- [1] C. Oshima, et al. Phys. Rev. Lett. 88, 038301 (2002).
- [2] P. Hommelhoff, et al. Phys. Rev. Lett. 96, 077401 (2006).
- [3] H. Yanagisawa, et al. Phys. Rev. Lett. 103, 257603 (2009).
- [4] H. Yanagisawa, et al. Phys. Rev. Lett. 107, 087601 (2011).
- [5] H. Yanagisawa, et al. Sci. Rep. 6, 35877 (2016).

Tue-14:40-O-OXID ●

From 2D to 3D Alumina: Interface Templated Growth of γ -Al₂O₃(111)-like Films

OXID Oxide surfaces and ultrathin oxide films

Wolf-Dietrich Zabka¹, Dominik Leuenberger¹, Gerson Mette^{1,2}, Jürg Osterwalder¹

¹ Department of Physics, University of Zürich, Switzerland

² Fachbereich Physik, Philipps-Universität Marburg, Germany

The properties of ultrathin oxide films, as well as those of molecules adsorbed on these ultrathin films can significantly change with increasing oxide film thickness [1-3]. Alumina (Al₂O₃) thin films grown by selective oxidation on a NiAl(110) substrate are a frequently used model system [4]. These oxide films consist of two atomic bi-layers of oxygen and aluminum (2L-alumina) [5]. A new multi-step oxidation procedure is used to increase the thickness of 2L-alumina from two atomic layers up to 1.5 nm, as measured by X-ray photoelectron spectroscopy (Fig. 1). The structure of the films is analyzed using X-ray photoelectron diffraction (XPD) and low-energy electron diffraction (LEED). XPD reveals changes in the atomic short range order: While increasing the thickness, we observe the local formation of a γ -Al₂O₃(111)-like structure (Fig. 2). LEED reveals that excellent crystallinity of the 2L-alumina interface is maintained during the film growth and that the complex long range order implied by the 2L-alumina interface remains. Based on the 2L-alumina model [5] and by finding structural analogies with γ -Al₂O₃ a blurred hexagonal structure in the LEED pattern is identified as evidence for a model of the γ -Al₂O₃(111) surface. Band structures measured by angle-resolved photoelectron spectroscopy reveal no significant changes in the electronic structure for the transition from 2L-alumina to thicker films. We conclude that these films are suited for the use as tunneling barriers and that the sequential preparation of the interface and the following layers provides a new route to synthesize novel oxide structures.

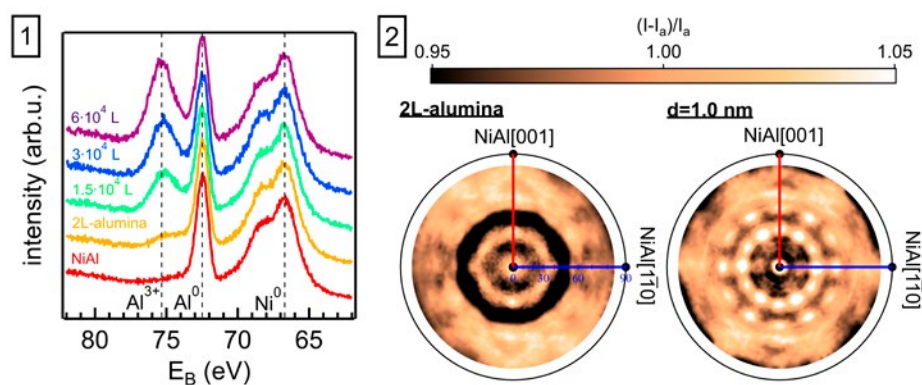


Fig. 1: Al 2p and Ni 3p core level spectra of NiAl(110), 2L-alumina/NiAl(110) and of thicker alumina films on NiAl(110). An increase of the Al³⁺ signal indicates continued oxide formation.

Fig. 2: Experimental O 1s XPD pattern of 2L-alumina (left) and a 1.0 nm thick film (right). The local formation of γ -Al₂O₃(111) is observed.

References:

- [1] C. Freysoldt, P. Rinke, and M. Scheer, Phys. Rev. Lett. 99, 086101 (2007).
- [2] M. Sterrer, T. Risse, M. Heyde, H.-P. Rust, and H.-J. Freund, Phys. Rev. Lett. 98, 206103 (2007).
- [3] O. T. Hofmann, P. Rinke, M. Scheer, and G. Heimel, ACS Nano 9, 5391 (2015).
- [4] H.-J. Freund, N. Nilius, T. Risse, and S. Schauermaier, Phys. Chem. Chem. Phys. 16, 8148 (2014).
- [5] G. Kresse, M. Schmid, E. Napetschnig, M. Shishkin, L. Köhler, and P. Varga, Science 308, 1440 (2005).

Thu-11:20-O-OXID ●**Adsorption of CO and water on magnetite Fe_3O_4 surfaces***OXID Oxide surfaces and ultrathin oxide films*

[Eman Zaki](#), [Francesca Mirabella](#), [Francisco Ivars-Barcelo](#), [Shamil Shaikhutdinov](#),
[Hans-Joachim Freund](#)

*Department of Chemical Physics, Fritz-Haber-Institut der Max-Planck-Gesellschaft, Faradayweg 4-6,
14195 Berlin, Germany*

Interaction of water with iron oxides received much attention in surface science community due to its importance in corrosion, geochemistry, and catalysis. In particular, magnetite (Fe_3O_4) surfaces were intensively studied, both experimentally and theoretically. The results revealed that water adsorption critically depends on surface preparation conditions, orientation and surface termination. It appears that some discrepancy still existing in the literature is originated from uncertainty in the atomic structure of oxide surfaces under study.

In this work, we made use of well-ordered $\text{Fe}_3\text{O}_4(111)$ and $\text{Fe}_3\text{O}_4(001)$ films grown on Pt(111) and Pt(001) substrates, respectively, characterized by LEED and AES. Adsorption studies were performed using temperature programmed desorption (TPD) and infrared reflection absorption spectroscopy (IRAS). Adsorption of CO as a probe molecule, corroborated by DFT calculations of the Sauer's group (HU Berlin), provide further evidence of the (111) surface structure previously determined on the basis of LEED I/V measurements. TPD and IRAS results of water adsorption on the (111) surface suggested water dissociation at low coverages following by molecular water adsorption and their clustering, ultimately resulting in a (2x2) periodic structure as observed by LEED. Coverage dependent desorption energetics were obtained from analysis of TPD spectra and compared with previously reported microcalorimetry data.

Thu-14:00-O-GRAP ●

Graphene/doped graphene from adsorbed molecules

GRAP Graphene and carbon-based 2D films

Tashfeen Zehra¹, Ali Syari'ati¹, Oleksii Ivashenko², Willem Van Dorp³, J.T.M De Hosson¹, Petra Rudolf¹

¹ Zernike Institute for advanced materials, University of Groningen, The Netherlands;

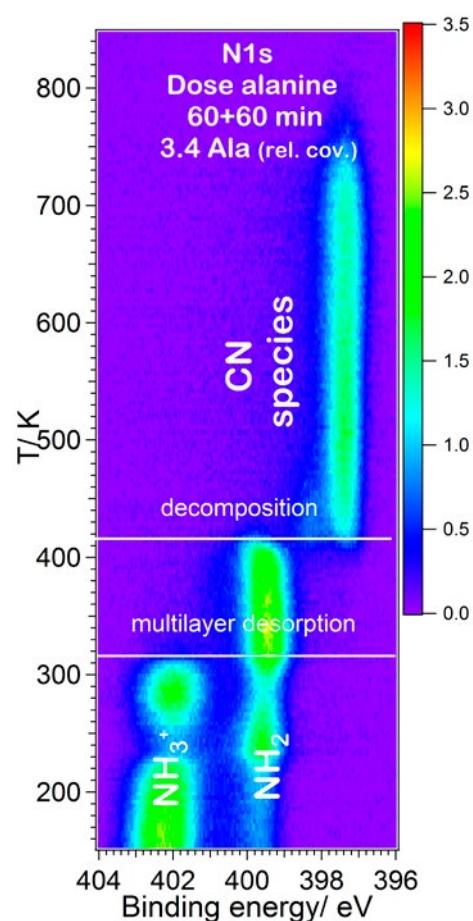
² University of Oslo, Norway;

³ Delft University of Technology, The Netherlands

Graphene is a promising candidate for a myriad of applications due to its unique electronic, mechanical, optical and thermal properties. Chemical doping is an important approach to tailor the properties of graphene. Usually graphene can be doped by two methods. Substitutional doping with atoms such as B and N can locally induce significant changes in the electronic properties and chemical reactivity [1] of graphene. Boron or nitrogen doping in the graphene network transform it into p- or n-type semiconductor, respectively, accompanied by opening of a band gap [2]. N-doping is extremely significant for enhanced catalysis for energy conversion/storage. The biocompatibility of carbon nanomaterials can also be enhanced by doping and is therefore favourable for biosensing applications [3]. The commonly used production method for graphene/doped graphene on metallic substrates is chemical vapour deposition, where growth starts at different points on the surface leading to defects, grain boundaries and wrinkles developing due to the different thermal expansion coefficients of substrate and graphene. Preparing large continuous layers of graphene on conducting and insulating substrates remains a challenge. A valid alternative to the chemical vapour deposition (CVD) method is graphene growth by decomposition of adsorbed molecules. Here, we illustrate two examples: graphene from the thermal decomposition of chemisorbed C₆₀ on copper and graphene/doped graphene from thiol SAMs on clean and/or oxidized copper. In the latter case the adsorbed layer has to be first crosslinked by UV light to prevent desorption during the thermal treatment to obtain graphene/doped graphene. In both cases the quality of the obtained material was verified by Raman spectroscopy; diffraction data (LEED and TEM) testify to the structural properties and XPS on the purity of the material.

References:

- [1] J. Y. Dai, J.M. Yuan, and P. Giannozzi, "Gas adsorption on graphene doped with B, N, Al, and S: A theoretical study", *Appl. Phys. Lett.* 95, 232105 (2009)
- [2] C. Zhang et al, "Synthesis of Nitrogen-Doped Graphene Using Embedded Carbon and Nitrogen Sources", *Adv. Mater.* 23, 1020 (2011).
- [3] S Y. Wang et al, "Nitrogen-doped graphene and its application in electrochemical biosensing", *ACS Nano* 4, 1790 (2010); H. Wang, T. Maiyalagan and X. Wang, "Review on Recent Progress in Nitrogen-Doped Graphene: Synthesis, Characterization, and Its Potential Applications", *ACS Catal.* 2 (5), 781 (2012).



Wed-9:20-O-ORGS ●

Conclusively addressing the CoPc electronic structure: a joint gas-phase and solid-state photoemission and absorption spectroscopy study

ORGS Organic molecules on solid surfaces

T. Zhang¹, I. Brumboiu², J. Lüder³, C. Grazioli⁴, V. Lanzilotto¹, E. Giangrisostomi⁵, R. Ovsyannikov⁵, Y. Sassa¹, I. Bidermane⁵, M. Stupar⁶, M. de Simone⁷, M. Coreno⁷, B. Ressel⁶, M. Pedio⁷, P. Rudolf⁸, B. Brena¹, C. Puglia¹

¹ Dept. of Physics and Astronomy, Uppsala University, Box 516, SE-751 20 Uppsala Sweden;

² Royal Institute of Technology, Dept. of Theoretical Chemistry and Biology, SE-106 91 Stockholm Sweden;

³ National University of Singapore, Dept. of Mechanical Engineering, 117575 Singapore;

⁴ University of Trieste, Dept. of Chemical and Pharmaceutical Sciences, 34127 Trieste, Italy;

⁵ Institute for Methods and Instrumentation for Synchrotron Radiation Research, Helmholtz-Zentrum Berlin;

⁶ University of Nova Gorica, Dept. of Physics, Vipavska Cesta 11c Ajdovščina 5270, Slovenia;

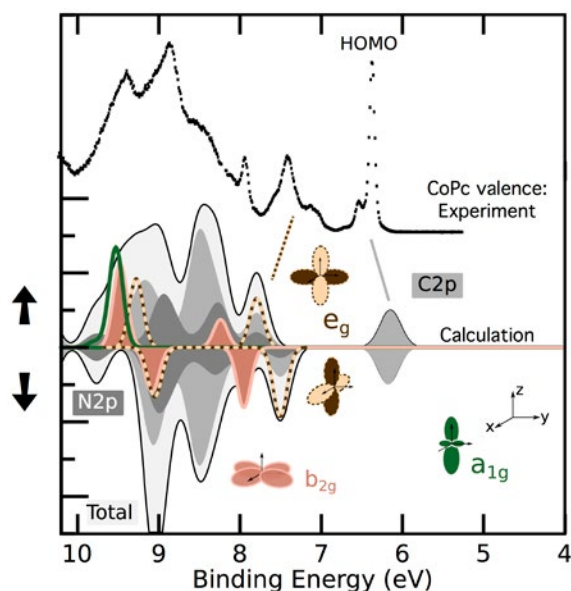
⁷ CNR-IOM, S.S. 14 Km 163,5, Basovizza, 34149 Trieste, Italy;

⁸ Zernike Institute for Advanced Materials, University of Groningen, Nijenborgh 4, 9747 AG Groningen, Netherland

The electronic configuration of the ground state of Cobalt Phthalocyanine (CoPc) is the focus of an ongoing debate. Controversial results provided by both experimentalists and theoreticians proposing a ground state configuration as ${}^2A_{1g}$ [1], a mix of ${}^2A_{1g}$ and 2E_g [2] or 2E_g [3]. Moreover, the character of the highest occupied molecular orbital (HOMO) of CoPc molecules is also still under discussion, since it has been suggested to be either metal 3d-like and localized on the central Co atom [4] or originated in the organic ring of the molecule [5]. Our high-resolution PhotoElectron Spectroscopy (PES) and XAS measurements of gas phase CoPc compared with single molecule theoretical simulations (Density Functional Theory as well as Multiplet Ligand-Field Theory calculations) clearly show that the ground state configuration can be correctly described by the ${}^2A_{1g}$ electronic configuration. In addition, valence photoelectron results of CoPc molecules in the gas phase have been compared to CoPc thin films deposited on an Au (111) single crystal. By varying the excitation photon energy, the valence photoemission results definitely enlightened that no Co 3d electrons contribute to the HOMO while Co 3d orbitals contribute mostly to the so-called interface state confirming it to be formed between the central Co atom of CoPc molecule and Au atom from Au(111) substrate.

References:

- [1] P Gargiani, Phys. Rev. B 87, 165407 (2013)
 [2] S Stepanow et al., Phys. Rev. B 83, 220401 (2011)
 [3] M. S. Liao et al., J. Chem. Phys. 114, 22 (2001)
 [4] M. Grobosch et al., J. Phys. Chem. C 113, 30 (2009)
 [5] S Bhattacharjee et al., Chem. Phys. 377, 96 (2010)



Thu-11:20-O-CATH ●

Simultaneously 2D spatially resolved activity and surface of a Pd(100) single crystal during CO oxidation

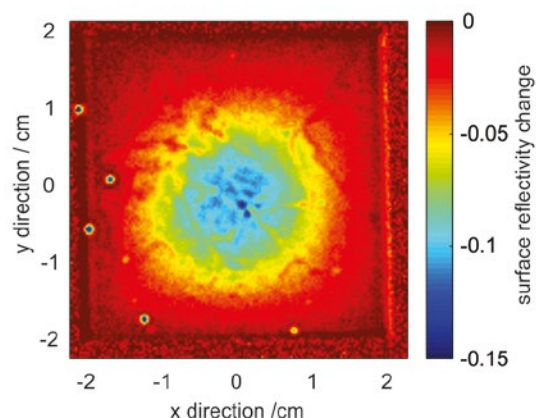
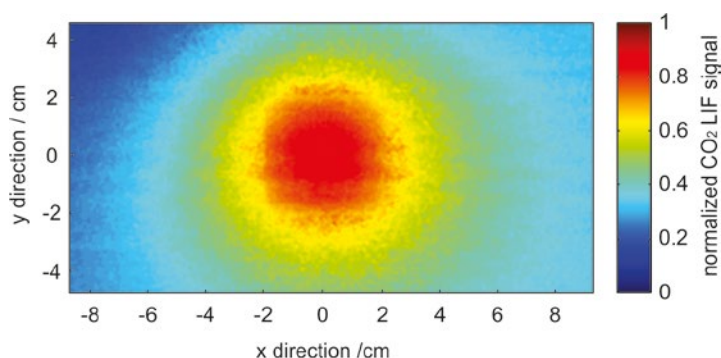
CATH Catalytic 2D-model studies under high pressures

Jianfeng Zhou¹, Sara Blomberg², Johan Gustafson², Edvin Lundgren², Johan Zetterberg¹¹ Division of Combustion Physics, Lund University, Lund, Sweden;² Division of Synchrotron Radiation Research, Lund University, Lund, Sweden

For a fundamental understanding of the mechanisms behind heterogeneous catalysis, a direct correlation between the reaction activity and the surface structure of a catalyst is generally needed. Therefore, we employed planar laser-induced fluorescence (PLIF) technique to spatially resolve the CO₂ distribution just above a Pd(100) surface during CO oxidation, and simultaneously monitored the reflectance of the surface. Both techniques provide high spatial (around 70 μm) and temporal (10 Hz) resolution. The combination of PLIF and surface reflectance makes it possible to follow dynamic change of both the gas phase and the surface on a sub-second scale at the same time, which provides us a direct correlation between the reaction activity and the surface structure of the sample on a macroscopic scale.

As reported in previous works [1, 2], thicker oxide forms on a Pd(100) surface under O₂ rich conditions, which leads to a rougher surface and thus lower surface reflectivity. We found that when the reaction is in the mass transfer limit (MTL) regime, a boundary layer is formed and significantly modifies the gas composition above the surface [3]. Interestingly, the thick oxide is mainly localized at the center of the sample just beneath the CO₂ cloud, as shown in Figure 1. It is clearly demonstrated that the formation of the thick oxide is sensitive to the variance of the gas composition, i.e. O₂ to CO ratio. Oscillating behavior of Pd(100) was recently revisited by Onderwaater et al. using surface X-ray diffraction technique [4]. We have also studied the oscillation of Pd(100) by combining PLIF and surface reflectance, and obtained new insights into the mechanisms. Most of our new finding will be discussed in the presentation.

Figure (top) CO₂ distribution 0.5 mm above the sample surface from top view; (bottom) reflectivity change of the surface, in the MTL regime. Sample dimension is 4 by 4 mm.



References:

- [1] Shipilin, M., et al., *The Journal of Physical Chemistry C*, 2015. 119(27): p. 15469-15476.
- [2] Onderwaater, W.G., et al., *Review of Scientific Instruments*, 2017. 88(2): p. 023704.
- [3] Zhou, J., et al., *Catalysts*, 2017. 7(1): p. 29.
- [4] Onderwaater, W.G., et al., *Catalysis, Structure & Reactivity*, 2017. 3(1-2): p. 89-94.

Wed-10:40-O-ORGS ●

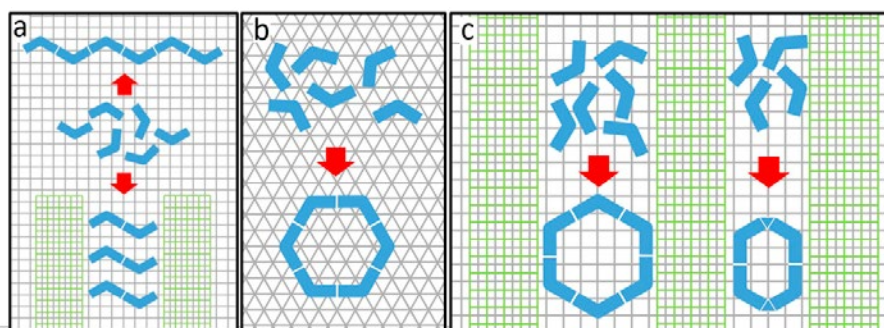
Tailoring the topology of low-dimensional organic nanostructures with surface templates

ORGS Organic molecules on solid surfaces

Qitang Fan¹, Junfa Zhu¹, J. Michael Gottfried²¹ National Synchrotron Radiation Laboratory and Collaborative Innovation Center of Suzhou Nano Science and Technology, University of Science and Technology of China, Hefei 230029, P.R. China;² Fachbereich Chemie, Philipps-Universität Marburg, Hans-Meerwein-Str., 35032 Marburg, Germany

The future of nanotechnology lies in the “bottom up” approach, which aims at building nanostructures at an atomic or molecular level so as to minimize the sizes of chips and other nano-devices. However, one of the long-term unresolved issues for “bottom up” nanotechnology is the precise control of the topologies of fabricated nanostructures. In this contribution, we will report our recent studies with regard to the control of the topologies of nanostructures formed *via* the on-surface Ullmann reaction or self-assembly of haloarenes, as shown in Scheme 1. The topic includes three aspects: control of the shape of the organometallic chain *via* lattice matching between the adsorbate nanostructure and the substrate;¹⁻³ tailoring the chains by employing super-gratings templates;⁴ and steering the covalent ring-chain competition in the reaction of precursors towards ring formation through adsorbate-substrate symmetry matching.⁵

This work was supported by the National Natural Science Foundation of China (21473178) and National Key Basic Research Program of China (2013CB834605)



Scheme 1. Illustrations for the topology regulations of on-surface nanostructures with different surface templates. (a) Bent precursors form six-membered (top) and two-membered (bottom) chains on flat and striped substrates, respectively. (b) Bent precursors form rings on six-fold symmetric substrate due to symmetry matching. (c) Bent precursors form rings with tunable sizes determined by the widths of the stripes on the striped substrate.

References:

- (1) Fan, Q.; Wang, C.; Han, Y.; Zhu, J.; Hieringer, W.; Kuttner, J.; Hilt, G.; Gottfried, J. M. Surface-Assisted Organic Synthesis of Hyperbenzene Nanotroughs *Angew. Chem.Int. Ed.* 2013, 52, 4668.
- (2) Fan, Q.; Wang, C.; Han, Y.; Zhu, J.; Kuttner, J.; Hilt, G.; Gottfried, J. M. Surface-Assisted Formation, Assembly, and Dynamics of Planar Organometallic Macrocycles and Zigzag Shaped Polymer Chains with C-Cu-C Bonds *ACS Nano* 2014, 8, 709.
- (3) Dai, J.; Fan, Q.; Wang, T.; Kuttner, J.; Hilt, G.; Gottfried, J. M.; Zhu, J. The role of the substrate structure in the on-surface synthesis of organometallic and covalent oligophenylene chains *Phys. Chem. Chem. Phys.* 2016, 18, 20627.
- (4) Fan, Q.; Dai, J.; Wang, T.; Kuttner, J.; Hilt, G.; Gottfried, J. M.; Zhu, J. Confined Synthesis of Organometallic Chains and Macrocycles by Cu-O Surface Templating *ACS Nano* 2016, 10, 3747.
- (5) Fan, Q.; Wang, T.; Dai, J.; Kuttner, J.; Hilt, G.; Gottfried, J. M.; Zhu, J. On-Surface Pseudo-High-Dilution Synthesis of Macrocycles: Principle and Mechanism *ACS Nano* 2017, DOI: 10.1021/acsnano.7b01870.

Thu-16:00-O-SEMI ●**Electronic states induced by cesium on atomically rough and flat GaAs(001) surfaces***SEMI Semiconductor surfaces and ultrathin layers*[A. G. Zhuravlev](#)^{1,2}, V. L. Alperovich^{1,2}¹ Novosibirsk State University, 630090 Novosibirsk, Russia;² Institute of Semiconductor Physics, 630090 Novosibirsk, Russia

The GaAs surface with adsorbed cesium is a model system for studying the mechanisms of metal-semiconductor interface formation and a basis for preparing *p*-GaAs(Cs,O) photocathodes with the state of negative effective electron affinity. On the GaAs(001) surfaces the evolution of the surface band bending φ under deposition of cesium was studied by photoreflectance (PR) spectroscopy [1]. This study revealed qualitative differences in the electronic surface states induced by cesium on the As-rich and Ga-rich surface reconstructions, and an unusual non-monotonic behavior («fine structure») in the evolution of φ with the increase of Cs coverage [1]. To clarify the origin of these phenomena and their relation to the morphology of the GaAs(001) surface, in the present work we studied the evolution of the band bending under Cs deposition on the atomically rough and flat GaAs(001) surfaces with various reconstructions. The experiments were performed on GaAs(001) epi-ready substrates and epitaxial layers. The morphology of the surfaces was studied *ex-situ* by the atomic force microscopy. The technique for preparation of atomically flat GaAs(001) surfaces by annealing in equilibrium conditions was developed. The comparison of the band bending behavior under Cs deposition on the atomically flat and rough surfaces proved that surface roughness produces defect-induced surface states which restrict the adatom-induced variations of band bending.

References:

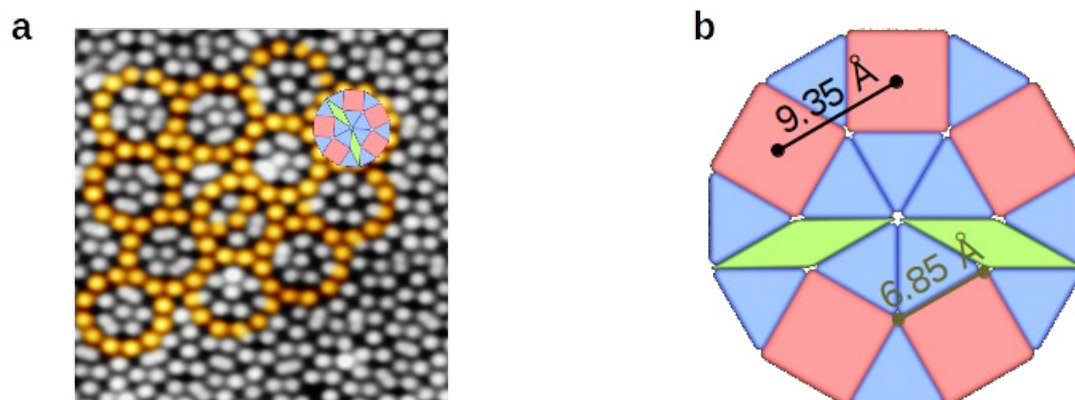
- [1] A. G. Zhuravlev, H. E. Scheibler, A. S. Jaroshevich, V. L. Alperovich, J. Phys.: Condens. Matter 22, 185801 (2010).

Thu-14:40-O-ORGS ●

C₆₀ adsorption on a two-dimensional oxide quasicrystal*ORGS Organic molecules on solid surfaces*Eva Maria Zollner¹, Stefan Förster¹, Rene Hammer¹, Klaus Meinel¹, Wolf Widdra^{1,2}¹ Martin-Luther-Universität Halle-Wittenberg, Halle, Germany;² Max-Planck-Institut für Mikrostrukturphysik, Halle, Germany

The recent observation of a two-dimensional oxide quasicrystal (OQC) at the interface to Pt(111) demonstrates that quasicrystalline structures can emerge in the heteroepitaxial growth of conventional periodic materials [1]. Under reducing conditions, a long-range ordered dodecagonal wetting layer is derived from ultrathin films of BaTiO₃ at the threefold Pt(111) substrate. Atomically-resolved scanning tunneling microscopy (STM) images reveal the formation of a Niizeki-Gähler tiling as shown in Fig. 1a [2,3]. The contrast in the STM image is given by the sublattice of the Ti atoms. The atoms exhibit an arrangement of squares, triangles, and 30° rhombs with a common edge length of 6.85 Å. The characteristic dodecagonal cluster is shown in Fig. 1b.

Due to the complexity of quasicrystalline materials, studies on the relation between aperiodic order and physical properties are challenging. Therefore, quasicrystal surfaces have been tested as templates for the growth of two-dimensional single element quasicrystals formed by molecular adsorbates. Recently, C₆₀ and Pentacene were reported to exhibit quasicrystalline networks on icosahedral Al-Cu-Fe and Ag-In-Yb [4]. Here we report the first adsorption studies on the BaTiO₃-derived OQC using C₆₀ molecules. Their van-der-Waals diameter of 10 Å matches roughly the distance between two neighboring squares (9.35 Å, shown in Fig. 1b). Different coverages of C₆₀ have been deposited on the OQC at room temperature and characterized by low-electron energy diffraction (LEED), x-ray photoemission spectroscopy (XPS), and STM. C₆₀ molecules form hexagonal islands at the OQC surface or absorb at step edges, which indicates a weak interaction with the OQC substrate. With increasing coverages, second layer islands are formed well before the monolayer is completed. At temperatures of 510 K C₆₀ thermal desorption sets in.



References:

- [1] S. Förster et al., Nature 502, 215 (2013).
- [2] N. Niizeki and H. Mitani, J. Phys. A: Math. Gen. 20 L405 (1987).
- [3] F. Gähler, in Quasicrystalline Materials (World Scientific, 1988).
- [4] J. A. Smerdon et al., Nano Lett. 14, 1184 (2014).



33rd EUROPEAN CONFERENCE ON SURFACE SCIENCE

POSTER PRESENTATIONS

Tue-PS1-01**Interstitial impurity induced magnetism on lead oxide surface**

[Elvis F. Arguelles](#)¹, [Shuichi Amino](#)², [Susan Aspera](#)³, [Hiroshi Nakanishi](#)³, [Hideaki Kasai](#)³,
[Wilson Agerico Dino](#)¹

¹ Department of Applied Physics, Osaka University, Osaka, Japan;

² A.L.M.T. Corp;

³ National Institute of Technology, Akashi College;

We investigated the possibility of employing the polycrystalline α PbO as a spintronics device by first principles calculations based on the density functional theory (DFT). In particular, we explored the effects of 3D transition metal atom, Fe on the structural and electronic properties of the layered α PbO (001) surface. Since it has been proven that ferromagnetic signals in experiments are often detected in thin films[1] we used a 2x2, 3-layered surface slab model of α PbO with 20 Å of vacuum space to simulate this environment in this study. The impurity atoms are placed in between the surface and subsurface of the crystal. The results show that the interstitial Fe interstitial forms shorter bonds with the oxygen atoms located at the surface and second layers. Also, this impurity is found to induce magnetism in the host crystal with magnetic moment value of 2.25 μ B, which is highly localised on the transition metal.

In the bonding process, the Fe's lower energy lying d states form overlaps with nearest neighbour oxygen atoms with non-bonding d states situated near or at the Fermi level and are spin split. These spin split orbitals induce spin polarisation of impurity states of oxygen atoms in the subsurface. Moreover, the magnetic order is determined using the energy difference between the antiferromagnetic and ferromagnetic states. The energy difference is 0.068 eV, suggesting that Fe interstitial impurities induce ferromagnetism in α PbO [2]. In this workshop, the effects of charge carriers to the magnetic properties will be briefly discussed. Finally, the position of the Fermi level in the density of states (DOS) suggests that in the case of α -PbO with Fe interstitials where the minority non-bonding d states are partially filled, the Zener's ferromagnetic double exchange mechanism may be dominant and stabilizing the ferromagnetic state.

References:

[1] M. Venkatesan, C. B. Fitzgerald, J. G. Lunney, and J. M. D. Coey, Phys. Rev. Lett. 93, 177296 (2007)

[2] E. F. Arguelles, S. Amino, S. Aspera, H. Nakanishi, and H. Kasai, J. Phys. Soc. Jpn. 84, 045002 (2015)

Tue-PS1-39**Enantioselective reactions on chirally-modified model surfaces:
a new molecular beam/surface spectroscopy apparatus**

[Smadar Attia](#)¹, [Evan J. Spadafora](#)², [Hans J. Freund](#)¹, [Swetlana Schauer](#)²

¹ Department of Chemical Physics, Fritz Haber Institute of the Max Planck Society, Berlin, Germany;

² Institute of Physical Chemistry, Christian Albrechts University of Kiel, Kiel, Germany

A molecular-level understanding of enantioselective processes on chiral surfaces is an important prerequisite for the rational design of new enantiospecific catalysts. Therefore, in this study, the reaction mechanisms, kinetics and dynamics of surface reactions were investigated using multi-molecular beam techniques and *in-situ* surface spectroscopic and microscopic tools on well-defined model surfaces in UHV.

A new UHV apparatus consisting of two independent UHV systems for the preparation and characterization of chirally modified model catalysts has been designed and built. This apparatus comprises three molecular beams (two effusive and one supersonic molecular beam), infrared reflection absorption spectroscopy (IRAS) as well as a number of standard tools for preparation and characterization of model surfaces, both single crystals and nanostructured surfaces consisting of metal nanoparticles supported on thin oxide films. Additionally, the sample can be transferred to an independent unit containing scanning tunneling microscope (STM).

First experiments were carried out at the newly setup UHV apparatus to investigate adsorption and reactivity behavior of a model chiral modifier (R)-(+)-1-(1-Naphthyl)ethylamine (NEA) and a prochiral molecule acetophenone over Pt(111). These processes were investigated over a broad range of coverage and temperature conditions. NEA was found to homogeneously distribute over Pt(111) surface at low coverage and to build island-like structures in the high coverage regime. Currently, co-adsorption of NEA with acetophenone is investigated with STM to follow the formation of NEA-acetophenone complexes on this chirally modified surface.

Spectroscopically, acetophenone was observed to strongly interact with the pristine Pt(111) surface resulting in strong changes of the IR spectra as compared to the unperturbed molecules in multilayers. Further experiments are currently in progress.

Thu-PS2-27**Advancement of sample preparation for atom probe tomography: analysis of nanoporous and single-atom-alloy catalysts**

[Cédric Barroo](#)^{1,2,3}, [Austin J. Akey](#)⁴, [David C. Bell](#)^{2,4}

¹ *Chemical Physics of Materials and Catalysis, Université libre de Bruxelles, 1050 Brussels, Belgium;*

² *John A. Paulson School of Engineering and Applied Sciences, Harvard University, Cambridge MA USA;*

³ *Department of Chemistry and Chemical Biology, Harvard University, Cambridge MA USA;*

⁴ *Center for Nanoscale Systems, Harvard University, Cambridge MA USA*

Atom probe tomography (APT) is a powerful technique for the characterization of composition of materials and their three-dimensional structure down to the atomic-scale. With the new developments in FIB-based sample preparation, there is a growing interest in the analysis of catalytic systems by APT. Our current research focuses on the use of nanostructured materials for sustainable catalysis applications, and more specifically, on metallic alloy catalyst materials that have dual functionality. The principal design feature of the catalyst material is to combine a minor amount of active metal that facilitates creation of reactive intermediates with a less active majority phase that transforms these intermediates to desirable products with high selectivity.

Gold-based catalysts with different architectures are currently being developed, and recent studies highlight the efficiency of nanoporous gold catalysts (npAu) for selective methanol oxidation at low temperatures. Ozone is used to activate the catalysts before reaction. Residual Ag is used in Au-based nanoporous catalysts to activate the oxygen dissociation. Due to the porous structure, the sample preparation requires new developments to analyse such samples by APT: using a combination of *in-situ* e-beam-directed chemical vapor deposition in the focused ion beam (FIB) and lift-out techniques, we were able to successfully image nanoporous gold samples by atom probe tomography, and to analyse the segregation of Ag atoms within the Au backbone.

In addition to this, we will present new progresses in the sample preparation and analysis of single atom alloy (SAA) catalysts: copper-based catalysts are currently being developed for selective dehydrogenation reactions. The typical concentration of Ni on supported Cu nanoparticles is 0.1 or 1%, and it might be difficult to analyse the distribution and the clustering of Ni with regular microscopy techniques, and APT seems to be particularly suited to determine the distribution of Ni within the nanoparticles. 15 nm CuNi_{0.01} nanoparticles were synthesized on graphite and then analysed by APT to reveal the presence of Cu, CuH and Cu_xO_y species. To determine the presence of Ni and/or the presence of clustering in this sample, further data treatment has been performed, as well as comparative STEM-EELS measurements.

As a conclusion, new sample preparation techniques developed in this work allow to perform APT study of samples of increasing complexity.

Tue-PS1-02

Hybrid SEM/AFM metrology for complex surface characterization

Peter Basa¹, Frank Hitzel², Fang Zhou³, Frank Hitzel²

¹ Semilab Semiconductor Physics Laboratory Co. Ltd., Prielle Kornélia u.2., 1117 Budapest, Hungary;

² Semilab Germany GmbH, DME SPM Products, Geysstraße 13, 38106 Braunschweig, Germany;

³ Carl Zeiss Microscopy GmbH, Zeiss Group, Carl-Zeiss-Straße 56, 73447 Oberkochen, Germany

Scanning Electron Microscopes (SEMs) combined with Focused Ion Beam (FIB) tools are today widely used for accurate manipulation/cutting and in-depth analysis of nanostructures. They provide a wide variety of physical parameters, however, they lack of obtaining quantitative electrical parameters of a sample, like conductivity, capacitance, work function, dopant level or similar, neither they can measure viscosity, adhesion forces or elastic modulus/hardness.

For obtaining such parameters on layers buried below the surface, a process resulting cross sectional preparation of the sample has to be done. This has three strong disadvantages: (1) it is a destructive method, (2) it is nearly impossible to target a certain area with high precision, and (3) it is very time consuming. Such difficulties could be overcome by using scanning probe microscope (SPM) metrology, however, integrating such precise probing system, like an atomic force microscope (AFM), to the vacuum chamber of a SEM tool, is not straightforward due to the related technical challenges.

In the recent years, the Semilab/ZEISS AFM Option in a ZEISS Crossbeam workstation was introduced as a unique solution on the market featuring a fully equipped AFM inside a crossbeam system [1]. Commonly, in this system the focused ion beam can be used to reveal the sub surface structure of a sample and enable electrical in-depth analysis by AFM [2,3].

In this study, we present an alternative, novel solution for accessing sub-surface layers: interactive manipulation. In the paper, case studies will be presented as demonstration of the new technique, using hard diamond tips for the modification of the surface silicon samples with electrical circuits, while controlling the force applied to the sample by the AFM feedback loop. The electrical properties of the modified sample surfaces were characterized by using the electron beam as current source, while scanning with AFM at constant distance from the sample using an electrically conductive tip.

In summary, the AFM in the SEM enables possibilities to access information of buried layers which no other system can provide. Moreover, depending on the type of AFM tip, either cutting or polishing behaviour can be achieved. This in many cases can make the crosssection preparation or FIB cutting unnecessary and results in uncontaminated exposition of surfaces.

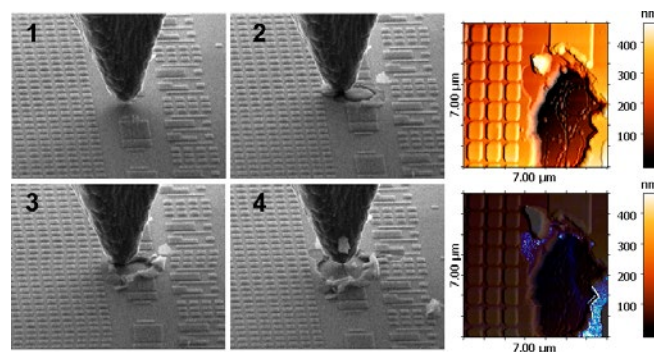


Fig. 1 Diamond tip modification of the Si sample surface, using *in-situ* monitoring of the process with SEM, and AFM images revealing the resulted structure topography during the process

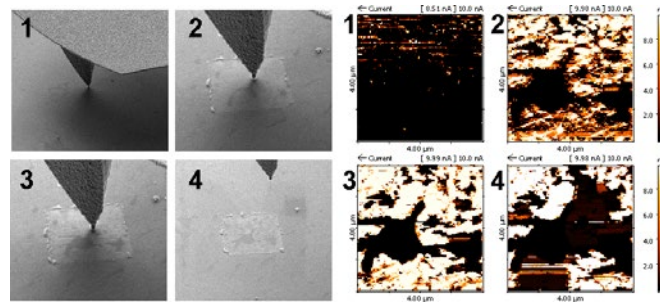


Fig. 2.: Diamond cantilever with relatively larger tip polishing the surface, and removing a few nm of material with every scan. The conductive AFM images show the step by step increase of sample conductance, thus, indicating the removal of the insulating surface layer

References:

- [1] N. Anspach, F. Hitzel, F. Zhou, Soeren Eyhusen, *Microsc. Microanal.* 20 (3), 2014
- [2] R. Saive, M. Scherer, C. Mueller, J. Schinke, M. Kroeger, W. Kowalsky, *Adv. Func Mat.* 23 (47) 2013, pp. 5854
- [3] R. Saive, C. Mueller, J. Schinke, R. Lovrincic, W. Kowalsky, *Appl. Phys. Lett.* 103, 243303 (2013)

Thu-PS2-22

Reduction and nitrogen implantation of graphene-oxide thin films in low pressure N-containing plasma

I. Bertóti, M. Mohai

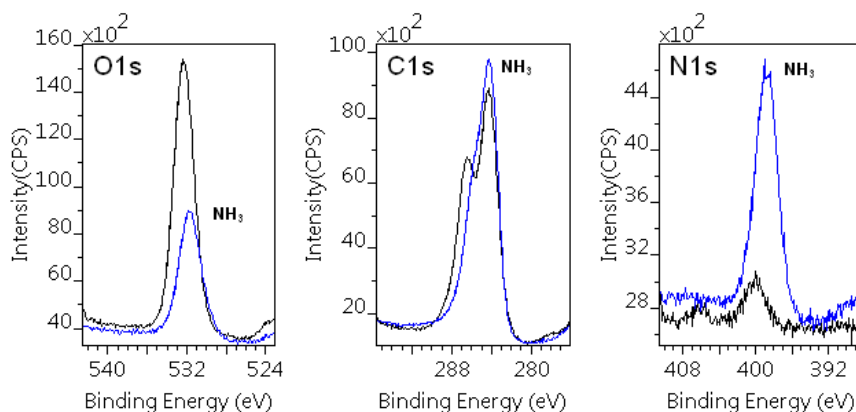
Institute of Materials and Environmental Chemistry, Research Centre for Natural Sciences, Hungarian Academy of Sciences, Budapest 1117, Magyar tudósok krt. 2, Hungary

It has been shown recently that nitrogen introduction into graphene (GR) and also simultaneous reduction of graphene oxide (GO) can be performed in nitrogen glow discharge plasma [1,2]. The resulting modified surface supposed to be further functionalized altering the properties of GO to make favourable for different applications.

In this work we performed low pressure plasma treatment of thin layers of commercial GO samples in two nitrogen containing gases, N_2 and NH_3 . Experiments were performed in the preparation chamber of the X-ray photoelectron spectrometer, allowing 'in situ' characterization of the treated surface. Reduction and introduction of nitrogen into the top surface of GO and GR was intensified by applying negative voltage on the sample between 0–300 V served for accelerating the positive plasma ions towards the sample.

Significant amount of nitrogen (≈ 10 atomic %) was built into the top few atomic layers of the GO samples at application of both types of plasma gases for a short 10–20 min reaction time.

At increasing the bias, the N-content increased in GR and GO, together with the decrease of the O content in GO. The high resolution C1s, O1s and N1s spectra are broad, representing existence of different chemical states (Fig. 1). The peak envelopes of the O1s and N1s lines could be decomposed essentially to three, while the C1s spectrum to five different, well separated peaks, with energy values being identical for all samples. The component peaks were assigned to specific chemical bonding states. The relative amounts of C–O and C–N bonding states changed significantly with advancement of the treatment performed at increasing biases. We attempted to establish interrelations among the different C–O and C–N states. The reasonable agreement found among the amounts of interconnected bonding states supported the validity of the suggested assignments.



Acknowledgement: This work was partly sponsored by the National Scientific Research Fund (OTKA) No. K-109558.

References:

- [1] I. Bertóti, M. Mohai, K. László, Surface modification of graphene and HOPG by nitrogen plasma: Quantitative XPS analysis of chemical state alterations, *Carbon* 84: 185–196, 2015.
- [2] M. Mohai, I. Bertóti, Modification of graphene-oxide surface in nitrogen and argon glow discharge plasma, *Surf. Interface Anal.* 2016, 48, 461–464

Tue-PS1-04**Nitrogen doping of titania nanomaterials using thermal and plasma activation**

Balázs Buchholcz¹, Kamilla Plank¹, Miklós Mohai², Ákos Kukovecz^{1,3}, János Kiss⁴, Imre Bertóti², Zoltán Kónya^{1,5}

¹ Department of Applied and Environmental Chemistry, University of Szeged, H-6720, Rerrich B. 1, Hungary;

² Hungarian Academy of Sciences (HAS), Research Centre of Natural Sciences, Institute of Materials and Environmental Chemistry, Budapest H-1117 Budapest, Magyar tudósok körútja 2.;

³ MTA-SZTE "Lendület" Porous Nanocomposites Research Group, Rerrich Béla tér 1, H-6720 Szeged, Hungary;

⁴ Department of Physical Chemistry and Materials Science, University of Szeged, H-6720, Aradi vértanúk tere 1, Hungary;

⁵ MTA-SZTE Reaction Kinetics and Surface Chemistry Research Group, University of Szeged, H-6720, Rerrich B. 1, Hungary

Among various semiconductors, titanium dioxide (TiO₂) as photocatalyst was studied excessively due to its advantages such as chemical and biological stability and of higher oxidative potentials. It is also widely proposed to solar cells and different photo-catalytic applications. Specific properties of titanias to meet complex requirements are often achieved by doping with different elements. N doping is one of the most popular way to decrease band-gap energy of the TiO₂. Recent development of titanium dioxide moved to a novel class of TiO₂-based one-dimensional layered titanate nanomaterials [1].

In this work Na-titanate nanotubes and nanowires were synthesized and their nitrogen doping was attempted using thermal and low pressure plasma activation. First the Na ions were replaced by hydrogen and layered nanotubes (100-120 nm length with 5-6 nm inner and 11-12 nm outer diameters), and nanowires (2-5 μm length with ca. 200 nm diameter) were obtained for these studies.

Thermal modification was performed at 300-500 K in order to preserve the as prepared preferable nanostructure. N-content in the range of around 10 at% could be achieved when NH₃ or NH₄F were used as precursors. In these cases O-Ti-N clusters (N1s at 399.5 eV) and NH groups were formed.

It has been shown recently that N₂⁺ bombardment of TiO₂ leads to incorporation of significant amount of N at room temperature avoiding use of any additional chemistry [2]. Based on these findings low pressure N₂ and NH₃ plasma treatment was explored for doping the surface of these nanotitanates by nitrogen. Implantation of the positive plasma ions was enhanced by 300 V negative bias applied to the sample layers deposited on conductive foil substrates. It turned out that while only 5-8 at% N is incorporated from N₂ plasma, significant oxygen removal and about 18 at% N-content can be achieved at NH₃ plasma treatment. Four different chemical states of N (mostly at N-Ti-N position, N1s at 396.3 eV) and also the reduced states of Ti are detected by XPS (Fig 1).

These latter findings were compared with the results obtained using thermally activated nitriding and interpreted involving, among others, the atomic specificity of these titanate nanophases.

Tue-PS1-05

Self-assembly of ordered graphene nanodot arrays

Luca Camilli¹, Jakob H. Jørgensen², Richard Balog², Andrew Cassidy², Liv Hornekær², Jerry Tersoff³, Jerzy T. Sadowski⁴, Adam Stoot⁵, Peter Bøggild⁵

¹ Center for Nanostructured Graphene, DTU Nanotech, Technical University of Denmark, DK-2800, Kongens Lyngby, Denmark;

² Department of Physics and Astronomy and Interdisciplinary Nanoscience Center iNANO, Aarhus University, 8000 Aarhus C, Denmark;

³ IBM T. J. Watson Research Center, Yorktown Heights, New York 10598, USA;

⁴ Center for Functional Nanomaterials, Brookhaven National Lab, Upton, New York 11973, USA;

⁵ Center for Nanostructured Graphene, DTU Nanotech, Technical University of Denmark, DK-2800, Kongens Lyngby, Denmark

The ability to fabricate nanoscale domains of uniform size in two-dimensional (2D) materials would enable new applications in nanoelectronics and the development of innovative metamaterials. However, achieving even minimal control of growth of 2D lateral heterostructures at such extreme dimensions has proven exceptionally challenging. Particularly intriguing is the evolution and arrangement of nanoscale domains within a two-dimensional layer made of boron, carbon and nitrogen (BCN). Previous work performed on ruthenium reported the evolution of graphene submonolayers subjected to progressive exposure to borazine vapors [1].

Here we show the spontaneous formation of ordered graphene nanodot arrays epitaxially embedded in a 2D boron-carbon-nitrogen (BCN) alloy [2]. A full set of complementary *in-situ* microscopy and spectroscopy techniques (including scanning tunnelling microscopy, X-ray photoemission spectroscopy and low-energy electron microscopy and diffraction) is used in this study.

The nanodots exhibit a strikingly uniform size of $1.6\text{nm} \pm 0.2\text{nm}$ and strong ordering, and the periodicity of the array can be tuned by adjusting the growth conditions (Figure 1). We use a model incorporating dot-boundary energy, a moiré-modulated substrate interaction, and long-range repulsion between dots to explain our findings.

This new 2D material, an ordered composite of uniform-size graphene nanodots laterally integrated within a continuous matrix, might hold promise for novel electronic and optoelectronic properties, with a variety of potential device applications.

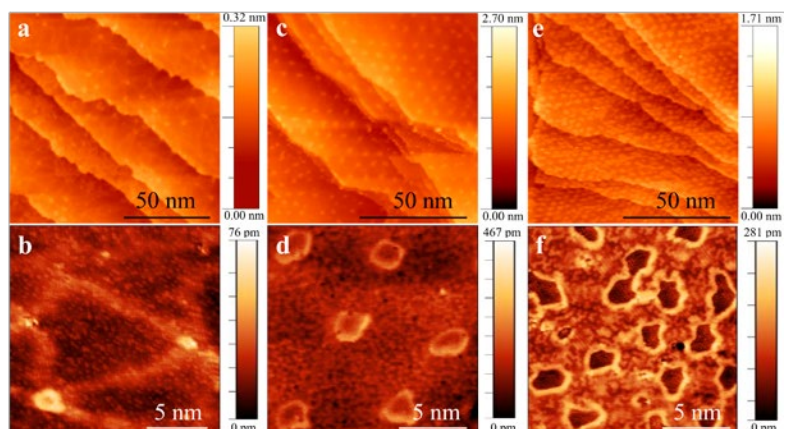


Figure: STM images of an Ir(111) surface after co-deposition of borazine and ethylene at various C fractions: (a, b) low, (c, d) medium and (e, f) high C fraction.

References:

- [1] J. Lu, et al. Nature Communications, 4 (2013) 2681
 [2] L. Camilli, et al. Nature Communications, In press (2017)

Thu-PS2-47
Effect of conduction band non-parabolicity on the intersubband transitions in ZnO/Mg_xZn_{1-x}O Quantum Well Heterostructures

 Younes Chrafh¹, Rahmani Khalid², Izeddine Zorkani³
¹ Sustainable development laboratory, Departement of Physics; Beni Mellal-Morocco;

² LIRST Faculty of Polydisciplinary, Beni Mellal-Morocco;

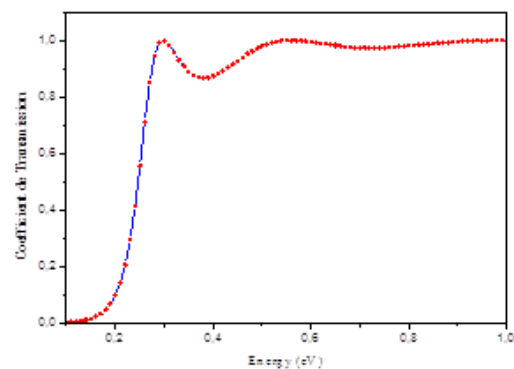
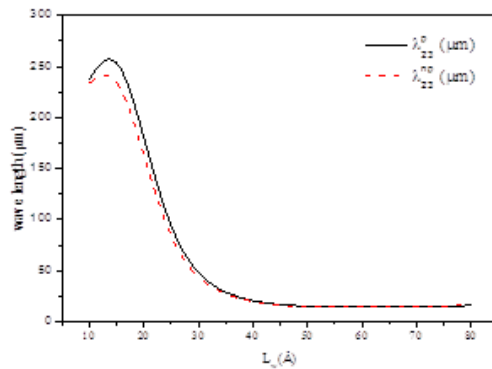
³ LPS, Faculty of Sciences Dhar Mehraz, Fès-Morocco

In this paper, we have calculated the electronic states and the intersubband transition energy in ZnO/Mg_xZn_{1-x}O quantum well structures (QW), with 20% of Magnesium in both the parabolic and the non-parabolic cases. Our calculations are performed in the context of the approximation of the envelope function formalism and using the finite difference method.

The results show that the intersubband transition energy increases rapidly with well width until $L_w=5\text{nm}$ and becomes almost constant (specially transitions E_{13} et E_{23}). The non-parabolicity effect is neglect.

Wavelength λ_{23} decreases with well width until $L_w=5\text{nm}$ and becomes constant. The non-parabolicity effect is more pronounced for small QW ($L_w \leq 5\text{nm}$) and less marked in narrow and large QW.

Also, we are studied the coefficient of transmission for 4(nm)/2(nm)/4(nm) geometry. We notice that when the height of barrier increases the coefficient of transmission decreases. It will be necessary to provide more energy to the electron so that it can cross the barrier. We also notice the variations related to a phenomenon of reflexion quantum.



Keywords:

Quantum well, Intersubband transitions, Conduction band, Non-parabolicity, Transmission coefficient, Wavelength.

References:

- [1] H. Akabli, A. Almaggoussi, A. Abounadi, A. Rajira, K. Berland, and T. G. Andersson, Superlattices and Microstructures 52, 70 (2012).
- [2] S.H. Park, D. Ahn, Intersubband energies in strain-compensated InGaN/AlInN quantum well structures; AIP Advances 6, 15014 (2016).
- [3] T.F. George, Computational studies of new materials II: from ultrafast processes and nanostructures to optoelectronics, energy storage and nanomedicine. World Scientific, Singapore ; Hackensack, NJ (2011).

Tue-PS1-38**Structural and Electronic modifications induced by reduction in cerium oxide nanoparticles**

[Jacopo Stefano Pelli Cresi](#)¹, [Maria Chiara Spadaro](#)^{1,2}, [Sergio D'Addato](#)^{1,2}, [Sergio Valeri](#)^{1,2}, [Lucia Amidani](#)³, [Federico Boscherini](#)^{4,5}, [Giovanni Bertoni](#)⁶, [Davide Deiana](#)⁷, [Paola Luches](#)²

¹ Dipartimento di Scienze Fisiche Informatiche e Matematiche, Università degli Studi di Modena e Reggio Emilia, Via G. Campi 213/a, 41125 Modena, Italy;

² Istituto Nanoscienze, Consiglio Nazionale delle Ricerche, Via G. Campi 213/a, 41125 Modena, Italy;

³ European Synchrotron Radiation Facility, BP 220, F-38043 Grenoble, France;

⁴ Department of Physics and Astronomy, University of Bologna, Viale C. Berti Pichat 6/2, 40127 Bologna, Italy;

⁵ Istituto Officina dei Materiali, Consiglio Nazionale delle Ricerche, Operative Group in Grenoble, c/o ESRF, BP 220, F-38043 Grenoble, France;

⁶ Istituto Materiali per Elettronica e Magnetismo, Consiglio Nazionale delle Ricerche, Parco Area delle Scienze 37/A, 43124 Parma, Italy;

⁷ Interdisciplinary Centre for Electron Microscopy, Ecole Polytechnique Fédérale de Lausanne, Station 12, 1015 Lausanne, Switzerland

Cerium dioxide is one of the most attractive oxides used in catalytic applications today. Its high reducibility (the ability of forming, filling and transporting oxygen vacancies) makes this material appealing for applications like fuel cells and biomedicine. A correct description of the structural and chemical modifications of cerium oxide confined into nanoparticles (NP) is very important in view of understanding the functionality of the material for its applications. In order to optimize the system, we investigated the reduction induced by thermal treatment in high vacuum of NP with diameter from 9 nm until 4 nm using a surface spectroscopy as XPS (x-ray photoelectron spectroscopy) and bulk spectroscopies as XANES (X-ray Absorption Near Edge Spectroscopy) and EXAFS (Extended X-ray Absorption Fine Spectroscopy) at the European Synchrotron Radiation Facility. The relatively low degree of reduction detected by XANES measurements on the cerium oxide NP before the reducing thermal treatment indicates that the bulk of the NP is well oxidized, although the Ce³⁺ species represent a non-negligible minority component. The comparison with the systematically higher values of Ce³⁺ concentration detected by XPS, which is a surface sensitive technique, indicates that the Ce³⁺ species are mainly localized near the surface. Thermal treatment in high vacuum has previously shown to induce a reduction detected by x-ray photoemission spectroscopy[1]. However, a mild reduction is observed by XAS which is sensitive to the whole NP volume. This suggests that the reduction process involves mainly the NP surface, while the bulk maintains the CeO₂ stoichiometry. EXAFS spectra, instead, show a systematic compression of the Ce-O interatomic distance with decreasing NP size that we relate to a reduced dimensionality effect.

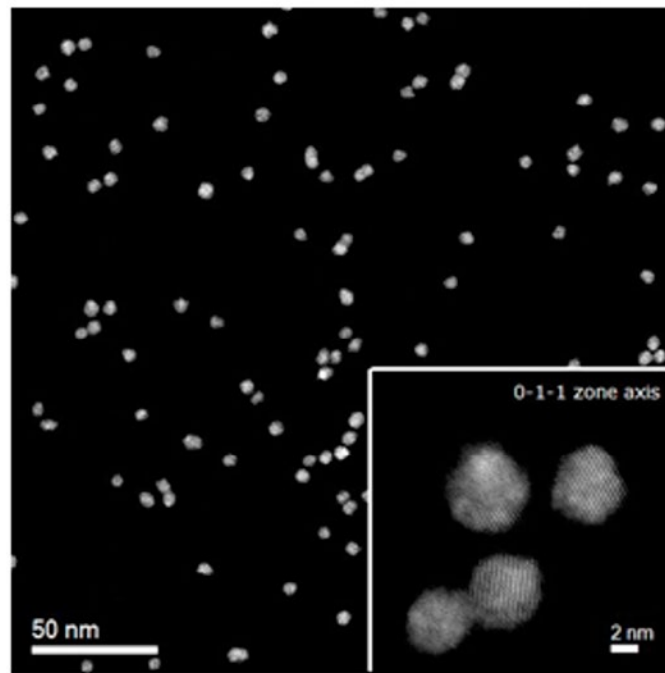


Fig. 1. STEM image of NP with 4nm diameter. The NP show a good monodispersion and a single crystalline structure.

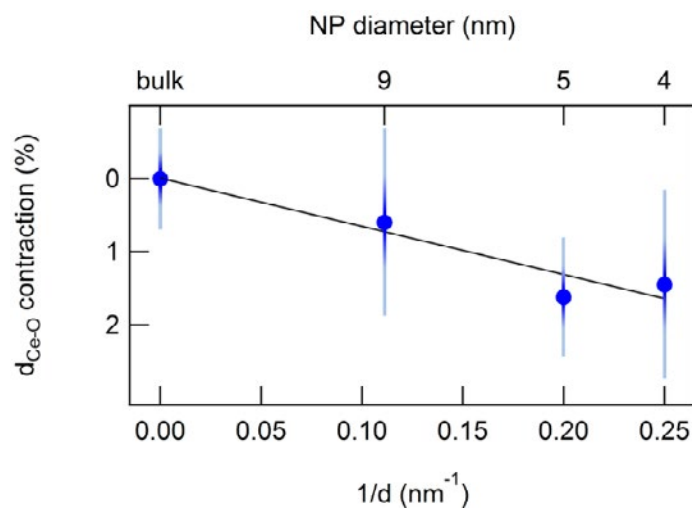


Fig. 2. STEM image of NP with 4nm diameter. The NP show a good monodispersion and a single crystalline structure.

References:

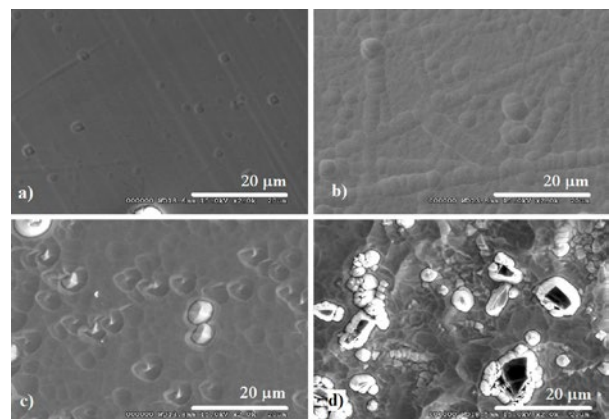
- [1] M. C. Spadaro, S. D. Addato, G. Gasperi, F. Benedetti, P. Luches, V. Grillo, G. Bertoni, and S. Valeri, "Morphology , structural properties and reducibility of size-selected CeO_{2-x} nanoparticle films," pp. 60–67, 2015.

Tue-PS1-06

Effect of growing conditions on surface modification of PbTe crystals caused by Ar⁺ ion bombardmentA Csik¹, D M Zayachuk², V E Slynko³¹ Institute for Nuclear Research, Hungarian Academy of Sciences (ATOMKI), Debrecen, Hungary;² Lviv Polytechnic National University, Lviv, Ukraine;³ Institute for Problems of Materials Science NASU, Chernivtsy branch, Chernivtsy, Ukraine

Ion bombardment is a widely used method for surface modification in microelectronic technologies and in studies of crystals and thin films. In this work we present results of the effect of Ar⁺ ion bombardment on the state of PbTe crystal surfaces depending on their growth conditions. Two types of crystal surfaces were studied: the surface of a crystal grown from vapor phase (free growing of the crystal) and a surface grown from a melt by the Bridgman method (growing of the crystal under mechanical impact caused by the quartz container). Different types of crystal surfaces were treated by Ar⁺ plasma: natural faceted surfaces corresponding to the crystallographic planes of high symmetry, natural lateral surfaces of crystal ingots, and surfaces which were mechanically processed during the cutting of the crystals. Sputtering experiments were carried out at the conditions of Secondary Neutral Mass Spectrometry. The surface morphology of samples after ion bombardment was analyzed by a Scanning Electron Microscopy.

We found that the growth environment of the PbTe crystal surfaces takes a very strong effect on the character of their modification under impact of Ar⁺ ion bombardment. The Figure shows the main results of our experiment which was performed by Ar⁺ ions with energy of 350 eV during 50 minutes of sputtering. Figure (a) corresponds to the natural (100) surface of the vapor phase crystal, Figure (b) and Figure (c) correspond to the lateral surfaces of the crystals grown from vapor phase and melt, respectively. Figure (d) corresponds to the surface processed mechanically. As it can be seen, the free natural facet surface was uniformly sputtered by Ar⁺ ion beam. The main surface modification was the emergence of single dislocation etch pit, the form of which was determined by crystallographic orientation of the surface. The lateral surface of the crystal grown from the vapor phase was also modified in similar way by sputtering (Figure (b)). The density of dislocation etch pits on the lateral surface was only much larger, and dislocation chains were dominated there. Occasionally one can observe small formations as islands of re-deposited phase in the dislocation etch pits. Sputtering process of the lateral surface of PbTe crystal grown from melt formed dimple reliefs on the surface (Figure (c)). Another pronounced effect was the appearance of an array of small microscopic structures on the surface as a result of re-deposition of sputtered Pb and Te atoms. It was observed that at a constant sputtering energy the average size of re-deposited microscopic surface structures decreased with the decrease of duration time, but their surface density increased. The same modifications were observed when the mechanically processed surface was bombarded (Figure (d)): while dimple reliefs were more developed, the density and average size of re-deposited structures became larger.



The work was supported by National Research, Development and Innovation Office of Hungary, project no. GINOP-2.3.2-15-2016-00041. The project is co-financed by the European Union and the European Regional Development Fund.

Tue-PS1-07**Nano-spectroscopy of phonon-polariton modes in boron nitride nanostructures**

[Daniel Datz](#)¹, [Gergely Németh](#)¹, [Áron Pekker](#)¹, [Kate Walker](#)², [Graham Rance](#)²,
[Andrei Khlobystov](#)², [Katalin Kamarás](#)¹

¹ *Institute for Solid State Physics and Optics, Wigner Research Centre for Physics, HAS, Budapest;*

² *School of Chemistry, University of Nottingham, Nottingham*

Scattering-type scanning nearfield optical microscopy (s-SNOM) is an effective device for optical imaging of nano-objects below the Abbe limit. The method is especially useful for detecting collective excitations in low-dimensional nanostructures due to surface enhanced scattering. In this study we examine the phonon-polariton excitations of a single, multi-walled boron nitride nanotube. The tubes were deposited on a silicon substrate under surface resonant conditions. Samples were investigated before and after a cleaning and opening procedure. We find that the characteristic phonon-polariton mode at 1380 cm^{-1} is present in both the cleaned and the uncleaned nanotubes. However, in the cleaned sample additional peaks appear at different wavenumbers, heavily localized along the nanotube. These peaks suggest that the cleaning procedure introduces defects in the structure of the nanotube, that can be detected by the localized phonon-polariton modes around the defect sites.

Thu-PS2-43
Oxide layer growth and hydrogen transfer processes at the surface of tungsten

Abdel El kharbachi^{1,2}, Loïc Marchetti^{3,4}, Frédéric Miserque³, Bernard Rousseau¹

¹ CEA, SCBM, Laboratoire de Marquage par le Tritium, 91191 Gif-sur-Yvette, France;

² Institute for Energy Technology, P.O. Box 40, NO-2027 Kjeller, Norway;

³ CEA, DEN, DPC, SCCME, Laboratoire d'Étude de la Corrosion Aqueuse, F-91191 Gif-sur-Yvette;

⁴ CEA, DEN, DTCD, SECM, Laboratoire d'Étude du Comportement à Long Terme des matériaux de conditionnement, F-30207 Bagnols-sur-Cèze, France

Tungsten is a particular metal. Among other, it does not form any hydride in the presence of hydrogen at moderate conditions; hence it constitutes a unique model for the study of bond-free metal–hydrogen interactions. In this work, we present an investigation of hydrogen absorption processes at the surface of tungsten. In particular, the aim is to track, using hydrogen isotopes detection methods, the mechanism governing the absorption of hydrogen in the presence of an oxide layer at the tungsten surface. Figure 1 shows the structural characterization of the W powders used in this study. The obtained powders by ball-milling were deoxidized and hydrogenated using the experimental set-up described elsewhere [1]. XPS analysis shows a well identified layer of WO_x ($2 \leq x \leq 3$), thickness of which is evolving upon the annealing process. The mechanism of interaction between O_2 and H-enriched W particles is presented and discussed according to the specific surface area of the W particles and ambient gas conditions. Questions related to surface limited processes are also addressed at the light of possible application in fuel cell devices.

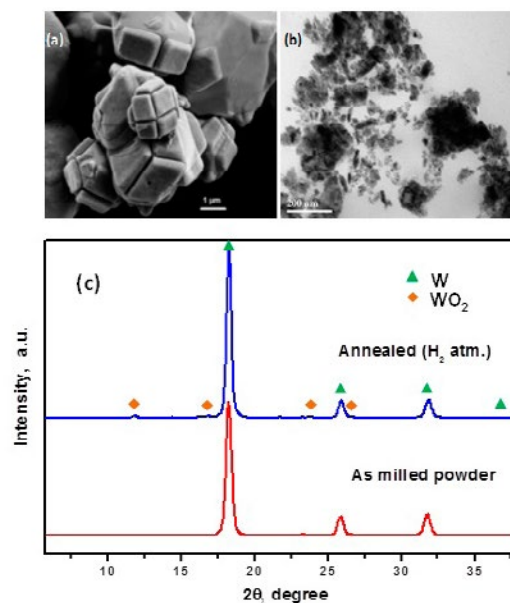


Fig. 1. Structural characterization of the W powders used in this study: (a) SEM image of the commercial powder, (b) TEM image of the milled powder and (c) XRD patterns of the as milled and annealed (750 K / H_2 atm.) W powders.

References:

- [1] A. El kharbachi, J. Chêne, S. Garcia-Argote, L. Marchetti, F. Martin, F. Miserque, D. Vrel, M. Redolfi, V. Malard, C. Grisolia, B. Rousseau, *Int. J. Hydrogen Energy* 39 (2014) 10525-10536.

Thu-PS2-10**Stochastic kinetic mean-field model – a new atomic scale simulation method**

[Bence Gajdics](#)¹, [Zoltán Erdélyi](#)¹, [Mykola Pasichny](#)², [Volodymyr Bezpalcuk](#)²,
[János J. Tomán](#)¹, [Andriy M. Gusak](#)²

¹ *Department of Solid State Physics, University of Debrecen, Debrecen, Hungary;*

² *Department of Physics, Cherkasy National University, Cherkasy, Ukraine*

We introduce a new model for evaluating the change in time of three-dimensional atomic configurations. The method is based on the kinetic mean field (KMF) approach [1], nevertheless we have transformed that model into a stochastic approach by introducing dynamic Langevin noise. The result is a stochastic kinetic mean field model (SKMF) which has very similar applicability and outcomes to lattice kinetic Monte Carlo (KMC). SKMF is, however, more cost-effective, the algorithm is easier to implement and its results are simpler to interpret. [2] The group made the software and the source code (together with tutorials) freely available to the scientific community at the <http://skmf.eu> webpage. [3] By modifying the program and using surface energies instead of periodic boundary condition, we are able to simulate samples having different shapes and sizes (e.g. nanospheres).

References:

- [1] Martin G., Atomic mobility in Cahn's diffusion model, *Phys. Rev. B* 41, 2279-2283 (1990)
- [2] Erdélyi Z., Pasichnyy M., Bezpalcuk V., Tomán J.J., Gajdics B., Gusak A.M., Stochastic Kinetic Mean Field Model, *Computer Physics Communications* 204: pp. 31-37. (2016), <http://dx.doi.org/10.1016/j.cpc.2016.03.003>.
- [3] <http://skmf.eu>

Tue-PS1-09**Synthesis, metalation and structures of tetrapyrroles at interfaces**

J. Michael Gottfried, Malte Zugermeier, Min Chen, Hans-Jörg Drescher, Benedikt P. Klein, Claudio K. Krug, Martin Schmid

Fachbereich Chemie, Philipps-Universität Marburg, Germany

Tetrapyrrole macrocycles such as porphyrins, phthalocyanines, naphthalocyanines, and corroles have gained high technological relevance [1]. Due to their versatile electronic and structural features, these macrocycles and their metal complexes are used as organic semiconductors in optoelectronic devices, including organic light-emitting diodes or organic photovoltaic cells [2]. The planar metal complexes also exhibit useful catalytic properties and can be used for surface functionalization. Here, we investigated structure and reactivity of various metal/tetrapyrrole interfaces and addressed the following topics:

(a) Metalation and oxidation state tuning of tetrapyrroles on single crystalline surfaces: Porphyrin and phthalocyanine monolayers react with coadsorbed metal atoms to form metal(II) complexes [1], while corroles can oxidize metal atoms to the +III oxidation state. This can be employed to control the electronic properties and reactivity of tetrapyrrole-functionalized surfaces.

(b) On-surface synthesis of tetrapyrroles: Adsorbed ortho-dicarbonitriles form naphthalocyanines by cyclotetramerization in the presence of iron. This reaction is useful to create tetrapyrroles directly on a surface by covalent linking of smaller subunits, especially when the target molecule is too large or fragile for vapor deposition.

(c) Structure: The molecular arrangement of tetrapyrroles in the monolayer is controlled by a complex interplay of molecule-substrate and molecule-molecule interactions.

(d) Buried interfaces: Tetrapyrroles represent useful model compounds for studying reactive buried metal/organic interfaces, which occur in organic electronic devices [3]. Insights into these complex surface and interface systems were obtained by various spectroscopic and microscopic techniques.

References:

- [1] J. M. Gottfried, Surface Chemistry of Porphyrins and Phthalocyanines, *Surf. Sci. Rep.* 70 (2015) 259-379.
- [2] J. M. Gottfried, Quantitative Model Studies for Interfaces in Organic Electronic Devices, *New J. Phys.* 18 (2016) 113022.
- [3] M. Chen, H. Zhou, B. P. Klein, M. Zugermeier, C. K. Krug, H.-J. Drescher, M. Gorgoi, M. Schmid, J. M. Gottfried*, Formation of an Interphase Layer During Deposition of Cobalt onto Tetraphenylporphyrin: A Hard X-Ray Photoelectron Spectroscopy (HAXPES) Study *Phys. Chem. Chem. Phys.* 18 (2016) 30643 - 30651.

Thu-PS2-04**X-ray photoemission studies of liquid model systems for Pt-Ga and Pd-Ga bimetallic dehydrogenation catalysts**

[Mathias Grabau](#)¹, [Jannis Erhard](#)², [Nicola Taccardi](#)³, [Sandra Krick Calderon](#)¹, [Christian Neiss](#)², [Peter Wasserscheid](#)³, [Andreas Görling](#)², [Hans Peter Steinrück](#)¹, [Christian Papp](#)¹

¹ *Physikalische Chemie 2, FAU Erlangen, Egerlandstraße 1-3, 91058 Erlangen;*

² *Theoretische Chemie, FAU Erlangen, Egerlandstraße 1-3, 91058 Erlangen;*

³ *Chemische Reaktionstechnik, FAU Erlangen, Egerlandstraße 1-3, 91058 Erlangen*

The use of binary alloys in well-functioning catalysts, in particular in applied industrial catalysis, is not a new concept. During the last decades, however, multi-metallic model systems have also attracted more and more the interest of surface scientists, seeking to understand the reasons for activity, selectivity and stability of certain catalyst systems on an atomic level [1,2,3]. In this study, we investigated liquid model catalysts consisting of bimetallic Pt-Ga and Pd-Ga alloys, among them a silica supported Pd-Ga system, in ultra-high vacuum using angle-resolved X-ray photoemission spectroscopy (ARXPS), and under reactive environments using near-ambient pressure XPS (NAP-XPS). It was shown that supported alloy catalysts outperform commercial catalysts in dehydrogenation of light alkanes [4].

For the liquid phase of Pd-Ga alloys, an inhomogeneous Pd distribution along the surface normal was derived by quantitative evaluation of ARXPS data collected in 0 and 80° emission at temperatures between 450 and 750 K. From these data, in combination with molecular dynamics simulations, we deduce a Pd depletion of the interface, which goes along with a Pd enrichment in the surface-near region below the interface. We also followed the oxidation of liquid Ga and the alloys in up to 1 mbar of oxygen *in situ* at different temperatures between room temperature and 550 K. Upon oxidation, a Pd-lean Ga₂O₃ film forms that covers the liquid-vacuum interface. This results in a redistribution of Pd towards the sample bulk. The redistribution of Pd is shown to be independent of pressure. Contrary, for the Pt-Ga system, enrichment of Pt within the Ga₂O₃ film by incorporation of Pt atoms or clusters is observed. The demonstrated behavior is independent of pressure or sample temperature, although, as is expected, the growth of Ga₂O₃ films shows strong temperature and pressure dependences.

XPS and online mass spectrometry studies on the reactivity of supported PdGa alloys will be discussed.

References:

[1] Clarke, J. K. A. *Chem. Rev.* 1975 75, 291- 305.

[2] Ponc, V. *Appl. Cat. A* 2001 222, 31-45.

[3] Zafeiratos, S.; Piccinin, S.; Teschner, D. *Catal. Sci. Technol.* 2012 2, 1787-1801.

[4] Taccardi, N. et al. 2017, submitted for publication.

Tue-PS1-10

Au-Pd nanoparticles and Au/Rh double layers on TiO₂(110)

Richard Gubó^{1,2}, Chi Ming Yim³, Michael Allan³, Chi Lun Pang³, László Óvári^{1,4},
András Berkó⁴, Geoff Thornton³

¹ ELI-ALPS, ELI-HU Nonprofit Ltd., 6720 Szeged, Dugonics tér 13., Hungary;

² Department of Applied and Environmental Chemistry, University of Szeged, Rerrich B. tér 1., H-6720 Szeged, Hungary, richardgubo@hotmail.com;

³ London Centre for Nanotechnology, University College London, 20 Gordon Street, London, WC1H 0AJ, U.K.;

⁴ MTA-SZTE Reaction Kinetics and Surface Chemistry Research Group, Rerrich B. tér 1., H-6720 Szeged, Hungary

Atomically dispersed bimetallic surface alloys are excellent nanocomposite materials for fine-tuning of the active centers in the homogeneous, heterogeneous, photo- and electro-catalysts. By systematic studies performed on 2D model systems, it is possible to study the structural and enhanced catalytic properties of alloyed, bimetallic systems. The formation and thermal evolution of nanoparticles on reducible oxide surfaces is a rather complex diffusion process due to the so-called decoration phenomenon where a reduced form of the oxide support covers metal nanoparticles. By applying STM, AES and LEED methods, in this work the thermally induced material transport processes are investigated and compared for two significantly different systems, namely for the bulk miscible Au-Pd and for the bulk-immiscible Au-Rh double films supported on rutile TiO₂(110).

In the case of monometallic Pd or Rh nanofilms (nanoparticles) the upward diffusion of Ti and O from TiO₂(110) is completed at around 850 K, which results in the formation of a uniform TiO_x atomically thin oxide layer on top of the metal layers, due to the strong metal support interaction (SMSI) [1, 2].

Regarding the Au-Pd system, a continuous 5 ML thick palladium film was prepared on TiO₂(110) using PVD at room temperature and it was further covered with 1 ML gold. According to the AES and STM measurements the bimetallic film de-wets around 850 K to form nanoparticles. In this temperature range the results suggest that there is penetration of gold into the subsurface regions of Pd, creating an Au-Pd core, Pd shell structure, due to the favorable miscibility of Au with Pd. Moreover, the nanoparticles are encapsulated with a TiO_x layer. However, by increasing the relative gold content (3 ML Pd/2 ML Au), a similar thermal treatment results in the formation of Au-Pd bimetallic nanoparticles with gold enrichment on top, which blocks the decoration process. These observations support the conclusions described previously in [3] and provide complementary information.

Regarding the Au-Rh system, a different behavior was observed. By preparing a 3 ML gold layer on a continuous rhodium film (30 ML) deposited on TiO₂(110) surface at room temperature, the thermal treatment induced only a strongly hindered TiO_x encapsulation due to the blocked oxygen diffusion up to 850 K, although it was possible to detect 3D TiO_x nanoclusters at higher temperatures (950 K). According to our LEIS, XPS and STM measurements, it was found that the gold layer (partially alloyed with Ti) is able to cover completely the Rh surface and to hinder its encapsulation by a 2D TiO_x nanofilm.

References:

- [1] L. Óvári, A. Berkó, R. Gubó, Á. Rácz, Z. Kónya: Journal of Physical Chemistry C 118 (2014) 12340.
- [2] R. A. Bennett, C. L. Pang, N. Perkins, R. D. Smith, P. Morrall, R. I. Kvon, M. Bowker, Journal of Physical Chemistry B 106 (2002) 4688.
- [3] R. Sharpe, J. Counsell, M. Bowker, Surface Science 656 (2017) 60.

Tue-PS1-11

Hydrogenation of CO₂ on Pt nanoparticles supported on NiO

Gyula Halasi^{1,2}, A. Sápi¹, D. Dobó¹, K. Baán¹, J. Kiss¹, Z. Kónya^{1,2}

¹ University of Szeged, Department of Applied and Environmental Chemistry – Szeged (Hungary);

² MTA - SZTE Reaction Kinetics and Surface Chemistry Research Group of the Hungarian Academy of Sciences at the University of Szeged – Szeged (Hungary)

The activation of CO₂ and its conversion into more valuable compounds is a great challenge for heterogeneous catalysis¹. Previous work found that earlier belief CO₂ does not dissociate on supported Rh at 300 K, but addition of H₂ to CO₂ induces its dissociation even at room temperature and leads to the formation of formate species. This result was confirmed on Rh(111) in UHV by several electron spectroscopic measurements². It was an important finding that the catalytic performance of the Pt metals in the hydrogenation of CO₂ is strongly affected by the nature of the supports. It appears that the interest in the carrier effect became more intensive nowadays thanks to the modern surface science methods. In this study measurements were performed by a Specs Near Ambient Pressure (NAP) X-ray Photoelectron Spectroscopy. The reaction was also followed by an *in situ* DRIFTS method. We have synthesized mesoporous-NiO with nanocrystalline structure by solvothermal hard-templating method, and have supported size-controlled Pt NPs on the NiO via capillary inclusion.

Our main purpose was to follow the effects of carbon dioxide hydrogenation on the surface of the mesoporous NiO-Pt interface. We are testing controlled size (~4,8 nm) Pt nanoparticles anchored on 3D mesoporous NiO supports in CO₂ reduction reactions. NAP-XPS demonstrated a strong correlation between the oxidation state and of the oxide support and the catalytic activity at the oxide-metal interface³.

We seek to look at the electronic structure of the Pt/NiO nanocatalyst under redox atmospheres (O₂ and H₂) and under the CO₂/H₂ reaction conditions using NAP-XPS to understand the catalytic processes under reaction conditions:

– What is the electronic structure of the 3D mesoporous NiO_x and Pt/NiO_x under different gases and pressures?

We had also performed *in situ* drift IR experiments and on the Pt samples occurred the formation of formate species. A significantly new absorption feature is detected at 5% Pt content. From 423 K a strong signal was detected at 1770 cm⁻¹, was contain C=O double bond, what can be assigned to formaldehyde (vCO). It is important that the formate was formed on NiO and the hydrogen was dissociated on Pt nanoparticles. We may assume that hydrogen atoms migrate to the metal-support interface and react with formate there. As adsorbed formyl was not detectable at low Pt content, we suppose that large amount of atomic hydrogen is necessary for this reaction.

The choice of the catalytic reaction is commensurate with the chemical nature of the NiO (i.e. a reducible metal oxide), and is anticipated to provide a knowledge to improved understanding of the 'support effect' in heterogeneous catalysis.

References:

- [1] W.M. Ayers, ed., Catalytic activation of carbon dioxide, ACS Symp. Ser. Vol. 363, American Chemical Society, Washington, DC, (1988).
- [2] F. Solymosi, G. Klivényi, Surf. Sci. 315 (1994) 255.
- [3] K. An, S. Alayoglu, N. Musselwhite, S. Plamthottam, G. Melate, A. E. Lindeman, G. A. Somorjai J. Am. Chem. Soc.135 (2013) 16689.

Thu-PS2-39**Toluene total oxidation over NiO nanoparticles on mesoporous SiO₂: catalytic reaction at lower temperatures and repeated regeneration**

[Sang Wook Han](#)¹, [Il Hee Kim](#)¹, [Ho Jong Kim](#)¹, [Byeong Jun Cha](#)¹, [Chan Heum Park](#)¹,
[Jae Hwan Jeong](#)¹, [Tae Gyun Woo](#)¹, [Hyun Ook Seo](#)^{2*}, [Young Dok Kim](#)^{1*}

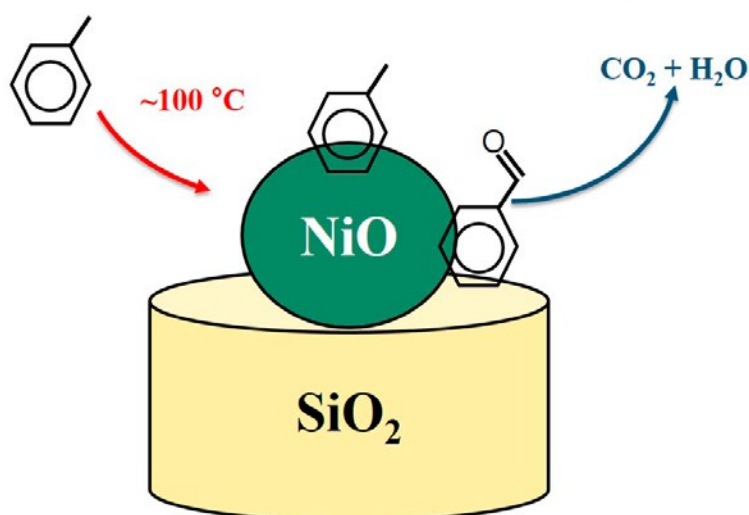
¹ Department of Chemistry, Sungkyunkwan University, 16419 Suwon, Republic of Korea;

² Department of Chemistry and Energy Engineering, Sangmyung University, 03016 Seoul, Republic of Korea

We deposited NiO via atomic layer deposition (ALD) on mesoporous SiO₂ particles with diameters of several hundred micrometers and a mean mesopore size of ~14 nm. NiO was deposited within the shell region of mesoporous SiO₂ particles with a shell thickness of ~11 nm. We annealed the as-prepared NiO/SiO₂ at 450 and 600 °C, respectively. These two samples were used as catalysts for the uptake of toluene molecules and their oxidative conversion to CO₂. In contrast to bare SiO₂, which showed almost no uptake of toluene vapor above 100 °C, NiO/SiO₂ showed significant uptake of toluene (even at 160 °C). The sample annealed at 450 °C was generally more reactive in toluene uptake and its subsequent conversion to CO₂. When the NiO/SiO₂ annealed at 450 °C was exposed to toluene vapor at 160 °C and then heated to 450 °C, CO₂ has emitted with almost no toluene desorption. We suggest that our catalysts can be used as building blocks for odor removal devices that operate below 200 °C. These catalysts can be regularly regenerated at ~450 °C.

[Capture of toluene at lower temperature (<200 °C)]

→ Total oxidation and CO₂+H₂O emission at higher temperature (450 °C)



Thu-PS2-33***In-situ* observation of water-induced reordering in ultrathin ionic liquid films**

Zoë Henderson¹, Alex S. Walton², Andrew G. Thomas³, Karen L. Syres¹

¹ *Jeremiah Horrocks Institute for Mathematics, Physics and Astronomy, University of Central Lancashire, Preston, Lancashire, United Kingdom, PR1 2HE;*

² *School of Chemistry, Photon Science Institute, University of Manchester, Manchester, M13 9PL;*

³ *School of Materials, Photon Science Institute, University of Manchester, Manchester, M13 9PL*

Ionic liquids (ILs) are salts that are liquid at, or around, room temperature; and are composed of ions that are held together by a strong Coulomb potential. ILs have very low vapour pressures, allowing them to be studied using ultra-high vacuum techniques. They are currently being investigated for a vast range of applications, including lubricants, corrosion protection, as an electrolyte in batteries and photovoltaic devices, and CO₂ capture and storage [1]. ILs also have potential applications in catalysis, and are an integral part of a homogeneous catalysis system known as Supported Ionic Liquid Phase (SILP) catalysis. This method requires only a very thin film of IL (with the desired homogeneous catalyst dissolved in the film) on the surface of a high-area, porous support material [2]. The ordering and structure of ILs is determined by the structure of the constituent ions, and for imidazolium-based ILs it has been seen that the cations arrange to form a layer of alkyl chains facing out towards the vacuum, creating a charged underlayer that contains the anion and imidazolium ring of the cation [3]. It is this ordering at the surface that is believed to govern the gas adsorption and uptake by ILs. Water is often present as a contaminant in ILs, and has shown to affect their physical properties [4]. In this work, the interaction of water with the IL 1-butyl-3-methylimidazolium tetrafluoroborate ([C4C1Im][BF4]) has been studied using near-ambient pressure X-ray photoelectron spectroscopy (NAPXPS). An ultrathin film of IL was deposited on rutile TiO₂ (110) at room temperature and exposed to water at 7 mbar at 283 K, corresponding to a relative humidity of ~70%. The ultrathin film was estimated to have a thickness of (10.8±0.9)Å, consisting of approximately three IL layers. Results indicate that water is trapped on the IL film, triggering a reordering of the ions at the surface. As water is pumped out of the near-ambient pressure cell, the IL begins to revert to its original surface structure.

References:

- [1] M. Armand, F. Endres, D. R. MacFarlane, H. Ohno, B. Scrosati, *Nature Materials*, 8, 621-629 (2009).
- [2] C. P. Mehnert, R. A. Cook, N. C. Dispenziere, M. Afeworki, *J. Am. Chem. Soc.*, 124, 12932-12933 (2002).
- [3] V. Lockett, R. Sedev, C. Bassell, J. Ralston, *Phys. Chem. Chem. Phys.*, 10, 1330-1335 (2008).
- [4] S. Rivera-Rubero, S. Baldelli, *J. Am. Chem. Soc.*, 126, 11788-11789 (2004).

Thu-PS2-46**Observation of shell structure in mixed Ar/Kr clusters studied by electron energy loss spectroscopy**Kazuma Kita ¹, Takato Hirayama ^{1,2}, Teppei Nomura ¹, Takayuki Tachibana ^{1,2}¹ Department of Physics, Rikkyo University, Tokyo 171-8501, JAPAN;² Research Center for Measurement in Advanced Studies (RCMAS), Rikkyo University, Tokyo 171-8501, JAPAN

The physics of clusters has attracted significant interests because they not only bridge the gap between atoms and solids, but also have specific physical properties. We have previously reported electron energy loss spectra of Ar clusters as a function of both incident electron energy and cluster size [1, 2]. These results clearly showed that the appearance cluster size of the bulk excitation peak was dependent on the incident electron energy. This characteristic feature was qualitatively explained by a simple model that takes into account the mean free path of the incident electrons in Ar clusters. We have also shown that the surface-excitation process can be effectively observed with an appropriate choice of cluster size and incident electron energy because of the relatively small mean free path of electrons. Here we report the results of the observation of a shell structure found in a mixed Ar/Kr cluster studied by electron energy loss spectroscopy.

Details of the experimental apparatus and procedure have been described elsewhere [1, 2]. Briefly, a mixed Ar/Kr cluster beam is generated by adiabatic coexpansion of the mixed argon and krypton gas through a conical nozzle attached to a pulse valve. The average cluster size is controlled by changing the stagnation pressure and the nozzle temperature, and is estimated using the Γ^* formula [3].

Figure shows the electron energy loss spectra of mixed Ar/Kr clusters. Primary mixtures with Kr in Ar ranging from 1 % to 50 % are used to produce the mixed clusters. The spectrum of Ar/Kr mixed gas is also shown as a reference. The spectra are normalized to the maximum intensity of each spectrum. Incident electron energy and the observation angle are 100 eV and 0 deg., and the stagnation pressure and the nozzle temperature are 0.2 MPa and 180 K, respectively. Although it is not possible to estimate the size of the Ar/Kr mixed cluster, the mean size for pure Ar and Kr clusters produced under these conditions are estimated to be 400 and 2000 atoms/cluster, respectively.

It is clearly shown that the intensity of Kr peak increases as the percentage of Kr increases. In the Kr 14% spectrum the relative intensity of the Kr peaks are much smaller than those in the Kr/Ar mixed gas spectrum (Kr 14 %). It suggests that the cluster has a core-shell structure (Kr core; Ar shell) due to the difference of the cohesive energy between Kr ($E_{\text{coh}} = 0.17$ eV/atom) and Ar ($E_{\text{coh}} = 0.08$ eV/atom). Such core-shell structure has already been found in Ar/Ne mixed cluster studied by photoelectron spectroscopy [4]. In Kr 50 % spectrum the Ar signal almost completely disappeared suggesting that all of Ar atoms are evaporated from the cluster surface by Kr condensation.

The results of the detailed analysis will be presented at the conference.

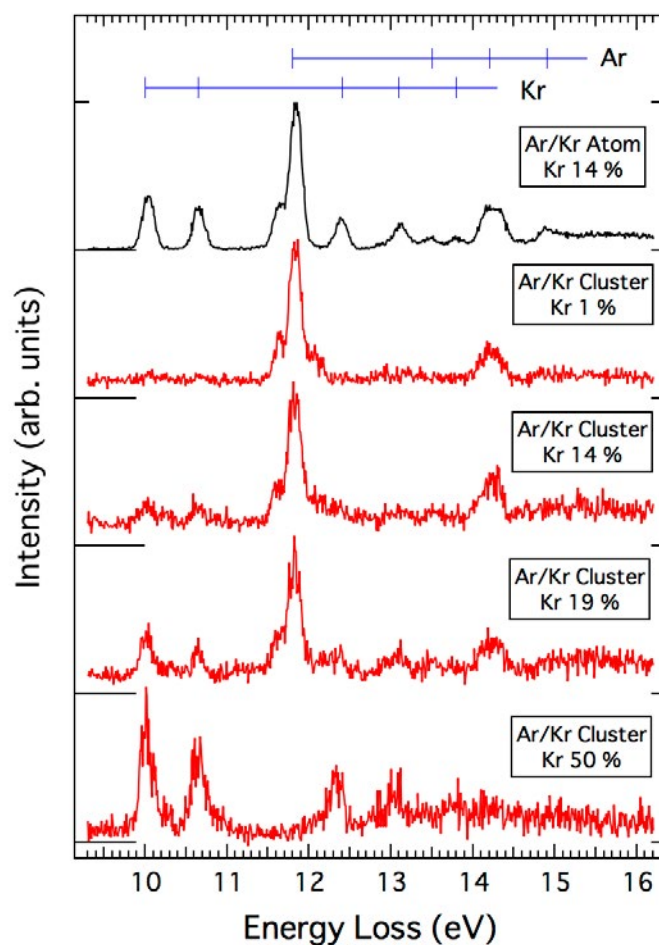


Figure: Electron energy loss spectra of Ar/Kr mixed clusters for Kr mixtures from 1% to 50 %.

References:

- [1] H. Kubotera, T. Sekitsuka, S. Sakai, T. Tachibana and T. Hirayama, *Appl. Surf. Sci.* 256, (2009) 1046-9.
- [2] H. Kubotera, T. Sekitsuka, S. Jinno, T. Tachibana and T. Hirayama, *J. Phys. Conf. Ser.* 288, (2011) 012012.
- [3] O. F. Hagen and W. Obert, *J. Chem. Phys.* 56, (1972) 1793.
- [4] M. Lundwall et al., *J. Chem. Phys.* 126, (2007) 214706.

Thu-PS2-07**Reforming of ethanol on Rh(111) surface and supported Rh nanoclusters**

[Yu-Yao Hsia](#)¹, [A. A. Ansari](#)¹, [Yu-Ling Lai](#)², [Yao-Jane Hsu](#)², [Meng-Fan Luo](#)¹

¹ *Department of Physics, National Central University, Taoyuan, Taiwan;*

² *National Synchrotron Radiation Research Center, Hsinchu, Taiwan*

Ethanol is readily extracted from biomass so becomes an attractive source to produce hydrogen. The steam reforming of ethanol catalyzed by metal catalysts, such as Pt, Pd, and Rh, yields high production of hydrogen but the process easily has CO poisoning and coke formation. The drawback can be solved with the oxidative steam reforming of ethanol controlled by the ethanol/water/oxygen molecular ratio, whereas its detailed kinetics remains unclear. To shed light on the reaction, we investigated the decomposition of ethanol co-adsorbed with atomic hydrogen and hydroxyl on Rh(111) single crystal and graphene-supported Rh nanoclusters, with synchrotron-based photoemission spectroscopy, infrared reflection absorption spectroscopy and temperature programmed desorption. The co-adsorbed atomic oxygen was shown to promote the formation of carbon dioxide and removal of atomic carbon; nevertheless, with increased atomic oxygen, the quantity of produced hydrogen decreased. Adsorbed water molecules were dissociated into hydroxyl groups when they were co-adsorbed with atomic oxygen less than 0.1 ML. The co-adsorbed hydroxyl increased methane but decreased ethylene produced in the reaction. The presentation also discuss the differences of the reaction on Rh(111) single crystal and graphene-supported Rh nanoclusters.

Tue-PS1-12

Charge transfer and orbital level alignment at inorganic/organic interfaces: the role of dielectric interlayers

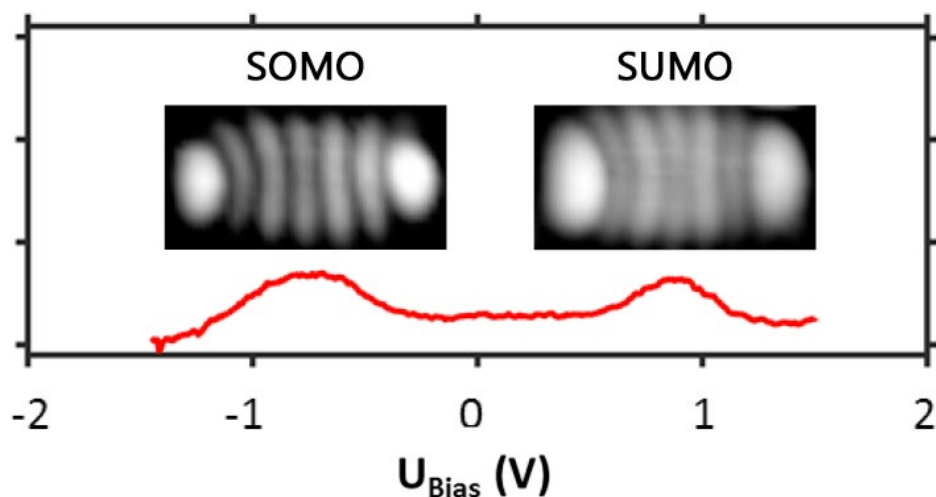
[Philipp Hurdax](#)¹, [Michael Hollerer](#)¹, [Daniel Lüftner](#)¹, [Thomas Ules](#)¹, [Sergey Soubatch](#)^{2,3}, [F. Stefan Tautz](#)^{2,3}, [Georg Koller](#)¹, [Peter Puschnig](#)¹, [Martin Sterrer](#)¹, [Michael G. Ramsey](#)¹

¹ Institute of Physics, University of Graz, NAWI Graz, Universitätsplatz 5, 8010 Graz, Austria;

² Peter Grünberg Institut (PGI-3), Forschungszentrum Jülich, 52425 Jülich, Germany;

³ Jülich Aachen Research Alliance (JARA), Fundamentals of Future Information Technology, 52425 Jülich, Germany

It is becoming accepted that ultrathin dielectric layers on metals are not merely passive decoupling layers, but can actively influence orbital energy level alignment and charge transfer at interfaces. As such, they can be important in applications ranging from catalysis to organic electronics. However, the details at the molecular level are still under debate. Here, we present a comprehensive analysis of the phenomenon of charge transfer promoted by a dielectric interlayer with a comparative study of pentacene adsorbed on Ag(001) with and without an ultrathin MgO interlayer¹. Using scanning tunneling microscopy and photoemission tomography supported by density functional theory we are able to unambiguously identify the orbitals involved and quantify the degree of charge transfer in both cases. Fractional charge transfer occurs for pentacene adsorbed on Ag(001), while the presence of the ultrathin MgO interlayer promotes integer charge transfer with the LUMO transforming into a singly occupied (SOMO) and singly unoccupied (SUMO) state separated by a large gap around the Fermi energy.



Acknowledgment: Supported by FWF (P21330-N20, P27649-N20, P27427)

References:

[1] ACS Nano, under review

Tue-PS1-13

Evaluation of electronic structure of the single molecule junction based on current voltage characteristics and thermopower

Y. Isshiki, Y. Komoto, S. Fujii, M. Kiguchi

Tokyo Institute of Technology, Department of Chemistry, Japan

The electronic structure of molecular junctions has significant impacts on their transport properties which have been expected to apply molecular devices such as switching, and transistor devices [1]. Despite the decisive role of the electronic structure, a complete characterization of the electronic structure remains a challenge. This is because there is no straightforward methods of measuring electron structure for an individual molecule trapped in a nanoscale gap between two metal electrodes. Herein, a comprehensive approach to obtain a detailed description of the electronic structure in single molecule junctions based on the analysis of current–voltage (I-V) and thermoelectric characteristics is described. It is shown that the electronic structure of the prototypical C_{60} single-molecule junction trapped between Au electrodes (Au- C_{60} -Au) can be resolved by analyzing complementary results of the I-V and thermoelectric measurement. Figure1, 2 show histograms of the I-V characteristics and the thermoelectric power of the Au- C_{60} -Au single molecule junctions. The conductance and I-V analysis revealed that the Au- C_{60} -Au single-molecule junction was highly conductive with electronic conductance of 0.033 and 0.003 G_0 . The thermoelectric measurement indicated that Seebeck coefficient is -12 mV/K (at 300 K). By analyzing the complementary results of the I-V and thermoelectric measurement, the charge transport was found to be mediated by a LUMO whose energy level was located 0.5 and 0.6 eV above the Fermi level of the Au electrode [2].

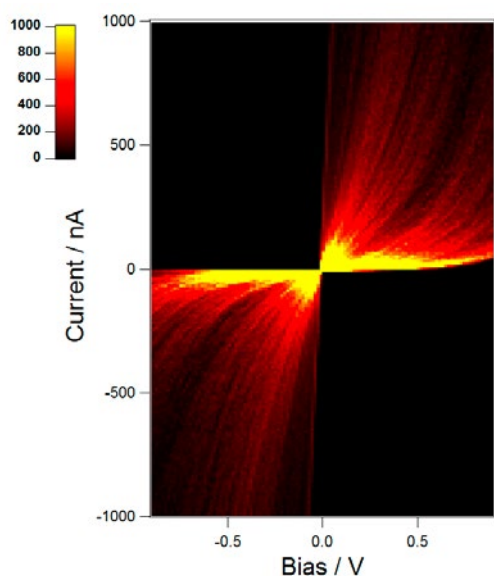


Figure1. Histograms of I-V curves of the Au-C60-Au single molecule junctions. The histograms are constructed from measurements on 2,664 junctions.

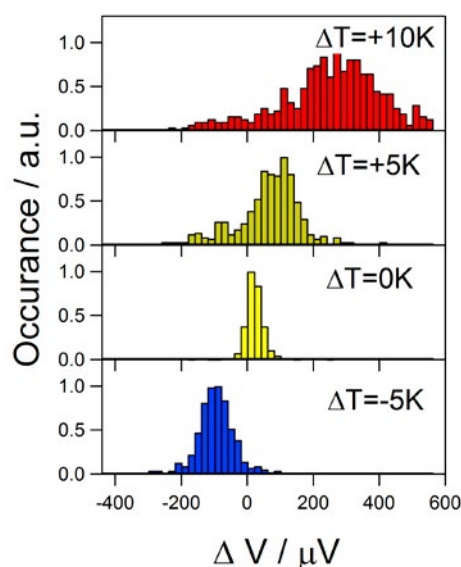


Figure2. Histograms of thermopower of the Au-C60-Au single molecule junctions.

References:

- [1] S. Fujii, T. Tada, Y. Komoto, T. Osuga, T. Murase, M. Fujita, M. Kiguchi, *J. Am. Chem. Soc.* 137 5939-5947 (2015)
 [2] Y. Komoto, Y. Isshiki, S. Fujii, T. Nishino, M. Kiguchi, *Chem. Asia J.* 12, 440-445 (2017)

Tue-PS1-08**Surface enrichment in gold/silver alloys: Study of the physicochemical influences using atom probe tomography**

Natalia Gilis¹, Luc Jacobs¹, Sten V. Lambeets¹, Eric Genty¹, Cédric Barroo², Thierry Visart de Bocarmé¹

¹ Chemical Physics of Materials and Catalysis (CPMCT), Université libre de Bruxelles, Faculty of Sciences, CP243, 1050 Brussels, Belgium;

² Interdisciplinary Center for Nonlinear Phenomena and Complex Systems (CENOLI), Université libre de Bruxelles, Faculty of Sciences, CP231, 1050 Brussels, Belgium

Bimetallic alloys are increasingly used in heterogeneous catalysis. This can be explained by that fact that new features emerge from the combination of two metals that are absent in the isolated parent metals. Synergic effects between the two combined elements creates a more efficient catalyst. One of the most interesting aspect of multicomponent materials in catalysis, is the fact that one could possibly control the catalytic properties of an alloy by controlling the nature and composition of the surface. The gold/silver alloy is an interesting example¹ since it combines a high activity and a large selectivity for a broad range of oxidation reaction. Examples have been reported from CO oxidation at low temperature to more complex oxygen-activated coupling reaction. The silver is crucial to provide the necessary oxygen dissociation without leading to a total oxidation. Thus, the gold/silver alloy is an interesting candidate for the selective oxidation of methanol to formaldehyde².

The study of the enrichment phenomenon is conducted by atom probe tomography (APT). This method allows us to establish the chemical composition profile of the alloy with a nanometric lateral resolution and an atomic depth resolution. The atom probe tomography setup is equipped with an *in-situ* reaction chamber allowing physicochemical treatments with temperature up to 800-900K and pressures up to 1bar. This overall approach allows us to treat our gold/silver (95/5 at.%) samples in condition close to the operating condition of the real catalyst and analyse the evolution of the composition on the surface and the bulk. In this way we aim to establish the physicochemical conditions that could be used to design the surface composition at will. Several thermal and chemical treatments were applied on Au-Ag samples to analyse the segregation behaviour. Our present research focusses on segregation triggered by high temperatures under UHV conditions, as well as segregation triggered by an oxidizing atmosphere, which in our case is N₂O. Results show that silver enrichment occurs in the presence of the oxygen rich gas and takes place at lower temperature than with annealing under UHV conditions. These results are in accordance with recent literature^{3,4}. Our results also show different segregation behaviors in the case of annealing or chemically triggered segregation. Indeed, the composition profile of N₂O-treated sample clearly shows - below the segregated silver layer - a layer which is Ag-depleted, before showing the expected bulk composition. In the case of annealed-samples, the Ag-depleted region is absent. This indicates that N₂O-segregated silver atoms are chemically pumped out from the bulk, just underneath the surface, while annealed-segregated silver atoms probably migrate at the surface from the shank of the tip to the apex part.

References:

1. Biener, J., Biener, M. M., Madix, R. J. & Friend, C. M. Nanoporous Gold: Understanding the Origin of the Reactivity of a 21st Century Catalyst Made by Pre-Columbian Technology. *ACS Catal.* 5, 6263–6270 (2015).
2. Rao, V. N. M. & Nielsen, N. A. Process for selective oxidation/dehydrogenation of methanol to formaldehyde using a metal catalyst. (1979).
3. Guisbiers, G. et al. Electrum, the Gold-Silver Alloy, from the Bulk Scale to the Nanoscale: Synthesis, Properties, and Segregation Rules. *ACS Nano* 10, 188–98 (2016).
4. Zugic, B. et al. Dynamic restructuring drives catalytic activity on nanoporous gold–silver alloy catalysts. *Nat. Mater.* 1, 1–8 (2016).

Thu-PS2-15**Thermally induced dewetting of three dimensional Cu islands on the Ag(111) surface**

Maciej Jankowski¹, Marta Mirolo¹, Wojciech Kwieciński², Kevin Hofhuis², Yorick Birkhölzer², Maurizio De Santis³, Herbert Wormeester², Aude Bailly³

¹ ESRF, 71 Avenue des Martyrs, Grenoble 38043, France;

² Physics of Interfaces and Nanomaterials, MESA+ Institute for Nanotechnology, University of Twente, P.O. Box 217, 7500AE Enschede, the Netherlands;

³ Institut Néel, CNRS and UGA, F-38000 Grenoble, France

We have investigated the growth and coalescence of three-dimensional copper islands grown on the Ag(111) surface by surface x-ray diffraction (SXR), scanning tunneling microscopy (STM), Auger electron spectroscopy (AES), and low energy electron diffraction (LEED). Deposition at room temperature of (sub) monolayer coverages of copper results in the formation of islands, with a thickness of a few monolayers [1]. These islands cover the Ag surface terraces and decorate the atomic steps. Concomitantly, the development of vacancy islands in the first layer of Ag(111) surface is also observed. The copper islands exhibit a Moiré pattern [2,3], which allows to accommodate a large lattice mismatch (12%) between silver and copper. Surface annealing at temperatures above 470 K leads to copper dewetting signaled by a strong decrease of the copper AES signal and the appearance of a copper Bragg peak in (00) crystal truncation rods recorded with SXR. STM observations revealed a dramatic decrease of the clusters density upon annealing correlated to the formation of high Cu crystallites, as a result of surface dewetting (see Fig. 1).

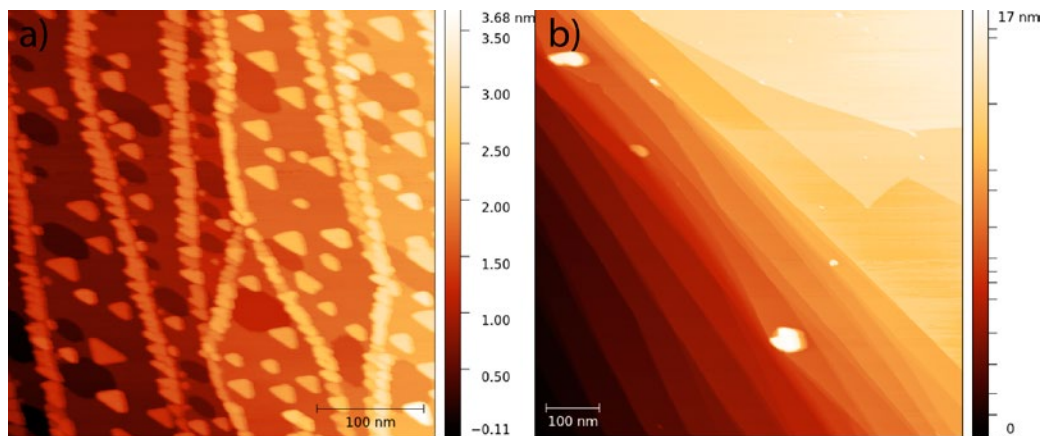


Figure 1: STM images illustrating the dewetting process in the case of a 0.4 ML of Cu on Ag(111) after deposition at room temperature (a) and after annealing at 570 K (b).

References:

- [1] F. Bocquet, C. Maurel, J.-M. Roussel, M. Abel, M. Koudia, L. Porte, Phys. Rev. B 71 (2005) 075405.
- [2] C. Maurel, M. Abel, M. Koudia, F. Bocquet, L. Porte, Surface Science 596 (2005) 45–52.
- [3] D.-A. Luh, C.-H. Huang, C.-M. Cheng, K.-D. Tsuei, Applied Physics Letters 102 (2013) 181601.

Tue-PS1-14

The sol aging time impact on the structural, optical and electrical properties of ZnO thin films

Tariq Jannane, Mohamed Manoua, Ahmed Liba, Nejma Fezouan

Sciences and Technologies Faculty, Sultan Moulay Slimane University, Material Physics Laboratory, BP 523, 23000 Beni Mellal, Morocco

Zinc oxide thin films were spin coated onto glass substrates by a sol gel process. The effect of aging times of the precursor solution on the structural, optical and electrical properties was investigated. Zinc acetate dehydrate, absolute ethanol and monoethanolamine (MEA) were used as a precursor source, solvent and stabilizer respectively. The increase of the aging time of the precursor solution showed the formation of films with three crystalline orientations (100), (002) and (101) corresponding to a wurtzite phase of zinc oxide, and indicating a good crystallization of our films. It was also found that the increase of aging time led to an increase in surface roughness, in addition of that it can also increase the films thickness. From the optical properties results, we revealed a reduction in the optical transmittance of the films while aging the deposition solution, and the optical band gap increases from 3,175 to 3,224 eV. Concerning the electrical properties, the minimum of ZnO films resistivity was obtained as $8,104 \times 10^{-2} \Omega \cdot \text{cm}$ for the aging time 48 hours, with $3,419 \times 10^{20} \text{ cm}^{-3}$ in free charge carriers density.

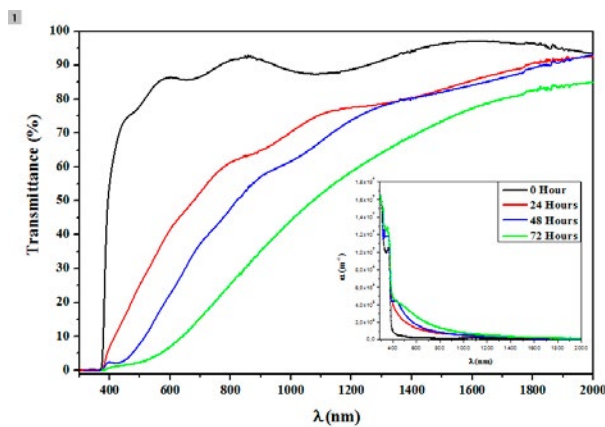


Figure 1. The XRD pattern of ZnO thin films at different aging time of the deposition solution.

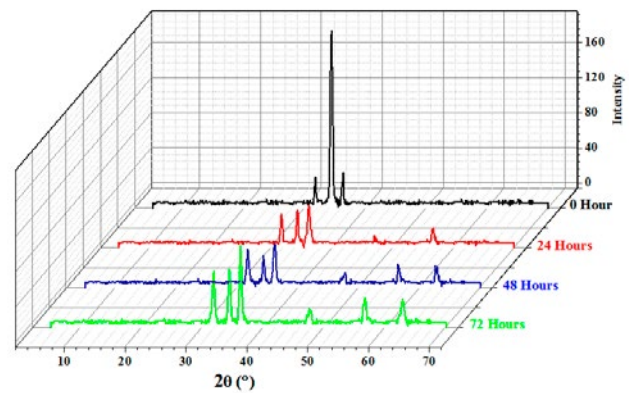


Figure 2. Variation of transmission and absorption coefficient versus the wavelength for ZnO thin films deposited at different aging time of the deposition solution.

References:

- [1] L. Znaidi, Materials Science and Engineering B 174 (2010) 18–30.
- [2] T. Jannane, M. Manoua, A. Liba, N. Fazouan, A. El Hichou, A. Almaggoussi, A. Outzourhit, M. Chaik., J. Mater. Environ. Sci 8 (1) (2017) 160-168.
- [3] J. Tauc, A. Menthe, J. Non-Cryst. Sol. 569 (1972) 8.
- [4] E. Burstein, Phys. Rev. 93 (1954) 632.
- [5] T.S. Moss, Proc. Phys. Soc. Lond. B. 67 (1954) 775.

Tue-PS1-15**Morphology and optical properties of porous gold nanoparticles coated with alumina layer**

[L. Juhász](#)¹, [B. Parditka](#)¹, [S.S. Shenouda](#)², [A. Kosinova](#)³, [D. Wang](#)⁴, [E. Baradács](#)¹,
[P. Schaaf](#)⁴, [E. Rabkin](#)³, [C. Cserhádi](#)¹, [Z. Erdélyi](#)¹

¹ Department of Solid State Physics, University of Debrecen, P.O. Box 2, H-4010, Debrecen, Hungary;

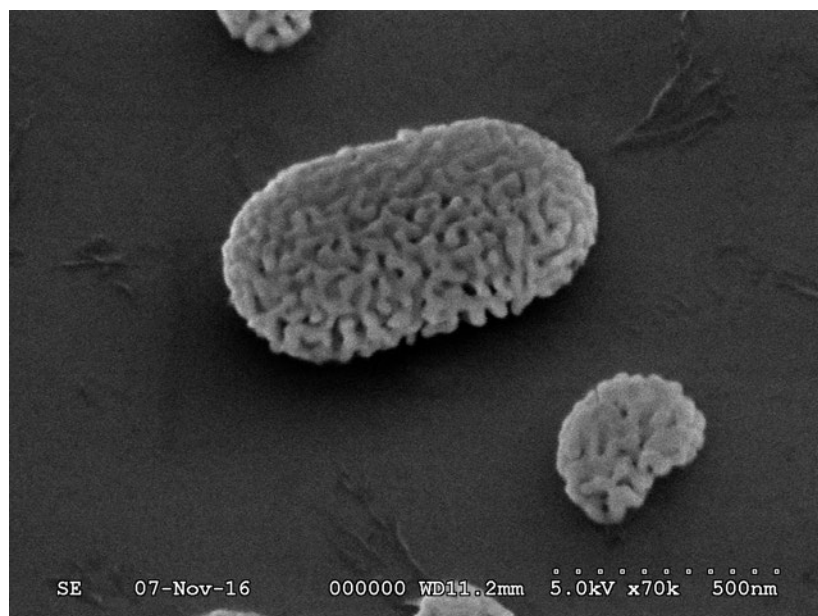
² Department of Physics, Faculty of Education, Ain Shams University, Cairo, Egypt;

³ Department of Materials Science and Engineering, Technion - Israel Institute of Technology, 32000 Haifa, Israel;

⁴ Chair Materials for Electronics, Institute of Materials Science and Engineering and Institute of Micro- and Nanotechnologies MacroNano[®], TU Ilmenau, Gustav-Kirchhoff-Str. 5, 98693 Ilmenau, Germany

Porous nanoparticles are very popular because of their high surface/volume ratio, moreover they have stronger plasmonical properties than their solid counterparts. Porous gold nanoparticles were fabricated on SiO₂/Si as well as on sapphire substrates with solid state dewetting and dealloying methods. They were coated with thin (~5 nm) alumina layer using plasma-enhanced atomic layer deposition (ALD) method. The samples were annealed for one hour in air at different temperatures. Changes in the morphology were investigated by Scanning Electron Microscope. Extinction spectra were measured by spectrophotometer in the spectral range of 300 nm – 2700 nm. The particles preserved their initial state even after annealing in the temperature range of 350 °C to 900 °C. As far the optical properties are concerned, significant change of plasmon peaks were observed due to the alumina coating, which did not change during the annealing.

In the poster presentation it will be shown how Al₂O₃ coating influences the optical and morphological properties of porous gold nanoparticles.



Tue-PS1-16**Photonic bandgap engineering and photo-induced emission in layered two-dimensional structures**

[Mousumi Upadhyay Kahaly](#), Saibabu Madas, Jiuwer Jilili, Sanjay Mishra

ELI-ALPS, Dugonics ter, Szeged, Hungary

We study electronic structures, tunability of photonic bands and associated magneto-optical properties of a class of two dimensional materials like graphene, phosphorene, borophene by employing density functional theory. We show how the electronic structures, and photonic band gap can be systematically tuned in these materials by the application of local strain along armchair or zigzag directions. Emergence of Dirac cone in the band structures of both borophene and phosphorene under appropriate strain makes these materials important for tunable electronic transport.

Further, a rigorous numerical formalism is applied to address the photo-thermionic effects in these systems under monochromatic excitation. In usual metals, free electron densities are high and the relative fraction of photoexcited hot electrons is low; thus such effects are not so prominent. However in materials, exhibiting semi-metallic behavior (when Dirac cone appears under/without strain) with linear band dispersion near the Fermi level, though the free electron densities are high, based on the physical conditions, the photoexcited densities can overwhelm them, and efficient enhancement of photo-induced thermalization of electrons under laser excitation is possible. Our results suggest prominent enhancement of photo-induced electron emission from these two-dimensional materials by suitably tuning the surface potential, work function etc.

Thu-PS2-28**Photon-stimulated desorption processes of polymers by vacuum ultraviolet emissions from a laser-produced plasma**

[Masanori Kaku](#)¹, [Kazuki Fuchigami](#)¹, [Masahito Katto](#)¹, [Atushi Yokotani](#)¹, [Wataru Sasaki](#)²

¹ *University of Miyazaki, Japan*

² *NTP, Inc.*

Short wavelength photons in the vacuum ultraviolet (VUV) spectral region would induce interesting photo-chemical reactions, since they have high photon energies. In certain photo-chemical interactions such as surface treatment of soft materials, low-power, incoherent lamp emission, rather than intense laser emission, may be adequate. Photochemistry of polymers was reported by using VUV emission sources such as rare gas resonance lamps, deuterium lamps, and so forth [1-3]. Emission spectra of these VUV lamps are, however, almost monochromatic, which may not be applicable to certain spectroscopy that requires continuous VUV emissions. In contrast to these monochromatic light sources, a synchrotron radiation source is presently one of the most versatile continuous emission sources, which can be used for surface physics and chemistry, and advanced spectroscopy. Photo-dissociation processes of several simple molecules such as H₂, O₂, N₂ and CO have been investigated by using such radiation [4]. This radiation source is, however, usually large and has limited use. Therefore, photon-stimulated desorption processes of solid materials such as polymers have not well been understood.

We have demonstrated a spectrally continuous VUV emission source in the wavelength between 115 and 200 nm using a laser-produced plasma (LPP) as a spectroscopic emission source. Despite lower brightness and coherence compared with those of synchrotron radiation, the LPP emission source can be easily operated in a compact size in a small-scale laboratory. We have proposed new photon-stimulated desorption surface spectroscopy using such broadband VUV emissions using the LPP [5]. Adsorbed atoms or molecules on material surfaces should be desorbed and dissociated as a result of absorption of the wavelength-selected high-energy VUV photons. Material surfaces would be analyzed by detecting desorbed and dissociated atoms or molecules. This photon-stimulated desorption surface spectroscopy should have superior characteristics over conventional thermal desorption spectroscopy in terms of energy and spatial resolutions with minimum heat effect. In this paper, we report new photon-stimulated surface spectroscopy system using the LPP. The irradiation wavelength dependence of mass spectra of polyethylene and polyvinyl chloride samples were demonstrated. We have found that the characteristic differences of the mass spectra were obtained in the wavelength shorter than 200 nm in each sample. Dissociation of atoms or molecules from material surfaces depended on bond energy or molecular structure.

References:

- [1] V. Skurat, *Nuclear Instruments and Methods in Physics Research B* 208, 27(2003).
- [2] C. Duca, G. Imoberdorf and M. Mohseni, *Photochemistry and Photobiology* 90, 238(2014).
- [3] C. Decker and M. Balandier, *European Polymer Journal* 18, 1085(1982).
- [4] Y. Hatano, *Phys. Repts* 313, 109(1999).
- [5] M. Kaku, D. Kai, M. Katto, A. Yokotani, S. Kubodera, and W. Sasaki, *Applied Physics B* 119, 427 (2015).

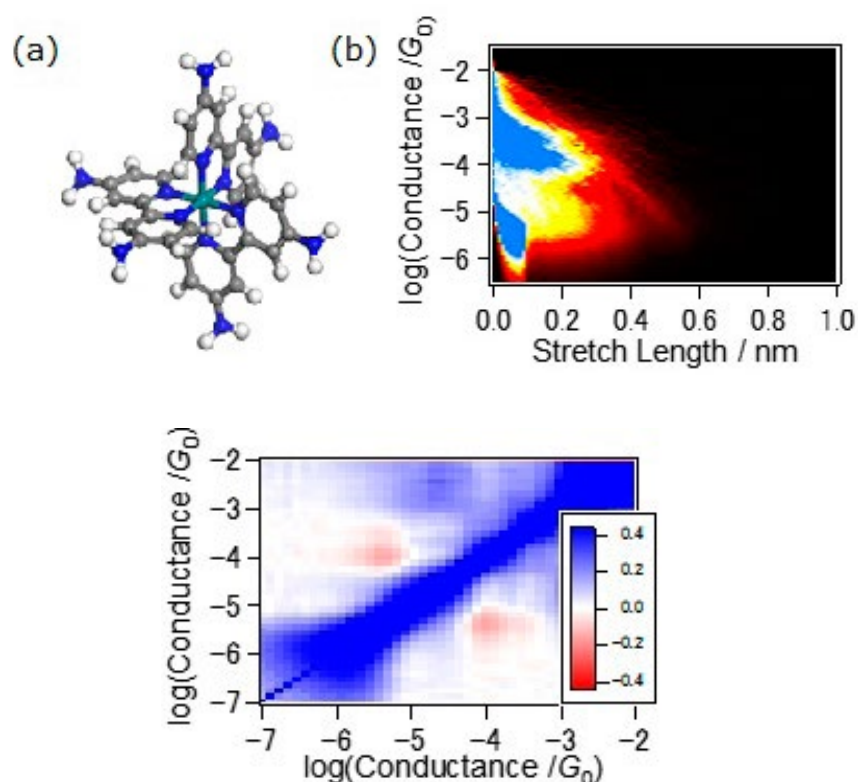
Thu-PS2-34

Single-molecule conductance measurement of Ru(bpy)₃ derivative

Yuki Komoto, Shintaro Fujii, Yusuke Tamaki, Osamu Ishitani, Manabu Kiguchi

Department of chemistry, Graduate School of Science, Tokyo Institute of Technology, 2-12-1 Ookayama, Meguro-ku, Tokyo 152-8551(Japan)

Dye-sensitized solar cells (DSCs) are attracting considerable attention because of their high light-to-electricity conversion efficiencies. The electron transport from the dye to the electrode plays the important role in determining the energy conversion efficiency of the DSCs. Here, we examined single-molecule transport property of a Ruthenium (II) bipyridyl complex (Fig. 1a) to understand the electron transport properties of the DSCs at atomic scale. Single-molecule conductance of the Ru complex sandwiched by Au electrodes via Au-N bonds was measured using scanning tunneling microscopy-based break junction technique. Figure 1b shows a 2D histogram of conductance traces during stretching process of Ru complex-junctions. The 2D histogram shows two distinctive single-molecule conductance of the Ru complex at $10^{-4} G_0$ (high conductance state) and $10^{-5} G_0$ (low conductance state) possibly due to difference in metal-molecule interface structures. The 2D conductance correlation histogram in Fig. 2 indicates that the point of intersection between the low and high conductance states has negative value. Hence, the two conductance states are structurally distinctive (i.e., the low conductance state is difficult to form after the high conductance state appeared). Considering the structure of the Ru complex, the origin of the difference between the two conductance states is that the Ru complex binds to Au electrodes using different Au-N bonding sites in the three bpy units. In conclusion, we determined the single-molecule conductance of the Ru complex. On the basis of the correlation analysis of the conductance behavior, it is suggested that electron transfer from the molecule to the electrode is significantly influenced by the adsorption structures.



Tue-PS1-17**Reaction pathways of adsorbed acetaldehyde on clean and modified Rh(111) surfaces**

[Imre Kovács](#)¹, [Arnold Péter Farkas](#)², [Ádám Szitás](#)³, [Zoltán Kónya](#)^{3,4}, [János Kiss](#)⁴, [Frigyes Solymosi](#)²

¹ University of Dunaújváros, 2401 Dunaújváros, Táncsics M. u. 1/A, Hungary;

² Department of Physical Chemistry and Materials Science, University of Szeged, 6720 Szeged, Aradi v. tere 1.;

³ Department of Applied and Environmental Chemistry, University of Szeged, H-6720 Aradi vértanúk tere 1, Hungary;

⁴ MTA-SZTE Reaction Kinetics and Surface Chemistry Research Group, University of Szeged, 6720 Szeged, Dóm tér 7;

The work was motivated by the findings that Rh is an effective catalyst in the reaction of CO+H₂ towards alcohols and C₂-oxygenates [1,2]. This compound was also formed by the partial oxidation of ethyl groups [3]. In this study, the interaction of CH₃CHO with clean, carbon, oxygen and potassium modified Rh(111) surfaces was studied to compare the different reaction mechanisms. The adsorbed molecular species were characterized by HREELS, besides EELS and work function ($\Delta\phi$) measurements. The products in the gas phase were detected by TPD with a quadrupole mass spectrometer.

The adsorption of acetaldehyde at 100 K resulted in the formation of η^1 -(O)-CH₃CHO_a and η^2 -(O,C)-CH₃CHO_a species. Upon increasing the temperature the first type of adsorbed molecules desorbed at 150 K. The remaining molecules formed polymers as a cyclic trimer, 2D, and three-dimensional species, too. Trimer molecules desorbed at T_p=225 K. Above this temperature intermediate (η^2 - CH₃CHO_a) acetaldehyde decomposed to the main products, CH₄, CO and to some adsorbed hydrogen and carbon. The inhibiting effect of surface carbon was found in the desorption of trimers and in CO formation. A direct surface reaction with preadsorbed oxygen led to the formation of acetate which was identified by HREELS. The product distribution changed, H₂O, CO₂ and acetic acid were also found by TPD. The thermal stability of adsorbed acetate increased with the oxygen coverage up to T_d= 325 K. The K atoms have a dramatic effect on the adsorbed acetaldehyde due to the extended electronic interaction. The amount of adsorbed molecules increased and the products of their thermal decomposition desorbed in a coincidence peak at 600 K and 630 K. A very similar interaction was found between K and HCOOH on Rh(111) surface [4].

References:

- [1] A. Kiennemann, R. Breault, J.-P. Hinderman, M. Laurin; J. Chem. Soc. Faraday Trans. 1 83, (1987) 2119.
- [2] Zs. Ferencz, A. Erdőhelyi, K. Baán, A. Oszkó, L. Óvári, Z. Kónya, C. Papp, H.-P. Steinrück, J. Kiss; ACS Catal. 4, (2014) 1205.
- [3] L. Bugyi, A. Oszkó, F. Solymosi; J. Catal. 159 (1996) 305.
- [4] F. Solymosi, J. Kiss, I. Kovács; The Journal of Phys. Chem., 92, (1988) 797.

Tue-PS1-18**Photo-switchable wettability and electric conductivity of self-assembled dithienylethene monolayers on Ag surface**

[S. Kumar](#)¹, [W. Danowski](#)², [B. L. Feringa](#)², [R.C. Chiechi](#)², [P. Rudolf](#)¹

¹ *Zernikhe institute for Advanced Materials, University of Groningen;*

² *Stratingh Institute for Chemistry, University of Groningen*

Dithienylethenes are photochromic molecules that show a change in structural configuration upon photo-radiation. Photo-switchable molecules have found numerous applications ranging from self-cleaning surfaces and biosensors to displacement of liquids in lab-on-a-chip devices, optical memories, photonic devices and logic units. Upon irradiation of the ring open form of a diarylethene with UV light a $6-\pi$ photocyclization reaction occurs, leading to ring closure. Upon irradiation of the closed form with visible light the reverse 'ring opening' reaction occurs. We developed a dithienylethene self-assembled monolayer (SAM) on a Ag surface. Here we report on the photo-switchable wettability of this dithienylethene-functionalized Ag surface. The SAMs were characterized by contact angle measurements and X-ray photoelectron spectroscopy (XPS), while their electrical properties (J(V)) were studied with liquid eutectic Ga–In (EGaIn) as a non-damaging, top-contact electrode. XPS analysis of the film revealed the presence of bound thiolate, which confirms the chemisorption of the dithienylethene switch on Ag. Changes in water contact angle of 10 ± 2 degree were observed as the surface-bound molecules switches from the ring closed to the ring open form under UV-visible radiation. The conductivity of these SAMs in both configurations also show marked differences.

Tue-PS1-19

Monolayer-to-thin-film transition in supramolecular assemblies on graphene

Zachary P. L. Laker¹, Alexander J. Marsden², Oreste De Luca², Luis M. Alves Perdigao², Giovanni Costantini², Neil R. Wilson¹

¹ Department of Physics, University of Warwick, Coventry, CV4 7AL;

² Department of Chemistry, University of Warwick, Coventry, CV4 7AL

Supramolecular assembly is intensively studied as a route to bottom-up synthesis of nanomaterials, among other areas. In these assemblies, molecules or ions interact through non-covalent forces (such as van der Waals and hydrogen bonding) to create macroscopic structures. In 2D assemblies, like monolayers of molecules, the substrate also plays a role in the self-assembly, which again interacts with the overlayers through non-covalent forces.[1,2]

Here, we investigate how supramolecular assembly affects the transition from monolayer to thin-film for the two organic molecules trimesic acid (TMA) and terephthalic acid (TPA) deposited onto graphene. The graphene is produced via chemical vapour deposition onto copper foils which enables both the monolayer and thin films to be studied: the graphene-copper is locally atomically flat for accurate STM measurements, but is also easily transferred to TEM supports for aberration-corrected TEM imaging and electron diffraction. We reveal that, despite the chemical similarity between the two molecules, different monolayer-to-thin-film transitions are seen for each of them. For TMA, the monolayer self-assembled chicken wire structure templates up through a film 20 nm thick, while for TPA, a quick transition to the bulk structure after only a few layers is seen. These results have important implications for how self-assembly can produce 3D structures, and for how STM can be coupled with TEM in order to directly measure the relation between 2D networks and their 3D counterparts.

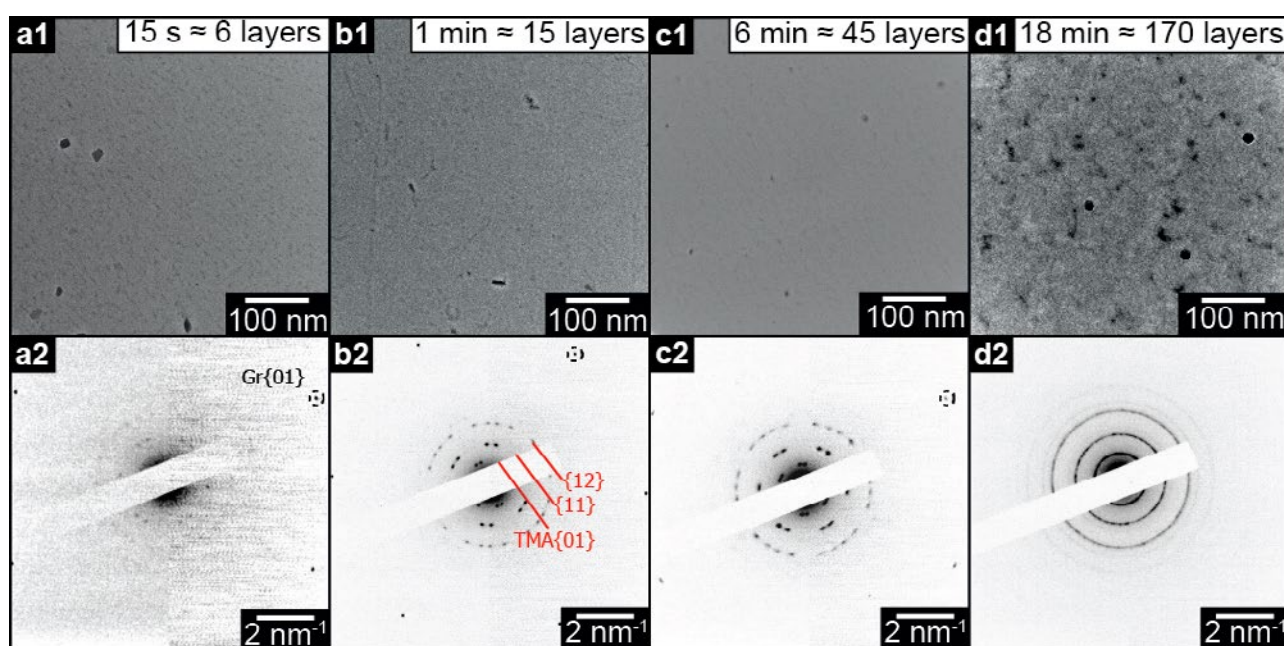


Figure 1: (a1) to (d1), brightfield TEM images of TMA thin films of increasing deposition time as marked, with corresponding low-dose selected-area electron diffraction patterns (a2) to (d2) on which graphene and TMA diffraction peaks are labelled.

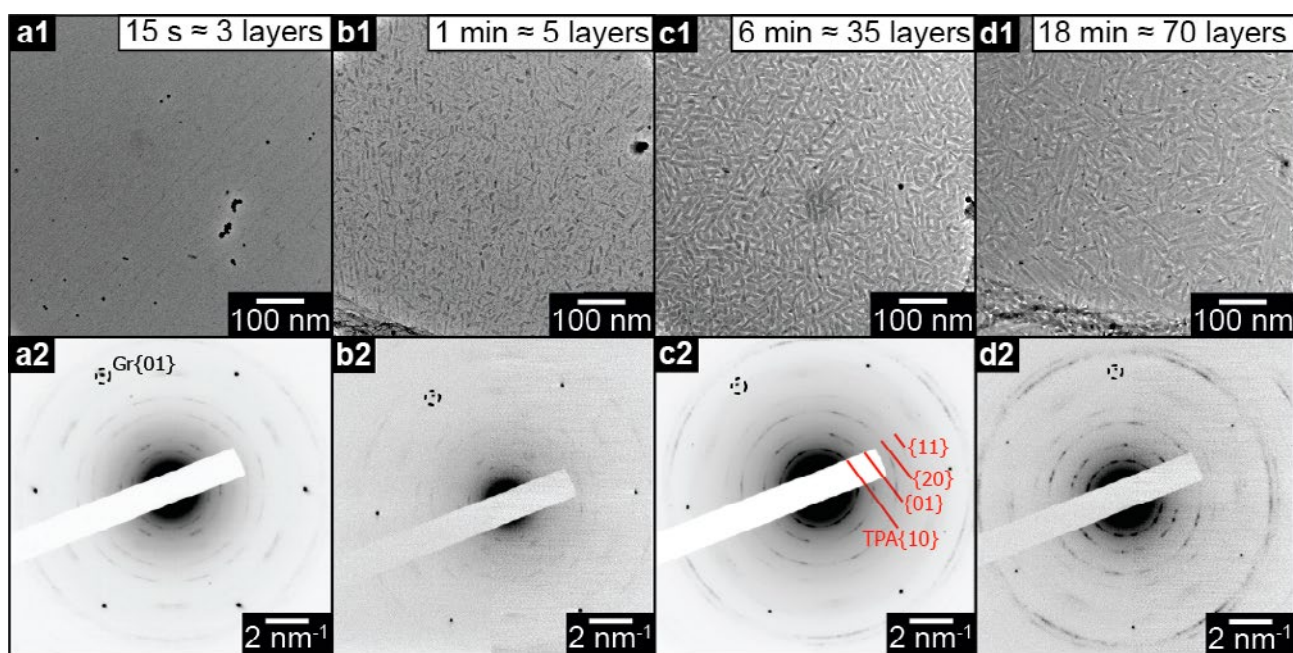


Figure 2: (a1) to (d1), brightfield TEM images of TPA thin films of increasing deposition time as marked, with corresponding low-dose selected-area electron diffraction patterns (a2) to (d2) on which graphene and TPA diffraction peaks are labelled.

References:

- [1] Pollard, A. J.; Perkins, E. W.; Smith, N. A.; Saywell, A.; Goretzki, G.; Phillips, A. G.; Argent, S. P.; Sachdev, H.; Müller, F.; Hufner, S.; et al. Supramolecular Assemblies Formed on an Epitaxial Graphene Superstructure. *Angew. Chemie - Int. Ed.* 2010, 49, 1794–1799.
- [2] MacLeod, J. M.; Lipton-Duffin, J. A.; Cui, D.; De Feyter, S.; Rosei, F. Substrate Effects in the Supramolecular Assembly of 1,3,5-Benzene Tricarboxylic Acid on Graphite and Graphene. *Langmuir* 2015, 31, 7016–7024.

Thu-PS2-29**Chiral recognition using field ion and field emission microscopy**

Natalia Gilis¹, Sten V. Lambeets¹, Jai Prakash², Eric Genty¹, Cédric Barroo³,
Thierry Visart de Bocarmé¹

¹ Chemical Physics of Materials and Catalysis (CPMCT), Université libre de Bruxelles, Faculty of Sciences, CP243, 1050 Brussels, Belgium;

² Department of Chemical Engineering, Indian Institute of Technology (IIT), 208016 Kanpur, India;

³ Interdisciplinary Center for Nonlinear Phenomena and Complex Systems (CENOLI), Université libre de Bruxelles, Faculty of Sciences, CP231, 1050 Brussels, Belgium

Chirality at surfaces has become an active research area targeting possible applications for enantioselective separation or detection. In this context, significant success has been achieved these past decades by developing new methods for a better understanding of enantiospecific interactions of chiral adsorbates with surfaces. „Chiral surfaces serve as media for enantioselective chemical processes. Their chirality is dictated by atomic- and molecular-level structure, and their enantioselectivity is determined by their enantiospecific interactions with chiral adsorbates. This Perspective describes three types of chiral metal surfaces: those modified by adsorption of chiral molecules, those templated by chiral lattices of adsorbed species, and those that are naturally chiral. A new paper in this issue of ACS Nano offers insight into the intermolecular interactions that govern chiral templating of surfaces. This Perspective then outlines three major challenges to the field of chiral surface science: development of methods for detection of enantiospecific interactions and enantioselective surface chemistry, preparation of high-area chiral metal surfaces, and the development of a fundamental, predictive-level understanding of the origin of enantioselectivity on chiral surfaces.” [1,2] Here, we propose a promising route to obtain a fundamental understanding of enantiospecific interaction of chiral molecules on metal surfaces using field emission based techniques. This technique has been chosen for its particular advantage to expose a wide range of structurally different facets in one atomically resolved picture. This diversity allows us to screen, with one sample, the interactions between a chemical species and a number of facets during the adsorption process.

Field Ion Microscopy (FIM) and Field Emission Microscopy (FEM) are the two methods used in this study. These two techniques allow to image the surface at the apex of a sharp metallic tip with a high resolution and in real space. In FIM mode, an imaging gas is ionized at the surface and the resulting atomically-resolved pattern shows a variety of facets with different structures inherent to the crystal lattice of the sample (Fig1.a). Kinks and steps of the surface are also shown on the ball-model of the tip on Fig 1c. In FEM mode, where the imaging principle is based on the emission of electrons (Fig 1.b), the brightness will vary in the presence of adsorbed species due to changes in the work function. It allows us to work with a wide range of temperature and pressure.

In order to observe the adsorption, the Pt surface is kept at temperatures between 150 and 300 K, and then exposed to vapors of D or L-alanine. The *in-situ* FEM pattern is recorded with a high-speed camera. The whole process is also performed in absence of alanine molecules to perform blank experiments (Fig 1. a and b). Therefore, the net adsorption sites can be imaged by removing the background image, as shown on Fig1d.

Our results show a clear preference of the alanine to adsorb on chiral facets. Although the 20 Å resolution of the FEM does not allow to unravel the edges of the facets of interest, the net images after exposures to one enantiomer of alanine show the occurrence of an enantioselective adsorption over sector of the same chiral symmetry. These results show that L-alanine has a strong tendency to adsorb onto R facets. Conversely, D-alanine adsorbs onto the S facets.

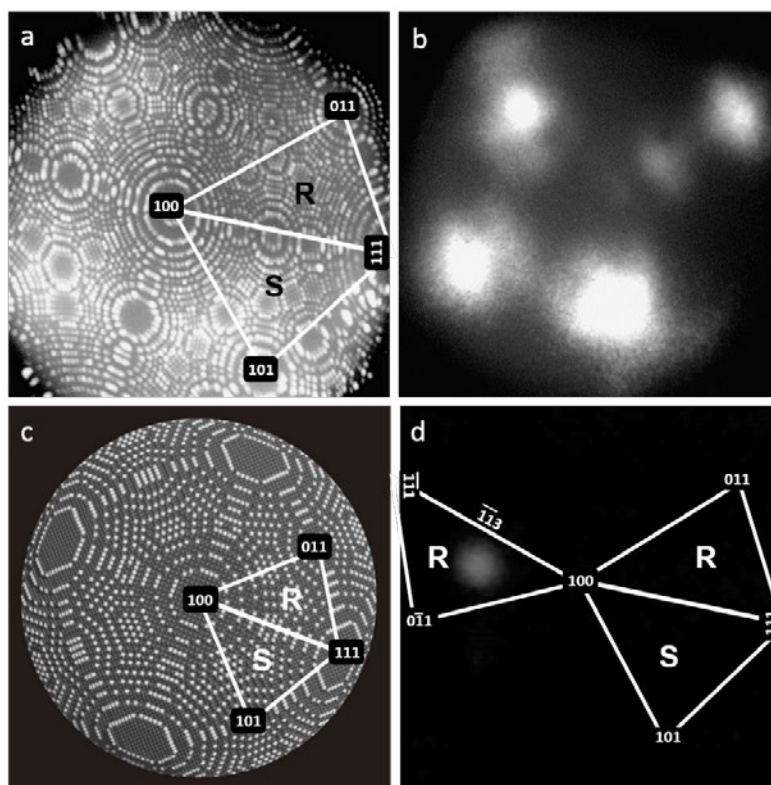


Figure 1. a) Field ion micrograph of a (100)-oriented platinum tip sample (imaging condition: $T = 50\text{K}$, $F = 35\text{V/nm}$, $P_{\text{Ne}} = 10^{-3}\text{Pa}$). (b) Field electron micrograph of a (100)-oriented platinum tip sample (imaging condition: $T = 50\text{K}$, $F = 3\text{V/nm}$, UHV). (c) Ball model depicting the field ion micrograph. (d) Image showing the net adsorption spot of L-alanine on a platinum tip at 300K ($P_{\text{Alanine}} = 3 \cdot 10^{-4}\text{Pa}$, $t_{\text{adsorption}} = 120\text{sec}$, $V = -1.8\text{V/nm}$)

References:

- [1] A.J. Gellman, Chiral surfaces: accomplishments and challenges., ACS Nano. 4 (2010) 5–10. doi:10.1021/nn901885n.
- [2] T. Mallat, E. Orglmeister, A. Baiker, Asymmetric Catalysis at Chiral Metal Surfaces, Chem. Rev. 107 (2007) 4863–4890.

Tue-PS1-20

Antiferromagnetic domains in epitaxial CoO ultra-thin layers grown on Pt(001)

Anne D. Lamirand, F. Maccherozzi, T. Forrest, A. Wilson, S. S. Dhesi

Diamond Light Source, Chilton, Didcot, Oxfordshire OX11 0DE, UK

Antiferromagnetic (AFM) spintronics is a new, rapidly developing and promising field in solid state physics. The intrinsic high frequencies of AFM dynamics and their insensitivity to external magnetic field are key assets for competing standard electronics. [1] However, the area is limited by the poor knowledge of the microscopic structure of the AFM thin films, especially in their surface and interfaces.[2] Here we used electron microscopy combined with linearly polarized x-ray to image both magnetic and crystalline domains in CoO layers grown on Pt(001).

Bulk CoO is AFM below $T_N=293\text{K}$. In the paramagnetic phase, it crystallizes in rock-salt structure with $a=4.26\text{ \AA}$. Below T_N , the structure becomes monoclinic. The concomitant changes in the structure and magnetic properties suggest that distortion and AFM are linked intimately by magnetostriction. As a film, the magnitude and orientation of its magnetic moment are highly sensitive to strain through the local crystal field [3].

CoO layers were prepared *in situ* by molecular beam epitaxy (MBE) under oxygen pressure on clean Pt(001) single crystal surface. Magnetic domains were observed by photoemission electron microscopy (PEEM) using x-ray magnetic linear dichroic (XMLD) contrast at Co- L_3 edge. Crystalline domains were measured by dark-field low-energy electron microscopy (LEEM). We observed that magnetic domains of CoO on Pt(001) match perfectly with crystalline domains indicating that the magnetic moments are pinned by the atomic structure. Crystalline domains correspond to twinned domains (2 hexagons rotated by 90°) on the square Pt surface. A strain-induced slight monoclinic distortion of the unit cell likely fixes the orientation of magnetic moments along $[010]_{\text{CoO}}$ in each domain through the local crystal field, leading to the magnetic domains shown in figure 1c [4].

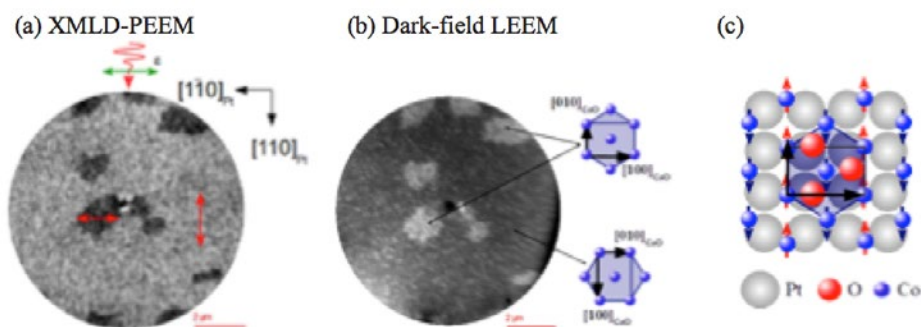


Figure 1: (a) CoO antiferromagnetic domains observed on $\text{Pt}(001)$ by PEEM using XMLD contrast at Co- L_3 edge. The magnetic orientation is represented by red arrows. (b) Dark field image of the same area measured by LEEM. Dark (bright) areas correspond to crystalline domains with $[010]_{\text{CoO}}$ oriented parallel to $[1 -1 0]_{\text{Pt}}$ ($[110]_{\text{Pt}}$). (c) Atomic and magnetic structures of CoO on $\text{Pt}(001)$.

References:

- [1] T Jungwirth et al, Nature Nanotechnology 11, 231–241 (2016)
- [2] A Fraile Rodriguez et al, Phys. Rev. B 92, 174417 (2015)
- [3] S. I. Csizsar et al, Phys. Rev. Lett. 95, 187205 (2005)
- [4] A. D. Lamirand et al, Phys. Rev. B 88, 140401(R) (2013)

Thu-PS2-41**Titanate nanotube supported plasmonic gold and rhodium particles for heterogeneous photocatalysis**

Balázs László¹, Kornélia Baán¹, Albert Oszkó^{1,4}, András Erdőhelyi¹, Zoltán Kónya^{2,3}, János Kiss^{1,3}

¹ Department of Physical Chemistry and Materials Science, University of Szeged, Aradi vértanúk tere 1., Szeged, H-6720, Hungary;

² Department of Applied and Environmental Chemistry, University of Szeged, Rerrich Béla tér 1., Szeged, H-6720, Hungary;

³ MTA-SZTE Reaction Kinetics and Surface Chemistry Research Group, Rerrich Béla tér 1., Szeged, H-6720, Hungary;

⁴ ELI-ALPS, ELI-HU Non-profit Ltd.- Szeged Hungary

The photocatalytic reactions in the $\text{CH}_4 + \text{H}_2\text{O}$ and in the $\text{CO}_2 + \text{H}_2$ systems were investigated in this research. The methane-water reaction could be important in energy storage while the CO_2 -reduction can be useful for CO_2 capture [1,2]. The photon-driven variants of these reactions could be promising alternatives of the thermal reactions in the future when the utilization of solar energy will be unavoidable.

Titanate nanotubes are attractive materials for photocatalysts because of their high surface area, elongated shape, good ion exchange capability and suitable semiconductor properties [3]. We modified them with Au and Rh co-catalysts in order to improve their photocatalytic activity. The catalysts were characterized with transmission electron microscopy, X-ray photoelectron spectroscopy and UV-VIS spectroscopy. The photoreactions were carried out in a flow-type photoreactor in gas phase. A mercury-arc UV source was used for excitation. *In-situ* infrared spectroscopy was used to investigate the surface composition of the catalysts during the reactions.

The metal modified catalysts showed increased activity in the reactions and the effect of the metals strongly correlated with their chemical and physical character. The size of the nanoparticles we used is on the borderline of molecular-like clusters and metallic particles. The molecular orbital interactions between the small metal clusters and the reactants and the metallic state with excitable plasmon resonance have to be also taken into account in this size range. We suggest that the photocatalytic excitation of the plasmon oscillation takes place in the reaction mechanisms in case of Au catalysts, but Rh acts in a more classical way.

Acknowledgements:

Financial support of this work by the Hungarian Research Development and Innovation Office through grants GINOP-2.3.2-15-2016-00013 and NKFIH OTKA K120115 is gratefully acknowledged.

Thu-PS2-37**Surface spectroscopic analysis of transition metal doped TiO₂ nanoparticles**

Lee Hangil

Department of Chemistry, Sookmyung Women's University, Seoul 140-742, Republic of Korea

The modified anatase TiO₂ nanoparticles to enhance their catalytic activities by doping them with the five transition metals (Cr, Mn, Fe, Co, and Ni) have investigated using various surface analysis techniques such as scanning transmission X-ray microscopy (STXM) and high resolution photoemission spectroscopy (HRPES). To compare catalytic activities of these transition metal-doped TiO₂ nanoparticles (TM-TiO₂) with anatase TiO₂ nanoparticle, we monitor their performances in the catalytic oxidation of 2-aminothiophenol (2-ATP) by using HRPES and on the oxidation of 2-ATP in aqueous solution by taking electrochemistry (EC) measurements. As a result, we clearly investigate that the increased defect structure induced by the doped transition metal are closely correlated with the enhancement of catalytic activities of TiO₂.

Tue-PS1-21**Atomistic modeling of alkali metals (Li, Na, K) intercalation into graphite**

[Olena Lenchuk](#), [Doreen Mollenhauer](#)

Justus-Liebig-University Gießen, Institute of Physical Chemistry, Heinrich-Buff-Ring 17, 35392 Gießen

Sodium-ion batteries (SIBs) are potential candidates for the energy-storage applications of the next generation [1]. Due to abundance of sodium in nature, sodium-ion batteries are considered as the best alternative power sources to traditionally used lithium-ion batteries. The intercalation chemistry of sodium and lithium is similar and therefore similar battery compounds can be used for both systems [2]. One of the challenges in SIBs is to design anode materials with high storage capacities. Graphite, which is commonly used as a negative electrode, hardly intercalates sodium ions. The sodium-rich binary graphite intercalation compounds (b-GICs) are energetically not stable [3-4]. The working hypotheses of the observed behavior include (1) mismatch between the graphite structure and the size of the Na ion and (2) unfavorable stretching of C-C bonds between two graphene layers. In the following study, we address these hypotheses and investigate the influence of alkali metals (AM = Li, Na, K) on graphite by means of density-functional theory calculations. The stability of AM-GICs with increasing concentration of alkali metals is evaluated by formation energies. The energetically preferable distribution of alkali metals in graphite and their influence of the graphite stacking sequence are carefully considered. The difference in bonding nature between Li, Na as well as K and graphite is estimated in a systematic way.

References:

- [1] M.D. Slater, D. Kim, E. Lee and C.S. Johnson, Sodium-Ion Batteries, *Adv. Funct. Mater.* 23 (2013) 947-958.
- [2] J.-Y. Hwang, S.-T. Myung and Y.-K. Sun, Sodium-ion batteries: present and future, *Chem. Soc. Rev.*, 2017.
- [3] K. Nobuhara, H. Nakayama, M. Nose, Sh. Nakanishi and H. Iba, First-principles study of alkali metal-graphite intercalation compounds, *J. Power Sources* 243 (2013) 585-587.
- [4] Zh. Wang, S.M. Selbach and T. Grande, Van der Waals density functional study of the energetics of alkali metal intercalation in graphite, *RSC Adv.* 4 (2014) 4069-4079.

Tue-PS1-22**Adsorption of CO and H₂O on Fe₃O₄ surfaces studied by density-functional theory**

[Xiaoke Li](#), [Joachim Paier](#)

Institut für Chemie, Humboldt-Universität zu Berlin, Unter den Linden 6, 10099 Berlin, Germany

Atomic level understanding on the interaction of CO and H₂O with oxide surfaces is of crucial importance in solving problems like hydrogen production and alternative energy conversion strategies. Fe₃O₄ (magnetite) represents a versatile oxide material due to many industrial applications [1,2]. This work reports results on periodic models of adsorbed CO and H₂O on various Fe₃O₄ surfaces. We study the adsorption thermodynamics and infrared spectra of the aforementioned adsorbed species in order to characterize these systems. We employ density-functional theory using the Perdew, Burke, Ernzerhof [3] gradient-corrected exchange-correlation functional including a correction for the Fe 3d levels by an onsite Hubbard-type U parameter. This approach was shown to perform accurately [4,5].

References:

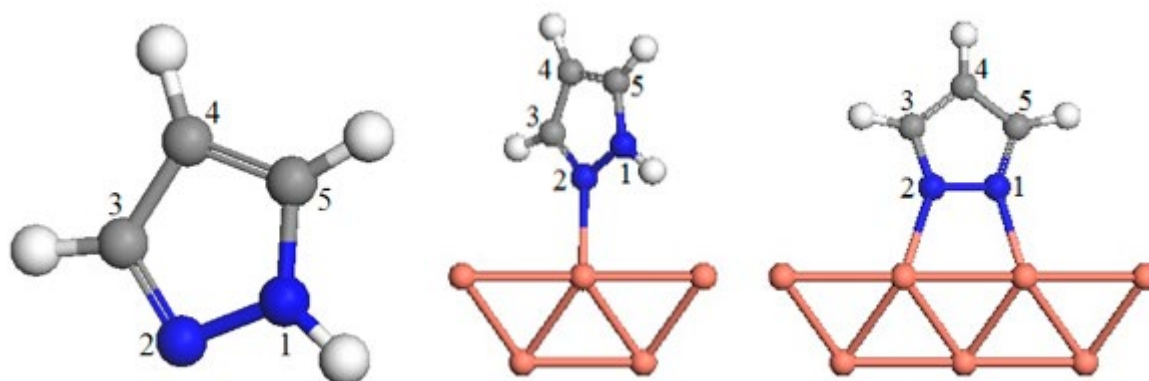
- [1] Xu, F., et al. *CrystEngComm*. 2013, 15, 4431.
- [2] Smit, E. de; Weckhuysen, B. *Chem. Soc. Rev.* 2008, 37, 2758.
- [3] Perdew, J. P.; Burke, K.; Ernzerhof, M. *Phys. Rev. Lett.* 1996, 77, 3865.
- [4] X. Li, J. Paier, *J. Phys. Chem. C* 2016, 120, 1056.
- [5] X. Li, J. Paier, J. Sauer, F. Mirabella, E. Zaki, F. Ivars-Barceló, S. Shaikhutdinov, H.-J. Freund, submitted.

Thu-PS2-06**Adsorption and thermal reaction of 1H-pyrazole on Cu(100)**

Jong-Liang Lin

Department of Chemistry, National Cheng Kung University, Taiwan

The studies of nitrogen-containing heterocyclic compounds are of importance in combustion chemistry, environmental protection, surface modification and corrosion inhibition of copper. Adsorption and thermal reaction of 1H-pyrazole ($C_3N_2H_4$) on Cu(100) have been investigated with temperature-programmed reaction/desorption, reflection-absorption infrared spectroscopy, X-ray photoelectron spectroscopy and calculation in the framework of density functional theory. 1H-pyrazole can be adsorbed on Cu(100) at 120 K, with intact molecule and the dissociative form of $C_3N_2H_3$ by 1N -H bond scission. At 250 K, only the $C_3N_2H_3$ intermediate with C_3N_2 ring structure exists on the surface. The theoretical result predicts that 1H-pyrazole is adsorbed on Cu(100), with the 2N atom located at atop site and the $C_3N_2H_3$ intermediate is bonded to the surface via the two N atoms near two neighboring copper atoms. The dehydrogenated 1H-pyrazole species ($C_3N_2H_3$) has the C_{1s} and N_{1s} binding energies at 285.3 and 400.0 eV, respectively, and has infrared absorptions at 981, 1255 and 1475 cm^{-1} from the ring bending, N-C stretching and C-H bending modes. The $C_3N_2H_3$ intermediate decomposes on Cu(100) at ~ 550 K, generating HCN, N_2 , CH_3CN and H_2 . No hydrocarbon products are found. These products reveal the dissociation pathways of the $C_3N_2H_3$ intermediate. The N_2 is from the cleavage of the 1N - 5C and 2N - 3C bonds. The HCN and CH_3CN products are due to the 2N - 1N and 3C - 4C bond scission.



Thu-PS2-45**Preformed cluster mobility as a probe for surface characterization**

[Julie Lion](#), [Pierre Billaud](#), [Alain Sarfati](#), [Nouari Kébaïli](#)

Laboratoire Aimé Cotton – UMR 9188 – CNRS, Université Paris-Sud et Ecole Normale Supérieure de Cachan, Bât 505, Campus d'Orsay F-91405 Orsay Cedex, France

An interesting and original approach step in the elaboration process of nanostructured materials consists of using preformed nanoparticles as elementary building blocks instead of atoms or molecules. In this case, the nanostructures obtained have shown that the morphology of islands grown on surfaces from soft-landed preformed clusters depends on the nature and temperature of the substrate, on the nature, size and flux of the clusters.

We have extended those studies to the benchmark deposition of metal clusters on different characteristic surfaces. It appears that, as the mobility of deposited clusters is highly influenced by the surface electronic and topological properties, then nanostructures obtained can also be seen as characteristic signature of local surface structure. Could we use the clusters, not only as building blocks, but also as a local probe for the surface characteristics is the main raised question here. The use of clusters deposition as probe for surface states characterization appears as an attractive and remarkable tool.

Thu-PS2-40**Surface plasmons on aluminum particles and silicon nanocrystals in off-stoichiometric SiO₂ films used to increase the conversion efficiency in silicon solar cells**

[Jesus Carrillo López](#), [José Alberto Luna López](#)

CIDS-ICUAP, Benemérita Universidad Autónoma de Puebla. Ed. 103 C, Col, San Manuel, Apdo. 1651, Puebla, Pue. México 72570

Currently, photovoltaic (PV) energy is one of the most attractive options for generating electricity using clean and renewable energy. However, PV energy is not yet economical compared to energy obtained through conventional sources. Therefore, it is essential to reduce manufacturing costs of solar cells, which constitute the PV modules. Research of silicon nanocrystals (Si NCs) has been actively conducted because Si NCs have shown intriguing properties such as bandgap control with nanocrystal size, very fast optical transition, and multiple carrier generation. Recently, we showed it is possible to increase the energy conversion efficiency of silicon solar cells by means of silicon rich oxide (SRO) films deposited on the solar cells surface. These films have the optical property of absorption below 300 nm radiation (UV), so that the absorbed energy by the SRO film is then reemitted as red light (photoluminescence). Silicon solar cells have a greater response in the 500 to 1000 nm spectral range, so that the redshift of the short wavelengths offers an increase in the efficiency of the silicon solar cell. On the other hand, the emerging field of plasmonics has yielded methods for guiding and localizing light at the nanoscale, well below the scale of the wavelength of light in free space. Now plasmonics researches are turning their attention to solar cells, where design approaches based on plasmonic can be used to increase the absorption in PV devices.

In this work we present the design and fabrication of a silicon solar cell structure, which uses the combined effects of a passivating Silicon Rich Oxide (SRO) Film Silicon with silicon nanocrystals embedded, and localized Surface Plasmons on aluminum particles deposited on the SRO film. Results on improved electrical and optical parameters, like as fill factor, efficiency and spectral response, are compared with those for conventional SiO₂ (SILOX technique) – covered silicon solar cells. Short Circuit Current, Open Circuit Voltage and Conversion Efficiency values for different aluminum nanoparticles sizes are presented. Also, the spectral response of the solar is presented and compared with simulation results based on a point dipole model.

References:

- [1] J. Carrillo, J. A. Luna, I. Vivaldo, M. Aceves, A. Morales, G. García, *Solar Energy Mat. And Solar Cells*, 100 (2012) 39-42
- [4] Harry A. Atwater, Albert Polman, *Nature Mater.* 9 (2010) 205-213
- [3] K. R. Catchpole, A. Polman, *OPTICS EXPRESS* vol. 16 no 26 (2008)

Thu-PS2-21**Multi-wall carbon nanotubes grown by USP-CVD: study of the growth time ratio against its length**

A. Garzon -Roman¹, J. A. Luna López¹, A. D. Hernández-de la Luz¹, M. E. Rabanal Jimenez²

¹ CIDS-ICUAP, Benemérita Universidad Autónoma de Puebla. Ed. 103 C, Col, San Manuel, Apdo. 1651, Puebla, Pue. México 72570;

² Materials Science and Engineering Department and IAAB, Universidad Carlos III de Madrid, 28911 Leganes, Spain

Multi wall carbon nanotubes (MWCNTs) are an allotropic form of carbon, MWCNTs are studied extensively since they were discovered in 1991 [1, 2]. Their potential applications are many and varied as [3]: hydrogen storage, field emission, composite materials, catalysts, nanoelectronic devices, printed electronics, supercapacitors, ultra-light composites [4-10], owing to their different properties such as: mechanical, electrical, thermal and chemical. These kinds of structures are built using different carbon-based precursors and metallic catalyzers; such structures are obtained by several methods, which allow the CNT synthesis. Among these methods, we find the dc arc discharge, laser ablation, PECVD, among others [2, 11-13]. There is some simple and inexpensive method, where it is possible to obtain high quality CNTs, but the main problem is the high temperature needed for the synthesis, others only can to be used to produce to the lab scale, but both need one additional process of purification. For large-scale production the Catalytic chemical vapor deposition technique (CCVD) has been is used [14–20] and this method working at low temperatures (<800°) is simple and cheap with median purity, but the CNTs grown contain some defects and there is sometimes a risk with the atmosphere used in the furnace. Spray pyrolysis (SP) is an appropriate technique for the preparation of different thin films as transparent conductor oxides [20-21], sulfides [22], and nitrides [23].

In this paper, the growth of Multi-Wall Carbon Nanotubes (MWCNTs) using toluene and ferrocene as precursors by ultrasonic spray pyrolysis with chemical vapour deposition (USP-CVD) is reported. The MWCNTs were synthesized on silicon substrates under optimal conditions. The investigation was performed using different growth times of 2, 3, 4, 5 and 10 minutes, in order to examine their effect on the quality of the nanostructures and length of the carbon nanotubes produced, these lengths were of 16, 29, 47, 80 and 142 μm , respectively. Structural, optical and morphological differences of the MWCNTs grown as vertical columns are studied and discussed. The micrographs were obtained using a Field Emission Scanning Electron Microscopy (FE-SEM) and High Resolution Transmission Electron Microscopy (HRTEM) and they correspond to the MWCNT growth times of 2, 3, 4, 5 and 10 minutes, for which we obtained their diameter of around of 18, 38, 40, 25 and 28 nm, respectively. The Raman spectra show the MWCNTs with a high quality, as is evidenced by the $I_{\text{D}}/I_{\text{G}}$ and $I_{2\text{D}}/I_{\text{G}}$ intensity ratios of 0.53 and 1.11, respectively.

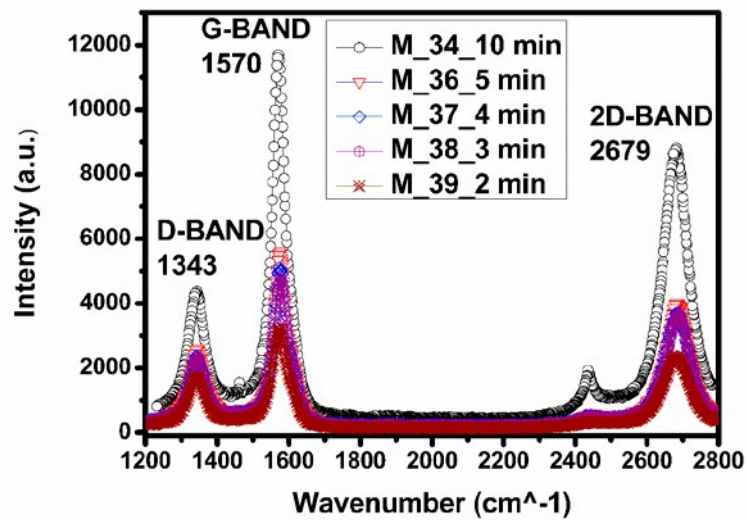


Fig. 1. Raman spectra of the CNTs grown on silicon substrates varying the growth time.

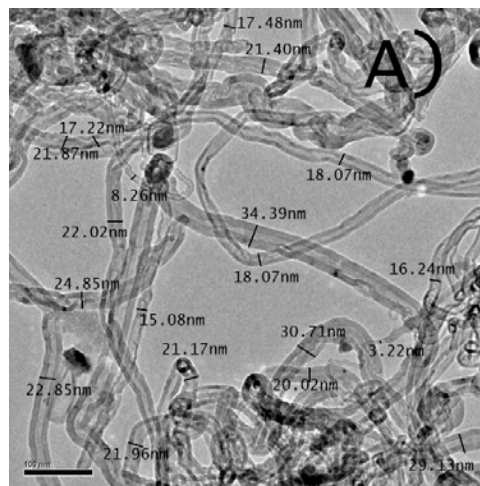


Fig. 2. The CNT TEM images obtained under different growth times conditions in low magnification, (a) 2 min.

References:

- [1] S. Iijima. Helical microtubules of graphitic carbon. *Nature* 1991; 354: 56-58.
- [2] Rakesh A. Afre, T. Soga, T. Jimbo, Mukul Kumar, Y. Ando, M. Sharon, Growth of vertically aligned carbon nanotubes on silicon and quartz substrate by spray pyrolysis of a natural precursor: Turpentine oil, *Chemical Physics Letters*, 414, 6-10, 2005.
- [3] L. F. Su, J. N. Wang, F. Yu, Z. M. Sheng, Hyuk Chang, Chanhok Pak, Continuous production of single-wall carbon nanotubes by spray pyrolysis of alcohol with dissolved ferrocene, *Chemical Physics Letters*, 420, 421-425, 2006.
- [4] A.C. Dillon, K.M. Jones. Storage of hydrogen in single-walled carbon nanotubes. *Nature* 1997; 386: 377-379.
- [5] H.M. Cheng, Q.H. Yang, C. Liu. Hydrogen storage in carbon nanotube. *Carbon* 2001; 39: 1447-1454.
- [6] S.J. Tans, A.R.M. Verschueren, C. Dekker. Room-temperature transistor based on a single carbon nanotube. *Nature* 1993; 393: 49-52.

Tue-PS1-24

Adsorption and dehydrogenation of naphthalene on nickel(111)

[K.M. Marks](#)¹, [M. Ghadami Yazdi](#)², [P.H. Moud](#)³, [W. Piskorz](#)⁴, [A. Kotarba](#)⁴, [T. Hansson](#)¹, [H. Öström](#)¹, [M. Göthelied](#)², [K. Engvall](#)³

¹ Stockholm University, Dept Physics, Chemical Physics, 106 91 Stockholm, Sweden;

² KTH, ICT, Materials Physics 16440 Kista, Sweden;

³ KTH, Dept of Chemical Engineering, 100 44 Stockholm, Sweden;

⁴ The Polish Academy of Theory and related phenomena;

The gasification of biomass is an important step in the production of renewable energy in the form of syngas from organic waste. To be able to use the gas product as an energy source the heavier hydrocarbons such as naphthalene, that are typically present, are a hindrance. An elegant way to remove these is by catalytically converting them to more useful molecules such as CO and H₂. [1] Nickel based catalysts are commonly used for the conversion of hydrocarbons and are considered a possible catalyst also for biomass gasification [2], but are notorious for being poisoned due to strong chemisorption. [3] Here we have used Scanning Probe Microscopy (STM), Temperature Programmed Desorption (TPD) and Density Functional Theory (DFT) to investigate the adsorption and dehydrogenation of naphthalene on Nickel (111) in Ultra High Vacuum (UHV).

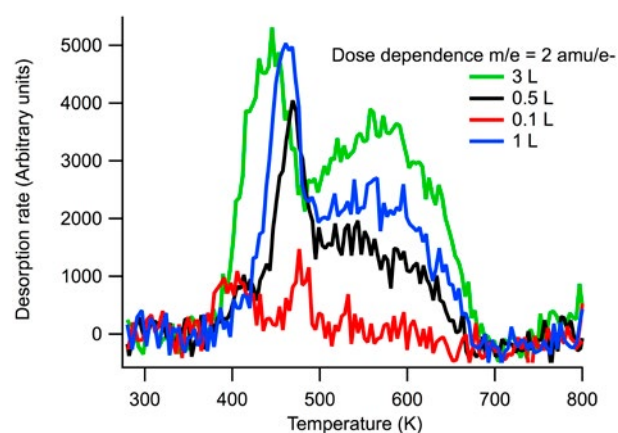
STM measurements show that at room temperature naphthalene adsorbs flat on the smooth terraces with the aromatic rings centered on top of Ni-atoms. Near terrace edges the layer is 0.25 Å higher because naphthalene adopts a tilted geometry; standing on its' side creating two Ni-C bonds and two hydrogen atoms. Preliminary DFT results confirm these findings.

Hydrogen production from naphthalene was monitored by measuring desorption of molecular hydrogen from the naphthalene covered surface. TPD of molecular hydrogen shows one sharp peak around 400 K and one broader peak above 500 K. The sharp peak broadens and shifts down in temperature with increased coverage in the first monolayer. After molecular hydrogen has been desorbed the surface is covered in carbon fragments that hinder further catalytic activity. This passivation was investigated by running multiple subsequent TPD cycles. Both peaks in the hydrogen TPD lose intensity after each cycle at different rates. After 6 cycles the catalytic activity with respect to hydrogen production was negligible.

Dosing naphthalene at 470 K increases the intensity of the second peak substantially. We calculated that through this dosing scheme the hydrogen production yield can be increased by 60% without increasing carbon passivation. We tentatively attribute this to closer packing of partially dehydrogenated molecules on the surface that potentially adsorb in a tilted geometry also on terrace sites. These studies add to the understanding of hydrogen production mechanisms that are important in gasification of biomass.

References:

- [1] Engvall, K., et al., Upgrading of Raw Gas from Biomass and Waste Gasification: Challenges and Opportunities. *Topics in Catalysis*, 2011. 54(13-15): p. 949-959.
- [2] Rostrup-Nielsen, J. and L.J. Christiansen, CONCEPTS IN SYNGAS MANUFACTURE. 2011, Singapore, UNITED STATES: World Scientific Publishing Company.
- [3] Bartholomew, C.H., Mechanisms of nickel catalyst poisoning. *Studies in Surface Science Catalysis*, 1987. 34: p. 81-104.



Tue-PS1-23 Ellipsometric and XPS study of Zr and ZrO₂

Tivadar Lohner¹, Péter Petrik¹, Attila Sulyok¹, Tamás Novotny², Erzsébet Perez-Feró², Benjámín Kalas¹, Emil Agócs¹, Miklós Menyhárd¹, Zoltán Hózer²

¹ Institute for Technical Physics and Materials Science, Centre for Energy Research, Hungarian Academy of Sciences, Konkoly Thege Miklós út 29-33, H-1121 Budapest, Hungary;

² Atomic Energy Research Institute, Centre for Energy Research, Hungarian Academy of Sciences, Konkoly Thege Miklós út 29-33, H-1121 Budapest, Hungary

Zirconium and its oxide have been applied in a broad range of fields. Zr and Zr alloy tubes for example are used in the nuclear industry as cladding for fuel elements, because Zr has low absorption cross section for neutrons. Understanding its oxidation during the operation of nuclear reactors is a major safety issue [1]. Zr tubes made of E110G alloy with diameters of 9.1 mm have been investigated in this study by spectroellipsometry using focusing (Fig. 1). The measurement series included not only the original (as received) material, but several cladding tubes have been oxidized in steam atmosphere at temperatures of 600°C and 800°C for different durations. Multi-sample and depth profiling optical models have been used to evaluate the measured ellipsometric spectra to determine the refractive index and the extinction coefficient in function of wavelength for both the Zr alloy and its oxide and the oxide thicknesses. A vertical inhomogeneity of the oxide properties has been found by the ellipsometric measurements as well as by depth-profiling X-ray photoelectron spectroscopy investigations (by applying low energy Ar ion bombardment) that have shown the formation of sub-oxides at the interface region of Zr and its surface oxide.

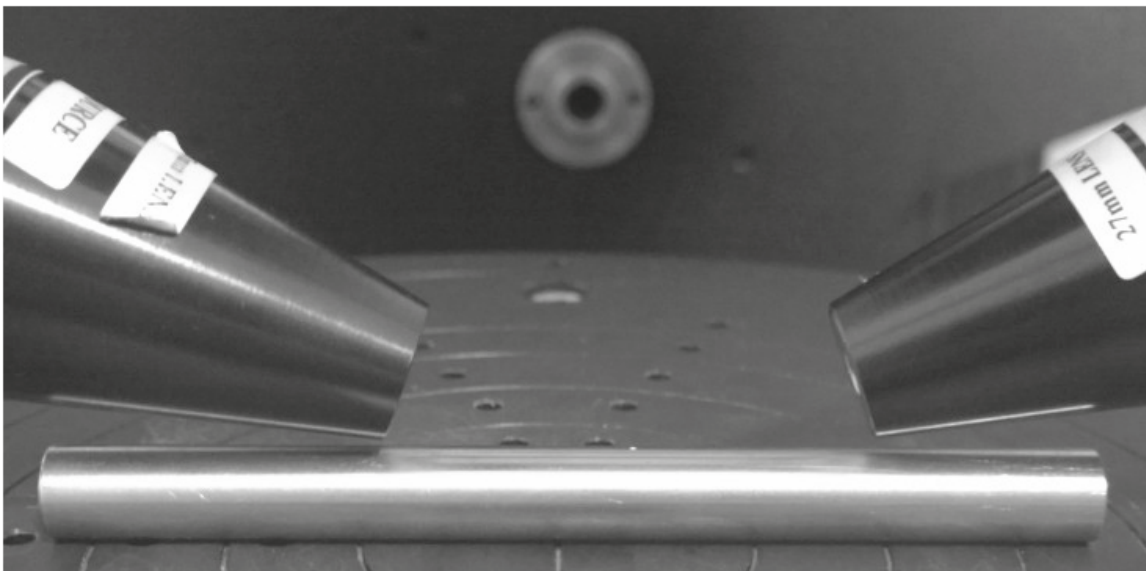


Fig. 1. Ellipsometric measurement of a Zr alloy tube for nuclear fuel cladding using focusing.

References:

- [1] Z. Hózer, Cs. Győri, L. Matus, M. Horváth, Ductile-to-brittle transition of oxidized Zircaloy-4 and E110 claddings, *Journal of Nuclear Materials* 373, 415–423 (2008).

Thu-PS2-09**XPS MultiQuant: multimodel XPS quantification software****M. Mohai**

Institute of Materials and Environmental Chemistry, Research Centre for Natural Sciences, Hungarian Academy of Sciences, Budapest, Hungary

Quantitative evaluation of XP spectra is a major issue in surface characterisation. Although lots of XPS quantification methods and programs are developed and published, usually the simplest ones are built into the commercial data systems broadly used in the practice. The aim of developing the XPS MultiQuant program was to give a freely available tool to the surface analysts, and producing the correct analytical results in most of the cases. Both the two main tasks of a quantification program: calculation of surface composition and layer thickness calculation can be performed.

Chemical composition

The surface chemical composition is calculated by the *infinitely thick homogeneous model*. The program [1] has a built-in library with all basic data for the quantification. All of the usual factors and correction methods, including cross section, asymmetry parameter, analyser transmission, IMFP, can be applied. Calculation for several samples or experimental data sets can be performed simultaneously. Chemical compositions can be presented in several ways, like *Atomic %*, *Atomic ratio* or *Mass %*, *Oxide %*, etc. A correction method can compensate the effect of adventitious carbon contamination up to 5 nm thick hydrocarbon layer [1].

Layer thickness

Several sample geometry models are available for layered structures on flat and curved surfaces. Setting up of a layer model by the program is easy and can be applied routinely [2-3]. The layer thickness calculations can transform the surface composition results into an other dimension. Thickness data, even they are not absolutely precise, give more information on the studied system.

Unique features

- Curved surfaces (spherical or cylindrical) and nanotubes, covered by thin overlayers, are frequently occurred and applied in the practice of surface analysis. XPS MultiQuant includes these special models to calculate layer structures on powders, fibres [2] and even on randomly stacked cylindrical shape nanotubes [3]. The layer thickness from an angle dependent experiment sets ('ARXPS') can be calculated together.
- The program can also be used for simulations: the integrated photoelectron intensity can be calculated for a defined composition and model layout.
- The software made to be ready to communicate with other XPS related applications through *XPS Reduced Data Exchange Files* [4].

XPS MultiQuant is freeware for non-commercial use and is available from the homepage of the program (<http://aki.ttk.mta.hu/XMQpages/XMQhome.htm>).

References:

- [1] M. Mohai, Surf. Interface Anal. 36, 828 (2004); doi:10.1002/sia.1775.
- [2] M. Mohai, I. Bertóti, Surf. Interface Anal. 36, 805 (2004); doi:10.1002/sia.1769.
- [3] M. Mohai, I. Bertóti, Surf. Interface Anal. 44, 1130 (2012); doi:10.1002/sia.4864.
- [4] M. Mohai, Surf. Interface Anal. 38, 640 (2006); doi:10.1002/sia.2198.

Thu-PS2-26

Iron phthalocyanine on ultrathin alumina template

[Fatema Mohamed](#)^{1,2}, Manuel Corva¹, Zhijing Feng¹, Nicola Seriani², Maria Peressi^{1,3}, Erik Vesselli^{1,3}

¹ Department of Physics, University of Trieste, Italy;

² International Center for Theoretical Physics, Trieste, Italy;

³ IOM-CNR, Trieste, Italy

The variety of applications of metal phthalocyanines (MPC) is a strong motivation to characterize their structure. Phthalocyanines (Pc) can accommodate a metal atom (M) in their tetrapyrrole cage, which can act as a biomimetic catalytic centre. These molecules adsorb on different surfaces and self-assemble in ordered structures, stable enough to provide optimal candidates to model single atom catalysis. We focus here in particular on Iron phthalocyanines on ultrathin alumina films. We characterize the ordered structures that can be formed depending on the coverage and on the presence of seeding Cu nanoclusters. The combination of ab-initio calculations and experiments allows to determine their relevant electronic properties and reactivity.

We acknowledge financial support from University of Trieste through the program "Finanziamento di Ateneo per progetti di ricerca scientifica – FRA 2016" and computational resources from CINECA through the IS CRA initiative and the agreement with the University of Trieste.

Tue-PS1-25**Insight into surface-confined 2D polymerization of a 1,2-bis(4-bromophenyl) ethyne on Ag(110) surface**

[Elaheh Mohebbi](#), [Silvia Carlotto](#), [Masoud Fakhrabadi](#), [Francesco Sedona](#), [Mauro Sambì](#), [Maurizio Casarin](#)

Department of Chemical Sciences, University of Padova, Via Marzolo 1, 35131, Padova, Italy

The bottom-up synthesis of covalently bonded organic nanostructures recently has become a promising approach to obtain surface-supported nanostructured two-dimensional (2D) networks [1]. The controlled assembly of highly ordered organic molecules is a subject of ongoing research, having many potential applications for the development of molecular nanotechnologies and optoelectronics such as organic light-emitting devices (OLEDs) and organic field-effect transistor (OFET) [2]. In the recent years, the research interests for surface-supported organic monolayers have been focused on the growth of graphene-like structures with the aim of inserting functional groups in the starting building units to allow the synthesis of well-ordered surface covalent organic frameworks (SCOFs) [3]. In this study, scanning tunneling microscopy (STM) measurements have been combined with DFT calculations to investigate the 1,2-bis(4-bromophenyl)ethyne as the precursor molecule in polymerization reaction leading to oriented graphene-like nanoribbons on Ag (110) surface. The calculations have been performed by using the generalized gradient approximation with the Perdew-Burke-Ernzerhof (PBE) functional as implemented in the Quantum ESPRESSO code. Long-range dispersion forces were introduced by using the empirical correction scheme proposed by Grimme to take account of van der Waals interactions. The STM analysis of the samples held at RT confirmed that monomers of 1,2-bis(4-bromophenyl)ethyne are completely debrominated on the Ag(110) surface and the resultant ph-C≡C-ph biradicals are linked by the Ag adatom.

The annealing of the organometallic structure at 473 K yields an extended conjugated polymeric phase by linking the neighboring ph-C≡C-ph biradical units, while the Ag adatoms were released. The bromine atoms are aligned between the organometallic structures on the top/bridge sites at RT and at the hollow positions at high temperature. The inclusion of the long-range dispersion forces provided a better agreement between simulated STM images and experimental evidences recorded at negative bias. In addition, a thorough analysis of the electronic structure revealed a noticeable electron density rearrangement at the interface region.

References:

- [1] Sedona, F, et al. ACS Nano 2010, 4, 5147.
- [2] Píš, I, et al. J. Phys. Chem. C 2016, 120, 4909.
- [3] Basagni, A, et al. ACS Nano 2016, 10, 2644.

Thu-PS2-18
Electrostatic shielding versus sterical ligand stabilization: tunable nanocrystal stabilization mechanisms

Lars Mohrhusen¹, Milena Osmić¹, Joanna Kolny-Olesiak², Katharina Al-Shamery¹

¹ Carl von Ossietzky University of Oldenburg, Institute of Chemistry, Physical Chemistry 1, Carl-von-Ossietzky-Straße 9-11, D-26129 Oldenburg, Germany;

² Carl von Ossietzky University of Oldenburg, Institute of Physics, Energy and Semiconductor Research Laboratory (EHF), Nanochemistry, Carl-von-Ossietzky-Straße 9-11, D-26129 Oldenburg, Germany

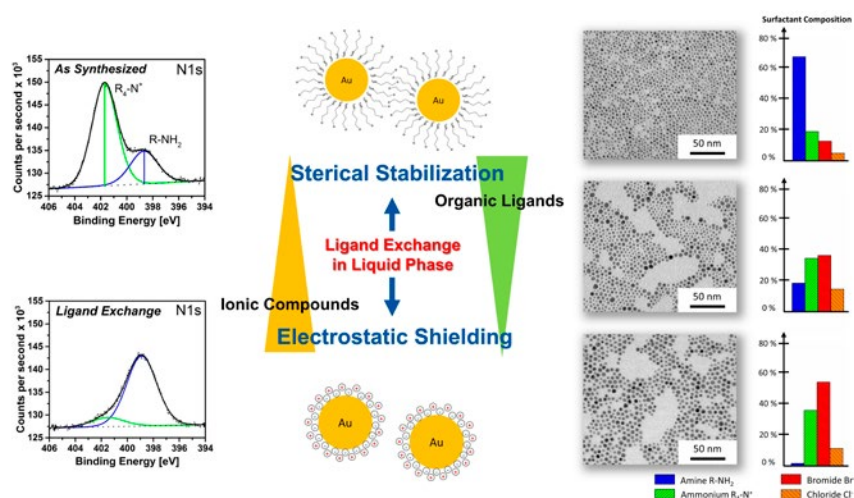
Metal nanomaterials enjoy great interest in almost every field of science and technology and are utilized in various applications such as biomedical sensing, optoelectronic devices, innovative coatings microelectronics. However, the requirements for well-defined nanoparticles are relatively high.^[1]

Colloidal metal nanoparticles are usually synthesized via the reduction of metal salt precursor compounds. Commonly organic capping agents are used to prevent agglomeration, but normally it is neglected that ionic compounds may coadsorb when present in the mixture. In order to address this issue, we developed a simple ligand exchange procedure in liquid phase under mild conditions. For this purpose we adopted a one-pot synthesis for the fabrication of noble metal nanoparticles initially developed by Jana and Peng and modified it by means of concentrations, various ligands and temperature control.^[2, 3]

The stabilization of such nanoparticles turned out to be a competitive combination of sterical ligand stabilization and electrostatic shielding. By means of transmission electron microscopy (TEM) and x-ray photoelectron spectroscopy (XPS) we could show that the ratio of ionic adsorbates to molecular ligands plays a key role for stabilization and ripening effects. Quantitative XPS studies demonstrate that we can adjust the ratio of both contributions via the ligand exchange procedure for production of nanoparticles with tailor-made surfactant composition.

The distinct properties of nanomaterials are dramatically influenced by the morphology and crystal orientation. However, high resolution TEM studies proved that the surfactant composition has no impact on the nanoparticle morphology.

Introducing a lack of stabilization by weaker sterical ligands offers an auspicious new way for the synthesis of porous nanomaterials. The finding that electrostatic shielding by ionic coadsorbates can be a crucial key shines new light to colloidal synthesis of nanomaterials in general.^[4]


References:

- [1] Y. Xia, Y. Xiong, B. Lim et al., *Angew. Chem.*, 121, 62-108 (2009).
- [2] N. R. Jana, X. Peng, *J. Am. Chem. Soc.*, 125, 14280-14281 (2003).
- [3] M. Osmić, J. Kolny-Olesiak and K. Al-Shamery, *CrystEngComm*, 16, 9907-9914 (2014).
- [4] L. Mohrhusen and M. Osmić, *RSC Adv.*, 7, 12897-12907 (2017).

Thu-PS2-30
Surface mobility and nucleation of a molecular switch: tetraaniline on hematite

Amirmasoud Mohtasebi, Peter Kruse

Department of Chemistry and Chemical Biology, McMaster University, 1280 Main Street West, Hamilton, Ontario, L8S 4L8, Canada

We have studied the mobility of different oxidation states of Phenyl-capped aniline tetramer (PCAT) on fully and partially oxidized iron oxide surfaces through the critical number of molecules required to form a stable island (i). Fully reduced (LB) and fully oxidized (PB) forms of PCAT are deposited on hematite(1000) single crystal surfaces via physical vapor deposition. Scaling behavior of the island-size distribution¹ in the aggregation regime (typically $0.1 < \theta < 0.5$) for both forms of the oligoanilines is demonstrated. Based on the distribution of the scaling function ($f_i(u)$), it is evaluated that four LB molecules, and seven PB molecules are required to form stable islands of LB and PB on hematite surfaces, respectively. Using the island density as a function of temperature, the activation energies of the critical nuclei of LB ($i = 4$) and PB ($i = 6$) on hematite(1000) are measured to be 1300 ± 5 meV and 527 ± 16 meV, respectively. This analysis reveals a higher energy barrier for the mobility of LB molecules in comparison to PB molecules on hematite(1000) surfaces. Using this information, the diffusion attempt frequency for each type of the islands was evaluated. In addition, the induced effect of the oxidation state of the iron oxide substrate (Fe_2O_3 or $\text{Fe}_2\text{O}_3 + \text{Fe}_3\text{O}_4$) on mobility of each state of PCAT was studied. For this aim, the changes in i value of LB and PB islands before and after reduction of iron oxide were evaluated.

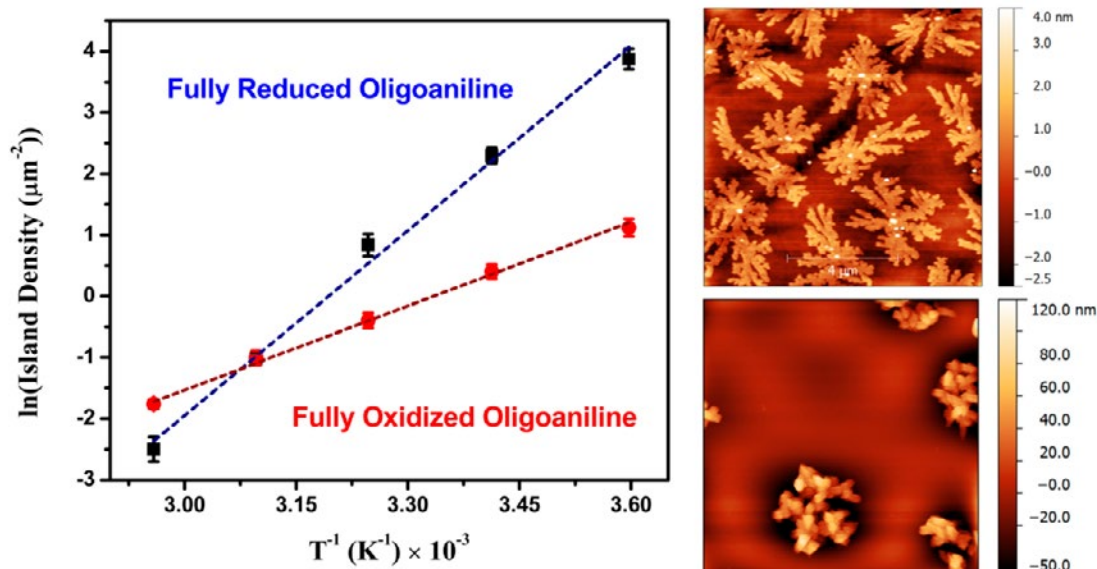


Figure: Island density of reduced and oxidized PCAT on hematite(1000) single crystal as function of surface's temperature.

References:

- [1] Ruiz, R.; Nickel, B.; Koch, N.; Feldman, L.; Haglund, R.; Kahn, A.; Family, F.; Scoles, G. Dynamic Scaling, Island Size Distribution, and Morphology in the Aggregation Regime of Submonolayer Pentacene Films. *Phys. Rev. Lett.* 2003, 91 (13), 136102-1-136102-4

Tue-PS1-26

Formate decomposition dynamics on Cu(111): importance of CO₂ bending vibrational mode

Fahdzi Muttaqien, Hiroyuki Oshima, Yuji Hamamoto, Kouji Inagaki, Ikutaro Hamada, and Yoshitada Morikawa

Department of Precision Science and Technology, Graduate School of Engineering, Osaka University, 2-1, Yamada-oka, Suita, Osaka 565-0871, Japan

One of the most important intermediate step in the methanol synthesis over Cu-based catalysts is CO₂ hydrogenation into formate (HCOO).¹ Formate synthesis has been experimentally clarified to occur by the Eley-Rideal mechanism,² which suggests that the reaction rate depends on the initial impinging CO₂ energy. Since formate synthesis and decomposition are reversible reactions, the initial impinging CO₂ energy must be related to the energy states of desorbed CO₂ from formate decomposition. Therefore, elucidation of formate decomposition dynamics is important for improving catalytic formate synthesis. We performed *ab initio* molecular dynamics analysis to elucidate the dynamics of formate decomposition on Cu(111). Here, we compared the results obtained using the Perdew-Burke-Ernzerhof (PBE) functional with those using the vdW density functionals (vdW-DFs), i.e., the original vdW-DF (vdW-DF1), optB86b-vdW, and rev-vdW-DF2 functionals. We also included the dispersion correction proposed by Grimme with PBE (PBE-D2). We first investigated the translational energy of desorbed CO₂ from the velocity of the center of mass of CO₂. Figure 1 summarizes the time evolution of CO₂ translational energy. The calculated translational energy using PBE, PBE-D2, vdW-DF1, rev-vdW-DF2, and optB86b-vdW are 0.30 eV, 0.05 eV, 0.18 eV, 0.16 eV, and 0.11 eV, respectively. Those calculated CO₂ translational energy using PBE-D2 and vdW-DFs are in reasonable agreement with the experimental estimation (0.10 eV),³ while PBE fails in predicting this energy.

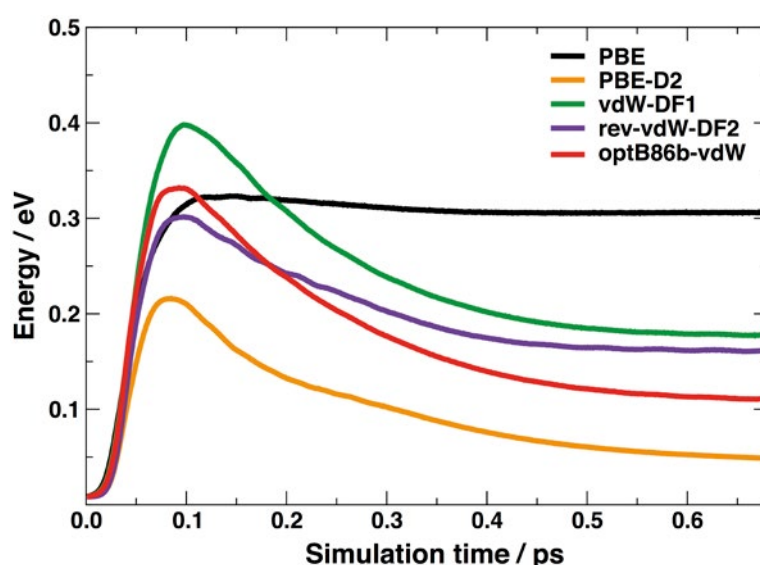


Figure 1. Time evolution of the translational energy of desorbed CO₂ from formate decomposition calculated using PBE, PBE-D2, and vdW-DFs.

We then explored the internal (rotational and vibrational) energies of CO_2 from formate decomposition. The rotational energy of CO_2 was calculated from its moment of inertia and its angular momentum. We obtained that the calculated CO_2 rotational energy varies in between 0.08–0.11 eV. The CO_2 rotational energy from formate decomposition is comparable with that from the CO oxidation on Pd and Pt surfaces (0.08–0.10 eV).⁴ The CO_2 vibrational energies are evaluated based on the time evolution of the desorbed CO_2 geometry, i.e., bond angle, total C–O bond length, and C–O bond length difference, as shown in Fig. 2. For the comparison, we also evaluated the vibrational frequencies of an isolated CO_2 . The calculated bending, symmetric stretching, and antisymmetric stretching energies are 0.25 eV, 0.11 eV, and 1.5 meV, respectively. The CO_2 bending and symmetric stretching energies are closed to the third excitation energy of the bending mode energy of an isolated CO_2 , respectively. Meanwhile, the antisymmetric stretching energy of desorbed CO_2 is much smaller than the zero-point energy of isolated CO_2 . These calculated CO_2 vibrational energies for formate decomposition are much different from those for CO oxidation on Pd and Pt surfaces: desorbed CO_2 has energies of 0.12–0.15 eV and 0.11–0.13 eV in the antisymmetric and symmetric bending modes, respectively.⁵ Therefore, our results suggest that formate synthesis can be enhanced by increasing the vibrational energy of the CO_2 bending mode, in contrast to CO_2 dissociation, in which the symmetric and antisymmetric stretching modes are more important.

In summary, the bending energy of desorbed CO_2 is twice larger than the translational energy. Since formate synthesis from CO_2 and H_2 , the reverse reaction of the formate decomposition, is experimentally suggested to occur by the ER mechanism, our results indicate that the reaction rate of formate synthesis can be enhanced if the bending vibrational mode of CO_2 is excited rather than the translational, rotational, and/or stretching modes. Accordingly, our study could provide useful guidance in controlling the initial impinged CO_2 energy for formate synthesis.

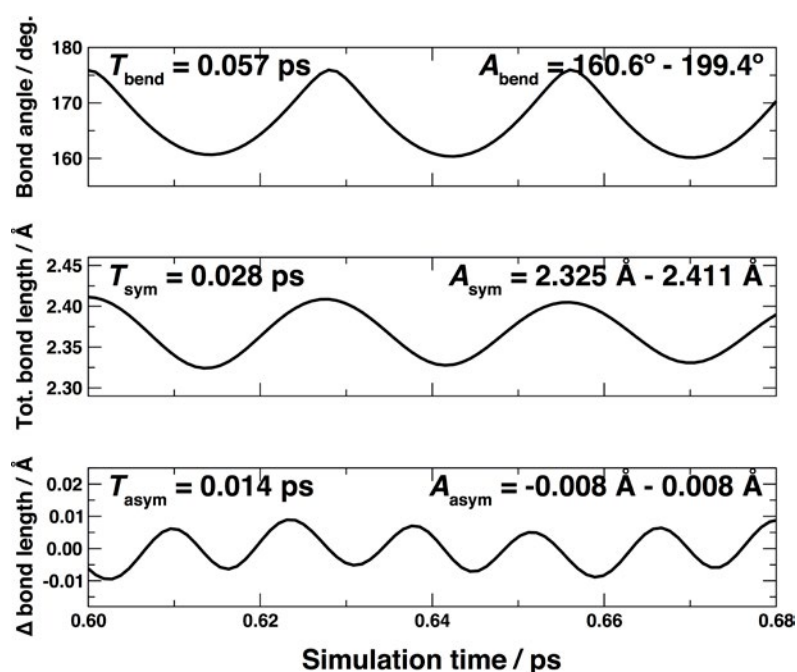


Figure 2. Time evolution of the CO_2 bond angle, total C–O bond length, and C–O bond length difference based on molecular dynamics trajectory calculated using optB86b-vdW functional. The periode (T) and amplitude (A) of each geometry data are shown in each panel.

References:

- [1] S. Kuld et. al., Science 352, 969 (2016).
- [2] H. Nakano, I. Nakamura, T. Fujitani, J. Nakamura, J. Phys. Chem. B 105, 1355 (2001).
- [3] J. Quan, T. Kondo, G. Wang, and J. Nakamura, Angew. Chem. Int. Ed. 56, 3496 (2017).
- [4] T. Yamanaka, Phys. Chem. Chem. Phys. 10, 5429 (2008).
- [5] K. Nakao, S. Ito, K. Tomishige, K. Kunimori, Catal. Today 111, 316 (2006).

Tue-PS1-27**Sol derived alumina and silica supported Au-Ag bimetallic catalysts: structure and activity in aerobic selective oxidation of benzyl alcohol**

G. Nagy¹, F. Somodi¹, G. Sáfrán¹, Z. Schay¹, T. Gál¹, A. Beck¹, L. Prati², C. Evangelisti³

¹ MTA Centre for Energy Research, H-1121 Budapest, Konkoly Thege Miklós street 29-33, Hungary;

² Dipartimento di Chimica, Università degli Studi di Milano, via C. Golgi 19, 20133 Milano, Italy;

³ Istituto di Scienze e Tecnologie Molecolari (ISTM-CNR), Via G. Fantoli 16/15, 20133 Milano, Italy

Gold is a well-recognised catalyst of selective alcohol oxidation. Combining with other metals may improve its properties. Earlier we reported synergetic effect of AuAg/SiO₂ of Au/Ag>3/1 atomic ratio in aerobic selective benzyl alcohol (BzOH) oxidation in toluene in base free conditions¹. In this work alumina supported analogues were studied and the effect of base addition to the reaction.

Bimetallic Au-Ag (Au/Ag=4/1; 1/1 atomic ratios, designated by Au4Ag1 and Au1Ag1, respectively) and corresponding monometallic aqueous sols were formed¹, and then adsorbed on alumina or silica. Alumina supported samples were prepared also by solvated metal atom deposition (SMAD) technique. For structural characterization of the samples UV-vis spectroscopy, HR-TEM, XPS, temperature programmed reduction (TPR), CO adsorption followed by DRIFT and its temperature programmed desorption by QMS was applied. The samples were tested in BzOH oxidation in toluene solution (30 mL 0.1 M BzOH, 15-30 mg catalyst, 80°C, O₂ bubbling, 1 atm) without or with addition of equimolar K₂CO₃ after calcination (400 °C/air/1h) and following reduction treatment (350 °C/H₂/30 min). The initial reaction rates were compared.

The mean particle sizes of Au-Ag and monometallic Au particles in the different catalysts varied between 2-5 nm, which did not change remarkably in the pretreatments. Ag particles in the monometallic Ag samples were much larger and polydisperse (5-17 nm). The formation of bimetallic particles with alloyed phase, and especially in Au1Ag1 systems and in SMAD samples, also silver segregated on the surface of bimetallic particles or separated as well was suggested by SPR bands in UV-vis and indirectly by XPS and TPR and CO adsorption measurements.

In BzOH oxidation only benzyl-benzoate was detected beside the main product benzaldehyde (>90% selectivity). In base free reaction all the catalysts deactivated quickly, because of poisoning by trace amount of benzoic acid. By added K₂CO₃ this could be avoided, the reaction rates increased, the complete conversion of BzOH could be reached. The monometallic Ag and the bimetallic Au1Ag1 samples had no or negligible activity in the reaction conditions applied. The alumina supported Au4Ag1=4/1 and Au catalysts' activity was similar in calcined and reduced state, in case of the silica supported samples the reduced form was more active. The alumina supported samples were much more active than the silica supported ones. The synergetic effect of the sol derived bimetallic Au4Ag1/SiO₂ significantly decreased on base addition, and on alumina support almost disappeared. The SMAD derived Ag4Ag1/Al₂O₃ was much less active, than Au/Al₂O₃.

Strong influence of the support, preparation method, Au/Ag molar ratio, the surface composition of bimetallic particles and K₂CO₃ addition to the reaction was demonstrated in evolution of synergetic Au-Ag bimetallic effect in benzyl alcohol oxidation.

Acknowledgements: This research has received funding from the Hungarian Science and Research Fund (OTKA K101854 and K101897).

References:

[1] Nagy G, Csay T, Horváth A, Frey K, Beck A, *Reac Kinet Mech Cat* (2015) 115:45-65

Tue-PS1-28**Effect of cationic species on the oxygen reduction reaction on Pt(111) electrode**

Masashi Nakamura, Tomoaki Kumeda, Nagahiro Hoshi

Chiba University

The ions in the electrical double layer strongly affect various electrochemical reactions. Recently, the structure of ions at the outer Helmholtz plane (OHP) has been studied using X-ray diffraction, and the effect of alkali metal cations at the OHP on the electrochemical reactions also has been investigated [1,2]. On Pt electrodes, the activities for the oxygen reduction reaction (ORR) in solutions containing Li^+ and Na^+ are lower than those in K^+ and Cs^+ solutions. Li^+ located at the OHP inhibited the surface oxidation of Pt(111) due to the stabilization effect between Li^+ and the surface oxygen species, whereas the high-order oxidation accompanied by surface roughness proceeded in solution containing Cs^+ [3]. Thus cationic effects on the surface oxidation result from the competitive interactions between the adsorption energy of oxygen-species and the binding energy of oxygen-species to cation.

In this study, activities for the ORR on Pt(111) have been investigated in alkaline solutions containing hydrophobic cations (tetramethylammonium (TMA^+) and tetrabutylammonium cation (TBA^+)). The ORR activities in the TMA^+ solution are as high as those in K^+ solutions. In the TBA^+ solutions, volcano type relationship between the ORR activity and the concentration of TBA^+ is found. The interfacial structure is determined using infrared spectroscopy and X-ray diffraction, which suggests that the interaction between the cation and Pt surface affects the ORR. We have found that similar interaction of TBA^+ with surface also activates the reactions in acidic solution.

References:

- [1] D. Strmcnik, K. Kodama, D. Vliet, J. Greely, V. R. Stamenkovic, N. M. Markovic, *Nat. Chem.*, 1 (2009) 466–472.
- [2] C. Stoffelsma, P. Rodriguez, G. Garcia, N. G. Araez, D. Strmcnik, N. M. Markovic, M. T. M. Koper, *J. Am. Chem. Soc.*, 132 (2010) 16127– 16133.
- [3] M. Nakamura, Y. Nakajima, N. Hoshi, H. Tajiri, O. Sakata, *ChemPhysChem*, 14 (2013) 2426-2431.

Tue-PS1-29**First principles study on the interaction between hydrogen atoms and the graphene buffer layer grown on the SiC(0001) surface**

[Jun Nara](#), [Takahiro Yamasaki](#), [Takahisa Ohno](#)

National Institute for Materials Science, Tokyo, Japan

Graphene is known as a promising future electronic device material, because it is expected to have high electron mobility and to contribute to the low energy consumption, which could help combat the global warming. Among graphene fabrication methods, thermal decomposition of SiC substrate, in which graphene sheets are formed after Si atom sublimation from SiC surface at high temperature, has an advantage in the sense that the graphene transfer process, which would degrade the graphene sheet, is not necessary for the device construction. Because the graphene buffer layer is covalently bonded to the SiC surface, it is necessary to decouple them by the intercalation of some guest materials. Hydrogen gas is mainly used for it. However there is no studies on the H atoms on the buffer layer with the experimentally observed periodicity of $(6\sqrt{3}\times 6\sqrt{3})R30^\circ$, while there are some studies on the much smaller one with the periodicity of $(\sqrt{3}\times\sqrt{3})R30^\circ$, in which graphene is largely expanded by about 8 %, and then the energetic of H adsorption is not clear on the buffer layer with the periodicity of $(6\sqrt{3}\times 6\sqrt{3})R30^\circ$.

In this paper, we investigated the interaction between hydrogen atoms and the graphene buffer layer with the periodicity of $(6\sqrt{3}\times 6\sqrt{3})R30^\circ$ by first-principles density functional calculation [1]. The honeycomb shape of pi bonds network between C atoms in graphene sheet is broken, because some of C atoms of buffer layer make covalent bonds with surface Si atoms, resulting in the different shape of pi network from the honeycomb one. We found that the H atom adsorption energy ranges between -0.35 eV and 0.94 eV depending on the adsorption sites. Adsorption energies are evaluated based on a H₂ molecule in vacuum, and the positive values mean stable states, while negative ones mean unstable states. The activation energy of the H₂ dissociative adsorption process is calculated as 1.0 eV. For the hydrogen intercalation temperature of about 1000 °C, this energy barrier is not large and H₂ molecule could adsorb on the buffer layer. The activation energy of the H diffusion on the buffer layer ranges from 1.7 eV to 2.3 eV depending on the diffusion path. While this energy values are larger than the one for the adsorption process, they are not so large at the intercalation temperature and H atoms could diffuse on the buffer layer. For the H penetration process from above to below the buffer layer, we obtained the activation energy of about 5 eV, which is quite large for the intercalation temperature, and H atoms could not penetrate to below the buffer layer. We also performed the molecular dynamics simulations for the buffer layer and found that the covalent bonds between the buffer layer and SiC substrate are often broken even at intercalation temperature, and then H atoms could diffuse in the room between the buffer layer and the SiC substrate.

References:

[1] PHASE code: <https://azuma.nims.go.jp/>

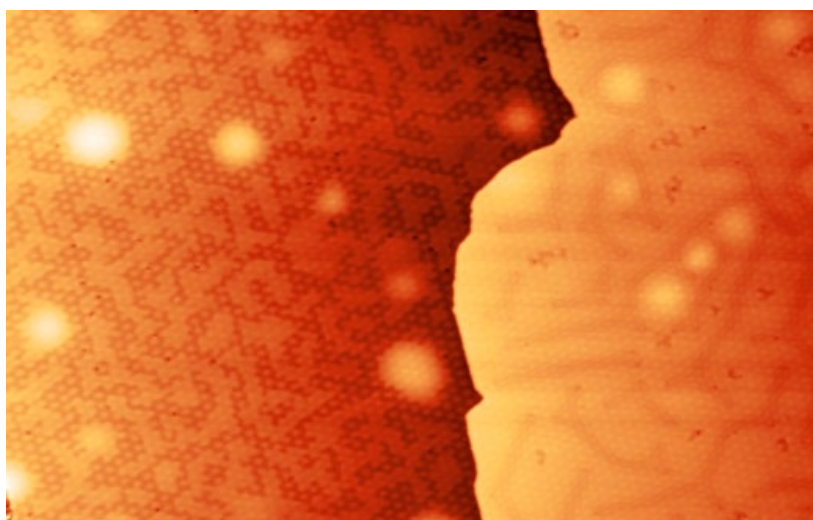
Tue-PS1-46 Gold intercalation in Graphene/Ir(111)

J.J. Navarro^{1,2}, F. Calleja¹, A.L. Vázquez de Parga^{1,2}, R. Miranda^{1,2}

¹ Instituto Madrileño de Estudios Avanzados en Nanociencia, Cantoblanco 28049, Madrid, Spain;

² Departamento de Física de la Materia Condensada and IFIMAC, Universidad Autónoma de Madrid, Cantoblanco 28049, Madrid, Spain

Atom intercalation in metal supported graphene is an effective way to decouple graphene from the underlying metal, giving a certain control over its doping and allowing the observation of inter- or intra-valley scattering processes [1]. In addition, if the intercalants are heavy-metal atoms, the intrinsic spin-orbit coupling of graphene could be enhanced to the point of turning it into a 2D topological insulator [2]. So far, by intercalation of gold and lead atoms it has been possible to enhance graphene's spin-orbit coupling to the order of 100 meV (including Rashba type), in particular in gr/Au/Ni(111) [3], gr/Pb/Ir(111) [4] and gr/Au/Pt(111) [5]. In this work we study the intercalation of gold in gr/Ir(111) by means of LEED and STM. We show that, under certain growth conditions, an Au-Ir interlayer alloy is formed underneath graphene, preserving the original moiré structure of graphene/Ir(111). In addition we explore the electronic structure of the intercalated system, observing inter-valley scattering processes that we use to estimate the Dirac point.



References:

- [1] I. Gierz et al, PRB 81, 235408 (2010)
- [2] C. Weeks et al, PRX 1, 021001 (2011)
- [3] D. Marchenko et al, Nat. Comms. 3, 1232 (2012)
- [4] F. Calleja et al, Nat. Phys. 11, 43 (2015)
- [5] I.I. Klimovskikh et al, ACS Nano 11, 368 (2017)

Thu-PS2-48**Particular behaviour of the GaAs wetting layer on AlGaAs substrate during droplet epitaxy**

Ákos Nemcsics¹, Lajos Tóth², Zoltán Erdélyi³

¹ Institute for Microelectronics and Technology, Obuda University; Tavaszmezo utca 17, H-1084 Budapest, Hungary;

² Institute of Technical Physics and Materials Science, Centre for Energy Research of HAS; P.O.B. 49, H-1525 Budapest, Hungary;

³ Department of Solid State Physics, University of Debrecen; PO.Box 400, H-4002 Debrecen, Hungary

Droplet epitaxy is a promising technology for nano-structure preparation [1]. Recently, no theoretical description is available yet for the underlying growth mechanism. In this work we are dealing with the composition of wetting layer during GaAs quantum dot (QD) formation on AlGaAs (001) surface. The atomic resolution investigation has shown few atomic embedded GaAs surface layers on the AlGaAs crystal surface between the QDs [2]. The existence of this GaAs surface layer was predicted earlier from the comparison of the photoluminescent measurement and the energy levels calculation [3]. The enrichment of aluminium on the surface is a similar demixing effect which was observed in the case of GaAs/AlGaAs [4]. This inverting layer can be explained with the nano segregation [5]. In this presentation we will show a model for a possible mechanism resulting in the enrichment of aluminium.

The work is supported by ERA-NET Concert Japan FemtoTera (NKFI NN114457) project.

References:

- [1] K. Watanabe, N. Koguchi, Y. Gotoh; Jpn. J. Appl. Phys. 39 (2000) L79
- [2] Á. Nemcsics, L. Tóth, L. Dobos, Ch. Heyn, A. Stemmann, A. Schramm, H. Welsch, W. Hansen; Superlattices and Microstructures 48 (2010) 351.
- [3] T. Mano, T. Kuroda, K. Mitsuishi, M. Yamagiwa, X.-J. Guo, K. Furuya, K. Sakoda, N. Koguchi, J. Cryst. Growth 301-302 (2007) 740.
- [4] W. Braun, Applied RHEED, Springer Verlag, Heidelberg, 1999.
- [5] D.L. Beke, Cs. Cserhádi, Z. Erdélyi, I.A. Szabó, Segregation in nanostructures (Chapter 7) in Nalwa HS (ed.) Nanoclusters and Nanocrystals - Stevenson Ranch: American Scientific Publishers pp. 211-252 (2003)

Tue-PS1-33

Soft X-ray spectroscopic study of electronic structure of Pd nanoparticles

*BAND Band structure of solid surfaces*Satoshi Ogawa¹, Kenta Otsuki¹, Shinya Yagi^{1,2}¹ Energy Engineering, Graduate School of Engineering, Nagoya University, Japan;² Institute of Materials and Systems for Sustainability, Nagoya University, Japan

In order to clarify the anomalous hydrogen absorption property of the Pd nanoparticles (NPs), we have investigated the electronic structure of the Pd NPs by the soft X-ray spectroscopy. Pd bulk exhibits the clear and sharp plateau region in the pressure-composition isotherm (PCI) of the hydrogen absorption. In contrast, the plateau is ambiguous in the PCI of the Pd NPs i.e. the plateau has the slope and the narrower width compared with that of the bulk one [1,2]. One of the suggested origins is the change of the electronic structure around the fermi level by the formation of the NPs [1]. We have carried out near Pd L₃-edge X-ray absorption fine structure (Pd L₃-edge NEXAFS) and X-ray photoelectron spectroscopy (XPS) measurements to investigate the unoccupied d-states and the valence band structure around the fermi level of the Pd NPs, respectively.

Pd L₃-edge NEXAFS measurements were carried out with Material Chemical State-Structural Analysis II at BL6N1, Aichi Synchrotron Radiation Center. The NEXAFS spectra were obtained by the total electron yield method using the drain current under the high vacuum ($\sim 5 \times 10^{-8}$ Pa). Figure 1 shows the Pd L₃-edge NEXAFS spectra of the Pd NPs and Pd sheet (Pd bulk). All spectra in Figure 1 were normalized with respect to height of the edge jump. The intensity of the white line in the L₃-edge NEXAFS spectrum reflects the DOS of the unoccupied d-state in the simple approximation. It can be seen that the intensity of the white line of Pd NPs is slightly lower than that of Pd bulk. This result represents that the unoccupied d-states near the Fermi level has decreased by the formation of Pd NPs which explains qualitatively that the hydrogen absorption amount of Pd NPs is lower than that of bulk. The unoccupied d-states are fulfilled by the electron of the hydrogen during the hydrogen absorption of Pd [3]. The decrease of the unoccupied d-DOS leads the decrease of the amount of the permitted hydrogen in the crystal lattice of Pd. The results of the valence band XPS will be also shown at the presentation.

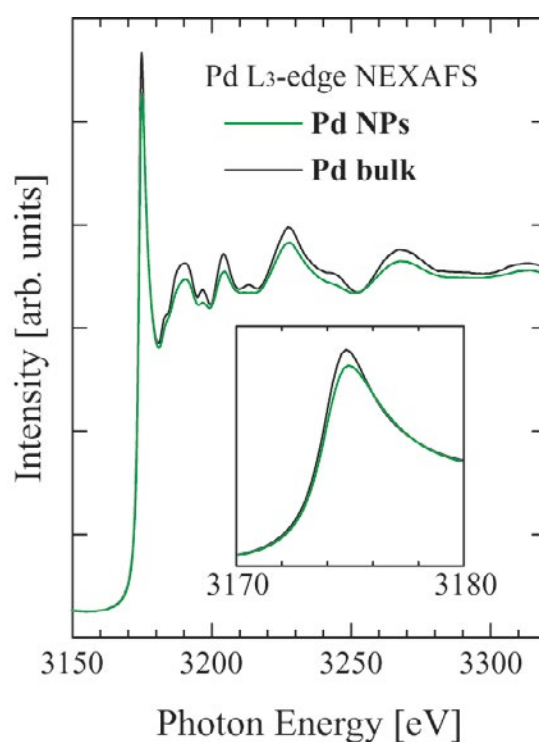


Figure 1 Pd L₃-edge NEXAFS of the Pd NPs and Pd bulk.

References:

- [1] M. Yamauchi, R. Ikeda, H. Kitagawa, and M. Takata, *J. Phys. Chem. C* 112, 3294 (2008).
- [2] S. Ogawa, T. Fujimoto, T. Kanai, N. Uchiyama, C. Tsukada, T. Yoshida and S. Yagi, *e-J. Surf. Sci. Nanotech.* 13, 343 (2015).
- [3] C. D. Gelatt, Jr., H. Ehrenreich, J.A. Weiss, *Phys. Rev. B* 17, 1940 (1978).

Tue-PS1-30
Regular and disordered surface vacancies on a ceria film surface

Reinhard Olbrich¹, Gustavo E. Murgida², Valeria Ferrari², Clemens Barth³, Ana M. Llois², Michael Reichling¹, M. Veronica Ganduglia-Pirovano⁴

¹ Fachbereich Physik, Universität Osnabrück, Barbarastr. 7, 49076 Osnabrück, Germany;

² Departamento de Física de la Materia Condensada, GlyA, CAC–CNEA, 1650 San Martín, Buenos Aires, Argentina; Consejo Nacional de Investigaciones Científicas y Técnicas – CONICET, C1033AAJ Buenos Aires, Argentina;

³ Aix-Marseille University, CNRS, CINaM UMR 7325, 13288 Marseille, France;

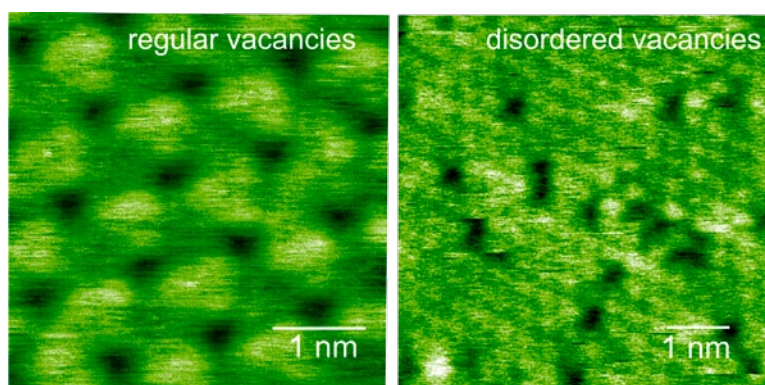
⁴ Instituto de Catálisis y Petroleoquímica, Consejo Superior de Investigaciones Científicas-CSIC, 28049 Madrid, Spain

Obtaining information about the defect structure of cerium oxide surfaces is of paramount importance in catalytic applications relying on the high oxygen storage capacity (OSC) of ceria. Oxygen vacancies observed with STM at the (111) surface facet of CeO₂ single crystals are discussed controversial [1] after fluorine impurities in ceria single crystals were found [2]. In STM measurements these fluorine impurities would not be distinguishable from oxygen vacancies [1]. NC-AFM measurements [3] have claimed that oxygen vacancies have a tendency to avoid the very surface layer but rather form a regular array in a subsurface layer effectively yielding a (2 × 2) surface reconstruction which was later confirmed by theoretical simulations [4]. We reveal surface vacancies that arise from annealing in an ultra-high vacuum (UHV) environment at various temperatures up to 1100K by direct imaging the surface of thick ceria films with a non-contact atomic force microscope. The oxygen vacancies can be separated in regularly arranged vacancies in form of surface reconstructions representing reduction stages ranging from CeO₂ to Ce₂O₃ [5] and in vacancies appearing at disordered surface positions representing a locally strong surface reduction. While the regular surface vacancies are stable the disordered vacancies rearrange to some extent over time. In contrast to the bulk crystals fluorine impurities have not been found [2] in film samples, hence, the observed irregularities can clearly be assigned to surface oxygen vacancies.

Acknowledgment: Support from the COST Action CM1104 is gratefully acknowledged.

References:

1. Kullgren, J., et al., Oxygen Vacancies versus Fluorine at CeO₂(111): A Case of Mistaken Identity? *Physical Review Letters*, 2014. 112(15): p. 156102.
2. Pieper, H.H., et al., Morphology and nanostructure of CeO₂(111) surfaces of single crystals and Si(111) supported ceria films. *Physical Chemistry Chemical Physics*, 2012. 14(44): p. 15361-15368.
3. Torbrügge, S., et al., Evidence of Subsurface Oxygen Vacancy Ordering on Reduced CeO₂(111). *Physical Review Letters*, 2007. 99(5): p. 056101.
4. Murgida, G.E. and M.V. Ganduglia-Pirovano, Evidence for subsurface ordering of oxygen vacancies on the reduced CeO₂(111) surface using density-functional and statistical calculations. *Physical Review Letters*, 2013. 110(24): p. 246101.
5. Olbrich, R., et al., Surface Stabilizes Ceria in Unexpected Stoichiometry. *The Journal of Physical Chemistry C*, 2017. 121(12): p. 6844-6851.



Thu-PS2-08**Synthesis of Pd nanoparticles by solution plasma method**

[K. Otsuki](#)¹, [S. Ogawa](#)¹, [E. Ikenaga](#)^{1,2}, [S. Yagi](#)^{1,2}

¹ Energy Engineering, Graduate School of Engineering, Nagoya University, Japan;

² Institute of Materials and Systems for Sustainability, Nagoya University, Japan

Introduction: In recent years, hydrogen energy is paid attention to a clean renewable energy. There is a problem of how to store hydrogen in the field of hydrogen energy. As one of useful methods, we have focused on the hydrogen storage material. Pd has been studied for the hydrogen storage material because it has high reaction rate with hydrogen [1]. It is possible to expect the improvements in reaction rate and temperature between metal and hydrogen by making the hydrogen absorption material into nanoparticle. The nanoparticles can be synthesized with clean surface by the solution plasma method [2]. In this study, we aim to synthesize the Pd nanoparticles with clean surface and controlled particle size by the solution plasma method.

Experimental: We synthesized the Pd nanoparticles by the solution plasma method, shown in Figure 1. A pulsed voltage was applied between the two Pd electrodes. A solvent and an electrolyte were water and NaOH, respectively. The concentration of electrolyte was 1 mmol/L. TEM (Transmission Electron Microscope) was used for the particle size estimation of the synthesized nanoparticles.

Results and Discussion: The Pd nanoparticles have been obtained by the solution plasma method. The color of the Pd colloidal solution is dark brown. In addition, a precipitate is not found in the Pd colloidal solution after synthesis. Figure 2 shows the TEM image of the Pd nanoparticles. The average particle diameter and the standard deviation are estimated to be 3.4 +/- 0.4 nm.



Figure 1. The photographic view of the experiment image synthesizing the Pd nanoparticles by the solution plasma method.

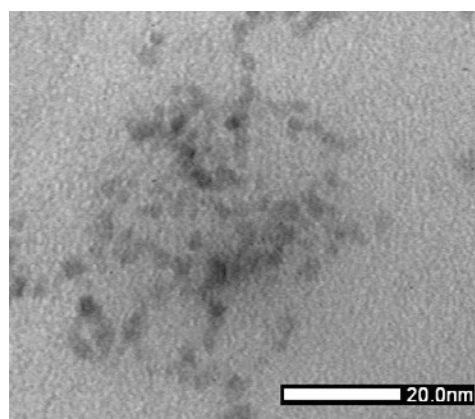


Figure 2. TEM image of the Pd nanoparticles.

References:

- [1] T. Aruga, Journal of the Surface Science Society of Japan, 27, (2006) 341-347.
- [2] N. Saito, J. Hieda, O. Takai, Thin Solid Films, 518, (2009) 912-917.

Thu-PS2-24

Metastable skyrmionic spin structures with various topologies and their electron charge/spin transport properties

Krisztián Palotás^{1,2,3}, **Levente Rózsa**^{4,5}, **Eszter Simon**³, **László Udvardi**³, **László Szunyogh**³

¹ Institute of Physics, Slovak Academy of Sciences, Bratislava, Slovakia;

² MTA-SZTE Reaction Kinetics and Surface Chemistry Research Group, University of Szeged, Szeged, Hungary;

³ Department of Theoretical Physics, Budapest University of Technology and Economics, Budapest, Hungary;

⁴ Institute of Applied Physics and Interdisciplinary Nanoscience Center, University of Hamburg, Hamburg, Germany;

⁵ Wigner Research Centre for Physics, Hungarian Academy of Sciences, Budapest, Hungary

Metastable localized spin configurations with topological charges ranging from $Q = -3$ to $Q = 2$ are observed [1] in a $(\text{Pt}_{0.95}\text{Ir}_{0.05})/\text{Fe}$ bilayer on Pd(111) surface by performing spin dynamics simulations, using a classical Hamiltonian parametrized by ab initio calculations [2]. It is demonstrated that the frustration of the isotropic exchange interactions is responsible for the creation of these various types of skyrmionic structures. The Dzyaloshinsky-Moriya interaction, present due to the breaking of inversion symmetry at the surface, energetically favors skyrmions with $Q = -1$, distorts the shape of the other skyrmionic objects, and defines a preferred orientation for them with respect to the underlying lattice.

By performing spin-polarized scanning tunneling microscopy (SP-STM) calculations, a direct connection between experimentally measurable SP-STM contrasts and different topologies of skyrmionic systems is established, highlighting the role of the local vorticity [3]. Moreover, the first results on high resolution scanning tunneling spin transfer torque (STT) microscopy simulations of the skyrmionic structures are also presented, employing a recently developed calculation method of tunneling STT [4].

Metastable localized spin configurations with topological charges ranging from $Q = -3$ to $Q = 2$ are observed [1] in a $(\text{Pt}_{0.95}\text{Ir}_{0.05})/\text{Fe}$ bilayer on Pd(111) surface by performing spin dynamics simulations, using a classical Hamiltonian parametrized by ab initio calculations [2]. It is demonstrated that the frustration of the isotropic exchange interactions is responsible for the creation of these various types of skyrmionic structures. The Dzyaloshinsky-Moriya interaction, present due to the breaking of inversion symmetry at the surface, energetically favors skyrmions with $Q = -1$, distorts the shape of the other skyrmionic objects, and defines a preferred orientation for them with respect to the underlying lattice.

By performing spin-polarized scanning tunneling microscopy (SP-STM) calculations, a direct connection between experimentally measurable SP-STM contrasts and different topologies of skyrmionic systems is established, highlighting

the role of the local vorticity [3]. Moreover, the first results on high resolution scanning tunneling spin transfer torque (STT) microscopy simulations of the skyrmionic structures are also presented, employing a recently developed calculation method of tunneling STT [4].

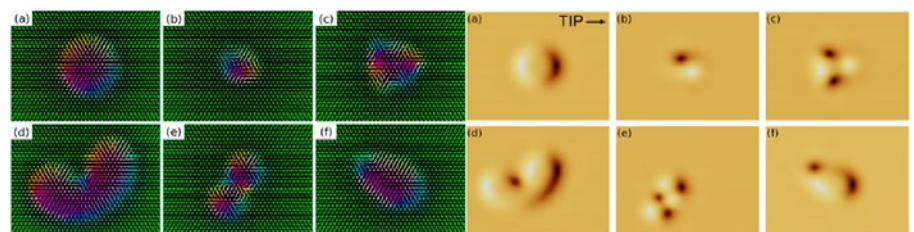


FIG: Metastable skyrmionic spin structures with various topological charges (Q) in the $(\text{Pt}_{0.95}\text{Ir}_{0.05})\text{Fe}/\text{Pd}(111)$ ultrathin magnetic film, and their SP-STM images with an in-plane magnetized tip: (a) $Q = -1$; (b) $Q = 1$; (c) $Q = 2$; (d) $Q = -2$; (e) $Q = -3$; (f) $Q = 0$. [arXiv:1609.07016]

References:

- [1] L. Rózsa et al., Phys. Rev. B 95, 094423 (2017).
- [2] L. Rózsa et al., Phys. Rev. Lett. 117, 157205 (2016).
- [3] K. Palotás et al., arXiv:1609.07016 (2016).
- [4] K. Palotás et al., Phys. Rev. B 94, 064434 (2016).

Tue-PS1-03

Oxygen reduction on carbon supported Pt_xSn electrodes with optimized Pt/Sn surface composition prepared by controlled surface reactionsIrina Borbáth¹, István Bakos¹, [Zoltán Pászti](#)¹, András Tompos¹, István Sajó²¹ Institute of Materials and Environmental Chemistry, Research Centre for Natural Sciences, HAS, Budapest, 1519, Hungary;² University of Pécs, Szentágotthai Research Centre, Pécs, H-7624, Hungary

Due to their excellent activity, Pt-Sn bulk alloys are among the most promising bimetallic systems for fuel cell applications. Crucial points in development of novel multicomponent catalysts are identification of the optimal surface composition and preparation of the corresponding catalysts.

Model Pt-Sn catalytic surfaces were prepared using electroless deposition of adsorbed tin atoms (via catalytic disproportionation of Sn²⁺ [1]) onto smooth polycrystalline Pt disc to clarify the relationship between the Pt/Sn surface composition and the oxygen reduction reaction (ORR) activity. According to the optimization results the most promising surface Pt/Sn atomic ratio was around 3, in agreement with our recent results demonstrating high activity of the Pt₃Sn phase in electrooxidation of C1-C2 alcohols or CO [2,3]. Exclusive formation of supported Sn-Pt alloy phases with different Sn/Pt ratios can be achieved by using Controlled Surface Reactions between hydrogen adsorbed on Pt sites and tetraethyltin [2-4]. Thus, efforts were made to adjust synthesis parameters in order to prepare carbon supported fcc Pt₃Sn alloy exclusively.

Sn-Pt/C electrocatalysts with desired Pt/Sn= 3 ratio have been prepared using commercial 20 wt.% Pt/C (20Pt/C (Q: Quintech)) and home-made 20Pt/C (H) catalysts. According to *in situ* XPS and *in situ* XRD studies the exclusive incorporation of Sn onto the Pt sites was achieved resulting in exclusive formation of Pt-Sn alloy. According to *in situ* XPS studies pre-treatment of the air exposed catalyst in H₂ even at 170°C resulted in complete reduction of the ionic tin to Sn⁰, suggesting alloy formation. After contact of Sn-Pt/C catalysts with air Sn tends to segregate to the surface, where it oxidizes to a certain extent. Reversible interconversion of PtSn ↔ Sn⁴⁺ + Pt in the presence of O₂ and H₂ was convincingly demonstrated by *in situ* XPS and *in situ* XRD studies.

The electrocatalytic performance of the alloy catalysts was tested in CO oxidation and the ORR [4]. Only minor changes of the surface composition of Sn-20Pt/C electrocatalysts were observed after 20 polarization cycles. Better performance in the CO electrooxidation for our Sn-Pt/C catalysts compared to the state-of-art CO tolerant PtRu/C benchmark was demonstrated. The increased activity in the ORR compared to the Sn-20Pt/C (Q) and both parent 20Pt/C catalysts is traced to the optimal balance between the oxidized and metallic components of the catalyst surface under working conditions.

References:

1. S. Szabó, *J. Electroanal. Chem.* **1984**, 172, 359-366.
2. S. García-Rodríguez, F. Somodi, I. Borbáth, J.L. Margitfalvi, M.A. Peña, J.L.G. Fierro, S. Rojas, *Appl. Catal. B-Environ.* **2009**, 91, 83-91.
3. I. Borbáth, D. Gubán, Z. Pászti, I.E. Sajó, E. Drotár, J.L. Gómez de la Fuente, T. Herranz, S. Rojas, A. Tompos, *Top. Catal.* **2013**, 56, 1033-1046.
4. I. Borbáth, D. Gubán, I. Bakos, Z. Pászti, G. Gajdos, I.E. Sajó, Á. Vass, A. Tompos, *Catal. Today* (2017) DOI: 10.1016/j.cattod.2017.01.011.

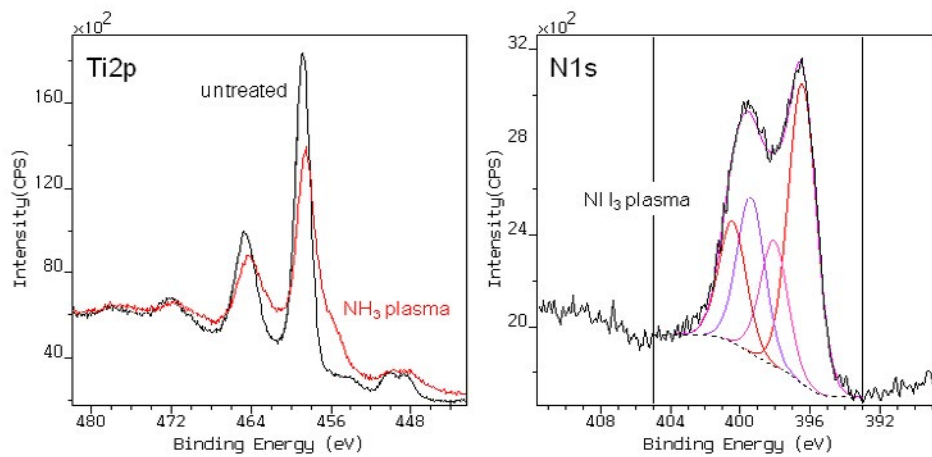


Figure 1 Ti 2p XP line and N 1s lines shape after NH₃ plasma treatment of titanate nanotubes.

References:

- [1] Á. Kukovecz, K. Kordás, J. Kiss, Z. Kónya, Surf. Sci. Rep. 71 (2016) 473-546.
- [2] I. Bertóti, Catal. Today (181 (2012) 95-101.

Tue-PS1-31

Spin relaxation length for medium energy electrons in Pd and LiF ultrathin films

[Pavlov A.V.](#)¹, [Ustinov A.B.](#)², [Petrov V.N.](#)¹

¹ Department of Experimental Physics, Institute of Physics, Nanotechnology and Telecommunications, Peter the Great St. Petersburg Polytechnic University, St. Petersburg, Russia;

² Department of Physical Electronics, Institute of Physics, Nanotechnology and Telecommunications, Peter the Great St. Petersburg Polytechnic University, St. Petersburg, Russia

The development of spintronics (the field of science that examines the behavior of systems, based not only on charge transfer, but on magnetic properties of nano-objects as well) requires study of various magnetic and electrical properties of nanoscale systems. One of the areas of research is connected with study of how efficiently polarized electrons pass through different solid state structures. Number of electrons that passed a certain distance without losing energy is governed by inelastic mean free path and is well studied. However, important and not sufficiently studied part of transport is connected with loss of spin-polarization. That is what this work targeted at.

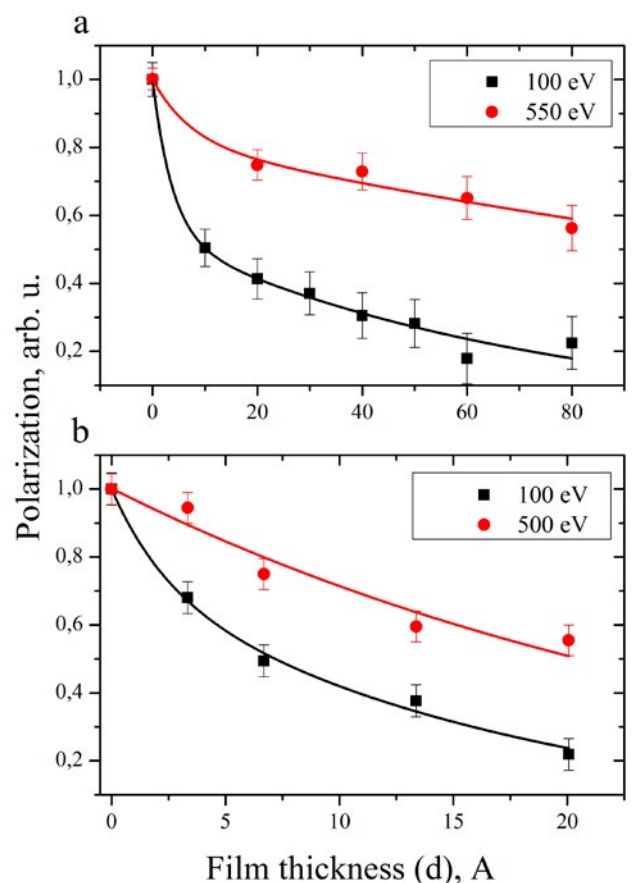
From literature it is known that spin relaxation length for medium energy electrons depends on electron shell occupation [1] and spin-orbit coupling [2]. Because of that Pd and LiF were chosen as a materials for study. They possess fully occupied atomic (molecular) shells and they are low-Z materials which reduces spin-orbit interaction.

In the study spin relaxation lengths in palladium and lithium fluoride were measured for electrons with energies in range between 35 and 600 eV. The basic idea behind the experiment is to measure polarization of secondary electrons emerging from ferromagnetic source through the film of investigated material.

Measurements were conducted as follows: thin films of examined material were deposited on a ferromagnetic single crystal, for different thicknesses of the film secondary electron spin-polarization was measured for different electron energies. Example of experimental dependencies for LiF/FeNi₃ and Pd/FeNi₃ are presented on figure 1 a and b respectively. To explain experimental dependencies quantitative model was developed. Experimental results and quantitative model were used for creation of a map of spin relaxation lengths in Pd and LiF for various energies and thicknesses.

Analysis show that the spin relaxation length exceeds the mean free path by a factor of 8 - 10 for LiF and by 2,5 - 3 for Pd. Greater value for LiF is understandable, because it's insulator and electron-electron interaction in it is much lower than for Pd. Also, Li and F have smaller Z, which reduces spin-orbit interaction.

The results of present studies can be used to create new solid-state polarization detectors (polarimeters) [3] and polarized positrons sources [4].



References:

- [1] D.T. Pierce, H.C. Siegmann, Hot-electron scattering length by measurement of spin polarization, *Phys. Rev. B.* 9 (1974) 4035.
- [2] R.J. Elliott, Theory of the Effect of Spin-Orbit Coupling on Magnetic Resonance in Some Semiconductors, *Phys. Rev.* 96 (1954) 266–279. doi:10.1103/PhysRev.96.266.
- [3] X. Li, O.E. Tereshchenko, S. Majee, G. Lampel, Y. Lassailly, D. Paget, J. Peretti, Optical detection of spin-filter effect for electron spin polarimetry, *Appl. Phys. Lett.* 105 (2014) 52402. doi:10.1063/1.4892073.
- [4] V.N. Petrov, S.N. Samarin, K. Sudarshan, L. Pravica, P. Guagliardo, J.F. Williams, Spin polarized low-energy positron source, *J. Phys. Conf. Ser.* 618 (2015) 12043. doi:10.1088/1742-6596/618/1/012043.

Tue-PS1-52**Paper-supported electrochemical analysis platform for ion and biosensing**

[Jouko Peltonen](#), [Emil Rosqvist](#), [Anna Fogde](#), [Petri Ihalainen](#), [Anni Määttänen](#),
[Jawad Sarfraz](#)

Laboratory of Physical Chemistry, Centre for Functional Materials, Åbo Akademi University, Turku, Finland

Printed or evaporated electrodes on a recyclable low-cost coated paper were used as an electrochemical platform for constructing biosensors and potentiometric ion sensors. Printed electrodes are easy and fast to prepare with possibility for upscaled production [1]. In contrast, evaporated electrodes can be made ultrathin and very smooth enabling supramolecular chemistry and optical applications (semitransparent electronics) [2].

The ion sensors consisted of a printed ion-selective electrode (ISE) and a reference electrode (RE). A poly(3,4-ethylenedioxythiophene) (PEDOT) layer, with poly(styrene sulfonate) (PSS) ions as counterions was deposited on the gold electrodes by electro-polymerization, drop-casting or ink-jet printing. The working electrode was modified by coating the PEDOT (PSS) layer with a K^+ -selective membrane, to obtain a solid-contact K^+ -ISE. The electrochemical characteristics were studied by amperometric, potentiometric and electrochemical impedance spectroscopic (EIS) measurements. The planar electrode platform is user-friendly and enables analysis of very small sample volumes [3].

Stable supramolecular biorecognition layers of biotin-functionalized tetraethylene-glycol polythiophene (b-TEGPT) and streptavidin were inkjet-printed on paper-based evaporated ultrathin gold film (UTGF) electrodes. The device was used for detecting complementary DNA oligomers and antibody-antigen complexes [2, 4].

Furthermore, self-supported latex films carrying UTGF electrodes were fabricated [5]. The latex films were transparent to visible light and also the thin Au electrodes were semi-transparent. The device was used for electrochemical impedance spectroscopy (EIS) measurements of protein adsorption. In addition, cyclic voltammetry measurements were carried out to determine active medicinal components, i.e., caffeic acid and piroxicam, a poorly water-soluble anti-inflammatory drug.

References:

- [1] A. Määttänen *et al.*, *Sensors and Actuators B* 160 (2011), 1404-1412.
- [2] P. Ihalainen *et al.*, *Applied Surface Science* 329 (2015), 321-329.
- [3] P. Sjöberg *et al.*, *Sensors and Actuators B* 224 (2016), 325-332.
- [4] P. Ihalainen *et al.*, *Applied Surface Science* 364 (2016), 477-483.
- [5] A. Määttänen *et al.*, *Applied Surface Science* 364 (2016), 37-44.

Thu-PS2-11**Reactivity of vanadium oxide monolayers on CeO₂(111) studied by density functional theory**

[Christopher Penschke](#), [Joachim Paier](#), [Joachim Sauer](#)

Humboldt-Universität zu Berlin, Unter den Linden 6, 10099 Berlin, Germany

The oxidative dehydrogenation of methanol to formaldehyde at vanadium oxides supported on cerium dioxide is a frequently studied model reaction for C-H bond activation.[1] The activity for this reaction decreases with increasing vanadia loading, and the system is inactive above monolayer coverage.[1-3] Reactivity descriptors obtained by virtue of density functional calculations under periodic boundary conditions showed the same trend for small vanadium oxide species on cerium dioxide (111).[4] Later mechanistic studies offered details about the support effect, proving that density functional theory is a valuable tool to gain insight into this catalyst system.[5] To further our understanding of the reactivity decrease at high vanadium coverage, we studied vanadium oxide monolayers on cerium dioxide (111). They present a limiting case with respect to activity, because in contrast to catalysts with lower vanadium loadings, the support is not accessible anymore. Structural models for the supported vanadium oxide monolayers are presented. Their activity is assessed by calculating oxygen defect formation energies and hydrogenation energies as reactivity descriptors. Furthermore, transition structures for hydrogen abstraction from adsorbed methoxide, which is the rate-determining step in the conversion to formaldehyde, and the corresponding activation barriers are analysed. The results suggest that monolayers are less reactive than the small ceria-supported vanadium oxide clusters, in agreement with experiment. Electronic and structural effects contribute to stability and activity of supported vanadium oxides.

References:

- [1] I. E. Wachs, *Catal. Today* 100, 79, (2005).
- [2] G. S. Wong, M. R. Concepcion, J. M. Vohs, *J. Phys. Chem. B* 106, 6451 (2002).
- [3] M. V. Ganduglia-Pirovano et al., *J. Am. Chem. Soc.* 132, 2345 (2010).
- [4] C. Penschke, J. Paier, J. Sauer, *J. Phys. Chem. C* 117, 5274 (2013).
- [5] T. Kropp, J. Paier, J. Sauer, *J. Am. Chem. Soc.* 136, 14616 (2014).

Thu-PS2-25

Investigation of oxide dispersion strengthened steel by photoelectron emission, Mössbauer spectroscopy, and X-ray diffraction

G. Pető, I. Dézsi, L.F. Kiss, Z.E. Horváth, D. Oszetzky, A. Nagy, G. Molnár, K. Balázs, Cs.S. Daróczy, A. Horváth

Institute of Technical Physics and Materials Science, MTA Centre for Energy Research, Budapest, Hungary

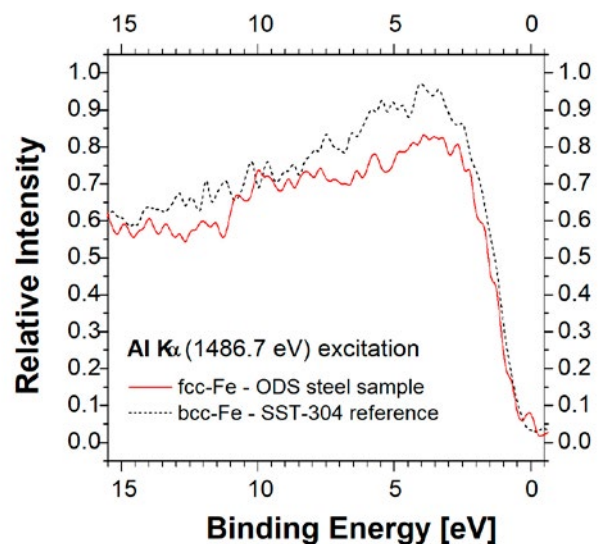
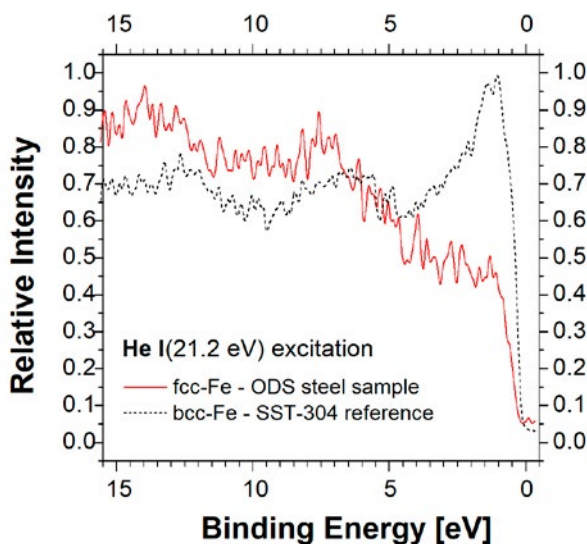
Oxide dispersion strengthened steels (ODS) have attracted attention for possible applications in the current fast nuclear reactors and for the first walls of the future fusion reactors. The valence band of α -Fe has ferromagnetic characteristics similar to bcc Fe, namely the large Fe 3d originated states at the Fermi level.

Our intention was to experimentally investigate these correlations for ODS steel. For this purpose, we have determined experimentally the valence band DOS vs. the atomic order, and the magnetic properties of the iron components in the ODS steel samples. The composition of the steel was Fe₁₈Cr₁₃Ni_{2.5}Mo_{3.2}Si_{0.1}C +1 wt% Y₂O₃.

The valence bands of the ODS steel sample and of a commercial Fe bcc and Cr based magnetic martensitic alloy sheet were measured by photoelectron emission, by a Foner-type magnetometer for their magnetic properties, and by X ray diffraction for their crystallographic structure. A similarly composed non-magnetic sheet and the ODS sample were studied by Conversion Electron Mössbauer Spectroscopy.

The electron emission intensity for the magnetic reference sample shown in Figs. 1(a) and (b) in the 0-5 eV binding energy range correlates well with the valence band emission of the Fe 3d bcc states, with a large peak at the Fermi level, in contrast to the missing peak for the fcc valence band emission.

This is the first experimental verification of the calculated valence band density of states and of the photoelectron emission of the fcc phase of iron. This work demonstrates that photoelectron emission can be used to distinguish Fe in various crystallographic structures with different magnetic properties.



Tue-PS1-32

Surface fluorination by C₆₀F₁₈ molecules adsorption on copper (001)

M. Petukhov¹, A. Oreshkin², D. Muzychenko², S. Oreshkin², S. Bourgeois¹, R. Bakhtizin³

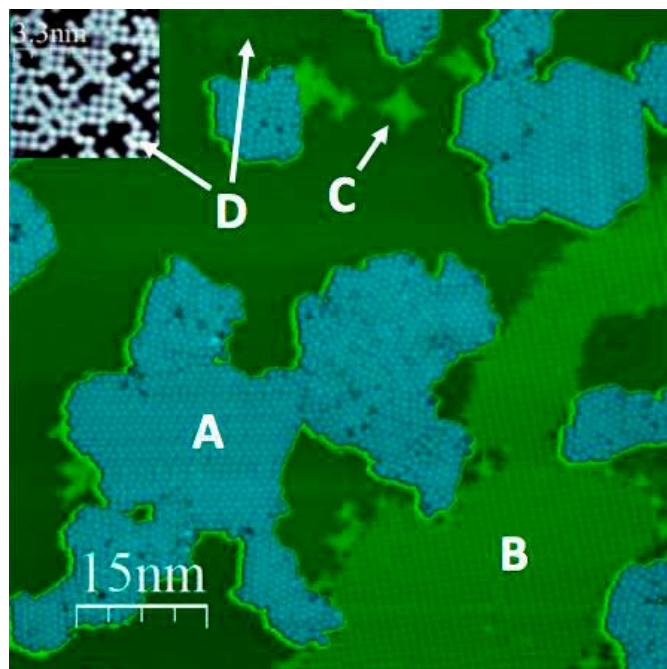
¹ University of Burgundy/Franche-Comté, Dijon, France;

² Moscow State University, Moscow, Russian Federation;

³ Bashkir State University, Ufa, Russian Federation

In recent years a particular attention was drawn to the study of physical and chemical properties of fluorinated fullerenes organic molecules due to technological development of new applications based on the local etching of the surface. Fluorination is the well known and attractive process for regulation of the energy levels of frontier orbitals of organic molecules [1]. In particular, the high reactivity of fluorinated fullerene has allowed to apply this molecules as a dopant to create a p-type conductivity in pentacene, which has been used to construct an organic light-emitting Schottky diode [2]. The creation of field-effect transistor based on the pentacene doping by fluorinated fullerene has been considered in [3]. Nevertheless, deeper understanding of structural and electronic properties of a thin molecular film of fluorinated fullerenes on a metallic surface is still required.

This study is dedicated to C₆₀F₁₈ molecules adsorption on the Cu(001) surface. The tortoise-shaped polar C₆₀F₁₈ molecule (electric dipole moment > 9 Debye) is very asymmetrical [4]. The C₆₀F₁₈ molecule has all fluorine atoms bound to only one hemisphere of C₆₀. The deposition of C₆₀F₁₈ molecules with a submonolayer coverage was performed on a clean Cu(001) surface at room temperature and studied by Scanning Tunneling Microscopy (STM). The observed complex structures are caused by C₆₀F₁₈ molecules self-assembling and a partial decay with detachment of fluorine atoms. The structure **A** (see figure; STM image $I_t=26$ pA; $U_b=-2.0$ V) corresponds to self-assembled fluorinated fullerene molecules, which have lost some fluorine atoms. The structure **D** corresponds to c(2×2) surface reconstruction determined by relative arrangement of F and Cu atoms. The structure **B** can be identified as a precursor phase of (√2×√2)R45°-F missing-row reconstruction. The structure denoted as **C** is most probably caused by initial adsorption of fluorine atoms on the substrate. We further discuss dynamics and interaction of the adsorbed molecules leading to fluorination of copper surface and molecules self-assembling.



References:

- [1] M.L.Tang, Z.Bao, Chem.Mater., 23, 446-455 (2011)
- [2] P.Pahner et al., Phys.Rev.B 88, 195205 (2013)
- [3] A.Gunther et al., Advanced Functional Materials, 26, 768-775 (2016)
- [4] I.S. Neretin et al., Angew.Chem.Int.Ed., 39,3273-3276 (2000)

Thu-PS2-38**Messenger atom action spectroscopy of solid surfaces**

[Agata Płucienik](#), [Zongfang Wu](#), [Matthias Naschitzki](#), [Walter Wachsmann](#),
[Helmut Kuhlenbeck](#), [Hajo Freund](#)

*Department of Chemical Physics, Fritz-Haber-Institut der Max-Planck-Gesellschaft, Faradayweg 4-6,
14195 Berlin, Germany*

Vibrational action spectroscopy employing infrared radiation from a free electron laser is successfully used since many years for the vibrational and structural characterization of gas phase aggregates. Despite the high sensitivity of this method, no relevant studies have yet been conducted for solid samples. An ultra-high vacuum (UHV), chamber incorporating surface science techniques, has been constructed at the free electron laser of the Fritz Haber Institute (FHI FEL). An aim is to apply this method to solid surfaces in order to learn about their vibrational, electronic and structural properties. As central components of heterogeneous catalysts, deposited metal clusters on oxide surfaces have been intensively investigated; yet in most cases little is known about their atomic structure, since it is experimentally not easily accessible. With messenger atom action spectroscopy, the vibrational modes of clusters are detected via infrared heating induced desorption of rare gas atoms attached to the clusters. A quadrupole mass spectrometer and a low temperature scanning probe microscope are available for the detection of the desorption process. Comparison of the experimental vibrational spectrum with quantum chemical calculations provides structural information and information about electronic properties. As the preliminary topics, we studied the action spectroscopy of rutile TiO₂(110), as well as V₂O₃(0001)/Au(111) in the middle infrared range at liquid helium temperature. The results of the former sample surface revealed a series of defect independent bulk vibrational states of TiO₂(110), which were not well recognized before. The results of the latter sample surface clearly demonstrated that our method is surface sensitive and capable of investigating a wide range of scientific topics.

Motivation: Incorporating the high sensitivity action spectroscopy method with surface science techniques to study the structural and electronic properties of the oxide film supported metal clusters model catalysts, in order to broaden our understanding of structure-reactivity relation of heterogeneous.

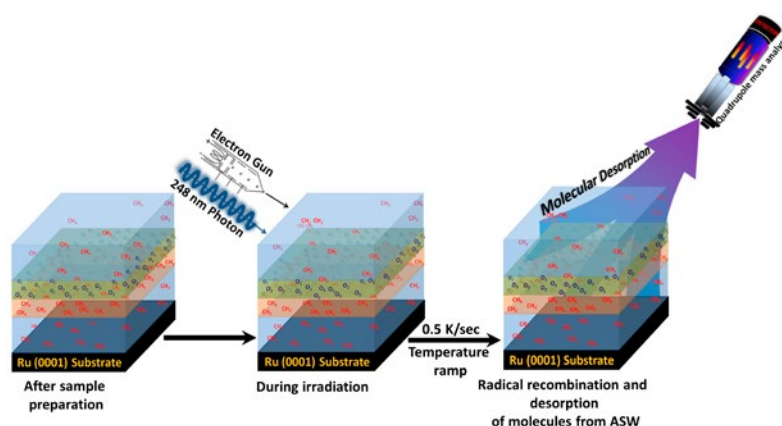
Tue-PS1-34

Photon and electron induced chemistry of molecules embedded within amorphous solid water (ASW)

Sujith Ramakrishnan, Micha Asscher

Department of Physical Chemistry, The Hebrew University of Jerusalem, Israel

Chemical reactions on solid surfaces are of interest in fields such as catalysis, atmospheric chemistry as well as astro-chemistry. In-order to understand the mechanism of the photon^[1] and electron induced chemistry^[2] and formation of organic molecules in the interstellar space a detailed understanding of photochemical reactions at the water ice-gas interface is imperative. Methane was chosen for our experiment because of its inert character with respect to chemical reactivity at atmospheric conditions which result in its accumulation in large quantities over the years underwater/underground in our planet and in the atmosphere of other planets in our solar system. Here we focus on the photochemical reaction and excitation mechanism of CH₄/ASW and CH₄/O₂/ASW on Ru(0001) substrate under UHV conditions using an excimer laser operating at 248nm. In addition, we compared the photon excitation with the effect of externally supplied electrons (5eV) by means of an energy tunable (1-100eV) electron gun^[3], as a model for secondary electrons generated by the UV light. The photo/electron induced products were detected via temperature programmed desorption (TPD) with D₂O used to form ASW^[4,5]. We demonstrated how methane conversion takes place in the vicinity of oxygen molecules entrapped in ASW analogous to conditions found in interstellar ice. The results reveal the role of reactive radical species that are formed during such excitation and its potential to activate C-H bond of methane to transform into various organic molecules. The main stable products are ethane, acetylene, and formaldehyde and hydroperoxyl radical. Interestingly the hydroperoxyl radical (HO₂ at mass33) is formed exclusively by photons.



References:

- [1] Moon, E.; and Kang, H. Metastable hydronium ions in UV irradiated ice. *The J.Chem.Phys.* 2012, 137, 204704.
- [2] Horowitz, Y.; Asscher, M. Electron induced chemistry of methyl chloride caged within amorphous solid water. *J. Chem.Phys.* 2013, 139, 154707.
- [3] Sieger, M.T.; Simpson, W.C.; Orlando, T.M. Production of O₂ on icy satellites by electronic excitation of low temperature water ice. *Nature.* 1998, 394, 554-556.
- [4] Livneh, T.; Romm, L.; Asscher, M. Cage formation of N₂ under H₂O overlayer on Ru (001). *Surf. Sci.* 1996, 315, 250.
- [5] R. S. Smith, C. Huang, E. K. L. Wong, and B. D. Kay. The molecular volcano: Abrupt CCl₄ desorption driven by the crystallization of amorphous solid water. *Phys. Rev. Lett.* 1997, 79, Number 5, 909-912.

Thu-PS2-17**Reversible interface formed on metal alloy oxide nanoparticles via lithiation**

[S.J. Rezvani](#)¹, [A. Di Cicco](#)², [R. Gunnella](#)², [F. Nobili](#)³, [S. Passerini](#)⁴, [L. Pasquali](#)¹,
[S. Nannarone](#)¹

¹ IOM CNR, S.S. 14, Km. 163.5, I-34012, Trieste, Italy;

² Dipartimento di Fisica, Università di Camerino, Camerino, Italy;

³ Dipartimento di Chimica, Università di Camerino, Camerino, Italy;

⁴ Helmholtz Institute Ulm (HIU), Albert-Einstein-Allee 11, 89081, Ulm, Germany

Transition metal oxide nanoparticles offering Li-ion storage through the combined conversion-alloying mechanism are interesting anode materials for lithium ion batteries due to their enhanced capacity compared to the conventional anode materials.

It is well known that the Li-ion anode materials often operate outside the voltage stability window of the electrolyte components. However, the electrolyte decomposition may lead to the formation of a protective layer at the interface of these nanoparticles with the electrolyte, called SEI (solid electrolyte interphase), which enable the reversible Li⁺ ion storage. [1]. The reductive decomposition of the electrolyte results in the formation of several compounds which can be present either in the whole SEI layer (e.g., LiF) or solely on the surface (e.g., LiC_x). The electronic insulation property of the SEI layer prevents the further reduction of the electrolyte salt and solvents, while its ionic conductivity allows the Li⁺ ion storage, i.e., the battery performance [2]. Improved performance (lower irreversible capacity) of the batteries employing such anode materials can be achieved if the complex set of chemical reactions could be rationalized and optimized. Hence, the detailed understanding of the nature and composition profile of the SEI layer formed on such nanoparticles, improving the understanding of the role of different components, may enhance the functionality of the Li ion battery electrodes.

We applied X-ray absorption spectroscopy (XAS) at the C, O, Li and F K-edges to study the composition of this superficial layer (SEI) on carbon coated ZnFe₂O₄ prototypical nanoparticles [3] during the first lithiation-delithiation cycle, and after several cycles. XAS spectra taken from samples at different stage of lithiation and delithiation. The line-shape evolution was also tracked at distinct stages before and during Li insertion. We demonstrate that apart from conventional SEI layer formed in these electrodes, a reversible superficial alkyl layer (ROCO₂Li) is formed within the lithiation process which can partly be responsible for the higher capacity of these materials.

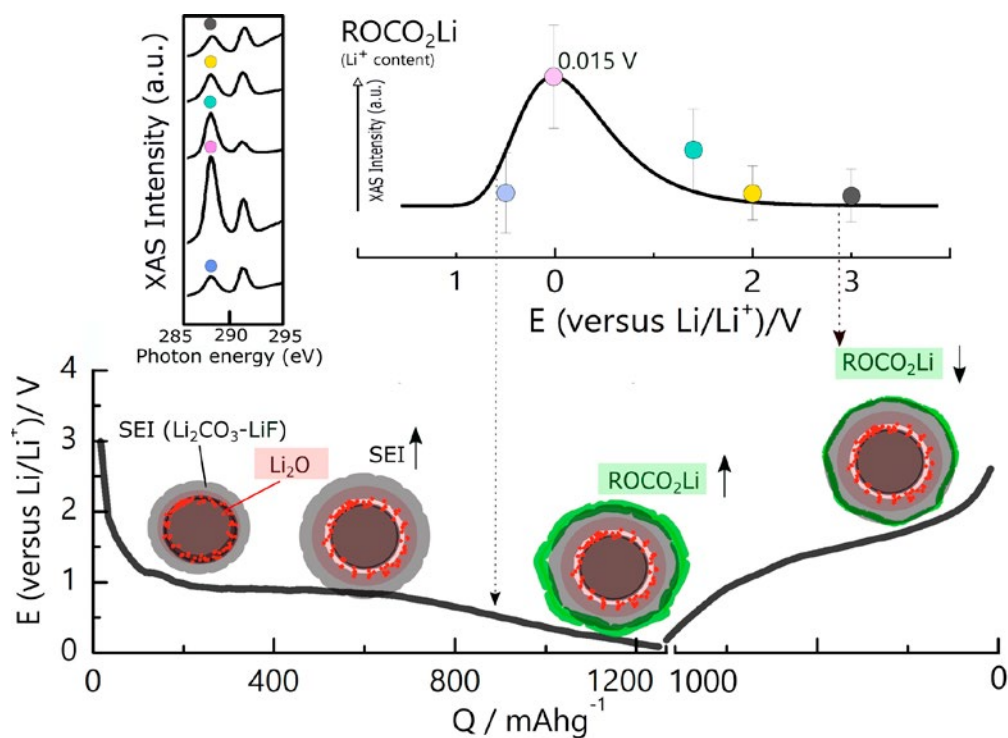


Figure 1 Trend of Li storage in the superficial SEI layer (below 0.7 V) by alkyl lithium carbonates as monitored by the corresponding intensity of the ROCO_2Li component at the XAS C K-edge [4].

References:

- [1] Peled, E.; Golodnitsky, D.; Ardel, G. *J. Electrochem. Soc.* 1997, 144, L208–L210.
- [2] Verma, P.; Maire, P.; Novak, P. *Electrochim. Acta* 2010, 55, 6332–6341.
- [3] Bresser, D.; Paillard, E.; Kloepsch, R.; Krueger, S.; Fiedler, M.; Schmitz, R.; Baither, D.; Winter, M.; Passerini, S. *Adv. Energy Mater.* 2013, 3, 513–523.
- [4] S. J. Rezvani, R. Gunnella, A. Witkowska, F. Mueller, M. Pasqualini, F. Nobili, S. Passerini, A. Di Cicco, *ACS Appl. Mater. Interfaces* 2017, 9, 4570–4576

Thu-PS2-20***In situ* XPS study of Ni-catalyzed graphitization on nano-crystalline diamond surface**

[O. Romanyuk](#)¹, [M. Varga](#)¹, [S. Tulic](#)², [T. Susi](#)², [T. Waitz](#)², [V. Skakalova](#)², [I. Izak](#)¹, [P. Jiricek](#)¹, [A. Kromka](#)¹, [B. Rezek](#)¹

¹ Institute of Physics, ASCR, Cukrovarnicka 10, 162 00 Prague, Czech Republic;

² Physics of Nanostructured Materials, Faculty of Physics, University of Vienna, Boltzmanngasse 5, 1090 Vienna, Austria

Graphene has attracted an enormous attention in recent years due to its unusual electronic properties. Similarly, diamond has also attracted researchers over the world due to extraordinary combination of its intrinsic properties. Combining both these materials in one system represented by “graphene-on-diamond” [1] can open new challenging fields in which such a system will benefit from their complementary properties.

In this work, the transformation of the surface layer of nano-crystalline diamond (NCD) caused by Ni catalyst was studied *in situ* by X-ray photoelectron spectroscopy (XPS). Thin NCD film (~60 nm) was grown on Si substrate by chemical vapor deposition (CVD) method. A 20 nm thick Ni film was evaporated on the NCD surface. The Ni/NCD and reference NCD samples were annealed up to 800 °C and cooled down to room temperature in the XPS chamber under vacuum 10⁻⁷ mbar. Photoelectron emission from C 1s, O 1s, and Ni 2p^{3/2} core-levels was measured during the annealing process with a ramping step of 100 °C. Three main stages of the Ni interaction with NCD surface have been resolved. First, desorption of oxygen from C-O and nickel oxide occurred at temperatures from 100 to 300 °C. Then, the Ni atomic concentration started to decrease at temperatures higher than 300 °C. Finally at 600 - 700 °C, Ni completely disappeared from the top-surface with annealing time.

During ramping up, the Ni 2p^{3/2} core-level peak was found at a constant position indicating that Ni carbides or other Ni phases are formed. On the other side, a significant shift of the C 1s peak maxima position depending on temperature has been observed. Figure 1 a) shows the C 1s core level peak variation with the annealing temperature. The C 1s peak of the as-received Ni/NCD sample is broad and weak in intensity, which is attributed to the carbon contamination on the sample surface. The first remarkable shift of the C1s peak was detected at 200 °C. Next the peak shift is observed at T > 300 °C when Ni starts to diffuse into the NCD film (i.e. its concentration decreases), and the formation of amorphous carbon is expected. The last significant change of the C 1s peak position maximum and its shape was observed at T > 600 °C. The C 1s peak maximum shifted back to lower binding energies and became asymmetric [2]. In this annealing stage, a graphitic C phase on sample surface is detected due to the Ni-catalyzed graphitization of the NCD film. The C 1s peak shape and intensity remain almost the same after the sample cooling down to room temperature. The Ni-catalyzed graphitization of the NCD film was also confirmed by Raman measurements (Figure 1 b): an obvious reduction in the Raman diamond peak intensity (1331 cm⁻¹) and evolution towards the D, G and 2D bands was observed. The possibility of graphene formation on NCD surface by controlled graphitization in UHV will be discussed.

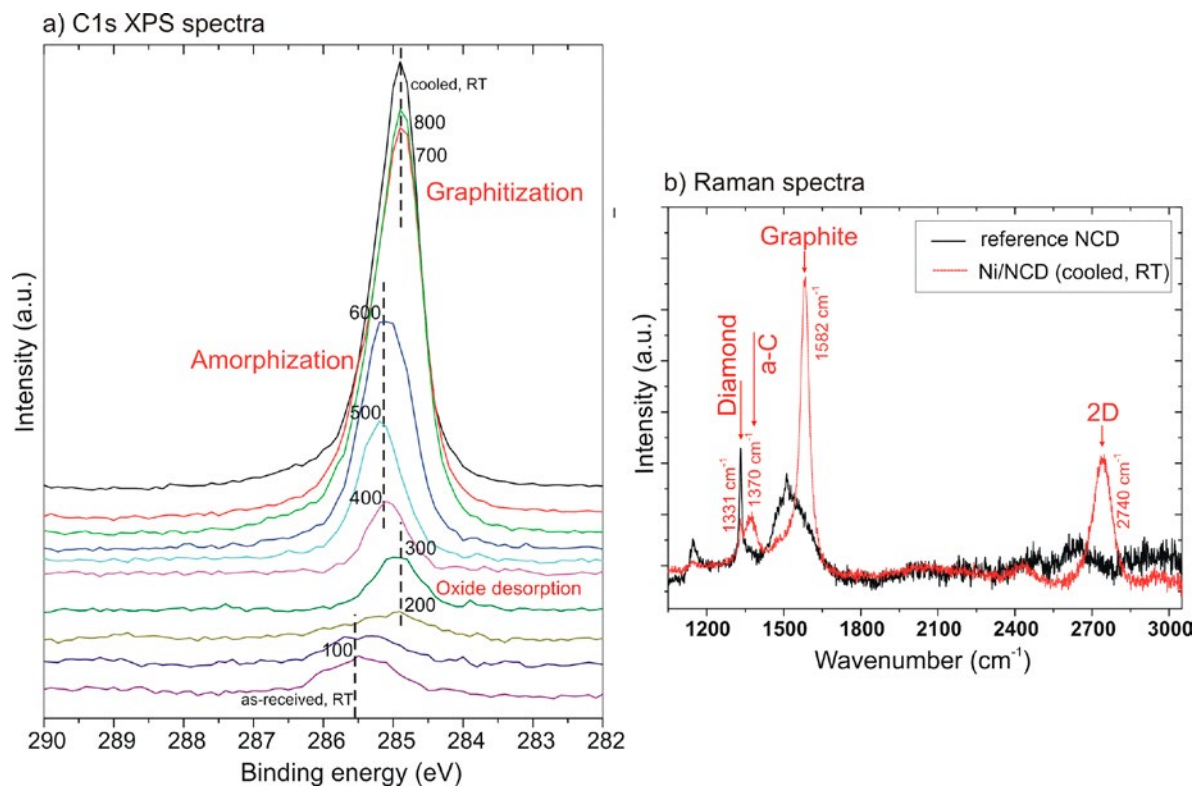


Figure 1 - a) C 1s core level peak dependence on annealing temperature in °C and b) Raman spectra measured on annealed reference NCD and Ni/NCD samples.

Acknowledgment: This work was supported by GACR-FWF bilateral project 16-34856L and FWF-I2344-N36.

References:

- [1] D. Berman, et.al., Nat. Comm. 7 (2016) 12099.
- [2] M. R. C. Hunt, PRB 78 (2008) 153408.

Thu-PS2-16**Temperature effect on transport and charging of low-energy electrons interacting with amorphous solid water films**

[Roey Sagi](#), [Micha Asscher](#)

Institute of Chemistry, Edmund J. Safra Campus, Givat-Ram, The Hebrew University of Jerusalem, Jerusalem 9190401, Israel

The charging process of molecular films has been extensively studied in recent years due to its importance in biological systems, ecology as well as in interstellar processes. We report here the charging effects of tens to hundreds layers thick Amorphous Solid Water (ASW) films grown on Ru(0001) as a result of low-energy electrons (5 eV) bombardment under ultra-high vacuum (UHV) conditions.

The charging of the ASW films was measured via contact potential difference (CPD) detection utilizing an *in-situ* Kelvin probe. Such systems have been found to obey the physics of a plate capacitor with nanometer range separation between the plates (nano-capacitor). The charging mechanism was studied as a function of the substrate temperature during film growth (T_{gr}) and during electrons irradiation (T_{irr}), both in the range of 50-120 K, and as function of film thickness. The through-the-film (electrons) transmission currents (I_e) and the charge accumulation were found to be strongly affected by the studied parameters. I_e shows varied intensity profiles for different growth temperatures such that for a given T_{gr} , the charging behavior depends on both film thickness and T_{irr} . This implies for a varying thickness of the effective negative electrode at the ASW/vacuum interface. Temperature Programmed-CPD (TP-CPD) measurements of charged films reveal a strong influence of T_{gr} on the discharge event. We propose that the electrons discharge from the top electrode to the grounded ruthenium is driven by the formation and propagation of cracks upon heating the films, a mechanism similar to release of trapped gasses inside ASW films. This allows charges to diffuse more easily on the walls of the pores and cracks until they reach the substrate.

Tue-PS1-35

Grafting unsaturated carbon groups on hydrogenated diamond under low-energy electron irradiation

Leo Sala, Lionel Amiaud, Céline Dablemont, Anne Lafosse

Institut des Sciences Moléculaires d'Orsay (ISMO), CNRS, Univ Paris-Sud, Université Paris-Saclay, F-91405 Orsay, France

Methods of grafting organic functional groups on semiconductor surfaces spur developments in the field of molecular electronics and biosensors. Organic groups allow for further functionalization of semiconductor surfaces to immobilize more complex molecular anchors for specific targets [1]. Often, these methods employ high energy irradiation which limits control over surface modifications due to numerous processes occurring at high energy as well as the high yield of low-energy secondary electrons which can also trigger various chemical processes. Using low-energy electrons, however, it is possible to isolate and understand a few of these mechanisms which initiate chemical processes for a more controlled modification of surfaces [2,3].

Hydrogenated diamond is a substrate of choice for the preparation of biosensors due to its biocompatibility in addition to its superior electrical, thermal, and mechanical properties [1,4,5]. This work demonstrates the grafting of organic groups containing sp^2 -hybridized carbon on the surface of inert hydrogenated diamond using benzylamine (structure in Fig. 1) and low energy electrons.

Benzylamine deposited on hydrogenated diamond was irradiated with low-energy electrons: 2.5, 9 and 11 eV, energies at which condensed benzylamine showed distinct reactive behaviors as identified from Electron Stimulated Desorption (ESD) yields of desorbing neutral fragments. After 9 and 11 eV treatment, enhanced sp^2 -hybridized carbon signal and phenyl ring-associated bending modes have been observed in the vibrational spectra of the treated surface as acquired through High Resolution Electron Energy Loss Spectroscopy (HREELS), alluding to the presence of phenyl and benzyl grafts (treatment procedure summarized in Fig. 1). At 11 eV, the density of grafted groups can be controlled by the irradiation dose and from this, the effective cross-section of the process could even be estimated. The competition between substrate activation and formation of reactive benzylamine fragments by electron irradiation at 9 and 11 eV was evaluated. Neutral dissociation and dissociative ionization mechanisms are plausibly involved in this functionalization process.

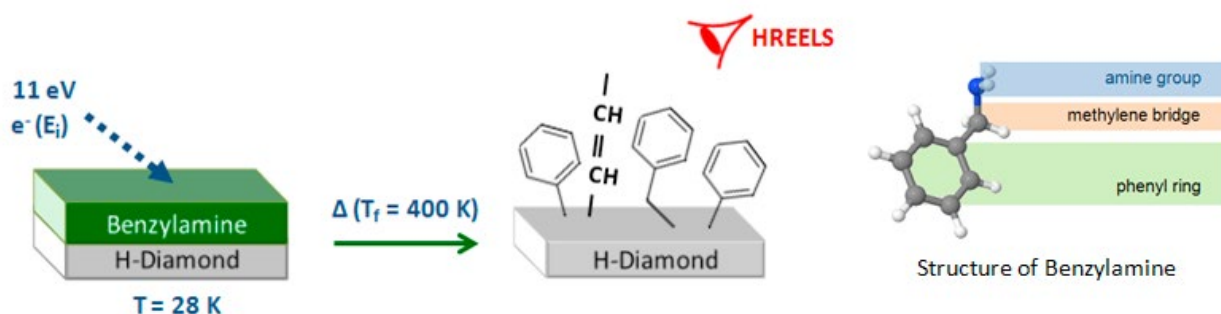


Figure 1. Electron-induced (11eV) functionalization of hydrogenated diamond by benzylamine, a potent source of sp^2 -hybridized C-containing groups.

References:

- [1] Szunerits, S. et al., *MRS Bull.* 39, 517–524 (2014).;
- [2] Arumainayagam, C. R. et al., *Surf. Sci. Rep.* 65, 1–44 (2010).;
- [3] Lafosse, A. et al., *Eur. Phys. J. D* 35, 363–366 (2005).;
- [4] Azria, R. et al., *Prog. Surf. Sci.* 86, 94–114 (2011).;
- [5] Arnault, J. C. et al., *Curr. Opin. Solid State Mater. Sci.* 21, 10–16 (2017).

Thu-PS2-03**BaZrO₃ inclusions in solution-derived YBa₂Cu₃O_{7-d} epitaxial thin films studied by X-Ray photoelectron spectroscopy**

[Antonino Santoni](#)¹, [Flaminia Rondino](#)¹, [Achille Angrisani Armenio](#)², [Antonella Mancini](#)², [Valentina Pinto](#)², [Giuseppe Celentano](#)², [Laura Piperno](#)³, [Giovanni Sotgiu](#)³

¹ FSN-TECFIS-MNF, ENEA C.R. Frascati, v. E. Fermi 45, 00044 Frascati, Italy;

² FSN, ENEA C.R. Frascati, v. E. Fermi 45, 00044 Frascati, Italy;

³ Engineering Department, Roma Tre University, Via Vito Volterra 62, 00146, Rome, Italy

The discovery of type II superconductivity [1] has opened the way for the development of high power superconducting electric devices. Such applications require high critical current densities even in high magnetic field conditions [2]. YBa₂Cu₃O_{7-d} (YBCO) is the most promising material for power applications because it is suitable for operation at liquid nitrogen temperature. Previous work has shown that the critical current of this material can be enhanced by incorporating a high density of extended defects acting as preferential sites where magnetic flux vortices (fluxons) can be effectively pinned, i.e. pinning centers. Defects in the form of nanoinclusions [3] embedded in the bulk superconductor have been demonstrated to behave as pinning centers. In particular, BaZrO₃ (BZO) has been demonstrated to be very effective for the creation of nanoscale defects in YBCO thin epitaxial films thanks to its chemical and structural stability with YBCO[4].

In this work, YBCO epitaxial thin films with different amounts of BZO secondary-phase nanoinclusions have been synthesized by chemical solution deposition (CSD) following the low-fluorine route in order to obtain less toxic, environment-friendly films [5]. In this context it is important to determine the Zr stoichiometry of the grown films as a function of thickness. To achieve this goal, X-Ray Photoelectron Spectroscopy (XPS) has been used, which proved to have the required sensitivity and accuracy for detecting Zr in small quantities. Furthermore, it was also found that mild Ar⁺-ion sputtering does not destroy the film Zr/Y stoichiometric ratio, therefore allowing the acquisition of depth profile data which can reveal the Zr distribution in the film.

References:

- 1] Wu, M. K. et al. Superconductivity at 93 K in a new mixed-phase Y-Ba-Cu-O compound system at ambient pressure. *Phys. Rev. Lett.* 58, 908–910 (1987).
- 2] Larbalestier, D., Gurevich, A., Matthew Feldmann, D. & Polyanskii, A. High-Tc superconducting materials for electric power applications. *Nature* 414, 368–377 (2001).
- 3] T. Haugan, P.N. Barnes, R. Wheeler, F. Meisenkothen, Addition of nanoparticle dispersions to enhance flux pinning of the YBa₂Cu₃O_{7-x} superconductor, *Nature*. (2004). doi:10.1038/nature02832.
- 4] J.L. MacManus-Driscoll, S.R. Foltyn, Q.X. Jia, H. Wang, A. Serquis, L. Civale, et al., Strongly enhanced current densities in superconducting coated conductors of YBa₂Cu₃O_{7-x} + BaZrO₃, *Nat Mater.* 3 (2004) 439–443. doi:10.1038/nmat1156.
- 5] V. Pinto, A.A. Armenio, L. Piperno, A. Mancini, F. Rizzo, A. Vannozzi, et al., Aging of Precursor Solutions Used for YBCO Films Chemical Solution Deposition: Study of Mechanisms and Effects on Film Properties, *IEEE Transactions on Applied Superconductivity.* 26 (2016) 1–5. doi:10.1109/TASC.2016.2542587.

Thu-PS2-05

Improvement in corrosion resistance of NiWP and NiWB films formed by electroless plating

Masami Shibata, Yuuta Miyazawa

University of Yamanashi, Japan

Electroless plating Ni alloy films with P and B of high content ratio are the amorphous structure, and therefore, the corrosion resistance is improved. In addition, it is known that the corrosion resistance of Ni film is also improved by W. Furthermore, it has been reported that the corrosion resistance is improved, when W is added to NiP and NiB films. However, the report on electroless plating NiWP and NiWB films with high W content is not found. In this study, it is a purpose to form electroless plating NiWP and NiWB films with high W content ratio and to evaluate the corrosion resistance.

The NiWP and NiWB films having various composition were prepared using the electroless plating method. The composition, crystal structure and surface morphology of the films were observed by EPMA, XRD and SEM, respectively.

The NiWP and NiWB films having various composition were obtained under the various plating conditions, as shown in Fig. 1. It rose to 15% and 25% at the W content rate in NiWP and NiWB, respectively. It is possible to produce the electroless plating NiWP and NiWB films with the high W content rate.

From the results of the XRD measurement, it was proven that these films were amorphous structure. After immersion in 5 M HCl solution for 72 hr, the surface of the electroless plating NiWP film does not change, which is difficult to be corroded in the hydrochloric acid. However, the pin-holes were formed at the NiP surface. Electrochemical behavior at the surface of NiP, NiB, NiWP and NiWB was measured in 1 M HCl solution, as shown in Fig. 2. The corrosion resistance of the electroless plating NiWP and NiWB films is improved, when high content of W is added to NiP and NiB.

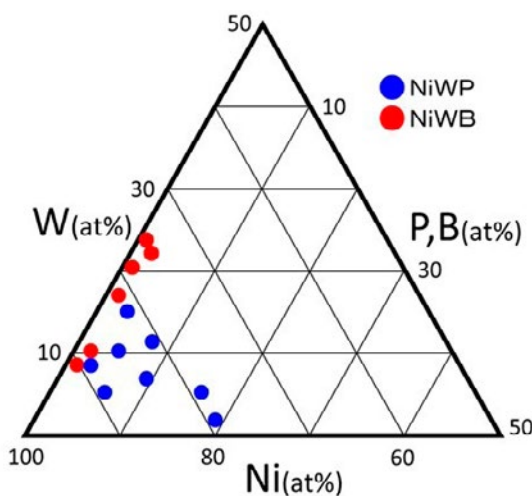


Fig. 1.

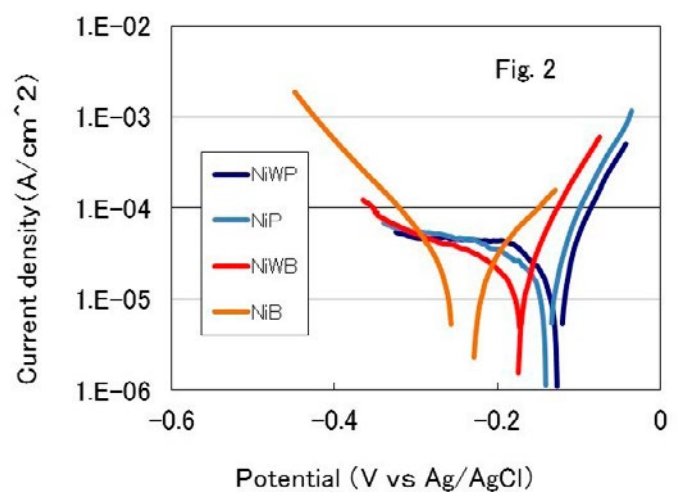


Fig. 2.

Thu-PS2-44
Influence of local surface potential on Kikuchi envelope and channeling of high-energy electrons on reconstructed surface

Yukichi Shigeta, Yuto Hagiwara

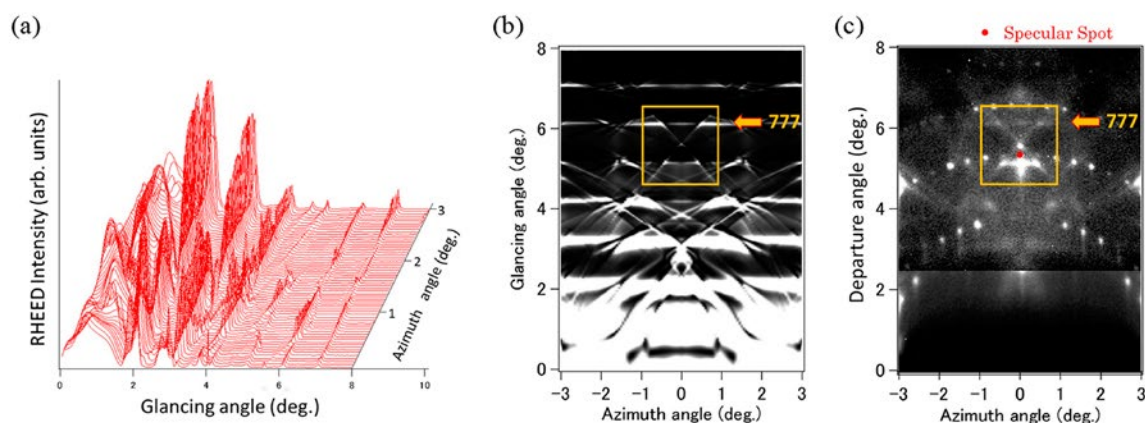
Yokohama City University, 22-2 Seto, Kanazawa-ku, Yokohama 236-0027, Japan

The reflection high-energy electron diffraction (RHEED) is a very useful tool to investigate the surface structure within a few layers underneath the surface [1-5]. In the RHEED pattern, Kikuchi pattern is also observed in addition to the diffraction spots. The Kikuchi pattern is composed of Kikuchi line, Kikuchi band and Kikuchi envelope [1,5 and 6]. The Kikuchi pattern is formed by diffracted waves resulting from secondary incident waves having various directions created by inelastic scattering of the primary incident wave. So the Kikuchi pattern includes much useful information about the surface structure, because the intensity distribution is formed by a set of the diffracted waves created under various incident conditions (various glancing and azimuth angles).

Especially, the Kikuchi envelope is considered to include useful information about the surface layer, because the envelope created under the surface wave resonance (SWR) condition for the reciprocal lattice rod [1,6]. Moreover, when the Kikuchi envelope under a resonance condition for the reciprocal lattice rod of the surface reconstructed structure at the topmost layer (SWR_s), the envelope will include valuable information about the topmost surface [7,8].

In this paper, we assume that the intensity of Kikuchi pattern is represented by calculated rocking curves for various azimuth angles based on the dynamical diffraction theory [1-3]. And we calculated the rocking curves for the Si(111) surface with the energy of 15 keV, as shown in Fig. 1(a), when the azimuth angle changes up to 3° from the [112] direction. The grayscale image of these curves is shown in Fig. 1(b), as a simulated Kikuchi pattern. And an observed RHEED pattern, when the specular spot is set in between the (666) and (777) Kikuchi lines, is also shown in Fig. 1(c). Each position of the Kikuchi lines and envelopes in the simulated pattern coincides with that in the observed pattern, respectively. And the intensity profile near the specular position surrounded by a square is well represented by the simulated pattern, where the cross section of the inelastic scattering will be larger than that in higher scattering angle.

For the Kikuchi envelope of the Si(111) $\sqrt{3}\times\sqrt{3}$ -Ag reconstructed surface under the SWRs condition, we found an influence of local potential formed by the Ag atoms at topmost surface on the position of the Kikuchi envelope. From the position shift, it is estimated that the surface wave for the SWRs propagates in the topmost layer within a thickness of 0.2 nm.



References:

- [1] A. Ichimiya and P. I. Cohen, "Reflection High Energy Electron Diffraction" (Cambridge University Press) 2004, (ISBN-10: 0521453739).
- [2] K. Yamaguchi, H. Mitsui, and Y. Shigeta, *J. Vac. Sci. Technol. A* 15, 1997, pp. 2569-2573.
- [3] Y. Fukaya and Y. Shigeta, *Phys. Rev. B* 65; 2002, 195415,
- [4] Y. Fukaya, Y. Shigeta, and K. Maki, *Phys. Rev. B* 61; 2000, 13000.
- [5] A. Ichimiya, *Surf. Sci.* 192; 1987, L893-L898.
- [6] A. Ichimiya, K. Kambe and G. Lehmpfuhl, *J. Phys. Soc. Jpn.* 49; 1980, pp. 684-688.
- [7] Y. Shigeta and K. Maki, *Surf. Sci.*, 152/153, 1007-1019 (1985).
- [8] Y. Shigeta, *Jpn. J. Appl. Phys.* 27; 1988, pp.908-911.

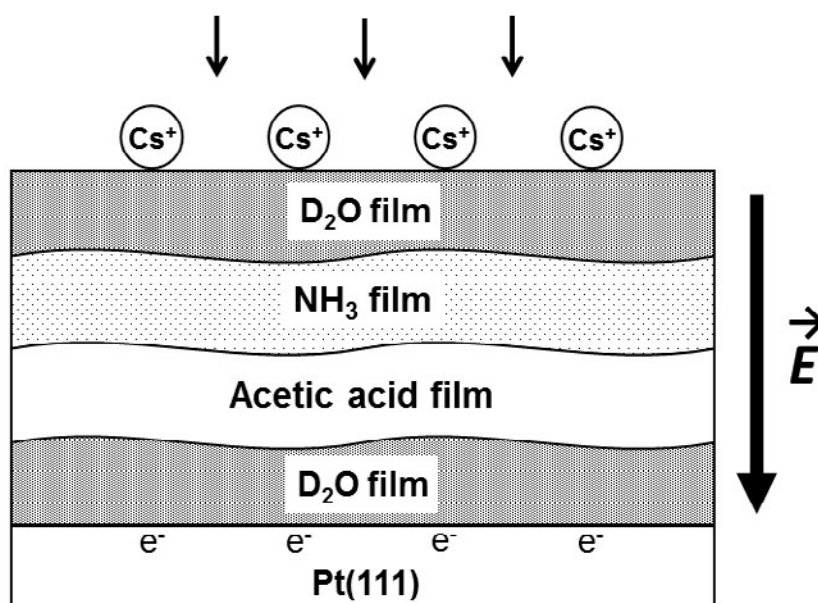
Tue-PS1-36

Effect of electric field on proton transfer at acid-base interface

Sunghwan Shin, Heon Kang

Department of Chemistry, Seoul National University, 1 Gwanak-ro, Gwanak-gu, Seoul 08826, South Korea

Although strong electric field plays a pivotal role in many chemical and biological phenomena, its operating mechanism is not yet fully understood at the molecular level. We study the effect of electric field on the acid-base reaction between acetic acid (AA) and ammonia (NH_3) by using the ice film capacitor method,¹ which can provide strong electric field ($\sim 10^8$ V/m) across a thin molecular film grown on a metal substrate in ultra-high vacuum. The field-induced reaction was examined at the interface of AA and NH_3 layers by making an ice film capacitor that contained AA and NH_3 films, as shown in Figure 1. To change the direction of applied field, the stacking sequence of AA and NH_3 films was reversed. The dissociation of AA was monitored by using reflection absorption infrared spectroscopy (RAIRS), which measured the intensities of vibrational bands of AA and acetate (AA^-) anion. RAIRS spectra showed that external electric field could enhance the acid dissociation and the proton transfer to NH_3 , but the enhancement effect depended on the direction of applied field. Interestingly, the proton transfer was enhanced when the direction of proton migration was opposite to the applied field. This dependency suggests that the reaction is induced by the reorientation of acid and/or base molecules, rather than by the electrostatic stabilization energy of charge transfer. The effect of molecular size was studied by comparing the results for formic acid and propionic acid. The dissociation of smaller acid was more strongly enhanced than that of larger acid, which supports the interpretation that the field-induced dissociation occurs via molecular reorientation.



References:

- [1] Shin, S.; Kim, Y.; Moon, E.-s.; Lee, D. H.; Kang, H.; Kang, H., J. Chem. Phys. 2013, 139, 074201.

Thu-PS2-01**New instrumentation for spin-integrated and spin-resolved momentum microscopy – METIS and KREIOS**

Marko Wietstruk¹, Violeta Simic-Milosevic¹, Andreas Thissen¹, Gerd Schoenhense²,
Andreas Oelsner³, Christian Tusche⁴

¹ SPECS Surface Nano Analysis GmbH;

² Johannes-Gutenberg-Universitaet Mainz;

³ Surface Concept GmbH;

⁴ Max-Planck-Institut fuer Mikrostrukturphysik Halle

Two new momentum microscopes are presented by SPECS: our newly developed time-of-flight momentum microscope METIS and the energy dispersive and filtered momentum microscope KREIOS. Both are using an optimized lens design which provides simultaneously highest energy, angular and lateral resolution. The lens provides a full 2π solid acceptance angle with highest angular resolution. In contrast to standard ARPES measurements with conventional hemispherical analyzers, electronic structure data from and beyond the 1st Brillouin zone is recorded without any sample movement. In addition the lens of such an instrument can work in a lateral imaging mode for microscopy as well. This enables navigation on the sample and reduces the size of the area under investigation in ARPES down to a few micrometers in diameter. This combination of large acceptance angle, high angular resolution and small acceptance area, makes this instrument the ideal tool for electronic structure studies on small samples or sample areas. The design is compact with a straight optical axis. Operation modes are (k_x, k_y, E_k) data acquisition by operation in energy filtered k-space imaging, (ToF-)PEEM mode, energy-filtered real space imaging and micro-spectroscopy mode.

The 3D (k_x, k_y, E_k) data recording is done with a 2-dimensional delayline detector, with a time resolution of 150 ps and count rates up to 8 Mcps. It uses channelplates with 40 μm spatial resolution. While the x,y position of an incoming electron is converted into k_x, k_y wave vector, the kinetic energy E_k is determined from the flight time t in METIS or obtained directly by the energy filter in KREIOS. Spin-resolved imaging is achieved by electron reflection at a W(100) spin-filter crystal prior to the 2-dimensional delayline detector. Electrons are reflected in the [010] azimuth at 45° reflection angle. Varying the scattering energy one can choose positive, negative, or vanishing reflection asymmetry.

Besides a description on how the instruments work data from both instruments on different single crystalline materials will be presented.

Tue-PS1-37**STM and STS study of thin Ag films grown on the Ga/Si(111)- $\sqrt{3}\times\sqrt{3}$ surface**

[S. Starfelt](#), [H.M. Zhang](#), [L.S.O. Johansson](#)

Department of Engineering and Physics, Karlstad University, SE-651 88 Karlstad, Sweden

Quantum Well States (QWS) are discrete electronic energy states formed by spatial confinement of the electrons in one dimension. QWS in thin films have been studied extensively for the past thirty years due to their importance both in low dimensional physics and device applications [1]. Metal films on semiconductor substrates, such as Ag on Si, where the Ag *sp* valence band is quantized into QWS, are examples of such systems. The growth of well-ordered silver films on Si substrates faces several challenges, such as requiring deposition at low temperature and avoiding the formation of strain in the film due to lattice mismatch and surface dangling bonds [2]. It has been shown that the Ga/Si(111)- $\sqrt{3}\times\sqrt{3}$ surface, formed by deposition of 1/3 monolayer (ML) of Ga on Si(111), is a good candidate to overcome these two obstacles [3]. Therefore, we have studied the atomic and electronic structures of both the bare Ga/Si(111)- $\sqrt{3}\times\sqrt{3}$ surface and Ag thin films deposited at room temperature (RT) conditions.

Scanning Tunneling Microscopy and Spectroscopy (STM/STS) measurements have been performed on the Ga/Si(111)- $\sqrt{3}\times\sqrt{3}$ surface as well as on silver films with thicknesses lower than 5 ML. STM images of the Ga/Si(111)- $\sqrt{3}\times\sqrt{3}$ surface highlight the importance of the annealing method for minimizing surface defects, such as Si substitution atoms. In addition, the STM images provide a means to confirm the Ag film thickness for studies of the electronic structures. STS measurements reveal the local electronic density of states of the silver film. For the filled states, the first visible peak just below the Fermi level in the STS spectra is identified as the Shockley surface state (SS). Below the SS, 2-3 peaks are visible in the spectra for all measured thicknesses in the energy range down to approximately -1.5 eV. Some of these peaks are attributed to QWS, belonging either to the fully confined or the resonant part of the quantum well state. The energy positions of these states have been tracked with respect to Ag film thicknesses.

In addition, Ultraviolet Photoelectron Spectroscopy (UPS) measurements have been performed on silver thin films deposited on the Ga/Si(111)- $\sqrt{3}\times\sqrt{3}$ surface, investigating the electronic energy dispersions in both ΓM and ΓK directions. The spectra reveal fully confined QWS outside of the bulk Si valence band region with parabolic dispersions. These QWS then couple with the substrate electronic structure and disperse upwards to follow the projection of the bulk Si valence bands. The combination of STM, STS and UPS measurements provides a comprehensive picture of the surface morphology and electronic structures of Ag films on the Ga/Si(111)- $\sqrt{3}\times\sqrt{3}$ surface in the low coverage regime.

References:

- [1] T.-C. Chiang, Surf. Sci. Rep. 39, 181-235 (2000)
- [2] I. Matsuda, Han W. Y., Jour. of Elec. Spec. and Rel. Phen. 126, 101-115 (2002)
- [3] He J.-H., Jiang L.-Q., Qiu J.-L., Chen L., Wu K.-H., Chin. Phys. Lett. 31, 128102 (2014)

Tue-PS1-51**Grazing incident excitations on aluminum and silicon surface**

[A.Sulyok](#)¹, [K. Tőkési](#)^{2,3}

¹ *Institute for Technical Physics and Materials Science, Centre for Energy Research, P.O. Box 49, H-1525 Budapest, Hungary;*

² *Institute for Nuclear Research, Debrecen, Hungary;*

³ *ELI-ALPS, Szeged, Hungary*

Precise knowledge of the energy losses of electrons as they travel within solids is fundamental in electron spectroscopy. The contributions of energy losses in the surface and the bulk region have to be taken into account in the interpretation of the surface sensitive electron spectra. Many authors have studied the combination of surface and bulk losses in various models [1-2]. The absolute intensities of surface and bulk plasmons strongly depend on the primary energy and on the geometrical conditions like angle of incidence of impacting and escaping electrons. Opposite to the bulk losses, the description of surface loss events hasn't been fully solved yet and especially the very grazing conditions are missing so far.

In this work the reflected electron energy loss spectra of aluminum and silicon are studied both experimentally and theoretically. The backscattered electron energy spectra were measured in reflected mode at energy range between 250eV and 2000eV and at wide range of incident angle including the very grazing geometry of 88° incident angle. We obtained a series of single and multiple surface and bulk plasmon losses in the measured spectra. For the interpretation of our spectra we performed Monte Carlo simulations, which is based on classical transport theory [3,4]. Electron trajectories, in the order of 10^9 , were calculated for the same conditions as the experiments, taking into account both elastic and inelastic collisions. The elastic scattering of electrons was described by cross sections derived from the static field approximation with non-relativistic Schrödinger partial wave analysis. For the case of inelastic scattering we used the dielectric response formalism where energy loss function was derived from experimental dielectric function to include all the possible losses.

References:

[1] F. Yubero and S. Tougaard, *Phys. Rev. B* 46 (1992) 2486.

[2] Y.F. Chen, *Surf. Sci.* 345 (1996) 213.

[3] Z.-J. Ding, R. Shimizu, *Surf. Sci.* 222 (1989) 313.

[4] K. Tőkési, D. Varga, L. Kövér, T. Mukoyama, *J. Electron Spectrosc. Relat. Phenom.* 76 (1995) 427.

Tue-PS1-40

Indium coverage on Si(111)- $\sqrt{7}\times\sqrt{3}$ -In surface

a

T. Suzuki^{1,2}, J. Lawrence², M. Walker³, J. M. Morbec⁴, P. Blowey², K. Yagyu¹, P. Kratzer⁴, G. Costantini²

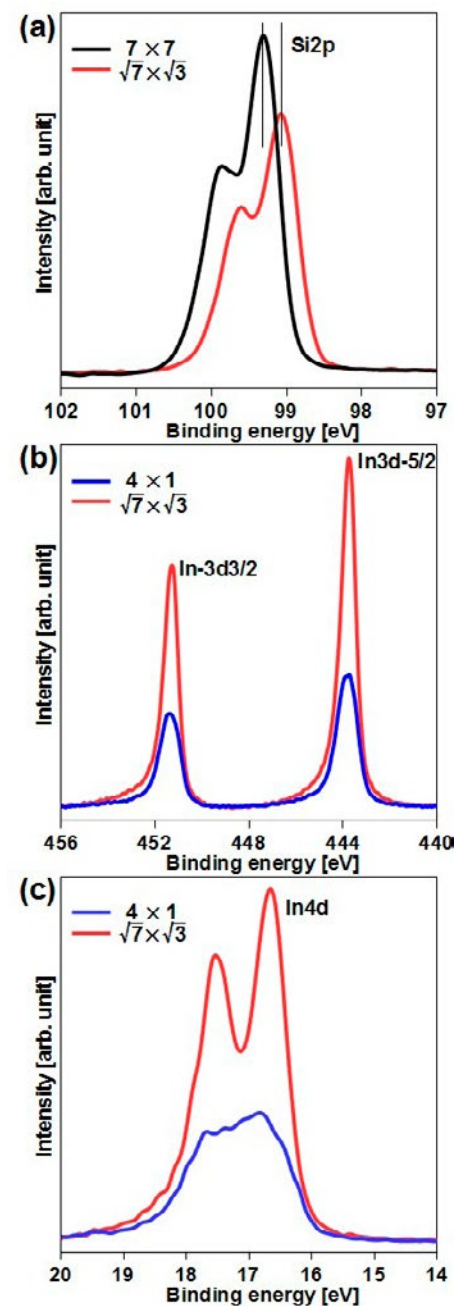
¹ Department of Electronics Engineering and Computer Science, Fukuoka University, Fukuoka 814-0180, Japan;

² Department of Chemistry, University of Warwick, Coventry, CV4 7AL, United Kingdom;

³ Department of Physics, University of Warwick, Coventry, CV4 7AL, United Kingdom;

⁴ Faculty of Physics, University of Duisburg-Essen, Lotharstrasse 1, 47057 Duisburg, Germany

The Indium coverage on Si(111)- $\sqrt{7}\times\sqrt{3}$ -In surface is investigated by means of X-ray photoelectron spectroscopy (XPS) and first-principles calculations. The coverage is estimated to be 2.9 ML from the attenuation of the Si 2p intensity, 2.0 ML and 2.1 ML from the ratio of the In 3d_{5/2} and In 4d intensities between the $\sqrt{7}\times\sqrt{3}$ and the 4 \times 1, and 2.3 ML from the thickogram, as shown in the figure. Therefore, all estimated values from the XPS measurements indicate that the In coverage of the $\sqrt{7}\times\sqrt{3}$ is rather a double layer (2.4 ML) than a single layer (1.2 ML). This was confirmed in our first-principles calculations, which predicted a deep minimum in the formation energy curve for a coverage of 2.4 ML (corresponding to a double layer of In with six In atoms in each layer, per unit cell); different coverages were found to be unlikely to form on the Si(111)- $\sqrt{7}\times\sqrt{3}$ surface. Moreover, we discuss its atomic structure by comparing experimental with simulated scanning tunneling microscopy (STM) images and scanning tunneling spectra (STS) with the calculated density of states (DOS). Our structural assignment agrees with previous studies except for the interpretation of experimental STM images. This means that both two different STM images previously reported to correspond to two different reconstructions (the „hex“ and the „rect“ phases), correspond to the “rect” phase, which shows different appearance depending on the bias voltage and the tunneling current used in the STM experiments.



Tue-PS1-41

Adhesion model of graphene islands on metal substrates based on Moiré-patterns

a

Márton Szendrő, Péter Süle

Hungarian Academy of Sciences, Centre for Energy Research, Institute for Technical Physics and Materials Science, Konkoly-Thege Miklós u. 29-33, Budapest, Hungary

One problematic aspect of graphene (GR) CVD growth on metal substrates is that GR is capable of creating rotational domains [1], separated by grain boundaries (GBs), sometimes even on a single crystal surface [2]. GBs worsen the electric properties of GR [3], therefore the nucleation of differently orientated islands is an undesirable phenomenon.

An interesting feature is, that the different existing orientations are very specific to the substrate (e.g: on Cu(111) the most commonly known orientations are: $R0^\circ$, $R7^\circ$, but for Ir(111) we have $R0^\circ$, $R14^\circ$, $R19^\circ$, $R23^\circ$, $R26^\circ$, $R30^\circ$)[4]. Even today there is no such a physical model that can somehow clarify the very basic nature of these orientations.

In order to understand these aspects, we have developed a continuum mathematical model that can calculate the adhesion energy of a GR island with a given size and orientation only by knowing the underlying Moiré-pattern that is formed between the atomic lattices. This approach agrees surprisingly well with DFT and CMD results. This shows that we have captured some very basic physical insights of the adhesion. Using our model, Monte-Carlo (MC) simulations can be carried out to perform GR growth simulations on several germs to analyze their distribution of orientation. These MC simulations are several orders of magnitude faster than Kinetic MC methods.

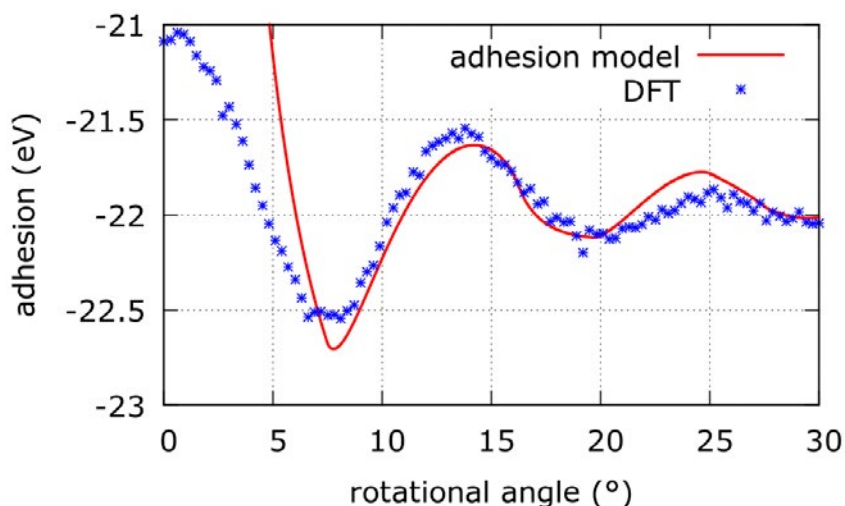


Figure 1: The dependence of the adhesion on the orientation of a GR nanoisland with a diameter of 2.2nm on Cu(111) surface. Our model (red line) is compared to DFT calculations (blue spots).

References:

- [1] M. Batzill, Surf. Sci. Rep. 67, (2012), 83.
- [2] Li Gao et al., Nano Letters 10(9) (2010), 3512-3516.
- [3] Vancsó, Péter, et al., Applied Surface Science 291,(2014), 58-63
- [4] Tetlow, H., et al., Physics Reports 542.3 (2014), 195-295

Thu-PS2-32**Formation of carbon nanostructures on metal deposits prepared by EBID**

[Imre Szenti](#)¹, [Fan Tu](#)², [Martin Dorst](#)², [Hubertus Marbach](#)², [János Kiss](#)³, [Zoltán Kónya](#)^{1,3}

¹ Department of Applied and Environmental Chemistry of the University of Szeged Rerrich Béla sq. 1, 6720 Szeged, Hungary;

² Physikalische Chemie II, FAU Erlangen-Nürnberg, Egerlandstr. 3, 910558 Erlangen, Germany;

³ MTA-SZTE Reaction Kinetics and Surface Chemistry Research Group, University of Szeged, Rerrich B. sq. 1, 6720 Szeged, Hungary

Carbon Nanotube (CNT) is the material lying between fullerenes and graphite as a member of carbon allotropes which exhibits special graphite like structure made up of individual coiled graphene sheets that form cylindrical structure. Single-wall or multi-wall carbon nanotubes can be prepared by catalytic chemical vapour deposition (CCVD) [1]. Control of the structure and location of individual CNTs with lithographic precision over large substrates is desired for their applications in electronic devices.

Thin films of Co and Fe nanostructures are widely-spread in catalytic applications. With our specific approach to focused electron beam induced processing (FEBIP), we are able to fabricate clean nanostructures on surfaces with full lithographic control, e.g., from adsorbed metal-organic precursor molecules like $\text{Fe}(\text{CO})_5$ [2]. In our ultra-high vacuum setup we can divide this nano-structuring process in two steps: the first part is the deposition of the non-volatile dissociation products of the precursors by the impact of the electron beam. Here we are able to control the lateral position and the size of the metal nanostructures. The second part is the autocatalytic growth of the metal particles. In this step we are able to control the corresponding enlargement of the patterns and increase the purity of metal particles [2]. By using EBID, we successfully fabricate well defined spatial arrangements of metal nanostructures, which we use as catalysts for the localized fabrication of secondary C-nanostructures by CCVD. The selective growth and structure of carbon nanostructures at the position of the metallic FEBIP deposits will be presented and discussed.

References:

- [1] Z. Kónya, Carbon Filaments and Nanotubes: common origins, differing applications? Dordrecht: Kluwer Academic Publishers, (2001). 85-109
- [2] H. Marbach, Appl. Phys. A, 117, (2014). 987

Tue-PS1-42**Adsorption, polymerization and decomposition of acetaldehyde on clean and carbon-covered Rh(111) surfaces**

[Ádám Szitás](#)¹, [Arnold Péter Farkas](#)², [Imre Kovács](#)³, [Zoltán Kónya](#)^{1,4}, [János Kiss](#)^{2,4}

¹ Department of Applied and Environmental Chemistry, University of Szeged, H-6720 Rerrich Béla tér 1, Hungary;

² Department of Physical Chemistry and Materials Science, University of Szeged, 6720 Szeged, Aradi Vértanúk tere 1, Hungary;

³ University of Dunaújváros, 2401 Dunaújváros, Táncsics M. u. 1/A, Hungary;

⁴ MTA-SZTE Reaction Kinetics and Surface Chemistry Research Group, University of Szeged, 6720 Szeged, Dóm tér 7, Hungary;

Acetaldehyde is one of the most abundant aldehydes in the atmosphere and a starting material for the catalytic production of many important chemicals. It has recently been found that it is an important surface and gas-phase product in the catalytic steam reforming of ethanol [1]. Noble metals, including Rh, are known as excellent catalysts for the dehydrogenation reactions. Therefore, to recognise its behaviour on single crystal surfaces is motivated by both applied and fundamental research reasons. The adsorption and dissociation of acetaldehyde were investigated by electron energy loss spectroscopy (EELS), temperature programmed desorption (TPD), high-resolution electron energy loss spectroscopy (HREELS) and $\Delta\phi$ measurements.

Our main purpose was to follow the adsorption properties of acetaldehyde on clean and carbon-covered Rh(111). The adsorption of acetaldehyde on clean Rh(111) surface produced various types of adsorption forms: η^1 -(O)-CH₃CHO and η^2 -(O,C)-CH₃CHO were developed and characterised by HREELS. η^1 -CH₃CHO desorbed at 150 K, another part of these species are incorporated in trimer, linear 2D polymer and three-dimensional surface species. Above 225 K acetaldehyde either desorbed (in monomer and trimer forms) or bonded as a stable surface intermediate (η^2 -CH₃CHO) on the rhodium surface. It is the first observation of the polymerization process of acetaldehyde on Rh(111). Similar behaviour was found on Ru(001) [2]. Surface carbon decreased the uptake of adsorbed acetaldehyde and inhibited the formation of the polymer. Nevertheless, it induced the C-O bond scission and CO formation with 40-50 K lower temperature. After higher acetaldehyde exposure on carbon contaminated surface at low carbon coverage regime, the η^1 (O)-acetaldehyde formation is the primary adsorption mode at 170 K, and at the same time, this is less stable and a part of these species desorbed from the surface as acetaldehyde after heating to 220 K.

References:

- [1] Zs. Ferencz, A. Erdőhelyi, K. Baán, A. Oszkó, L. Óvári, Z. Kónya, C. Papp, H.-P. Steinrück, J. Kiss, Effects of Support and Rh Additive on Co-Based Catalysts in the Ethanol Steam Reforming Reaction, *ACS Catal.* 4, (2014) 1205-1218.
- [2] M. A. Henderson, Y. Zhou, J. M. White, Polymerization and decomposition of acetaldehyde on ruthenium(001), *J. Am. Chem. Soc.* 111, (1989) 1185-1193.

Thu-PS2-12**Collision-induced enhancement of polyimide corrosion in sub-low Earth orbit (LEO) space environment**

[Masahito Tagawa](#), [Ryota Okura](#), [Yusuke Fujimoto](#), [Kazuki Kita](#), [Kumiko Yokota](#)

Kobe University, Kobe, Japan

Materials used in the exterior surfaces of spacecraft orbiting in the low earth orbit (LEO) experienced severe erosion by the hyperthermal collision with atomic oxygen (AO) which is the major atmospheric species in LEO [1]. Due to the high-orbital velocity of spacecraft (8 km/s), the impact energy of AO to the spacecraft surface reaches as high as 5 eV, which is higher than the interatomic bonding energy of many materials. Thus, the chemical reactions occurred at the spacecraft ram surface are under the effect of high-impact energy. Many flight projects have been conducted to clarify the erosion properties of materials in LEO, for example, Materials International Space Station Experiment (MISSE) series [2].

On the other hand, much effort has been paid for simulating the materials degradation in a ground-based facility. A microwave or radio frequency oxygen plasma source has been used for material screening test, however, this type of simulation facility does not simulate the collision energy of AO in LEO. In order to simulate the impact energy of AO, a laser-detonation method has been applied [3]. The laser-detonation hyperthermal beam source used for accelerating electrically neutral atoms is based on the laser thruster technology. The laser-detonation atomic beam source used in this study is equipped with a custom-built piezoelectric pulsed supersonic valve (PSV) system and a carbon dioxide laser. The PSV introduces the target gas into the nozzle throat through a 1 mm hole. The laser light is focused on the ejected gas in the nozzle throat using a concave Au mirror located 50 cm from the nozzle. Once plasma is formed in the nozzle by the inverse Bremsstrahlung process, the photon energy in the laser pulse is absorbed by the plasma behind the shock. Thus, the detonation wave propagates in the laser incident direction. Moreover, the thermal energy of the high-temperature plasma is converted to kinetic energy up to 15 eV by the nozzle. Hyperthermal Ar and AO beams, thus generated, were used for polyimide corrosion studies in sub-LEO where 5 eV AO and 9 eV N₂ collide to polyimide surface simultaneously. It was clearly indicated that the mass-loss (etching) of polyimide was increased with increasing the Ar flux. Also synergistic effect of simultaneous exposures of AO and Ar on the polyimide erosion was confirmed (Enhancement of erosion rate as high as factor of 3 was observed). These results suggested that the collision-induced desorption process would be the rate-limiting process in the erosion of polyimide in sub-LEO environment. It has been suggested by the ASTM standard that the estimation of polyimide etching is carried out based on the AO fluence [4]. However, the experimental result obtained in this study clearly indicates that the flux of N₂ (or other heavy molecules) needs to be considered for the estimation of polyimide erosion. Since polyimide is a reference material to measure AO fluence and erosion yields of many material tests both on ground and in orbit, it is quite important to understand the erosion yield and mechanism of polyimide for the accurate evaluation of survivability of materials in space.

A part of this study was supported by KAKENHI from JSPS under contract Nr. 25289307, 26289322, 15K14252 and 15K14253. Financial support through the Coordination Funds for Promoting Aerospace Utilization from the MEXT was also appreciated.

References:

- [1] J. C. Yang, K. K. de Groh, MRS Bulletin, 35 (2010) 12.
- [2] K. K. de Groh, B. A. Banks et al., High Performance Polymers, 20 (2008) 388.
- [3] M. Tagawa, T. K. Minton, MRS Bulletin, 35 (2010) 35.
- [4] Standard practices for Ground Laboratory Atomic Oxygen Interaction Evaluation of Materials for Space Applications, ASTM E2089-00 (2006).

Thu-PS2-36**Investigation of carbendazim removal from water media by multiwalled carbon nanotubes and magnetite modified multiwalled carbon nanotubes**

Valéria Guzsvány¹, Ana Tasić¹, Miroslav Bogosavljev¹, Olga Vajdle¹, Laszló Nagy², Ákos Kukovecz², Zoltán Kónya²

¹ University of Novi Sad, Faculty of Sciences, Department of Chemistry, Biochemistry and Environmental Protection, Trg D. Obradovića 3, 21000 Novi Sad, Serbia;

² University of Szeged, Department of Applied and Environmental Chemistry, Rerrich Béla tér 1, 6720 Szeged

Benzimidazole fungicides, such as carbendazim (methyl-benzimidazol-2-ylcarbamate, MBC), are systemic pesticides that are widely used for the pre- or post- harvest protection of various fruits and vegetables (1, 2). Because of the very intensive application there is the requirement for their collection and removal in/from the water media. In this study multiwalled carbon nanotubes (MWCNTs) and by 10% w/w magnetite modified MWCNTs (Fe₂O₃-MWCNTs) were tested as possible adsorbents for the above purpose. The investigations were performed by different weight (5, 10 and 15 mg) of suspended nanomaterials in 20.0 mL of bidistilled water. In all cases the initial concentration of MBC was 2.4 µg/mL. The MBC removal was monitored by a simply HPLC-DAD method from the water phase of the samples which were taken at following time intervals: 0.0; 1.0; 2.5; 5.0; 7.5; 10.0; 15.0; 20.0; 30.0 and 40.0 minutes from by magnetic stirrer mixed suspensions. The samples were deep-frozen immediately after their fast sampling and filtering by syringe filters 0.22 µm. The samples for the analysis were defrosted just before the chromatographic measurements. It was found that the amount of the used nanomaterials influences significantly the MBC removal. The most intensive changes in the MBC concentration were observed in the first 5 minutes of contact time in the case of both nanomaterials at their lower concentrations, but in the case of their highest investigated concentration nearly 2.5 minutes were appropriate for the removal of cc. 99% of the target analyte. The magnetic behavior of the composite material helped for the removal of adsorbents. Special attention was paid to the appearance of the degradation intermediates, especially in the case of the Fe₂O₃-MWCNTs application.

Acknowledgement: Financial support of the projects of Ministry of Education, Science and Technological Development of R. Serbia ON172059, ON172012 and CEEPUS CIII-CZ-0212-09-1516 is gratefully acknowledged.

References:

- [1] WHO/FAO Joint Meeting on Pesticides Residues (JMPR) Report (1994) Carbendazim (072).
- [2] Vega, A.B., Frenich, A.G., Vidal, J.L.M., Monitoring of pesticides in agricultural water, soil samples from Andalusia by liquid chromatography coupled to mass spectrometry, *Anal.Chim.Acta*, 2005, 538, 117-127.

Thu-PS2-19**Gap opening in graphene buffer layer induced by structural superperiodicity**

Maya N. Nair^{1,2}, Antonio Tejada^{1,2}, Maya N. Nair^{1,2}, Irene Palacio¹, Arlensíú Celis^{1,2}, Alberto Zobelli², Alexandre Gloter², Stefan Kubsky¹, Jean-Philippe Turmaud³, Matthew Conrad³, Claire Berger^{3,4}, Walter de Heer³, Edward H. Conrad³, Amina Taleb-Ibrahimi¹

¹ *Synchrotron SOLEIL, Saint-Aubin, 91192 Gif sur Yvette, France;*

² *Laboratoire de Physique des Solides, Université Paris-Sud, CNRS, UMR 8502, F-91405 Orsay Cedex, France*

³ *School of Physics, The Georgia Institute of Technology, Atlanta, Georgia 30332-0430, USA;*

⁴ *CNRS/Grenoble University Alpes, Grenoble, 38042, France*

The disadvantage of graphene for using digital electronics is the lack of bandgap, which is necessary to perform on-off switching operations in transistors. This problem has therefore motivated many different approaches to opening a gap ranging from chemical modification by doping, functionalization with atoms, molecules or a substrate to patterning graphene into nanoribbons. In this context, the buffer layer of graphene grown on SiC(0001) can reveal itself promising. The buffer layer consists of a honeycomb lattice carbon layer attached periodically to the substrate, and it has been observed the presence of a gap [1,2]. The origin of this bandgap was unclear.

To understand the bandgap opening in buffer layer, we used different experimental techniques such as scanning tunneling microscope (STM), high-resolution scanning transmission electron microscope (HR-STEM) and angle-resolved photoemission spectroscopy (ARPES). We show that the band structure in the buffer has an electronic periodicity related to the structural periodicity observed in our STM images and in X-ray diffraction [3,4]. Our HR-STEM measurements show the bonding of the buffer layer to the SiC at specific locations separated by 1.5 nm. This is consistent with the quasi 6×6 periodic corrugation observed in the STM images. This surface periodicity promotes band foldings in the superperiodic Brillouin zone edges as seen by photoemission and confirmed by our calculations.

References:

- [1] K. V. Emtsev, F. Speck, T. Seyller, and L. Ley, *Phys. Rev. B* 77, 155303 (2008).
- [2] M.S. Nevius, M. Conrad, F. Wang, A. Celis, M.N. Nair, A. Taleb-Ibrahimi, A. Tejada, and E.H. Conrad, *Phys. Rev. Lett.* 115, 136802 (2015)
- [3] M. Conrad, F. Wang, M. Nevius, K. Jinkins, A. Celis, M. Narayanan Nair, A. Taleb-Ibrahimi, A. Tejada, Y. Garreau, A. Vlad, A. Coati, P. F. Miceli, and E. H. Conrad, *Nano Lett.* 17, 341 (2017).
- [4] M. N. Nair, I. Palacio, A. Celis, A. Zobelli, A. Gloter, S. Kubsky, J-P. Turmaud, M. Conrad, C. Berger, W. A. de Heer, E. H. Conrad, A. Taleb-Ibrahimi, and A. Tejada *Nano Lett.* 17, 2681 (2017).

Tue-PS1-43**Electron spectroscopic study of carbon fiber – polyacrylate composites**

József Tóth¹, Tamás Károly², István Péter Nagy²

¹ Institute for Nuclear Research, Hungarian Academy of Sciences, Debrecen, Hungary;

² Institute of Physical Chemistry, University of Debrecen, Hungary

Electrically conductive composites of carbon fiber - copolymers synthesized from acryl amide (AA) and triethylene glycol dimethacrylate (TGDMA) by frontal polymerization method [1], [2], [3] were studied with conventional Al K alpha X-ray excited Photoelectron Spectroscopy (XPS) and Reflection Electron Energy Loss Spectroscopy (REELS) by the help of a home-made electron spectrometer equipped with a home-made X-ray tube. The doping carbon fibers and the liquid of the monomers were mixed before the polymerization. The conductive copolymer was used as an electrode material instead of Cr-content electrode in our department. The knowledge of such type of copolymers can be used during the development of environment-friendly polymer accumulators and biopolymers as well.

In the case of biopolymers used in dentistry the copolymer is not doped with carbon material and the polymerization starts with deep blue light radiation instead of heat, but the frontal polymerization is also exothermic. That type of polymers are filler materials for the dentistry. In the clinical usage that is also very important to achieve hundred percent conversion of the monomers into polymer, not to cause any hazardous health effects by the monomer.

The carbon fiber- copolymer composites with different molar ratios of TGDMA/AA [4] were produced and electric conductivity measurements were carried out as well.

In the electron spectroscopic studies, the XPS spectra of O 1s and C 1s showed very strong characteristic features as a function of the TGDMA/AA ratios. The partial C/O atomic concentration ratios were determined and assigned to different chemical forms of the carbon and oxygen chemical bondings. Correlations were found between the different strength chemical bonds (C, CH_x; carbonyl; carboxyl) in the C1s and O 1s complex peaks as a function of the TGDMA/AA molar ratios.

In the REELS measurements the π - π^* and the σ + π (σ + π)* transitions showed characteristic features depending on the chemical bondings of the copolymer. In the REELS the fine structure of the elastic peaks of carbon standards was measured as well with high energy resolution [5]. The REELS energy scale was calibrated very precisely with XPS by the help of polycrystalline Cu, Ag and Au specimens using the binding energy standards originating from the NIST (USA) and the NPL (UK) XPS databases.

In these days the interface bonding and the mechanism of the conductivity of the carbon fiber- copolymer composites are exciting questions. Because of that, further studies, including the creation of theoretical models for the molecular structures, are in progress on the carbon fiber-copolymer composites.

References:

- [1] N. M. Chechilo, R. J. Khvilivitskii, N. S. Enikolopyan, Dokl. Akad. Nauk SSSR 1972, 204, 1180-1181.
- [2] J. A. Pojman, I. P. Nagy, C. Salter, J. Am. Chem. Soc. 1993, 115, 11044-11045.
- [3] J. Tóth, T. Károly, I. P. Nagy, JVC-15, 15-20 June, 2015, Vienna.
- [4] T. Károly, I. P. Nagy, J. Tóth, "Eur. Congr. on Advanced Materials and Processes", 2005, Prague.
- [5] J. Tóth, I. Cséry, L. Kövér, D. Varga, L. Stobinski, B. Lesiak, P. Herczegh, JVC-14, 4-8 June, 2012, Dubrovnik, Croatia.

Thu-PS2-02**Energy loss function of samarium derived from reflection electron energy loss spectroscopy**

H. Xu¹, K. Tőkési^{2,3}, M. Menyhárd⁴, Z.J. Ding¹

¹ National Laboratory for Physics Sciences at Microscale and Department of Physics, University of Science and Technology of China, Hefei 230026, Anhui, P.R. China

² Institute for Nuclear Research, Hungarian Academy of Sciences (ATOMKI), P.O. Box 51, Debrecen;

³ ELI-ALPS, ELI-HU Non-profit Ltd., Szeged (Hungary);

⁴ Institute for Technical Physics and Materials Science Centre for Energy Research, Hungarian Academy of Sciences (MTA), P.O. Box 49, H-1525 Budapest, Hungary

The internal properties of solids are commonly studied by the response of various kinds of energetic beams. The optical, the electronic properties and the energy loss functions of the sample are mostly studied by reflection spectroscopy, absorption spectroscopy and spectroscopic ellipsometry techniques. Nowadays these technique are routinely carried out with commercial equipment. The handbook edited by Edward D. Palik [1] included optical constants of most elements in the periodic table along with many common compounds. However, with the demands of scientific development, standard optical techniques have reached their limitations. At the same time, in nano-science requires characterization techniques with high spatial resolution. This is impossible by using photon probe because it is difficult to focus the incident beam. Since the advent of electron energy-loss spectroscopy (EELS), it was realized that the energy loss functions and thereby the optical properties of a solid sample from an EELS spectra can be obtained. EELS are routinely carried out under UHV conditions and it is not as sensitive to surface roughness as optical reflection experiments. Furthermore, electrons can easily be focused even in the sub-nanometer range. More importantly, the energy range of optical data obtained with EELS experiments are directly determined by the range of the EELS spectrum, which is typically from 0 eV to 100 eV or larger. In this work, the energy loss function of samarium in the energy range between 0 eV and 100 eV were studied and obtained from the spectra measured by the reflection electron energy loss spectroscopy technique. For this reason, a recently developed reverse Monte Carlo technique was employed to resolve the electron energy loss features buried in the REELS spectra [2] of samarium. Critical analysis and comparisons were made among our current electron loss functions (ELFs) with the limited available literature data. The accuracy of the ELFs was checked by applying the Thomas-Ritchie-Kuhn (f-sum rule) and the perfect-screening sum rules (p-sum rule).

This work was supported by the National Natural Science Foundation of China (No. 11574289) and Special Program for Applied Research on Super Computation of the NSFC-Guangdong Joint Fund (2nd phase), and by the European Cost Actions CM1405 (MOLIM) and MP1306 (MPNS). We also thank the supercomputing center of USTC for support in performing parallel computations.

References:

- [1] E.D. Palik, Handbook of Optical Constants of Solids (Academic Press, New York,1985).
- [2] Da, Y. Sun, S. F. Mao, Z. M. Zhang, H. Jin, H. Yoshikawa, S. Tanuma, and Z. J. Ding, J. Appl. Phys. 113, 214303 (2013).

Thu-PS2-14
Fabrication and characterization of the substrateless GaN-on-Si LEDs with a metal can package

Chia-Lung Tsai, Yi-Chen Lu, Chia-Yu Yu and Yen-Chen Tu

Department of Electronic Engineering and Green Technology Research Center, Chang Gung University, Taoyuan 333, Taiwan

Through good control of the thermally induced tensile stress via the use of the step-graded AlGaIn buffers incorporated with three low-temperature-grown AlN interlayers, we present the successful growth of a 5.5- μm -thick crack-free InGaIn LED epilayer on 6-inch Si substrates. According to the full width at half-maximum values of (0002) and (10-12) XRD reflections, the corresponding screw and edge dislocation density of GaN-on-Si LEDs are comparable to those of previous findings [1]. Otherwise, an anomalous optical behavior of "S-shaped" (redshift-blueshift-redshift) variations in the temperature-dependent photoluminescence spectra is observed in our InGaIn LEDs. Such result implies that the influence of the material defect-related recombination centers on output performance of the fabricated LEDs is limited due to injected carriers tend to recombine radiatively at the localized states caused by indium compositional fluctuation in InGaIn wells [2]. Further improvement in light output power of GaN-on-Si LEDs can be done by stripping the Si substrates along with the use of a highly reflective metal as the bottom reflectors. Nevertheless, it was found that the presence of the output power roll-off in the light intensity-current curve of the transistor outline (TO)-packaged thin-film LEDs is relatively apparent as compared to that of GaN-on-Si LEDs with the same metal can package (TO-46). In the experiment, the completed LED chips with an epitaxy side-up configuration were all packaged onto the TO headers using Ag paste. Due to the poor thermal conductivity of the Ag paste ($2\text{--}25\text{ Wm}^{-1}\text{K}^{-1}$), the heat generated at the p-n junction of thin-film LEDs cannot easily be conducted to the TO-46 and thus their capacity for high power operation is restricted. However, in addition to serving as the growth substrate, Si can also be used to facilitate heat dissipation of InGaIn LEDs due to its high thermal conductivity ($\sim 150\text{ Wm}^{-1}\text{K}^{-1}$) and specific heat capacity ($\sim 700\text{ Jkg}^{-1}\text{K}^{-1}$) [3]. Therefore, at elevated current levels, the influence of joule heating on this device would be rather slight despite the Ag paste was used as die attach adhesives.

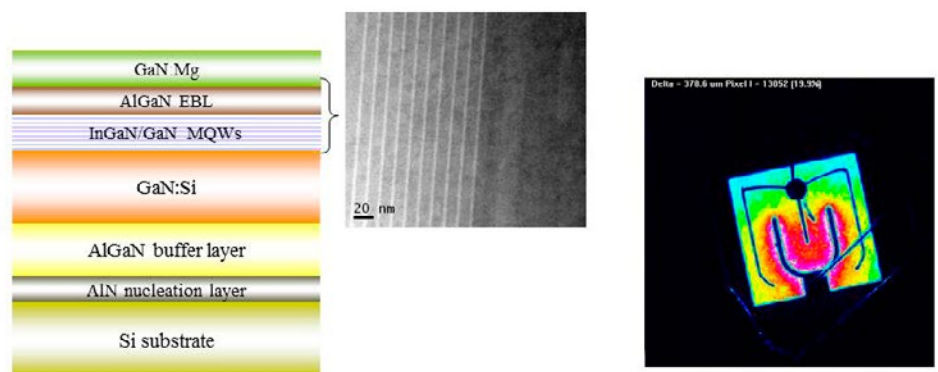


Fig. 1 InGaIn LEDs grown on Si (111) substrate and their emission pattern.

References:

- [1] D. Zhu, C. McAleese, M. Häberlen, C. Salcianu, T. Thrush, M. Kappers, A. Phillips, P. Lane, M. Kane, D. Wallis, T. Martin, M. Astles, N. Hylton, P. Dawson, and C. Humphreys, *J. Appl. Phys.*, 109, 014502 (2011).
- [2] Y. H. Cho, G. H. Gainer, A. J. Fischer, J. J. Song, S. Keller, U. K. Mishra, and S. P. DenBaars, *Appl. Phys. Lett.*, 73, 1370 (1998).
- [3] S. M. Sze, *Physics of Semiconductor Devices*, 2nd Edition, Appendix H, John Wiley & Sons, New York (1981).

Thu-PS2-35**Epitaxial growth of fullerene on the organic single crystal**

Ryohei Tsuruta¹, Yuta Mizuno², Yuta Togami¹, Soichiro Yamanaka¹, Toshiaki Mori¹, Tomoyuki Koganezawa³, Takuya Hosokai⁴, Yasuo Nakayama¹

¹ Department of Pure and Applied Chemistry, Tokyo University of Science, Japan;

² Graduate School of Advanced Integration Science, Chiba University, Japan;

³ Japan Synchrotron Radiation Research Institute, Japan;

⁴ National Institute of Advanced Industrial Science and Technology, Japan

Structural design of pn heterojunctions is an important issue for improving the performance of organic electronic devices. Especially for organic photovoltaics, controlling the morphological size scale at the pn heterojunction to be comparable to the exciton diffusion length (10-100 nm) is important [1,2]. For smarter design of the heterojunction structures, understanding on detailed mechanisms of the interface formation composed of two molecular materials is demanded. However, molecular behaviors at the heterojunctions have not been clarified yet, as most of past studies used polycrystalline organic thin films as substrates, and thus any molecular-scale fine information is hidden by the non-uniform nature of the interface structures. In this work, the crystal structures of well-defined organic semiconductor pn heterojunctions were examined by using the organic single crystal surface as substrates (Fig. 1); namely epitaxial overlayers of a typical n-type molecular semiconductor fullerene (C_{60}) built on single crystals of pentacene ($C_{22}H_{14}$) and rubrene ($C_{42}H_{28}$), which are both representative p-type organic semiconductor materials, were examined by grazing incidence x-ray diffraction (GIXD) method at SPring-8 BL46XU and BL19B2 (Proposal No. 2015A1685, 2015B1624, 2016A1676, 2016B1612).

Pentacene and rubrene single crystal substrates were produced by gas-phase recrystallization in a purified nitrogen stream. The crystals were fixed onto Si wafers, where the crystal surface of pentacene and rubrene is known to be the (001)/(00-1) and (001), respectively, and these were subsequently introduced into an ultrahigh vacuum chamber. C_{60} was evaporated up to 20 nm thick on these organic single crystal substrates. GIXD measurements were conducted at BL46XU or BL19B2, SPring-8, in the ambient atmosphere at room temperature [3,4].

The GIXD results indicated that C_{60} forms fcc crystalline overlayers in the (111)-orientation [3]. Two-dimensional GIXD measurements by rotating the sample azimuthal angle revealed that the fcc- C_{60} {2-20} diffraction spots appeared at every sixty degree of the angle. This means that C_{60} grows epitaxially on the pentacene single crystal surface. An inter-lattice relationship between the C_{60} overlayer and pentacene single crystal is derived based on the present GIXD results as shown in Fig. 2(a), where the C_{60} molecules align along the [-110] direction of pentacene. An in-plane mean crystallite size of C_{60} deposited on the pentacene single crystals at room temperature is larger than 100 nm, which is significantly greater than the case of the C_{60} overlayers formed on polycrystalline films of pentacene [4]. The crystallite size was regulated depending on the growth temperature up to 150 nm or wider, as shown in Fig. 2(b). In this presentation, we also discuss the variation in the growth behaviors of the C_{60} overlayers depending on the crystallographic structures of the organic molecules.

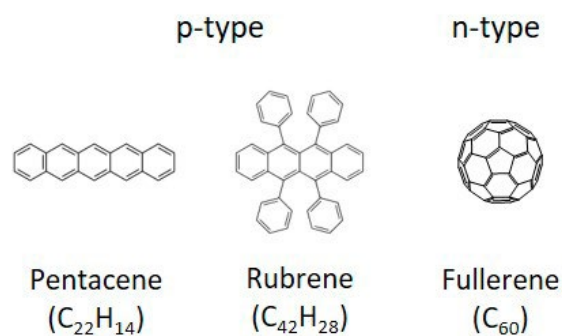


Fig1. Molecular structure of pentacene, rubrene and fullerene

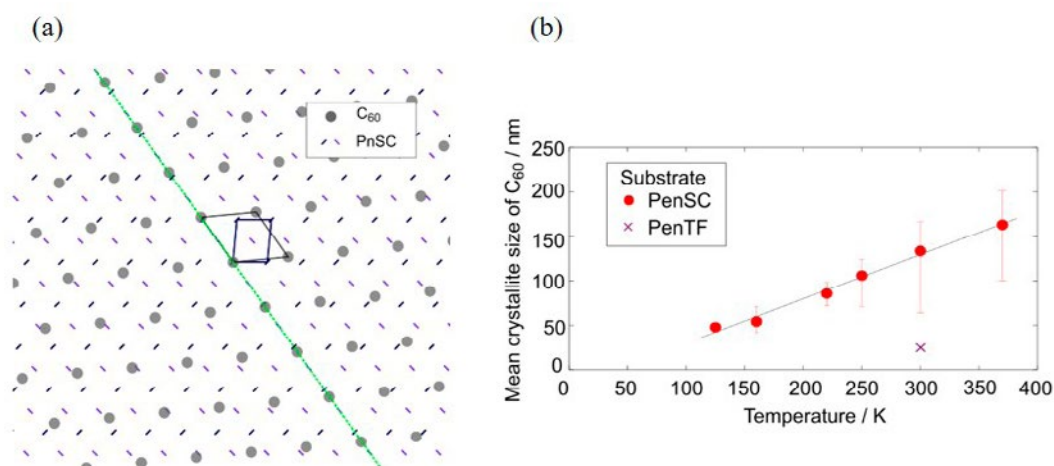


Fig2. (a) The inter-lattice relationships of the C₆₀ overlayers on the pentacene single crystal. (b) In-plane mean crystallite Sizes of C₆₀.

References:

- [1] M. Hiramoto, et al., Appl. Phys.Lett., 58 (1991) 1062.
- [2] P. Peumans, et al., Nature 425 (2003) 158.
- [3] Y. Nakayama, et al., ACS Appl. Mater. Interf. 8 (2016) 13499.
- [4] R. Tsuruta, et al., J. Cryst. Growth, in press (DOI: 10.1016/j.jcrysgro.2016.10.031.)

Thu-PS2-23**Plasmon-induced electron emission from a carbon nanotube under polarized laser: a real-time first-principles study**

[Kazuki Uchida](#), [Kazuyuki Watanabe](#)

Department of Physics, Tokyo University of Science, 1-3 Kagurazaka, Shinjuku, Tokyo 162-8601, Japan

Laser-assisted field emission (LAFE) from metallic nanotips with femtosecond laser pulse illumination has attracted great interest [1], since the emitted electrons are localized spatially and temporally, which are utilized for applications such as ultrafast electron microscopy. Recently, interesting observations of LAFE from a nanotip based on carbon nanotube (CNT) have been reported [2]. Regarding the observation, microscopic mechanism of photoabsorption excitations followed by electron emission, which critically depends on the laser polarization, is unknown and to be clarified.

Motivated by the experiment on LAFE from CNT-based nanotip, we aim to elucidate the microscopic mechanism and investigated the laser-polarization dependence of electronic excitation dynamics in a finite CNT using a time-dependent density functional theory simulation in real space and time [3].

The results in the present study are summarized as follows: 1. In the optical absorption spectra of finite (3, 3) CNT, an absorption peak emerges at the energy of the plasmon excitation in the near-infrared light region for the light polarized to the direction parallel to the CNT axis. By applying the laser of energy corresponding to plasmon excitation (on resonance) to the CNT, we found electric-field enhancement around the CNT and energy transfer to the CNT remarkably large compared with those under laser of off-resonance energy. The properties are consistent with the presence of plasmon peak in the absorption spectra. In contrast to the absorption spectra for the laser of *parallel* direction, there is no absorption in the infrared and visible light regions in the *perpendicular* direction. 2. Dynamics of electronic excitations of CNT under the laser of on-resonance energy highly depends on the direction of laser polarization. The absorbed energy and the number of excited electrons significantly increase with decreasing the relative angle of laser polarization to the CNT axis, manifesting neither one-photon nor multi-photon but plasmon excitations as the excitation mechanism. 3. The energy spectra of emitted electrons is broadened to high-energy region, which indicates that the electrons are emitted and accelerated toward the vacuum by plasmon-induced electric field near the CNT edges.

To conclude, we demonstrated by real-time first-principles simulations that laser-induced electron emission from a carbon nanotube is governed by plasmon excitations and highly sensitive to the direction of laser polarization.

References:

- [1] M. Krüger, M. Schenk, M. Förster, and P. Hommelhoff, *J. Phys. B: At. Mol. Opt. Phys.* 45, 074006 (2012).
- [2] M. R. Bionta, B. Chalopin, A. Masseboeuf, and B. Chatel, *Ultramicroscopy* 159, 152 (2015).
- [3] K. Uchida, E. P. Silaeva, and K. Watanabe, *Appl. Phys. Express* 9, 065101 (2016).

Thu-PS2-42**First-principle study of angle-resolved secondary electron emission from atomic sheets**

[Yoshihiro Ueda](#), [Yasumitsu Suzuki](#), [Kazuyuki Watanabe](#)

Department of Physics, Tokyo University of Science, 1-3 Kagurazaka, Shinjuku-ku, Tokyo 162-8601, Japan

Angle-resolved secondary electron emission (ARSEE) is one of the experimental methods that have a possibility to probe the surface band structures above the vacuum level. It has been considered that the emitted secondary electrons have information of the band structure at the emission time and thus the peaks in the spectra of angle-resolved secondary electrons can be interpreted in terms of the band structure. In a recent study [1], it was reported that the ARSEE spectra obtained from the graphene on Ni substrate partially reproduced the band structure calculated by the density functional theory (DFT) simulation. In this study, our objective is to reveal the dynamical process of ARSEE by means of first principles simulation and examine the validity of above interpretation of the ARSEE. To this end, we calculate the energy spectra of secondary electrons using the time-dependent DFT (TDDFT) and compare the results with the band structures.

We have recently developed a new method using TDDFT to study the electron scattering processes [2]. The method represents the incident electron as a wave packet and evolves it using the time-dependent Kohn-Sham equations. Our method can describe the dynamics of both of the target and incident electrons, which is necessary for correct simulation of electron scattering from nanostructures. Compared with the conventional scattering theory approach, the TDDFT method has an advantage in that multiple and inelastic scatterings are automatically included in its framework.

By applying this TDDFT approach, we have calculated the k-point resolved energy spectra of secondary electrons emitted from three different atomic sheets, graphene, h-BN, and silicone, and then constructed the ARSEE spectra based on them. We have found that the ARSEE spectra coincide with some part of the band structure calculated by DFT, although there are also non-negligible differences. We found that the ARSEE spectrum has clear dependence on the type of atomic sheets, and concluded that the difference in the ARSEE spectra reflects the difference in the band structures. We also calculated the time evolution of the occupation of k-point resolved Kohn-Sham eigenstates, and revealed that there is a clear relationship between the time-resolved occupation of excited states and k-point resolved energy spectra of secondary emitted electrons.

References:

- [1] M. Pisarra, et al., Carbon 77, 796-802 (2014).
- [2] Y. Ueda, Y. Suzuki, K. Watanabe, Phys. Rev. B 94, 035403 (2016).

Tue-PS1-50**Comparison of multiwalled carbon nanotubes modified with silver and gold particles as surface modifiers of carbon paste electrode for hydrodynamic chronoamperometric determination of H₂O₂**

Valéria Guzsvány¹, Olga Vajdle¹, Milana Gurdeljević¹, Péter Pusztai², Dániel Madarász², László Nagy², Zoltán Kónya²

¹ Department of Chemistry, Biochemistry and Environmental Protection, Faculty of Sciences, University of Novi Sad, Trg D. Obradovića 3, 21000 Novi Sad, Serbia;

² Department of Applied and Environmental Chemistry, University of Szeged, Rerrich Béla tér 1, 6720 Szeged, Hungary

Two composite materials made from multiwalled carbon nanotubes and silver (Ag-MWCNT) and gold particles (Au-MWCNT) were synthesized and characterized by XRD and SEM/EDS measurement techniques. The SEM micrographs obtained for the Ag-MWCNT and Au-MWCNT confirmed a very similar carbon based frameworks where the multiwalled carbon nanotubes are densely and randomly oriented. In the cases of both investigated materials the Ag and Au particles are surrounded by the carbon nanotubes forming on such way the composite, where the average diameter of the modifier particles in the case of the both composites was between 50 and 200 nm. The XRD confirmed the presence of Au and Ag particles in the composites. Thanks to the EDS measurements the modifier content was found as nearly 5 mass % expressed as Ag and Au. The Ag-MWCNT and Au-MWCNT together with the basic MWCNT material were applied as surface modifiers of simply carbon paste electrode (made from paraffin oil and graphite powder) by drop coating method. Such prepared voltammetric working electrodes, Ag-MWCNT-CPE, Au-MWCNT-CPE, MWCNT-CPE and bare CPE, were characterized by cyclic voltammetry (CV) in acetate and phosphate buffer solutions as supporting electrolytes (pH 4.50 and 7.50, 0.1 M) in the absence and presence of the H₂O₂ target analyte. Hydrodynamic chronoamperometric experiments were performed at selected working potential values, in accordance with the CV outlines, for the development of analytical methods for determination of H₂O₂. In the case of the Ag-MWCNT-CPE the most promising working potential values in the acetate buffer solution were -0.40 V and +0.80 vs SCE, and in phosphate buffer -0.30 V and +0.60 V. As for the Au-MWCNT-CPE it is applicable in acetate buffer solution in the working potential span from -0.10 V to -0.30 V vs SCE and from +0.70 V vs SCE and higher values, and in the phosphate buffer solution only from +0.50 V vs SCE and higher potential values. In all cases the investigations were performed in the concentration range of the H₂O₂ from 30 to 200 µg/cm³. The sensitivity of the obtained methods is higher than the case with the results obtained by the MWCNT-CPE and bare CPE. The relative standard deviation of the measurements was lower than 10%.

Acknowledgement: Financial support of the projects of Ministry of Education, Science and Technological Development of R. Serbia ON172059, ON172012 and CEEPUS CIII-CZ-0212-09-1516 is gratefully acknowledged.

Tue-PS1-44**Interaction of Au, Rh and Au-Rh alloys with the hexagonal boron nitride monolayer studied on Rh(111)**

Gábor Vári¹, Richárd Gubó², János Kiss³, Arnold Farkas^{2,4}, László Óvári^{2,3}, András Berkó³, Zoltán Kónya^{1,3}

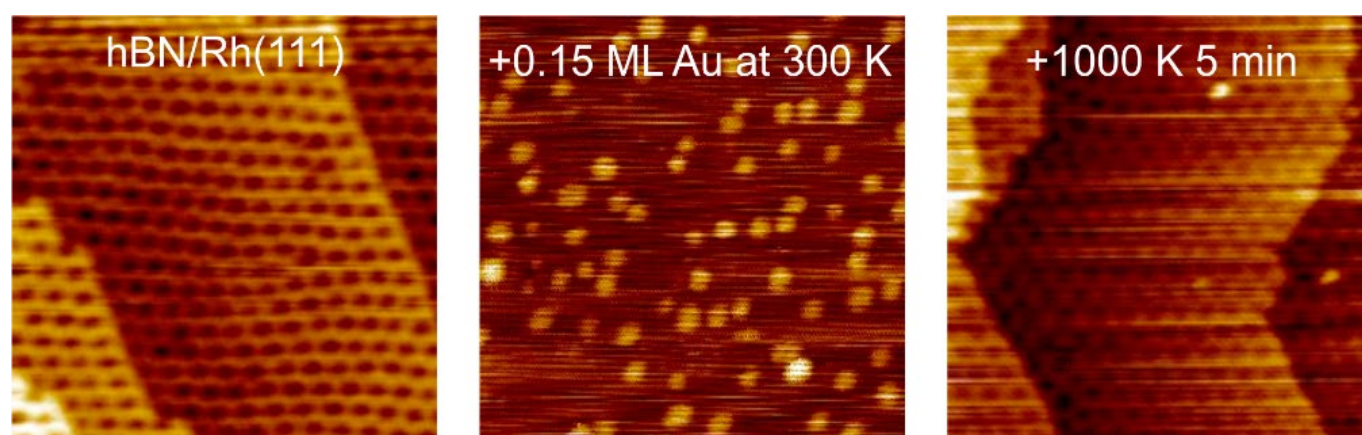
¹ Department of Applied and Environmental Chemistry, University of Szeged, Szeged, Hungary;

² Ultrafast 4D Imaging Group, ELI Attosecond Light Pulse Source, Szeged, Hungary;

³ MTA-SZTE Reaction Kinetics and Surface Chemistry Research Group, Szeged, Hungary;

⁴ Department of Physical Chemistry and Materials Science, University of Szeged, Szeged, Hungary

Two dimensional monolayers (MLs) of hexagonal boron nitride (h-BN) are promising insulator components for nanoelectronics, while calculations predict a particularly high thermal conductivity for this nanomaterial. The h-BN monolayer has a similar structure and lattice constants as those of graphene. On certain low index transition metal surfaces like Rh(111), monolayer h-BN forms a periodically corrugated surface structure, called “nanomesh”, which consists of “wires” and “pores” [1,2]. This phenomenon allows its application as a nanotemplate, with a hexagonal periodicity of 3.2 nm and a pore size of 2 nm in case of Rh(111) [3]. The existence and the extent of corrugation sensitively depend on the substrate to h-BN lattice mismatch and the strength of interaction between them [4]. For Rh(111) the lattice mismatch is 7%, and the interaction is rather strong. For metals of the copper group, however, the h-BN film is flat, because of the weak interaction. This difference in the h-BN growth and morphology strongly motivated our work dealing in part with bimetallic Au-Rh surfaces. In our earlier study we dealt with the growth of gold on Rh(111) surface and subsequent thermal effects, studied by scanning tunneling microscopy (STM), X-ray photoelectron spectroscopy (XPS) and low energy ion scattering spectroscopy (LEIS) [5]. The latter technique reveals the elementary composition of the outermost atomic layer. In that study we proved that gold and rhodium form surface alloy above 6-700 K, in spite that these metals are bulk immiscible.



Here we report on the growth of gold and rhodium on the h-BN/Rh(111) surface and on subsequent thermal effects studied by the same techniques mentioned above. The h-BN monolayer was formed on Rh(111) by the decomposition of borazine at high temperatures (1000-1050 K). Gold forms 1-2 atomic layer thick nearly 2D nanoparticles, when it is evaporated in small amounts (~0,15 ML) on the nanomesh at 300 K. Gold clusters are preferentially stabilized at the edge of the pores. At higher coverages, the growth is strongly three dimensional. Even though typically on inert surfaces small gold particles are

characterized by a Au 4f_{7/2} binding energy higher than the bulk value due to final state effects [6], in this case the gold peak was observed at a rather low position (83.7 eV), indicating significant electronic interaction either with h-BN or with the rhodium substrate through the h-BN monolayer. Indeed, previous density function theory (DFT) calculations indicated an electron transfer from boron nitride to gold [7,8]. The intercalation of gold is the dominant process upon stepwise thermal annealing to 1050 K, but agglomeration and evaporation also occur to a limited extent. Interestingly, though gold and rhodium form a surface alloy after intercalation, the presence of ~ 0.15-0.50 ML of Au below the h-BN layer does not significantly influence the nanomesh structure (see figure; image size: 50 nm × 50 nm). At higher gold doses a partial or full flattening of the nanomesh was observed.

We also investigated the growth of h-BN on Au-Rh alloyed surfaces varying the gold content between 0.25 ML and 4 ML. In these measurements gold was evaporated on Rh(111) at 500 K, followed by annealing at 1000 K for 5 min. This treatment resulted in surface alloying at smaller coverages, while a continuous Au cover layer was formed at 4 ML. Subsequently, the surface was gradually exposed to borazine at 1000 K. The exposure was increased until the whole metal surface was covered by h-BN, as shown by LEIS, but not above 260 L. Decomposition of borazine on the alloyed surface led to the attenuation of both Rh and Au LEIS (normalized) intensities, but with a substantially different slope, revealing a much more efficient coverage of Rh atoms compared to gold. Moreover, the attenuation of the normalized Au signal slowed down with increasing Au content, suggesting the importance of the spill-over of h-BN or borazine fragments from Rh to Au. It was shown by STM measurements that up to a gold coverage of to 0.5 ML, the nanomesh structure is only slightly disturbed, but larger and larger parts are flattened at higher Au doses.

LEIS studies on the growth of rhodium on h-BN/Rh(111) indicated a predominantly 3D growth, similar to the gold case. When small amounts of rhodium (up to 1 ML) were deposited on h-BN/Rh(111), intercalation was nearly complete upon annealing to ~900 K, while dewetting of the h-BN layer set in at ~1050 K. At higher rhodium doses, complete intercalation could not be reached at any temperatures, probably because of the higher stability of larger Rh nanoparticles formed at room temperature.

References:

- [1] M. Corso et al. *Science* 303 (2004) 217.
- [2] R. Laskowski et al. *J. Phys.: Condens. Matter* 20 (2008) 064207.
- [3] I. Brihuega et al. *Surf. Sci.* 602 (2008) L95.
- [4] F. Müller et al. *Phys. Rev. B* 82 (2010) 113406
- [5] L. Óvári et al. *Phys. Chem. Chem. Phys.* 18 (2016) 25230
- [6] J. Kiss et al. *e-J. Surf. Sci. Nanotech.* 12 (2014) 252.
- [7] H.-P. Koch et al. *Phys Rev. B* 86 (2012) 155404.
- [8] M. Patterson et al. *Phys. Rev. B* 89 (2014) 205423

Tue-PS1-45**Transmission surface diffraction for operando studies of heterogeneous interfaces**

[Tim Wiegmann](#)¹, [Finn Reikowski](#)¹, [Jochim Stettner](#)¹, [Jakub Drnec](#)², [Veijo Honkimäki](#)², [Fouad Maroun](#)³, [Philippe Allongue](#)³, [Olaf M. Magnussen](#)¹

¹ *Institute of Experimental and Applied Physics, Kiel University, 24098 Kiel, Germany;*

² *Experimental Division, ESRF, 71 Avenue des Martyrs, 38000 Grenoble, France;*

³ *Physique de la Matière Condensée, Ecole Polytechnique, CNRS, 91128 Palaiseau, France*

Processes at the buried interface between solids and liquid or gaseous environments often involve structural changes that are heterogeneous on the micrometer scale. We present a novel *in-situ* X-ray diffraction technique that uses high-energy photons and a transmission geometry for atomic-scale studies under these conditions with micrometer spatial resolution. The potential of this new technique is illustrated by *in-situ* studies of surface phase transitions and electrodeposition processes. [1]

For large, single-crystal samples of high surface quality, surface X-ray diffraction under grazing incidence (GID) is a powerful tool for *in-situ* investigations of the atomic arrangement at the interface. By employing high photon energies (up to 150 keV) and large 2D detectors, a large portion of reciprocal space can be accessed in a single image. [2] However, GID is very sensitive to shifts in beam position and the large beam footprint prohibits spatially resolved measurements.

We propose an alternative geometry termed *Transmission Surface Diffraction* (TSD), in which the X-ray beam impinges along the surface normal and passes through the sample, which, at modern synchrotron sources, allows for a beam footprint of micrometer dimensions. Combined with high photon energies, this geometry gives access to the full $q_z = 0$ plane of reciprocal space in a single acquisition, with diffraction peaks at intersections with CTRs or adlayer rods (Fig. 1). This is particularly suitable for the operando monitoring of unknown, incommensurate 2D phases, as no searches in reciprocal space are required and the demand on alignment precision is low.

Proof-of-principle experiments show that TSD is capable of revealing structural changes with a sensitivity down to single monolayers. This was demonstrated in [1] by operando monitoring of different electrochemical processes at the surface of a Au(111) electrode, such as the formation of the $(22 \times \sqrt{3})$ surface reconstruction, the deposition and dissolution of Co or Bi adlayers, and the potential-dependent transition of a Bi UPD layer from a (2×2) to a $(p \times \sqrt{3})$ phase. As the full in-plane geometry is captured in a single detector image, structural changes and epitaxy of different phases can be easily identified, even for incommensurate structures with many domains.

The small beam footprint can be exploited to measure structural properties of adlayers such as layer thickness, strain, and grain size with (currently) 20 μm spatial resolution. As a demonstration, the properties of a Bi(012) film deposited on Au(100) in a microfluidic electrochemical cell were mapped over the electrode surface, revealing heterogeneities that can be associated with diffusion-limited deposition under laminar flow.

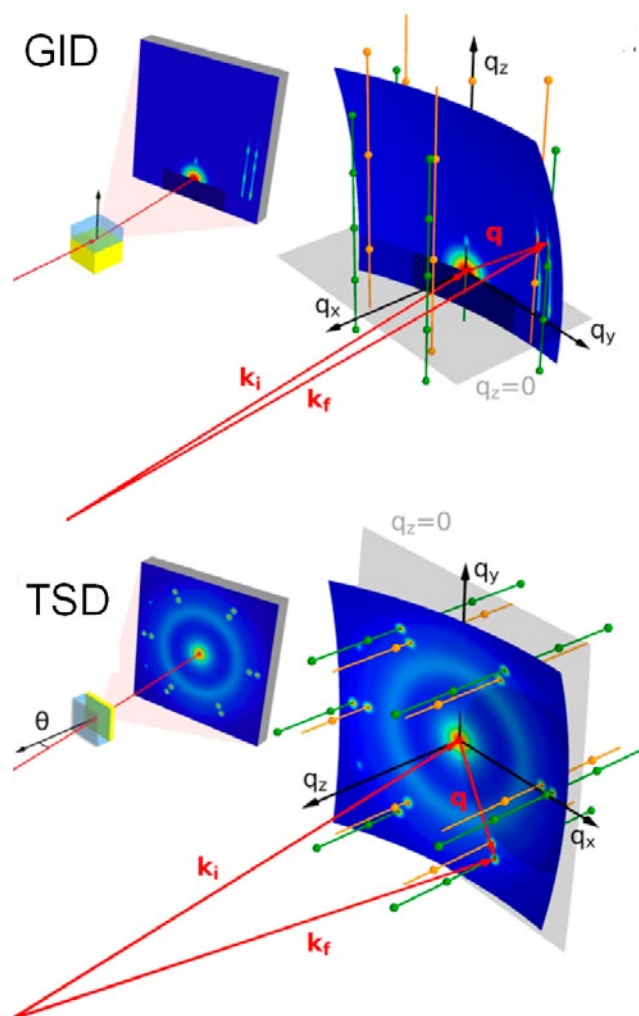


Figure: Schematic of the scattering geometry in real and reciprocal space for GID and transmission surface diffraction.

References:

- [1] F. Reikowski et al.: Transmission Surface Diffraction for Operando Studies of Heterogeneous Interfaces. *J. Phys. Chem. Lett.* 2017, 8, 1067-1071.
- [2] J. Gustafson et al.: High-Energy Surface X-ray Diffraction for Fast Surface Structure Determination. *Science* 2014, 343, 758-761.

Tue-PS1-47**Decomposition of methanol on vanadium nanoclusters supported by graphene grown on Ru(0001)**

[Yu-Cheng Wu](#), [Yi-Cheng Huang](#), [Meng-Fan Luo](#)*Department of Physics, National Central University, Taoyuan, Taiwan*

The catalytic decomposition of methanol (CH_3OH) is extensively investigated because the principal reaction is applied in direct methanol fuel cells (DMFC), which offer a prospect of efficient conversion of methanol to electricity, and because it can serve as a source of hydrogen. As the performance of DMFC or the production of hydrogen is governed largely by the catalyzed reaction, a knowledge of the detailed reaction kinetics and a correlation between reactivity and structure of the catalysts are desirable. To respond to the demand, we investigated adsorption and reaction of methanol on vanadium nanocluster supported on graphene grown on Ru(0001) single crystal, a realistic model system, under ultrahigh vacuum conditions and with infrared reflection absorption spectroscopy and temperature programmed desorption. In the presentation, we show detailed reaction kinetics and compare the results to those from vanadium single crystal and thin films.

Tue-PS1-48**Spin-orbital entanglement and optical spin control in solid surfaces**

[Koichiro Yaji](#)¹, [Kenta Kuroda](#)¹, [Katsuyoshi Kobayashi](#)², [Fumio Komori](#)¹, [Shik Shin](#)¹

¹ *Institute for Solid State Physics, The University of Tokyo;*

² *Department of Physics, Ochanomizu University*

Strongly spin-orbit coupled (SOC) materials such as topological insulators and Rashba systems are intensively studied not only because of fundamental interests but also technological directions. In a standard model of the spin texture of the SOC materials, the spin is locked to the momentum of an electron. However, recently, the spin-orbital entangled states were discovered in topological surface states. Here we show the spin-orbital texture of a Bi(111) surface state and a general description of the spin-orbital texture of the SOC systems in the mirror symmetry. Moreover, we establish a model of three-dimensional spin-rotation effect in photoemission process [1].

Spin- and angle-resolved photoelectron spectroscopy with a laser light (laser-SARPES) was performed at the Institute for Solid State Physics, The University of Tokyo [2]. In our system, the electrons are excited 6.994-eV photons, which correspond to the 6th harmonic of a Nd:YVO₄ quasi-continuous wave laser. The photoelectrons are analyzed by a ScientaOmicron DA30L analyzer equipped with an electron deflector function. To analyze the spin polarization three-dimensionally, two very-low-energy-electron-diffraction (VLEED) type spin detectors are orthogonally placed each other. The combination of the high-performance spectrometer and the high-photon-flux laser achieves an energy resolution of 1.7 meV for SARPES. In the present study, the energy and angular resolutions were set to 6meV and 0.7°, respectively. The laser-SARPES measurements were performed in a mirror plane of the Bi(111) surface. We observed the spin polarization only in the direction perpendicular to the mirror plane with *p*- and *s*-polarized lights. We also found the reversal of the spin polarization upon switching the light polarization from *p* to *s*. Thus, a spin-polarized branch consists of the linear combination of $|\text{even}, \uparrow\rangle$ and $|\text{odd}, \downarrow\rangle$ states, as in the other spin-orbit coupled surface states [3,4]. On the other hand, even if the mirror symmetry governs the spin orientation in the initial states, rotating the electric-field vector of the incident linearly polarized light can break the mirror symmetry of the experimental geometry, which leads to the three-dimensional spin rotation in photoexcited states. This is produced by the spin-dependent quantum interference of the wavefunctions, resulting from simultaneous excitation of the $|\text{even}, \uparrow\rangle$ and $|\text{odd}, \downarrow\rangle$ states.

References:

- [1] K. Yaji et al., Nat. Commun. 8, 14588. (2017).
- [2] K. Yaji et al., Rev. Sci. Instrum. 87, 053111 (2016).
- [3] K. Kuroda et al., Phys. Rev. B 94, 165162 (2016).
- [4] R. Noguchi et al., Phys. Rev B 95, 041111(R) (2017).

Tue-PS1-49**Orange up-conversion in TiO₂-ZnO composite ceramics fabricated by metal organic decomposition**Shin-Ichi Yamamoto, Toshihiro Nonaka*Ryukoku University, Japan*

Up-conversion (UC) phosphors can convert near-infrared light into visible light, and this property has attracted considerable research attention in recent years for application in various fields ranging from bioimaging to solar cells. In this context, the rare earth (RE) ion combination of Er³⁺ and Yb³⁺ has been frequently reported to successfully yield emission. In this regard, in our previous study, we investigated the dependence of UC emission on the molar ratio of Yb³⁺ and Er³⁺ [1].

The solid-state reaction method is often used in the fabrication of UC devices. On the other hand, in this study, we adopt metal organic decomposition (MOD) method for fabrication because of its low initial cost and the ease of controlling the composition.

The phenomenon of photon up-conversion (UC) has attracted considerable research interest for its application to fields as diverse as bioimaging and photovoltaics. In this study, we report on the concentration dependence of Zn₂TiO₄:Yb³⁺, Er³⁺ on UC emission. Upon investigating Mg, Ti, and Zn as potential UC host materials, we find that the combination of Ti and Zn yields the most increase in luminous efficiency. Further, as a result of varying the molar ratio, a high-intensity emission spectrum is observed for the ratios of Zn : Ti = 44 : 56 and 50 : 50. The samples prepared in this study exhibit excellent moisture resistance, and they can be utilized in solar cells and lighting equipment.

In the previous stage of our study, strong UC emission was obtained when the mol ratio was Ti : Zn = 1 : 1. The mol ratios of Ti and Zn were set to 25 : 75, 31 : 69, 38 : 62, 44 : 56, 50 : 50, 56 : 44, 62 : 38, 69 : 31, and 75 : 25 in that order, and the corresponding UC phosphors were evaluated for emission. Mol ratios of 25 : 75, 50 : 50, and 75 : 25 correspond to ratios of 1 : 3, 1 : 1 and 3 : 1, respectively, in the previous experimental stage.

The PL characteristics of the above mentioned Ti/Zn phosphors are shown in Fig. 1. From Fig. 1, we note that UC emission is obtained with molar ratio range of Ti : Zn = 44-56 : 56-44. In other words, UC emissions were observed when the mol ratio of the host materials (Ti : Zn) varied by ±6% from 1:1 ratio. However, maximum UC emission was obtained with Ti : Zn = 1:1, wherein Ti and Zn are mixed in equal parts.

The X-Ray diffraction (XRD) measurement results of the UC phosphors composed of segmented TiO₂ and ZnO are shown in Fig. 2. The curves in Fig. 2 correspond to mixing ratios of 25 : 75, 31 : 69, 38 : 62, 44 : 56, 50 : 50, 56 : 44, 62 : 38, 69 : 31 and 75 : 25 from top to bottom. The XRD results in Fig. 2 indicate the presence of TiO₂, ZnO, RE₂Ti₂O₇, and ZnTiO₄, where RE₂Ti₂O₇ represents Yb₂Ti₂O₇ and Er₂Ti₂O₇. In this paper, we write Yb₂Ti₂O₇ and Er₂Ti₂O₇ as RE₂Ti₂O₇ because the peaks of Yb₂Ti₂O₇ and Er₂Ti₂O₇ exist at the same θ value.

TiO₂ is formed with increase in Ti beyond the ratio of Ti : Zn = 50 : 50. On the other hand, ZnO is observed with increase in ZnO from the ratio of Ti : Zn = 50 : 50. The peaks corresponding to RE₂Ti₂O₇ and Zn₂TiO₄ are observed for all samples, but the shapes of the peaks vary. The integrated intensity of RE₂Ti₂O₇ decreases for Ti : Zn = 50 : 50. Further, the integrated intensity of Zn₂TiO₄ increases with increase in ZnO.

In our study, we examined the feasibility of using Zn₂TiO₄ as a host material for UC emission. When Mg, Ti, and Zn were used as single-component host materials, UC emission was not obtained. Thus, we subsequently examined various combinations of Mg, Ti, and Zn. The emission intensities were observed to increase for Zn : Ti ratios of 44 : 56 and 50 : 50. We believe that our findings can significantly contribute to developments in UC phosphors.

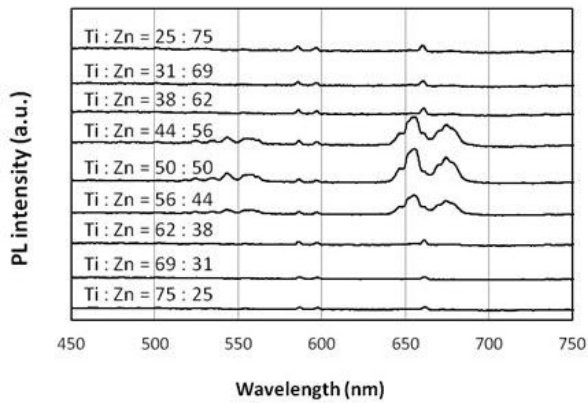


Fig. 1 Emission spectrum obtained with segmented TiO_2 and ZnO as host materials.

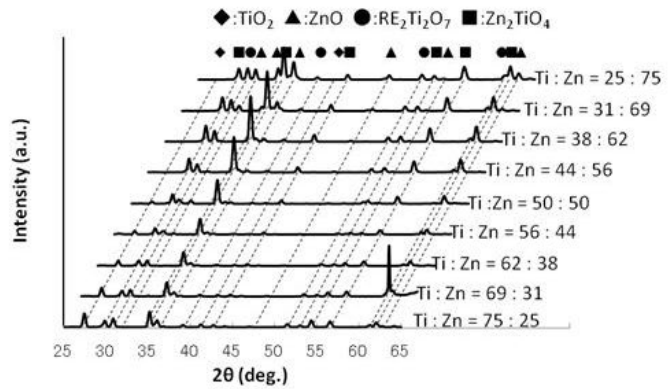


Fig. 2 X-ray diffraction (XRD) measurement results of up-conversion (UC) phosphors composed of segmented TiO_2 and ZnO .

References:

[1] T. Nonaka, T. Kanamori, K. Ohyama, and S. Yamamoto, *Jpn. J. Appl. Phys.* 54, 03CA02 (2015).

Thu-PS2-31
Perfluoropentacene films on gold surfaces grown by supersonic molecular beam deposition

Adem Yavuz¹, Gianangelo Bracco², Mehmet Fatih Danisman³

¹ *Micro and Nano Technology, Middle East Technical University, Ankara, Turkey;*

² *Department of Physics, University of Genoa, Genoa, Italy;*

³ *Chemistry, Middle East Technical University, Ankara, Turkey*

Here we will present a study of perfluoropentacene (PFP) films on gold surfaces with different morphologies and coatings.

Specifically, we used gold films on mica, template-stripped gold surfaces and thiol-coated gold surfaces as substrates. We will discuss wetting properties and morphologies of PFP films grown on these substrates by means of supersonic molecular beam deposition.

The effect of PFP deposition rate, deposition energy, and film thickness will be discussed. Finally, construction of a new helium diffraction setup that will be used for characterizing PFP films will be discussed.

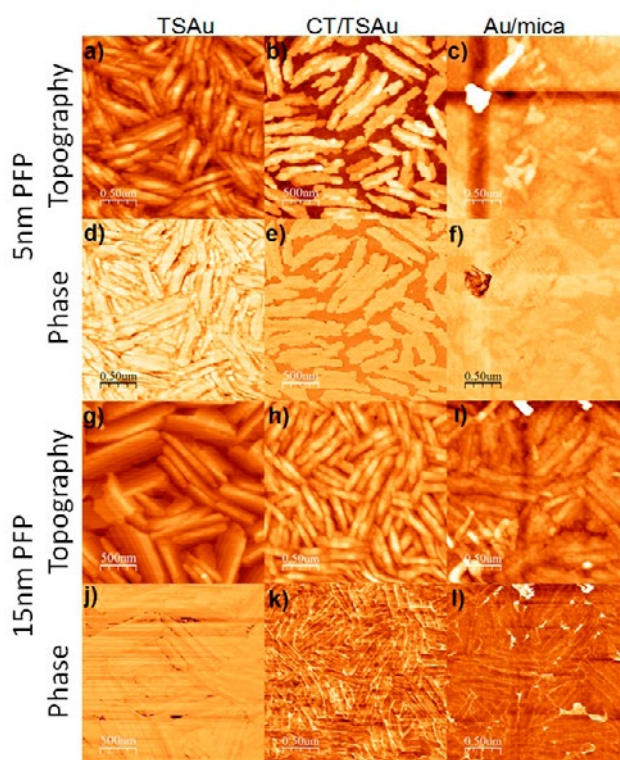


Figure 5 nm and 15 nm PFP films obtained with deposition rate of 0.05 \AA/s on TSAu (a, g), CT-SAMs/TSAu (b, h) and Au/mica (c, i) surfaces, and phase images for PFP films on TSAu (d, j), CT-SAM/TSAu (e, k) and Au/mica (f, l)

Thu-PS2-13**Surface degradation of fluoroethylenepropylene (FEP) films in sub-low earth orbit (LEO) environment; origin and mechanism**

[Kumiko Yokota](#), [Yusuke Fujimoto](#), [Ryota Okura](#), [Kazuki Kita](#), [Masahito Tagawa](#)

Kobe University, Kobe, Japan

Polyimide and fluoroethylenepropylene (FEP) are very common polymeric materials used in spacecraft for thermal control purposes. These materials are used on the exterior surface of spacecraft and directly exposed to severe space environment. There are many environmental factors in space, however, atomic oxygen (AO), which is the major (>99%) species in upper atmosphere of the Earth at the altitude of 500 km, is believed one of the most hazardous factors for polymer survivability. FEP and polyimide located in the ram surface of spacecraft are exposed to 8 km/s collisions of AO (collision energy of 5 eV). In order to evaluate the survivability of materials, many flight experiments have been performed by space shuttle and International Space Station (ISS). Many flight tests indicated that FEP is much durable in low Earth orbit (LEO) space environment compared with many hydrocarbon polymers such as polyimide. However, ground-based studies using plasma asher or laser-detonation sources gave inconsistent results, i. e., FEP erodes much faster than in space. The origin of this inconsistency in material tests in space and on ground is still in discussion. Somehow, FEP showed good durability in space, it was selected as the radiator material of the world's first sub-LEO test satellite (supper-low altitude test satellite, SLATS), which will be launched in Dec. 2017 by Japan Aerospace Exploration Agency (JAXA). However, the neutral gas environment in upper atmosphere of the Earth depends strongly on the altitude and solar activities. In the altitude of 200 km, where SLATS is orbiting, major atmospheric components are AO and N₂. The densities of AO and N₂ are increased by 10³ and 10⁴ times, respectively, compared to those in the altitude of 450 km where many material exposure tests have been performed by ISS. The fraction of N₂ is as high as 50% in the altitude of 200 km, however, the effect of N₂ on the AO-induced degradation of FEP has not been considered seriously on the design and material selection of SLATS. One of the reasons is that N₂ is chemically inactive unlike AO. It has been considered that 9 eV N₂ collision is not problematic for polymeric materials. However, it has recently been reported that the erosion of polyimide was significantly accelerated by the presence of N₂ under AO exposure. The erosion property of FEP in sub-LEO, where simultaneous collisions of AO and N₂ occurs, has not been fully understood. In this study, simultaneous exposures experiments of AO and Ar, which is simulating N₂ collision in Sub-LEO, were performed on FEP/Ag film samples.

We used the laser-detonation AO beam source, which is a standard method to create 5 eV AO beam, in order to simulate the collision energy of the spacecraft and the neutral molecules in LEO. In this method, CO₂ laser pulse was focused on the target gas to accelerate molecules and generate a beam that reproduced the collisional velocity in LEO space environment. A number of particles per unit flight time was counted by the quadrupole mass spectrometer (QMS), and the beam composition and average kinetic energy of the beam was analyzed from the obtained time-of-flight (TOF) spectra. Two laser-detonation sources were combined in order to shoot AO and Ar beams independently. The reason for using Ar instead of N₂ is that N₂ is decomposed to N atom which reduces the collision energy.

A FEP film on which Ag was deposited on the backside (FEP/Ag, Sheldahl Co.) was used as a specimen. The thickness of this film is 25 μm. This sample was cut from the same manufacture lot of the samples used for SLATS. Erosion was evaluated by measuring the mass of the film before and after exposures. Simultaneous AO and Ar beam exposures were carried out for 15 hours. Fraction of Ar was 70% balance AO. The average kinetic energy was 2.7 eV for AO beam and 9.0 eV for Ar beam. The largest mass-

loss was observed in the simultaneous AO+Ar exposure condition. Surprisingly, the mass-loss by AO is less than one half of that by Ar, which simulated the N₂ collision in sub-LEO. It was also confirmed that strong synergistic effect of AO and Ar on FEP/Ag erosion was not observed in AO+Ar simultaneous exposure conditions. These results suggested that the erosion mechanism of FEP by AO and that by Ar act independently. The results of computational chemistry reported by Troya also supports this conclusion. Currently, ASTM recommends to estimate the erosion of FEP in the based only on the AO fluence. However, it was clearly indicated that FEP erosion was more affected by Ar (or N₂ in sub-LEO) fluence than by AO fluence. Therefore, it is necessary to assess the FEP erosion based not only AO fluence but also N₂ fluence in the sub-LEO environment.

A part of this study was supported by KAKENHI from JSPS under contract Nr. 25289307, 26289322, 15K14252 and 15K14253. Financial support through the Coordination Funds for Promoting Aerospace Utilization from the MEXT was also appreciated.



33rd EUROPEAN CONFERENCE ON SURFACE SCIENCE

INDEX

| A | |
|---------------------------|--|
| Abd-el-Fattah Z | Wed-16:40-0-SAMA |
| Acres M | Tue-9:00-I-CORR |
| Acres R G | Wed-11:40-0-ORGS |
| Agócs E | Tue-PS1-23 |
| Aguilar P C | Tue-14:00-0-ORGS, Wed-11:00-0-BAND |
| Ahmad A | Thu-15:20-0-ENER |
| Ahsan A | Thu-9:20-0-MOLA |
| Aitchison H | Tue-17:00-0-MOLA |
| Akey A J | Thu-PS2-27 |
| Akhtar N | Tue-11:40-0-OXID |
| Akiyama R | Wed-16:00-0-BAND |
| Albertin S | Thu-14:20-0-CATH |
| Aldahhak H | Tue-14:00-0-ORGS |
| Alev O | Tue-16:40-0-OXID |
| Alexa P | Tue-10:40-0-ORGS1 |
| Al-Hada M | Tue-9:40-I-NAEX |
| Allan M | Tue-PS1-10 |
| Allegretti F | Tue-14:00-0-ORGS |
| Allongue P | Tue-PS1-45 |
| Alonso C | Wed-9:00-0-GRAP |
| Alperovich V L | Thu-16:00-0-SEMI |
| Al-Shamery K | Thu-PS2-18 |
| Parlak E A | Wed-16:00-0-ORGS |
| Alves Perdigao L M | Tue-PS1-19 |
| Amati M | Tue-9:40-I-NAEX |
| Amiaud L | Tue-PS1-35 |
| Amidani L | Tue-PS1-38 |
| Amino S | Tue-PS1-01 |
| Ana-Cristina G-H | Thu-11:40-0-GRAP |
| Andryushechkin B V | Wed-11:20-0-OXID |
| Anggara K | Thu-16:20-0-CATL |
| Angot T | Wed-16:20-0-GRAP |
| Antici P | Mon-17:00-0-ELI-ALPS |
| Armenio A A | Thu-PS2-03 |
| Ansari A A | Thu-PS2-07 |
| Antczak G | Wed-9:00-0-ORGS |
| Araby M I | Wed-11:20-K-GRAP |
| Arafune R | Mon-14:40-0-BAND |
| Arasu N P | Tue-9:20-0-ORGS |
| Arguelles E F | Wed-9:00-0-COMP, Tue-PS1-01 |
| Arita M | Wed-16:20-0-BAND |
| Aspera S | Tue-PS1-01 |
| Asschauer U | Thu-9:40-0-OXID |
| Asscher M | Tue-16:00-I-PISC, Tue-PS1-34, Thu-PS2-16 |
| Atodiresei N | Wed-16:40-0-ORGS |
| Atti S | Thu-15:00-0-OXID |

| Attia S | Tue-PS1-39 |
|---------------------|--|
| Aulická M | Tue-9:40-0-ENER |
| Ayani C G | Tue-10:40-0-EG2D, Wed-11:00-0-BAND |
| B | |
| Baán K | Tue-PS1-11, Thu-PS2-41 |
| Bachellier N | Tue-9:20-0-MAGN |
| Bachmann P | Tue-16:20-0-CATL |
| Bahr S | Mon-14:40-0-NAEX |
| Bailly A | Thu-PS2-15 |
| Bakhtizin R | Tue-PS1-32 |
| Bakos I | Tue-PS1-03, Thu-9:00-0-OXID |
| Balajka J | Thu-9:40-0-OXID |
| Balázs K | Thu-PS2-25 |
| Balmes O | Thu-14:20-0-CATH |
| Balog R | Tue-PS1-05, Wed-10:40-0-GRAP, Wed-11:00-0-GRAP |
| Baltic R | Tue-9:40-0-MAGN |
| Bana H V | Tue-11:00-0-EG2D |
| Bao X | Wed-11:00-0-OXID |
| Baradács E | Tue-PS1-15 |
| Baraldi A | Tue-11:00-0-EG2D |
| Barragán A | Thu-14:40-0-ENER |
| Barroo C | Mon-15:20-0-CATL, Tue-11:20-0-EG2D, Tue-17:20-0-CATL, Tue-PS1-08, Thu-PS2-27, Thu-PS2-29 |
| Barth C | Tue-PS1-30, Thu-14:40-0-OXID |
| Barth J V | Tue-14:00-0-ORGS |
| Bartynski R | Thu-15:00-0-ORGS |
| Basa P | Tue-PS1-02 |
| Battistig G | Thu-14:40-0-SAMA |
| Bauer U | Tue-16:20-0-CATL |
| Bauer A | Wed-11:20-0-ORGS |
| Bayat A | Wed-16:20-0-SAMA |
| Bechstedt F | Thu-16:20-0-SEMI |
| Beck A | Tue-PS1-27 |
| Behm R J | Fri-11:20-Plen-7 |
| Behmenburg H | Thu-10:00-0-GRAP |
| Beinik I | Thu-10:00-0-OXID |
| Bell D C | Thu-PS2-27 |
| Bellec A | Tue-17:20-0-ORGS, Wed-16:00-0-GRAP |
| Belza W | Thu-10:40-0-ORGS, Thu-11:20-0-SEMI |
| Berber S | Wed-16:00-0-ORGS |
| Bercha S | Wed-11:40-0-ORGS |
| Berger J | Tue-11:00-0-ORGS2 |
| Berger C | Thu-PS2-19 |
| Bergmann K | Tue-10:40-I-MAGN |

| | |
|-----------------------|---|
| Berkó A | Mon-15:00-0-CATL, Tue-PS1-10, Tue-PS1-44 |
| Bertoni G | Tue-PS1-38 |
| Bertóti I | Tue-PS1-04, Thu-PS2-22 |
| Bertram M | Tue-14:40-0-ELCH |
| Bertran F | Tue-15:00-0-OXID |
| Beser U | Tue-11:40-0-ORGS2 |
| Bettermann H | Tue-14:40-0-BIMS |
| Bezpalchuk V | Thu-PS2-10 |
| Bichler M | Thu-11:40-0-OXID |
| Bidermane I | Wed-9:20-0-ORGS |
| Bignardi L | Tue-11:00-0-EG2D |
| Billaud P | Thu-PS2-45 |
| Birkhölzer Y | Thu-PS2-15 |
| Birnal P | Thu-11:40-0-ORGS |
| Biró L P | Tue-15:00-0-EG2D |
| Bisson R | Wed-16:20-0-GRAP |
| Blaha P | Thu-11:40-0-OXID |
| Bloch J | Thu-15:00-0-OXID |
| Blomberg S | Thu-11:20-0-CATH, Thu-14:20-0-CATH, Thu-14:40-0-CATH |
| Blowey P | Tue-PS1-40 |
| Blügel S | Wed-16:40-0-ORGS |
| Boatner L A | Thu-9:20-0-OXID |
| Bocquet M-L | Tue-9:20-0-MAGN |
| Bodek L | Mon-14:20-0-ORGS |
| Boggild P | Tue-PS1-05 |
| Bogosavljev M | Thu-PS2-36 |
| Bokányi E | Tue-14:00-0-BIMS |
| Bollmann T R J | Tue-14:20-0-EG2D |
| Bondarchuk A | Tue-11:20-0-ELCH |
| Borbáth I | Tue-PS1-03, Thu-9:00-0-OXID |
| Borbon A P | Thu-10:40-0-CATH |
| Borg A | Tue-16:40-0-PISC |
| Boscherini F | Tue-PS1-38 |
| Bourgeois S | Tue-PS1-32, Thu-11:40-0-ORGS |
| Bracco G | Thu-PS2-31 |
| Brambilla A | Tue-11:00-0-ORGS1 |
| Brena B | Wed-9:20-0-ORGS |
| O'Brien P | Thu-15:00-0-ENER |
| Bruix A | Thu-9:00-0-CATH |
| Brumboiu I | Wed-9:20-0-ORGS |
| Brummel O | Tue-14:40-0-ELCH |
| Brune H | Tue-9:40-0-MAGN |
| Buchholcz B | Tue-PS1-04 |
| Buck M | Tue-17:00-0-MOLA |
| Bussetti G | Tue-11:00-0-ORGS1 |
| Büyükköse S | Wed-16:00-0-ORGS |

C

| | |
|------------------------|---|
| Cabailh G | Tue-11:20-0-OXID, Tue-17:20-0-OXID |
| Cabo A G | Wed-10:40-0-GRAP |
| Caciuc V | Wed-16:40-0-ORGS |
| Cai L | Thu-16:20-0-ORGS |
| Cakirlar C | Wed-16:00-0-ORGS |
| Calleja F | Tue-10:40-0-EG2D, Tue-15:00-0-ORGS, Tue-PS1-46, Thu-11:20-0-GRAP |
| Calloni A | Tue-11:00-0-ORGS1 |
| Camilli L | Tue-PS1-05 |
| Campbell C T | Thu-14:20-0-ORGS, Fri-9:20-Plen-5 |
| Camuka H | Tue-17:40-0-OXID |
| Canimkurbey B | Wed-16:00-0-ORGS |
| Capelli R | Wed-16:20-0-ORGS |
| Carey S J | Thu-14:20-0-ORGS |
| Carla F | Tue-14:20-0-EG2D, Tue-16:20-0-ELCH |
| Carlotto S | Tue-PS1-25 |
| Carrier X | Tue-17:20-0-OXID |
| Casarin M | Tue-PS1-25 |
| Cassidy A | Tue-PS1-05, Wed-16:20-0-GRAP, Wed-10:40-0-GRAP, Wed-11:00-0-GRAP |
| Catrou P | Wed-9:40-0-OXID |
| Celentano G | Thu-PS2-03 |
| Celis A | Thu-PS2-19 |
| Cha B J | Tue-17:00-0-OXID, Thu-PS2-39 |
| Chab V | Tue-10:00-0-CORR |
| Chacon C | Tue-17:20-0-ORGS, Wed-16:00-0-GRAP |
| Chan W-Y | Tue-9:00-0-NAEX |
| Chandola S | Thu-16:20-0-SEMI |
| Chang C-S | Tue-9:00-0-NAEX |
| Charalambidis D | Mon-17:00-0-ELI-ALPS, Thu-10:00-0-LASE |
| Chasse A | Wed-16:20-0-SAMA |
| Chen W-C | Wed-16:20-0-BAND |
| Chen M | Tue-PS1-09 |
| Cheng C-M | Wed-16:20-0-BAND |
| Chenot S | Tue-11:20-0-OXID |
| Chiang T-C | Wed-16:20-0-BAND |
| Chiechi R C | Tue-PS1-18 |
| Cho Y | Thu-9:40-0-SAMA |
| Choi J J | Tue-16:00-0-OXID |
| Chrafih Y | Thu-PS2-47 |
| Adamsen K C | Thu-10:00-0-OXID |
| Chulkov E V | Wed-11:00-0-BAND |
| Ciccacci F | Tue-11:00-0-ORGS1 |
| Cichon S | Tue-10:00-0-CORR |
| Cieslik K | Thu-10:40-0-ORGS |
| Cirera B | Tue-11:20-0-ORGS1 |

| | |
|------------------------|---|
| Coati A | Tue-14:40-0-EG2D |
| Comelli G | Thu-10:40-1-GRAP |
| Conrad M | Thu-PS2-19 |
| Conrad E H | Thu-PS2-19 |
| Constantini G | Tue-14:00-0-EG2D, Tue-PS1-19, Tue-PS1-40 |
| Coraux J | Tue-15:00-0-OXID |
| Coreno M | Wed-9:20-0-ORGS |
| Cornish A | Thu-14:00-0-ORGS |
| Corso M | Wed-16:40-0-SAMA |
| Corva M | Thu-PS2-26 |
| Cossaro A | Wed-9:20-0-GRAP, Thu-9:00-0-MOLA |
| Cresi J S P | Tue-PS1-38 |
| Cruguel F H | Thu-9:00-0-MOLA |
| Crumlin E | Thu-10:40-0-CATH |
| Csizmadia T | Mon-17:00-0-ELI-ALPS |
| Cyganik P | Tue-17:20-0-MOLA |
| Cserháti C | Tue-PS1-15, Thu-16:20-0-ENER |
| Csík A | Tue-9:40-0-BIMS, Tue-PS1-06 |
| D | |
| Dablemont C | Tue-PS1-35 |
| D'Addato S | Tue-PS1-38 |
| Danisman M F | Thu-PS2-31 |
| Danowski W | Tue-PS1-18 |
| Dappe Y J | Tue-15:00-0-OXID |
| Daróczy C S | Thu-PS2-25 |
| Datz D | Tue-PS1-07 |
| De Bocarmé T V | Mon-15:20-0-CATL, Thu-PS2-29 |
| De Decker Y | Mon-15:20-0-CATL |
| De Heer W | Thu-PS2-19 |
| De Hosson J T M | Thu-14:00-0-GRAP |
| De La Torre B | Mon-14:00-0-ORGS |
| De Luca O | Tue-PS1-19 |
| De Santis M | Thu-PS2-15 |
| De Simone M | Wed-9:20-0-ORGS |
| Deák L | Tue-15:20-0-OXID |
| Dedkov Y | Wed-11:20-0-ORGS |
| Deiana D | Tue-PS1-38 |
| Deimel P S | Tue-14:00-0-ORGS |
| Dékány I | Tue-10:00-0-ENER |
| Del Cueto M | Wed-16:00-0-SAMA |
| Deleporte E | Thu-14:40-0-ENER |
| Delhaye G | Wed-9:40-0-OXID |
| Demir Ü | Tue-11:40-0-ELCH |
| Denecke R | Wed-16:20-0-SAMA |
| Deniz O | Tue-11:40-0-ORGS2, Tue-17:00-0-PISC |
| Deuermeier J | Wed-10:40-0-BAND |

| | |
|----------------------------|--|
| Dézsai I | Thu-PS2-25 |
| Dhesi S S | Tue-PS1-20 |
| Di Cicco A | Thu-PS2-17 |
| Di Giovannantonio M | Tue-11:40-0-ORGS2, Tue-17:00-0-PISC, Wed-9:20-0-GRAP |
| Díaz C | Wed-16:00-0-SAMA |
| Diebold U | Tue-16:00-0-OXID, Wed-16:40-0-OXID, Thu-9:20-0-OXID, Thu-9:40-0-OXID, Thu-11:40-0-OXID |
| Dietrich P | Mon-14:40-0-NAEX |
| Diller K | Tue-9:40-0-MAGN |
| Dinelli F | Wed-16:20-0-ORGS |
| Ding Z J | Tue-11:00-0-ORGS |
| Dino W A | Tue-PS1-01, Wed-9:00-0-COMP, Thu-15:20-0-ENER |
| Dobó G D | Tue-9:20-0-NAEX, Tue-PS1-11 |
| Dobrik G | Tue-15:00-1-EG2D |
| Dogan H Ö | Tue-11:40-0-ELCH |
| Dombi P | Mon-17:00-0-ELI-ALPS, Thu-10:00-0-LASE |
| Rivera M D | Tue-10:00-0-CORR |
| Domenichini B | Thu-11:40-0-ORGS |
| Domján A | Tue-10:00-0-ENER |
| Donati F | Tue-9:40-0-MAGN |
| Dorst M | Thu-PS2-32 |
| Dostert K-H | Tue-16:40-0-K-CATL |
| Dreiser J | Tue-9:40-0-MAGN, Tue-10:40-0-ORGS1 |
| Drescher H-J | Tue-PS1-09 |
| Dresler C | Wed-16:20-0-SAMA |
| Drnec J | Tue-PS1-45, Thu-14:20-0-CATH |
| Dubau M | Wed-11:40-0-ORGS |
| Duchon T | Tue-9:40-0-ENER |
| Dumergue M | Mon-17:00-0-ELI-ALPS |
| Dumslaff T | Tue-11:40-0-ORGS2 |
| Duncan D A | Tue-14:00-0-ORGS |
| Dung N V | Thu-11:40-0-GRAP |
| Duò L | Tue-11:00-0-ORGS1, Tue-14:00-1-OXID |
| Düll F | Tue-16:20-0-CATL |
| Dvorák F | Thu-14:20-0-OXID |
| E | |
| Ebeling R | Wed-16:40-0-ORGS |
| Ebrahimi M | Wed-9:20-0-GRAP |
| Echavaren A | Tue-16:00-0-ORGS |
| Ecija D | Tue-11:20-0-ORGS1, Tue-17:20-0-PISC |
| El Kharbaci A | Thu-PS2-43 |
| Ellis G J | Wed-9:00-0-GRAP |
| El-Sayed A | Wed-16:40-0-SAMA |
| Eltsov K N | Wed-11:20-0-OXID |

| | |
|----------------------------|--|
| Engelund M | Tue-16:00-0-ORGS |
| Engvall K | Tue-PS1-24 |
| Erdélyi Z | Tue-14:00-0-BIMS, Thu-16:20-0-ENER, Wed-10:00-0-BIMS, Tue-PS1-15, Thu-PS2-10, Thu-PS2-48 |
| Erdőhelyi A | Thu-PS2-41 |
| Erhard J | Thu-PS2-04 |
| Erler P | Wed-11:20-0-ORGS |
| Esser N | Thu-16:20-0-SEMI |
| Estelle M | Thu-11:40-0-GRAP |
| Etzkorn M | Tue-10:40-0-ORGS1 |
| Evertsson J | Tue-16:20-0-ELCH, Tue-16:40-0-ELCH |
| F | |
| Fabris S | Thu-14:20-0-OXID |
| Fagot-Revurat Y | Tue-15:00-0-OXID, Wed-9:20-0-GRAP |
| Faisal F | Tue-14:40-0-ELCH |
| Fakhrabadi M | Tue-PS1-25 |
| Falta J | Thu-14:00-0-OXID |
| Fan Q | Wed-10:40-0-ORGS |
| Farkas A P | Mon-15:00-0-CATL, Tue-PS1-17, Tue-PS1-42, Tue-PS1-44 |
| Farkas B | Mon-17:00-0-ELI-ALPS |
| Farnesi Camellone M | Thu-14:20-0-OXID |
| Farstad M H | Tue-16:40-0-PISC |
| Fasel R | Tue-11:40-0-ORGS2, Tue-17:00-0-PISC |
| Fatayer S | Thu-9:20-0-MOLA |
| Felici R | Tue-16:20-0-ELCH |
| Feng B | Wed-16:20-0-BAND |
| Feng Z | Thu-PS2-26 |
| Feringa B L | Tue-PS1-18 |
| Ferrari V | Tue-PS1-30, Thu-14:40-0-OXID |
| Fertey P | Thu-14:40-0-ENER |
| Fester J | Tue-16:20-0-OXID |
| Fezouan N | Tue-PS1-14 |
| Figueroba A | Tue-9:40-0-ENER |
| Finazzi M | Tue-11:00-0-ORGS1 |
| Fischer P | Thu-9:40-0-LASE |
| Flavell W R | Thu-15:00-0-ENER |
| Flege J I | Thu-14:00-0-OXID |
| Fleig J | Wed-16:40-0-OXID |
| Floreano L | Tue-10:00-0-CORR, Tue-11:00-0-ORGS1, Thu-9:00-0-MOLA |
| Flores F | Thu-15:00-0-ORGS |
| Foelske-Schmitz A | Tue-15:00-0-ELCH |
| Fogde A | Tue-PS1-52 |
| Fogg J | Tue-16:00-0-ELCH |
| Fonin M | Wed-11:20-0-ORGS |
| Forrest T | Tue-PS1-20 |

| | |
|-------------------------------|---|
| Fortunato E | Wed-10:40-0-BAND |
| Foster A S | Wed-10:40-0-COMP |
| Foti G | Mon-14:00-0-ORGS |
| Fournée V | Thu-16:00-0-CATH |
| Förster S | Wed-16:20-0-SAMA, Thu-14:40-0-ORGS |
| Föttinger K | Thu-9:40-0-CATH |
| Franceschi G | Wed-16:40-0-OXID |
| Franchini C | Wed-16:40-0-OXID |
| Franke M | Wed-11:40-0-OXID |
| Franz D | Thu-11:40-0-CATH |
| Freund H-J | Tue-16:40-0-K-CATL, Tue-PS1-39, Thu-11:20-0-OXID, Thu-PS2-38 |
| Fuchigami K | Thu-PS2-28 |
| Fujii S | Tue-10:40-0-ORGS2, Tue-11:20-0-ORGS2, Thu-PS2-34 |
| Fujii J | Wed-16:00-0-BAND |
| Fujimoto Y | Thu-PS2-12, Thu-PS2-13 |
| Fukidome H | Thu-9:20-0-CATH |
| Fukuda T | Tue-14:20-0-BIMS |
| Fukutani K | Wed-9:00-0-COMP |
| Füle M | Mon-17:00-0-ELI-ALPS |
| Fülöp L | Mon-17:00-0-ELI-ALPS |
| G | |
| Gajdics B | Tue-14:00-0-BIMS, Wed-10:00-0-BIMS, Thu-PS2-10 |
| Gajic R | Thu-15:20-0-ORGS |
| Gál T | Tue-PS1-27 |
| Galbács G | Tue-9:20-0-NAEX |
| Galeotti G | Wed-9:20-0-GRAP |
| Gallego J M | Tue-11:20-0-ORGS1 |
| Galloway E | Tue-9:40-0-CORR |
| Ganduglia-Pirovano M V | Tue-16:00-0-CATL, Tue-PS1-30, Thu-14:40-0-OXID |
| García López V | Mon-15:00-0-SAMA |
| García-Hernández M | Wed-9:00-0-GRAP |
| Garcia-Lekue A | Tue-16:00-0-ORGS |
| Garnier L | Tue-9:20-0-MAGN |
| Garreau Y | Tue-14:40-0-EG2D |
| Garzon-Roman A | Thu-PS2-21 |
| Gasperi G | Thu-14:00-0-OXID |
| Gaudry E | Thu-16:00-0-CATH |
| Gauquelin N | Thu-14:00-0-SEMI |
| Gellmann A J | Wed-9:00-0-BIMS, Wed-11:00-0-ORGS |
| Gelsomini C | Wed-16:20-0-ORGS |
| Genser J | Thu-15:20-0-ORGS |
| Genty E | Tue-11:20-0-EG2D, Tue-17:20-0-CATL, Tue-PS1-08, Thu-PS2-29 |
| Gerhold S | Wed-16:40-0-OXID |

| | | | |
|-------------------------|--|--------------------------------|---|
| Gerstmann U | Tue-14:00-0-ORGS | Hamada I | Tue-17:00-0-ORGS, Tue-PS1-26 |
| Getzlaff M | Tue-14:40-0-BIMS | Hamamoto Y | Tue-17:00-0-ORGS, Tue-PS1-26 |
| Giangrisostomi E | Wed-9:20-0-ORGS | Hammer B | Thu-9:00-0-CATH, Thu-11:20-0-ORGS, Thu-15:20-0-OXID |
| Giesen C | Thu-10:00-0-GRAP | Hammer R | Thu-14:40-0-ORGS |
| Giglia A | Wed-16:20-0-ORGS | Han S W | Tue-17:00-0-OXID, Thu-PS2-39 |
| Gillis N | Tue-11:20-0-EG2D, Tue-17:20-0-CATL | Hansson T | Tue-PS1-24 |
| Girard Y | Tue-17:20-0-ORGS, Wed-16:00-0-GRAP | Hao X | Wed-16:40-0-OXID |
| Ghadami M | Tue-PS1-24 | Hardacre C | Tue-16:20-0-ORGS |
| Glatzel T | Mon-14:20-0-ORGS | Harlow G S | Tue-16:20-0-ELCH, Tue-16:40-0-ELCH |
| Gleeson M | Thu-9:40-0-MOLA | Harsh R | Tue-17:20-0-ORGS |
| Gloter A | Thu-PS2-19 | Hasegawa Y | Wed-16:00-0-BAND |
| Godlewski S | Mon-14:20-0-ORGS, Tue-16:00-0-ORGS | Hasegawa S | Wed-16:00-0-BAND |
| Goikolea E | Tue-11:20-0-ELCH | Hayashi H | Tue-17:00-0-PISC |
| Goldoni A | Tue-11:00-0-ORGS1 | Hejral U | Tue-16:40-0-ELCH, Thu-11:40-0-CATH, Thu-14:20-0-CATH |
| Golek F | Wed-9:00-0-ORGS | Held G | Thu-14:00-0-ORGS |
| Goniakowski J | Tue-11:20-0-OXID | Henderson Z | Tue-16:20-0-ORGS, Thu-PS2-33 |
| Gopakumar T G | Thu-10:00-0-MOLA | Hermansson K | Thu-10:40-1-OXID |
| Gopinath C S | Thu-11:00-0-CATH | Hernández-de la Luz A D | Thu-PS2-21 |
| Gottfried J M | Tue-11:40-0-ORGS1, Tue-PS1-09, Wed-10:40-0-ORGS | Heuken M | Thu-10:00-0-GRAP |
| Görling A | Thu-PS2-04 | Hikasa M | Wed-11:40-0-BAND |
| Göthelied M | Tue-PS1-24 | Hirayama T | Thu-PS2-46 |
| Grabau M | Thu-PS2-04 | Hirjibehedin C F | Mon-15:20-0-SAMA |
| Grazioli C | Wed-9:20-0-ORGS | Hitzel F | Tue-PS1-02 |
| Gregoratti L | Tue-9:40-1-NAEX | Hoffmann G | Tue-9:00-0-NAEX |
| Grill L | Mon-15:00-0-SAMA | Hofhuis K | Thu-PS2-15 |
| Gronborg S S | Thu-9:00-0-CATH | Hollerer M | Tue-PS1-12 |
| Groot I M N | Mon-15:20-0-NAEX | Hogan C | Thu-16:20-0-SEMI |
| Gross L | Mon-14:40-0-SAMA | Holst B | Tue-11:40-0-OXID |
| Grönbeck H | Thu-10:40-0-CATH | Honkimäki V | Tue-PS1-45 |
| Grumelli D | Tue-10:40-0-ORGS1 | Horakova K | Tue-10:00-0-CORR |
| Grunder Y | Tue-16:00-0-ELCH | Hornekær L | Tue-9:40-0-ORGS, Tue-16:40-0-ORGS, Tue-PS1-05, Wed-10:40-0-GRAP, Wed-11:00-0-GRAP, Wed-16:20-0-GRAP |
| Gubó R | Tue-PS1-10, Tue-PS1-44 | Horváth A | Thu-PS2-25 |
| Guitián E | Mon-14:40-0-SAMA, Tue-16:00-0-ORGS | Horváth Z E | Tue-15:00-1-EG2D, Thu-PS2-25 |
| Gunnella R | Thu-PS2-17 | Hoshi N | Tue-PS1-28 |
| Gurban S | Thu-14:40-0-SAMA | Hosokai T | Thu-PS2-35 |
| Gurdeljević M | Tue-PS1-50 | Hózer Z | Tue-PS1-23 |
| Gusak A M | Thu-PS2-10 | Hötger D | Tue-10:40-0-ORGS1 |
| Gustafson J | Thu-10:40-0-CATH, Thu-11:20-0-CATH, Thu-11:40-0-CATH, Thu-14:20-0-CATH, Thu-14:40-0-CATH, Thu-15:20-0-OXID | Hsia Y-Y | Thu-PS2-07 |
| Gutzler R | Tue-10:40-0-ORGS1 | Hsu Y-J | Thu-PS2-07 |
| Guzsvány V | Tue-PS1-50, Thu-PS2-36 | Hu Z | Thu-16:20-0-CATL |
| H | | | |
| Hagiwara Y | Thu-PS2-44 | Huang Y-C | Tue-PS1-47 |
| Hagman B | Thu-10:40-0-CATH | Hulva J | Tue-16:00-0-OXID, Thu-11:40-0-OXID |
| Hakl J | Tue-9:40-0-BIMS | Humbolt V | Tue-17:20-0-OXID, Thu-9:00-0-MOLA |
| Halasi G | Tue-9:20-0-NAEX, Tue-PS1-11 | Hurdax P | Tue-PS1-12 |

| | |
|------------------------|---|
| Hussain H | Tue-9:00-I-CORR |
| Huth P | Wed-16:20-O-SAMA |
| Hutter H | Wed-16:40-O-OXID |
| Hwang C | Tue-15:00-I-EG2D |
| I | |
| Ichinokura S | Wed-16:00-O-BAND |
| Ideta S | Wed-11:40-O-BAND |
| Ihalainen P | Tue-PS1-52 |
| Imori T | Wed-16:20-O-BAND |
| Ikenaga E | Thu-PS2-08 |
| Inagaki K | Tue-17:00-O-ORGS, Tue-PS1-26 |
| Isshiki Y | Tue-10:40-O-ORGS2, Tue-PS1-13 |
| Ito S | Wed-16:20-O-BAND |
| Ivars-Barcelo F | Thu-11:20-O-OXID |
| Iwaoka M | Wed-16:00-O-BAND |
| Izak I | Thu-PS2-20 |
| J | |
| Jacobs L | Tue-11:20-O-EG2D, Tue-17:20-O-CATL, Tue-PS1-08 |
| Jacques V | Thu-14:40-O-ENER |
| Jain R | Thu-11:00-O-CATH |
| Jakub Z | Thu-11:40-O-OXID |
| Janas A | Thu-14:00-O-SEMI |
| Jankowski M | Tue-14:20-O-EG2D, Thu-PS2-15 |
| Jannane T | Tue-PS1-14 |
| Jany B R | Thu-11:20-O-SEMI, Thu-14:00-O-SEMI |
| Jelinek P | Mon-14:00-O-ORGS, Tue-10:40-I-NAEX, Tue-11:00-O-ORGS2 |
| Jemli K | Thu-14:40-O-ENER |
| Jensen P A | Tue-9:40-O-ORGS |
| Jeong J H | Tue-17:00-O-OXID, Thu-PS2-39 |
| Jethwa S J | Thu-11:20-O-ORGS |
| Jilili J | Tue-PS1-16 |
| Jiricek P | Thu-PS2-20 |
| Joachim C | Tue-16:00-O-ORGS |
| Johann C | Thu-11:40-O-GRAP |
| Johánek V | Thu-14:20-O-OXID |
| Johansson L S O | Tue-PS1-37 |
| Jorgensen J H | Tue-16:40-O-ORGS, Tue-PS1-05, Wed-10:40-O-GRAP, Wed-11:00-O-GRAP |
| Jorgensen M S | Thu-15:20-O-OXID |
| Joucken F | Tue-17:20-O-ORGS, Wed-16:00-O-GRAP |
| Jöhr R | Mon-14:20-O-ORGS |
| Juhász K L | Tue-9:20-O-NAEX |
| Juhász L | Tue-PS1-15, Thu-16:20-O-ENER |
| Jung T A | Thu-9:20-O-MOLA |

| | |
|---------------------|--|
| Jupille J | Tue-11:20-O-OXID |
| Jurczyszyn L | Mon-14:40-O-ORGS |
| K | |
| Kahaly M U | Tue-PS1-16 |
| Kahaly S | Mon-17:00-O-ELI-ALPS |
| Kaku M | Thu-PS2-28 |
| Kalas B | Tue-PS1-23 |
| Kalita G | Wed-11:20-K-GRAP |
| Kálomista I | Tue-9:20-O-NAEX |
| Kamarás K | Tue-PS1-07 |
| Kaminski D | Tue-14:20-O-EG2D |
| Kanematsu H | Tue-15:20-O-ORGS |
| Kang Ha | Thu-11:00-O-SEMI |
| Kang He | Thu-11:00-O-SEMI |
| Károly T | Tue-PS1-43 |
| Karthäuser S | Wed-16:40-O-ORGS |
| Kasai H | Tue-PS1-01, Wed-9:00-O-COMP, Thu-15:20-O-ENER, Thu-16:00-O-ORGS |
| Katto M | Thu-PS2-28 |
| Kawaguchi N | Tue-17:00-O-ORGS |
| Kawai H | Tue-16:00-O-ORGS |
| Kawai M | Mon-14:00-O-BAND |
| Ke C-R | Thu-15:00-O-ENER |
| Kébaili N | Thu-PS2-45 |
| Kera S | Wed-11:40-O-BAND |
| Kern K | Tue-10:40-O-ORGS1 |
| Kettner M | Thu-9:40-O-LASE |
| Khalakhan I | Wed-11:40-O-ORGS |
| Kharche N | Wed-9:20-O-GRAP |
| Khlobystov A | Tue-PS1-07 |
| Kibis L | Thu-16:00-O-CATH |
| Kierren B | Tue-15:00-O-OXID |
| Kiguchi M | Tue-10:40-O-ORGS2, Tue-11:20-O-ORGS2, Tue-PS1-13, Thu-PS2-34 |
| Kilic V | Thu-11:40-O-CATH |
| Kim I H | Tue-17:00-O-OXID, Thu-PS2-39 |
| Kim H J | Tue-17:00-O-OXID, Thu-PS2-39 |
| Kim Y D | Tue-17:00-O-OXID |
| Kim Y | Thu-16:00-O-ENER |
| King M | Tue-9:40-O-CORR |
| Kishida I | Tue-14:20-O-BIMS |
| Kishida R | Thu-16:00-O-ORGS |
| Kiss J | Mon-15:00-O-CATL, Tue-PS1-04, Tue-PS1-11, Tue-PS1-17, Tue-PS1-42, Tue-PS1-44, Thu-PS2-32, Thu-PS2-41 |
| Kiss L F | Thu-PS2-25 |
| Kita K | Thu-PS2-12, Thu-PS2-13, Thu-PS2-46 |
| Kitazawa M | Wed-11:20-K-GRAP |

| | |
|-------------------------|---|
| Kizaki H | Tue-10:00-0-MAGN |
| Kjaervik M | Mon-14:40-0-NAEX |
| Klappenberger F | Tue-14:00-0-ORGS |
| Kleimeier N F | Wed-11:20-0-BAND |
| Klein A | Wed-10:40-0-BAND |
| Klein B P | Tue-11:40-0-ORGS1, Tue-PS1-09 |
| Klötzer B | Tue-16:00-0-OXID |
| Kobayashi K | Mon-14:20-0-BAND, Tue-PS1-48, Wed-16:20-0-BAND |
| Kobayashi T | Tue-15:20-0-ORGS |
| Kocan P | Mon-14:40-0-ORGS, Tue-14:20-0-ORGS |
| Koch R | Tue-14:00-0-ORGS |
| Koga M | Wed-16:00-0-BAND |
| Koganezawa T | Thu-PS2-35 |
| Koitaya T | Thu-9:20-0-CATH |
| Koller G | Tue-PS1-12 |
| Kolmer M | Tue-16:00-0-ORGS |
| Kolny-Olesiak J | Thu-PS2-18 |
| Kolsbjerg E L | Thu-11:20-0-ORGS |
| Koltsov A | Tue-11:20-0-OXID |
| Komori F | Mon-14:20-0-BAND, Tue-9:00-0-MAGN, Tue-PS1-48, Wed-16:20-0-BAND |
| Komoto Y | Tue-10:40-0-ORGS2, Tue-PS1-13, Thu-PS2-34 |
| Kondo T | Tue-15:20-0-ELCH |
| Kondratyuk P | Wed-9:00-0-BIMS |
| Kónya Z | Mon-15:00-0-CATL, Tue-9:20-0-NAEX, Tue-15:20-0-OXID, Tue-PS1-04, Tue-PS1-11, Tue-PS1-17, Tue-PS1-42, Tue-PS1-44, Tue-PS1-50, Thu-PS2-32, Thu-PS2-36, Thu-PS2-41 |
| Koós A A | Tue-15:00-0-EG2D |
| Koshmak K | Wed-16:20-0-ORGS |
| Kosinova A | Tue-PS1-15 |
| Kotarba A | Tue-PS1-24 |
| Stig Koust S | Thu-10:00-0-OXID |
| Kovács I | Tue-17:40-0-MOLA, Tue-PS1-17, Tue-PS1-42 |
| Kovács A | Thu-10:00-0-GRAP |
| Köck E-M | Tue-16:00-0-OXID |
| Kötz R | Tue-15:00-0-ELCH |
| Krasteva A | Wed-9:20-0-COMP |
| Kratochvilova I | Tue-10:00-0-CORR |
| Kratzer P | Tue-10:00-0-ORGS, Tue-PS1-40 |
| Kratzer M | Thu-11:20-0-SEMI, Thu-15:20-0-ORGS |
| Krause P P | Tue-17:40-0-OXID |
| Kraushofer F | Thu-11:40-0-OXID |
| Krejci O | Mon-14:00-0-ORGS |
| Kremer G | Tue-15:00-0-OXID |
| Krick Calderon S | Thu-PS2-04 |
| Kroes G J | Wed-16:00-0-SAMA |

| | |
|----------------------|---|
| Krok F | Thu-10:40-0-ORGS, Thu-11:20-0-SEMI, Thu-14:00-0-SEMI |
| Kromka A | Thu-PS2-20 |
| Krooswyk J D | Mon-14:00-0-CATL |
| Krug C K | Tue-11:40-0-ORGS1, Tue-PS1-09 |
| Kruppe C M | Mon-14:00-0-CATL |
| Kruse P | Thu-PS2-30 |
| Krzykawska A | Tue-17:20-0-MOLA |
| Krzyzewski F | Wed-9:20-0-COMP |
| Kubicek M | Wed-16:40-0-OXID |
| Kubsky S | Thu-PS2-19 |
| Kuhlenbeck H | Thu-PS2-38 |
| Kuk Y | Wed-14:00-Plen-3 |
| Kukovecz Á | Tue-9:20-0-NAEX, Tue-PS1-04, Thu-PS2-36 |
| Kumar M | Thu-14:20-0-SEMI |
| Kumar S | Tue-PS1-18 |
| Kumeda T | Tue-PS1-28 |
| Kuroda K | Mon-14:20-0-BAND, Tue-PS1-48 |
| Kühnle A | Mon-15:00-0-ORGS |
| Kwieciński W | Thu-PS2-15 |
| Kyhl L | Wed-10:40-0-GRAP, Wed-11:00-0-GRAP |
| L | |
| Lackner P | Tue-16:00-0-OXID |
| Lacovig P | Tue-11:00-0-EG2D |
| Lafosse A | Tue-PS1-35 |
| Lagarde P | Thu-11:40-0-ORGS |
| Lagoute J | Tue-17:20-0-ORGS, Wed-16:00-0-GRAP |
| Lai Y-L | Thu-PS2-07 |
| Laker Z P L | Tue-14:00-0-EG2D, Tue-PS1-19 |
| Lambeets S V | Tue-11:20-0-EG2D, Tue-17:20-0-CATL, Tue-PS1-08, Thu-PS2-29 |
| Lambin Ph | Tue-15:00-0-EG2D |
| Lamirand A D | Tue-PS1-20 |
| Lancok J | Tue-10:00-0-CORR |
| Lanzilotto V | Wed-9:20-0-ORGS |
| Larciprete R | Tue-11:00-0-EG2D |
| László B | Thu-PS2-41 |
| Lauritsen J V | Tue-16:20-0-OXID, Thu-9:00-0-CATH, Thu-10:00-0-OXID |
| Lawrence J | Tue-PS1-40 |
| Lazzari R | Tue-11:20-0-OXID |
| Le T H L | Tue-11:20-0-OXID |
| Le Bolloch D | Thu-14:40-0-ENER |
| Le Breton J-C | Wed-9:40-0-OXID |
| Le Fèvre P | Tue-15:00-0-OXID |
| Lédée F | Thu-14:40-0-ENER |
| Ledieu J | Thu-16:00-0-CATH |
| Lee M | Thu-14:40-0-ENER |

| | |
|------------------------|---|
| Lee H | Thu-PS2-37 |
| Leichtweiss T | Tue-17:40-0-OXID |
| Lenchuk O | Tue-PS1-21 |
| Leong J X | Thu-15:20-0-ENER |
| Lépine B | Wed-9:40-0-OXID |
| Lepine F | Mon-17:00-0-ELI-ALPS |
| Lesiak B | Wed-9:40-0-GRAP |
| Leuenberger D | Tue-14:40-0-OXID |
| Leung L | Thu-16:20-0-CATL |
| Lewis D J | Thu-15:00-0-ENER |
| Li X | Tue-PS1-22 |
| Liao C-C | Tue-9:00-0-NAEX |
| Liba A | Tue-PS1-14 |
| Libuda J | Tue-9:40-0-ENER, Tue-14:40-0-ELCH |
| Lim T | Thu-16:20-0-CATL |
| Limot L | Tue-9:20-0-MAGN |
| Lin J L | Thu-PS2-06 |
| Linderoth T R | Thu-11:20-0-ORGS |
| Lindsay R | Tue-9:00-0-CORR, Thu-15:20-0-OXID |
| Linepé W | Tue-16:20-0-ELCH |
| Linpé W | Tue-16:40-0-ELCH |
| Lion J | Thu-PS2-45 |
| Lipton-Duffin J | Wed-9:20-0-GRAP |
| Lirst R K | Thu-PS2-47 |
| Lisi S | Tue-15:00-0-OXID, Thu-11:40-0-GRAP |
| Liu R-Y | Wed-16:20-0-BAND, Thu-9:20-0-CATH |
| Liu N | Thu-9:40-0-MOLA |
| Lizzit S | Tue-11:00-0-EG2D |
| Llois A M | Tue-PS1-30, Thu-14:40-0-OXID |
| Lobo-Checa J | Wed-16:40-0-SAMA |
| Lohner T | Tue-PS1-23 |
| López J C | Thu-PS2-40 |
| López J A L | Thu-PS2-40 |
| López M F | Wed-9:00-0-GRAP |
| Lopez-Elvira E | Wed-9:00-0-GRAP |
| Lorente N | Tue-9:20-0-MAGN |
| Lu S-M | Tue-9:00-0-NAEX |
| Lu Y-C | Thu-PS2-14 |
| LU C-Y | Thu-PS2-14 |
| Lu H | Tue-17:00-0-MOLA |
| Lucas C | Tue-16:00-0-ELCH |
| Luches P | Tue-PS1-38, Thu-14:00-0-OXID |
| Luna López J A | Thu-PS2-21 |
| Lundgren E | Tue-16:20-0-ELCH, Tue-16:40-0-ELCH, Thu-10:40-0-CATH, Thu-11:20-0-CATH, Thu-11:40-0-CATH, Thu-14:20-0-CATH, Thu-14:40-0-CATH, Thu-15:20-0-OXID |
| Luo M-F | Tue-PS1-47, Thu-PS2-07 |

| | |
|-------------------------|---|
| Lustemberg P | Tue-16:00-0-CATL |
| Lüder J | Wed-9:20-0-ORGS |
| Lüftner D | Tue-PS1-12, Thu-15:20-0-ORGS |
| Lykhach Y | Tue-9:40-0-ENER |
| Lytken O | Wed-11:40-0-OXID |
| M | |
| Ma T | Wed-11:00-0-OXID |
| Määttänen A | Tue-PS1-52 |
| Maccherozzi F | Tue-PS1-20 |
| Madarász D | Tue-PS1-50 |
| Madas S | Tue-PS1-16 |
| Madry B | Tue-14:00-0-ELCH |
| Magda G Z | Tue-15:00-0-EG2D |
| Magnussen O M | Tue-PS1-45 |
| Maier F | Wed-9:40-0-NAEX |
| Maier M | Wed-11:20-0-ORGS |
| Major B | Mon-17:00-0-ELI-ALPS |
| Majrik K | Tue-10:00-0-ENER |
| Majzik Z | Mon-14:40-0-SAMA |
| Malik I H | Thu-10:00-0-MOLA |
| Malterre D | Tue-15:00-0-OXID |
| Mancini A | Thu-PS2-03 |
| Mándi G | Wed-11:20-0-COMP, Thu-PS2-24 |
| Manoua M | Tue-PS1-14 |
| Mao Z | Thu-14:20-0-ORGS |
| Marbach H | Thu-16:00-0-ELAM, Thu-PS2-32 |
| Marchetti L | Thu-PS2-43 |
| Mark A | Thu-9:40-0-LASE |
| Márk G I | Tue-15:00-0-EG2D |
| Marks K M | Tue-PS1-24 |
| Maroun F | Tue-PS1-45 |
| Marsden A J | Tue-PS1-19 |
| Martin N M | Thu-11:40-0-CATH |
| Martin F | Wed-16:00-0-SAMA |
| Martinez J I | Wed-9:00-0-GRAP, Thu-15:00-0-ORGS |
| Martín-Gago J A | Wed-9:00-0-GRAP |
| Martín-Jiménez A | Tue-17:20-0-PISC |
| Martins R | Wed-10:40-0-BAND |
| Masuda T | Tue-15:20-0-ORGS |
| Mataigne J M | Tue-11:20-0-OXID |
| Matkovic A | Thu-15:20-0-ORGS |
| Matolin V | Tue-9:00-0-ENER, Tue-9:40-0-ENER, Wed-11:40-0-ORGS |
| Matolinová I | Wed-11:40-0-ORGS |
| Matsuda I | Wed-16:20-0-BAND, Thu-9:20-0-CATH |
| Matvija P | Mon-14:40-0-ORGS, Tue-14:20-0-ORGS |
| Mazur P | Wed-9:00-0-ORGS |
| Meinel K | Wed-10:00-0-OXID, Thu-14:40-0-ORGS |

| | |
|---------------------------|--|
| Mendez J | Wed-9:00-0-GRAP |
| Menyhárd M | Tue-PS1-23, Thu-14:40-0-SAMA |
| Meriggio E | Tue-17:20-0-OXID |
| Merte R L | Thu-10:40-0-CATH, Thu-11:40-0-CATH, Thu-15:20-0-OXID |
| Messaykeh M | Tue-11:20-0-OXID |
| Mészáros G | Mon-17:00-0-ELI-ALPS |
| Méthivier C | Tue-17:20-0-OXID, Thu-9:00-0-MOLA |
| Mette G | Tue-14:40-0-OXID |
| Meunier V | Wed-9:20-0-GRAP |
| Meyer B | Thu-9:20-0-OXID |
| Meyer Ernst | Mon-14:20-0-ORGS, Tue-PS1-33 |
| Meyer Erik | Mon-14:40-0-CATL |
| Meyer G | Mon-14:40-0-SAMA |
| Mihály J | Tue-10:00-0-ENER |
| Miller J B | Wed-9:00-I-BIMS |
| Minkowski M | Wed-9:40-0-COMP |
| Mirabella F | Thu-11:20-0-OXID |
| Miranda R | Tue-10:40-0-EG2D, Tue-17:20-0-PISC, Tue-15:00-0-ORGS, Tue-PS1-46, Wed-11:00-0-BAND, Thu-11:20-0-GRAP |
| Mirolo M | Tue-14:20-0-EG2D, Thu-PS2-15 |
| Miserque F | Thu-PS2-43 |
| Mishra S | Tue-11:40-0-ORGS2, Tue-17:00-0-PISC, Tue-PS1-16 |
| Misják F | Tue-14:00-0-BIMS, Wed-10:00-0-BIMS |
| Mitlin S | Tue-16:00-I-PISC |
| Mittal A K | Thu-14:20-0-SEMI |
| Miwa J A | Thu-9:00-I-SEMI |
| Miyamachi T | Tue-9:00-0-MAGN |
| Miyazawa Y | Thu-PS2-05 |
| Mizuno Y | Wed-11:40-0-BAND, Thu-PS2-35 |
| Mohai M | Tue-PS1-04, Thu-PS2-09, Thu-PS2-22 |
| Mohamed F | Thu-PS2-26 |
| Mohebbi E | Tue-PS1-25 |
| Mohrhusen L | Thu-PS2-18 |
| Mohtasebi A | Thu-PS2-30 |
| Molinari E | Fri-10:10-Plen-6 |
| Mollenhauer D | Tue-PS1-21 |
| Molnár G | Thu-PS2-25 |
| Mondal S | Mon-17:00-0-ELI-ALPS |
| Montes E | Wed-10:00-0-COMP |
| Morbec J M | Tue-10:00-0-ORGS, Tue-PS1-40 |
| Morchutt C | Tue-10:40-0-ORGS1 |
| Moraeu L | Tue-15:00-0-OXID |
| Moreira R | Mon-14:40-0-CATL |
| Mori T | Thu-PS2-35 |
| Morikawa Yoshitada | Tue-10:00-0-MAGN, Tue-PS1-26 |

| | |
|--------------------------|---|
| Morikawa Yoritada | Tue-17:00-0-ORGS |
| Moud P H | Tue-PS1-24 |
| Mouras R | Thu-9:40-0-MOLA |
| Mousavi S F | Thu-9:20-0-MOLA |
| Mukai K | Thu-9:20-0-CATH |
| Munkhtsog M | Tue-15:20-0-ORGS |
| Munoz-Ochando I | Wed-9:00-0-GRAP |
| Muntwiler M | Tue-11:40-0-ORGS2 |
| Murata M | Wed-11:40-0-BAND |
| Murgida G E | Tue-PS1-30, Thu-14:40-0-OXID |
| Muttaqien F | Tue-17:00-0-ORGS, Tue-PS1-26 |
| Muzas A S | Wed-16:00-0-SAMA |
| Muzychenko D | Tue-PS1-32 |
| Müllegger S | Tue-14:00-0-ORGS |
| Müllen K | Tue-11:40-0-ORGS2 |
| Myslivecek J | Thu-14:20-0-OXID |
| Mysyk R | Tue-11:20-0-ELCH |
| N | |
| Nagy A | Thu-PS2-25 |
| Nagy G | Tue-PS1-27 |
| Nagy I P | Tue-PS1-43 |
| Nagy L | Tue-PS1-50, Thu-PS2-36 |
| Nair M N | Thu-14:40-0-ENER, Thu-PS2-19 |
| Nakamura M | Tue-PS1-28 |
| Nakamura J | Tue-15:20-0-ELCH |
| Nakanishi H | Tue-PS1-01 |
| Nakashima S | Tue-9:00-0-MAGN |
| Nakayama Y | Wed-11:40-0-BAND, Thu-PS2-35 |
| Nakayama K | Wed-9:00-0-COMP |
| Nakazawa T | Mon-14:00-0-BAND |
| Namatame H | Wed-16:20-0-BAND |
| Nannarone S | Wed-16:20-0-ORGS, Thu-PS2-17 |
| Nara J | Tue-PS1-29 |
| Narayanan-nair M | Tue-14:40-0-EG2D |
| Nardi M V | Wed-16:20-0-ORGS |
| Narita A | Tue-11:40-0-ORGS2 |
| Naschitzki M | Thu-PS2-38 |
| Navarro J J | Tue-10:40-0-EG2D, Tue-15:00-0-ORGS, Tue-PS1-46, Thu-11:20-0-GRAP |
| Neff J L | Mon-15:00-0-ORGS |
| Neiss C | Thu-PS2-04 |
| Neitzel A | Tue-9:40-0-ENER |
| Nemcsics Á | Thu-PS2-48 |
| Nemes-Incze P | Tue-15:00-I-EG2D |
| Németh A | Thu-14:40-0-SAMA |
| Németh G | Tue-PS1-07 |
| Netzer F P | Wed-16:00-K-OXID |
| Neyman K M | Tue-9:40-0-ENER, Tue-15:00-I-BIMS |

| | |
|---------------------------|---|
| Nicklin R E | Thu-14:00-0-ORGS |
| Nieckarz D | Tue-14:40-0-ORGS |
| Niedermaier I | Wed-9:40-K-NAEX |
| Nijs T | Thu-9:20-0-MOLA |
| Nikiel M | Thu-14:00-0-SEMI |
| Nobili F | Thu-PS2-17 |
| Noguera C | Tue-11:20-0-OXID |
| Nomura T | Thu-PS2-46 |
| Nonaka T | Tue-PS1-49 |
| Norris A | Wed-11:00-0-BAND, Thu-11:20-0-GRAP |
| Novotny T | Tue-PS1-23 |
| Nowakowska S | Thu-9:20-0-MOLA |
| Nowicki M | Tue-14:00-I-ELCH |
| Nürnberg D | Thu-9:40-0-LASE |
| O | |
| O'Dwyer K | Thu-9:40-0-MOLA |
| Brien C O | Tue-16:40-K-CATL |
| Oelsner A | Thu-PS2-01 |
| Ogawa S | Wed-16:40-0-BAND, Thu-PS2-08 |
| Ohno T | Tue-PS1-29 |
| Okada M | Tue-15:20-0-ORGS |
| Okura R | Thu-PS2-12, Thu-PS2-13 |
| Olbrich R | Tue-PS1-30, Thu-14:40-0-OXID |
| Olszowski P | Mon-14:20-0-ORGS |
| Ondracek M | Tue-11:00-0-ORGS2 |
| Oreshkin A | Tue-PS1-32 |
| Oreshkin S | Tue-PS1-32 |
| Ormaza M | Tue-9:20-0-MAGN |
| Ortega J | Wed-16:40-0-SAMA, Thu-15:00-0-ORGS |
| De La Morena R M O | Tue-17:00-0-MOLA |
| Oshima H | Tue-PS1-26 |
| Osmic M | Thu-PS2-18 |
| Ossowski J | Tue-17:20-0-MOLA |
| Ostadal I | Mon-14:40-0-ORGS, Tue-14:20-0-ORGS |
| Osterwalder J | Tue-14:40-0-OXID |
| Osvay K | Mon-11:30-I-ELI-ALPS, Mon-17:00-0-ELI-ALPS |
| Oszetzky D | Thu-PS2-25 |
| Oszkó A | Thu-PS2-41 |
| Otero R | Tue-11:20-0-ORGS1, Tue-17:20-0-PISC |
| Otero-Irurueta G | Wed-9:00-0-GRAP |
| Otsuki K | Wed-16:40-0-BAND, Thu-PS2-08, Tue-PS1-33 |
| Óvári L | Mon-15:00-0-CATL, Tue-PS1-10, Tue-PS1-44, Thu-10:00-0-LASE |
| Over H | Tue-16:00-0-CATL, Tue-17:40-0-OXID |
| Ovsyannikov R | Wed-9:20-0-ORGS |
| Owczarek S | Tue-17:20-0-CATL |
| Öström H | Tue-PS1-24 |

| | |
|-------------------------|--|
| Öznülüer T | Tue-11:40-0-ELCH |
| Öztürk ZZ | Tue-16:40-0-OXID, Wed-16:00-0-ORGS |
| P | |
| Paier J | Wed-11:40-0-COMP, Tue-PS1-22, Thu-PS2-11 |
| Palacio I | Wed-9:00-0-GRAP, Thu-PS2-19 |
| Palotás K | Wed-11:20-0-COMP, Thu-PS2-24 |
| Pandey S N | Thu-14:20-0-SEMI |
| Pang C L | Tue-PS1-10 |
| Panhwer M | Tue-11:20-0-ELCH |
| Papageorgiou A C | Tue-14:00-0-ORGS |
| Papp C | Tue-16:20-0-CATL, Thu-PS2-04 |
| Parditka B | Tue-PS1-15, Thu-16:20-0-ENER |
| Park Y | Thu-11:00-0-SEMI |
| Park C H | Tue-17:00-0-OXID, Thu-PS2-39 |
| Parkinson G | Tue-16:00-0-OXID, Thu-11:40-0-OXID |
| Pasichny M | Thu-PS2-10 |
| Pasquali L | Wed-16:20-0-ORGS, Thu-PS2-17 |
| Passerini S | Thu-PS2-17 |
| Paszkievicz M | Tue-14:00-0-ORGS |
| Pászti Z | Tue-10:00-0-ENER, Tue-PS1-03, Thu-9:00-0-OXID |
| Patthey F | Tue-9:40-0-MAGN |
| Pavlicek N | Mon-14:40-0-SAMA |
| Pavlov A V | Tue-PS1-31 |
| Pavlova T V | Wed-11:20-0-OXID |
| Payne M | Wed-9:00-I-BIMS |
| Pécz B | Thu-10:00-0-GRAP |
| Pedio M | Wed-9:20-0-ORGS |
| Pekker Á | Tue-PS1-07 |
| Peltonen J | Tue-PS1-52 |
| Cresi J S P | Tue-PS1-38 |
| Pena D | Mon-14:40-0-SAMA, Tue-16:00-0-ORGS |
| Penner S | Tue-16:00-0-OXID |
| Penschke C | Wed-11:40-0-COMP, Thu-PS2-11 |
| Perepichka D F | Wed-9:20-0-GRAP |
| Peressi M | Thu-PS2-26 |
| Perez-Feró E | Tue-PS1-23 |
| Pérez D | Mon-14:40-0-SAMA, Tue-16:00-0-ORGS |
| Pérez E M | Tue-15:00-0-ORGS |
| Persson M | Mon-15:20-0-SAMA |
| Pető J | Tue-15:00-I-EG2D, Thu-PS2-25 |
| Petrik P | Tue-PS1-23 |
| Petrov V N | Tue-PS1-31 |
| Petukhov M | Tue-PS1-32, Thu-11:40-0-ORGS |
| Pfaff S | Thu-14:20-0-CATH |
| Pham V D | Wed-16:00-0-GRAP |
| Philippe D | Thu-11:40-0-GRAP |
| Piantek M | Mon-15:20-0-SAMA |

| | |
|----------------------------|------------------------------------|
| Piccolo L | Thu-16:00-0-CATH |
| Picone A | Tue-11:00-0-ORGS1 |
| Pieczrak B | Mon-14:40-0-ORGS |
| Pignedoli C A | Tue-17:00-0-PISC |
| Pinfold H | Tue-14:00-0-EG2D |
| Pinto V | Thu-PS2-03 |
| Piperno L | Thu-PS2-03 |
| Piquero-Zulaica I | Wed-16:40-0-SAMA |
| Piskorz W | Tue-PS1-24 |
| Pivetta M | Tue-9:40-0-MAGN |
| Plank K | Tue-PS1-04 |
| Plucienik A | Thu-PS2-38 |
| Pochet P | Tue-15:00-0-OXID |
| Polak M | Tue-17:40-0-BIMS |
| Polanyi J C | Thu-16:20-0-CATL |
| Popova H | Wed-9:20-0-COMP |
| Popova O | Thu-9:20-0-MOLA |
| Pradier C-M | Thu-9:00-0-MOLA |
| Prakash J | Thu-PS2-29 |
| Prince K C | Tue-9:40-0-ENER, Wed-11:40-0-ORGS |
| Puglia C | Wed-9:20-0-ORGS |
| Puschnig P | Tue-PS1-12, Thu-15:20-0-ORGS |
| Pussi K | Thu-15:20-0-OXID |
| Pusztai P | Tue-9:20-0-NAEX, Tue-PS1-50 |
| R | |
| Rabanal Jimenez M E | Thu-PS2-21 |
| Rabkin E | Tue-PS1-15 |
| Rácz A | Thu-14:40-0-SAMA |
| Radności G | Tue-14:00-0-BIMS, Wed-10:00-0-BIMS |
| Radovic M | Wed-10:40-0-OXID |
| Ragazzon D | Tue-16:40-0-PISC |
| Ramakrishnan S | Tue-PS1-34 |
| Ramapanicker I R | Thu-10:00-0-MOLA |
| Rameshan Christoph | Thu-9:40-I-CATH |
| Ramsey M G | Tue-PS1-12 |
| Daud W R W | Thu-15:20-0-ENER |
| Rance G | Tue-PS1-07 |
| Rangan S | Thu-15:00-0-ORGS |
| Rauls E | Tue-14:00-0-ORGS |
| Rault J | Tue-15:00-0-OXID |
| Raval R | Wed-14:50-Plen-4 |
| Rawle J | Thu-15:20-0-OXID |
| Reichling M | Tue-PS1-30, Thu-14:40-0-OXID |
| Reikowski F | Tue-PS1-45 |
| Repain V | Tue-17:20-0-ORGS, Wed-16:00-0-GRAP |
| Ressel B | Wed-9:20-0-ORGS |
| Resta A | Tue-14:40-0-EG2D |

| | |
|------------------------------|--|
| Rezek B | Thu-PS2-20 |
| Rezvani S J | Thu-PS2-17 |
| Rice D | Thu-9:40-0-MOLA |
| Rijnders G | Tue-14:20-0-EG2D |
| Risse T | Mon-14:40-0-CATL |
| Riva M | Wed-16:40-0-OXID |
| Rodriguez-Fernandez J | Tue-16:20-0-OXID, Thu-9:00-0-CATH |
| Rojo T | Tue-11:20-0-ELCH |
| Romanyuk O | Thu-PS2-20 |
| Rondino F | Thu-PS2-03 |
| Rosei F | Wed-9:20-0-GRAP |
| Rosenow P | Tue-11:40-0-ORGS1 |
| Rosmi M S | Wed-11:20-K-GRAP |
| Rosqvist E | Tue-PS1-52 |
| Rousseau B | Thu-PS2-43 |
| Rousset S | Tue-17:20-0-ORGS, Wed-16:00-0-GRAP |
| Rozbořil F | Mon-14:40-0-ORGS, Tue-14:20-0-ORGS |
| Rubinovich L | Tue-17:40-0-BIMS |
| Rudolf P | Tue-PS1-18, Wed-9:20-0-ORGS, Thu-14:00-0-GRAP |
| Ruffieux P | Tue-11:40-0-ORGS2, Tue-17:00-0-PISC |
| Ruggieri C | Thu-15:00-0-ORGS |
| Rullik R | Tue-16:20-0-ELCH |
| Rupprechter G | Thu-9:40-I-CATH |
| Rusponi S | Tue-9:40-0-MAGN |
| Rzysko W | Tue-14:40-0-ORGS |
| S | |
| Sabik A | Wed-9:00-0-ORGS |
| Sack C | Tue-16:00-0-CATL |
| Sadowski J T | Tue-PS1-05 |
| Sadowski J | Thu-15:00-I-SEMI |
| Sansone G | Mon-17:00-0-ELI-ALPS |
| Saeyes M | Tue-16:00-0-ORGS |
| Sáfrán G | Tue-PS1-27 |
| Sagi R | Thu-PS2-16 |
| Saha P | Thu-10:00-0-MOLA |
| Sajdi P | Tue-10:00-0-CORR |
| Sajó I | Tue-PS1-03, Thu-9:00-0-OXID |
| Sakamoto K | Wed-16:00-0-BAND |
| Sala L A | Tue-PS1-35 |
| Salavagione H J | Wed-9:00-0-GRAP |
| Salazar N | Thu-9:00-0-CATH |
| Salomon E | Wed-16:20-0-GRAP |
| Sambi M | Tue-PS1-25 |
| Sanchez-Portal D | Tue-16:00-0-ORGS |
| Sandell A | Tue-16:40-0-PISC |
| Santoni A | Thu-PS2-03 |
| Sápi A | Tue-9:20-0-NAEX, Tue-PS1-11 |

| | |
|------------------------|---|
| Sarfati A | Thu-PS2-45 |
| Sarfraz J | Tue-PS1-52 |
| Sasaki W | Thu-PS2-28 |
| Sassa Y | Wed-9:20-0-ORGS |
| Sauer M | Tue-15:00-0-ELCH |
| Sauerbrey M | Thu-14:00-0-OXID |
| Sawada H | Tue-17:00-0-ORGS |
| Schaaf P | Tue-PS1-15 |
| Schaefer A | Tue-16:40-0-PISC, Thu-10:40-0-CATH, Thu-15:20-0-OXID |
| Schauermann S | Tue-16:40-K-CATL, Tue-PS1-39 |
| Schay Z | Tue-17:40-0-MOLA, Tue-PS1-27 |
| Schieffer P | Wed-9:40-0-OXID |
| Schiller F | Wed-16:40-0-SAMA |
| Schindler K-M | Wed-16:20-0-SAMA |
| Schmid Michael | Tue-16:00-0-OXID, Wed-16:40-0-OXID |
| Schmid Martin | Tue-11:40-0-ORGS1, Tue-PS1-09 |
| Schmidt W G | Tue-14:00-0-ORGS |
| Schoenhense G | Thu-PS2-01 |
| Schöfberger W | Tue-14:00-0-ORGS |
| Schöniger M | Tue-11:40-0-ORGS1 |
| Schubert S | Mon-15:20-0-SAMA |
| Schumann F O | Wed-10:00-0-OXID |
| Schweke D | Thu-15:00-0-OXID |
| Sebók D | Tue-9:20-0-NAEX |
| Sedona F | Tue-PS1-25 |
| Seiler S | Thu-9:20-0-OXID |
| Selloni A | Thu-9:40-0-OXID |
| Sen I | Wed-9:00-I-BIMS |
| Seo H O | Tue-17:00-0-OXID, Thu-PS2-39 |
| Seriani N | Thu-PS2-26 |
| Serrate D | Mon-15:20-0-SAMA |
| Setvin M | Thu-9:20-0-OXID |
| Sevciková K | Wed-11:40-0-ORGS |
| Sezen H | Tue-9:40-I-NAEX |
| Shaikhutdinov S | Thu-11:20-0-OXID |
| Shenouda S S | Tue-PS1-15, Thu-16:20-0-ENER |
| Shevlyuga V M | Wed-11:20-0-OXID |
| Shi H | Thu-15:00-I-CATH |
| Shibata M | Thu-PS2-05 |
| Shibuya R | Tue-15:20-0-ELCH |
| Shigeta Y | Thu-PS2-44 |
| Shimoyama Y | Tue-15:20-0-ELCH |
| Shin Sunghwa | Tue-PS1-36 |
| Shin Shik | Tue-PS1-48 |
| Shiozawa Y | Thu-9:20-0-CATH |

| | |
|--------------------------|---|
| Shipilin M | Thu-10:40-0-CATH, Thu-11:40-0-CATH, Thu-14:20-0-CATH, Thu-15:20-0-OXID |
| Shukla N | Wed-11:00-0-ORGS |
| Sicot M | Tue-15:00-0-OXID |
| Silien C | Thu-9:40-0-MOLA |
| Simic-Milosevic V | Mon-14:40-0-NAEX, Thu-PS2-01 |
| Simonsen F D S | Tue-9:40-0-ORGS |
| Simpson G J | Mon-15:00-0-SAMA |
| Singer F | Wed-11:20-0-ORGS |
| Singha A | Tue-9:40-0-MAGN |
| Skakalova V | Thu-PS2-20 |
| Skála T | Tue-9:40-0-ENER, Wed-11:40-0-ORGS, Thu-14:20-0-OXID |
| Skov A W | Tue-9:40-0-ORGS, Tue-16:40-0-ORGS |
| Slynko V E | Tue-PS1-06 |
| Sobotík P | Mon-14:40-0-ORGS, Tue-14:20-0-ORGS |
| Solymosi F | Tue-PS1-17 |
| Somers M F | Wed-16:00-0-SAMA |
| Someya T | Wed-16:20-0-BAND, Thu-9:20-0-CATH |
| Somodi F | Tue-PS1-27 |
| Somorjai G A | Mon-9:30-Plen-1 |
| Sotgiu G | Thu-PS2-03 |
| Soubatch S | Tue-PS1-12 |
| Soulimane T | Thu-9:40-0-MOLA |
| Spadafora E J | Tue-PS1-39 |
| Spadaro M C | Tue-PS1-38 |
| Späth F | Tue-16:20-0-CATL |
| Speiser E | Thu-16:20-0-SEMI |
| Stara I | Tue-11:00-0-ORGS2 |
| Starfelt S | Tue-PS1-37 |
| Stary I | Tue-11:00-0-ORGS2 |
| Steinhauer J | Tue-16:20-0-CATL |
| Steinrück H-P | Wed-9:40-K-NAEX, Wed-11:40-0-OXID, Tue-16:20-0-CATL, Thu-PS2-04 |
| Stepanow S | Tue-10:40-0-ORGS1 |
| Sterrer M | Tue-PS1-12 |
| Stetsovych O | Tue-11:00-0-ORGS2 |
| Stettner J | Tue-PS1-45 |
| Stierle A | Thu-11:40-0-CATH |
| Stirling A | Tue-17:40-0-MOLA |
| Stolz S | Tue-11:40-0-ORGS2 |
| Stoot A | Tue-PS1-05 |
| Stumm C | Tue-14:40-0-ELCH |
| Stupar M | Wed-9:20-0-ORGS |
| Su W-B | Tue-9:00-0-NAEX |
| Such B | Mon-14:20-0-ORGS |
| Suchkova S | Thu-16:20-0-SEMI |
| Suchorski Y | Thu-9:40-I-CATH |

| | |
|-------------------------|---|
| Suemitsu M | Thu-9:20-0-CATH |
| Sulyok A | Tue-PS1-23, Tue-PS1-51, Thu-14:40-0-SAMA, Thu-PS2-02 |
| Sun Q | Thu-16:20-0-ORGS |
| Sun Z | Tue-16:20-0-OXID |
| Surnev S | Wed-9:00-I-OXID, Wed-16:00-K-OXID |
| Susi T | Thu-PS2-20 |
| Suzer S | Mon-14:00-I-NAEX |
| Suzuki T | Tue-PS1-40 |
| Suzuki Y | Thu-PS2-42 |
| Süle P | Tue-PS1-41 |
| Svec M | Mon-14:00-0-ORGS, Tue-11:00-0-ORGS2 |
| Swart I | Tue-11:40-0-ORGS1 |
| Syari'ati A | Thu-14:00-0-GRAP |
| Syres K L | Tue-16:20-0-ORGS, Thu-PS2-33 |
| Szabelsi P | Tue-14:40-0-ORGS |
| Szabó T | Tue-10:00-0-ENER |
| Szabová L | Thu-14:20-0-OXID |
| Szajna K | Thu-10:40-0-ORGS, Thu-11:20-0-SEMI, Thu-14:00-0-SEMI |
| Szamosvölgyi Á | Tue-9:20-0-NAEX |
| Szanyi J | Thu-15:00-I-CATH |
| Szendró M | Tue-PS1-41 |
| Szenti I | Tue-15:20-0-OXID, Thu-PS2-32 |
| Szítás Á | Mon-15:00-0-CATL, Tue-PS1-17, Tue-PS1-42 |
| Szymonski M | Mon-14:20-0-ORGS, Tue-16:00-0-ORGS |
| T | |
| Taccardi N | Thu-PS2-04 |
| Tachibana T | Thu-PS2-46 |
| Tagawa M | Thu-PS2-12, Thu-PS2-13 |
| Tajiri H | Mon-15:00-0-NAEX |
| Takagi N | Mon-14:00-0-BAND |
| Takahashi Y | Tue-9:00-0-MAGN, Wed-11:20-K-GRAP |
| Takáts V | Tue-9:40-0-BIMS |
| Takayama A | Wed-16:20-0-BAND |
| Takeuchi K | Thu-9:20-0-CATH |
| Tálas E | Tue-10:00-0-ENER |
| Taleb-Ibrahimi A | Mon-15:00-I-BAND, Tue-14:40-0-EG2D, Thu-14:40-0-ENER, Thu-PS2-19 |
| Tamaki Y | Thu-PS2-34 |
| Tanaka K | Wed-11:40-0-BAND |
| Tang S-J | Wed-16:20-0-BAND |
| Tanemura M | Wed-11:20-K-GRAP |
| Taniguchi M | Wed-16:20-0-BAND |
| Tapasztó L | Tue-15:00-I-EG2D |
| Tariq Q | Wed-11:40-0-OXID |
| Tashima K | Thu-9:20-0-CATH |
| Tasic A | Thu-PS2-36 |

| | |
|------------------------|---|
| Tautz F S | Tue-PS1-12 |
| Taylor R | Tue-16:20-0-ORGS |
| Tebi S | Tue-14:00-0-ORGS |
| Tedstone A A | Thu-15:00-0-ENER |
| Teichert C | Thu-11:20-0-SEMI, Thu-15:20-0-ORGS |
| Tejeda A | Thu-14:40-0-ENER, Thu-PS2-19 |
| Terstoff J | Tue-PS1-05 |
| Thissen A | Mon-14:40-0-NAEX, Thu-PS2-01 |
| Thomas A G | Tue-16:20-0-ORGS, Thu-15:00-0-ENER, Thu-PS2-33 |
| Thomsen S D | Thu-9:00-0-CATH |
| Thornton G | Tue-PS1-10, Thu-15:20-0-OXID |
| Timm M J | Thu-16:20-0-CATL |
| Toccoli T | Wed-16:20-0-ORGS |
| Tofail S A M | Thu-9:40-0-MOLA |
| Togami Y | Thu-PS2-35 |
| Tomán J J | Tue-14:00-0-BIMS, Wed-10:00-0-BIMS, Thu-PS2-10 |
| Tomellini M | Wed-9:20-0-GRAP |
| Tompos A | Tue-10:00-0-ENER, Tue-PS1-03, Thu-9:00-0-OXID |
| Tonchev V | Wed-9:20-0-COMP |
| Tonks J | Tue-9:40-0-CORR |
| Tonner R | Tue-11:40-0-ORGS1 |
| Torun I | Tue-16:40-0-OXID |
| Totani R | Thu-9:00-0-MOLA |
| Tóth J | Tue-PS1-43 |
| Tóth L | Thu-PS2-48 |
| Tour J | Mon-15:00-0-SAMA |
| Tovt A | Thu-14:20-0-OXID |
| Tőkési K | Tue-PS1-51, Thu-PS2-02 |
| Travaglia E | Tue-11:00-0-EG2D |
| Trenary M | Mon-14:00-I-CATL |
| Tricot S | Wed-9:40-0-OXID |
| Trippé-Allard G | Thu-14:40-0-ENER |
| Tsai T-R | Tue-9:00-0-NAEX |
| Tsai C-L | Thu-PS2-14 |
| Tsaousis P | Thu-14:00-0-ORGS |
| Tsud N | Tue-9:40-0-ENER, Wed-11:40-0-ORGS |
| Tsukamoto S | Wed-16:40-0-ORGS |
| Tsuruta R | Thu-PS2-35 |
| Tu Y-C | Thu-PS2-14 |
| Tu F | Thu-PS2-32 |
| Tusche C | Thu-PS2-01 |
| Tulic S | Thu-PS2-20 |
| Turban P | Wed-9:40-0-OXID |
| Turcsányi Á | Tue-10:00-0-ENER |

| | |
|-----------------------------|--|
| Turmaud J-P | Thu-PS2-19 |
| Tzallas P | Mon-17:00-0-ELI-ALPS |
| U | |
| Uchida K | Thu-PS2-23 |
| Ueba T | Wed-11:40-0-BAND |
| Ueda Y | Thu-PS2-42 |
| Ueno N | Wed-11:40-0-BAND |
| Ules T | Tue-PS1-12 |
| Umezawa K | Tue-14:20-0-BIMS |
| Unger W | Mon-14:40-0-NAEX |
| Urgel J I | Tue-11:40-0-ORGS2, Tue-17:00-0-PISC |
| Urhan B K | Tue-11:40-0-ELCH |
| Ustinov A B | Tue-PS1-31 |
| Utsumi Y | Tue-15:20-0-ORGS |
| V | |
| Vad K | Tue-9:40-0-BIMS |
| Vajdle O | Tue-PS1-50, Thu-PS2-36 |
| Valerie G | Thu-11:40-0-GRAP |
| Valeri S | Tue-PS1-38, Thu-14:00-0-OXID |
| Van Aert S | Thu-14:00-0-SEMI |
| Vancsó P | Tue-15:00-0-EG2D |
| Van Der Heijden N | Tue-11:40-0-ORGS1 |
| Van Dorp W | Thu-14:00-0-GRAP |
| Vantalon D | Thu-11:40-0-ORGS |
| Van Tendeloo G | Thu-14:00-0-SEMI |
| Varga M | Thu-PS2-20 |
| Varga E | Tue-9:20-0-NAEX |
| Vári G | Mon-15:00-0-CATL, Tue-PS1-44 |
| Varju K | Mon-17:00-0-ELI-ALPS |
| Vasiljevic N | Tue-16:00-0-ELCH |
| Vass Á | Thu-9:00-0-OXID |
| Vasseur G | Wed-9:20-0-GRAP |
| Vázquez H | Mon-14:00-0-ORGS, Tue-9:20-0-ORGS, Wed-10:00-0-COMP |
| Vázquez de Parga A L | Tue-10:40-0-EG2D, Tue-15:00-0-ORGS, Tue-PS1-46, Wed-11:00-0-BAND, Thu-11:20-0-GRAP |
| Vedmedenko E Y | Thu-14:00-0-ENER |
| Veltruská K | Tue-9:40-0-ENER |
| Van den Bos K H W | Thu-14:00-0-SEMI |
| Verbeek J | Thu-14:00-0-SEMI |
| Verdini A | Tue-10:00-0-CORR, Tue-11:00-0-ORGS1, Wed-9:20-0-GRAP, Thu-9:00-0-MOLA |
| Vergeer K | Tue-14:20-0-EG2D |
| Verlhac B | Tue-9:20-0-MAGN |
| Vertesy G | Thu-14:40-0-SAMA |
| Verucchi R | Wed-16:20-0-ORGS |

| | |
|-----------------------|--|
| Vesselli E | Thu-PS2-26 |
| Vilas-Varela M | Mon-14:40-0-SAMA |
| Vinithra G | Thu-10:00-0-MOLA |
| Vinogradov N A | Tue-16:20-0-ELCH |
| Vishwakarma R | Wed-11:20-0-K-GRAP |
| De Bocarmé T V | Tue-11:20-0-EG2D, Tue-17:20-0-CATL, Tue-PS1-08 |
| Vlad A | Tue-14:40-0-EG2D |
| Vorokhta M | Wed-11:40-0-ORGS |
| W | |
| Wachsmann W | Thu-PS2-38 |
| Wäckerlin C | Tue-9:40-0-MAGN, Thu-9:20-0-MOLA |
| Wagner M | Thu-9:20-0-OXID |
| Waitz T | Thu-PS2-20 |
| Wakamatsu Y | Wed-11:20-0-K-GRAP |
| Walczak L | Mon-14:00-0-BAND |
| Walker M | Tue-PS1-40 |
| Walker K | Tue-PS1-07 |
| Walton A S | Thu-15:00-0-ENER, Thu-PS2-33 |
| Wandelt K | Tue-14:00-0-ELCH |
| Wang D | Tue-PS1-15 |
| Wang J | Mon-14:00-0-SAMA |
| Wang X | Thu-15:00-0-CATH |
| Waser R | Wed-16:40-0-ORGS |
| Wasserscheid P | Thu-PS2-04 |
| Watanabe K | Thu-PS2-23, Thu-PS2-42 |
| Watson D | Thu-14:00-0-ORGS |
| Wechsler D | Wed-11:40-0-OXID |
| Weinelt M | Thu-9:00-0-LASE |
| Weingarth D | Tue-15:00-0-ELCH |
| Wella S A | Tue-17:00-0-ORGS |
| Wendt S | Thu-10:00-0-OXID |
| Wenzel G | Wed-11:20-0-BAND |
| Widdra W | Wed-10:00-0-OXID, Wed-16:20-0-SAMA, Thu-14:40-0-ORGS |
| Widmer R | Tue-11:40-0-ORGS2 |
| Wiegmann T | Tue-PS1-45, Thu-14:20-0-CATH |
| Wietstruk M | Thu-PS2-01 |
| Willhammar T | Thu-14:00-0-SEMI |
| Wilson N R | Tue-14:00-0-EG2D, Tue-PS1-19 |
| Wilson A | Tue-PS1-20 |
| Winter R | Wed-11:20-0-ORGS |
| Wolf M | Mon-10:40-Plen-2 |
| Woo T G | Tue-17:00-0-OXID, Thu-PS2-39 |
| Wormeester H | Thu-PS2-15 |

| | |
|--------------------------|--|
| Wrana D | Thu-10:40-0-ORGS, Thu-11:20-0-SEMI |
| Wu Z | Thu-PS2-38 |
| Wu Y-C | Tue-PS1-47 |
| X | |
| Xia X | Tue-14:00-0-EG2D |
| Xie L | Tue-11:00-0-ORGS |
| Xu W | Tue-11:00-0-ORGS, Thu-16:20-0-ORGS |
| Xu H | Thu-PS2-02 |
| Yadav R P | Thu-14:20-0-SEMI |
| Yagi S | Wed-16:40-0-BAND, Thu-PS2-08, Tue-PS1-33 |
| Yagy K | Tue-PS1-40 |
| Yaji K | Mon-14:20-0-BAND, Tue-PS1-48 |
| Yajima A | Wed-9:00-0-COMP |
| Yaakob Y | Wed-11:20-K-GRAP |
| Yakimova R | Thu-10:00-0-GRAP |
| Yamada H | Tue-17:00-0-PISC |
| Yamamoto S | Thu-9:20-0-CATH |
| Yamamoto S-I | Tue-PS1-49 |
| Yamanaka S | Thu-PS2-35 |
| Yamasaki T | Tue-PS1-29 |
| Yamashita S | Wed-9:00-0-COMP |
| Yamasue K | Thu-9:40-0-SAMA |
| Yanagisawa H | Thu-10:40-0-LASE |
| Yang D | Wed-11:00-0-ORGS |
| Yaoita Y | Wed-16:00-0-BAND |
| Yavuz A | Thu-PS2-31 |
| Yildiz B | Wed-16:40-0-OXID |
| Yim C M | Tue-PS1-10 |
| Yivlialin R | Tue-11:00-0-ORGS1 |
| Yokota K | Thu-PS2-12, Thu-PS2-13 |
| Yokotani A | Thu-PS2-28 |
| Yoshida K | Wed-11:40-0-BAND |
| Yoshida Y | Wed-16:00-0-BAND |
| Yoshimoto S | Thu-9:20-0-CATH |
| Yoshinobu J | Thu-9:20-0-CATH |
| Yu C-Y | Thu-PS2-14 |
| Zaba T | Tue-17:20-0-MOLA |
| Zabka W-D | Tue-14:40-0-OXID |
| Zacharias H | Thu-9:40-0-LASE |
| Zajac L | Mon-14:20-0-ORGS |
| Zaki E | Thu-11:20-0-OXID |
| Zalkind S | Thu-15:00-0-OXID |
| Zaluska-Kotur M A | Wed-9:20-0-COMP, Wed-9:40-0-COMP |
| Zayachuk D M | Tue-PS1-06 |
| Zboril R | Mon-14:00-0-ORGS |

| | |
|-----------------------|---|
| Zehra T | Thu-14:00-0-GRAP |
| Zetterberg J | Thu-11:20-0-CATH, Thu-14:20-0-CATH, Thu-14:40-0-CATH |
| Zhang Chi | Thu-11:00-0-ORGS |
| Zhang Chu | Thu-10:40-0-CATH, Thu-11:40-0-CATH, Thu-15:20-0-OXID |
| Zhang T | Wed-9:20-0-ORGS |
| Zhang Y | Tue-14:00-0-ORGS, |
| Zhang Yituo | Wed-16:00-0-BAND |
| Zhang W | Thu-14:20-0-ORGS |
| Zhang H M | Tue-PS1-37 |
| Zhao W | Thu-14:20-0-ORGS |
| Zhao Y | Wed-11:00-0-ORGS |
| Zharnikov M | Tue-17:00-0-MOLA |
| Zhidomirov G M | Wed-11:20-0-OXID |
| Zhou J | Thu-11:20-0-CATH, Thu-14:20-0-CATH, Thu-14:40-0-CATH |
| Zhou F | Tue-PS1-02 |
| Zhu J | Wed-10:40-0-ORGS |
| Zhuravlev A G | Thu-16:00-0-SEMI |
| Zilberberg L | Tue-16:00-1-PISC |
| Zobelli A | Thu-PS2-19 |
| Zollner E M | Wed-16:20-0-SAMA, Thu-14:40-0-ORGS |
| Zolnai Z | Thu-14:40-0-SAMA |
| Zorkani I | Thu-PS2-47 |
| Zugermeier M | Tue-PS1-09 |
| Zuzak R | Tue-16:00-0-ORGS |